ISBN: 978-605-83575-0-1

# 2016 BOOK OF PROCEEDINGS

## Chapter 2

ICENS

INTERNATIONAL CONFERENCE ON ENGINEERING AND NATURAL SCIENCES

24-28 May 2016 / Sarajevo

**Organized by**



EUROPE CONGRESS

www.europecongress.org

**Supported by**

ZENITH GROUP

CNR GROUP

where innovation starts

TURKISH AIRLINES

ICENS
INTERNATIONAL CONFERENCE ON ENGINEERING AND NATURAL SCIENCES
24-28 May 2016 /Sarajevo

# Design and Improvement of Route Plans with Multiple Automated Guided Vehicles for Mechatronics Education

**Barış GÖKÇE[1], Ercan ŞİMŞİR[1]**

Afyon Kocatepe University, Faculty of Technology

***Abstract***

*In this study, an automated guided vehicle model which can move freely with wireless control system and which comprises the transferring and storing of the items with easily changeable direction system for the purpose of being used for Mechatronics education. In this study, it has been assumed that the item will be transferred to the automated guided vehicle model from its position to another position. Besides, this system is controlled by computer remotely with wireless control system. Thus, apart from the person who controls the system, the fully automatic, suitable for needs and fast process of transferring and storing has become easier without the help of any human beings. This study whose prototype has been made will be a model for Mechatronics education and it has been aimed that it will be a step for the further studies.*

**Keywords:** Automated Guided Vehicles**,** Route Plans

## 1. INTRODUCTION

Depending on the fast improvement of the technology, smart machine design and producing has gained importance fitting for the purpose of high cost and instead of human power. The development of all these studies has led to the common usage of robot and automatization in the developed countries [1]. Recently the development of technology and industry has shown its real effect with the development robots and their usage when necessary. As these robotic studies have improved, it has been understood that robots are necessary for different application areas. The robot which reaches to a target whose coordination are known without crashing barriers has been aimed to reach the target with no human power in a mapped area. While carrying on its mission the robot will continue along its way by detecting the barriers and passing over them without moving away from its target [2]. With this system, the creating storing areas with high and narrow corridors has been effective on increasing the capacity. Transportation with no operator and risk could be done apart from standard height with the increase of capacity paralleling with height. In this study, an education robot design which both helps the storing problems to be solved and contributes to mechatronics education has been made. In addition to a software which positions the robot in the storing system has been improved.

Machines, robots and all mechanisms carrying out certain functions depend on mechatronics system components to perform in a smart way [3].

Automated guided vehicle decreases the cost and increases the productivity by helping a production facility or store automatization to become mechanical. First automated guided vehicles were invented by Berret Electronic in 1953. An AGV can pull the objects with a trailer attached to its back size separately. These trailers were used in order to carry raw materials and manufactured goods. AGVs can also store the objects on a ground and those

products can be placed on conveyors and can be pulled turning upside down. AGVs can be used nearly all kind of ındustries ıncluding paste paper, metal, newspaper and general production. Materials such as food, linen or drugs which can be transported are ıncluded in this process.

AGVs are the vehicles which are used in transportation within the factories in the fields of production and installation and storing. In principle AGVs should be divided in two [4].

- Those which transport freely,
- Those which depend on a route.

First type vehicles use laser or infra-red ray equipment identifying its position by using the reflected ray via the mirrors on the walls and position predictions. In addition, a communication net which is installed on the floor to arrange the calibration can be used. This system can be established by using kits fulfilling transmitter and receiver duties, magnets or chess board shaped figures which can be carried optically [4].

Nowadays AGVs are used in any other transportation duties (stores, container stations, external transferring system). The source of information about the design and control of AGV system in production, distribution, load transfer and transportation has been dealt with. Most of the patterns have been understood to be applicable for the problems in the production centres. It has been proved that the present patterns and some of the new patterns are successful in big AGV systems. In fact, new analytical and simulation patterns should be improved for big AGV systems to deal with the problems such as extended calculating time, unity, congestion, getting stuck, delay and finite planning time [5].

Figure 1 shows the directing flexibility of mobile pack transporter with trailer, automated guided vehicles are used in many production systems, especially in the facilities with various and complex process routes. In the recent years, there are a lot of studies related to AGV problems one of which is vehicle accidents. One of the strategies to prevent those accidents is to separate the route of the vehicles and to use the “one area strategy” which enables the vehicles to function alone. The vehicles do not help each other in the systems in which traditional one area strategy is used and when there appears a load imbalance of the vehicle, immobile area strategy cannot respond to the demand because of this limitation [6].

*Figure 1. Mobile pack transporter with AGV trailer.*

## 2. MATERIAL AND METHOD

The route planning training set of unmanned multiple automated guided vehicles consist of four main areas like its production, software and design as it is shown in Figure 2. Those areas are computer based solid pattern layout, its prototype production, computer control and electronic control card. Each area has been examined and the rate of cost and performance had been emphasized as its being economical.

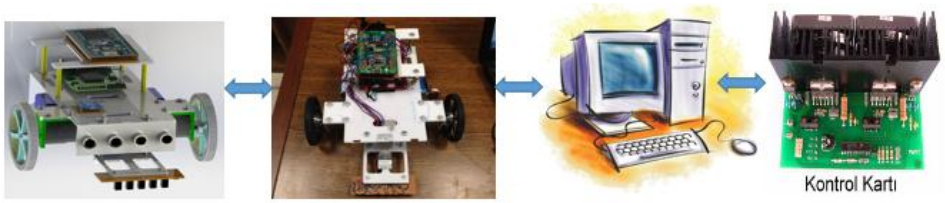


*Figure 2. The model of multiple automated guided vehicles.*

### *2.1. Bottom Sachet System*

In this training robot study, materials which have been used for the construction of sub-chassis have been mentioned in robot locomotor system. U plate which is 110x95x3 mm in size has been fixed in parallel with T plate which is 200x110x4 mm in size which is reinforced with a material M4x40 mm. As it is seen in Figure 3, four dead shores are added between the parallel Plexiglas plates and bottom sachet plate has been fixed. There are cable vessels and holes on the bottom sachet plate in order to provide convenience in installation.

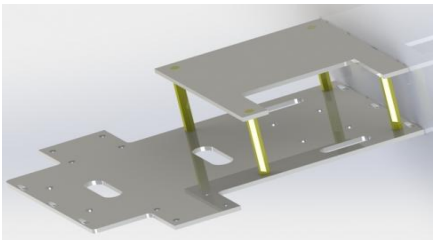

*Figure 3. Installation model of bottom and top plate.*

Shaft driver which has been installed on a polo wheel Φ 90x10 mm in size has been fixed with motor shaft. The installed Wheel has been shown in Figure 4.

*Figure 4. The installed Wheel.*

The system which will enable the movement on the black band has been prepared on the bottom sachet by locating ARM control cart 90x55x3 mm in size through vessels as it is seen in Figure 5.

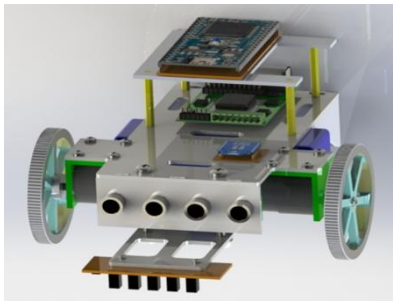

*Figure 5. The design of the automated guided system.*

### *2.2. Functioning Principle of the System*

The aim of this study is to Show that two vehicles move without crashing each other and carry the predetermined load from a certain location. Besides, the robots turn back to the desired location by certain movements. After the distance between the two robots and the in and out destination are determined, the destination of the defined robot is questioned from the database. Then, the signals are converted into a language which can be understood by driver cards in order for automated guided vehicles to go to the determined location. DC motor has been aimed to function with this process. This information has been sent to the controller of the DC motor. For this reason, the system functions. By keeping the distance between the vehicles, they are enabled to move without crashing. Vehicles and the place they move in has been shown in Figure 6.

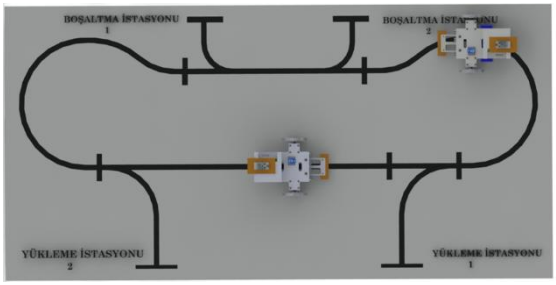


*Figure 6. The solid works design of the vehicles and their movement system.*

### *2.3. Motion System with Line Tracking*

The schematic circuit, showing the monitor system of tracking and drawing and being created for the automated guided vehicles, has been illustrated in the Figure 7. 8 entry gear socket; GND gathering pin numbered 8 and pin numbered 7 has 5-

volt supply voltage. Pins numbered 6.5.4.3.2. are used to take a reading coming from the sensors and the pin numbered 1 has been left empty. It has been enabled that both robots can move on the floor set up black tape.

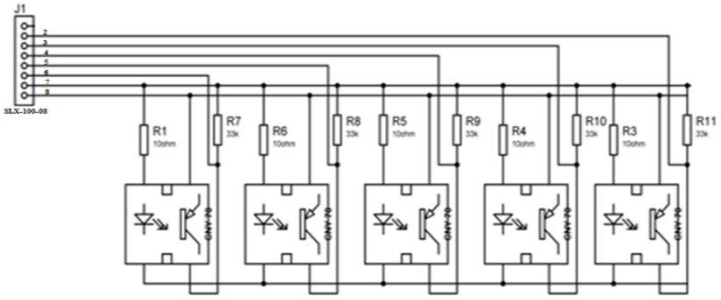


*Figure 7. Schematic circuit of line tracking.*

### *2.4. Control of PID*

In this study, PID has been used. These terms explain three functions applied on a mistake, which are basis rate, integral, mathematical derivative. The vehicle has been enabled to move to the line without any rolling. According to the information from sensors, deviation of target movement is calculated. Hence, the deviation can be minimalized.

The robot which isn't applied PID can move on the line without any rolling in low speed. When the speed of robot is increased, rolling and off-road can be observed. Thus PID is used to enable the robot move on the line properly.

The control of PID has been shown in the Figure 8. If the mathematical template which belongs to a system can be improved, it can be possible to apply lots of model design techniques to calculate control variance which will explain the temporary and permanent situation and their features of closed loop. Hence if the mathematical model cannot be created and the system is complicated, then analytic approach for the model of PID control is impossible [7].

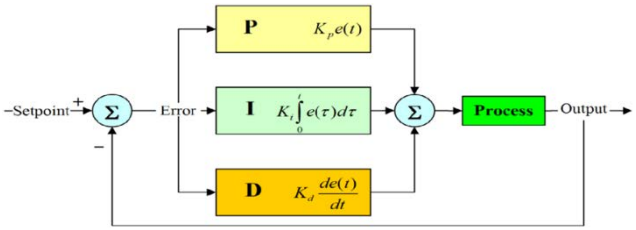


*Figure 8. PIC controller of a system.*

## 2.4.1. Ziegler – Nichols rules for the settings of PID Control

Ziegler-Nichols advices rules to calculate modulating gain Kp, integral time Tİ, derivative Ta considering temporary characteristic of answers. Measurements will be taken into consideration to calculate the parameters of PID controller. Ziegler-Nichols uses two ways for the settings rules. 25% carry in maximum is aimed in both ways. This aim is shown in the Figure 9 [7].

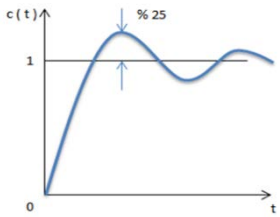


*Figure 9. Cure of step replication, maximum 25% transport [7].*

The factors -such as friction, weight- of parts used in the set of mechanic system has not been regarded before the system has been set. It has been considered that troubles can be seen in tracking the black line and in the speed of mechanic speed on the condition that these are added to the system. These troubles have been tried to be minimalized with a few interferences. The interfaces done were greasing the place where friction is seen, minimizing the friction. The automated guided vehicle which is able to move without human beings is shown in the Figure 10.

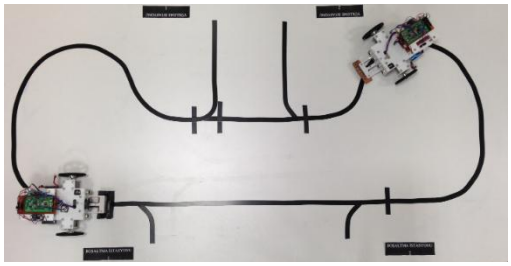

*Figure 10. The system of automated guided vehicle moving without human beings.*

### *2.5. Creating the Movement Information*

After robots are defined, it is decided which defined robots will be taken to the which entry- exit units of a computer. Then to reach this coordinate, all the necessary movements are calculated. Movements calculated are turned into a signal which can be understood by the drivers. Encoder DC motor has been aimed to move with the turning process. This information has been sent to the sensitive DC motor controller. All these control processes are really critical. The coordinate information calculated before is sent to the related encoder DC motor. Hence robot has been enabled to move.

In this study, loading and discharge stations are detected on the path for two automated guided vehicles, which can be seen in the Figure 11. In this system, car numbered 1 takes the products from the loading station numbered 1 and moves towards the discharge station without any human being's help. The car numbered 2 uses the same path at the same time. If the second car encounters the first car, while moving on the path, the second car stops at a suitable distance to avoid any crash or follows the other car. The car numbered 2 get the products from the second station and moves towards second discharge station.

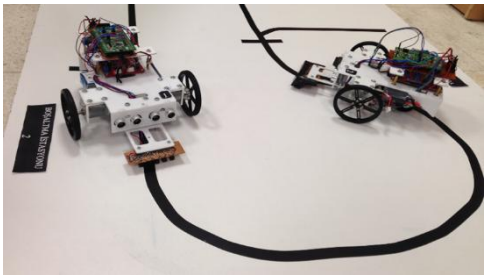

*Figure 11. The movements of the automated guided vehicles on the path.*

The working principle of the robot depends on moving on the lines while keeping the line in the middle. Robot determines its position according to the black line detecting the sensor periodically. It is illustrated in the Figure 12.

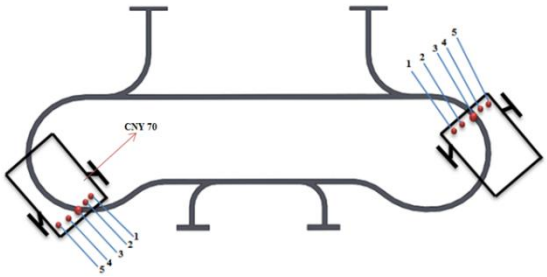


*Figure 12. The movement of the robot forward.*

### *2.6. Interface of Vehicle Control*

C# computer program has been used as an interface in this study. As it is seen in Figure 13, the vehicle numbered 1 takes the product from the second loading station with no human interfere and moves towards the second dumping offloading station. The information about the location of the vehicles has been transferred to the control interface. Besides, the vehicle numbered 2 takes the product from the loading station with no interfere and moves towards the offloading station. We can see the information about their movement on interface with the lines "vehicle communication 1" and "vehicle communication 2".

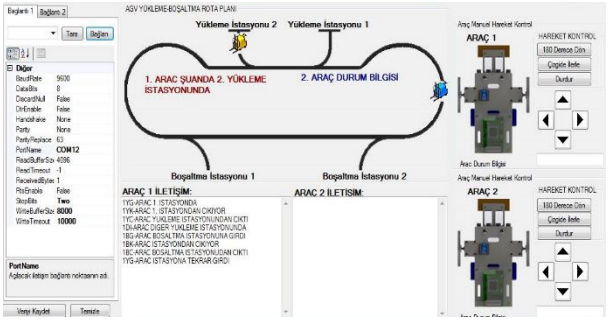


*Figure 13. The control interface of the vehicles on the system.*

## 3. DISCUSS AND CONCLUSION

It is significant to use the current technology on the mobile robot systems and to up bring experts on this field and improved them. Techniques used on the mobile robots are updated for the development of the working fields. To perform the current form with the robots used in daily life cause the loss of time while they are set, financial problems, and the robots wear off and energy loss. Producing portable robots provide the problems to be solved. Besides that, portable robots are used for the visual education as they are real-like. These portable robots provide us to apply the methods taught, observe the results, analyse the data in education without regarding real robot system necessary.

Robots have been enabled to move properly on the black line in the system of design and improvement of the path plans and automated guided multiple vehicles. Robots are activated in different speed and applied more than one supply voltage. Supply voltage, 12 volts, applied on the DC motors are observed to decrease the speed of the working performance. The best supply voltage has been found as 15.7 volts.

It is required that both vehicles should move on the determinate path without crashing each other. The robot completes its target after taking the materials from the entry station and then transmitting them to exit station. The distance between stations and the main road should be set properly to enable the robots turn back with 1800 from the exit station.

In this study, the process is not only reforming and product development and also transporting of the products, planning and improvement of the path, making a model of the system and the usage of the automatization technology. It is possible to decrease the labour force and expenses on the transport of products and planning of the auto vehicle path.

The practice of the modelled robot sets an example for the students in mechanical engineering, electrical and electronic engineering. As it is really had to understand lessons at the mechatronics engineering without applied course and laboratory practice. Besides, it is necessary to produce real-like vehicles and use them in laboratory. In the end, it will be beneficial for the students to have portable vehicles in the laboratory. Thus, this system is suitable to be improved and enlarged. It sets an example for courses of mechatronics engineering as well as being a robot application.

## 4. REFERENCES

[1]. Akpınar, Ö. *Image Processing* Based *A Cartesian Robot Design For Storage,* Sakarya University, Master of Science Thesis, Sakarya, 2008.
[2]. Yorulmaz, S. and Yılmaz, A. *A Robot Project That Found The Targets*. Chamber Of Electrical Engineers Project Competition 3, İstanbul, 2007.
[3]. Öztürk, F.Ş. , Afyon Kocatepe University, Master of Science Thesis Afyonkarahisar, 2014.
[4]. Mantel, R. J. and Landeweerd H. R. A. *Design and Operational Control of an AGV System*. International Journal of Production Economics, 41: 1–3, 257–266, 1995.
[5]. Vis, I.F.A. *Survey of Research in the Design and Control of Automated Guided Vehicle Systems*. European Journal of Operational Research 170: 9, 677–709, 2006.
[6]. Chin HO,Y. and We Liao T. *Zone Design and Control For Vehicle Collision Prevention and Load Balancing in a Zone Control AGV System*. Computers&Industrial Engineering, 56: 1-7, 257-266, 2009.
*[7].* Soygüder, S. *PID control of a SCARA robot by using programmable logic controller*. Fırat University, Master of Science Thesis Elazığ, 2004.

# Investigation of Wind Energy Potential Using Weibull Parameters

*B. Yanıktepe[1], İ. Aladağ[2], C. Özalp[2], C. Aladağ[2]*

***Abstract***

*Turkey is not prevailing country for energy issue and electric energy consumption is getting ascended quickly in the sense of population growth rate and the development of industry. Even tough Turkey has extensive ratio of energy resources for example l , l , l, ., h . O h , w bl T k ' future energy demand are playing significance role owing to both energy dependency and disadvantages from the fossil fuels. On this issue, especially wind energy which has high potential in Turkey from renewable energy sources has still invested. In this study, wind energy distribution according to Weibull parameters are researched in Osmaniye. shape and scale factors are determined using graphical method.*

**Keywords: Weibull distribution, Osmaniye, Turkey**

## 1. INTRODUCTION

Turkey's electricity consumption has inreased rapidly in recent years owing to population growth rate and the development of industry. Even though Turkey has extensive ratio of energy resources for example petroleum, natural gas, coal, etc., they are finite. Therefore, Current trend in energy policy of Turkey has started to look for alternative energy resources espacially wind and solar energy. So that the research of wind energy has gained prominence quickly in Turkey which has high rate potential [1].

Analysis of wind characteristics studied for a specific period of time such as monthly, seasonal, and yearly based on the wind data of the location that is obtained. In the past fifteen years, different mathematical methods were used to investigate of wind characteristics considering with many locations. In the evaluation of wind energy for a specified region, the usage of two parameters Weibull distribution is an essential instrument in order to determine whether wind energy is a reasonable or not. Many studies for different locations were done so as to determine the shape (k) and scale (c) parameters of Weibull distribution for the region [2-4].

Seguro and Lambert studied Weibull distribution by using three methods for estimating shape and scale parameters. They determined the wind energy analysis considering with the graphical method, maximum likelihood method, and the modified maximum likelihood method. Their results showed that both maximum likelihood method and modified maximum likelihood method can provide more accurate results than graphical method [5]. Yaniktepe et al. investigated the wind energy potential for Osmaniye region by using 44 months meteorological data. And they calculated the two parameters of Weibull distribution applying graphical method. Frequency distribution for wind direction and the average power density values for different directions are presented in this study [6]. Akdag and Guler developed a novel method (NEPFM) to determine Weibull parameters efficiently and accurately. Comparison was made between NEPFM method and eight methods considering various data set. The result in their study indicated that the NEPFM method is slightly better fit than compared parameter estimation methods [7]. Islam et al. carried out a study about the wind potential assessment in two different regions in Malaysia. They determined monthly scale and shape parameters

for each year. Finally, they found wind power density values for the regions. A maximum power density of 67.40 (W/m$^2$) was encountered at Kudat region [8].

This paper presents an investigation of wind energy potential as a consequence of the Weibull distribution in the location of near Osmaniye. the shape (k) and scale (c) parameters were calculated using graphical method. Wind power densities were also determined of location.

[1] *Corresponding author: Osmaniye Korkut Ata University, Department of Energy Systems Engineering, 80000, Osmaniye, Turkey.* byaniktepe@osmaniye.edu.tr

[2] *Osmaniye Korkut Ata University, Department of Energy Systems Engineering, 80000, Osmaniye, Turkey.* ilyasaladag@osmaniye.edu.tr, coskunozalp@osmaniye.edu.tr, cananaladag@osmaniye.edu.tr

## 2. MATERIAL AND METHOD

The location, measurement, data and calculation method are given below in detail.

### *2.1. Location, Measurement Station and Collected Wind Speed Data*

Wind speed distribution is a very significance parameter for consideration the wind energy potential of a region. In this study, ten minutes time-series wind data for the location near Osmaniye has been analyzed. The location of region to investigate, where the measurement station is installed, can be seen in Figure 1.

Measurement station was installed in the region and wind speed value at approximately 80 m height were recorded during a nine months period between the April, 10st 2012 and December , 30th 2012. The collected data were recorded as 10 min average values using an data logger and weather data transfer utility. The direction of the wind as well as air pressure and temperature values were also measured and recorded for the observation period.


*Figure 1. Location of region in Osmaniye, Turkey*

### *2.2. Weibull Distribution*

Equations (1-2) using measured data were calculated monthly average wind speed values and standard deviations.

$$v_m = \frac{1}{N}\left[\sum_{i=1}^{N} v_i\right] \tag{1}$$

$$\sigma = \left[\frac{1}{N}\sum_{i=1}^{N}(v_i - v_m)^2\right]^{0,5} \tag{2}$$

where $v$ is wind speed, $v_i$ observed wind speed, $v_m$ is average wind speed (m/s), $N$ is total number of wind speed and $\sigma$ is standard deviations (m/s).

Weibull distribution for the probability density function can be characterized in terms of wind speed at a given location within a specified time period and it is given below,

$$f_w(v) = \frac{k}{c}\left(\frac{v}{c}\right)^{k-1} \exp\left[-\left(\frac{v}{c}\right)^{k}\right] \tag{3}$$

where $f_w(v)$ is the probability of having a wind speed of $v$ (m/s), $k$ and $c$ is a shape factor and scale factor respectively. The relationship between shape factor $k$, scale factor $c$ and the mean wind speed $v_m$ is shown as it is given below formula:

$$v_m = c\Gamma\left(1+\frac{1}{k}\right) \tag{4}$$

Remark tahat the gamma function , has the features of

$$\Gamma(1+x)=x\Gamma(x) \text{ and } \Gamma(x)=\int_0^{\infty}\zeta^{x-1}\exp(-\zeta)d\zeta$$

Furthermore, cumulative probability function of the Weibull distribution $F_w(v)$ is figured out as given below,

$$F_w(v)=1-\exp\left[-\left(\frac{v}{c}\right)^k\right] \quad (5)$$

As shown equations (3-5), the Weibull distribution has two-parameter. These are shape and scale parameters. In this study to calculate the shape "k" and scale "c" parameters of the Weibull distribution from the observed wind data the after methods are applied [9,12],

Equation (6) can be shown as,

$$\ln\left[-\ln\left(1-F_w(v)\right)\right]=k\ln v-k\ln c \quad (6)$$

İn this place, if $x=\ln v$ , $y=\ln\left[-\ln\left(1-F_w(v)\right)\right]$, $A=k$ and $B=-k\ln c$ are to be accepted, there becomes a linear equation. Afterwards, $y=Ax+B$ is acquied from the equation (6). Moreover, the equation of $c=\exp(-B/A)$ is estimated from the equation of $B=-k\ln c$. The least square method is applied to estimated the $A$ and $B$ are estimated as follow:

$$A=\frac{\sum_{I=1}^{N}\left(x_i-\bar{x}\right)\left(y_i-\bar{y}\right)}{\sum_{i=1}^{N}\left(x_i-\bar{x}\right)^2} \quad (7)$$

İn this place, $\bar{x}$ (mean of x values) and $\bar{y}$ (mean of values) are found by,

$$\bar{x}=\frac{1}{n}\sum_{i=1}^{N}f_i x_i \quad , \quad \bar{y}=\frac{1}{n}\sum_{i=1}^{N}f_i y_i \quad (8)$$

From the graphical method, by using linear least-squares regression model with regression coefficient or regress variable taken as wind speed to compute the best fitted line. Plotting $\ln v$ counter $\ln\left[-\ln\left(1-F_w(v)\right)\right]$ should output a flat line. $k$ is the slope of the line and $-k\ln c$ is the intersection of the y–axis. The obtained graph as an example for the mean value of nine months is shown in Fig. 2, $k$ and $c$ parameters in equation (5) of the Weibull distribution can be readily calculated using the wind speed data of Osmaniye location as 1.93 and 6,09 respectively.

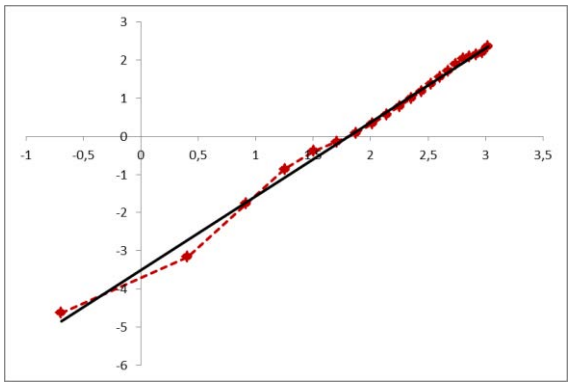


*Figure 2. Linearized curve and fitted line comparison*

### *2.3. Calculation of Wind Power Density*

Wind power is dependent upon the cubic of wind speed. Therefore, the power density for observed data can be estimated using the following equation [10, 11]:

$$P(v) = \frac{1}{2}\rho A v^3 \quad (9)$$

Where $\rho$ is the standard density of air, 1.225 kg/m$^3$, the theoretical power depended on the Weibull probability function per unit area is given by [10],

$$P_w = \frac{1}{2}\rho c^3 \left(1+\frac{3}{k}\right) \quad (10)$$

## 3. RESULTS AND DISCUSSION

Wind speed potantial of Osmaniye location was studied using Weibull distribution. The monthly avarage values of wind speed and the standard deviations obtained from equations (1-2) using observed data, also shape (k) and scale (c) parameters of the Weibull distribution were estimated using equations (4-5). All estimated monthly parameters are shown in Table 1. The monthly average wind speeds are observed maximum values in May and June with the magnitudes of 7.80 m/s and 7.28 m/s and the lowest values of 3.55 m/s and 3.82 m/s are occured in August and September. Also the highest value of standard deviation is 3.89 m/s and the lowest value is determined as 1.09 m/s for wind speed data at Osmaniye region. The Weibull parameters have been well fitted by the linear regression model (Graphical method) for the given location. Shape parameter of Weibull distribution has been determined in the range of 1.34 to 3.54 and it is lowest in December and highest in August. Scale parameter of Weibull distribution has been determined in the range of 4.67 m/s to 7.91 m/s.

*Table 1. Parameters, calculated from wind speed data of Osmaniye location*

| | $V_m$ (m/s) | σ ( / ) | c (m/s) | k |
|---|---|---|---|---|
| April | 7,00 | 2,66 | 7,04 | 2,30 |
| May | 7,80 | 2,94 | 7,91 | 2,19 |
| June | 7,28 | 2,85 | 7,33 | 2,47 |
| July | 6,99 | 2,66 | 6,87 | 2,43 |
| August | 3,55 | 1,29 | 4,67 | 3,54 |
| September | 3,82 | 1,09 | 5,07 | 3,43 |
| October | 4,89 | 2,52 | 5,89 | 2,24 |
| November | 5,80 | 2,85 | 5,98 | 1,87 |
| December | 6,29 | 3,89 | 5,87 | 1,34 |

Figure 6 shows monthly variation of the power densities based on actual data and Weibull function for nine months period. It showed that the wind power density values has maximum average value of 415.97 W/m$^2$ in May and minimum value of 41.45 W/m$^2$ for the month of August. As can be seen from this figure, the values of power densities spring season of year are higher than the other seasons.

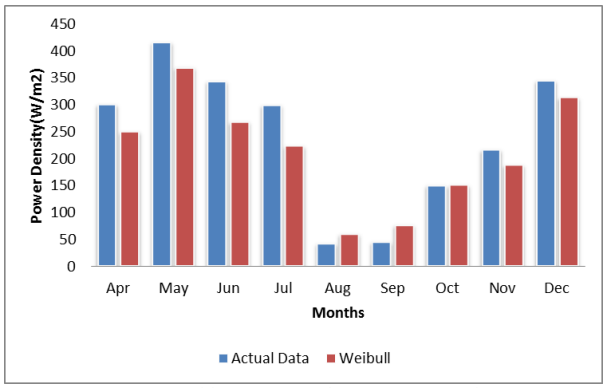


*Figure 6. Monthly variation of average power densities*

## 4. CONCLUSIONS

In current research, monthly average wind speeds have been observed for a region of Osmaniye. Shape parameter *k* and scale parameter *c* of the Weibull distribution were detemined using graphical method by measuring wind speed at 80m height.

Results are concluded as it is given below,

- The mean wind speeds range between 3.55 and 7.80 m/s. The lowest values of mean wind speed were in August, September, October. On the other hand, the highest amounts of mean wind speed were seen May, June, April. The average wind speed for spring, summer and autumn seasons is 7.4 m/s, 5.94 m/s and 4.83 m/s respectively.
- The values of c have been observed higher as compared to the value of k in all the months. The monthly values of k parameter ranged from 1.34 to 3.54. Also, c values varied from 4.67 to 7.91 m/s.
- The wind power density has maximum average value of 415.97 $W/m^2$ in May and minimum value of 41.45 $W/m^2$ for the month of August.
- Weibull and actual data are almost the same rate values.

## REFERENCES

[1]. Yanıktepe B., Özalp C., Kaşka Ö. and Köroğlu T. "An assessment of Wind Power Potential in Osmaniye, Turkey" *6th I l A v T h l S (IATS'11)*, pp. 82-88, 16- 18 May 2011, Elazığ, Turkey.

[2]. Gokcek M., Bayulken A. and Bekdemir S., "Investigation of wind characteristics and wind energy potential in Kirklareli, Turkey", *Renewable Energy*, vol. 32, pp. 1739-1752, 2007.

[3]. Guler O., "Wind energy status in electrical energy production of Turkey", *Renewable and Sustainable Energy Reviews*, vol. 13, pp. 473– 478, 2009.

[4]. Bilir L., İmir M., Devrim Y., Albostan A., "An investigation on wind energy potential and small scale wind turbine performance at İncek region - Ankara, Turkey", *Energy Conversion and Management*, vol. 103, pp. 910-923, 2015.

[5]. Seguro J.V., Lambert T.W., " Modern estimation of the parameters of the Weibull wind speed distribution for wind energy analysis. *J. Wind. Eng. Ind. Aerod.* , vol. 85 pp.75-84, 2000.

[6]. Yaniktepe B., Koroglu T., Savrun M.M., " Investigation of wind characteristics and wind energy potential in Osmaniye, Turkey", *Renew. Sust. Energy Rev.*,vol. 21, pp. 703–11, 2013.

[7]. Akdağ S. A., Güler Ö., " A novel energy pattern factor method for wind speed distribution parameter estimation", *Energy Conversion and Management*, vol. 106, pp. 1124-1133, 2015.

[8]. Islam M.R., Saidur R., Rahim N.A., "Assessment of wind energy potentiality at Kudat and Labuan, Malaysia using Weibull distribution function", *Energy*, vol. 36, pp. 985–92, 2011.

[9]. Ahmed Shata, "Theoretical investigation and mathematical modelling of a wind energy system case study for Mediterranean and Red Sea", M.Sc. Thesis, Technical University of Berlin, 2008.

[10]. Celik A. N., "A Statistical analysis of wind power density based on the Weilbull and Rayleigh models at the southern region of Turkey," *Renewable Energy*, vol.29, pp. 593-604, 2003.

[11]. Akpinar Kavak E., Akpinar S., "An Assessment of Wind Turbine Characteristics and Wind Energy Characteristics for Electricity Production," *Energy Sources, Part A*, vol. 28, pp. 941–953, 2006.

[12]. Mohammadi K., Alavi O., Mostafaeipour A., Goudarzi N., Jalilvand M., "Assessing different parameters etimation methods of Weibull distribution to compute wind power density", *Energy Conversion and Management*, vol. 108, pp. 322-335, 2016.

# A Comparative Study of Joint Clearance Effects on Robotic Systems Having 2D and 3D Motion Necessities

***Selçuk Erkaya***[3]

***Abstract***

*Due to the advances in technology, robots are used in industrial applications where high accuracy, repeatability and stability of operations are required. Even in an accurate design and manufacturing process, clearance in a joint cannot be completely eliminated in articulated systems owing to the relative motion necessity of links. This is a main reason of accuracy loss for a robotic manipulation. In this study, effects of joint clearance are investigated on the system dynamics. Theoretical analysis is performed for a small clearance size. By using the nonlinear spring-damper characteristic, contact model in revolute joint with clearance is established and the friction effect is performed using the Coulomb friction model. 2D and 3D motion sensitivities are compared relative to each other by considering with and without joint clearance. The results show that even if the clearance size is small, it has a crucial role on motion sensitivity of robotic manipulations.*

**Keywords:** Contact force, joint clearance, manipulation accuracy, motion sensitivity, rigid impact.

## 5. INTRODUCTION

Due to the advances in technology, robots are used in industrial and medical applications where where high accuracy, repeatability and stability of operations are desired. The possible sources of errors in robots are summarized as assembly errors, resolution of the servo actuators, backlash in the reducers and clearances in the joints [1]. In the kinematic and dynamic analyses of the robot manipulator systems, each joint is characterized as perfect adjustments, that is, clearance, wear, deformations etc. are not considered. However, the clearances always exist in the joint connections due to assemblage, wear and manufacturing errors [2-6]. A reasonable clearance for the joints at link connections of mechanical system is necessary to allow the relative motion of the connected links. In the presence of clearance at a revolute joint, the two kinematic constraints are eliminated, and two degrees of freedom consisting of the horizontal and vertical displacements of the journal center relative to bearing center are added to the mechanism motion.

An error analysis for a parallel device was proposed to predict the accuracy of the parallel devices with the static and dynamic errors [7]. The optimal allocation of joint tolerances was investigated by considering the positional and directional errors of the robot end effector and the manufacturing cost. The unknown joint variables were modelled as interval parameters due to the inherent uncertainty [8]. The effects of joint clearance on the parallel robot's accuracy were investigated. An analytical model was presented to predict easily the pose error for a given external load, a nominal pose and the structural parameters of the 3-UPU parallel manipulator [9]. Due to the clearances and elastic deformations in parallel manipulators, a procedure was proposed to calculate the positional. A 5R planar mechanism was used for an example to perform the validity of proposed procedure [10]. The effect of joint flexibility on the dynamic performance of a serial spatial robot arm with

rigid links was studied by using three developed models. Theoretical and simulation studies showed that joint damping was outlined as a major source of inaccuracies, causing trajectory error without a proper feedback controller [11]. The trajectory of a mobile robot having clearance joint was studied. The ANFIS approach was used to model the clearance characteristics and the system kinematics were investigated. To decrease the effects of clearance on the desired trajectory, an optimisation process was also outlined by using genetic algorithms [12]. The effects of joint clearance and link flexibility on the kinematics and dynamics of conventional articulated mechanisms were extensively performed with analytical and numerical studies [5, 12, 13]. For improving the mechanism precision, optimisation methods were also introduced to decrease the deviations owing

[3] *Corresponding author: Mechatronics Engineering Department, Erciyes University, Engineering Faculty, 38039 Kayseri/TURKEY.* serkaya@erciyes.edu.tr

to the clearance joint [14, 15]. Artificial neural networks were used to model the vibration characteristics of a mechanism with joint clearance [16]. Both theoretical and experimental studies about joint clearance were presented [17].

## 6. MOTION EQUATION OF ROBOT MANIPULATOR WITH JOINT CLEARANCE

The existence of clearances in the joints of mechanical systems is inevitable due to the assemblage, manufacturing errors and wear. A reasonable clearance for the joints at link connections of mechanical system is necessary to allow the relative motion of the connected links. Radial clearance in a joint, as shown in Fig. 1, can be defined as the difference between journal and bearing radii.

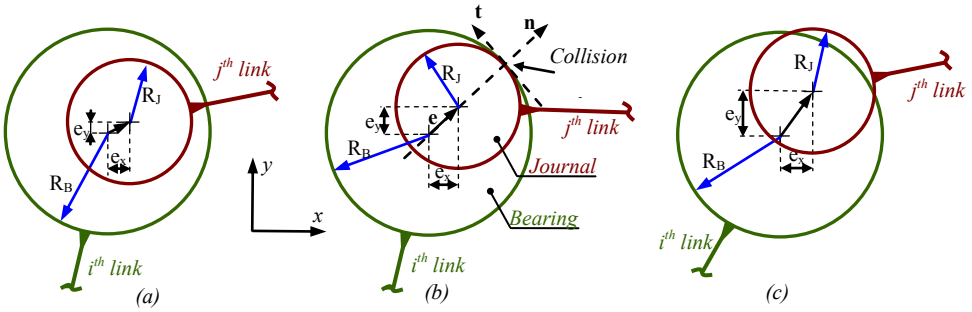


*Figure 1. Different motion types of journal inside the bearing: (a) free flight mode, (b) contact with impact mode, (c) contact with relative penetration (continuous contact mode)*

The magnitude of the clearance vector represents the relative displacement between journal and bearing centers. Three different types of motion between the journal and bearing can be observed during the dynamics of the revolute joint clearance, (i) free flight mode, that is, journal and bearing are not in contact and journal moves freely within the bearing's boundaries (Fig. 1(a)), (ii) impact mode, which occurs at the end of the free flight mode (Fig. 1(b)), (iii) continuous contact mode, in which contact is always maintained although the relative penetration depth between the bearing and journal (Fig. 1(c)). If there is no lubricant, the journal can move freely within the bearing until contact between the two bodies takes place. When the journal impacts the bearing wall, normal and tangential contact forces are developed. The bearing and journal are parts of the $i^{th}$ and $j^{th}$ bodies, respectively. The relative penetration depth ($\delta$) between the journal and bearing is given as

$$\delta = e - c \tag{1}$$

in which $e$ is the magnitude of the clearance vector between the bearing and journal centres, and $c$ is the radial clearance ($c=R_B-R_J$). In a joint with clearance, the force is explained by two different situations. The first one is no contact forces ($F_C$) when the journal and bearing are not in contact with each other. The second is, when the contact between the two bodies occurs; the contact-impact forces are modelled according to a nonlinear dissipative force model based on the Hertzian contact theory (normal force, $F_N$) together with Coulomb's friction law (tangential force, $F_T$). These two conditions can be given as [2],

$$\begin{aligned} \mathbf{F_C} &= 0 \quad \text{if} \quad \delta < 0 \\ \mathbf{F_C} &= F_N + \mathbf{F_T} \quad \text{if} \quad \delta \geq 0 \end{aligned} \tag{2}$$

The normal force is expressed as [2]

$$F_N = K\delta^{(3/2)} + D\dot{\delta} \tag{3}$$

where the first term represents the elastic force component and the second term explains the energy dissipation. K is the generalised stiffness parameter and D is the hysteresis damping coefficient. The

generalised stiffness parameter K depends on the geometry and physical properties of the contacting surfaces. The stiffness parameter K is defined by [18]

$$K=\frac{4\left(E_i E_j\right)}{3\left(E_j\left(1-\nu_i^2\right)+E_i\left(1-\nu_j^2\right)\right)}\left(\frac{R_i R_j}{R_i-R_j}\right)^{1/2} \tag{4}$$

$\nu$ and E are the Poisson's coefficient and the Young's modulus associated with each body (journal and bearing). The hysteresis damping coefficient is outlined as [2]

$$D=\left\{3\left(1-\zeta^2\right)K\delta^{3/2}\right\}/\left\{4v_0\right\} \tag{5}$$

where $\zeta$ is the restitution coefficient and $v_0$ is the initial impact velocity. Friction force acts when contacting bodies tend to slide relative to each other. This force is tangential to the contact surface and is opposite to the sliding velocity. The friction force model is given as [19].

$$\mathbf{F_T}=-\mu\left(\upsilon_T\right)F_N\boldsymbol{\upsilon}_T/\left|\upsilon_T\right| \tag{6}$$

where $\mu(\upsilon_T)$ is the coefficient of dynamic friction. It is a function of relative tangential sliding velocity ($\upsilon_T$) in the collision plane. This expression is defined as:

$$\mu\left(\upsilon_T\right)=\begin{cases}-\mu_d sign\left(\upsilon_t\right) & for \quad \left|\upsilon_t\right|>\upsilon_d \\ -\left\{\mu_d+\left(\mu_s-\mu_d\right)\left(\frac{\left|\upsilon_t\right|-\upsilon_s}{\upsilon_d-\upsilon_s}\right)^2\left[3-2\left(\frac{\left|\upsilon_t\right|-\upsilon_s}{\upsilon_d-\upsilon_s}\right)\right]\right\}sign\left(\upsilon_t\right) & for \quad \upsilon_s\le\left|\upsilon_t\right|\le\upsilon_d \\ \mu_s-2\mu_s\left(\frac{\upsilon_t+\upsilon_s}{2\upsilon_s}\right)^2\left(3-\frac{\upsilon_t+\upsilon_s}{\upsilon_s}\right) & for \quad \left|\upsilon_t\right|<\upsilon_s\end{cases} \tag{7}$$

where $\mu_s$ and $\mu_d$ are the static and dynamic friction coefficients, respectively. $\upsilon_s$ and $\upsilon_d$ denote the critical velocities of the static and maximum dynamic frictions, respectively.

A six-axis industrial robot was considered for the theoretical analysis. This robot is mainly used for laser cutting, welding, handling, assembly etc. The robot manipulator has six degrees of freedom when all joints are perfect, as shown in Fig. 2. Joint clearance leads to different motion modes such as free-flight, impact and continuous contact. Therefore, the dynamic model of the robot manipulator must be developed considering joint clearance.

$$\mathbf{M}\left(q(t)\right)\ddot{\mathbf{q}}(t)+\mathbf{C}\left(q(t),\dot{q}(t)\right)\dot{\mathbf{q}}(t)+\mathbf{Q}\left(\dot{q}(t)\right)+\mathbf{G}\left(q(t)\right)=\mathbf{F}(t)+\mathbf{F_C}\left(\delta,\dot{\delta}\right) \tag{8}$$

where $\mathbf{q}$ is the generalised coordinate column matrix. $\mathbf{M}(q(t))$ denotes the inertia matrix of the robot manipulator. $\mathbf{C}(q(t),\dot{q}(t))$ is the vector of centrifugal and Coriolis terms. $\mathbf{Q}(\dot{q}(t))$ represents the friction term, which consists of the viscous and dynamic frictions. $\mathbf{G}(q(t))$ and $\mathbf{F}(t)$ denote the vector of gravity term and the generalized force matrix, respectively. $\mathbf{F_c}(\delta,\dot{\delta})$ is the contact force which comprises the normal and tangential components. The characteristics of the robot manipulator are outlined in Table 1.

*Table 1. Characteristics of robot manipulator*

| Robot | Length | Mass | Mass moment of inertia characteristics [kgm$^2$] |
|---|---|---|---|

| Links | [mm] | [kg] | $J_{xx}$ | $J_{yy}$ | $J_{zz}$ | $J_{xy}$ | $J_{yz}$ | $J_{zx}$ |
|---|---|---|---|---|---|---|---|---|
| Link 1 | 680 | 74.08 | 3.26 | 0.32 | 3.25 | $1.84\ 10^{-3}$ | 0.145 | $-1.32\ 10^{-3}$ |
| Link 2 | 402 | 43.51 | 0.336 | 1.407 | 1.362 | $-5.28\ 10^{-3}$ | $-7.46\ 10^{-3}$ | $9.78\ 10^{-3}$ |
| Link 3 | 268 | 7.87 | $1.83\ 10^{-2}$ | $6.46\ 10^{-2}$ | $5.89\ 10^{-2}$ | $1.83\ 10^{-5}$ | $4.02\ 10^{-6}$ | $3.68\ 10^{-3}$ |
| Link 4 | 115 | 2.22 | $2.09\ 10^{-3}$ | $4.9\ 10^{-3}$ | $4.86\ 10^{-3}$ | $7.61\ 10^{-10}$ | $1.13\ 10^{-9}$ | $5.56\ 10^{-4}$ |

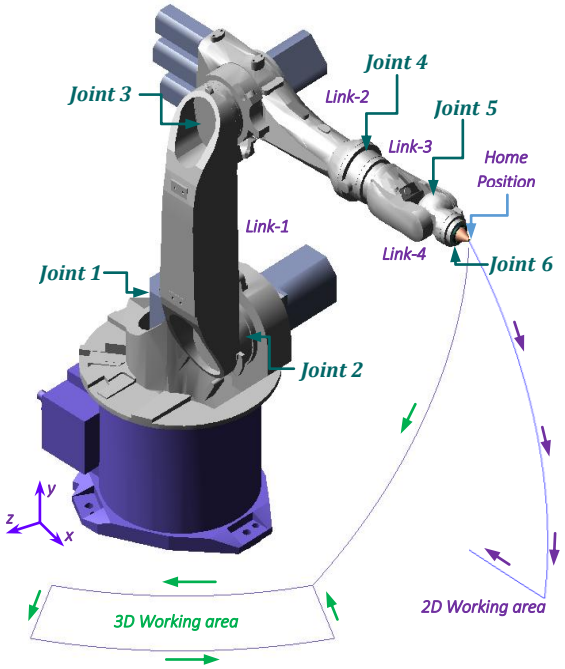


*Figure 2. Robot manipulator*

## 7. RESULTS

A theoretical investigation of joint clearance effects on the motion accuracy of robot manipulators with joint clearance was implemented for 2D and 3D motion necessities. As an imperfect joint characteristic, the value of joint clearance in joint 5 was considered as 0.2 mm for necessary comparison. The working period was adjusted as 2 and 6 seconds for fulfilling the 2D and 3D required tasks, respectively. All simulations were performed in an Intel Xeon computer. To evaluate the force and moment components, joints 2 and 3 are selected for each motion type of robotic system. The dynamic simulation parameters of the robot manipulator with joint clearance are outlined in Table 2.

*Table 2. Simulation parameters of robot manipulator*

| Description | Value | Description | Value |
|---|---|---|---|
| Dynamic friction coefficient | 0.01 | Young's modulus | 71.7 GPa |
| Restitution coefficient | 0.9 | Integration step size | $1x10^{-3}$ s |
| Poisson's coefficient | 0.33 | Integration tolerance | $1x10^{-5}$ |

Force components with and without clearance are outlined in Figs. 3 and 4. As seen from figures, for each motion necessity, the existence of joint clearance causes impulse type contact forces. These forces occur during a small time interval [5, 6]. Also, 3D motion necessity in a robotic system having joint clearance leads to an increasing at the force peak frequency relative to 2D motion necessity. In particular, these peaks are seen at the beginning of the motion and there is an instant change in force characteristics. This force characteristic not only decreases the performance of robot manipulator such as motion sensitivity and repeatability, but also leads to degradation of its vibration and noise quality.

The effects of clearance on torque characteristics are given in Figs. 5 and 6. As seen from figures, the robot manipulator with joint clearance has some peaks on torques [5, 6]. These peaks are seen especially at the instant change of torques. Naturally, due to the more torque changing in 3D motion, the peak frequency of torque is bigger than the 2D path motion.

## 8. CONCLUSIONS

As an imperfect joint characteristic, clearance in a joint causes deterioration on the whole system performance. All simulations show that much more computation time is necessary in the case of the imperfect joint approach. Even if the clearance size is small, it has a crucial role on motion sensitivity of robotic manipulations. Additional degrees of freedom originating from clearance lead to different motion modes. These are sources of uncertainties in robotic manipulations. The impulsive behaviour arising from a joint with clearance has a clear effect on the force and torque characteristics. The dynamics of the robot manipulator are obviously different for the case of different motion necessity. Especially, 3D motion is more chaotic relative to 2D motion in the robotic system having joint with clearance.

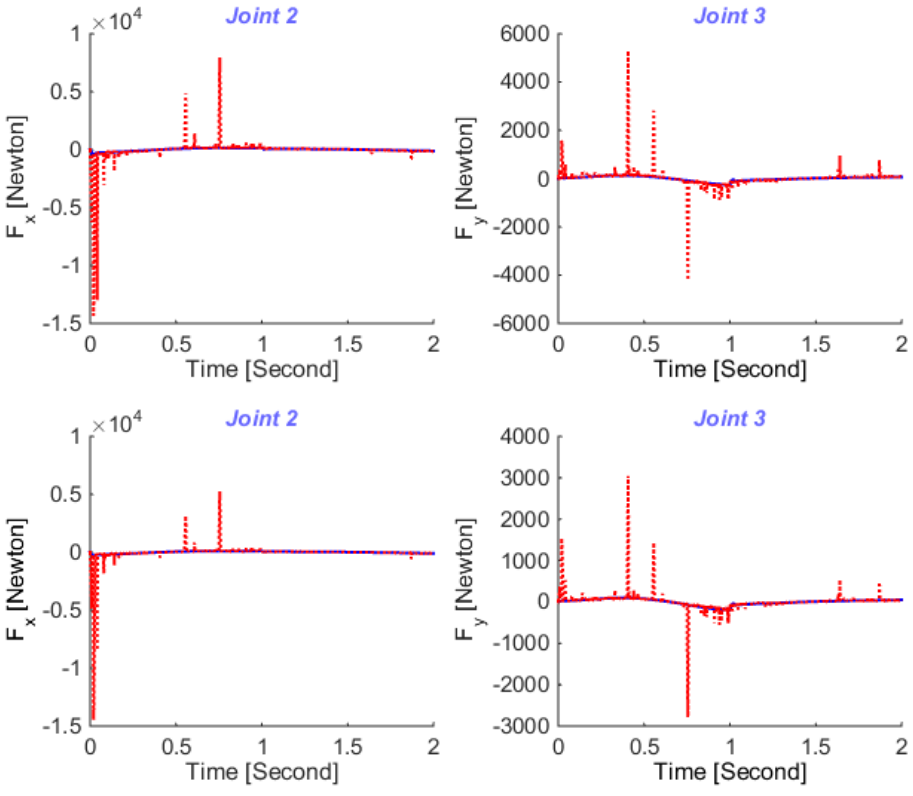


*Figure 3. Force components for the 2D motion path necessity*

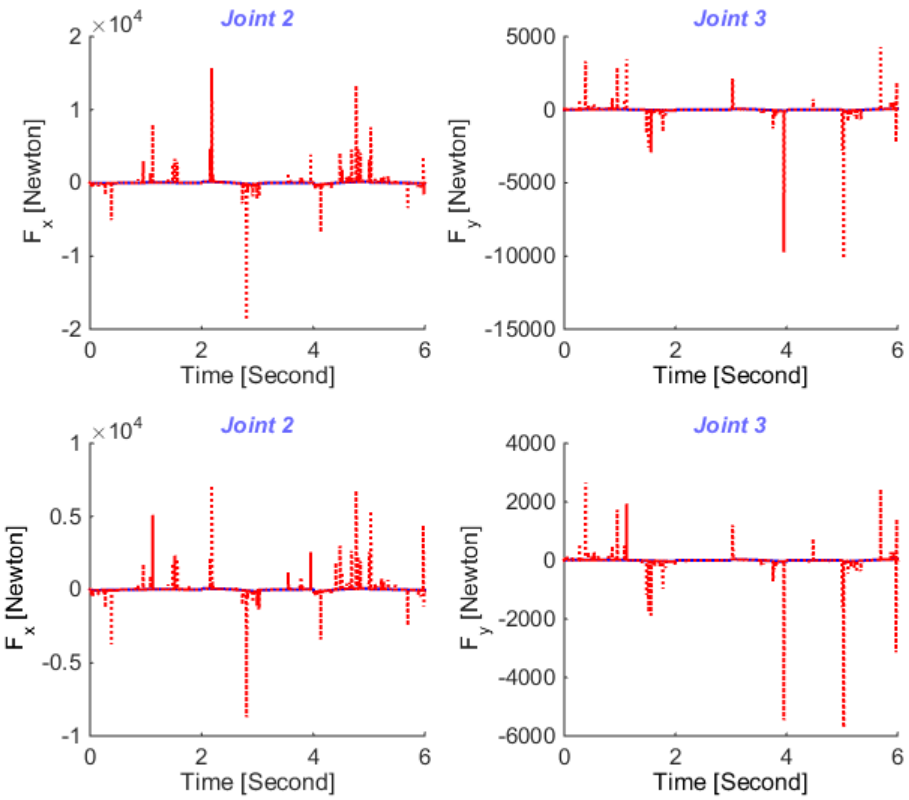


*Figure 4. Force components for the 3D motion path necessity*

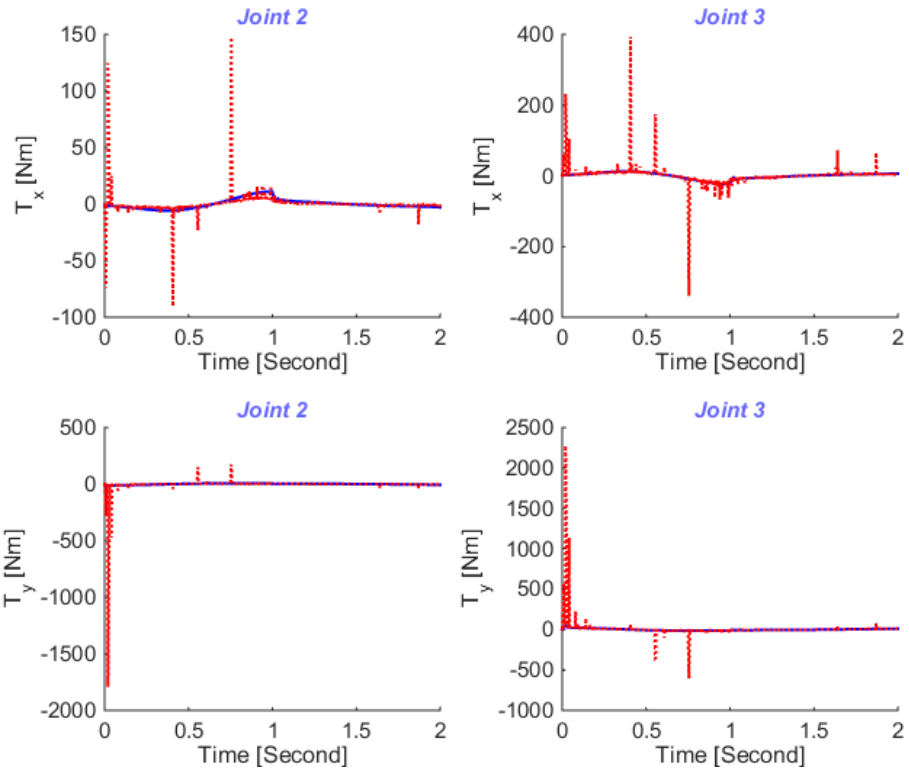


*Figure 5. Torque components for the 2D motion path necessity*

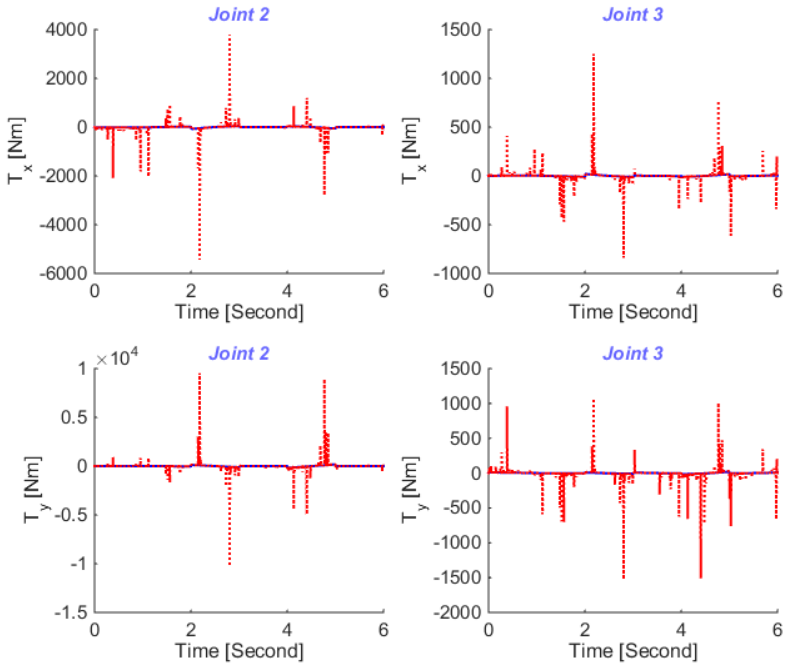


*Figure 6. Torque components for the 3D motion path necessity*

## REFERENCES

[1]. Tsai, C. H. **Hou, K. H. Chuang, H. T., "**Fuzzy control of pulsed GTA welds by using real-time root bead image feedback,*" J. Mater. Process. Technol*., 176, 158–167, 2006.

[2]. P. Flores, J. Ambrosio, H. C. P. Claro, H. M. Lankarani, C. S. Koshy, "A study on dynamics of mechanical systems including joints with clearance and lubrication," *Mech. Mach. Theory.,* 41, 247-261, 2006.

[3]. P. Flores, "Modeling and simulation of wear in revolute clearance joints in multibody systems," *Mech. Mach. Theo*., 44, 1211–1222, 2009.

[4]. S. Erkaya, I. Uzmay, "A neural–genetic (NN–GA) approach for optimising mechanisms having joints with clearance," *Multib. Sys. Dyn*., 20, 69–83, 2008.

[5]. S. Erkaya, I. Uzmay, "Investigation on effect of joint clearance on dynamics of four-bar mechanism," *Nonlin. Dyn*., 58, 179–198, 2009.

[6]. S. Erkaya, "Investigation of joint clearance effects on welding robot manipulators," *Robotics Comp. Integ. Manufac.*, 28, 449-457, 2012.

[7]. S. R. Lim, K. Kang, S. Park, W. C. Choi, J. B. Song, D. Hong, J. K. Shim, "Error analysis of a parallel mechanism considering link stiffness and joint clearances," *KSME Int. J.*, 16(6), 799-809, 2002.

[8]. W. Wu, S. S. Rao, "Uncertainty analysis and allocation of joint tolerances in robot manipulators based on interval analysis," *Reliab. Eng. Sys. Saf*., 92, 54–64, 2007.

[9]. A. Chebbi, Z. Affi, L. Romdhane, "Prediction of the pose errors produced by joints clearance for a 3-UPU parallel robot," *Mech. Mach. Theory.*, 44(9), 1768-1783, 2009.

[10]. J. Aginaga, O. Altuzarra, E. Macho, X. Iriarte, "Assessing position error due to clearances and deformations of links in parallel manipulators," *J. Mech. Des*., 135(4), 041006, 2013.

[11].M.H. Zahera, S.M. Megaheda, "Joints flexibility effect on the dynamic performance of robots," *Robotica.*, 33(7), 1424-1445, 2015.

[12]. S. Erkaya, "Trajectory optimization of a walking mechanism having revolute joints with clearance using ANFIS approach," *Nonlinear Dyn*., 71(1-2), 75-91, 2013.

[13]. S. Erkaya, S. Doğan, "A Comparative Analysis of Joint Clearance Effects on Articulated and Partly Compliant Mechanisms," *Nonlinear Dyn*., 81(1), 323-341, 2015.

[14]. S. Erkaya, İ. Uzmay, "Determining link parameters using genetic algorithm in mechanisms with joint clearance," *Mech. Mach. Theory*., 44, 222-34, 2009.

[15]. S. Erkaya, İ. Uzmay, "Optimization of transmission angle for slider-crank mechanism with joint clearances," *Struc. Multidis. Opt*., 37, 493-508, 2009.

[16]. S. Erkaya, "Prediction of vibration characteristics of a planar mechanism having imperfect joints using neural network," *J. Mech. Sci. Tech*., 26(5), 1419-1430, 2012.

[17]. S. Erkaya, İ. Uzmay, "Experimental investigation of joint clearance effects on the dynamics of a slider-crank mechanism," *Multibody Sys. Dyn*., 24, 81-102, 2010.

[18]. W. Goldsmith, "Impact; the theory and physical behaviour of colliding solids," *Edward Arnold Ltd*., London, 1960.

[19]. Z. F. Bai, Y. Zhao, "A hybrid contact force model of revolute joint with clearance for planar mechanical systems," *Int. J. Nonlinear Mech*., 48, 15–36, 2013.

# A Mechatronic Device for Preventing the Surgical Operation in Intussusception

*Selçuk Erkaya[4], Bilal Özak[5], Selim Doğanay[6] and Kazım Gümüş[7]*

***Abstract***

Intussusception case is a common abdominal emergency for children. It is necessary to make prompt diagnosis and management. The majority of intussusceptions in children can be treated safely with nonsurgical operations. This study proposes design and prototype manufacturing of a mechatronic air feeder device which is named as pneumatic reduction device. This device can control the pressure and flowrate. Working stability in millibar level is also possible. By using this device, it is aimed to solve the invagination problem, frequently experienced in children between six months and two years old, without surgical operation. This device was tested in laboratory condition and it was seen that it can quickly reach necessary pressure level in spite of change in volume and it can preserve this pressure level stably.

**Keywords:** Intussusception, invagination, mechatronics, pneumatic reduction device

## 9. INTRODUCTION

The treatment of intussusception in children is vital. In case of the treatment process, in first step, water or compressed air is used to open the intertwined and clogged bowel in the patient's rectum. If it is not succeeded by this way, surgery becomes inevitable due to the intestinal blood problems. Surgery is an undesired phenomenon since it specially increases mortality and morbidity risks, also length of hospital stay and the cost of treatment increase. Nonsurgical reduction of intussusception dates back to the time of Hippocrates, and various reduction procedures have been used since then [1-3].

The prototype which is produced in this study is unique in domestic. There is no any company which produces this product in a foreign country or supplies in domestic according to detailed research on the internet and interviews with Pediatric Surgery and Pediatric Radiology departments of Erciyes University [4-6]. It is reached the conclusion that manual pneumatic devices are using instead of hydrostatic devices for reduction of intussusception. It has been observed that important medical centers, which work on reduction of intussusception with air/water, try to produce these devices for their needs [7]. Although barium enema can be considered as a standard care for the diagnosis and therapeutic reduction of intussusception, alternative procedures has been introduced to the literature. Among them, pneumatic reduction with fluoroscopic guidance is claimed to be quick, safe, and clean, and it has been reported to have a high success rate [8-12]**.** There are academic studies about how to use manual pneumatic devices and about the effectiveness of treatment [13]. Studies on these cases, it can be seen that the maximum pressure of insufflation recommended for this pathology is 120 mmHg and the effectiveness of pneumatic reduction procedure is more than 90% [10-14]. Experimental and clinic studies outlined that the amount of liquid emerging from the patient's anus during the pneumatic reduction process is less than that of hydrostatic reduction [15-16]. This is crucial by considering the hygiene

and used device's continuity/working life. Also air is preferred instead of water because air causes a limited perforation and it is less dangerous in the peritoneal cavity in case of the perforation of reduction [17]. In case of intussusception, reduction with air is quicker, cleaner and more acceptable. Also, potentially risk of perforation is lesser and the application time is smaller than that of reduction with water [18]. In an analysis of cases in 2007, the effectiveness of hydrostatic reduction of intussusception is 85.3% but the effectiveness of pneumatic reduction is 88.2%. This study emphasizes the importance of pneumatic reduction in intussusception cases [19]. As a result of the study which is conducted on 44 cases, it is stated that the average pressure is 110.4 mmHg in pneumatic reduction process [20]. After the process, the length of hospital stay for children by pneumatic reduction is shorter than hydrostatic reduction. In another study which is experienced on 150 cases, the

[4] *Corresponding author: Erciyes University, Engineering Faculty, Mechatronics Engineering Dept., 38039 Kayseri/TURKEY. serkaya@erciyes.edu.tr*

[5] *Amasya University, Faculty of Technology, Mechatronics Engineering Dept., Amasya/TURKEY, ozakbilal@gmail.com*

[6] *Erciyes University, Faculty of Medicine, Paediatric Radiology Dept., Kayseri/TURKEY, selimdoganay@gmail.com*

[7] *Erciyes University, Biomedical Imaging Research Center, Kayseri/TURKEY, kzgumus@gmail.com*

effectiveness of pneumatic reduction with manual pneumatic device is around 86% [21]. In the literature, pneumatic and hydrostatic reduction of intussusception the methods of perforation and success rates have been evaluated. Pneumatic reduction is more advantageous than hydrostatic reduction; thereby, pneumatic reduction is more preferable [10, 22-24].

According to the factors such as shortness of the length of hospital stay, the risk result from the air in the peritoneal cavity in perforation is less compared to the water, application success rate show the effectiveness of pneumatic reduction in intussusception cases. In response to these cases, developing a mechatronic device which provides easy implementation for medical doctor, is going to be beneficial. For instance, medical doctors will be able to concentrate all the attention on the trouble region, time to reach the required pressure value will be short like 2-3 minutes, the success rate of opening the bowel will increase.

## 10. INTUSSUSCEPTION AND REDUCTION

Invagination can be described as a bowel problem. In general, the third quarters of invagination patients are younger than 1 year old. Invagination mostly occurs between 6 months and 2 years old babies. Male infants and toddlers, who are suffering from invagination, are more than female ones. Under the 5 years old patients, invagination is the cause of surgical operation at 25 percent. Frequently, it is occur at the tissue of small bowel joint with large bowel. The last part of small bowel is penetrating to the first part of large bowel. The general symptoms of intussusception are blood on the feces, uneasiness and vomiting. On the early stages of sickness, firstly nonsurgical methods must be applied. On the other hand, on the later stages of sickness, may be required an operation because of the cardiovascular problem at the bowel surface. The potential risks which are caused by surgical operation can be followed as;

- Especially, the increasing at the mortality and morbidity risks (operation based complications)
- The increasing at the costs and the length of hospital stay.
- The necessity of a general hospital to perform the operation.
- Complications arising from anesthetize applying to the babies

The bowel regularly acts in a coordinated contraction and relaxation. These relations in the bowel help the materials that inside the bowel to be transferred to the anus. This process continues at a certain speed and pattern. Conditions which lead to increases of intestinal motility such as diarrhoea or medication use break the regular act of bowel. Therefore, large and small bowels may frequently entwine together. If the incoming part of the bowel cannot go back and stay, then the result of this situation defines as invagination (Figure 1). This intestinal problem may be seen all ages.

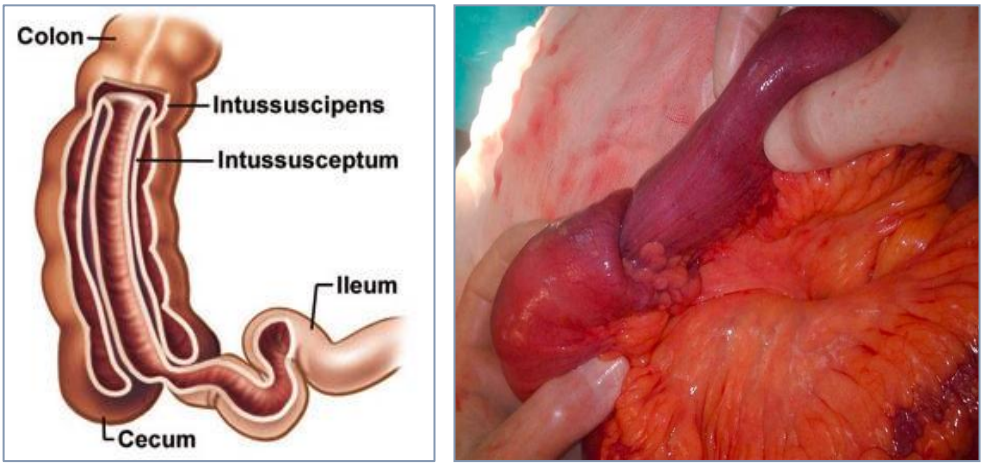


*Figure 1. Intussusception (a) Schematic presentation [25] (b) View on the case [26]*

If it is not attempted on time, stopping of bleeding after a while, it results in the death of that tissue there. The *necrosis* that occurred in the wall of bowel may result in a perforation. In this case, the stool

placed in the bowel spreads into the abdomen and a very serious intra-abdominal infection (peritonitis) and an inflammation of blood (sepsis) occur, which threat the life.

Without the necessity of a surgical operation, and even the staying of kid in the hospital, the solution of the problem is specified as reduction which is a process of clearing the occluded area away by inserting from the anus. The process of manual aerating into the bowel is predicted on the physical performance of the medical doctor. Reaching the necessary pressure values and taking it constant, or not being able to focus on the problematic area of bowel, more time necessity show the ineffectuality of manual air reduction device. In the thematic literature, there are manual air reduction devices which are used for this process (Figure 2). Also, it is possible to see the devices which are used water instead of air. Aerating of occluded bowel is carried out by inserting a cannula from anus. The occluded area during the operation is monitored by the medical imaging devices (ultrasound and/or scopy).

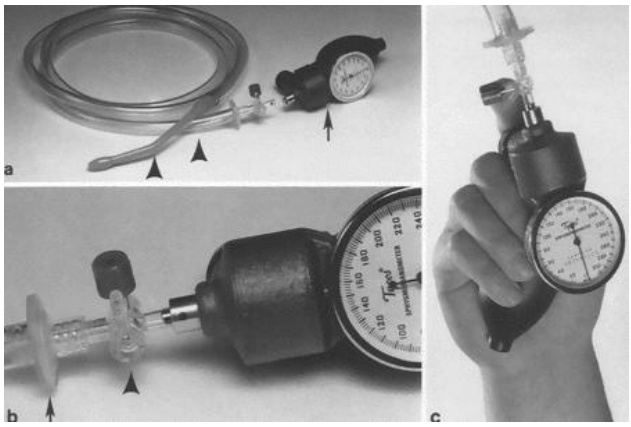


*Figure 2. Manual device with air feeder*

The process of aerating into the bowel is performed by a medical doctor. It is rather difficult both reaching the pressure level sensitively which is necessary to aerate and being increased gradually (from 70 mmHg to 110 mmHg), and taking it constant in that pressure level for a certain period (until the occluded bowel is threated). This process needs about 20 minutes. Also, the medical doctor might not be able to focus on the occluded bowel because he makes a physical effort and might be distracted. These are the negative reflections encountered frequently in the intervention with the manual systems. In the automatic devices with water feeder, it might be seen some problems, such as hygiene problems because of the outing of water from the anus, impairments of the electronic equipment used in monitoring owing to the water and the complications resulted from the water coming into the abdomen area are relatively (compared to intervention with the air) more dangerous.

A prototype model of the automatic device with air feeder, which can control the pressure and flowrate and can be used with the aim of treatments in invagination, is given in Figure 3.

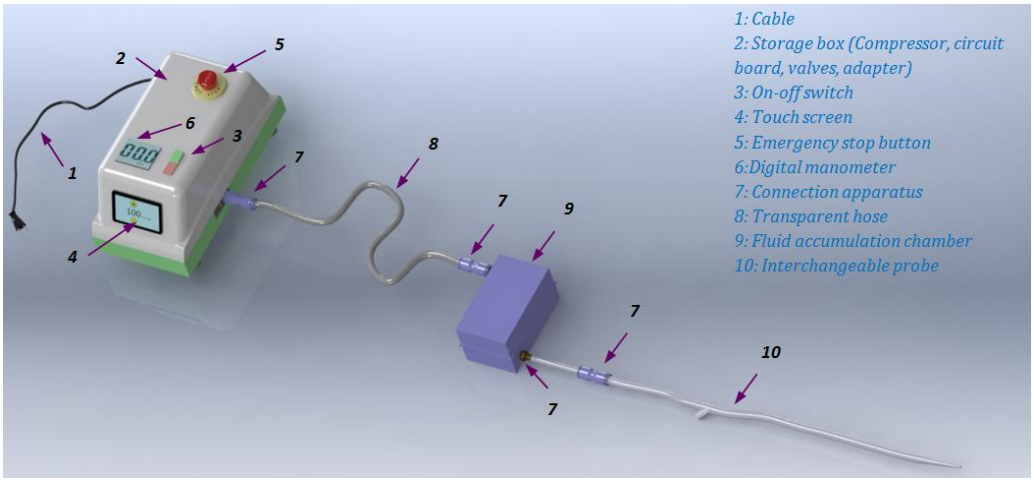


*Figure 3. The solid model of low pressure, flow controlled pneumatic reduction device [27]*

The main components of the system are; Electronic control unity, mini compressor, digital manometer to monitor the level of pressure, pressure switch, solenoid valve, pressure level adjusting button, LCD control panel, emergency button, pneumatic connection components and trompe, changeable cannula and effusion tank to prevent the damaging of fluid coming from the bowel because of the pressurized environment.

## 11. CONCLUSIONS AND RECOMMENDATIONS

The various reasons for using air instead of water during the opening process of occluded bowel can be mentioned as follows; the high possibility of complications caused by bowel perforation and subsequently the leaking liquid in the peritoneal cavity during the water usage [17], the excessive liquid coming from the anus [15, 16], the high possibility of medical equipment getting damaged by this excessive liquid, the success rate of reduction with air being higher [19]. The device produced as a prototype, which has been experimentally tested at the laboratory conditions and registered by Turkish Patent Institute (TPE), can be applicable easily and effectively to intussusception cases no need surgery operations. Complications and increasing costs arising from stay in hospital and surgery operation can be prevented by this device.

The disadvantages of this manual device are the difficulty of reaching a desired pressure and holding this pressure as stable, and the more time needed to achieve this. In addition to these, users (medical doctors) may not be able to focus on the occluded bowel because of the physical effort used on manual air supply. There are also various systems that use water instead of air. But in these systems there are some possible negative effects such as hygiene and equipment breakdowns (Figure 4) because of the extra amount of liquid coming from the patient's anus. Besides, there is a necessity of an expert radiologist at the operation team during the reduction with water process. Providing the required air through a compressor in the reduction with air operation in intussusception is a difference compared to the existing type that provides air manually and used in the thematic literature. Because, all the physical efforts and the attentions of the users (medical doctors) will focus on the occluded bowel for necessary threating by the usage of developed device. The time required in the manual air systems for reduction will be further shortened (about 1/10 level).

*Figure 4. Imaging systems which are used during the reduction of intussusception process*

Additionally, the device which has low and adjustable pressure, can sensitively supply the desired pressure range. It has an electronic control unit, pressure switch and solenoid valve. Pressure level can be monitored digitally. The pressure value is properly kept under the strength of human bowel by solenoid valve, that is, the pressure shall not exceed the upper limit of the resistance of human bowel due to an incorrect setting during application.

## ACKNOWLEDGMENT

This study is a part of the research project FYL-2015-6280. The authors wish to express their thanks for financial support being provided by the Scientific Research Projects Coordination Unit of Erciyes University, in carrying out this study.

## REFERENCES

[1]. D. P. Frush, J. Y. Zheng, V. G. McDermott, G. S. Bisset III, "Nonoperative treatment of intussusception: historical perspective," *AJR Am J Roentgenol*., 165, 1066–1070, 1995.
[2]. W. H. McAlister, "Intussusception: even Hippocrates did not standardize his technique of enema reduction," *Radiology*., 206, 595–598, 1998.
[3]. G. Del-Pozo, J. C. Albillos, D. Tejedor, et al., "Intussusception in children: current concepts in diagnosis and enema reduction," *RadioGraphics*., 19, 299–319, 1999.
[4]. (2016) EPO European Patent Office website [Online]. Available: www.epo.org
[5]. (2016) USPTO US Patent and Trademark Office website [Online]. Available: www.uspto.gov
[6]. (2016) TPE Turkish Patent Intstitute [Online]. Available: www.tpe.gov.tr
[7]. (2016) Youtube [Online]. Available: http://www.youtube.com/watch?v=N5RxjkzFh0Y
[8]. C. H. Yoon, H. J. Kim, H. W. Goo, "Intussusception in Children: US-guided Pneumatic Reduction—Initial Experience," *Radiology*., 218, 85–88,2001.
[9]. J. Z. Guo, X. Y. Ma, Q. H. Zhou, "Results of air pressure enema for the reduction of intussusception: 6,396 cases in 13 years," *J Pediatr Surg*., 21, 1201–1203, 1986.
[10]. D. R. Kirks, "Air intussusception reduction: the winds of change," *Pediatr Radiol*., 25, 89–91,1995.
[11]. W. E. Shiels, D. K. Maves, G. L. Hedlund, D. R. Kirks, "Air enema for diagnosis and reduction of intussusception: clinical experience and pressure correlates," *Radiology*., 181, 169–172, 1991.
[12]. M. Stein, D. J. Alton, A. Daneman, "Pneumatic reduction of intussusception: 5-year experience," *Radiology*., 183, 681–684, 1992.
[13]. W. H. Shiels, G. S. Bisset, D. R. Kirks, "Simple device for air reduction of intussusception," *Pediatric Radiology*., 20, 472-474, 1990.
[14]. R. E. Storey, I. C. Salama, *"Design of a Pneumatic Device for Intussusception Reduction in Children," The Internet Journal of Third World Medicine., 1(2), 2004.*
[15]. K. Maoate, S. W. Beasley, "Perforation during gas reduction of intussusception," *Pediatric Surgery International,* 14, 168–70, 1998.
[16]. W. E. Shiels, C. K. Maves, G. L. Hedlund, D. R. Kirks, "Air Enema for diagnosis and reduction of intussusception clinical experience and pressure correlates," Radiology., 181, 169–72, 1991.
[17]. (2016) Ali Gurtuna website [Online]. Available: http://www.aligurtuna.com/invajinasyon-bagirsak-dugumlenmesi-1976.html

[18]. S. D. Heenan, J. Kyriou, M. Fitzgerald, E. J. Adam, "Effective Dose at Pneumatic Reduction of Paediatric Intussusception," *Clinical Radiology*., 55, 811-816, 2000.
[19]. R. J. Thomas, S. Rakhesh, "An air insufflation device for reduction of intussusception in children," *Journal of Indian Association of Pediatric Surgeons*., 13(3), 94-96, 2008.
[20]. F. A. Abantanga, M. Amoah, A. O. Adeyinka, B. Nimako, K. P. Yankey, "Pneumatic reduction of intussusception in children at the Komfo Anokye Hospital, Kumasi, Ghana.," *East African Medical Journal.,* 85(11), 550-555, 2008.
[21]. S. Arslan, C. Turan, S. Doğanay, M. Güzel, Ö. Yandım, A. B. Doğan, A. Aslan M. Küçükaydın, "The Effectiveness of Pneumoreduction for Intussusception," *Annali Italiani di Chirurgia*., 5, 459-463, 2014.
[22]. A. Daneman, O. Navarro, "Intussusception, Part 1: A review of diagnostic approaches," *Pediatric Radiology*., 33, 79–85, 2003.
[23]. A. Daneman, O. Navarro, "Intussusception, Part 2: An update on the evolution of management," *Pediatric Radiology*., 34, 97–108, 2004.
[24]. A. Daneman, O. Navarro, "Intussusception, Part 3: Diagnosis and management of those with an identifiable or predisposing cause and those that reduce spontaneously," *Pediatric Radiology*., 34, 305–312, 2004.
[25]. (2016) Yoursurgery website [Online]. Available: http://www.yoursurgery.com/ProcedureDetails.cfm?BR=1&Proc=81
[26]. S. Akbulut, M. M. Sevinc, B. Cakabay, S. Bakir, A. Senol, "Giant inflammatory fibroid polyp of ileum causing intussusception: a case report," *Cases Journal*., 2:8616 doi: 10.4076/1757-1626-2-8616, 2009.
[27]. S. Erkaya, S. Doğanay, K. Z. Gümüş, "İnvajinasyonda Pnömatik redüksiyon cihazı," TPE Faydalı model, Tescil No: 2014/00795.

# Heart Sounds Analysis by Using Linear Prediction Cepstral Coefficients

*Fatma Z. Göğüş* [1] *and Gülay Tezel* [1]

***Abstract***

*The analysis of heart sounds has an important role to recognize the signs of various pathological conditions of heart. Along with the development of the signal analysis techniques, analysis of heart sounds and determination of the pathological heart sounds have become possible in the digital environments. In this study, following the filtering and segmentation pre-process, 9 different heart sound data were analyzed using linear prediction coding technique. Weighted cepstral coefficients derived from linear prediction parameters were evaluated characteristic features of heart sound data. Reduction of features was performed using principal component analysis. Artificial neural network, k nearest neighbor and support vector machine algorithms were used to classify heart sounds into 9 different types. As a result of analyzing and classification, the accuracy of over 90% with each classifier was obtained for identification of 9 different heart sounds.*

**Keywords:** Artificial Neural Network, Cepstral Coefficient, Heart Sounds, K-nearest Neighbor, Linear Prediction Coding, Support Vector Machine

## 12. INTRODUCTION

Heart sounds are produced while pumping blood to the lungs and body [1]. The sounds are caused opening and closing of the heart valves and mechanical activities such as movement of blood between the heart chambers and vibration of the heart muscles. These sounds carry important information about the pathological conditions of heart, heart valves and cardiovascular system. For this reason, interpretation of heart sounds is very important for diagnosing of various heart diseases. Cardiac auscultation, which based on listening and assessment of heart sounds, is the most common diagnostic tool in diagnosing cardiovascular diseases [2]. In the process of auscultation, heart sounds are listened through a stethoscope from the auscultation points. Fig. 1 shows auscultation of heart. The heart sounds listened by physicians are used to diagnose diseases. Although there are several advantages of auscultation such as cheapness, reliability efficiency, this tool has many limitations and problems [3]. Recognition and interpretation of the findings obtained by auscultation depend on personal expertise. Many factors such as physician's age, experience, education, ability to distinguish sounds, environmental factors and fatigue can affect the interpretation of findings. Also human ear is not the sensitive against sounds at certain frequencies [4]. This is another limitation of auscultation. Due to these reasons, auscultation is insufficient for the diagnosing of some cardiac diseases.

Advances in computer technology and improved methods in acoustic pattern recognition and signal processing [5] overcome many restrictions of auscultation. Thus, interpretation of heart sounds has become more objective and reliable. There are many studies about the heart sound analysis and detection of pathological conditions of cardiac. Autoregressive (AR) method is an effective method used most of these studies [1], [6]. With this technique, analysis and feature extraction process has been performed and effective results have been achieved in many studies about the heart sounds [1], [6].

*Figure 1. Auscultation of heart*

AR approach is closely related to linear predictive coding (LPC) technique. LPC technique is one of the parametric analysis techniques. It models the signal as output of the all-pole filter [7]. It is used generally for analysis of echoes, speech sounds and musical sounds. However, it is adapted to heart sound analysis by Agostinho and Souza in 1997 [7]. Since that time, this technique has been used in various studies that deal with heart sound analysis [8]. Cepstral coefficients derived from the LPC method are the strong characteristic features of the heart sounds. These coefficients are called linear prediction cepstral coefficients (LPCC) and often used as a biometric for human identification from the heart sounds [9, 10]. Although analysis of heart sounds with cepstral coefficients provide high performance in the biometric recognition area, this analysis form is rarely used in the biomedical area for detection of pathological conditions. Because of this reason, in this study, it is intended to show that LPCC belonging to heart sounds can produce successful performances in the biomedical field, too.

In this study, 9 different heart sounds are analyzed and classified in the digital environment for identification of heart sound types associated with several pathological states. Block diagram shown in Fig. 2 summarizes the study schematically.

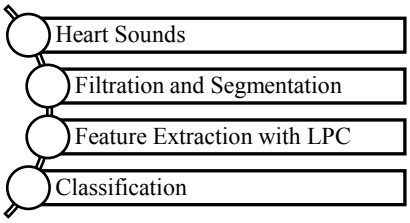


*Figure 2. Block diagram of study*

In this study, after the heart sounds were pre-processed with filtering and segmentation, they were subjected to analysis by the LPC method. As a result of analysis, the weighted cepstral coefficients were derived from the LPC parameters. These coefficients were considered as features of the heart sounds. Principle component analysis (PCA) was used to reduce dimensions of features.

For testing the reliability of the analysis results, different classification algorithms; artificial neural network (ANN), k-nearest neighbor (KNN) and support vector ma-chine (SVM) algorithms were used. Identification of 9 different heart sound types was carried out via classification of features.

As a result of the classification procedure, it is observed that the heart sounds are well represented by weighted cepstral coefficients and different types of heart sounds are identified with a high rate.

Finally, classification algorithms were compared on the basis of classification ac-curacy.

## 13. MATERIALS AND METHODS

### *13.1. Used Heart Sound Data*

Nine different heart sounds which were used in study named "A Novel Feature Extraction Method for Heart Sounds Classification"[11] were also used in this study. Used heart sounds are normal heart sounds (S1 and S2) (NHS), third heart sound (S3), fourth heart sound (S4), opening snap (OPS), aortic stenosis (AST), midsystolic click and late systolic murmur (MCC-LSM), ventricular septal defect (VSD), atrial septal defect (ASD) and patent ductus arteriosus (PDA). The duration of these sounds is 14 or15 sec. and sampling frequency is 44100 Hz. Each of sounds contains 17 heartbeats.

Fig. 3 shows used a heartbeat sounds.

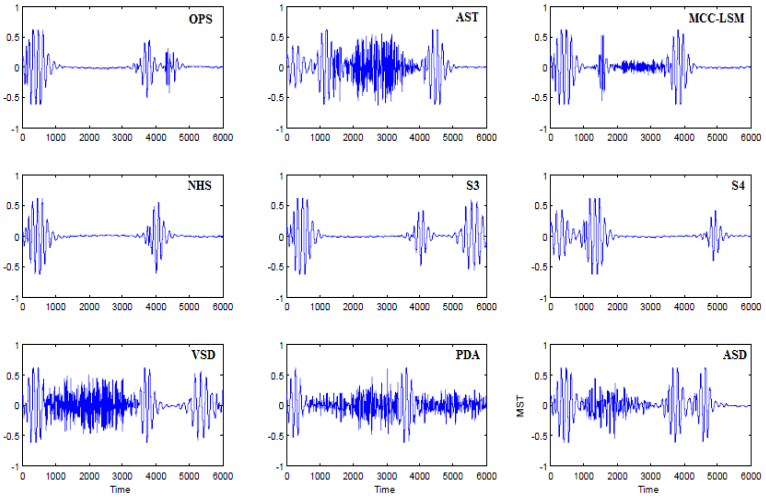


*Figure 3. Used heart sounds*

### *13.2. Pre-Processing*

Heart sound signals are generally in the range of 20-600 Hz. While normal heart sounds are dispersed in the frequency range 20-100Hz, abnormal heart sounds and murmurs are usually scattered throughout the frequency range 30-600Hz [12]. In this reason, our heart sound data were filtered using a band-pass filter Butterworth, with 3rd order and cut-off frequencies set at 20Hz and 600Hz [12].

Following the filtering process, each of heart sounds was segmented into a little duration of complete one cycle of heart beat. In this way, 9 x17, in other words, 153 heart sound signals were obtained.

### *13.3. Feature Extraction Methods*

#### *2.3.1. Linear Predictive Coding (LPC)*

The basic idea behind the LPC analysis method is that each sample of signal can be expressed as a linear combination of a few past samples of the signal [13]. LPC method is formulated as shown in equation 1.

$$s[n] = a_1 s[n-1] + a_2 s[n-2] + ... + a_p s[n-p] \quad (1)$$

According to equation 1, signal sample at time n, s[n], can be approximated a linear combination of the past p signal samples. a1, a2,…,ak are the LPC parameters.

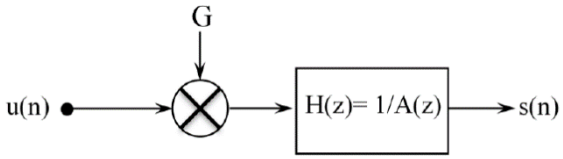


*Figure 4. LPC synthesis model*

According to the LPC synthesis model expressed by Fig. 4, when the normalized input signal u(n) is scaled by the gain G (power of a signal) and acted as input the all pole system, output signal s[n] is produced [14]. Thereby, equation 1 is rearranged as in equation 2 [14].

$$s[n] = \sum_{k=1}^{p} a_k s[n-k] + Gu[n] \quad (2)$$

In the analysis process with LPC, signals are separated into short frames and pre-diction parameter estimation is performed for every frame. The number of parameters is determined by the degree of the LPC method. There are two methods for estimation of LPC parameters. These are covariance and autocorrelation methods. According to the results of a study [14], it is expressed that the filter is designed with autocorrelation parameters is stable. However, this guarantee cannot be given for filters designed with covariance parameters [14]. Also autocorrelation method requires less calculation than covariance [15]. Therefore, the autocorrelation method was preferred for parameter estimation in this study.

#### *2.3.2. Linear Prediction Cepstral Coefficients (LPCC)*

Cepstrum is defined as the inverse Fourier transform function of the logarithmic Fourier transform of a signal. Due to the nature of the sound signals, they can be modelled by Cepstrum coefficients. Cepstrum coefficients can be obtained by Fourier transform. They also calculated based on the linear prediction parameters [16]. Cepstral coefficients which are calculated LPC parameters are referred as the linear prediction cepstral coefficients (LPCC).

LPCC values are obtained through Fourier transform of the linear prediction parameters [15]. These values are computed as in equation 3 [16].

p is the number of LPC parameters.

$$LPCC(p) = LPC(p) + \sum_{k=1}^{p-1} \left( \frac{k-p}{p} \right) LPCC(p-k) LPC(k) \quad (3)$$

The calculation process of LPCC values is shown as schematic in Fig. 5 [15].

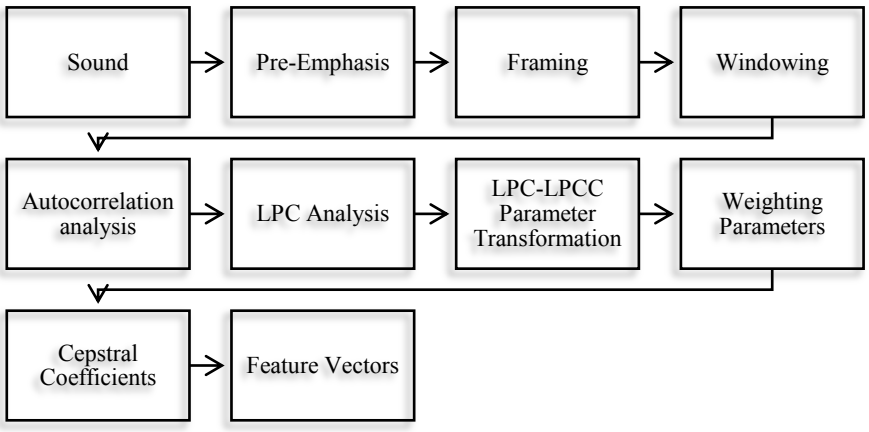

*Figure 5. Calculation process of LPCC values*

### *2.3.3. Principle Component Analysis (PCA)*

Principle component analysis (PCA) expresses a variety of original variables by using new variables. The new variables are linear component of the original variables and dimension of these new variables are fewer than that of original variables [12]. There are relationship and dependence among original variables, but there is no relationship between the new variables. These low dimensional new variables are referred to as principal components [12]. The first principal component has the highest variance value [17]. Other components are ranked from highest variance to lowest variance [17]. Because PCA produces lower dimensional variables, it can be used for reducing the dimension of features.

## *13.4. Feature Extraction of Heart Sounds*

It is important to determine the LPC degrees. In this study, LPC algorithms with different degrees were applied to 9 different heart sounds. Because of the best representation of heart sounds, the degree of the algorithm is determined as 35 Fig. 6 shows heart sounds spectrums and LPC spectrums with different degrees. As shown in Fig. 6, LPC spectrum with 35th degree is more similar to spectrum of heart sound.

Each of the 153 heart sounds was divided into 20 frames. Every frame contains approximately 40 msec sounds. With a framing process, non-static heart sound signal is rendered more stable. However, signal discontinuity may occur at the beginning and end of the frames. Therefore, the windowing process was applied to all frames to minimize signal discontinuity. Hamming window was used for windowing process. After the windowing process, LPC parameters were estimated for every frame by using the Autocorrelation Levinson Durbin method.

When compared with LPC parameters, cepstral coefficients provide more reliable and robust representation of sound signals [18]. Moreover, various factors such as noise can be minimized and major differences between cepstral values can be eliminated by weighting cepstral coefficients. Therefore, LPC parameters found by the autocorrelation method were transformed into weighted Cepstral coefficients by using the equation 3.

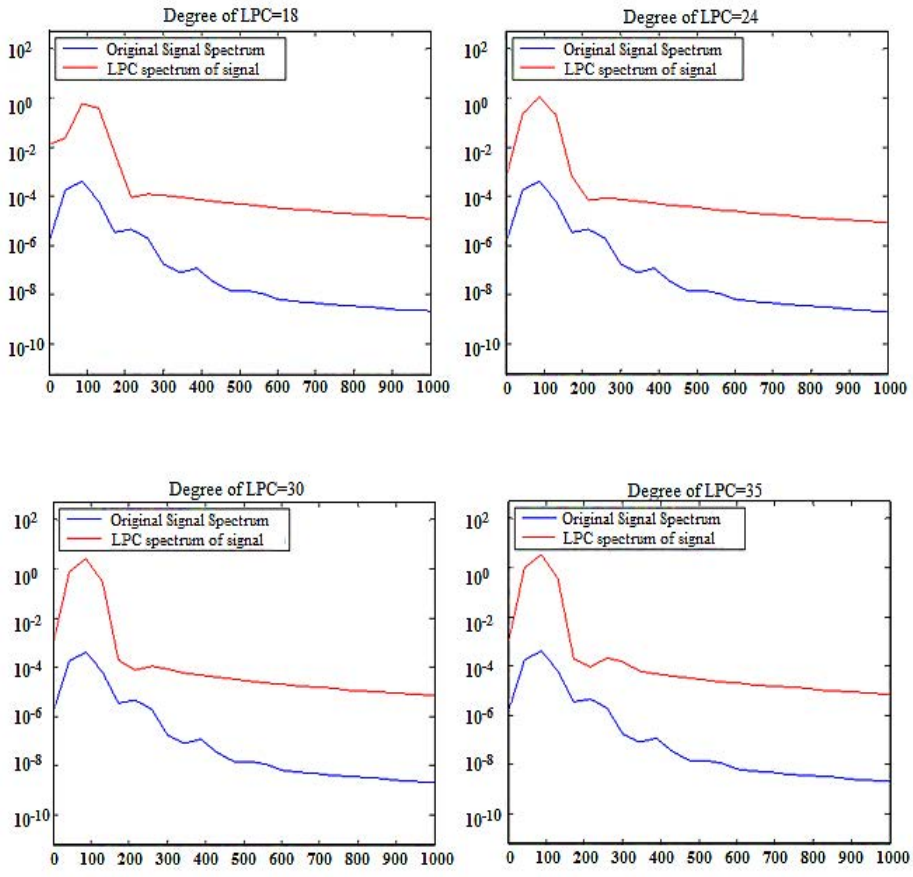


*Figure 6. Spectrums*

As a result of performed operations, 20 frames belonging to every sound and 35 weighted cepstral coefficients belonging to every frame were obtained. In other words, 20 x 35 feature values were obtained from each of the 153 heart sounds.

Because of the high dimensionality of features at the extraction stage, the classification cannot be performed effectively and quickly. Feature amount must be reduced for an effective classification result. Therefore, PCA was used to achieve feature reduction. With this method, the number of features was diminished to 25.

Feature extraction of heart sounds can be summarized as shown in Fig. 7.

## 14. RESULTS AND DISCUSSIONS

Heart sounds are a bio signals providing information about the mechanical activity of the heart. Therefore, the identification of heart sounds is an important step for detection of pathological conditions of heart. In this study, it is intended to recognize normal and abnormal 9 different heart sounds. To accomplish this intent, LPC method was applied to each of the heart sounds and the sounds were analyzed. The weighted cepstral coefficients obtained by the LPC method were considered as features of the heart sounds.

ANN, KNN and SVM algorithms commonly used for classification of biomedical sounds and they produce high performance. That's why, ANN, KNN and SVM algorithms were used to classify heart sounds into 9 different types in this study. Orange canvas toolbox [19] was used for classifiers. This toolbox is available for free at www.ailab.si/orange.

Classification results of features values by ANN, KNN and SVM are shown in Table 1.

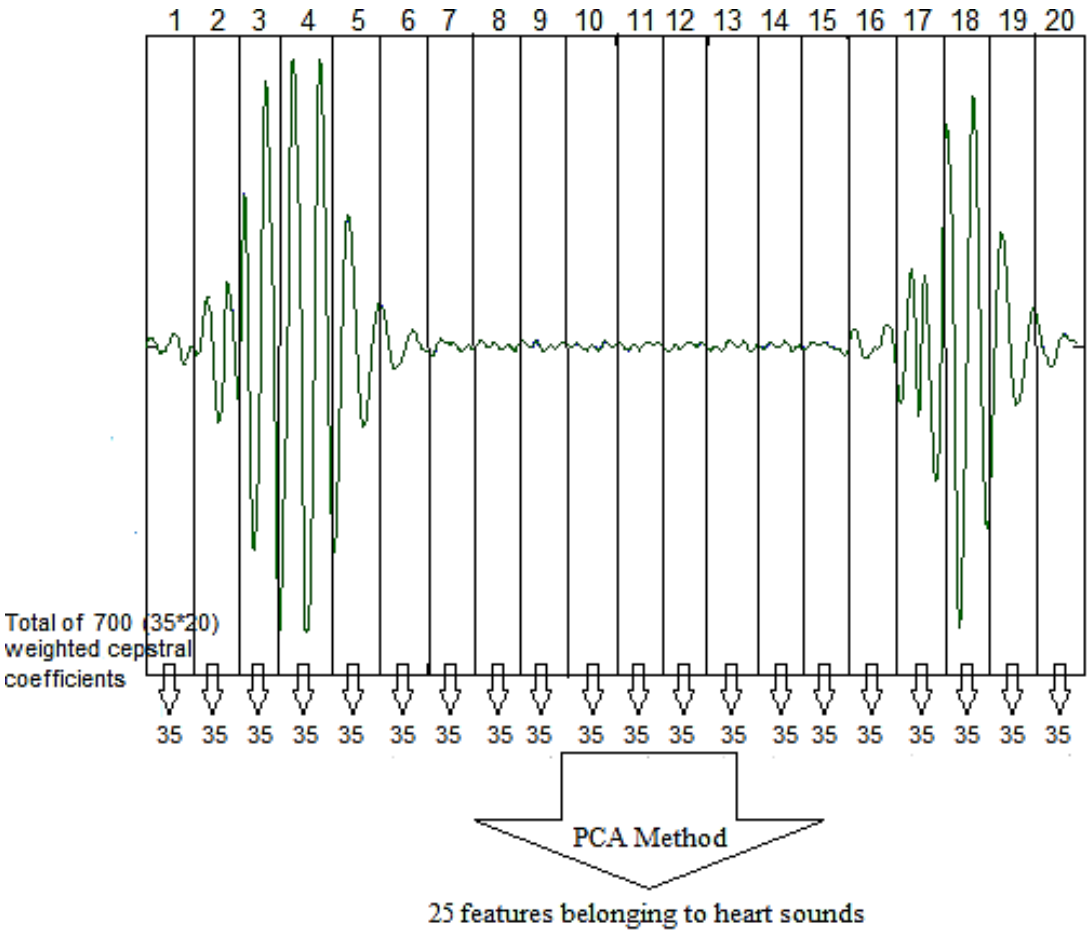


*Figure 7. Feature extraction diagram of heart sounds*

*Table 1. Classification accuracies of heart sounds using ANN, KNN and SVM.*

| Classification Algorithm | Classification Accuracy (%) |
|---|---|
| Artificial Neural Network (ANN) | 100 |
| Support Vector Machine (SVM) | 100 |
| K-Nearest Neighbor (KNN) | 95.42 |

Classification process was carried out with 1000 iterations and 10 cross-validations. ANN with 3-layer was used. The input layer has 20 neurons, hidden layer contain 21 neurons and output layer include 9 neurons. k value was determined as 6 for KNN. Cost (c) value is determined as 1.00 and kernel function is selected linear for the SVM classifier.

As seen from Table 1, the highest accuracy rate for the recognition of different heart sounds as %100 was obtained by SVM and ANN classification algorithms. All sound samples were classified correctly by these two classifiers. When the confusion matrix belonging to classification of heart sounds by KNN is examined, it is observed that 7 of the 153 heart sounds are misclassified.

SVM and ANN algorithms produce equal correct classification rate as %100. Although the KNN algorithm produces high classification accuracy, it is less successful than SVM and ANN for recognition of the different heart sounds.

## 15. CONCLUSIONS

Analysis of heart sounds is very important for the diagnosis of cardiac diseases such as heart failure. Many digital signal processing algorithms are used for analysis of heart sounds. Due to ease of use, less memory requirement and producing effective results, LPC is a digital signal processing method for analyzing the sound signals.

In this study, analysis of 9 different heart sounds was carried out by LPC method. Weighted cepstral coefficients obtained by using the LPC method were considered as characteristic features of heart sounds. ANN KNN and SVM algorithms were used to recognize 9 different heart sounds by classifying the resulting feature values. As a result of the classification process, it is observed that weighted cepstral coefficients represent well the heart sound data. Also we can say that as in the field of biometric recognition, analysis of heart sounds with LPCC has high performance in the biomedical field. This analysis technique gives useful information about the pathological conditions of heart.

The results obtained from this study are very promising for defining different types of heart sound associated with various pathological conditions. Therefore, it can be said that detection of various pathological conditions is performed by analysis of heart sounds in a digital environment. However, more experimental work is required, especially with larger data sets in order to develop and commercialize real-time computer based sound analysis and disease diagnostic systems.

## ACKNOWLEDGEMENT

The authors would like to thank Asst. Assoc. Dr. Yücel Koçyiğit for his data sharing with us. Also, we are grateful to Prof. Dr. Bekir Karlık for his support and encouragement.

## REFERENCES

[8]. B. Ergen, *Linearity analysis of heart sounds by power and higher order spectrum estimation techniques*, Fırat Üniversity Journal of Engineering., vol. 23, no. 1, pp. 53-60, 2011.
[9]. Y. Wang, W. Li, J. Zhou, X. Li and Y. Pu, *Identification of the normal and abnormal heart sounds using wavelet-time entropy features based on OMS-WPD*, Future Generation Computer Systems, vol. 37, pp. 488-495, 2014.
[10]. İ. Güler, H. Polat and U. Ergün, *Combining neural network and genetic algorithm for prediction of lung sounds*, Journal of Medical Systems, vol. 29, no. 3, pp. 217-231, 2005.
[11]. A. R. A. Sovijarvi, J. Vanderschoot and J. E. Earis, *Standardization of computerised respiratory sound analysis*, Eur. Respir. Rev., vol. 10, no. 77, pp. 585-590, 2000.
[12]. H. Pasterkamp, S. S. Kraman and G. R. *W k , R v b h h* , Am J Respir Crit Care Med., vol. 156, pp. 974-987, 1997.
[13]. M. Akay, J. L. Semmlow, W. Welkowitz, M. D. Bauer and J. B. Kostis, *Detection of coronary occlusions using autoregressive modeling of diastolic heart sounds*, Biomedical Engineering. IEEE Transactions on.,vol. 37, no. 4, pp. 366-373, 1990.
[14]. M. C. Agostinho and M. N. Souza, *A new heart sound simulation technique*, Engineering in Medicine and Biology Society. Proceedings of the 19th Annual International Conference of the IEEE., vol. 1,pp. 323-326,1997.

[15]. G. Redlarski, D. Gradolewski and A. Palkowski, *A system for heart sounds classification*, PLoS One, vol. 9, no. 11, pp. 1-12, 2014.
[16]. X. M. Guo, Y. Duan and L. Zhong, *Study of human identity recognition based on HMM and WNN*, Appl. Res. Comput., vol. 27, pp. 4561-4564, 2010.
[17]. L. Zhong, J. Wan, Z. Huang, X. Guo and Y. Duan, *Research on biometric method of heart sound signal based on GMM*, Chinese Journal of Medical lnstrumentation, vol. 37, no. 2, pp. 92-95, 2013.
[18]. Y. Kocyigit, *A novel feature extraction method for heart sounds*, Proceedings IWBBIO, vol. 1, pp. 34-41, Granada 7-9 April, 2014.
[19]. F.Z. Göğüş, *Analysis and classification of biomedical sounds*, Selcuk Üniversity, The Graduate School Of Natural And Applied Science, Computer Engineering Deparment. MS Thesis. pp. 49, 2015.
[20]. M. Bahoura, *Pattern recognition methods applied to respiratory sounds classification into normal and wheeze classes*, Computers in biology and Medicine., vol. 39, pp. 824-843, 2009.
[21]. M. A. Özkan, *Secure voice communication over GSM*, Istanbul Technical University. Faculty of Electrical and Electronics. Graduation Thesis. pp. 20, 2011.
[22]. O. Eray, *The speech recognition application with support vector machines*, Pamukkale Üniversity. The Graduate School Of Natural And Applied Science, Electrical and Electronics Deparment. MS Thesis. pp. 21, 2008.
[23]. H. Artuner, *The design and implementation of a turkish speech phonome clustering system*, Hacettepe University. The Graduate School Of Natural And Applied Science, Computer Science and Engineering Department. PhD Thesis, pp. 68, 1994.
[24]. I. Yazar, H. S. Yavuz, and M. A. Çay, *Face recognition applications of principle component analysis method and some of its classical and robust variants*, Journal of Engineering and Architecture Faculty of Eskişehir Osmangazi University, vol. 22, no. 1, pp. 49-63, 2009.
[25]. L. Rabiner, B. H. Juang, *Fundamentals of Speech Recognition. Englewood Cliffs*, NJ: Prentice-Hall, 1993.
[26]. J. Demšar, T. Curk, A. Erjavec, Č. Gorup, T. Hočevar, M. Milutinovič, M. Možina, M. Po-lajnar, M. Toplak, A. Starič, M. Stajdohar, L. Umek, L. Žagar, J. Žbontar, M. Žitnik and B, Zupan, Orange: data mining toolbox in Python. JMLR, vol. 14, no. 1, pp. 2349–2353, 2013.

# Application on Forest Waste Biosorbent for the Removal of Zinc(II)

*Handan UCUN ÖZEL[8], Ercan BERBERLER[9], Halil Barış ÖZEL[10]*

***Abstract***

*The aim of this study is to evaluate the potential use of forest waste as a biosorbent for removal of Zinc(II) ions from aqueous solution. With this purpose, used of forest waste were obtained from oriental beech (Fagus orientalis Lipsky.) forests. The biosorption properties of Zinc(II)onto forest waste were investigated by using batch techniques. Biosorption studies indicated that the biosorption efficiency decreased with increasing initial concentration of Zinc(II), but the biosorption capacity increased. The biosorption efficiency of Zinc(II) from solution with forest waste dose of 3 g $L^{-1}$ varied from 41.9 % to 33.2% for an increase of the Zinc(II) ion concentration from 10 to 50 mg $L^{-1}$. It is said that the results of this study indicate the possibilities that exist in the clean-up of the environment with the use of natural resources. Forest waste was screened as a potent candidate for biosorbent capable of removing Zinc ions efficiently.*

**Keywords:** Zinc(II), Forest Waste, Biosorption, Heavy Metal, Biosorbent

## 16. INTRODUCTION

Metals like Cd, Hg, Pb, Cr, Ni, Cu, Zn, and Co are, at elevated concentrations, detrimental to human health and ecosystem stability, and threshold values have been set for these metals for wastewater discharged into environment and for drinking water [1]. The removal of heavy metals from aqueous effluents so as to avoid their toxic and bioaccumulation effects to environment is usually realized by means of physical, chemical treatment and biological processes [2]. The removal of heavy metals from contaminated wastewater is generally accomplished chemical precipitation as sulphides and hydroxides, chemical oxidation or reduction, ion exchange, lime coagulation, evaporative recovery. All these processes have several disadvantages including high-energy requirements, high energy consumptions or expensive synthetic resins and chemicals requirements. The search is still on for an efficient, yet cost-effective treatment option. Biosorption is a widely used technology to remove of heavy metals. Biosorption by inexpensive biomaterials promises to be an excellent alternative. These biomaterials are bacteria, fungi, algae, industrial wastes, agricultural wastes, natural residues, and other biomaterials [3]-[10].

Zinc is an essential trace element for all forms of life. However, an excess of zinc in the human body may cause a range of serious illnesses including anemia, damage to pancreas, lungs, decreased immune function, ranging from impaired neuropsychological functions, grows retardation and stunting, impaired reproduction, immune disorders, dermatitis, impaired wound healing, lethargy, loss of appetite and loss of hair [2]. Zinc may be found in wastewater discharges from acid mine drainage, galvanising plants, as a leachate from galvanised structures and natural ores, and from municipal wastewater treatment plant discharges. Zinc is not biodegradable and travels through the food chain via bioaccumulation. Therefore, there is significant interest regarding zinc

[8] *Corresponding author: University of Bartin, Department of Environmental Engineering, Faculty of Engineering, 74100, Bartin/ Turkey. hanucun@yahoo.com*

[9] *University of Bartin, Department of Environmental Engineering, Faculty of Engineering, 74100, Bartin/ Turkey. ercanberberler@gmail.com*

[10] *University of Bartin, Department of Silviculture, Faculty of Forestry, 74100, Bartin, Turkey. halilbarisozel@yahoo.com*

removal from wastewaters and its toxicity for humans at levels of 100–500 mg/day. World Health Organization (WHO) recommended the maximum acceptable concentration of zinc in drinking water as 5.0 mg/L [10], [11].

Oriental beech or eastern beech (*Fagus orientalis* Lipsky.) belongs to the family Fagaceae. It is a deciduous broad-leaved tree which reaches height of 30-40 meters. Stem diameter can reach about 1 m at breast height. Height growth of oriental beech at early ages is slow. The maximum growth rate is usually achieved at the age of 30- 40 years, but under shelter, this could take longer, even 60 years. If oriental beech experiences fast growth during the early stages, then growth will end at about 100 years of age, whilst for stands growing more slowly over the early stages, the growth will continue until the age of 160-200 years. Oriental beech is indigenous to the Balkans in the west, through Anatolia (Asia Minor), to the Caucasus, northern Iran and Crimea. Oriental beech is a shade-tolerant species that occurs in Turkey, Syria and north of Asia Minor and Iran, in mild mountainous or marine climates with high humidity. Moist and acid clay soils inhibit its regeneration, and late frost, early heavy snow, and direct sunlight damage the seedlings. As a sapling, F. orientalis is much more resistant to frost, sunburn and drought stress than European beech (*F. sylvatica* Lipsky). In Turkey, the species is distributed in Trachia and in the south of Marmara Sea and throughout the Black Sea Regions where it is possible to find oriental beech both as pure stands and mixed forests with conifers and other deciduous broadleaves [12], [13].

This study investigates the potential use of forest waste from oriental beech (*Fagus orientalis* Lipsky.) forest as biosorbent for removal of Zn(II) ions from aqueous effluents. The biosorption of Zn(II) ions from aqueous solutions on forest waste was studied as function of initial Zn concentrations and biosorbent dosages.

## 17. *MATERIALS AND METHODS*:

### *17.1. Biosorbent preparation*

In this study, forest wastes were collected on natural pure oriental beech (*Fagus orientalis* Lipsky.) forest stands in the Bartin-Yenihan range forest district in the Western Black Sea Region in Turkey and used as a low-cost and abundant biosorbent. The forest wastes as combined materials were collected on the forest floor and forest wastes were prepared as biosorbent after various procedures. Firstly, forest wastes were washed with deionized water several times to remove surface impurities and then dried at 80 $^{o}$C for 24 h. The dried forest wastes were ground and sieved to particle size of 500 µm. Required biosorbent amount for the experiments was obtained from this dried mass by weighing precision and used as biosorbent.

### *17.2. Reagent preparation*

The Zinc stock solution was prepared by dissolving analytical grade $ZnSO_4 \cdot 7H_2O$ in 1 L of deionized water. Zinc solutions at the desired concentrations were prepared by adequate dilution of the stock solutions with deionized water.

### *17.3. Experiments*

Biosorption experiments were performed in the batch system. Biosorption experiments were carried out in 250 mL Erlenmeyer flasks using 100 mL metal-bearing solution with a known quantity of the dried biosorbent. The biosorption of Zn(II) ions from aqueous solutions on forest waste was studied as function of initial Zn concentration(10-50 mg/L) and biosorbent dosage (1.0-4.0 g/L). The biosorption medium was stirred at constant speed (150 rpm) for 2.0 h at 25 $^{o}$C and pH 6.0. The samples were taken at definite time and were filtered immediately to remove forest waste. The Zn(II) in the remaining solution was analyzed. The Zn(II) removal efficiency were calculated using the following equation;

$$\%Zn\ removal = \frac{C_o - C_e}{C_o} * 100 \quad (1)$$

The adsorption capacity of the Zn was calculated as follows;

$$q_e = \frac{(C_o - C_e)V}{m} \quad (2)$$

where $q_e$ is the mass of adsorbed metal per unit mass of adsorbent (mg/g); $C_o$ and $C_e$ are the initial and equilibrium Zn concentration (mg/L), respectively, V is the volume of the Zn solution (L) and m is the biosorbent mass (g) [2], [4], [15].

### *17.4. Analysis*

After being filtered, the concentrations of unadsorbed Zn(II) ions in the effluent were determined using an atomic absorption spectrophotometer.

## 18. RESULT AND DISCUSSION

### *18.1. Biosorption capacity*

The biosorption capacity, as it is a measure of the amount of metal ions bound by unit weight of biomass increased first with increasing of the initial concentration of metal ions and reached a saturation value [11]. Biosorption capacity (mg Zn adsorbed/g biomass) of the forest waste for removal of the Zn(II) at pH 6.0 and 150 rpm for 2.0 h was presented in Figure 1. In order to determine the biosorption capacity of forest waste, biosorption experiments were carried out at a fixed forest waste dose of 3.0 g/L and different Zn(II) concentrations ranging from 10 to 50 mg/L. The biosorption capacity of Zn(II) initially increased rapidly with increasing concentration Zn(II). It is thought that will increase its adsorption capacities even at the higher Zn(II) concentrations. The biosorption capacity of forest waste at the Zn(II)concentrations from 10 mg/L to 50 mg/L increased from 1.4 mg/g to 5.53 mg/g, respectively. Similar findings were reported for Zn uptake by other types of biosorbents [9], [11], [14].

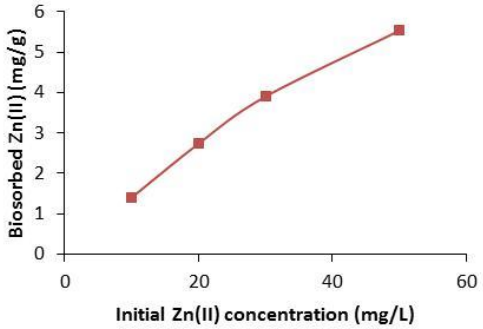


*Figure 2. Biosorption capacity of forest waste for Zn(II)*

The biosorption efficiency of forest waste was also determined for different initial Zn(II) ion concentrations (Fig.2). From 10 mg/L to 50 mg/L Zn ion solutions, the biosorption of 41.9 % zinc were achieved with 3.0 g/L forest biosorbent. The rate of biosorption is a function of initial concentration of ions. The biosorption efficiency of Zn(II) ions to the forest biosorbent decreased as the initial concentration of Zn(II) ions was increased.

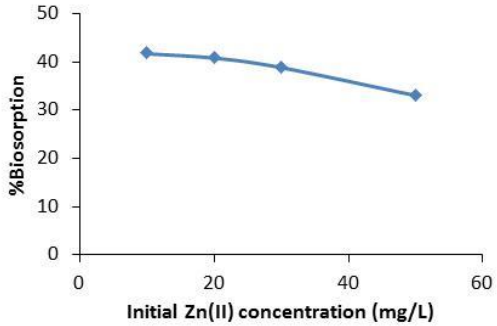


*Figure 2. Biosorption efficiency of forest waste for Zn(II)*

### *18.2. Effect of biosorbent dosage on Zn(II) biosorption*

The influence of initial biosorbent dose on the biosorption efficiency and biosorption capacity of forest waste was studied for Zn(II) concentration of 30 mg/L and a content of 1.0-4.0 g/L of biosorbent. The experimental results are illustrated in Fig. 3 and Fig.4.

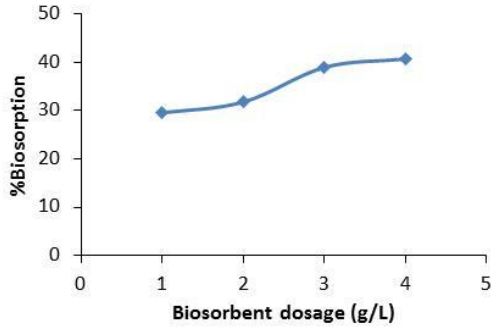


*Figure 3. Effect of initial biosorbent dose on biosorption efficiency of forest waste for Zn(II)*

The increase in forest waste dose from 1.0 to 4.0 resulted in a rapid increase in biosorption efficiency. The maximum Zn(II) uptake was observed at 3.0 and 4.0 g/L. It is thought that will not increase its biosorption efficiency at the higher biosorbent doses. Because, it may be that further increase in dose results in clumping of the biosorbent particles, which can result in loss of available surface area for metal ion uptake. This condition was observed by some researchers [2], [9], [11], [14].

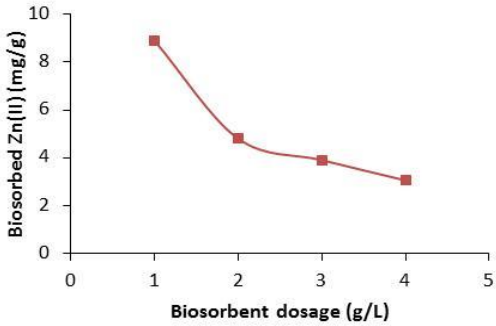


*Figure 4. Effect of initial biosorbent dose on biosorption capacity of forest waste for Zn(II)*

Zn(II) binding capacity values showed a reverse trend and therefore, its magnitude decrease with increment in biomass dosage. Their maximum value was 8.9 mg/g, therefore obtained for the lowest biosorbent dosage (1.0 g/L). Bozic et al. [8] have repoted that the maximum adsorption capacity of Zn adsorption on beech sawdust was found to be 2 mg/g. this value obtained by beech sawdust was lower than value of this study. An increase in Zn(II)/biosorbent ratio caused a decrease in biosorption efficiency.

## 19. CONCLUSIONS

The biosorption of Zn(II) metal ions from aqueous solution was performed by using oriental beech (*Fagus orientalis* Lipsky.) forest wastes biomass. The results indicated that oriental beech (*Fagus orientalis* Lipsky.) forest wastes biomass may be used as an inexpensive and effective for the removal of zinc from aqueous solutions. The zinc biosorption of the forest waste biomass was influenced by the initial metal concentration and biosorbent dosage. For used experimental conditions, the attained maximum biosorption capacity was as 8.9 mg/g and maximum biosorption efficiency was as 41.9%.

## REFERENCES

[27]. K. Conrad, and H.C.B. Hansen, "Sorption of zinc and lead on coir", *Bioresour. Technol*., vol. 98 pp. 89–97, 2007.
[28]. C. Paduraru, L. Tofan, C. Teodosiu, I. Bunia, N. Tudorachi, and O. Toma, "Biosorption of zinc (II) on rapeseed waste: Equilibrium studies and thermogravimetric investigations," *Process Safety and Environmental Protection*, vol. 94, pp. 18-28, 2015.
[29]. H. Ucun, Y.K. Bayhan, Y. Kaya, A. Cakici, and O.F. Algur, "Biosorption of chromium(VI) from aqueous solution by cone biomass of *Pinus sylvestris*," *Bioresour. Technol*., vol. 85 (2), pp. 155–158, 2002.

[30]. H. Ucun, "Equilibrium, thermodynamic and kinetics of reactive black 5 biosorption on loquat (*Eriobotrya japonica*) seed," *Sci Res Essays*, vol. 6 (19), pp. 4113-4124, 2011.
[31]. H. Ucun Ozel, "Biosorption of Cd (II) ions by Nordmann fir cones," *Fresenius Environmental Bulletin*, vol. 21 (9), pp. 2527-2535, 2012.
[32]. D. Park, Y. S. Yun, and J. M. Park, "The past, present, and future trends of biosorption," *Biotechnology and Bioprocess Engineering*, vol. 15 (1), pp. 86-102, 2010.
[33]. J. Kumar, C. Balomajunder, and P. Mondall, "Application of agro-based biomasses for zinc removal from wastewaters-a review," *Clean – Soil, Air, Water*, vol. 39 (7), pp. 641–652, 2011.
[34]. D. Božić, M. Gorgievski, V. Stanković, N. Štrbac, S. Šerbula, and N. Petrović, "Adsorption of heavy metal ions by beech sawdust–kinetics, mechanism and equilibrium of the process," *Ecological Engineering*, vol. 58, pp. 202-206, 2013.
[35]. T. Limcharoensuk, N. Sooksawat, A. Sumarnrote, T. Awutpet, M., Kruatrachue, P. Pokethitiyook, and C. Auesukaree, "Bioaccumulation and biosorption of Cd 2+ and Zn 2+ by bacteria isolated from a zinc mine in Thailand," *Ecotoxicology and environmental safety*, vol. 122, pp. 322-330, 2015.
[36]. Y.P. Kumar, P. King, V.S.K.R. Prasad, "Zinc biosorption on *Tectona grandis* L.f. leaves biomass: equilibrium and kinetic studies," *Chem. Eng. J,*. vol. 124 pp. 63–70, 2006.
[37]. H. Ucun, O. Aksakal, and E. Yildiz, "Copper (II) and zinc (II) biosorption on Pinus sylvestris L," *Journal of Hazardous Materials*, vol. 161 (2), pp. 1040-1045, 2009.
[38]. G. Kandemir, and Z. Kaya, "EUFORGEN Technical Guidelines for genetic conservation and use of oriental beech (*Fagus orientalis*)," *Bioversity International*, Rome, Italy. p. 6, 2009.
[39]. M. Tabari, P. Fayaz, K. Espahbodi, J, Staelens, and L. Nachtergale, "Response of oriental beech (*Fagus orientalis* Lipsky) seedlings to canopy gap size," *Forestry*, vol. 78 (4), pp. 443-450, 2005.
[40]. S. Jiang, L. Huang, T. A. Nguyen, Y. S. Ok, V. Rudolph, H. Yang, and D. Zhang, "Copper and zinc adsorption by softwood and hardwood biochars under elevated sulphate-induced salinity and acidic pH conditions," *Chemosphere*, vol. 142, pp. 64-71, 2016.
[41]. O. Aksakal, H. Ucun, and Y. Kaya, "Application of *Eriobotrya japonica* (Thunb.) Lindley (Loquat) seed biomass as a new biosorbent for the removal of malachite green from aqueous solution," *Water. Sci. Technol*., vol. 59, pp. 1631-1639, 2009.

## BIOGRAPHY

***Handan UCUN ÖZEL*** *works as an associate professor and head of department at Bartin University, Department of Environmental Engineering.*

*Ucun Özel received her BSc and MSc in Environmental Engineering in 1998 and 2001, from Atatürk University, Erzurum, Turkey, respectively. She received her PhD in 2008 from same university and worked as a researcher assistant in the same university. In 2009, she relocated to Bartin University; she is still as an associate professor on Waste Water Treatment at Bartin University, Environmental Engineering Department.*

*She may be contacted at handanucun@bartin.edu.tr or hanucun@yahoo.com*

ICENS
INTERNATIONAL CONFERENCE ON ENGINEERING AND NATURAL SCIENCES
24-28 May 2016 /Sarajevo

# A Research on Determining the User Satisfaction with the Parks Built for the Disabled: The Sample of the City of Malatya

***Atilla Atik*[1], Fürüzan Aslan[1], Bülent Yılmaz[1]***

*[*]: Corresponding Author: atikatilla@hotmail.com*
*[1]: Inonu University Faculty of Fine Arts and Design Department of Landscape Architecture, 44280, Malatya-Turkey.*

## *Abstract*

*In the city center of Malatya are a total of 94 parks providing active service in accordance with the figures pertaining to the year 2015. A h k l h ''Th P k h bl '', wh h w b b bl viduals in particular.*

*In this study, it was aimed on the basis of the participatory approach that the view, wish and satisfaction levels of the disabled individuals '' Th P k h bl M l '', wh h w h b b h isabled individuals living in the City of Malatya, be determined. Within this context, a survey study was conducted on the disabled individuals living in this city. According to the data obtained from the survey study, it was determined that 69.5% of the disabled individuals living in the city center of Malatya had found The Park of the Disabled insufficient in terms of its areal size. 51.4% of the participants found the number of equipments insufficient, whereas 32.4% of them found the equipment qualities insufficient; on the other hand, 58.1% of them expressed the view that the park was in an inconvenient location in terms of transportation. Accordingly; in Malatya, almost 13.9% of the population of which consist of disabled individuals, it is necessary to develop the Park of the Disabled in terms of its areal size, the number and the quality of the equipments as well as easy transportation. Separately, the fact that there is only one park designed to be used solely by the disabled individuals in the city impairs the urban quality of life in terms of disabled individuals.*

**Keywords:** The Disabled, Urban Park, Design, Participatory Approach.

## 1. INTRODUCTION

According to the "World Report on Disability (2010)" by the World Health Organisation (WHO), more than a billion people or about 15% of the world's population are estimated to live with some form of disability [1]. So far today, the definition of disability has been made in different ways by different people, institutions or organizations. According to three major international organizations, which are The United Nations (UN), The World Health Organization (WHO) and The International Labour Organization (ILO), the definition of a disabled or handicapped person is as follows:

The United Nations (UN) gives the definition of a disabled person over the term 'handicapped' and defines this term as such: *" wh bl h h h l h /h w h /h l l l as the result of any flaw that occ h /h h l l b l h l l l "* [2]. The International Labour Organization (ILO) also gives the definition of a disabled person over the term 'handicapped' and defines an individual *"wh j b specific to him/her and the sustenance of this job have greatly declined, and whose expectations of being able to progress in his/her own job have considerably weakened as the result of an accepted h l l b l "* as a handicapped person [3]. The World Health Organization (WHO), on the other hand, exhibited a medical approach in defining the handicapped by sticking to their own study field, and by considering disability as a disease, they defined the concepts by classifying them separately [4].

In Turkey, according to TurkStat, the ratio of the disabled to the total population is 12.29%, which makes nearly 10 million people all over the country [5].

The greatest obstacles for the disabled in taking part within the society are transportation and physical environmental problems. The physical environment in which the disabled live is of great importance due to the physical dysfunctioning/impairments they possess as well as the restrictions caused by these incapabilities. Roads, pavements, public buildings, parks and gardens, schools, the residential settlements, transportation vehicles and several physical environmental factors like these pose serious obstacles against the disabled in their participation within the society [6].

The principles of The European Urban Charter, while identifying how cities should look like for the purpose of owning the rights defined through the European citizen rights, also lay emphasis on the architectural arrangements in order to allow the disadvantaged groups ignored in our cities, such as the disabled, the elderly and children users, to benefit from urban areas and structures. Within the principles of The European Urban Charter, it is aimed that unobstructed, habitable, functional and accessible urban areas and structures be constituted, that awareness towards the disabled be raised, and that the urban quality of life be enhanced in cities [7].

In Turkey, the insufficiency of the architectural arrangements that should allow the disabled to realize their civil rights vested in them through the Law, such as education, health, occupation, entertainment and sports, cause the disabled population to

remain uneducated to a large extent, thus, leading them to participate in production and labour force less and less. While, in the developed countries, the disabled comprise 7-8% of the population, this percentage is about 12% in Turkey [5, 7].

Open-green area systems situated in a city can be defined as the areas that areally comprise or need to comprise a major part of a city, and that are vegetated by local managements by being arranged in the way that they will meet the recreational requirements of people during the time remaining behind their general activities like working and sheltering in order to allow them to make use of their leisure time like walking around, entertainment, physical activities. These areas are the cultural or natural places used commonly by those living in cities [8].

There are many various services and benefits provided for the society by the open-green areas in a city. Until today, there have been many studies conducted by the researchers from different disciplines who aimed to find out these services and benefits. Among these, the studies suggesting that the open-green area systems in a city have positive and direct effects on those living in the city, such as reducing stress and psychological disorders in terms of psychology [9, 10], reducing obesity [11, 12], increasing physical activity [13], protecting health order [14], and boosting the perception of life quality [15], can be given as the examples to these.

As in all developed countries, today in Turkey, necessary arrangements for the disabled are also being performed in the parks, which are among the most important elements of the active green-area systems in cities, for the purpose of meeting the recreative requirements of the disabled individuals. Depending on this, the quality and the quantity of the roads and equipments with accessible design features are being continuously increased in all the parks available in cities. Besides, in order for the disabled individuals to make use of all the activities in the parks of today's cities, The whole design was implemented by taking into consideration the physical limitations of the disabled, and special importance is attached to the construction of the parks planned to be of service to only the disabled individuals by taking into account various disabled groups.

In this study, on the basis of the participatory approach, it was aimed that the view, wish and satisfaction levels of the disabled individuals regarding '' The Park of the Disabled in Malatya'', which was constructed for the purpose of being used by the disabled individuals living in the City of Malatya, be determined. Thus, according to the findings obtained as the result of this study, it was planned that various opinions and suggestions regarding the park of the disabled be presented to the institutions and the people in decision-making positions who were in charge of designing, planning and managing the parks.

## 2. MATERIALS AND METHODS

This study was conducted for the purpose of determining the user satisfactions, expectations and suggestions in '' The Park of the Disabled in Malatya'' located in the city center of Malatya, Turkey. To that end, a face-to-face survey study was performed with the disabled individuals residing in the city center of Malatya.

In determining the sampling size, the proportional approach determined with the help of Formula 1 was benefited from [16].

$$n = \frac{Np(1-p)}{(N-1)\sigma_{px}^2 + p(1-p)} \qquad (1)$$

In the Formula; n, sampling size, N, population size; $\sigma_{px}^2$, variance; p represent the ratio of the disabled users visiting the park of the disabled.

To conduct research with a large population, the $p = 0.5$ value was accepted for $p(1\text{-}p)$ to be the largest value [16, 17].

According to TUIK's (Turkish Statistical Institute) data over the Population and Settlements pertaining to the year 2011, the number of people with at least one disablement in Turkey is 420 227 in the Eastern Anatolian Region and 69 376 in Malatya [18].

Using the above formula, the minimum sample size was calculated to be 94 people at 10% error and 95% confidence interval. This sample size was increased by about 10% to 105 people [17].

The survey consists of 11 questions, and the first 7 questions are about the socio-demographic characteristics of the participants and the identification of the disabled groups. The remaining 4 questions, however, were prepared for the purpose of determining the views of the participants regarding the size of "The Park of the Disabled in Malatya", the quantity-quality status of the components of park equipments as well as accessibility through convenient transportation.

## 3. RESULTS AND DISCUSSION

The data obtained as the result of the survey and some statistical information pertaining to these data are given in Table 1.

Table 1. The results of the questionnaire.

| Socio-demographic characteristics | Name of characteristics | Number | % | Sdt. Dev. | Scale |
|---|---|---|---|---|---|
| **Gender** | Female (1) | 34 | 32.4 | | |
| | Male (2) | 71 | 67.6 | | |

| | | | | | |
|---|---|---|---|---|---|
| | ***TOTAL*** | ***105*** | ***100*** | ***0.470*** | ***1-2*** |
| **Marital Status** | Single (1) | 66 | 62.9 | | |
| | Married (2) | 39 | 37.1 | | |
| | ***TOTAL*** | ***105*** | ***100*** | ***0.486*** | ***1-2*** |
| **Age** | ≤20 (1) | 25 | 23.8 | | |
| | 21-40 (2) | 45 | 42.9 | | |
| | 41-60 (3) | 29 | 27.6 | | |
| | ≥61 (4) | 6 | 5.7 | | |
| | ***TOTAL*** | ***105*** | ***100*** | ***0.852*** | ***1-4*** |
| **Education Level** | Illiterate (1) | 20 | 19.0 | | |
| | Primary School (2) | 27 | 25.7 | | |
| | Secondary school (3) | 34 | 32.4 | | |
| | High school (4) | 7 | 6.7 | | |
| | Vocational school (5) | 9 | 8.6 | | |
| | University graduate (6) | 8 | 7.6 | | |
| | ***TOTAL*** | ***105*** | ***100*** | ***1.451*** | ***1-6*** |
| **Occupation** | Housewife (1) | 11 | 10.5 | | |
| | Public officer (2) | 10 | 9.5 | | |
| | Worker (3) | 14 | 13.3 | | |
| | Retired (4) | 5 | 4.8 | | |
| | Self-employed (5) | 18 | 17.1 | | |
| | Unemployed (6) | 47 | 44.8 | | |
| | ***TOTAL*** | ***105*** | ***100*** | ***2.455*** | ***1-6*** |
| **Income Level** | ≤1000 TL (1) | 78 | 74.3 | | |
| | 1000-2000 TL (2) | 16 | 15.2 | | |
| | 2000-3000 TL (3) | 10 | 9.5 | | |
| | ≥3000 TL (4) | 1 | 1.0 | | |
| | ***TOTAL*** | ***105*** | ***100*** | ***0.697*** | ***1-4*** |
| **Disability Group** | Orthopedic (1) | 43 | 41.0 | | |
| | Hearing (2) | 5 | 4.8 | | |
| | Mental (3) | 33 | 31.4 | | |
| | Visually impaired (4) | 19 | 18.1 | | |
| | Speech and language (5) | 5 | 4.8 | | |
| | ***TOTAL*** | ***105*** | ***100*** | ***1.746*** | ***1-5*** |
| **Is the park sufficient as areal size for you?** | No (0) | 73 | 69.5 | | |
| | Yes (1) | 32 | 30.5 | | |
| | ***TOTAL*** | ***105*** | ***100*** | ***0.426*** | ***0-1*** |
| **What is your opinion about the number of equipments in the park?** | Rather insufficient (1) | 23 | 21.9 | | |
| | Insufficient (2) | 31 | 29.5 | | |
| | Neutral (3) | 30 | 28.6 | | |
| | Sufficient (4) | 13 | 12.4 | | |
| | Quite sufficient (5) | 8 | 7.6 | | |
| | ***TOTAL*** | ***105*** | ***100*** | ***1.101*** | ***1-5*** |
| **What is your opinion about the qualities of equipments in the park?** | Rather insufficient (1) | 11 | 10.5 | | |
| | Insufficient (2) | 23 | 21.9 | | |
| | Neutral (3) | 28 | 26.7 | | |
| | Sufficient (4) | 25 | 23.8 | | |
| | Quite sufficient (5) | 18 | 17.1 | | |
| | ***TOTAL*** | ***105*** | ***100*** | ***1.319*** | ***1-5*** |
| **The Park of the Disabled in Malatya is in well-located.** | Strongly Disagree (1) | 7 | 6.7 | | |
| | Disagree (2) | 16 | 15.2 | | |
| | Neutral (3) | 21 | 20.0 | | |
| | Agree (4) | 49 | 46.7 | | |
| | Strongly Agree (5) | 12 | 11.4 | | |
| | ***TOTAL*** | ***105*** | ***100*** | ***1.309*** | ***1-5*** |

According to the data obtained from the survey study, 69.5% of the disabled individuals living in the city center of Malatya expressed the view that the park of the disabled, located in the city center of Malatya, was not large enough in terms of its areal size.

"The Park of the Disabled in Malatya", which was designed for the purpose of being used by the disabled living in this city, is situated in an area of 2500 $m^2$. The green areas established to meet the recreational needs of the city people may show territorial or regional differences in terms of planning and design features. However, the main objective in planning such areas is to allow the city folk to meet with Nature and to fulfill their longing for Nature [19].

The sufficiency of the green areas in cities have been evaluated by several researchers. Gökyer and Bilgili, in their study conducted for determining the sufficiency and accessibility of the green areas in the city center of Bartın, Turkey, evaluated the parks smaller than 8000 $m^2$ as non-standard places [20].

Emür and Onsekiz (2007) stated that a living environment of quality along with the urban fabric were the result of a balanced spatial relationship among structures, transportation facilities as well as open and green areas. Accordingly; the type, size, fitting (equipment) and functional levels of the use of open and green urban areas has a significant impact on determining the effect of green areas on the urban quality-of-life [21]. As an efficient element in terms of creating a lively environment within the city, in establishing human/environment relationship in the hectic city center and in constituting an urban circulation and activity areas, parking areas, due to the fact that they are socially reduced to a living space/location, can be characterized as one of those significant components of the urban quality-of-life in the sense of the presence of open and green areas [22].

According to TUIK's (Turkish Statistical Institute) 2011 data, the park of the disabled in Malatya, the city in which 69 376 disabled individuals live in total, is rather insufficient/poor in terms of both its areal size and of being the only park that provides provincial-wide service for the disabled. Also according to the result of the survey, the majority of the disabled individuals living in Malatya state the fact that this park is rather poor in terms of its areal size. While only 20% of the participants expressed their positive opinions as to the sufficiency of the number of equipments/fittings in the park, 51.4% of them said they had negative opinions over this matter, whereas the remaining 28.6% said that their opinions about this subject were neutral. Accordingly, the majority of the disabled in Malatya find the number of equipments in the park of the disabled rather insufficient. Although most of the participants find the number of equipments insufficient, they still state the fact that the equipments within the park are qualitatively sufficient.

On the other hand, when the park in question is evaluated in terms of its positional accessibility, 58.1% of the participants expressed positive opinions, whereas 21.9% of them were negative in this matter and 20% of them stated that they were neutral about this subject. Accordingly, the majority of the participants are of the opinion that "The Park of the Disabled in Malatya" is in well-located spot in terms of its positional accessibility. However, even though the views expressed by most of the participants were towards the fact that the park was well-located in terms of accessibility, Aslan and Atik (2015), in their study, reported that 63.8% of the disabled individuals in Malatya were not even aware of the fact that there was a park constructed to provide service solely for them [23].

Keleş (1998) defines the open areas located within the city as urban components where people keep on living, that which remains outside the closed spaces on which constructions were built, those left in their own natural condition, or those that are spared for resting and relaxing purposes, except for agricultural and residential ones. The green areas in cities are the places spared as resting, wandering spots as well as game areas for humans, and such places can be defined as communal areas, such as the alleys arranged by the urban managements and wooded roads, built for preventing the city from becoming a heap of stones [24].

In the City of Malatya, about 13.9% of the population of which consist of disabled individuals, the fact that there is only one single park designed to be used only by the disabled impairs the urban quality-of-life a great deal in terms of the disabled individuals.

In a study conducted by Dikmen (2011) in the City of Yozgat, Turkey, within the context of the Transportation and Circulation Principles of the European Urban Charter, the challenges confronted by the disabled in transportation, circulation and access into the structures in the urban area as well as the architectural arrangements required to be performed in order to eliminate these challenges were discussed, the implementation level of the arrangements for the disabled, which were specific to the city of Yozgat, were questioned, and suggestions were made for the purpose of elevating the quality-of-life and the participation of the disabled in the social and urban life [7].

In the survey study conducted by ÖZİ (2010) for determining the convenience of the built environments and urban services for the disabled, 90.1% of the participants expressed the view that public transport vehicles, buildings, main roads, streets and pavements were not convenient for the disabled [25].

In a study in which the problems that a visually-impaired individual confronts in Turkey in order to minimize the restrictions for use and circulation in parks were discussed, the design criteria were specified in line with the behaviours and requirements of the individual, and finally, solution proposals for implementation were developed [26].

In Turkey, in the sample of the city of Istanbul, the expectations of the disabled individuals regarding the areas of activity in urban parks were evaluated, and through the survey study conducted, it was determined that the majority of the participants had wished the urban parks to provide the opportunity for them to become socialized [27].

Philippa et al. (2009) states that the structural environments in cities increase the movement difficulties for the elderly individuals [28].

## 4. CONCLUSIONS

The expression in the 61st clause of 1982 Constitution stating, "The State takes measures for providing protection for the disabled and allowing them to conform to social life", was included in the Constitution as a direct regulation for the disabled; in addition, along with the regulation in the 60th Clause titled as Social Security within 1982 Constitution, which stated: "Everybody has a social security right. The State takes the necessary precautions to ensure this security and establishes the governance", the State was assigned the duty to perform any type of regulation to allow the disabled individuals to conform to social life [29]. Accordingly, the number of the parks designed to provide service for the disabled in the city center of Malatya are proposed to be maximized in line with equality and affirmative action towards the disabled by also taking into consideration the population rate of the disabled in the city.

Separately, this park with the areal size of only 2500 $m^2$ can be characterized as a non-standard one, as was remarked by several researchers. However, when the current localization status around it is taken into consideration, there is no possibility for this park to be enlarged. For this reason, the areal size of the new parks to be designed for the disabled in the city must also be in accordance with the standards and expectations.

In conclusion, the disabled individuals should be able to make optimum use of the urban parks - which are important public areas for use in elevating the urban quality of life - in order to be able to meet their social needs without excluding themselves from social life but along with the whole society, yet, independently, and this depends on the existence of the parks designed only through the evaluation of various disabled groups.

## REFERENCES

[1] WHO, World Report on Disability (Summary), http://www.who.int-/disabilities/world_report/2011/accessible_en.pdf: pp. 7-8, 2011.
[2] M. Öztürk, *Tü k ' E ll G ç ğ* , MÜSİAD Cep Kitapları, 2011, vol. 30.
[3] ILO, *ILO Sözl ş , S k l M l k R h b l v İ h* , no. 159, 1983.
[4] WHO, International Classification of Impairments, Disabilities and Handicaps, Geneva, 1980.
[5] (2015) The "Turkish State Meteorological Service" website. [Online]. Available: http://www.meteor.gov.tr/
[6] K. Karataş, "The disabled want to live in cities free," *Ufkun Ötesi*, vol. 2, no. 4, pp. 10-13, 1998.
[7] Ç. B. Dikmen, "Examining the accessibility of handicapped to urban areas and buildings within the context of transportation and circulation principles of European urban charter: Yozgat sample," *NWSA*, vol. 6, pp. 838-858, 2011.
[8] M. Dil, "İstanbul'un yeşil alan sisteminin, planlama kriterleri açısından irdelenmesi," Master of Science Thesis, İstanbul Teknik Üniversitesi, Fen Bilimleri Enstitüsü, İstanbul, Turkey, 2004.
[9] M. Annerstedt, P. Ostergren, J. Bjork, P. Grahn, E. Skarback and P. Wahrborg, "Green qualities in the neighbourhood and mental health - results from a longitudinal cohort study in Southern Sweden," BMC Public Health, vol. 12, p. 337, 2012.
[10] C. Ward Thompson, J. Roe, P. Aspinall, R. Mitchell, A. Clow and D. Miller, "More green space is linked to less stress in deprived communities: evidence from salivary cortisol patterns," Landscape and Urban Planning, vol. 105, no. 3, pp. 221-229, 2012
[11] T. S. Nielsen and K. B. Hansen, "Do green areas affect health? Results from a Danish survey on the use of green areas and health indicators," Health and Place, vol. 13, pp. 839-850, 2007.
[12] J. Bell, J. Wilson and G. Liu, "Neighborhood greenness and 2-year changes in body mass index of children and youth," American Journal of Preventive Medicine, vol. 35, p. 547, 2008.
[13] R. Mitchell, "Is physical activity in natural environments better for mental health than physical activity in other environments?," Social Science & Medicine, vol. 2012, pp. 1-5, 2012.
[14] R. Mitchell and F. Popham, "Effect of exposure to natural environment on health inequalities: an observational population study," The Lancet, vol. 372, pp. 1655-1660, 2008.
[15] H. Tinsley, D. Tinsley and C. Croskeys, "Park usage, social milieu, and psychosocial benefits of park use reported by older urban park users from four ethnic groups," Leisure Sciences, vol. 24, pp. 199-218, 2002
[16] P. Newbold, "*Statistics for Business and Economics*, Prentice-Hall, New Jersey, USA, 1995.
[17] B. Miran, "*Basic statistics*," Aegean University Printing Office, İzmir, 2003.
[18] (2011) The "Turkish Statistical Institute" website. [Online]. Available: http://www.turkstat.gov.tr/
[19] B. C. Bilgili and E. Gökyer, "*Urban green space system planning*," Landscape Planning, Published by InTech, 2013.
[20] E. Gökyer and B. C. Bilgili, "A research on assessment of accessibility of green areas: The case of Bartın Province," *SDU Faculty of Forestry Journal,* vol. 15, pp. 140-147, 2014.
[21] H. Emür and D. Onsekiz, "The importance of open and green areas in the components of urban life quality-the analysis of park areas in Kayseri/Kocasinan district," *Sosyal Bilimler Enstitüsü Dergisi*, vol. 22, pp. 367-396, 2007.
[22] N. Sırtkaya, " Samsun, Ordu ve Rize kentlerinin bazı kıyı parklarındaki bitki kompozisyonlarının mekânsal yapı yönünden incelenmesi," Master of Science Thesis, Akdeniz University, Department of Landscape Architecture, Trabzon, Turkey, 2007.
[23] F. Aslan and A. Atik, "Determination of the awareness level of individuals about the parks designed for the disabled," *ICENS 2015,* paper, p. 251.
[24] R. Keleş, "*K b l T l Sözlüğü*," İmge Kitabevi Yayınları, Ankara, Turkey, 1998.
[25] ÖZİ, "T.C. Başbakanlık Özürlüler İdaresi Başkanlığı, Özürlülük Eğitimi: Toplum Özürlülüğü Nasıl Anlıyor Temel Araştırması, T.C. Başbakanlık Özürlüler İdaresi Başkanlığı Yayınları, 2010.
[26] S. Bekiroğlu, "Görme Özürlülerin Kullanımına Yönelik Park Tasarım Kriterleri," Peyzaj Mimarlığı Kongresi/Ankara, 2000.
[27] N. Özdingiş, "İstanbul Kent Parklarının Bedensel Özürlüler Açısından Değerlendirilmesine Yönelik Bir Araştırma," Master of Science Thesis, Çevre Tasarımı Yüksek Lisans Programı, Fen Bilimleri Enstitüsü, Bahçeşehir Üniversitesi, İstanbul, Turkey, 2007.
[28] C. Philippa, A. A. Jennifer and L. Paula,"Urban built environments and trajectories of mobility disability: Findings from a national sample of community-dwelling American adults (1986–2001)," *Social Science & Medicine*, vol. 69, pp. 964–970, 2009.
[29] S. Çinarli, "*E ll l Yö l k K H z l ,"* Kazancı Hukuk Yayıne-vi, İstanbul, Turkey, 2010.

ICENS
INTERNATIONAL CONFERENCE ON ENGINEERING AND NATURAL SCIENCES
24-28 May 2016 /Sarajevo

# Historic Battalgazi District; its tourism potential, problems and solution proposals, Malatya, Turkey

***Bülent Yılmaz*[1], Atilla Atik[1], Fürüzan Aslan[1]***

*[*]: Corresponding Author: bulent.yilmaz@inonu.edu.tr*
*[1]: Inonu University Faculty of Fine Arts and Design Department of Landscape Architecture, 44280, Malatya-Turkey.*

***Abstract***

*Historical surroundings are among important elements for the sustainability of cultural heritage. Contribution of such city parts to cultural tourism is also large since they function as a bridge between past and future. It is emphasized in Convention Concerning the Protection of World Cultural and Natural Heritage (UNESCO 1972) that such unique values are not only owned by the geography they are located but also by commonly all mankind. In this respect, cultural tourism is an effective tool to protect historical and cultural heritage and may provide significant economic incomes.*

*Battalgazi District (Ancient Malatya) is evaluated whose history dates back to Palaeolithic period in the scope of the present study. The District has been one of the most important junctions from Antique period to date between Anatolia, Middle East and Eurasia geography. As the first settlement area of the city of Malatya, Battalgazi District, tries to sustain its historical tissue inherited today. Historical tissue in the District cannot reflect its cultural identity completely due to various reasons such as lack of maintenance and wrong restorations. Performance of historical remains the district shelters in its body is very low and inefficient. Aim of the present study is to offer solution proposals for Battalgazi district to develop tourism by determining its cultural tourism potentials. Thus, cultural tourism may overtake responsibility to protect cultural heritage.*

**Keywords:** Cultural tourism, historical environment, Battalgazi, Malatya.

## 1. INTRODUCTION

Tourism has been studied for its economic, environmental, cultural, and social impacts. Rarely has tourism been explicitly examined as a possible catalyst for social movement participation [1-14]. Countries prefer to develop strategies and competitive and marketable local touristic products to get more share from tourism sector by considering their own potentials. Tourism activities in Turkey began to develop in 1980s based initially on sea, sand and sun (3-S) aiming sightseeing and entertainment. At present, more than half of the foreign visitors to Turkey still come for this aim [15]. As a result of such a situation, alternative types of tourism to 3-S began to be suggested in many places [16]. In this respect, culture tourism as a type of alternative tourism is growing day by day with the changing travel trends and tourist expectations. Desires to see and visit more distinctive and authentic places have caused increase in the number of travels to cultural sites. Culture tourism is expected to develop since culture tourists are willing to discover cultural richness [17, 18].

Culture tourism as a concept can involve several sub-topics. Historical and archaeological remains reflecting the history of a given area, historic and religious centres, museums, festivals and special days, local handicrafts can be counted among such subthemes. Such topics can serve as cultural capital in a country. Many cities may own a long historical background. Formation of cities may date back to centuries ago even antique ages. Historical and archaeological urban tissue and architectural examples in a region can bear valuable clues about the history of the mentioned area and its close proximity and serve as important cultural heritage in a city by providing scenes related to living conditions and social life [19-21].

Culture includes everything human produces against nature to survive together with it. Formation of different cultures in different places resulted in tourism and in the last years, concepts such as cultural heritage, heritage tourism, historical tourism, cultural tourism have been suggested by various sides of the tourism sector. However, basic point is the complete use of cultural sources for touristic purposes [22]. Cultural tourism is a form of tourism which is emphasized on for not only its income increasing effects but also for the preservation of cultural values [23]. However, despite positive and constructing effects of culture tourism on the conservation and restitution of historical and cultural values, culture tourism is known to have sometimes destroying and devastating effects on them by causing an unplanned tourism development [15, 24-25].

Historical and cultural environment is defined to be the views of cultural values humans created throughout their history and reflected on physical environment [26]. Historical city centres can bear an accumulation of many historical and cultural experiences gained in a process from their inceptions and transfer to date. However, such areas are taken under the effects of new and bad developments due to their locations in the entire city and remain inefficient to meet spatial needs required by modern life style. Such type of developments may turn these areas into depression zones from physical, economic and social aspects [27].

The aim of the present study is to determine tourism potential of Battalgazi, a historical settlement and offer suggestions to improve such potentials. It is also aimed in the study to attract attention to historical structures in the area which suffer

seriously from problems like false restoration and differentiations in social structure and suggest solution proposals for the creation of liveable historical areas.

## 2. MATERIALS AND METHODS

Main material of the study is Battalgazi district, the first settlement area of Malatya, and sheltering important historical tissues. Battalgazi is located in Upper Euphrates sub- region of East Anatolia inside the official border of Malatya province [28]. Surface area of the district is 213 km$^2$ and it is 9 km away from city centre. The area is surrounded by Karakaya Dam Lake in the north, Kale and Pötürge districts in the east and Yeşilyurt district in the west and south (Figure 1).

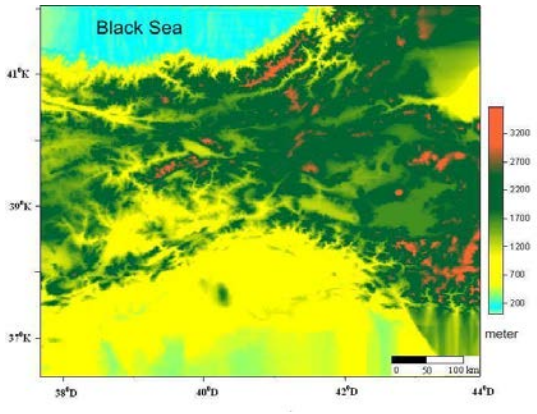


*Figure 1 Location of study area*

Historical remains were introduced by reviewing related literature to Battalgazi known also to be Ancient Malatya in the scope of the study. Their locations were determined through field surveys and photographs. Importance of historical works in the history of the region and cultural heritage tried to be determined.

## 3. RESULT AND DISCUSSION

The city of Malatya, so-called history books, was 9 km northwest of present city with the name Ancient Malatya (Battalgazi) [29]. The region covering Malatya was under the sovereignty of historical states such as Assyrian, Urartian, Persian, Hittite, Roman, Byzantine, Arabic, Seljuk and Ottoman.

In 2nd Century BC, Roman Empire carried the city of Malatya from Aslantepe to today's Battalgazi and surrounded it with walls. The city was attacked many times since it remained to be a border location in the east of the country and many civilisations took the city under their control. Photographs and information of the historical works in the district are given below (Figure 2).

*( ) K l S l ( w ll):* Fortress remaining from Roman Era began to be constructed in 79 AD and was completed around 530 – 540 after a very long lasting construction period. The fortress lost its defencing properties from Ottoman Period onwards and was demolished largely in 19th century. The fortress had originally 95 constellations and 11 gates [30]. Cut stones in regular edges used in the fortress walls can now be seen in the walls of houses and gardens. In some parts walls are restored today.

*(b) Armourer Mustafa Paşa Caravanserai:* This structure was built by Armourer of Ottoman Emperor Murad IV, Mustafa Paşa, in 1632 in Battalgazi (Ancient Malatya). Construction material of the rectangular – shaped and structure with an arcaded yard and indoor extension of the yard is cut stone. Closed with a vault roof system, the structure is made up of two parts used distinctly in winter and summer [30]. It is one of the most important monumental structures of Battalgazi. Caravanserai, in a good physical condition after a restoration today, is used for meetings, autograph sessions, discourses and exhibitions.

*(c) Ulu Cami (mosque):* This Mosque was constructed by Seljuk Sultan Alaaddin the 1st in 1224. It sustains the heritage of Great Seljuk Empire in Anatolia. It is the only structure which has a domed shrine, yard and iwan together. The mosque restored in 1970s takes place in a social complex together with Sahabiye Kübra Madrasah, remains of which are in the south facet of the Madrasah [30].

*(d) Melik Sunullah Minaresi (Minaret)*: Normally the Minaret belongs to a mosque constructed by Çerkez, the son of Abdullah Hüsnü in Battalgazi in 1394 but demolished completely today. The Minaret is constructed using bricks and called preacher centre by local people [30].

*(e) Emir Ömer Masjid:* It was built in Battalgazi in 1556 with a rectangular plan and is used and visited today as tomb not masjid. It has a flat roof and stone walls. Tomb shelters a burial chamber [30]. It is a typical example of Ottoman architecture [31].

*(f) Karahan Mosque*: According to its identity tablet, the structure was constructed in 1583 by Hüsrev Bey, the colonel of Malatya in Ottoman period on a square plan. The Mosque built in Battalgazi and restored in 1900 has a narthex surrounded by porticos [30].

*(g) Ak Minare Cami (White Minaret Mosque)*: The Mosque constructed of cut stone by Himmet, the son of Zaim Yusuf in 1572 is a structure from Ottoman time. Minaret of the Mosque which is the only mosque with solitary dome collapsed [30, 31].

*(h) Sütlü Minare (Milky Minaret)*: Even though it has no tablet, the Minaret in Battalgazi is considered to belong to 17th Century in Ottoman period when considered construction techniques and materials used. The mosque it was once connected is now demolished. The Minaret facing demolishing threats has a one balcony [30, 31].

*(i) Namazgah (small praying house)*: The structure built in 1243 managed to survive and reach to date by preserving its original situation. All the historical structures in Battalgazi were constructed from cut stones. In the Namazgah, which was constructed in Seljuk's period for voyagers to pray comfortably along the route, shelters a shrine and s seven-staged pulpit (minbar) [30].

*(j) M l Ş h Al B M q* : The mosque was constructed by colonel Şah Ali Bey in 1591 Battalgazi in the south of Alacakapı Wall Gate in convenience with a square plan and a flat wooden ceiling [31].

*(k) S Z T b :* Even though it has no tablet on it, it is understood that it is a Seljuk time structure due to its construction technique. Pyramid was constructed in Battalgazi in the form of a conic polygon and from stone material [30].

*(l) K l Kü b (Bl T b ):* Its tablet cannot be read. It was constructed in nearly 1300s as a monumental grave from stone and brick material in a square plan. Downstairs of the two – storey Tomb serves as mummy place and upstairs is for visit. Dome of the Tomb estimated to be covered by a conic shape looks like a half moon inside [30].

*(m) Halfetih Minaresi (Minaret):* Minaret constructed completely from brick material is from 13th century. It is estimated to be the part of mosque or madrasah around it. It is similar Ulu Cami in its structure technique and construction material. It is so – called "Hötüm Dede" by locals in Battalgazi [30].

*(n) Toptaş M q* : The Mosque constructed in the neighbourhood in the same name in Battalgazi was restored many times and deviated heavily from its original form. According to the dates in its tablets it was restored in 1681 and 1827. The Mosque has a roof and a Minaret constructed in 1960s [30].

*(o) Sahabiye-i Kübra Madrasah*: Ruins in the south of Battalgazi Ulu Cami belong to this Madrasah. According to art historians, it was constructed in the era of Seljuk Sultan Keykavus. It is estimated to take place in a complex together with Ulu Cami [30].

*(p) Ahmet Duran Masjid and Tomb*: It was constructed in 1792 from wooden material. It is visited densely by locals by considering its holly aspects. The person who gave his name to the structure is said to be one of Seyit Battalgazi's commanders [30].

*( ) K k K şler Ş h l ğ (F B h M ) :* A cemetery from 13th century Seljuk's time was surrounded with a stone and concrete wall by Battalgazi Municipality and taken under protection. People believe this area belongs to 40 Seljuk soldiers [30].

*(s) Nefise Hatun Türbesi (Tomb):* The Tomb constructed out of Battalgazi city walls in Meydanbaşı point is from 14th century. The Tomb covered with a pendentive doomed roof was constructed from regularly cut stones and bricks. The burial chamber belongs to Hacı Nefise Hatun, daughter of Emir Sühnab Bey [31].

*(t) B l z M k (H B l z ):* It is in Meydanbaşı neighbourhood in Battalgazi. Evliya Çelebi, a famous Turkish voyager, mentioned about this structure in his book, Seyahatname, as that it was in Aspuzu vineyards and it stood for 700 years strongly due to Battalgazi's holly soul [31].

*(u) Aslantepe Tumulus*: It is in Orduzu location 4 km away from Malatya citty centre. It hosts 27 cultural layers from Neolithic (8.000 BC) to Roman Age. Excavations have regularly been going on since 1961.

*Figure 2. Photographs of historical structures in Battalgazi*

Economic activities in Battalgazi are performed based on agricultural sector. Share of tourism sector is not significant in the total economic District even though it shelters the mentioned historical and archaeological values serving as the potentials for cultural tourism [21]. The number of tourists in Malatya is at an ignorable level when compared to that of the country [Table 1, 32, 33].

*Table 1. Tourist number in Malatya Turkey*

| | **Years** | **Domestic Tourists** | **Foreign Tourists** |
|---|---|---|---|
| Malatya | 2010 | 5 846 | 3 956 |
| | 2011 | 6 324 | 3 814 |
| | 2012 | 5 701 | 3 895 |
| | 2013 | 3 710 | 2 289 |
| | 2014 | 3 393 | 1 934 |
| Turkey | 2010 | 10 921 427 | 28 632 204 |
| | 2011 | 11 592 653 | 31 456 076 |
| | 2012 | 11 731 463 | 31 782 832 |
| | 2013 | 12 474 218 | 34 910 098 |
| | 2014 | 12 768 914 | 35 257 859 |

It is important for the continuity of cultural heritages reaching successfully to date to transfer historical structures to generations next. Introduction of cultural tourism to the area may prevent historical tissue from leaving unattended and improving the physical conditions of the structures constructed in this tissue. The point to be considered should be the prevention of cultural values. Even though there are various legal regulations to conserve cultural heritages in Turkey, they are not applied efficiently in practice. Such a situation is also valid for Battalgazi district. The most important problem may be accepted to be the good intended but amateur approaches of local authorities and NGOs. Restorations perceived to be not original should be avoided and told to be not an acquirement. Several of restored historical structures can exhibit views not belonging originally to them. Local construction workers not knowing how to repair and restore such structures harm to these buildings and remains and cause them to lose their real identity. In addition, majority of historical structures are captured in narrow streets and settlement zones. Especially, the stones of city walls are used as the construction material in the walls of some houses and gardens. As the result of such unconscious activities, the district faces the danger of losing its cultural tissue. Such a situation may be thought to be a primary problem for the development of cultural tourism.

## 4. CONCLUSIONS

Only 20% of park areas in the city have shelter water surface. Historical and cultural heritage in Turkey offers an important potential for cultural tourism. It is an indispensable responsibility to transfer such heritage to generations next by preserving and improving historical sites in order to develop cultural tourism. Historical tissue of Battalgazi district, an important part in Malatya city, may serve as an important culture tourism circle. In this context, conscious activities both nongovernmental organisations and local authorities will perform related to cultural heritage are of great importance.

## REFERENCES

[1] I. Light and C. C. Wong, "Protest or work: dilemmas of the tourist ındustry in American Chinatowns," *American Journal of Sociology*, vol. 80, pp. 1342-1368, 1975.
[2] G. Wall and C. Wright, *The Environmental Impacts of Outdoor Recreation*, University of Waterloo, Department of Geography, Publication Series No. 11, 1977.
[3] E. de Kadt, Tourism, *Passport to Development?* Perspectives on the Social and Cultural Effects of Tourism in Developing Countries. New York: Oxford University Press, 1979.
[4] A. Mathieson and G. Wall, *Tourism: Economic, Physical, and Social Impacts*, New York: Longman Press., 1982.
[5] A. Milman and A. Pizam, "Social ımpacts of tourism on central Florida," *Annals of Tourism Research,* vol. 15, pp. 191–204, 1987.
[6] V. Smith, *Hosts and Guests: The Anthropology of Tourism*, Philadelphia: University of Pennsylvania Press, 1989.
[7] E. Boo, *Ecotourism: Potentials and Pitfalls*. Washington DC: World Wildlife Fund, 1989.
[8] B. Martin and M. Uysal, "An examination of the relationship between carrying capacity and the tourism lifecycle: management and policy ımplications," *Journal of Environmental Management*, vol. 31, pp. 327–332, 1990.
[9] B. H. Farrell and D. Runyan, "Ecology and Tourism," *Annals of Tourism Research,* vol. 18, pp. 26–40, 1991.
[10] C. M. Hall, *Tourism and Politics: Policy, Power, and Place*, Chichester: Wiley, 1994.
[11] L. Tonkin, "Can community action groups produce structural change in the Blue Mountains Tourism Industry?" *Australian Geographical Studies*, vol. 33, pp. 287-298, 1995.
[12] E. Chambers, *Tourism and Culture: An Applied Perspective Albany*, NY: State University of New York Press, 1997.
[13] R. Wyllie, *Tourism and Society*, State College PA: Venture Publishing, 2000.
[14] N. G. McGehe, "Alternative tourism and social movements," *Annals of Tourism Research*, vol. 29, pp. 124-143, 2002.
[15] B. Gülcan, "Türkiye'de kültür turizminin ürün yapısı ve somut kültür varlıklarına dayalı ürün farklılaştırma ihtiyacı," *İşl A ş l* , vol. 2, pp. 99-120, 2010.
[16] T. Kiper, "Safranbolu Yörük Köyü peyzaj potansiyelinin kırsal turizm açısından değerlendirilmesi," Doktora Tezi, Ankara Üniversitesi, Fen Bilimleri Enstitüsü, Ankara, Turkey, 2006.
[17] S. Wang, Y. Y. Fu, A. Cecıl, S.S.H. Avgoust, "Residents' perceptions of cultural tourism and quality of life- a longitudinal approach," *Tourism Today*, vol. 2006, pp. 47-61, 2006.
[18] S. Meydan Uygur, E. Baykan, "Kültür turizmi ve turizmin kültürel varlıklar üzerindeki etkileri," *T v T z Eğ F kül Dergisi*, vol. 2007, pp. 30-49, 2007.
[19] C. Weber, "Interaction model application for urban planning," *Landscape and Urban Planning,* vol. 63, pp. 49-60, 2003.
[20] K. Taylor, "Cultural heritage management: A possible role for charters and principles in Asia," *International Journal of Heritage Studies,* vol. 10, pp. 417-433, 2004.
[21] B. Yılmaz, S. Sarıçam, F. Aslan, A. Atik, "Landscape characteristics of Battalgazi archaeological and historical settlement in Malatya, Turkey, its protection problems and solutions," *Journal of Environmental Protection and Ecology,* vol. 15, pp. 1181-1190, 2014.
[22] G. Emekli, "Avrupa Birliği'nde turizm politikaları ve Türkiye'de kültürel turizm," *E C ğ* , vol. 14, pp. 99-107, 2005.
[23] Y. I. Öztürk, I. Yazıcıoglu, "Gelişmekte olan ülkeler için alternatif turizm faaliyetleri üzerine teorik bir çalışma," *Gazi Üniversitesi Ticaret ve Turizm Eğitim Fakültesi Dergisi*, vol. 2, pp. 183-195, 2002.
[24] M. Kousis, "Tourism and the environment a social movements perspective," *Annals of Tourism Research,* vol. 27, pp. 468-489, 2000.
[25] R. Engelhardt, W. Jamıeson, B. Kaldun, J. Koch-Schulte, P. Sunalaı, E. Meleısea, "*The effects of tourism on culture and the environment in Asia and the Pacific*," Tourism and Heritage Site Management in Luang Prabang, Bangkok:Office Of Regional Advisor, United Nations Educational, Scientific and Cultural Organization, 2004.
[26] R. Keleş, C. Hamamcı, "*Çevrebilim*," İmge Kitabevi, Ankara, Turkey, 1997.
[27] R. Z. Çetin, "Tarihi kent merkezlerinde yeniden canlandırma politikaları üzerine değerlendirme, İzmir Kemeraltı Örneği," Master of Science Thesis, Dokuz Eylül Üniversitesi, Fen Bilimleri Enstitüsü, İzmir, Turkey, 2012.
[28] Ö. Arslan, "Battalgazi İlçesinin (Malatya) beşeri ve ekonomik coğrafyası," Master of Science Thesis, Fırat Üniversitesi, Sosyal Bilimler Enstitüsü, Elazığ, Turkey, 2006.
[29] Y. Durgun, "Geleneksel Malatya evleri üzerine bir inceleme. Master of Science Thesis, Gazi Üniversitesi, Fen Bilimleri Enstitüsü, Ankara, Turkey, 2006.
[30] Ö. Y. Yakar, F. Fırat, N. Bozdağ, A. E. Baydoğan, "*S l, Kül ü l v Ek k Yö l İl M l* ," TC Malatya Valiliği, İl Planlama ve Koordinasyon Müdürlüğü, Malatya, Turkey, 2004.
[31] H. Demirbağ, F. Fırat, "*M B ş ğ M l* ," Malatya Valiliği Malatya Kitaplığı Yayınları. Kültür-Sanat Dizisi 2, Malatya, Turkey, 2013.
[32] (2015) "Republic of Turkey Ministry of Culture and Tourism" website. [Online]. Available: http://www.kultur.gov.tr/?_dil=1/
[33] (2015) "Turkish Statistical Institute" website. [Online]. Available: http://www.turkstat.gov.tr/

# Examining The Arboreal Taxa used in Landscape Design Works of the City of Malatya

*Atilla Atik*[*1], Fürüzan Aslan[1], Bülent Yılmaz[1]*

[*]: *Corresponding Author: atikatilla@hotmail.com*
[1]: *Inonu University Faculty of Fine Arts and Design Department of Landscape Architecture, 44280, Malatya-Turkey.*

***Abstract***

*In the scope of this study, the arboreal plant taxa which are used in open urban area landscape design in the city center of Malatya in Turkey, have been examined. In the light of the data received from the Parks and Gardens Management of Malatya Metropolitan Municipality, the types that were purchased by the relevant units of the municipality to be used in landscape design like the city parks, child ' l , roadside planting, square designs for the years 2011-2012-2013 and 2014 have been determined. According to the data obtained, it was observed that 83 strains belonging to 29 families and 50 stocks were used in these design works. 25 out of these 83 strains were gymnosperm and 58 were angiosperm. Again, among these 83 strains, 37 were shrub species and 46 were tree species.*

**Keywords:** Urban green area, Plant material, Biological diversity, Malatya.

## 1. INTRODUCTION

Throughout history, arboreal plants, especially trees have attracted the attention of human beings, and have been used actively in agricultural areas as well as for landscape design works [1, 2]. Today, depending on the increasing population and dense urbanization, the need for open green areas have increased more than ever [2]. There have been a great number of studies from various disciplines conducted on the positive effects of trees in urban areas on the urban ecosystems of any size and any intensity.

Davies et al. (2011) and Paoletti et al. (2011) reported that trees and other vegetation in open urban green areas have the duty of being a carbon sink against the carbon release stemming from industrial activities because of their carbon-binding properties [3, 4]. Gidlöf-Gunnarsson & Öhrström (2007) reported that a vegetation form with especially arboreal taxa had effects that could decrease the noise in a city [5].

Today, about 31% of the Earth's land area consist of forests [6]. The total area of Turkey is 78 356 000 ha, and 1.78% of it consists of water. In this context, the total land area is 76 963 000 ha. The country has the 1.14% of the total land area of the Earth, and is in the 37$^{th}$ row in terms of area size [7].

Due to its geographical location and distinct topography varying across very limited distances, Turkey is much richer than most of the surrounding countries in terms of plant biodiversity. The number of plant taxa distributed across Turkey is close to the number of plant taxa spread in the whole of the European continent. According to the latest inventory information, Turkey hosts nearly 12,000 plant taxa. This is also a result of the diversity of plantation habitats [8, 9].

Not only does this case provide a wide range of plant material selection in rural and urban landscaping in Turkey but also the climatic, edaphic, physiographic and biological changes at short distances make it necessary to select appropriate and adaptive species in regional, urban and even suburban scales.

The plant materials used in landscape designing works are green building elements having aesthetic features and providing various functional features to the environment as well. Urban population growth and urban sprawl, one of the largest problems of especially developing countries, further increase the importance of using plant materials in the landscaping works in urban areas. Today, selection of plants, knowing their dendrologic and ecological features and demands, is perceived as the most important indicator on the effective use of limited resources [2].

In this study, especially in Malatya, with limited conditions in plant breeding and variety selection due to its climate-induced handicap, the plant materials consisting of arboreal taxa used in landscaping works were identified. The results obtained from this study has a expansive effect in terms of revealing the plant diversity used in the city center and creating resources for studies to be conducted to determine the adaptability of the species planted, as well.

## 2. MATERIALS AND METHODS

This study was conducted to determine arboreal plant taxa used in urban open green spaces for 4 years between 2011-2014 by the Parks and Gardens Management of Malatya Metropolitan Municipality.

Malatya is located in the Upper Euphrates River Valley of Eastern Anatolia Region in Turkey. A substantial portion of the land of Malatya lacks vegetation. Formerly, an important part of the province was covered with forests, while this cover has

disappeared in time. Because the natural conditions greatly complicate self-renewal of forests, steppes are formed in patches. 367.253 hectares of provincial land area (30%) are covered with forests and heathland, and 125.156 ha of it (10%) with grasslands. Malatya mountains extending in east-west direction that cover the southern lands of provinces from longitudinally, disordered woods dominated by oak, and coppice forests starts to turn into order woods and coppice woods. Cranberries, a species of coniferous trees which has been disapprearing in Eastern Anatolia, are found in mountain slopes overlooking the Sultansuyu Valley, at the western end of Malatya Mountains. The plateaus situated on Malatya mountains and the plains having a half-lowland quality located in areas close to Malatya Plain are covered with rich meadow grasses. The natural vegetation in the mountains surrounding the southwest of the province and in the plateaus have virtually disappeared. No other vegetation other than disordered forest remains consisting dominantly of oaks can be found in this region. This vegetation is occasionally accompanied by wild fruit trees, poplars and willows found around water sources and in the valleys. In areas where plant growing is practiced, orchards are more common than the natural vegetation. The mountains surrounding the northern part of Malatya are considered richer than the western part, and to a lesser extent, Pütürge and Doğanşehir in terms of vegetation. In these areas are deciduous forests mostly of oak, most of which are of a disordered nature. fruit trees, willows and poplars, along with a thick layer of soil, are observed in this part [10].

According to Thornthwaite climate classification; a continental climate type, indicated by D,B'2,s,b'2, semi-arid, mesothermal, and having a moderate level of excess water in winter and an evaporation rate of 58% in summer [11].

According to Address Based Population Registration System, total population of the province of Malatya in 2014 is 769.544. The provincial average of annual population growth in the 7-year period from 2007 to 2014 has been determined as 9.2% and the total increase in the same period as 48.7. The population of the city of Malatya in 2014 is 583.579 [12]. The city center, especially in recent years, lets in a mass migration from rural areas and neighboring provinces.

While the main material of the study consists of the data obtained from the Parks and Gardens Directorate of Malatya Metropolitan Municipality, observational studies were also conducted on different types of open-green areas in the city. Additionally, evaluation of plant materials used in various open-green areas and similar studies done on the subject in Malatya city center constitute the auxillary material for the study.

## 3. RESULT AND DISCUSSION

The list of arboreal plant taxa list used in the landscape design works in urban open-green areas by Parks and Gardens Directorate of Metropolitan Municipality of Malatya during the 4-year period between 2011-2014 is given in Table 1.

Table 1. Arboreal Taxa used in the urban open-green areas of Malatya between the years 2011-2014.

| **Turkish name of plants** | **Latin name of plants** | **Label** |
|---|---|---|
| Abelya | *Abelia grandiflora* | Ag |
| Doğu Karadeniz Göknarı | *Abies ordmanniana* | An |
| Dişbudak Yapraklı Akçaağaç Flamingo Akçaağacı | *Acer negundo flamingo* | Ane |
| Çınar Yapraklı Akçaağaç | *Acer platanoides* | Ap |
| Japon Akçaağacı | *Acer palmatum* | Apa |
| Kırmızı Çizgili Akçaağaç | *Acer capillipes* | Ac |
| Bayaz Çiçekli At Kestanesi | *Aesculus hippocastanum* | Ah |
| Gülibrişim-İpek Ağacı | *Albizzia julibrissin* | Aj |
| Kadıntuzluğu | *Berberis thunbergii* | Bt |
| Salkım Huş | *Betula pendula roth* | Bp |
| Şimşir | *Buxus baccata* | Bb |
| Adi Şimşir | *Buxus sempervirens* | Bs |
| Himalaya Sediri | *Cedrus deodora* | Cd |
| Atlas Sediri | *Cedrus atlantica* | Ca |
| Toros Sediri | *Cedrus libani* | Cl |
| Erguvan | *Cercis siliquastrum* | Cs |
| Japon Ayvası | *Chaenomeles japonica* | Cj |
| Mavi Servi | *Cupressus arizonica* | Car |
| Limoni Servi | *Cupressus macrocarpa goldcres altuni* | Cm |
| Leylandi | *Chamacparis leylandi* | Cp |
| Kara Servi - Akdeniz Servisi | *Cupressus sempervirens* | Cs |
| Dağ Muşmulası | *Cotoneaster horizontalis* | Ch |
| Ateş ağacı | *Delonix regia* | Dr |
| Altuni Taflan | *Euonymus japonica* var. *Aurea* | Ej |
| Gümüşi Taflan | *Euonymus varigeta* | Ev |
| Kalem Ağacı | *Euphorbia triucali* | Et |
| Altınçanak | *Forsythia intermedia* | Fi |
| Amerika Dişbudağı | *Fraxinus americana* | Fa |
| Adi Dişbudak | *Fraxinus excelsior* | Fe |
| Hatmi | *Hibiscus syriacus* | Hs |
| Kış Yasemini | *Jasminum nudifolium* | Jn |
| Adi Yasemin | *Jasminum officinale* | Jo |

| | | |
|---|---|---|
| Yatay Ardıç | *Juniperus chinensis* var. *pfitzeriana* | Jc |
| Yatay Ardıç | *Juniperus horizontalis* | Jh |
| Ardıç | *Juniperus indica* | Ji |
| Ardıç | *Juniperus sabina* | Js |
| Ardıç | *Juniperus conferta* | Jco |
| Yatay Ardıç | *Juniperus davurica* | Jd |
| Ardıç | *Juniperus squamata* | Jsq |
| Oya Ağacı | *Lagerstroemia indica* | Li |
| Akdeniz Defnesi | *Laurus nobilis* | Ln |
| Karayemiş | *Lauroceracus officinalis* | Lo |
| Lavanta | *Lavandula angustifolia* | La |
| Ligüstrum | *Ligustrum japonicum* | Lj |
| Ligüstrum | *Ligustrum ovalifolium* | Lov |
| Ligüstrum | *Ligustrum vulgare* | Lv |
| Lale Ağacı | *Liriodendron tulipifera* | Lt |
| Küçük Yapraklı Hanımeli | *Lonicera nitida* | Lni |
| Hanımeli | *Lonicera sempervirens* | Ls |
| Manolya | *Magnolia grandiflora* | Mg |
| Tesbih ağacı | *Melia azedarach* | Ma |
| Çınar Yapraklı Dut | *Morus platanifolia* | Mp |
| Ters Dut | *Morus nigra pendula* | Mn |
| Zakkum | *Nerium oleander* | No |
| Pavlonya | *Paulownia tomentosa* | Pt |
| Filbahri | *Philadelphus coronarius* | Pc |
| Alev Ağacı | *Photinia fraseri red robin* | Pf |
| Batı Ladini | *Picea abies* | Pa |
| Doğu Ladini | *Picea orientalis* | Po |
| Mavi Ladin | *Picea pungens* | Pp |
| Karaçam | *Pinus nigra* | Pn |
| Ehrami Karaçam | *Pinus nigra* var. *Pyramidata* | Pni |
| Yıldız Çalısı | *Pittosporum tobira nana* | Pto |
| Londra Çınarı | *Platanus acerifolia* | Pac |
| Doğu Çınarı | *Platanus orientalis* | Por |
| Douglas Göknarı | *Pseudotsuga menziesii* | Pm |
| Pırnal Meşesi | *Quercus ilex* | Qi |
| Top Akasya | *Robinia pseudoacacia umbriculifera* | Rp |
| Salkım Söğüt | *Salix babylonica* | Sb |
| Mamut Ağacı | *Sequoiadendron giganteum* | Sg |
| Japon Soforası | *Sophora japonica* | Sj |
| Keçi Sakalı | *Spiraea bumalda* | Sbu |
| Keçi Sakalı | *Spiraea vanhouttei* | Sv |
| Leylak | *Syringa vulgaris* | Svu |
| Porsuk | *Taxus baccata* | Tb |
| Çit Mazı | *Thuja orientalis* | To |
| Piramit Mazı- Boylu Mazı | *Thuja plicata* | Tp |
| Büyük Yapraklı Ihlamur | *Tilia platyphyllos* | Tpl |
| Gümüşi Ihlamur | *Tilia tomentosa* | Tt |
| Palmiye | *Trachycarpus fortunei* | Tf |
| Yıldız Çiçekli Yasemin | *Trachelospermum jasminoides* | Tj |
| Kartopu | *Viburnum opulus* | Vo |
| Kartopu | *Viburnum tinus* | Vt |

According to Table 1; 83 different arboreal taxa were used in the landscape design works in the urban open-green areas of Malatya between the years 2011-2014.

A total of 83 species were used in the landscaping works in the city center of Malatya between the years 2011-2014 in terms of purchase and planting activities. While the number of plant species planted in 2011 during this period was 12, this value shows an upward trends with 33 in 2012, 39 in 2013, and 40 in 2014. In addition, when plant pruchases for the specified period are studied, the number of species purchased was found to be 4 in 2011, 6 in 2012 and 54 in 2013 and 9 in 2014.

If we classify the plant taxa used in landscaping works in section; it is understood that 25 of the species belong to gymnospermae section, while 58 to angiospermae species. The section-besed distributions of the species used in Figure 1 are given in percentage.

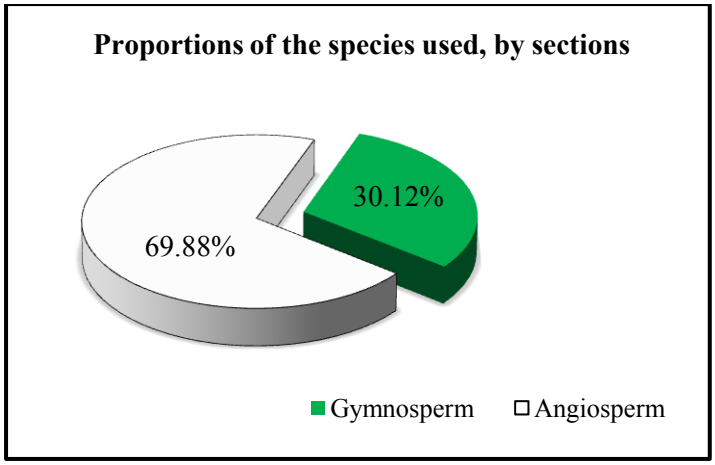


*Figure 1. The sectional distribution of the species used in landscaping work in Malatya city center.*

It was determined, when classified according to their forms; 46 of the the species used in landscaping work carried out in Malatya city center were in the form of tree, while 37 of them were arboreal taxa in shrub or creeping forms. The distribution of the species shown in Figure 2 according to their forms is given by percentage.

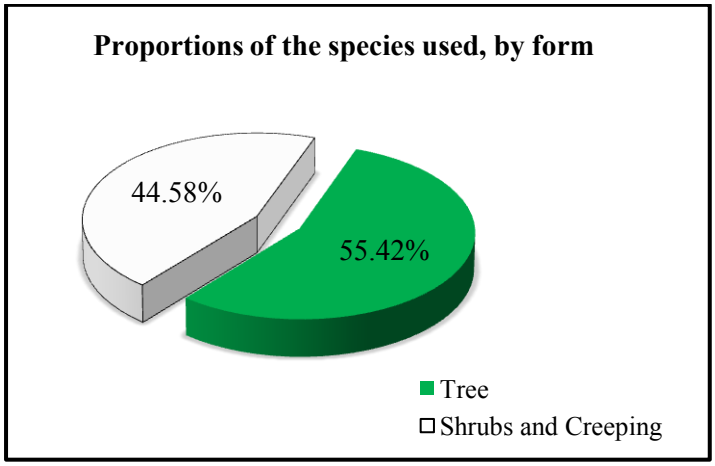


*Figure 2. The distribution of the species used in landscaping work in Malatya city center according to their forms.*

In Figure 3a, b, c and d; photographs of plant material used in the landscaping work of various types of open-green areas in Malatya city are presented.

3a. Akpınar Square - *Albizzia julibrissin*

3b. Sümer Park - *Nerium oleander*

3c. Ring Road Pavement – *Morus platanifolia*

3d. Sümer Park – *Cedrus libani*

Within the scope of this study, in which the progressive use and demand of the arboreal plant material used in landscaping works in open-green areas in the city center of Malatya province were evaluated in terms of section, form and species; a total of 83 species, as gymnosperm and angiosperm, were determined to be in tree and shrub-creeping form.

In the study of Yilmaz and İrmak (2004), to determine the plant species used in the open-green areas of the Province of Erzurum, which is located in the same geographical region as Malatya, 60 species of plants, used for different purposes, were identified. It was reported by the researchers that only ten of these species are commonly used in open-green areas [2].

In the study of Acar and Sari (2010), which was conducted in Trabzon, located in the Black Sea Region in Turkey and having different climatic characteristics from those of Malatya, a total of 232 distinct plant taxa were identified in residential gardens in the city [13].

In a survey conducted by Aslan et al. (2013), aimed to determine the outdoor plant preferences of Malatya people, a total of 83 plant species were determined to exist in the gardens of the respondents in the survey [14].

## 4. CONCLUSIONS

With its growing population, the city of Malatya is faced with a rapid restructuring process. One of the most important parallels for an upgraded quality of urban life in this fast growth process is the presence of active green spaces in the city. According to Welch (1994) Atik et al. (2013) and Aslan et al. (2013); the socio-economical and geographic structure of a city, and the preferences of city administration in area using are the most important factors on plant species diversity [14-16]. In the city of Malatya, the severe and drought summer period due to its continental climate, high temperature differences between

day and night and especially the danger of frost emerge as the factors limiting plant species diversity. Therefore, ecological requirements of the species to be used in the selection of species in the region should be examined in detail, and adaptation success of the species used in similar climatic conditions should be investigated in the city. ıt is recommended that the local government cooperate with the universities and research institutes in the region on these issues. Within the scope of this cooperation, adatability of these species should be determined by experimenting on the species thought to be purchased domestically or imported from other countries in order to increase the plant biodiversity in the region.

In addition to this, the region houses 206 endemic species according to 30 families, and is noted for its high level of endemism [17]. Therefore, it is recommended that native species grown in the region and in particular endemic species be primarily given special attention in the selection of plant material to be used in urban open-green spaces.

## REFERENCES

[1] S. Ürgenç, *G l Pl v Ağ çl T k ğ* . İstanbul Üniversitesi Yayınları, No. 3644, İstanbul, Turkey.
[2] H. Yılmaz and M. A. Irmak, "Erzurum Kenti Açık-Yeşil Alanlarında Kullanılan Bitki Materyalinin Değerlendirilmesi," *Ekoloji*, vol. 13, no. 52, pp. 9-16, 2004.
[3] Z. Davies, J. Edmondson, A. Heinemeyer, J. Leake and K. Gaston, "Mapping an urban ecosystem service: Quantifying above-ground carbon storage at a city-wide scale," *Journal of Applied Ecology*, vol. 48, no. 5, pp. 1125-1134, 2011.
[4] E. Paoletti, T. Bardelli, G. Giovannini and L. Pecchioli, "Air quality impact of an urban park over time," *Procedia Environmental Sciences*, vol. 2011, no. 4, pp. 10-16, 2011.
[5] A. Gidlof-Gunnarsson and E. Ohrstrom, "Noise and well-being in urban residential environments: The potential role of perceived availability to nearby green areas," *Landscape and Urban Planning*, vol. 83, pp. 115-126, 2007.
[6] FAO, "Global Forest Resources Assessment 2010," Main Report. Food and Agriculture Organization of the United Nations, 378 pp., Rome, Italy, 2010.
[7] A. Atik, F. Aslan and S. Allahverdi, "*Forest Assets throughout the World and Turkey*. Environment and Ecology at the Beginning of the 21st Century, St. Kliment Ohridski University Press Sofia, ISBN: 978-954-07-4001-0, Chapter 41, pp. 559-571, 2015.
[8] S. Erik and B. Tarıkahya, "Türkiye florası üzerine," *Kebikeç*, vol. 17, pp. 139-163, 2004.
[9] M. Avcı, "Diversity and endemism in Turkey's Vegetation," *C ğ* , vol. 13, pp. 27-55, 2005.
[10] (2015). Malatya. Available: http://www.on5yirmi5.com/
[11] (2015) The "Turkish State Meteorological Service" website. [Online]. Available: http://www.meteor.gov.tr/
[12] (2015) The "Turkish Statistical Institute" website. [Online]. Available: http://www.turkstat.gov.tr/
[13] C. Acar and D. Sarı, "Evaluation of Plant Species in Urban Residential Landscapes Based on Their Characteristics for Landscape Preferences; A Sample of Trabzon City," *Ekoloji*, vol. 19, no. 74, pp. 173-180, 2010.
[14] F. Aslan, L. G Kaya, B. Yılmaz and A. Atik, "A research on determination of outdoor plants preference of the Malatya urban community," *E-Journal of New World Sciences Academy-Social Sciences*, vol. 8, no. 1, pp. 33-49, 2013.
[15] J. M. Welch, "Street and trees of Boston: a comparison of urban forest structure," *Landscape and Urban Planning*, vol. 29, pp. 131-143, 1994.
[16] A. Atik, F. Aslan and B. Yılmaz, "Some demographic characteristics and their relationship with out door plant material: a case study from Malatya City, Turkey," *Comprehensive Research Journal of Agricultural Science*, vol. 1, pp. 20-25, 2013.
[17] (2015) "Turkish Plants Data Service" website. [Online]. Available: http://www.tubives.com/

# Determining the Relation between Lighting and Park Security with the Help of Logistic Regression Analysis

*Atilla Atik*[1], Fürüzan Aslan[1], Bülent Yılmaz[1]*

[*]: *Corresponding Author: atikatilla@hotmail.com*
[1]: *Inonu University Faculty of Fine Arts and Design Department of Landscape Architecture, 44280, Malatya-Turkey.*

## Abstract

*The purpose of this study is determining the relation between the lighting and park security in parks, which are one of the most important elements of urban open green area systems. In the scope of the study, a questionnaire has been prepared and applied to determine the viewpoints of the users on security and lighting in Abdullah Gul Park, which is one of the biggest and the most developed parks in the city center of Malatya in Turkey. The logistic regression method has been used to determine the relation between the lighting and park security. According to the logistic regression model, which has been established with the data obtained in the questionnaire study, the effects of the lighting on the viewpoints of the users on park security is 61.8%.*

**Keywords:** Lightning, Security, Urban park, Malatya.

## 1. INTRODUCTION

Safe life, which is one of the basic needs of human beings, is not limited by the planning of the areas in a city, but is related with the planning of the safe areas to live in. Insufficient lighting cause the people living in the area feel unsafe in urban areas during nights [1].

According to the data provided by FAO for the year 2015, around 54% of the 7.3 billion world's population live in urban areas [2]. Urban areas may be converted into total criminal areas due to insufficient lighting during nights. Designing safe urban areas is extremely important in decreasing the fear created by the crime that develop due to the physical and social structure of the city [1].

Urban open green areas are defined as the areas that response to the recreational needs of the people in terms of the leisure times spent on the general activities except for accommodation and working [3]. Parks, natural or artificial woods around the city, orchards, trees in streets and squares, road slope and median trees, cemeteries, house gardens, school gardens, green roofs, the hardens of the private or public work places, and sports complexes may also be included in this definition [4].

Parks, which are among the most important elements of active urban green area systems, are used not only during daytime but also at nights. The sustaining of the contribution of the parks to the needs and urban life quality of the human beings during daytime depends on lighting in parks at nights. Today, the importance of outdoor areas increase with each day. People living in houses and similar places may use the gardens during daytime and may also use them during nights with the same comfort and security. Moreover, lighting is provided in parks, streets and sports areas at nights to provide different usage areas for people [5].

Lighting is the basic conditions for parks to be used at nights. The use parks as passage, trip, game and making use of several opportunities by the city people is only possible with a lighting. Security appears as an important problems before us in parks where there are no lighting systems or the lighting system is insufficient.

A questionnaire has been performed in the scope of this study in Abdullah Gul Park in Malatya city center. With this questionnaire, the relation between the park security and the lighting system has been determined by using the regression analysis.

## 2. MATERIALS AND METHODS

In determining the sampling volume, the rate approach determined with the help of Formula 1 has been made use of [6].

$$n = \frac{Np(1-p)}{(N-1)\sigma_{px}^2 + p(1-p)} \quad (1)$$

In the Formula; n is the size of the sampling; N is the size of the universe; $\sigma_{px}^2$ is the variance[11]; p is the rate of the handicapped users visiting Abdullah Gul Park[12] [6, 7].

Questionnaire forms were completed using face to face method in all neighbourhoods of the city in order to include almost all the views from all parts of the city. According to Addresses Based Population Recording System of Turkish Statistics Institution (TSI), population of the city is 769 544 in 2014. The total population of the city center of Malatya, which is divided into two districts as Battalgazi and Yeşilyurt Municipalities, for the year 2014 is 583579 people [8]. When considered this value, sample size was calculated in 10% error and 90% confidential interval to be 96 people minimum.

The questionnaire consisted of 9 questions, and the first 6 questions were intended to determine the socio-demographic properties of the participants the remaining 3 questions consisted of 1 dependent and 2 independent variables, and were intended to determine the relation between the park security and the lighting.

The Regression Analysis Method, in which the relations that are valid for the subject are investigated, requires that the data are in accordance with the true nature of the data. Although the analysis methods that may be used in situations where the dependent variable could be double (0, 1) are limited in number, the most frequently used ones are the Logistic Regression (=LR), Logit, Probit and Linear Probability Models [9].

Logistic Regression is a method used as an alternative to Linear Regression Analysis due to the disruption of the normality assumption in case there is two-class or multiple-class discrete variables. The assumption being not limited, the ease in the use, the model obtained with the analysis being very flexible, and being easily interpreted increased the interest in the method [10, 11].

## 3. RESULT AND DISCUSSION

With the evaluation of the questionnaire forms, the question "*Do you feel yourself safe at nights in Abdullah Gul park?*", which is the dependent variable in the model, was answered by the participants, and when the answers are examined it has been determined that 68.8% of the participants said "No", and 31.2% said "Yes". In this context, the majority of the people of the city stated that they did not feel themselves safe in Abdullah Gul Park at nights.

The statement "*I find the night lighting in Abdullah Gul Park sufficient*" is the independent variable that is influential on the viewpoints of the participants on the security of the park. 26.0% of the participants stated that they definitely did not agree to this statement; 30.2% of them stated that they did not agree with it; 28.1% stated that they agreed; and 12.5% stated that they had neutral opinions on the issue. In this context, the majority of the people in the city find the lighting in Abdullah Gul Park insufficient.

In order to determine the relation between the lighting and security, the summary of the data in the two-variable logistics regression model is given in Table 1. According to the R square value in Table 1 (0.618), the lighting has had an influence on the viewpoints of the participants on the security of the park was 61.8%.

*Table 1. Model summary.*

| Step | -2 Log likelihood | Cox & Snell R Square | Nagelkerke R Square |
|---|---|---|---|
| 1 | 63.614[a] | 0.440 | 0.618 |

a. Estimation terminated at iteration number 20 because maximum iterations has been reached. Final solution cannot be found.

The classification table in which the specifity and sensitivity values of the model were obtained is given in Chart 2. In this context, our model estimated 54 people out of 66 people who did not feel themselves safe in Abdullah Gul Park in an accurate way (*specifity 81.8%*), and estimated 27 out of 30 people who did feel themselves safe (*sensitivity 90.4%*). In this context, the general estimation rate of the model is 84.4%.

*Table 2. Classification Table[a]*

| | | | Predicted | | |
|---|---|---|---|---|---|
| | | | *Do you feel yourself safe at nights in Abdullah Gul park?* | | Percentage |
| | Observed | | No | Yes | Correct |
| Step 1 | *Do you feel yourself safe at nights in Abdullah Gul park?* | No | 54 | 12 | 81.8 |
| | | Yes | 3 | 27 | 90.0 |

[11] In order to determine the highest sampling volume; [1]This value has been taken as 1.645 $_{Sp}^2$=0.05.

[12] *To conduct research with a large population, the p = 0.5 value was accepted for p (1-p) to be the largest value.*

| | |
|---|---|
| Overall Percentage | **84.4** |

[a.] The cut value is 0.500

The history of the city that reflects the cultural heritage, modern buildings and artistic values are visible with all their glory during daytime. These values define the culture and civilization level of the people living in the city and leave the city deprived of the beauties when darkness falls in. for this reason, the symbolic urban values that define the character of the city must be lit to increase the time in which people can see them [12].

Yılmaz et al. (2014) conducted a study in Antalya, Turkey, and reported that the lighting elements in a park existing at a sufficient level in terms of their lighting level and number could change the perceptions of people on the park. This situation influences the usage density of the park directly. Again, he stated that according to the data obtained in the study, lighting was directly related with security [13].

According to Arifoğlu and Sözen (2000), lighting parks for security reasons is not sufficient. The design of the lighting must be conducted by considering the amusing and relaxing elements to attract attention [14].

## 4. CONCLUSIONS

The city of Malatya has a profile that shows that it is growing in a fast pace in terms of population and constructions. One of the most important elements in the life quality of a city is security. The fact that people feel safer in well-lit areas during nights in open areas has been revealed in many studies. However, according to the data obtained from this study, it has been determined upon the user evaluations that the lighting in Abdullah Gul Park, which is the most developed park of the city with its area and opportunities, is not sufficient. Another situation which depends on this finding and which has been proven to have an association with this situation in statistical terms is the fact that people do not feel safe in Abdullah Gul Park. According to these results, the lighting systems in Abdullah Gul Park and in all of the other parks in the city must be reviewed by the Parks and Gardens Management of the Metropolitan Municipality, which is responsible for the maintenance and running of the parks in the city. First of all, it is recommended that the faults and missing points that stem from the lighting systems of the parks are projected again. In addition, the failures and breakdowns in the present lighting system must be determined and repaired. All of these procedures and operations must be repeated in a systematic manner with regular intervals.

## REFERENCES

[1] E. Ataç, "Kent, Güvenlik ve Güvenli Kent Planlaması; Bursa Örneği," Master of Science Thesis, Gazi Üniversitesi, Fen Bilimleri Enstitüsü, Şehir ve Bölge Planlama Anabilim Dalı, Ankara, Turkey, 2008.
[2] (2015) "FAO, United Nations, Department of Economic and Social Affairs, Population Division" website. [Online]. Available: http://www.fao.org/
[3] M. Dil, "İstanbul'un yeşil alan sisteminin, planlama kriterleri açısından irdelenmesi," Master of Science Thesis, İstanbul Teknik Üniversitesi, Fen Bilimleri Enstitüsü, İstanbul, Turkey, 2004.
[4] C. Konıjnendıjk, M. Annerstedt, A. B. Nielsen and S. Maruthaveeran, "Benefits of Urban Parks. A Systematic Review," A Report for IFPRA, 2-7, 2013.
[5] N. Çelik ve I. Koç, "Kent İçi Açık ve Yeşil Alanlarda Aydınlatma Elemanlarının İrdelenmesi," Yılsonu Ödevi, Ankara Üniversitesi Ziraat Fakültesi, Ankara, Turkey, 45 p., 1992.
[6] P. Newbold, "*Statistics for Business and Economics*, Prentice-Hall, New Jersey, USA, 1995.
[7] B. Miran, "*Basic statistics*," Aegean University Printing Office, İzmir, 2003.
[8] (2015) The "Turkish Statistical Institute" website. [Online]. Available: http://www.turkstat.gov.tr/
[9] D. N. Gujarati, "*Basic Econometrics*," United States Military Academy, West Point, 1995.
[10] K. Özdemir "*P k P l l İ k l V A l z* ," Kaan Kitabevi, Eskişehir, Turkey, 1999.
[11] M. Cankurt ve B. Miran, "Aydın yöresinde çiftçilerin traktör satın alma eğilimleri üzerine bir araştırma," *Ege Üniversitesi Ziraat Fakültesi Dergisi*, vol. 47, no. 1, pp. 43-51, 2010.
[12] L. D. Öztürk, "*K A l İlk l* ," Yıldız Teknik Üniversitesi Mimarlık Fakültesi Baskı İşliği, İstanbul, Turkey, 112 p., 1992.
[13] T. Yılmaz, F. Şavklı, R. Olgun and E. Özdamarlar, "The effects of lighting on park use preferences," *İ ö ü Ü v S v T* , vol. 4, no. 9, pp. 15-20, 2014.
[14] N. Arifoğlu ve M. S. Sözen "Yaya mekanlarında aydınlatma," *3. Ul l A l K* , pp. 132-138, 2000.

ICENS
INTERNATIONAL CONFERENCE ON ENGINEERING AND NATURAL SCIENCES
24-28 May 2016 /Sarajevo

# Examining the Intracity Parks in Terms of the Existence and Size of Water: The Example of the City of Malatya

***Atilla Atik*[1], Fürüzan Aslan[1], Bülent Yılmaz[1]***

*[*]: Corresponding Author: atikatilla@hotmail.com*
*[1]: Inonu University Faculty of Fine Arts and Design Department of Landscape Architecture, 44280, Malatya-Turkey.*

***Abstract***

*The services and benefits of the open and green areas in cities for the residents of the city have been examined and revealed with a great number of studies conducted by authors from various disciplines. Parks, on the other hand, are accepted as the most important elements of this open and green area systems. Especially in the designs of the parks in hot climate areas the issue of water has a wide area of use. In this study, the existence and size of water element in the 94 parks located in the city of Malatya, which has the half-dry climate type in Thornthwaite Climate Classification, and which is a transitional area between the Eastern Anatolian and Southeastern Anatolian Regions and the contributions of the parks to the city as a surface of water have been examined.*

**Keywords:** Open green area, Urban park, Water, Malatya.

## 1. INTRODUCTION

The density of the buildings increase in almost every city in global scale depending on the density of the human beings. In this process, open green area systems, which are among the important symbols of the urban life quality, increase with each growing day. Urban open green area systems consist of elements of different function, shape and size [1]. According to Konijnendijk et al. (2013) the green areas in cities cover the parks as well as natural or artificial forest areas surrounding the cities, orchards, street trees, and the trees in squares, road slope and refuge, trees, cemeteries, house gardens, school gardens, green roofs, gardens of the work places of the public or private sector, and sports complexes [2].

Urban open green areas are the areas that are planted by local administrations in a way that may cover the recreational needs of people in times other than general activities such as accommodation and working for the purpose of having a trip, fun, bodily activities and leisure activities. These are natural areas used by the people living in it as mutual areas, and which shapes or has to shape an important part of a city. These areas may be in function areas, and the elements from trees to forests and other elements are all included in the definition of green areas [3].

The current regulation related with urban open green area symbols in Turkey is the one that was enacted on 14.11.2015 with the number 29532 in Official Gazette with the title "Regulation on the Changes to be made on the Planned Area Types Building Regulation". The regulation includes the changes made in previous 15 regulations with the dates 02.11.1985 with the number 8916 in Official Gazette with the title "Planned Areas Type Building Regulation", the first one being on 12.08.1987 with the number 19542 released in the Official Gazette. In the 7$^{th}$ Item of the Regulation which has the title of "Urban Area Definitions and Area Use Conditions" and in "Social and Cultural Infrastructure Areas" which is the 2$^{nd}$ Item, these areas are classified under 5 main groups, which are green areas, sports and game areas, socio-cultural facility areas, worshipping places, and cemeteries. The green areas in this classification are defined as "the total of game gardens, children's gardens, recreational areas, travel areas, picnic areas, entertainment areas, recreation areas and coastal areas. The fairs, botanic and animal gardens and regional parks are also included in this classification". These elements are given under 3 titles, which are children's gardens, parks and picnic-recreational areas. The parks, which are covered under the title of "the green areas in the city" in the relevant regulation, are defined as "*The green areas are determined in the construction plan and organized by considering the natural ground or evened soil ground together with forestation and plants with a soil layer with sufficient depth covering the standards; the car parks, pools, open sports and game areas, public toilets so long as the 1$^{st}$ floor does not exceed h=4,50 m and the basement areas does not exceed 0,03 n total; provided that the relevant materials are produced from detachable elements; on which open tea gardens, buffets, pergola, mukhtarship, security hut, sportsmen cabins, taxi stops, transformer and similar establishments may be built; and the areas where the green plant and recreational needs of the residents are covered*" [4].

According to Atik et al. (2014), the benefits of the open green areas in cities for the people living in them have been investigated by a great number of studies [1]. Among these, the study conducted by Annerstedt et al. (2012) and Ward et al. (2012) the open green area systems decrease the stress and psychological disorders of the people living in the cities; Nielsen and Hansen (2007) and Bell et al. (2008) reported that these systems decreased the rate of obesity; Mitchell (2012) reported that these systems increased physical activity; Mitchell and Popham (2008) reported that these systems had effects that could

protect the health system; Maas et al. (2006) and Stigsdotter et al. (2010) reported that they increased the life quality perception of people; Tinsley et al. (2002) and Hung and Cromption (2006) reported that they had direct influences on people in terms of psycho-social effects [5-6].

The hard tissue, which consist of various structures in a city and green areas, and watery areas, which compose the soft tissue define the general characteristics of a city. Today, the qualities and quantities of the green areas in cities are accepted as the indication of the welfare and civilization. In this context, many countries try to plan and organize the urban areas and ecology in a style that is most proper for the mental and physical needs of the people [7].

Konijnendijk et al. (2013) defines the city parks as the areas the majority of which is covered with water and the rest covered with plant, and which are spared for the use of the people of the city as urban open green areas [2]. According to this definition, the natural and/or artificial water surfaces areas in the city parks are the elements of the urban open green area systems. Water joins the atmosphere by vaporizing and increases the relative humidity in the air. The cities and the watery areas around them soften the climate and decrease the difference between the temperature during the night and day. In this context, water has the quality of increasing the microclimatic comfort level of the cities. It is known that especially in hot climates, pools, lakes and similar structures create positive media in the atmosphere [8, 9].

During the history of the mankind, water was important as the source of life in previous periods, and in various periods in residential periods, it has become the indispensable part of life, which is parallel to different developmental levels, different needs [10, 11].

Water is the most important source of all creatures as well as of the mankind, and has been an important element in landscape design from the past until today. Many researchers report that water has the effects of being therapeutic, and relaxing, taking away from stress. Meanwhile, the elements that have water surfaces are used as a flexible material that may be used is parks, gardens etc. that has various sizes; they are the focus of interest even in small-sized usage areas. For this reason, water is defined as the most active and exciting elements in landscape design [12].

Water has a wide area of use in landscape architecture, and is an indispensable elements especially in hot climates. Water may be used as micro-climate agent in all size landscape designs as well as being a sound barrier [13].

Water is generally used as an element that ensures rich design possible in landscape design. In addition, the accessory elements that consist of water and water elements increase the recreational use in places, and make the landscape become more attractive [14]. Especially in a city like Malatya, which has a half-dry and dry climate, water elements make the landscape design become more valuable [15].

In the context of this study, the existence and the size of water elements in the city center of Malatya; and in addition to this, the parks and water surface area rate per capita have been determined.

## 2. MATERIALS AND METHODS

Malatya is located in the Upper Euphrates Basin of the Eastern Anatolia Region of Turkey, and its neighbors are Elazığ and Diyarbakir in the East, Adıyaman in the south, Kahramanmaraş in the west, Sivas and Erzincan in the north. 47% of the city area consist of meadows and ranges, 34% of it consist of agricultural areas [16, 17].

According to Malatya Meteorology Regional Management, whose elevation from the sea level is 950 m and the distance to the city center is 8 km, the annual average temperature is 13.8°C for many years (1954-2013). The highest temperature is recorded in July (27.4°C), and the lowest temperature is recorded as January (0.0°C). The highest temperature average value is 34.0°C (July), and the lowest temperature average value is -2.9°C (January). The number of annual average rainy days is 92, the days with frost is 69, and the annual average rainfalls is 381.7 mm. according to the Thornthwaite Climate Classification, continental climate, which is shown with D,B'2,s,b'2, sub-arid, mesothermal, water excess rate being in winter, vaporization rate in summer season is 58%, dominates the city [18].

According to the Address-Based Population Registry System, the total population of Malatya in 2014 is 769544. The average increase in the population in the city between the years 2007-2014 for 7 years has been 9.2%, and the total increase in the same period has been determined as 48.7‰. Malatya Centrum Municipality became metropolitan municipality in 2012, and the city center was divided into two as Battalgazi and Yeşilyurt Municipality. The total population of these municipalities was 583579 in 2014 [19].

The name list, total area size and address information of the 94 parks located in the city center of Malatya, which is the subject matter of the study, were obtained from the Malatya Metropolitan Municipality, Park and Gardens Management. The list was organized with the data obtained and constitutes the basis of the study. All the parks in the list were marked in the Google Earth Satellite Map and on the construction plan of the city, and the quality and quantity of the watery areas were determined.

## 3. RESULT AND DISCUSSION

The names and the geographical distributions of the 94 parks in the city center are given in Figure 1. According to the data obtained at the end of the study, there are natural or artificial water surfaces only in 19 (%20.21) of the parks in Malatya city center. All of the water surfaces in these parks are in the quality of being artificial and accessory pools. The rest of the parks (75 parks (79.79%) did not have natural or artificial landscape elements for the purpose of forming a water surface (Figure 2).

The names, rates, neighborhoods, surface areas and water surface areas are given in Chart 1. It was determined that only in 15 neighborhoods of the 85 neighborhoods in Malatya Metropolitan Municipality borders had parks with water surfaces, and the remaining 80 neighborhoods did not have artificial or natural water surfaces (Table 1, Figure 3). This means that there are parks with water surfaces in 15,9% of the neighborhoods in Malatya city center. When Table 1 is examined it becomes obvious that the number of the parks with water surfaces is 3 in Hamidiye Neighborhood, 2 in Inönü and Zafer Neighborhoods, and 1 in the remaining 12 parks.

The surface areas of the parks with water surface vary between 350 $m^2$ - 26740.18 $m^2$. The water surface areas in these parks is between 3-300 $m^2$. The biggest park is Hurriyet Park in Zafer Neighborhood (Figure 3); and the smallest one is Kanalboyu I Park in Ucbaglar Neighborhood. When the sizes of the parks are considered, it is observed that the park with the biggest water surface is Kanalboyu I Park, which constitutes the 3.43% of the total park area; and the smallest one is Abdullah Gul Park located in the Inönü Neighborhood, which constitutes the % 0.31 of the total park area (Figure 4) (Chart 1).

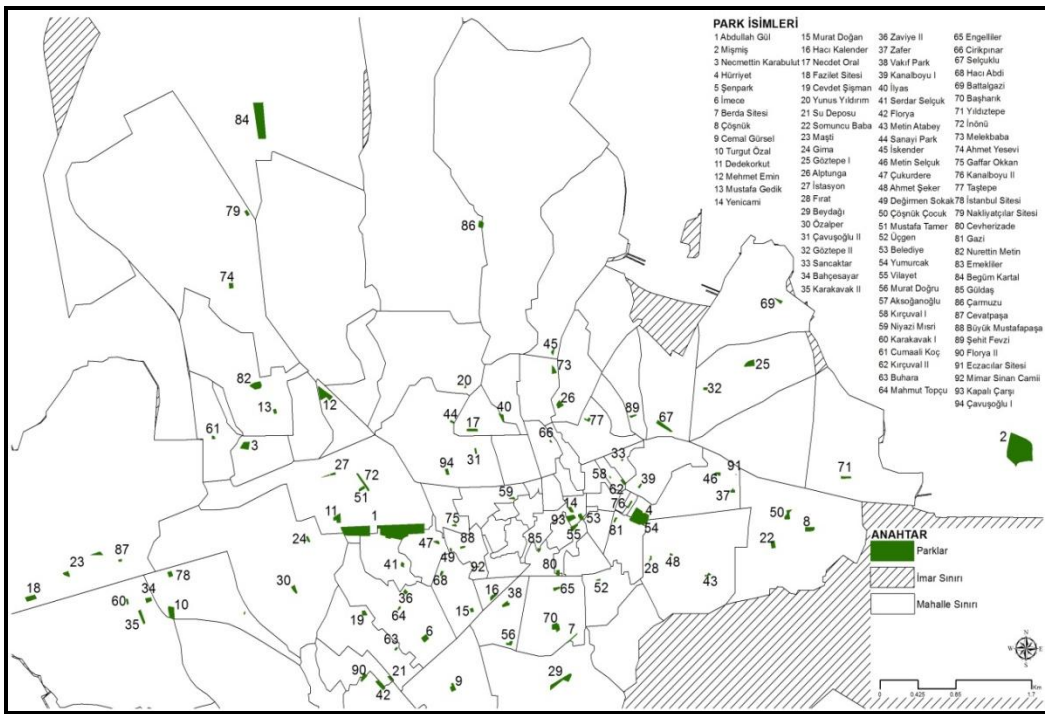


*Figure 1. The Geographical Distribution of the Parks in Malatya.*

*Table 1. The position and area information of the parks with water surface in Malatya city center.*

| Park No | The Name of the Park | Neighborhood | Park General Area ($m^2$) | The Water Surface Area in the Park ($m^2$) | Water Surface Per Area (%) |
|---|---|---|---|---|---|
| 1 | Çöşnük | Çöşnük | 4663.32 | 70 | 1.50 |
| 2 | Mehmet Emin | Fatih | 12636.29 | 100 | 0.79 |
| 3 | Begüm Kartal | Yaka | 10923 | 40 | 0.37 |
| 4 | Hürriyet | Zafer | 26740.18 | 300 | 1.12 |
| 5 | Gima | Özalper | 1550 | 25 | 1.61 |
| 6 | Çavuşoğlu I | Çavuşoğlu | 2290 | 15 | 0.66 |
| 7 | Fazilet Sitesi | Cevatpaşa | 5970.94 | 27 | 0.45 |
| 8 | Nakliyatçılar Sitesi | H. Ahmet Yesevi | 5951 | 27 | 0.45 |
| 9 | Zafer | Zafer | 1840 | 30 | 1.63 |
| 10 | Yenicami | Hamidiye | 1645.82 | 30 | 1.82 |
| 11 | Emekliler | Hamidiye | 2843 | 10 | 0.35 |
| 12 | Gazi | Kernek | 1133.08 | 25 | 2.21 |
| 13 | Kanalboyu II | Küçük Şahinbey | 931.63 | 30 | 3.22 |
| 14 | Kanalboyu I | Üçbağlar | 350 | 12 | 3.43 |

| | | | | | |
|---|---|---|---|---|---|
| 15 | Turgut Özal | Turgut Özal | 5633.81 | 50 | 0.89 |
| 16 | Hacı Kalender | Ataköy | 3010.90 | 75 | 2.49 |
| 17 | Güldaş | Hamidiye | 670 | 3 | 0.45 |
| 18 | Dedekorkut | İnönü | 8452.16 | 75 | 0.89 |
| 19 | Abdullah Gül | İnönü | 97299 | 300 | 0.31 |
| **TOTAL** | | | **194534.13** | **1244** | **0.64** |

Bold lines represent the Neighborhoods which have parks with more than 1 water surface.

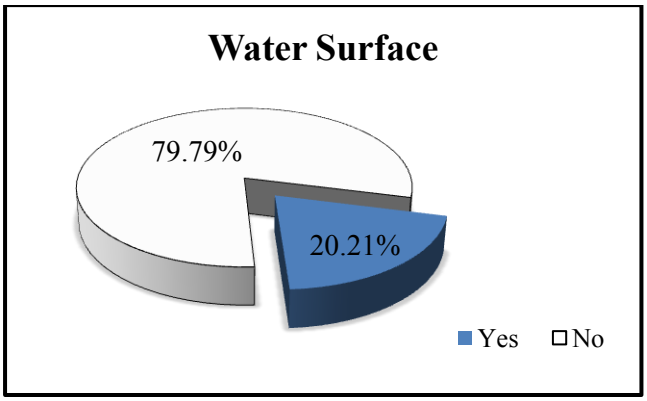


*Figure 2. Water existence of the parks in the city center of Malatya.*

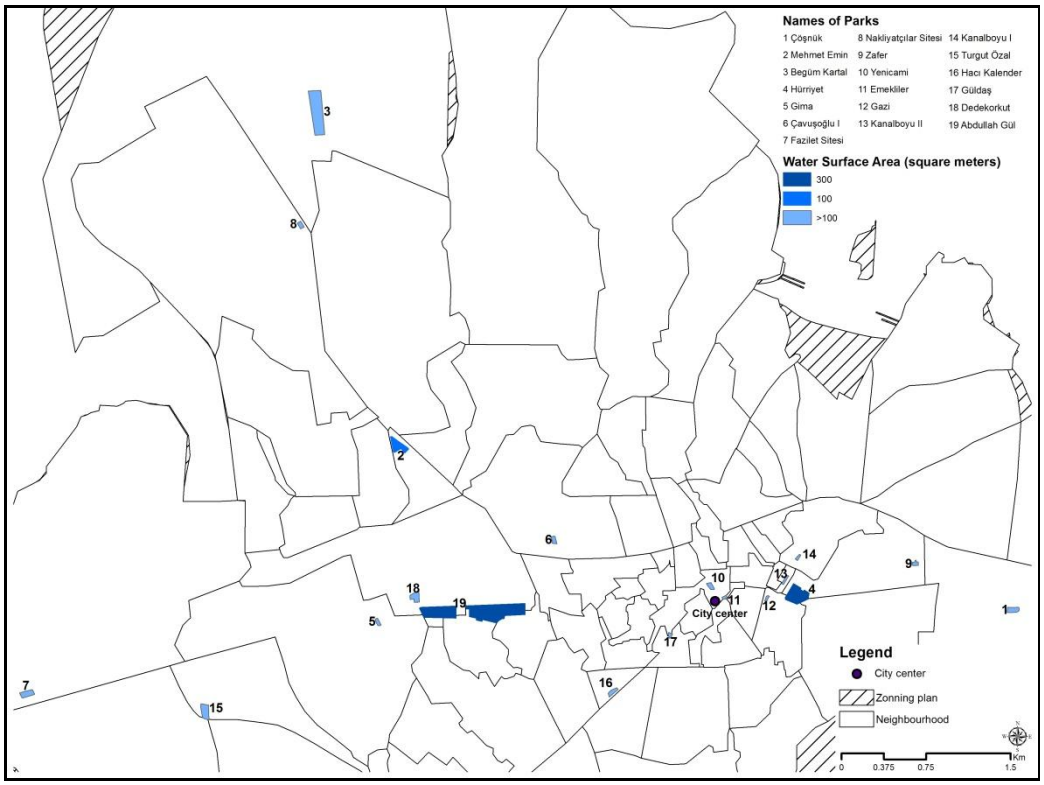


*Figure 3. The distribution of the parks with water surface.*

*Figure 3. Ornamental pool in Hürriyet Park.*

*Figure 4. Ornamental pool in Abdullah Gül Park.*

When Chart 1 is examined it is observed that the total area of the 19 parks with water surfaces is 194531.13 $m^2$, the total water surface area is 1244 $m^2$; and the rate of the water surface area to the general park area is 0.64%.

The existence of water in city parks has important functions in terms of esthetics. Water exists as ornamental pools, various water games and artificial lakes in park designs, and is a dominant and important element in visual quality [20] and has a positive influence in perceiving the landscape as an attractive object [21, 22]. Forming a focal point, recreation, circulation control, audio-visual filtering and cooling are the important factors of water surfaces, and the sound, debit, vision and color of water give calmness and excitement for people [23]. Yılmaz et al. (2013) conducted a study in Akdeniz University Campus on water elements and reported that 73% of the users thought that water elements had a relaxing influence [17].

## 4. CONCLUSIONS

The rate of water existence at a rate of 20% in the parks in the city supports the idea claiming that the landscape designs so far have not cared for water elements. The city center of Malatya is 15 km air distance far from Karakaya Dam Lake, which is located in the Northern/North-Eastern part of the city, 260 km far from the nearest sea, the Mediterranean. When the climate data of the Malatya Meteorology Station are considered, it is observed that the annual precipitation is lower than 400 mm, and there is sub-arid climate in the city according to the Thornthwaite Climate Classification. When the abovementioned climatic and geographical data are considered together, it is observed that the city of Malatya longs for water and humidity both in terms of vision and for climatic reasons. When considered in this aspect, it is recommended that the climate in the city must be cared for and the designs and planning of the parks or various green areas in the city center and water surface areas must be given due importance.

## REFERENCES

[1] A. Atik, B. Yılmaz, E. Taçoral, Ş. İ. Bayazıt and M. Kılıç, *Urban Forests and Their Contributions to Urban Sustainability*. Urban and Urbanization, St. Kliment Ohridski University Press Sofia, ISBN: 978-954-07-3772-0, pp. 134-148, 2014.

[2] C. Konıjnendıjk, M. Annerstedt, A. B. Nielsen and S. Maruthaveeran, "Benefits of Urban Parks. A Systematic Review," A Report for IFPRA, 2-7, 2013.

[3] M. Dil, "İstanbul'un yeşil alan sisteminin, planlama kriterleri açısından irdelenmesi," Master of Science Thesis, İstanbul Teknik Üniversitesi, Fen Bilimleri Enstitüsü, İstanbul, Turkey, 2004.

[4] Anonymous, "Planlı Alanlar Tip İmar Yönetmeliğinde Değişiklik Yapılmasına Dair Yönetmelik," Resmi Gazete, Tarih: 14.11.2015, Sayı: 29532.

[5] M. Annerstedt, P. Ostergren, J. Bjork, P. Grahn, E. Skarback and P. Wahrborg, "Green qualities in the neighbourhood and mental health - results from a longitudinal cohort study in Southern Sweden," *BMC Public Health*, vol. 12, p. 337, 2012.

[6] C. Ward Thompson, J. Roe, P. Aspinall, R. Mitchell, A. Clow and D. Miller, "More green space is linked to less stress in deprived communities: evidence from salivary cortisol patterns," *Landscape and Urban Planning*, vol. 105, no. 3, pp. 221-229, 2012.

[7] A. Gül and V. Küçük, "Kentsel Açık-Yeşil Alanlar ve Isparta Kenti örneğinde İrdelenmesi," Süleyman Demirel Üniversitesi, Orman Fakültesi Dergisi, vol. 2, pp. 27-48, 2001.

[8] A. Zaloğlu, "Ankara kent parklarında suyun gösteri elemanı olarak irdelenmesi," Master of Science Thesis, Ankara Üniversitesi Fen Bilimleri Enstitüsü, Ankara, Turkey, 2006.

[9] T. Yılmaz, B. Zırhlıoğlu and R. Olgun, "Üniversite yerleşke alanlarında su kullanımlarının incelenmesi: Akdeniz Üniversitesi örneği," Inonu University Journal of Art and Design, vol. 3, no. 7, pp. 13-21, 2013.

[10] M. Z. Hattapoğlu, "Su olgusunun yerleşmeler evrimindeki yeri ve günümüzde bir kentsel tasarım elemanı olarak yeniden yorumlanması," Master of Science Thesis, Mimar Sinan Güzel Sanatlar Üniversitesi, Fen Bilimleri Enstitüsü Fakültesi, İstanbul Turkey, 2004.

[11] H. E. Oktay, R. Erdoğan, and F. B. Oktay, " Kent ve su," Inonu University Journal of Art and Design, vol. 5, no. 11, pp. 119-125, 2015.

[12] T. Rees and P. May, *S B hç l T K b* , Yapı Endüstri Merkezi Yayınları, İstanbul, Turkey, p. 144, 2002.

[13] G. Uzun, *Ç v T S K ll* , Çukurova Üniversitesi Ziraat Fakültesi, Adana, Turkey, vol. 179, p. 239, 1997.

[14] J. Ingels, *Landscaping Principles and Practises*, (Seventh Edition). Cengage Learning Products, USA, p. 573, 2009.
[15] F. Aslan and A. Atik, *Qualitative and Quantitative Evaluation of the Parks in Malatya City*. Tourism, Environment and Sustainability, St. Kliment Ohridski University Press, Sofia, Bulgaria, Chapter 3, pp. 35-45, 2015.
[16] Anonymous 2010a, "Kayısı Araştırma Raporu," Fırat Kalkınma Ajansı, Malatya, TR. 63 p.
[17] Anonymous 2010b, "Malatya Provincial Environmental Status Report," Malatya Governorship Provincial Directorate of Environment and Forestry, Malatya, 366 p.
[18] (2015) The "Turkish State Meteorological Service" website. [Online]. Available: http://www.meteor.gov.tr/
[19] (2015) The "Turkish Statistical Institute" website. [Online]. Available: http://www.turkstat.gov.tr/
[20] S. Yamashita, "Perception an devaluation of water in landscape: use of Photo-Projective Method to compare child and adult residents' perceptions of a Japanese river environment," *Landscape and Urban Planning*, vol. 62, pp. 3-17, 2002.
[21] E. L. Shafer, Jr. J. F. Hamilton and E. A. Schmidt, "Natural resources preferences: a predictive model," *J. Leisure Res*., vol. 1 pp. 1-19, 1969.
[22] E. H. Zube, D. G. Pitt, T. W. Anderson, *Perception and Measurement of Scenic Resources on the Southern Connecticut River Valley*. The Institute for Man and Enviroment, University of Massachusetts, Amherst, MA. 1974
[23] N. K. Booth, *Basic elements of landscape architectural design*. New York: Elsevier, 315 p. 1983.

# Comparison of the Oil Agglomeration Results for the Enriched Coals

***Selma Düzyol*[13],**

***Abstract***

*The success of the enrichment process is depended on the several parameters. Many factors are taken into consideration to decide on which method is applied for the beneficiation of any mineral. The particle size of mineral is one of these factors. Dense medium is the most common separation method in order for cleaning of coarse coal. This method is based on the density differences between the coal and inorganic materials. However, dense medium separation for fine particles loses its effectiveness due to the decrease in the gravitational forces on the fine particles. Oil agglomeration is a well-accepted method for the enrichment of fine mineral particles. In this method, the mineral particles which are naturally hydrophobic or rendered hydrophobic by surface active agent together with the oils used and agglomerated. The various parameters such as type and amount of oil, stirring speed, agglomeration time, pH, solid rate etc. influence the success of the process.*

*In this study, the oil agglomeration of enriched coals which had +18 mm and -18+0.5 mm of particle sizes obtained from the Tuncbilek (Kutahya) coal washery plant along with the raw coal sample were investigated and correlated. The agglomeration time, stirring speed and amount of oil were also examined for each sample.*

**Keywords:** *Coal, oil agglomeration, kerosene, combustible recovery*

## 20. INTRODUCTION

Coal which meets the energy need of countries is one of the important basic materials. It can be utilized either as extracted from the mines or after going through a number of coal preparation processes according to the demand. Coal is rarely used as mined off. The coal preparation process based on the increase of coal quality includes size reduction and enrichment of coal via ash rejection. The coal size is a significant factor for determining the enrichment method(s). Most coal beneficiation techniques are established on the differences in the physical properties between the coal and its impurities. The most common application of physical enrichment of coal is gravity method using the difference in the specific gravity and in surface properties of components. A commercial coal processing plant includes sizing and screening, specific gravity-based cleaning and dewatering. The method commonly used in coal preparation plants in Turkey is the heavy medium separation achieved by setting the desired density using magnetite.

While the method developed for fine particles enrichment is flotation, it loses its efficiency for ultra-fine particles. Oil agglomeration is highly effective method for the beneficiation of ultra-fine coal particles. The differences in surface properties of coal and its mineral matter (hydrophobic or hydrophilic) are considered in both flotation and oil agglomeration techniques. Oil agglomeration processes rely on the wettability of the coal particles by bridging agent, such as oils [1-3]. These oil-wetted coal particles are brought together by stirring and the agglomerated forms having larger sizes are obtained. These agglomerates are easily separated from the

inorganic impurities by sieving with a residual of ash. However, the major disadvantage of oil agglomeration is that the large amount of oil is consumed during the process.

In the present paper, different coal samples were selected in order for further understanding of oil agglomeration technique. Enriched coal samples with two different sizes such as coarse (+18 mm) and fine (-18+0.5 mm) and raw coal sample were obtained from the coal washery plant in Tuncbilek (Kutahya). Therefore, the oil agglomeration experiments were performed on these coal samples.

## 21. METARIALS AND METHODS

### *21.1. Coal Samples*

In this study, the coal samples mentioned above were used for experimental works. The cleaned (coarse and fine) and raw coal samples were ground by using steel rod mill under the size of 75 micrometer. After milling, the size distribution of each

[13]*Corresponding author: Selcuk University, Department of Mining Engineering, 42075, Konya, Turkey. selmad@selcuk.edu.tr*

sample was identified by screen analysis and given in Fig. 1. The $d_{80}$ values of samples (80% of the sample falls within) were obtained from Figure 1 and given in Table 1 with the ash contents of samples. As seen from Table 1, the ash contents of enriched coals in two different sizes were varied depending on the enrichment sizes. In other words, the ash content of enriched fine sized coal sample was lower.

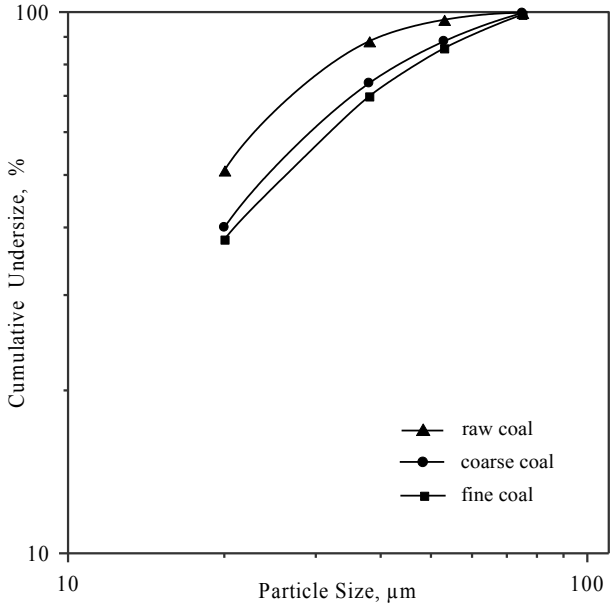


*Figure 3. Particle size distribution of coal samples*

*Table 2. Sample specifications*

| Coal Sample | $d_{80}$ (µm) | Ash (%) |
|---|---|---|
| Raw | 32.5 | 50.5 |
| Coarse | 44 | 17.9 |
| Fine | 48 | 11.4 |

### *21.2. Oil Agglomeration Experiments*

The oil agglomeration experiments were performed in the 400 $cm^3$ volume of cylindrical vessel. Four baffles were attached to the interior surface of vessel in order to increase the collision effect. It is known that the presence of baffles in the agglomeration unit reduces power consumption and assists to produce more turbulence [4,5]. 5 gram samples of coal and 300 $cm^3$ distilled water were used for the preparation of the suspension. Kerosene was added into the solution after the 3 minutes stirring period and the coal agglomerates was separated from the solution by a test sieve (75 µm). The agglomerates were washed by the tap water and dried in an oven at 105º. Finally, the dried agglomerates were weighed and then the ash contents were determined from the ash analysis.

The combustible recovery (CR) which implies the success of the oil agglomeration process was determined by the following equation.

$$CR\% = \frac{M_c(1-A_c)}{M_f(1-A_f)} \quad (1)$$

where $A_c$ is the ash content of agglomerate, $A_f$ is the ash content of feed, $M_c$ is the mass of agglomerated coal and $M_f$ is the mass of feed.

## 22. RESULTS AND DISCUSSIONS

### *22.1. The Effect of Agglomeration Time*

The effect of agglomeration time on the oil agglomeration was investigated and obtained results were given in Fig. 2. The stirring speed and oil amount were kept constant at 1000 rpm and 31.6% (w/w), respectively. For coarse and fine coal, the increasing agglomeration time resulted in the increasing in CR%. Whereas, 5 minutes of agglomeration time could be enough for raw coal, 15 minutes of agglomeration time was almost effective for the coarse coal sample. The ash content of coal

samples did not change much with time. The ash contents were determined between 22-25%, 9-10% and 8% for raw, coarse and for fine coal samples, respectively. In fact, the increase in the agglomeration time enhanced the collision rate between the coal particles and agglomerates [5-9]. Therefore strong agglomerates occurred. As seen from the Fig. 2, the best results were reached for the fine sized coal at 10 minutes of agglomeration time.

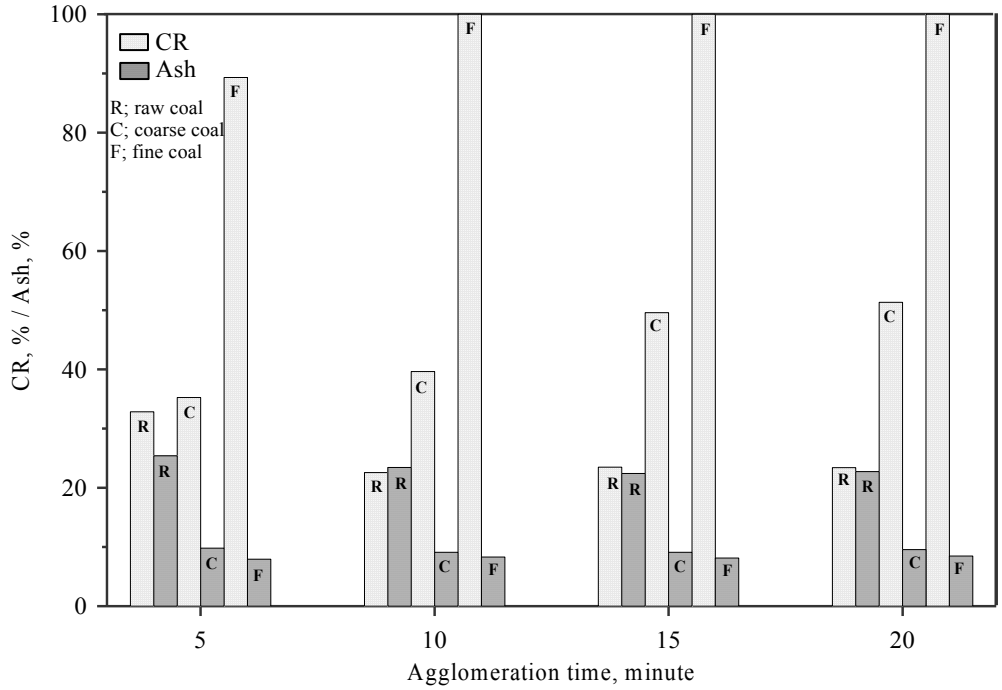


*Figure 2. The effect of agglomeration time on the CR% and ash content of coal samples (conditions; stirring speed:1000 rpm, oil amount: 31.6% (w/w)*

### *22.2. The Effect of Stirring Speed*

The results of oil agglomeration for different stirring speed were given in Fig. 3, comparatively. An increase was onserved in CR% for three samples with the rising of stirring speed. To disperse the bridging oil into small droplets, strong agitation should be required. Therefore, successful agglomeration could be created due to the collision among the oil-coated particles [10,11]. Similar results were reached by the researchers in the literature [9,12-14]. It can be seen from the Fig. 3, the maximum CR% was achieved at 1000 rpm for raw and fine coal and 1500 rpm for coarse coal. It was also concluded that the ash content of samples did not change much.

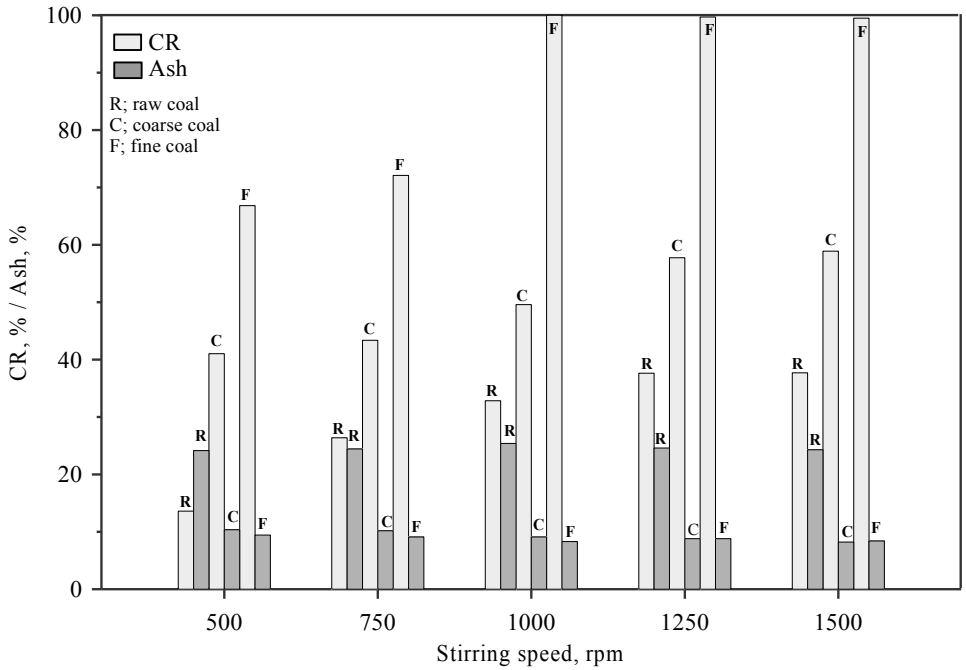

*Figure 3. The effect of stirring speed on the CR% and ash content of coal samples (conditions; oil amount: 31.6% (w/w), agglomeration time: 5 min for raw coal sample, 15 min for coarse coal sample, 10 min for fine coal sample)*

### *22.3. The Effect of Oil Amount*

The effect of oil amount was investigated and obtained results were given in Fig.4. The increase in oil amount enhanced the oil agglomeration of coal samples therefore reached CR% of samples were raised. The ash contents were also decreased with the further addition of oil. Oil amount was strongly affected the agglomerate structure, therefore oil agglomeration behavior especially CR% [15]. Small agglomerates were reached at the low concentrations and the CR% was low due to the weak and small agglomerate structure. The best results were gained at 47.7% of oil amount for raw and coarse coal samples and 31.6% of oil amount for fine coal sample.

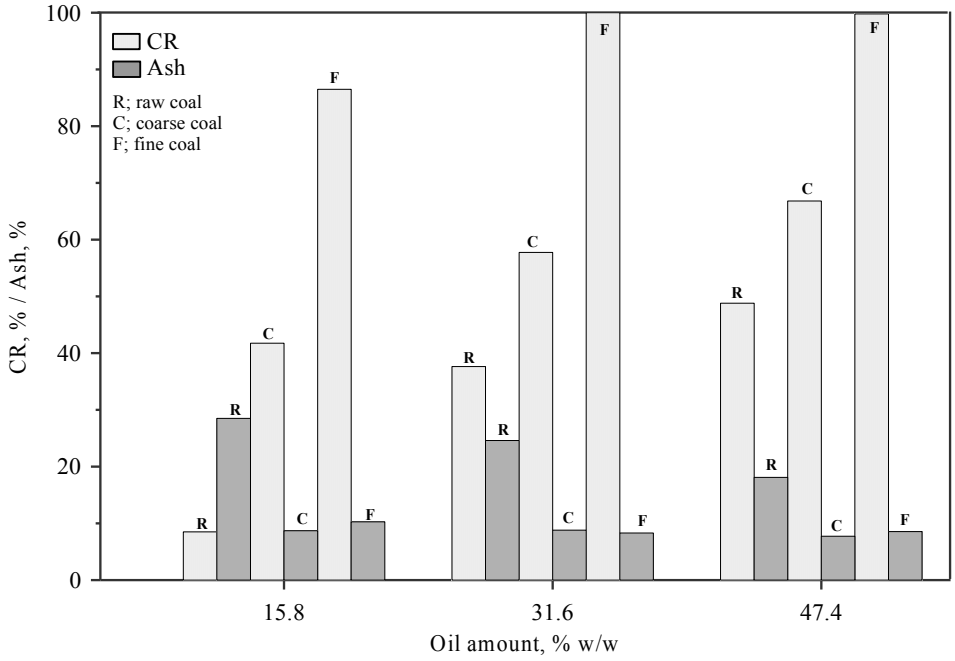


*Figure 4. The effect of oil amount on the CR% and ash content of coal samples (conditions; stirring speed: 1000 rpm for raw and fine coal samples, 1500 min for coarse coal sample)*

## 23. CONCLUSIONS

The oil agglomeration behaviors of enriched coal samples together with raw coal sample were investigated, compared and following conclusions were obtained;

- Whereas the increasing of agglomeration time has a positive effect on the enriched coal samples, it causes a decreases in the CR% for raw coal.
- The CR% of three samples is increased with the rising stirring speed while the ash contents of these samples are decreased.
- The oil amount is strongly enhanced the recovery by the oil agglomeration of samples. The obtained ash contents are 18.1% and 7.7% for raw and coarse coal samples, respectively at 47.4% oil amount and 8.3% for fine coal at 31.6% of oil amount. The CR% values are also determined as to be 48.8% and 66.8% for raw and coarse coals, respectively at 47.4% oil concentration and 100% for fine coal at 31.6% oil concentration.
- The fine coal presents the best oil agglomeration behavior due to the liberalization among the enriched coals. It can be concluded that this liberalization increases the selectivity of coal and mineral matter and therefore the oil agglomeration.

## ACKNOWLEDGMENT

The financial support given by the Scientific Research Project Fund of Selcuk University (project no: 16701175) on the present work is greatly acknowledged.

## REFERENCES

[42]. C. E. Capes and K. Darcovich, “A survey of oil agglomeration in wet fine coal processing”, *Powder Technology*, vol. 40, pp. 43–52, 1984.

[43]. J. S. Laskowski, "Coal flotation and fine coal utilization", *Developments in Mineral Processing*. vol. 14, ed: Elsevier, 2001.
[44]. J. S. Laskowski, "Chapter 12 - Oil assisted fine particle processing", *Developments in Mineral Processing*. vol. 12, J. S. Laskowski and J. Ralston, Eds., ed: Elsevier, pp. 361–394. 1992.
[45]. Z. Yu, "Flocculation, hydrophobic agglomeration and filtration of ultrafine coal", University of British Columbia, 1998.
[46]. S. Duzyol and C. Sensogut, "Investigation of the oil agglomeration of Eskiceltek lignites in Turkey". *Proceedings of 14th International Multidisciplinary Scientific GeoConference & EXPO, SGEM*, vol. 3, pp. 889–896, 2014.
[47]. Y. Cebeci, U. Ulusoy, and S. Simsek, "Investigation of the effect of agglomeration time, pH and various salts on the cleaning of Zonguldak bituminous coal by oil agglomeration", *Fuel*, vol. 81, pp. 1131–1137, 2002.
[48]. E. Sahinoglu and T. Uslu, "Amenability of Muzret bituminous coal to oil agglomeration", *Energy Conversion and Management*, vol. 49, pp. 3684–3690, 2008.
[49]. G. Chary and M. Dastidar, "Optimization of experimental conditions for recovery of coking coal fines by oil agglomeration technique", *Fuel*, vol. 89, pp. 2317–2322, 2010.
[50]. S. Duzyol, "Investigation of oil agglomeration behaviour of Tuncbilek clean coal and separation of artificial mixture of coal–clay by oil agglomeration", *Powder Technology*, vol. 274, pp. 1–4, 2015.
[51]. C. Capes and R. Germain, "Selective oil agglomeration in fine coal beneficiation", *Physical cleaning of coal*, ed: Marcel Dekker New York, pp. 293–351, 1982.
[52]. R. D. Coleman, B. D. Sparks, A. Majid, and F. N. Toll, "Agglomeration-flotation: recovery of hydrophobic components from oil sands fine tailings", *Fuel*, vol. 74, pp. 1156–1161, 1995.
[53]. N. Gence, "Coal recovery from bituminous coal by aggloflotation with petroleum oils", Fuel, vol. 85, pp. 1138–1142, 2006.
[54]. Y. Cebeci and I. Sonmez, "Application of the Box-Wilson experimental design method for the spherical oil agglomeration of coal", *Fuel*, vol. 85, pp. 289–297, 2006.
[55]. N. Aslan and I. Unal, "Multi-response optimization of oil agglomeration with multiple performance characteristics", *Fuel Processing Technology*, vol. 92, pp. 1157–1163, 2011.
[56]. S. Duzyol, C. Sensogut, A.O. Aksu, H.S. Erisir and K. Aspir, "Beneficiation of Tuncbilek lignites by oil agglomeration". *Proceedings of the 19th Coal Congress of Turkey*, pp. 237–244 2014 (in Turkish).

# An İnvestigation Of The Effect Of Zeolite On Physical And Mechanical Properties Of Autoclaved Aerated Concrete

***Osman Ünal[14], Kadir Güçlüer[15]***

***Abstract***

*Autoclaved aerated concrete is the construction material that is contained in lightweight concrete class. Zeolites are raw materials which has a puzzolanic properties. The new generation of building materials production, it is important for scientists working in this field. For this purpose, in this study it is investigated that the effect of zeolite additive in autoclaved aerated concrete pr . Z l w l h . S l 7 b h order the determine for physical and mechanical properties subjected to the bulk density, ultrasound pulse velocity and compressive strength. As a result, compressive strength and bulk density value of samples are same to commercial autoclaved aerated concrete that were observed.*

**Keywords:** Zeolite, Autoclaved Aerated Concrete, Physical and Mechanical Properties

## 24. INTRODUCTION

Nowadays, lightweight concrete (LWC) is widely used in building construction due to its low density, low thermal conductivity, low shrinkage and high heat resistance. There are many advantages in low density, for example reduction of dead load, faster building rate and lower haulage cost. Autoclaved aerated concrete (AAC) is the LWC production by creating gas bubbles in a cement slurry and cured in high-pressure steam curing (autoclaved). Generally, aerated concrete is made from quartz-rich sand, lime, cement and aluminium powder as pore-forming agent [1].

Autoclaved aerated concrete (AAC), from the group of lightweight concretes, is a mixture of quartzite sand and cement, lime and gypsum (calcium sulphate dihydrate) with a trace amount of aluminium powder to bind the material. There is a growing interest in the use of mineral admixtures for cement [2].

Autoclaved aerated concrete (AAC) is a lightweight and highly porous wall material with excellent insulation ability [3]. Autoclaved aerated concrete (AAC) has attracted the attention of the construction industry in view of its low weight, excellent thermal insulation and sound absorption [4].

The uses of waste by-products from various industrial processes as a component of concrete have been investigated prior to this. To increase the range of waste materials reused as raw materials in concrete, and lower production costs, several previous works have investigated the possibility of traditional raw materials replace- ment in AAC by using industrial waste such as efflorescent sand and phosphorescent slag, iron ore

tailings, air-cooled slag, siliceous crushed stone, lead–zinc tailings, coal bot- tom ash, copper tailings and blast furnace slag and calcium fly ash and natural zeolite [5].

Zeolites are found in nature, and the zeolite mineral stilbite was first discovered in 1756 by the Swedish mineralogist A.F. Cronstedy [6]. Zeolites has own low weight, highly porous, firm and solid homogenous structure. Its pozzolanic reactivity, ion make change, adsorption properties preferred in many industrial fields, including the construction industry [7].

İn this study, it is investigated that the effect of zeolite on physical and mechanical properties of autoclaved aerated concrete.

[14] *Afyon Kocatepe University, Department of Civil Engineering, 03200, Afyonkarahisar, Turkey. unal@aku.edu.tr*

[15] *Corresponding author: Afyon Kocatepe University, Department of Civil Engineering, 03200, Afyonkarahisar, Turkey. kgucluer@hotmail.com.tr*

## 25. MATERIAL AND METHOD

The zeolites used in this study has obtained from Manisa-Gördes region in Turkey. İt is physical properties are given Table 1, chemical properties are given Table 2 and particle size of zeolite are given Figure 1. CEM I 42.5 R type cement was used in this study. Physical properties are given Table 1, and chemical properties are given Table 2.

*Table 3. Physical properties of zeolite and cement*

| | Specific Gravity (gr/cm$^3$) | Blaine surface area (cm$^2$/gr) |
|---|---|---|
| **Zeolite** | 1,72 | 2522 |
| **Cement** | 3,10 | 3074 |

*Table 4. Chemical properties of zeolite and cement*

| Component (%) | $SiO_2$ | CaO | $Al_2O_3$ | $Fe_2O_3$ | MgO | $K_2O$ | $Na_2O$ |
|---|---|---|---|---|---|---|---|
| **Zeolite** | 71,9 | 2,0 | 13,2 | 1,4 | 1,1 | 3,5 | 0,3 |
| **Cement** | 19,2 | 62,8 | 3,8 | 4,2 | 3,4 | 0,3 | - |

Particle size distribution of zeolite $d_{10}$=5,054 µm, $d_{50}$=28,240 µm and $d_{90}$=103,200 µm values was measured with Malvern Mastersizer 2000 device to "laser diffraction method''. (Fig 1.)

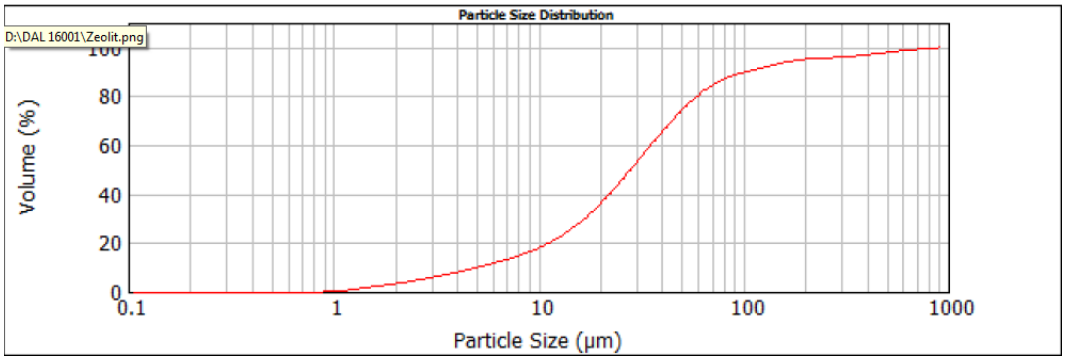


*Figure 4. Particle size diagram of zeolite*

While the mixture is produced, primarily used aggregate, cement and gypsum were subject to the homogeneously dry mixture. After the mixture came to the consistency of the ready state by the addition of lime and aluminum powder mixture was stirred from 1-2 minutes with the help of mixer. Then, the mixture which the prepared mold height 7 cm sides cube molds into 2/3 is placed at the level of fill. Then the samples were allowed to cure in an oven at 75 $^0$C (Fig 2). Samples removed from the mold was subjected to curing for 8 hours at 172 $^0$C temperature and 8 bar of steam pressure in autoclave for determining of physical and mechanical properties.

*Figure 2. samples were allowed to cure in an oven*

## 26. FINDINGS

### *26.1. Bulk Density Findings*

Bulk density of the samples is calculated with the formula (1) and bulk density values are given in Figure 3.

$$\Delta = \frac{W}{V} \quad (gr/cm^3) \quad (1)$$

**Δ:** Bulk density ($gr/cm^3$) **W:** Oven dry weigth (gr) **V:** Volume of sample ($cm^3$)

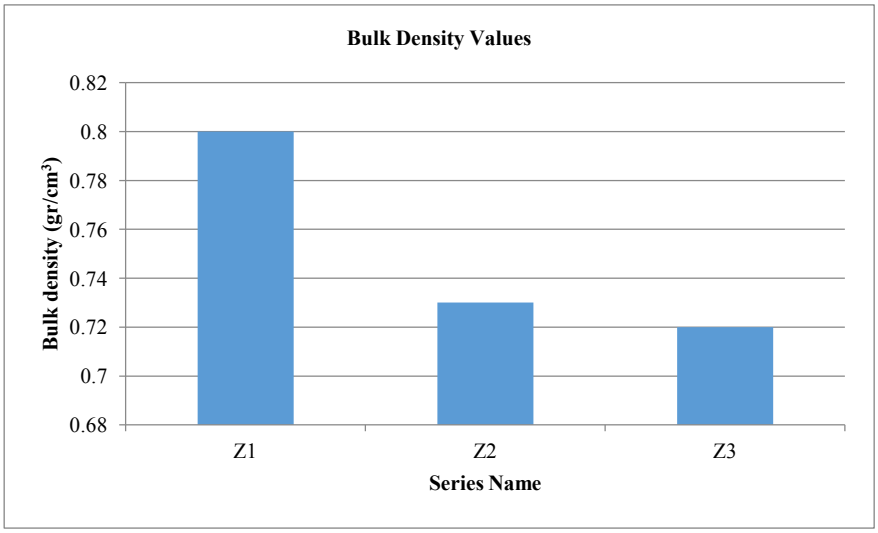


*Figure 3. Bulk density values of series*

Bulk density values of series range from 0.8 $gr/cm^3$ to 0.72 $gr/cm^3$. With the fall of the cement dosage in the series, the bulk density values also decreases. Bulk density values of the samples are similar to commercial aerated concrete examples, they are floating in the water situation (Fig 4).

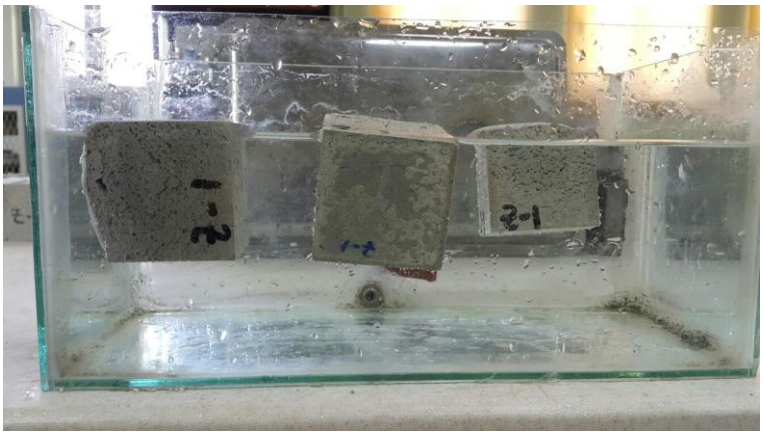

*Figure 4. Samples of water floating state*

### *26.2. Compressive Strength Findings*

Compressive strength values of experiment samples is calculated with formula (2). İn this place $f_c$ is the compressive strength value (MPa), P is the load (Newton) and the A is the surface area($mm^2$). Compressive strength values of samples are given Figure 5.

$$f_c = \frac{P}{A} \quad (2)$$

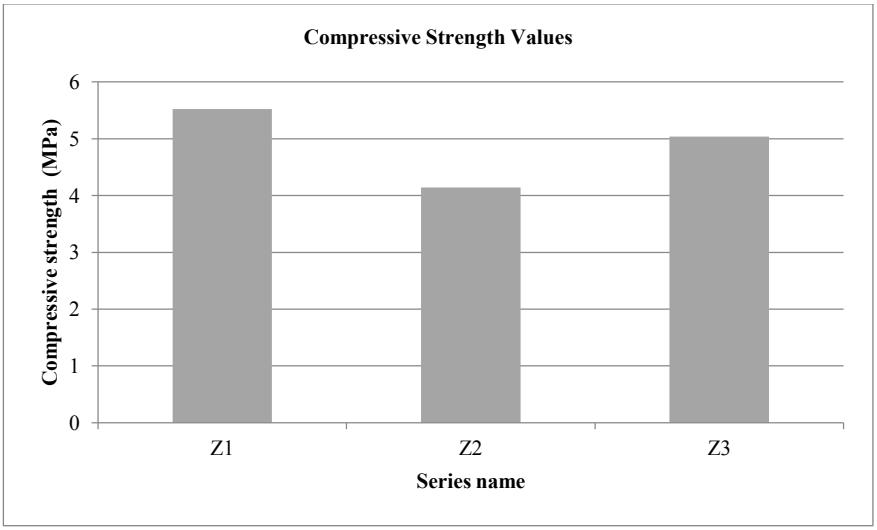


*Figure 5. Compressive strength values of series*

Compressive strength values of series range from 5.52 MPa to 4.14 MPa. In the series, compressive strength values decreases with the decline of cement dosage were observed.

The intended use of the zeolite in this study, to observe the formation of the Tobermorite and CSH ($CaO\text{-}SiO_2\text{-}H_2O$) phase in the autoclave at high temperature and steam pressure. According to the XRD results (Fig 6), under the 172 $^0$C and 8 bar steam pressure, has been observed that the development of the CSH structure in the microstructure of material. Tobermorite plate started the development has been observed when examine the SEM analyzed(Fig 7).

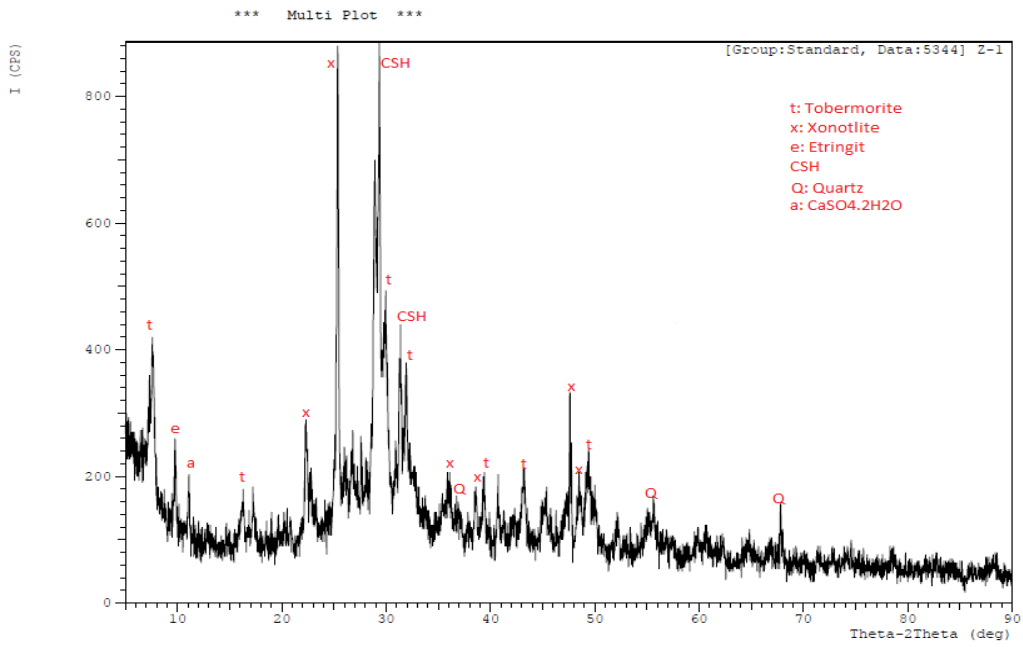


*Figure 6. XRD patterns of Z1 series*

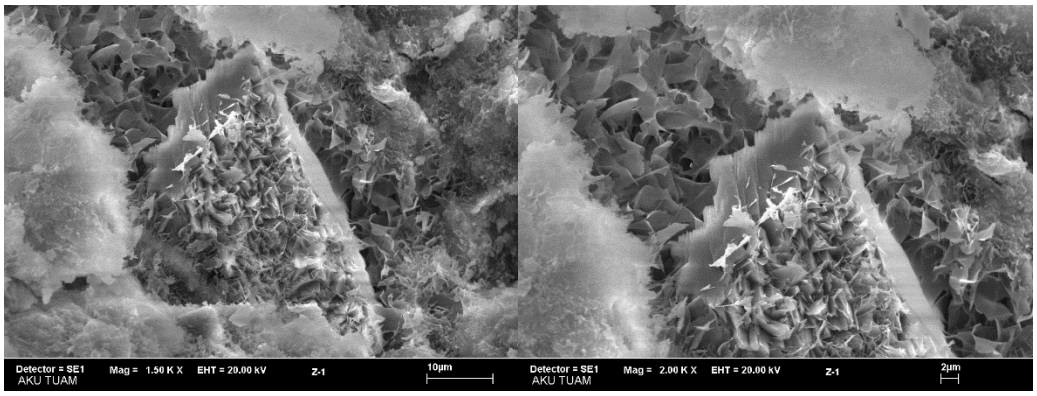


*Figure 7. SEM figures of Z1 series*

## 27. RESULTS AND DISCUSSION

This study is used as a raw material of the zeolite, bulk density and compressive strength values it reached similar conclusion commercial autoclaved aerated concrete.

Tobermorite plates found in microstructure study shows positive results on the pozzolanic activity of the zeolite. The development of the tobermorite plates will be more intense when working at higher temperatures and steam pressure.

Conservation of raw materials and the application of different production methods in construction material studies will be more useful in terms of our science world.

## ACKNOWLEDGMENT

The authors thanks to Afyon Kocatepe University BAPK department for support this study with the number of 15. FEN BİL.21 project.

## REFERENCES

[57]. Kurama H., Topçu İ., B., Karakurt C. (2009). *Propeties of The Autoclaved Aerated Concrete Produced From Coal Bottom Ash*. Journal of Material Processing Technology, 209**:** 767-773.

*[58].* Owsiak, Z., Soltys, A., Sztaboroski, P., Mazur, M., *Properties of autoclaved aerated concrete with halloysite under industrial conditions*, Procedia Engineering 108 ( 2015 ) 214 – 219.

[59]. Huang, X., Ni, W., Cui, W., Wang, Z., Zhu, L. Preparation of autoclaved aerated concrete using copper tailings and blast furnace slag. Construction and Building Materials 27 (2012) 1–5.

[60]. Song, Y., Guo, C., Qian, J., Ding, T. *Effect of the Ca-to-Si ratio on the properties of autoclaved aerated concrete containing coal fly ash from circulating fluidized bed combustion boiler*. Construction and Building Materials 83 (2015) 136–142
[61]. Thongta, A., Maneewan, S., Punlek, C., Ungkoon, Y., Investigation of the compressive strength, timelag sand decrement factors ofAAC-lightweight concrete containing sugar sediment waste" Energy andBuildings84(2014)516–525.
[62]. Auerbach S., Carrado K., Dutta P., 2003. ''Handbook of Zeolite Scıence and Technology''.Marcel Dekker Inc., New York 12701, U.S.A.
*[63]*. Kibaroglu,U.,(2015).*http://www.oocities.org/kibaroglu/calismalar/zeolit.htm*

# Numerical Analysis of $SiO_2$/Water Nanofluid Flow over Backward Facing Step

*Recep Ekiciler [16], Kamil Arslan[17]*

***Abstract***

*Two-dimensional numerical simulation of steady state laminar forced convection flow and heat transfer in a duct having backward facing step (BFS), using $SiO_2$/water nanofluid is presented in detail. This study was conducted for effects of nanoparticle volume fraction on flow and heat transfer characteristics. The Reynolds number was ranged from 75 to 225. Both of the step and inlet heights of the duct were 4.8 mm. As the downstream wall was subjected to constant and uniform heat flux of 2000 W/m$^2$, the other walls were insulated. The nanoparticle volume fraction was varied from 1.0% to 4.0%. The average and local values of Nusselt number and Darcy friction factor were obtained for each nanoparticle volume fractions. Velocity and temperature profiles were analyzed. It is found from the results of numerical simulation that the Nusselt number increases with increasing the nanoparticle volume fraction; however, there is no change on Darcy friction factor.*

**Keywords: Backward facing step, Forced convection, Heat transfer, Laminar flow, $SiO_2$/water nanofluid.**

## 28. INTRODUCTION

The phenomena of flow separation and subsequent reattachment which occur due to a sudden expansion in flow passages such as backward facing steps have been recognized as important industrial situations. This complex flow structure present in heating or cooling applications such as cooling electronic equipment, cooling turbines blades, combustion chambers, chemical processes, cooling of nuclear reactors, wide angle diffusers, high performance heat exchangers, energy systems equipment, and flow in valves [1].

The phenomena of flow separation and reattachment caused by sudden changes in geometries is very popular in engineering applications. There are many publications about the flow over backward facing step to understand flow characteristics of geometry. Goldstein et al. [2] conducted an experimental study to investigate the reattachment point under laminar and subsonic flow conditions over a step. They noticed that the reattachment point and boundary displacement thickness change with Reynolds number. Denham and Patrick [3] investigated 2D laminar flow over the BFS. Water is used for working fluid. The channel's expansion ratio and aspect ratio is equal to 3 and 20, respectively. The Reynolds number was changed between 50-250. They observed that the flow characteristics of BFS resemble to other 2D geometries having sudden expansion. Yet both recirculation length and mass flow rate circulating were smaller. At Re=229, they noticed a fluctuation, which shows the beginning of transition to turbulent separated boundary layer. Armaly et al. [4] studied the effect of Reynolds number on velocity distributions and length of reattachment. The work was numerically done as two-dimensional under laminar, transitional and turbulent flow conditions. Air was flowed in the channel has aspect ratio of AR=36. They observed that length of reattachment strongly depended on Reynolds number. Reattachment length increases to Re=1200 and then occurs velocity fluctuations. At higher Reynolds

[16] *Corresponding author: Karabuk University, Mechanical Engineering Department, 78050, Karabuk, Turkey.* recepekiciler@karabuk.edu.tr
[17] *Karabuk University, Mechanical Engineering Department, 78050, Karabuk, Turkey.* kamilarslan@karabuk.edu.tr

numbers 3D effects was dominant near the sidewalls. Numerical predictions were compared with the experimental results. They realized that numerical and experimental results were in good agreement. Chen et al. [5] investigated the influence of the step height on flow and heat transfer characteristics in 2D BFS channel under turbulent forced convection flow conditions. The Reynolds number was 28000. Uniform and constant heat flux ( $q''_w$ =270 W/m$^2$) was exposed to the stepped wall downstream from the step and the other walls were kept at adiabatic. Step heights were 0.019, 0.038 and 0.076 m. They observed that bulk temperature, maximum turbulent kinetic energy, primary and secondary recirculation regions increase while the step height increases. Mahdi et al. [6] studied to explore heat transfer mechanism and flow behavior due to expansion ratio and Reynolds number over 2D BFS. The study was done on laminar incompressible flow conditions. They found that separation zone size and reattachment length increases with increasing expansion ratio and Reynolds number. As long as Reynolds number increases, Nusselt number increases, too.

Recently, nanofluids have been used for enhancing heat transfer. Nanofluids are novel heat transfer fluids having nanoparticles whose sizes change from 1 nm to 100 nm suspended base fluids. The first scientist who used nanofluid was Choi [7]. Nanofluids are used for increasing thermal conductivity to enhance heat transfer. Due to this, nanoparticles are chosen as either metallic or metal oxide materials which have high thermal conductivity. In ducts with backward-facing step, heat transfer applications have been increased by using nanofluids. Abu-Nada [8] may be approved the first scientist conducted a numerical study concerning heat tranfer by using nanofluids in ducts with backward-facing step. In this study, five different nanoparticles (Cu, Ag, $Al_2O_3$, CuO, and $TiO_2$) were used with volume fractions between 0.05% to 2.0%. Water was the base fluid. Duct was thougth 2D and its expansion ratio was 2. The range of Reynolds number was 200-600. He reported that Nusselt number increases with increasing volume fractions. Al-aswadi et al. [9] studied numerically 2D laminar forced convection flow of nanofluids in channel with BFS. The base fluid was water. They conducted this study by using Au, Ag, $Al_2O_3$, Cu, CuO, $SiO_2$, $TiO_2$ and diamond nanoparticles with 0.05 volume fraction. The study was performed for Re=50, 100 and 175. Step height and expansion ratio of he devised channel were 4.8 mm and 2, in respectively. All the walls were insulated. They presented effects of Reynolds number and nanofluids types on pressure drop, velocity distribution and friction coefficient. They noticed that the highest wall shear stress is observed for $SiO_2$/water nanofluid. They found that nanofluids prepared nanoparticle with low density increas velocity much more compared to nanofluids prepared nanoparticle with high density. Also, they obtained that Reynolds number and skin friction coeffcient are inversely proportional. Heshmati et al. [10] investigated a numerical simulation of a two dimensional duct having backward-facing step devised slotted baffles on the top wall. Flow was performed for laminar mixed convection condition. Working fluids were $SiO_2$/water, $Al_2O_3$/water, CuO/water and ZnO/water nanofluids. Nanoparticles were added obvious volume fraction ($\varphi$=1.0-4.0%) and their diameters range were at 20–50 nm. Also, Constant and uniform heat flux ( $q''_w$ =10000 W/m$^2$) was applied to downward of the step wall while the other walls and slotted baffle were insulated. The main purpose of the study was that effects of the slotted baffle's positions (with a vertical solid baffle, with a solid inclined baffle, with two inclined slotted baffle), nanofluid's volume fractions and diameters on heat transfer. They observed that $SiO_2$/water nanofluid having 4% nanoparticle volume fraction and 20 nm nanoparticle diameter enhances heat transfer much more amoung the other nanofluids. In addition, they found that maximum Nusselt number is obtained in duct with inclined slotted baffle.

It is obtained from the above literature review that the case of forced convective heat transfer over horizontal BFS utilizing $SiO_2$/water nanofluid seems not to have been investigated in the past and this has motivated the present study. The present study deals with 2D laminar forced convective flow over a

backward-facing step (BFS) in a horizontal rectangular cross-sectioned duct by using different nanopaticles volume fractions (1.0%-4.0%) of $SiO_2$/water nanofluid. Results of interests such as Nusselt number, Darcy friction factor, velocity and temperature distributions for laminar forced convection flow over a horizontal BFS are reported to illustrate the effect of nanoparticles volume fractions of $SiO_2$/water nanofluid on these parameters.

## 29. MATHEMATICAL MODELING

### *29.1. Geometrical Configuration*

A duct having backward facing step was modeled to analyze in this study. Both the step height ($s$) and inlet height ($h_s$) of the duct were 4.8 mm. Total length ($H$) of duct was 9.6 mm. As the downstream wall was subjected to constant and uniform heat flux, the other walls were insulated. The schematic diagram of the backward facing step is presented in Figure 1.

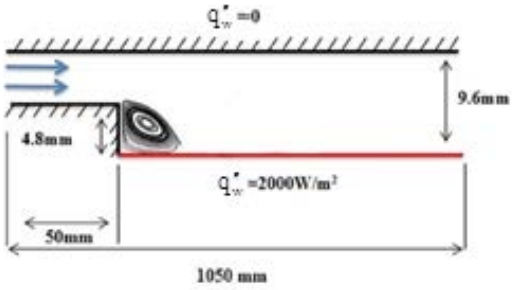


*Figure 1. Schematic diagram of the backward facing step*

### *29.2. Governing Equations and Boundary Conditions*

In the mathematical modeling of single-phase steady-state incompressible laminar flow, the following governing equations are used.

Contunity: $div(\rho\vec{V}) = 0$ (1)

Momentum: $div(\rho\vec{V}\vec{V}) = -grad\,P + div(\mu\, grad\,\vec{V})$ (2)

Energy: $div(\rho C_P\vec{V}T) = div(k\, grad\,T)$ (3)

In the governing equations, the buoyancy effect, viscous dissipation and radiation heat transfer are assumed to be negligible. Constant inlet velocity is applied and the inlet velocity can be calculated by specified Reynolds number as follows.

$$U_{inlet} = \frac{\mu Re}{\rho D_h} \quad (4)$$

where $\mu$ [Pa.s] is the viscosity, $\rho$ [kg/m$^3$] is the density of the nanofluid. $D_h$ is the hydraulic diameter and $D_h$=$H$.

Constant heat flux of 2000 W/m$^2$ is applied to the downstream wall of backward facing step.

### *29.3. Thermophysical Properties*

To solve the governing equations, the thermophysical properties of nanofluid should be defined. The effective density and specific heat of $SiO_2$-water nanofluid can be defined with following equations [11]

$$\rho_{eff} = \varphi\rho_s + (1-\varphi)\rho_f \quad (5)$$

$$(Cp)_{eff} = \frac{(1-\varphi)(\rho C_p)_f + \varphi(\rho C_p)_s}{(1-\varphi)\rho_f + \varphi\rho_s} \quad (6)$$

where $\varphi$ is the nanoparticle volume fraction, $C_P$ [J/kgK] is the specific heat. The subscripts *eff*, *s* and *f* denote effective, nanoparticle and base fluid, respectively.

The effective thermal conductivity of $SiO_2$-water nanofluid can be calculated by the following equation is given by Vajjha and Das [12] as:

$$k_{eff} = k_{static} + k_{brownian} \tag{7}$$

The $k_{static}$ is presented by Ghasemi and Aminossadati [13] as:

$$k_{static} = k_f \left[ \frac{(k_s + 2k_f) - 2\varphi(k_f - k_s)}{(k_s + 2k_f) + \varphi(k_f - k_s)} \right]$$

Thermal conductivity resulting from Brownian motion is offered by Vajjha and Das [12] as:

$$k_{brownian} = 5x10^4 \beta\varphi\rho_f Cp_f \sqrt{\frac{KT}{\rho_s d_p}} f(T,\varphi) \tag{8}$$

where

$$f(T,\varphi) = (2.8217x10^{-2}\varphi + 3.917x10^{-3})\frac{T}{T_o} + (-3.0669x10^{-2}\varphi - 3.91123x10^{-3}) \tag{9}$$

where $T$ is the fluid temperature, $T_o$ is the reference temperature and $K$ is the Boltzman constant.

Corcione [12] presented viscosity of nanofluid equation as:

$$\frac{\mu_{eff}}{\mu_f} = \frac{1}{1 - 34.87(d_p / d_f)^{-0.3}\varphi^{1.03}} \tag{10}$$

where

$$d_f = \left[ \frac{6M}{N\pi\rho_{fo}} \right]^{1/3} \tag{11}$$

where $\mu_f$ and $\mu_{eff}$ are viscosity of base fluid and nanofluid, respectively. $d_f$ is the base fluid equivalent diameter and $d_p$ is diameter of nanoparticle. $N$ is the Avogadro number, $M$ is the base fluid's molecular weight, and $\rho_{fo}$ is the mass density of the base fluid calculated at $T$=293 K. The nanoparticle diameter was taken as 65 nm.

The effective thermal expansion of nanofluid is presented by Corcione [11] as:

$$\beta_{eff} = \frac{(1-\varphi)(\rho\beta)_f + \varphi(\rho\beta)_s}{(1-\varphi)\rho_f + \varphi\rho_s} \tag{12}$$

Thermal expansion value of $SiO_2$ can be calculated from $\beta_s = 1.9526(100\varphi)^{-1.4594}$.

Average Nusselt number, Darcy friction factor and heat transfer coefficient are calculated as:

$$Nu = \frac{hD_h}{k} \tag{13}$$

$$f = \frac{\Delta P(D_h / L)}{\rho U^2_{inlet} / 2} \tag{14}$$

$$h = \rho U_{inlet} A_c C_p (T_{mo} - T_{mi}) / A_s (T_w - T_m) \tag{15}$$

where $\Delta P$ is the pressure difference between inlet and outlet of the duct, $L$ is the total length of the duct, $A_c$ is the cross-section area of the duct, $L$ is the length of the heated wall, $T_{mo}$, $T_{mi}$ and $T_w$ are mean temperatures of outlet, inlet and heated wall temperature of duct, respectively.

The thermophysical properties for base fluid and nanoparticle are given in Table 1.

*Table 1. Thermophysical properties for base fluid and nanoparticle [14, 15]*

| Material | $\rho(kg/m^3)$ | $C_p(J/kgK)$ | $k(W/mK)$ | $\mu(Ns/m^2)$ |
|---|---|---|---|---|
| Water | 997 | 4179 | 0.613 | 0.000855 |
| $SiO_2$ | 2200 | 703 | 1.2 | - |

### *29.4. Numerical Method and Code Validation*

Hexahedral mesh distribution was utilized in the modeling of backward facing step. Finite volume method was used to carry out the numerical computation. The governing equations were solved with boundary conditions. SIMPLE algorithm was used to resolve velocity and pressure coupling. To discretize the momentum and energy equation, Green Gauss Cell Based Method was applied. The convergence criterion of $10^{-6}$ was used in the iteration of governing equations. No convergence problems were observed during the calculations.

The mesh independence study was performed for the duct having backward facing step by refining the mesh number until the variation in both average Nusselt number and average Darcy friction factor are less than 0.08%. To obtain the optimum mesh number, a grid independence study was conducted using eight different mesh numbers changing from $3.4x10^2$ to $5.7\ x10^5$ for Re=225. Changing of Nusselt number and average Darcy friction factor values with mesh number for pure water flow is given in Figure 2 as an illustration. It was observed that a further refinement of mesh number from $4.4x10^4$ to $5.7x10^5$, the changing of average Nusselt number and average Darcy friction factor is negligible. If Figure 2 is observed, optimum mesh number with minimum computational time and maximum accuracy approximately can be seen at $4.4x10^4$.

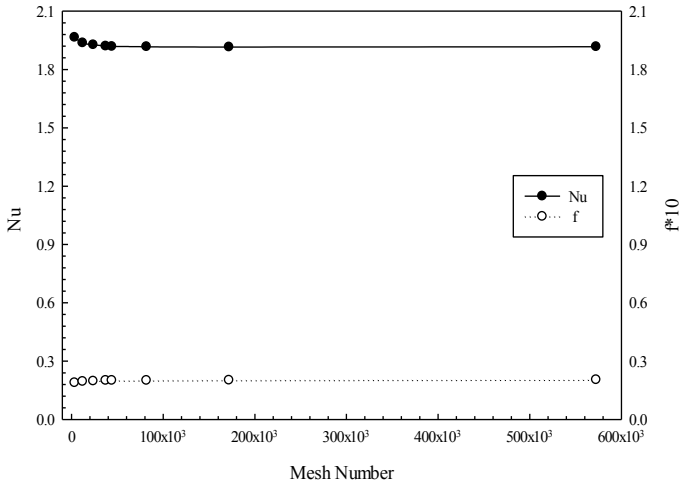


*Figure 2. Mesh independency validation*

To validate the code, the numerical results were compared with the data given by Togun et al. [16] and illustrated in Figure 3. As can be seen from Figure 3, the results obtained by present study show good agreement with the results obtained by Togun et al. [16].

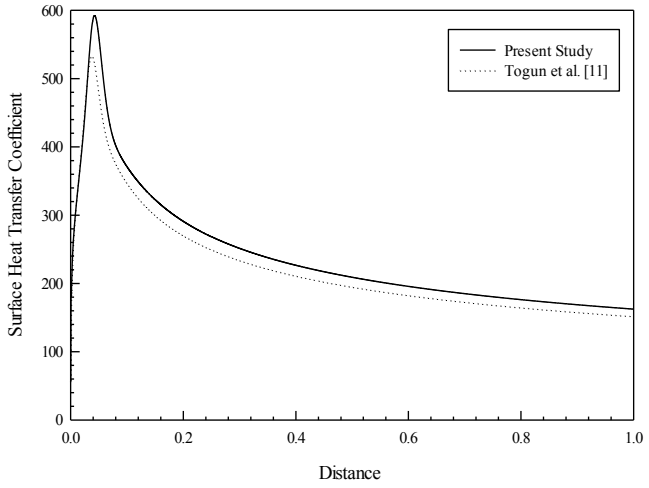


*Figure 3. The comparison of the surface heat transfer coefficient values obtained by present study with that of Togun et al. [16] at Re=225*

## 30. RESULTS

Laminar forced convection flow and heat transfer characteristics of $SiO_2$ nanofluid over a 2D horizontal backward facing step was numerically investigated. The nanoparticle diameter was 65 nm. The effects of the nanoparticle volume fractions on the average Nusselt number and average Darcy friction factor are presented in Figure 3 and Figure 4, respectively. As seen in Figure 3, the average Nusselt number increases with increasing both nanoparticle volume fractions and Reynolds number. Nanoparticle volume fraction of 4.0% has the highest average Nusselt number. Pure water has the lowest average Nusselt number. These results can show that adding nanoparticles inside the base fluids enhance the heat transfer. It can be obtained from Figure 4 that the average Darcy friction factor decreases with increasing Reynolds number. Also, changing nanoparticle volume fraction does not affect the average Darcy friction factor. Pure water has higher average Darcy friction factor compared to nanofluids. This means that $SiO_2$/water nanofluid has lower pumping power in comparison to pure water.

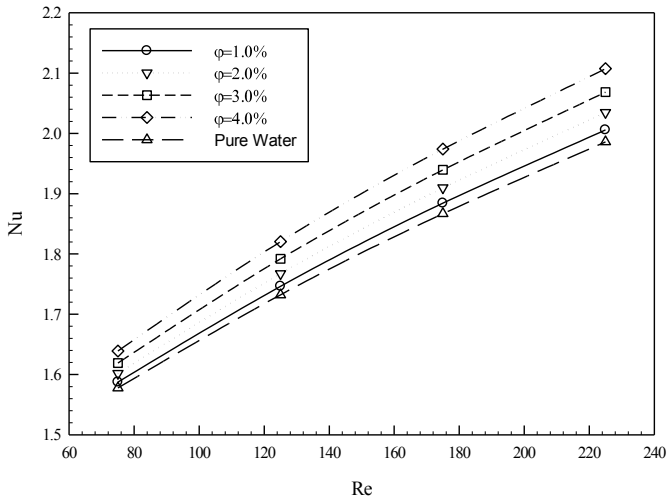


*Figure 3. Average Nusselt number for different nanoparticle volume fractions of $SiO_2$/water nanofluid*

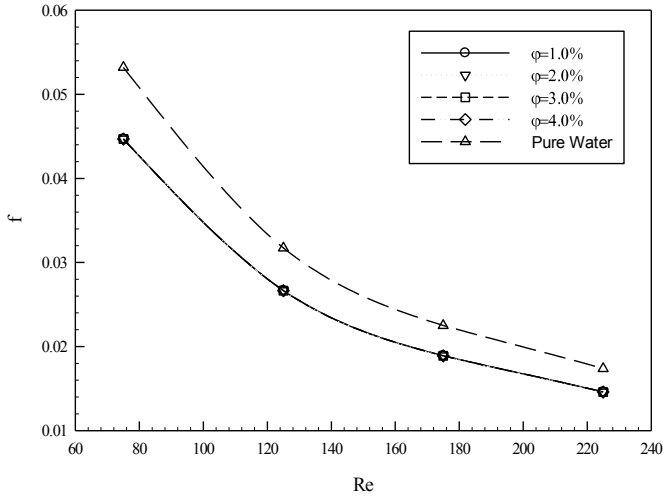


*Figure 4. Average Darcy friction factor for different nanoparticle volume fractions of $SiO_2$/water nanofluid*

The local Nusselt number distributions were presented along the heated wall in Figure 5. In the presented figure, four different nanoparticle volume fractions ($_{\varphi}$=1.0%-4.0%) were used as the Reynolds number was kept constant at 225. It was noticed that the local Nusselt number is realized to increase steeply to its maximum value at the separation point and then it decreases with keeping away from the step of the duct having BFS until the reattachment point and then it takes a fixed shape when the flow is being thermally fully developed condition. This is due to the fluid flow separation which leads to enhance the heat transfer [17]. The local Darcy friction factor distributions were presented along the heated wall in Figure 6. In this figure, four different nanoparticle volume fractions ($_{\varphi}$=1.0%-4.0%) were used for Re=225. It was obtained that the local Darcy friction factor decreases the minimum value and increases 0.05 levels and then it decreases 0.04 levels and finally increases until it reaches a point where the local Darcy friction factor remains constant along the rest of heated wall. This shows that the local Darcy friction factor asymptotically approaches the hydrodynamically fully developed condition. Also, it is noticed that the local Darcy friction factor is independent from nanoparticle volume fractions.

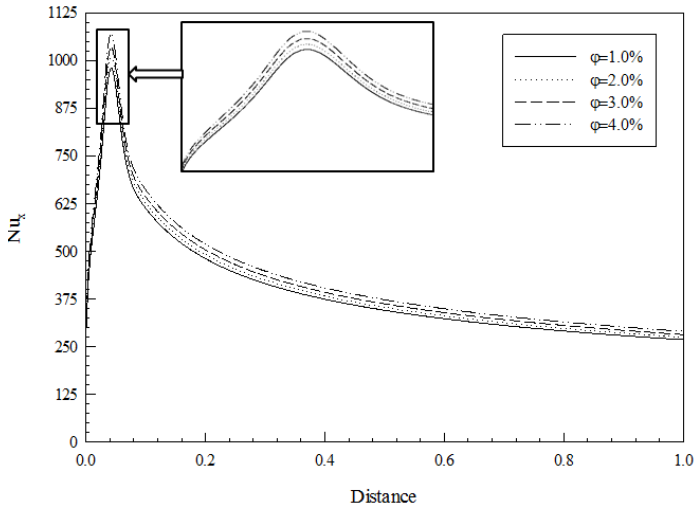


*Figure 5. Local Nusselt number distributions for different nanoparticle volume fractions along the heated wall at Re=225*

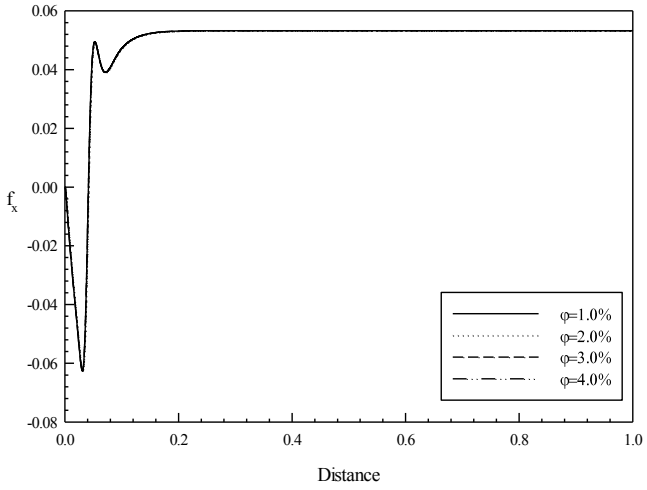


*Figure 6. Local Darcy friction factor distributions for different nanoparticle volume fractions along the heated wall at Re=225*

Streamlines inside the duct for different Reynolds numbers and different nanoparticle volume fractions of $SiO_2$/water nanofluid were presented in Figure 7 and Figure 8, respectively. It was noticed from Figure 8 that changing of Reynolds number markedly affects the size of the recirculation zones for volume fraction of 4.0%. As the Reynolds number increases, the size of the recirculation zone increases. Also, the contours of streamlines for different nanoparticle volume fractions at Re=225 are given in Figure 8. It can be obtained from the figure that, variation of nanoparticle volume fraction does not affect the size of the recirculation zones. Also, flow velocity increases with increasing nanoparticle volume fraction because of increasing viscosity of nanofluid.

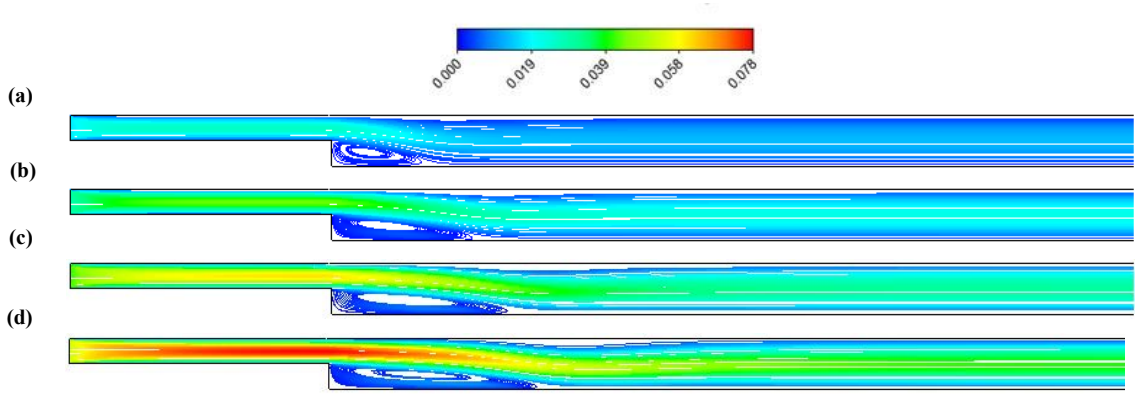


*Figure 7. Streamlines for different Reynolds number of $SiO_2$/water nanofluid for volume fraction of 4.0%; (a) Re=75, (b) Re=125, (c) Re=175, (d) Re=225*

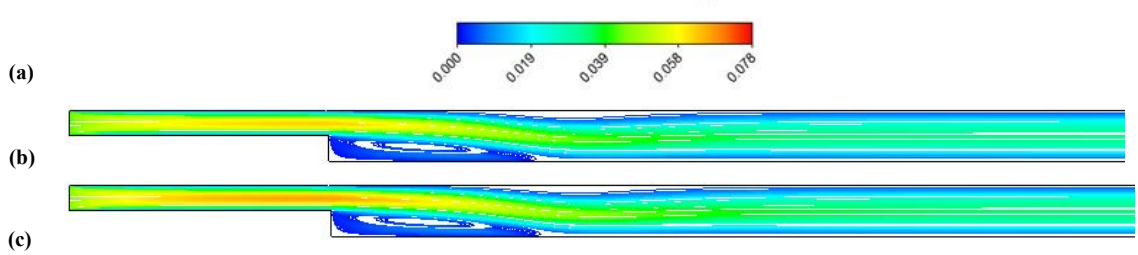

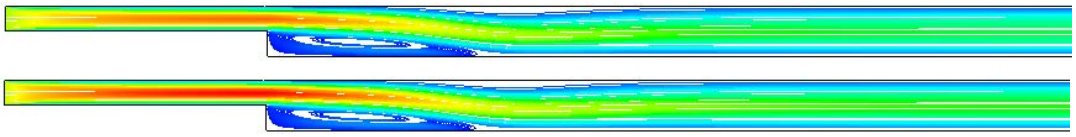


*Figure 8. Streamlines for different nanoparticle volume fractions of $SiO_2$/water nanofluid at Re=225; (a) $\varphi$ =1.0%, (b) $\varphi$ =2.0%, (c) $\varphi$ =3.0%, (d) $\varphi$ =4.0%*

## 31. CONCLUSIONS

Numerical simulation of steady state laminar forced convection flow and heat transfer in a 2D duct having backward-facing step (BFS) was presented. $SiO_2$/water nanofluid was used as working fluid. Effect of Reynolds number and nanoparticle volume fraction on convective heat transfer were investigated in detail. It was noticed from the numerical simulation results that $SiO_2$/water nanofluid enhances heat transfer. The average Nusselt number increases with increasing the Reynolds number and nanoparticle volume fractions. Also, average Darcy friction factor decreases with increasing Reynolds number. There is no effect of changing of nanoparticle volume fractions on average Darcy friction factor.

## REFERENCES

[64]. A.A. Al-aswadi, H.A. Mohammed, N.H. Shuaib, Antonio Campo, "Laminar forced convection flow over a backward facing step using nanofluids", *International Communications in Heat and Mass Transfer*, vol. 37, pp. 950-957, 2010.
[65]. R. J. Goldstein, V. L. Ericsen, R. M. Olson, E. R. G. Eckert, "Laminar separation reattachment, and transition of the flow over a downstream-facing step", *J. Basic Eng.*, vol. 92, pp. 732–741, 1970.
[66]. M. K. Denham, M. A. Patrick, "Laminar flow over a downstream-facing step in a two-dimensional flow channel", *Trans. Inst. Chem. Eng.*, vol. 52, pp. 361–367, 1974.
[67]. B. F. Armaly, F. Durst, J. C. F. Pereira, B. Schonung, "Experimental and theoretical investigation of backward-facing step flow" *J. Fluid Mech.,* vol. 127, pp. 473–96, 1983.
[68]. Y. T. Chen, J. H. Nie, B. F. Armaly, H. T. Hsieh, "Turbulent separated convection flow adjacent to backward-facing step—effects of step height", *International Journal of Heat and Mass Transfer*, vol. 49, pp. 3670–3680, 2006.
[69]. E. Pulat, M. Diner, "Geri basamak akışının nümerik analizi", *Mühendislik Bilimleri Dergisi*, vol.7, pp. 29-34, 2001.
[70]. A. A. Mahdi, H. A. Neema, B. Kadhem, "The effecting of a sudden step change on heat transfer coefficient", *Journal of Thi-Qar University*, vol. 4, pp. 39-64, 2008.
[71]. S. U. S. Choi, "Enhancing thermal conductivity of fluid with nanoparticles", *ASME FED*, vol.231, pp. 99-105, 1995.
[72]. A. A. Al-aswadi, H. A. Mohammed, N. H. Shuaib, A. Campo, "Laminar forced convection flow over a backward facing step using nanofluids", *International Communications in Heat and Mass Transfer*, vol. 37, pp. 950–957, 2010.
[73]. A. Heshmati, H. A. Mohammed, A. N. Darus, "Mixed convection heat transfer of nanofluids over backward facing step having a slotted baffle", *Applied Mathematics and Computation*, vol. 240, pp. 368-386, 2014.
[74]. M. Corcione, "Heat transfer features of buoyancy-driven nanofluids inside rectangular enclosures differentially heated at the sidewalls", *Int. J. Therm. Sci.,* vol.49, pp. 1536–1546, 2010.
[75]. R. S. Vajjha, D. K. Das "Experimental determination of thermal conductivity of three nanofluids and development of new correlations", *Int. J. Heat Mass Transfer,* vol.52, pp. 4675–4682, 2009.
[76]. B. Ghasemi, S. M. Aminossadati, "Brownian motion of nanoparticles in a triangular enclosure with natural convection", *Int. J. Therm. Sci.*, vol. 49, pp. 931–940, 2010.
[77]. F. P. Incropera, D. P. DeWitt, "Introduction to Heat Transfer 3rd ed.", *John Wiley&Sons Inc.*, New York, pp. 75-370, 1993.
[78]. B. H. Salman, H. A. Mohammed, A. S. Kherbeet, "Heat transfer enhancement of nanofluids flow in microtube with constant heat flux", *International Communications in Heat and Mass Transfer*, vol, 39, pp. 1195–1204, 2012.
[79]. H. Togun, T. Abdulrazzaq, S. N. Kazi, A. Badarudin, M. K. A. Ariffin, M. N. M. Zubir, "Numerical study of heat transfer and laminar flow over a backward facing step with and without obstacle", *International Journal of Mechanical, Aerospace, Industrial, Mechatronic and Manufacturing Engineering*, vol. 8, 2014.
[80]. H. A. Mohammed, A. A. Al-aswadi, M. Z. Yusoff, R. Saidur, Mixed convective flows over backward facing step in a vertical duct using various nanofluids bouyancy-assisting case, *Thermophys. Aeromech.,* vol. 42(1), pp. 1-30, 2012.

## BIOGRAPHY

Kamil ARSLAN is an Associate Professor of Mechanical Engineering Department at Karabük University, Turkey. He received his Ph.D. from Mechanical Engineering Department, Gazi University, Turkey, in 2010. He is active in both teaching and research in the area of thermal sciences. Also, he is interested in computational fluid dynamics, experimental methods in heat transfer and nanofluids.

# Remote Control of Lighting Usıng Programming Language Matlab, ZigBee Technology and PIC18F452 Microcontroller

*Edin Mujčić[1], Dženita Nuhić[2], Mujo Hodžić[3]*

***Abstract***

*Microcontrollers are used in automated products and devices, such as automobile engine control systems, remote controls, office machines, power tools, toys and other systems that are embedded. Also, the ZigBee networks are very suitable for network applications. ZigBee is a low-cost, low-power, wireless mesh network standard targeted at the wide development of long battery life devices in wireless control and monitoring applications. Bearing in mind the numerous advantages and ease of linking these two technologies, the remote control of lighting is practically implemented. Lighting assembly is made from more types of light sources. The PIC18F452 microcontroller and transistor amplifiers are used to control lighting. XBee modules are used for serial communication to PIC18F452 microcontroller and computer. The graphical user interface, designed in the programming language MATLAB, is used for remote control of lighting. In this way, the user has a complete overview of the state of lighting at any time.*

**Keywords: PIC18F452 microcontroller, XBee modules, XCTU, lighting, graphical user interface**

## 32. INTRODUCTION

The occurence of microcontrollers and microprocessors are regarded as one of the greatest technical achivements that characterized twentieth century. Main difference between microcontrollers and microprocessors is that they are the first optimized for speed and performance with computer programs, while microcontrollers are optimized towards integration of a large number of circuits real-time control, mass production, low cost and low power consumption [1]. Microcontrollers are also more resistant on variation of voltage, temperature, humidity, vibration, etc. Huge advantage is reflected in the fact that can be programmed, beside Assembler, and in high-level programming languages: C, Pascal, Basic, etc. [2]. This increases number of users who can write programs and thus also apply [1],[3]. They are used in a wide variety of modern devices such as: robots, telecommunication devices, satellites, cars, measuring instruments, mobile phones, cameras, etc. Also they are widely used in many home devices such as washing machines, microwave ovens, breadmakers, etc. [3].Today on market there are few major manufacturers microcontroller which in its production program have different microcontroller families. The most popular of them are Intel, Motorola, Amtel and Microchip. In this paper is used PIC18F452 microcontroller [4]- [10].

XBee radio module is a brand company Digi International which fully implement the Zigbee protocol [11]. XBee is tiny RF (radio frequency) module that has been developed and specifically designed to provide a simple and cost-effective performance of ZigBee wireless technology. It requires minimal energy to operate and provides reliable data transmission between devices [12]-[15]. Available are different protocols and characteristics of RF modules, which allow the user great flexibility to choose the best option for their needs. Family Xbee module is composed (March 2016) from 18 different modules of different qualities [16].

Remote control of lighting is achieved using XBee modules, where a module is connected to the computer, and the other is attached to the model. Communication is achieved by using wireless networks established between them using ZigBee network.

In programming language MATLAB is created a graphical user interface for lighting control. The user interface sends data using the serial port. On the serial port the XBee module is connected. XBee module is programmed using a programming language X-CTU. Received data from the MATLAB programming language, using XBee wireless communication module is sent to the second XBee module which is connected to the PIC18F452 microcontroller. The PIC18F452 microcontroller is controlling lighting system.

**33. PIC18F452 MICROCONTROLLER**

The PIC18F452 microcontroller is a modern microcontroller with a large storage space and a large number of I/O lines, implemented in CMOS technology. In CMOS technology, consumption is noticeable only in the transition from the state of logic zero in the state of logical units, or vice versa. Consequently, the PIC18F452 microcontroller has a low power consumption. Also, microcontroller made in this technology is resistant to impulse noise at the I/O lines and the power supply. In figure 1 (a) shown the appearance PIC18F452 microcontroller in 40-pin DIP package and in figure 1 (b) shown the appearance PIC18F452 microcontroller in 44-pin TQFP package.

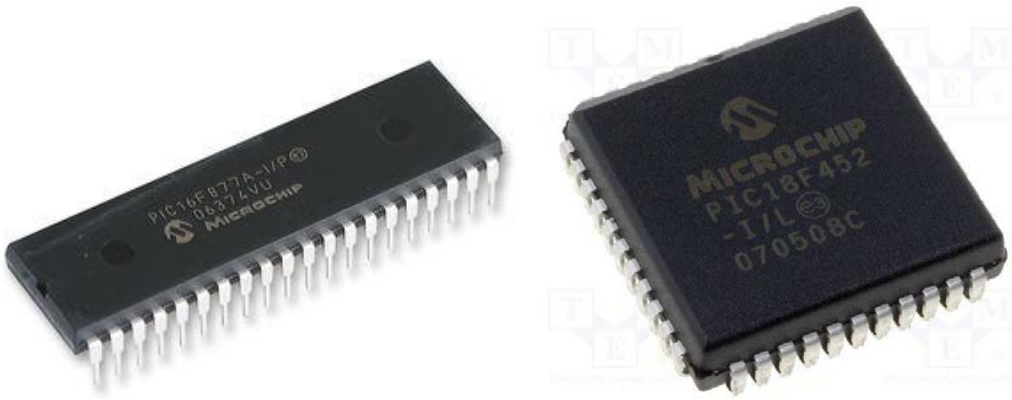


*Figure 1. (a) The PIC18F452 microcontroller 40-pin DIPpackage (b) The PIC18F452 microcontroller 44-pin TQFP package*

In this paper, PIC18F452 microcontroller in 40-pin DIP package is used. In Figure 2 shown the pin diagram of PIC18F452 microcontroller and pins description.

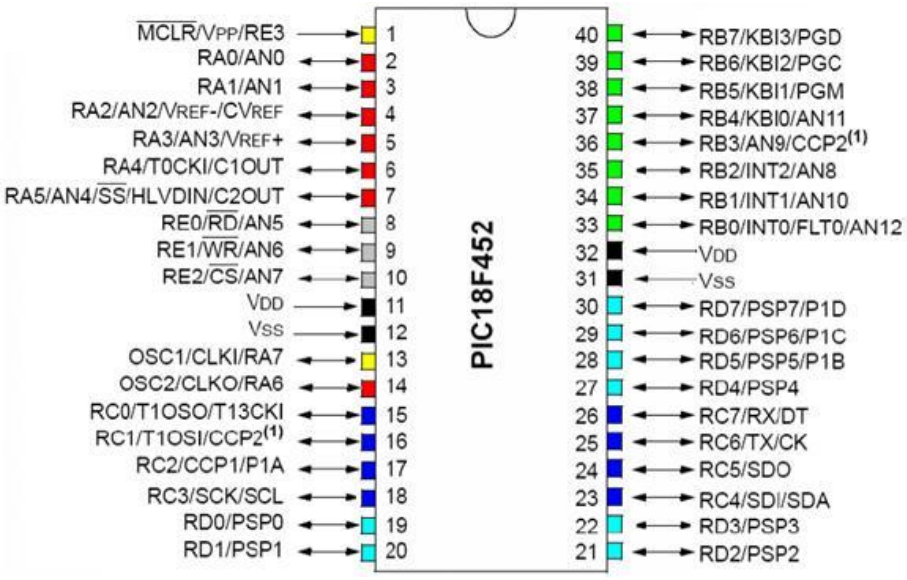


*Figure 2. Pin diagram of PIC18F452 microcontroller and pins description [8]*

From Figure 2 we see that the PIC18F452 microcontroller has, in addition to the basic pins for power supply, connect the oscillator and reset, 34 digital I/O pins, 8 analog inputs and two ten-bits inputs and two PWM modules.

Written program should be placed in the microcontroller memory. Programming microcontrollers is done by entering the instruction in the EPROM according to the instructions of the microcontroller used, and according to a set of instructions that are supported by the central unit. In this paper, the code written in assembly language, using MPLab integrated development environment. Hexadecimal file, using programmer MPLAB ICD2, is transferred to PIC18F452 microcontroller. The code is not listed in this paper because of its size.

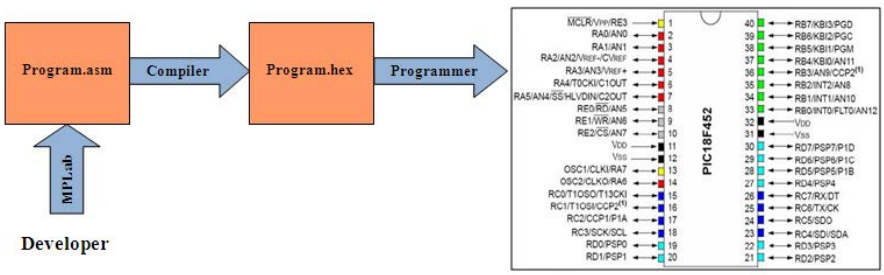


*Figure 3. A method of programming PIC18F452 microcontroller*

On Figure 3 the steps to programme the microcontroller PIC18F452 are shown.

## 34. XBEE MODULES

XBee radio module is a brand of company Digi International to fully implement the Zigbee protocol [11]-[13]. XBee is a tiny RF (radio frequency) module that has been developed and specifically designed to provide a simple and cost-effective performance of ZigBee wireless technology. Requires minimal energy to operate and provide reliable data transfer between

devices [14]. Different protocols and features of RF modules are available, which allow the users great flexibility to choose the best option for their needs.

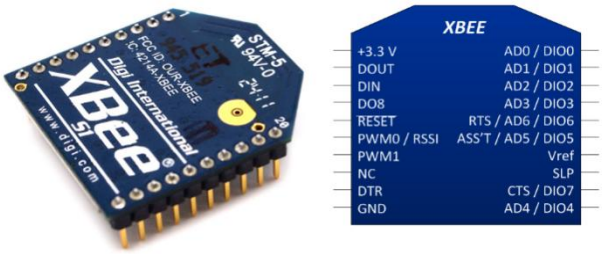


*Figure 4. XBee Module 24*

XBee/XBee PRO modules have 20 pins (see Figure 4). For work of XBee module four basic pin connections are sufficient - power supply Vcc (3.3 V), ground GND, Data input DIN and Data output DOUT. Other pins are used as input-output pins for the analog and/or digital data as well as control pins (sleep, status, reset, etc.).

Characteristics of XBee module 24 are [12]:

- Supply Voltage 2.8 – 3.4 V
- Indoor/Urban Range Up to 30 m
- Outdoor RF line-of-sight Range Up to 90 m
- Transmit Power Output (software selectable) 1 mW (0 dBm)
- Operating Frequency ISM 2.4 GHz
- Seven 10-bit ADC input pins
- 8 digital I/O pins
- 128-bit encryption
- AT or API command set
- ...

To program XBee module programming tool X-CTU is used. X-CTU set program is shown in Figure 5.

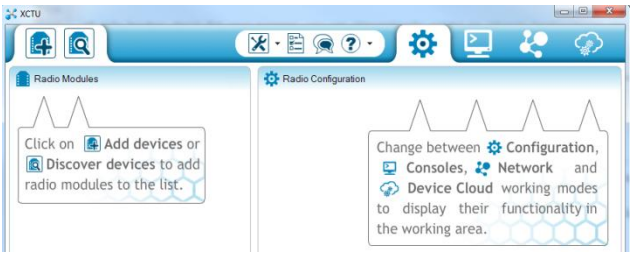


*Figure 5. Appearance of XCTU program*

Table 1 shows how to configure the XBee modules to communicate with each other.

*Table 5. Configure the XBee modules to communicate with each other*

| | Xbee 1 | Xbee 2 |
|---|---|---|
| **PAN ID** | 3010 (or any number in the range of 0-FFFF) | 3010 (or any number in the range of 0-FFFF) |
| **CH** | C | C |
| **MY Address** | 1 | 2 |
| **DH** | 0 | 0 |
| **DL** | 2 | 1 |

Besides basic configuration it is necessary to set a large number of parameters for proper and safe operation of the ZigBee network.After programming the XBee modules they are ready to communicate with each other. In our project XBee modules are used to send data from the computer to the PIC18F452 microcontroller.

## 35. REMOTE CONTROL OF LIGHTING USING PROGRAMMING LANGUAGE MATLAB, ZIGBEE TECHNOLOGY AND PIC18F452 MICROCONTROLLER

In programming language MATLAB is created a graphical user interface for lighting control. The graphical user interface sends data using the serial port. On the serial port the XBee module is connected. XBee module is programmed using a programming tool X-CTU. Received data from the MATLAB programming language, using XBee wireless communication module is sent to the second XBee module which is connected to PIC18F452 microcontroller. The PIC18F452 microcontroller is controlling lighting system. This is shown in Figure 6.

.

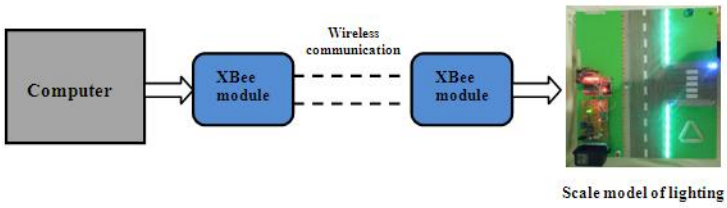


*Figure 6. Block diagram of model of lighting*

In order to use the PIC18F452 microcontroller for lighting control, amplification of its output signal must be made. We used MOSFET transistors IRFZ 44 and relays to do so. After designing in the programming language Circuit Wizard, development and soldering necessary parts receive the energy part of the system as shown in Figure 7.

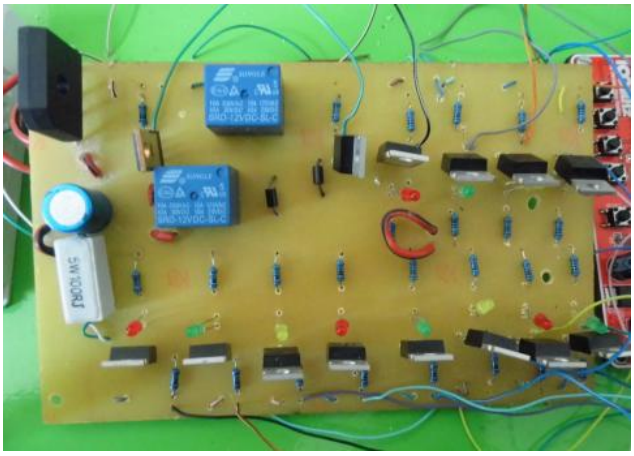

*Figure 7. The appearance of the energy part of lighting control system*

For the PIC18F452 microcontroller is used a develop board for 40-pin PIC microcontrollers shown in Figure 8

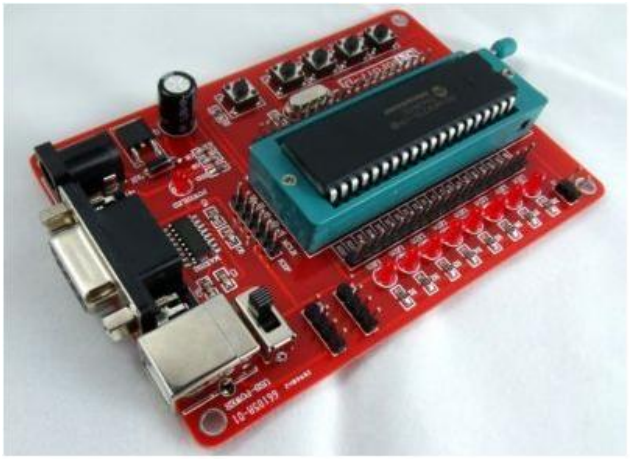

*Figure 8. Development board for 40-pin microcontrollers with the PIC18F452 microcontroller*

After connecting and testing we're getting circuit for remote control of lighting shown in Figure 9.

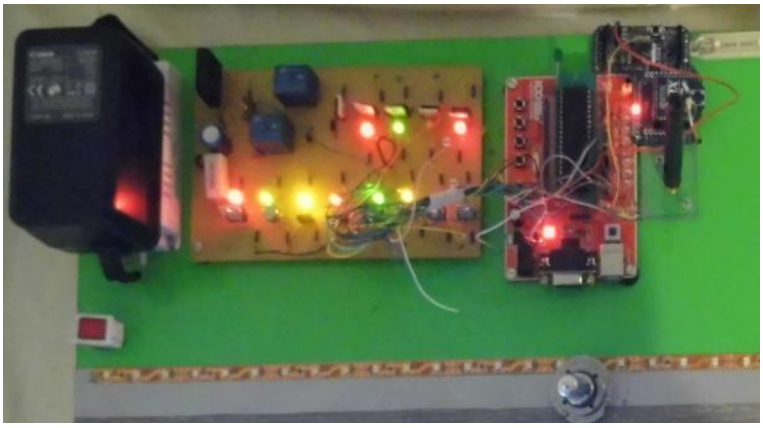

*Figure 9. The appearance of the finished circuit for remote control of lighting*

From Figure 9 we see that XBee module wirelessly receives signals from XBee module connected to the serial port. The received control signals are sending to the PIC18F452 microcontroller where these signals are being processed and sent to the individual outputs from the PIC18F452 microcontroller.The processed signals are then amplified and sent to individual consumers on the board that is used to verify the work designed system for remote control of lighting. Consumers are at the lighting: incandescent bulbs, LEDs, LED modules and LED strips.

## 36. EXPERIMENTAL RESULTS

In this part of the paper experimental verification of work created system was carried out. User is using the graphical interface created in programming language Matlab, controls the work of the remote system lighting. Pressing the green buttons (see figure 10) turn on light bulbs, LED strips or LED modules and pressing the red buttons turn off the specified lighting. Panel (white or yellow color) at the end of each pair of on-off changes color depending on whether it is on or off lighting. The yellow color of the panel means that turn on bulbs (LED strip, LED module) which spatially corresponds included on-off pair.

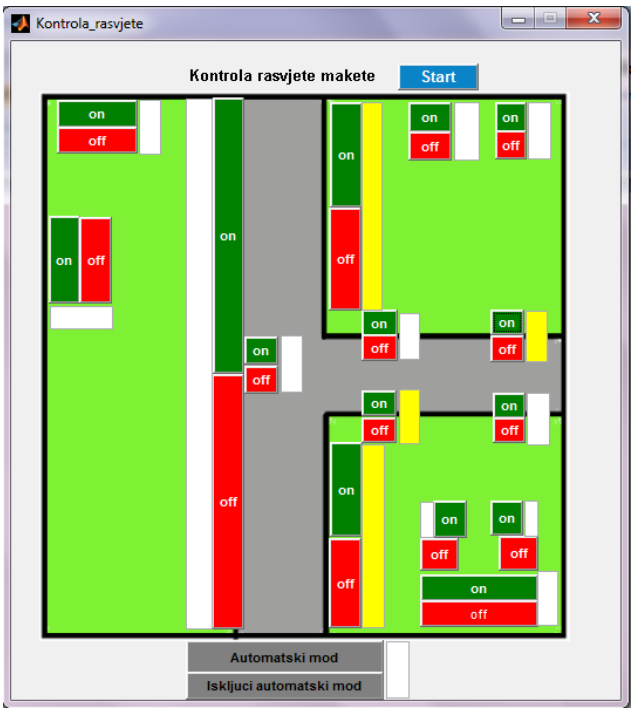


*Figure 10. The graphical user interface with the turn on four bulbs (LED strips, LED bulbs)*

Figure 11 shows the appearance of the model lighting for this case. We see that they include two LED strips along the street, and two LED bulbs equivalent to yellow panels on the graphical interface shown in Figure 10. From this we can conclude that the project to a remote control model of lighting works well. At any time, the user knows which the buld (LED strip, LED Module) is turned on and which one is not.

*Figure 11. The appearance of created system for remote control of lighting*

We can also select the mode "Automatski mod" (see figure 10) in which the light bulbs (LED strips, LED modules) turn on/turn off the pre-programmed order. Pressing the button titled "Iskljuci automatski mod" again switches to manual operation system for remote control of lighting.

## 37. CONCLUSION

Based on the experimental analysis, we can conclude that the system designed for remote control of lighting works well. With minimal changes (suiting real system) designed system can be used to control lighting of smart house.

## REFERENCES

[81]. Mikrokontroler [Online]. Available: http://sh.wikipedia.org/wiki/Mikrokontroler
[82]. Uvodnipojmovi-programiranje mikrokontrolera [Online]. Avaliable http://mikrokontroleri.weebly.com/uvodni-pojmovi---programiranje.html
[83]. D. Đorđević, Ž. Đorđević: *Komunikacijamikrokontrolera PIC16F877 preko SPI modula,* Elektronskifakultet, Niš, 2007
[84]. I. Dogan, *Advanced PIC Microcontroller Projects in C,* Elsevier, Burlington, USA, 2008.
[85]. "PIC18F42X, Data Sheet", FLASH-Based 8-Bit CMOS Microcontroller, 2003.
[86]. L. Chartrand, H. W. Huang, *PIC Microconteroller: An Introduction to Software & Hardware Interfacing*, Mankato, 2005.
[87]. A. E. TakiEl_Deen, A. M.Fanni, "Implementation of AES Algorithm in MicroController Using PIC18F452," *Journal of Computer Engineering (IOSR-JCE),* Vol. 15, pp. 35-38, Nov. 2013.
[88]. Modulo micro PIC18F452 [Online]. Avaiable: http://www.monografias.com/trabajos104/modulo-micro-pic18f452/modulo-micro-pic18f452.shtml
[89]. A. Abdullah, Md. G. Anwar, T. Rahman, S Aznabi, "Water level Indicator with alarms using PIC microcontroller", *American journal of engineering research (AJER),* vol. 4, pp.88-92, 2015.
*[90].* A. G. Samanta, "Interfacing Of PIC 18F252 Microcontroller with Real Time Clock via I2C Protocol", *Journal of Engineering Research and Applications*, Vol. 4, Issue 7, pp. 152-156, July 2014.
[91]. XBee terminology [Online]. Available: https://docs.digi.com/display/XBJLIB/XBee+terminology
[92]. XBee/XBee PRO RF Modules [Online]. Available: http://ftp1.digi.com/support/documentation/90000982_S.pdf
[93]. K. Sohraby, D. Minoli, T. Zanati, *Wireless sensor networks*, Wiley, 2007.
[94]. XBee/XBee PRO RF Modules [Online]. Available: https://www.sparkfun.com/datasheets/Wireless/Zigbee/XBee-Datasheet.pdf
[95]. P.V. Mane-Deshmukh, B.P. Ladgaonkar, S. C. Pathan, S. S. Shaikh, "Microcontroller PIC18f4550 Based Wireless Sensor Node to Monitor Industrial Environmental Parameters", *International Journal of Advanced Research in Computer Science and Software Engineering*, Vol. 3, Issue 10, pp. 943-950, Oct. 2013.
[96]. XBee [Online]. Available: https://en.wikipedia.org/wiki/XBee

# Evaluation of Antioxidant Capacity of *Paronchia argyroloba* Seeds

***Idris Arslan*[18], Ali Zeytunluoğlu[19]***

***Abstract***

*The genus Paronychia Miller (Illecebraceae) is distributed in warm and dry regions of the world. Paronychia species are found in Irano-Turanian and East-Mediterranian phytogeographic regions and is represented by 28 species, 20 of which are endemic to Turkey & East Aegean Islands.*

*The main objective of the present study was to analyze the antioxidant capacity and phenolic content of aqueous and methonolic extracts of Paronchia argyroloba naturally grows in Anatolia region. TEAC (trolox equivalent antioxidant capacity), TPC (total phenolic content) and DPPH (free radical scavenging activity) of each extracts were investigated. As a results, a positive correlation was determined between total phenolic content and antioxidant capacity.*

**Keywords: *Paronchia argyroloba*, ABTS$^{+\cdot}$ , DPPH, TOC**

## 38. INTRODUCTION

The genus *Paronychia* Miller (Illecebraceae) is distributed in warm and dry regions of the world. *Paronychia* species are found in Irano-Turanian and East-Mediterranian phytogeographic regions and is represented by 28 species, 20 of which are endemic to Turkey & East Aegean Islands [1-2]. In the Red data book of turkish plants, the status of 12 endemic *Paronychia* species has been described [3].

*Paronychia argyroloba* is an annual plant and naturally found in Tavas/Denizli region ant its environments.

It was reported that *Paronychia* species shows a broad spectrum of different activities, such as antidiabetic, antimicrobial, antiulser, antianorexia and antioxidant [4-6].

*Figure 1. (a) Morphological apperance of Paronchia argyroloba (b) Seeds of Paronchia argyroloba*

It seems that the among the main constituents oleanane-type saponins are widely found. Gypsogenic acid-derived triterpenoidal saponins from *Paranochia* genus was reported [7]. Also, there is a report on the isolation and characterizattion of four new tritepenoidal saponins from *Paronychia anatolica* subsp. *balansae* roots [8].

To the best of our knowledge, there is no report on antioxidant capacity and total phenolic content of *Paronchia argyroloba* plant species. The main objective of the present study was to analyze the antioxidant capacity and phenolic content of methonolic extracts of *Paronchia argyroloba* naturally grows in Anatolia region.

[18] *Corresponding author: Pamukkale University, Department of Biomedical Engineering, 20170, Pamukkale/Denizli, Turkey.* iarslan@pau.edu.tr

[19] *Pamukkale University, Electron Microscopy Center, 20170, Pamukkale/Denizli, Turkey.* azeytun@pau.edu.tr

## 39. MATERIAL AND METHODS

### *39.1. Plant materials*

The plant samples (*Paronchia argyroloba*) was collected from Çakıroluk region, Tavas-Denizli, Turkey. 3.0 g of the powder plant material was solved in 100 ml of distilled water. The mixture was stirred on the hot-plate in temperature of 50-60 °C for 2.5 hours and then filtered by the double-layered cheesecloth. Obtained filtrate was centrifuged at 5000 rpm for 10 min and then the supernatant collected in a dark glass bottle in frozen (- 20 °C) until use.

3.0 g of the powder plant material was solved in 500 ml of methanol (90 %). The mixture was stirred on the hot-plate in room temperature for 2.5 hours and then then filtered using Whatman filter paper No. 1. The filtrate was concentrated in a rotary evaporator at 60°C. The resulting extracts were stored at −20°C until the analysis.

### *39.2. Total phenolic content*

Total phenolic content of methanolic extract obtained from *P.argyroloba* was determined using modified of microscale Folin-Ciocalteau's method described by Slinkard & Singleton with slight modifications [9]. Briefly, 20 µl of plant extract were mixed with 100 µl of Folin–Ciocalteu reagent and the mixture was incubated for 1 min in room temperature and then added of 80 µl of 7.5% (*w/v*) sodium carbonate. The mixture was allowed to stand for a further 30 min in the dark, and absorbance was measured at 760 nm. All measurements were carried out in triplicate and calculations were based on a calibration curve obtained with gallic acid. Total phenolic content was expressed as mg.g-1 gallic acid equivalent using the equation obtained from the calibration curve y=0.00427×-0.0138, $R^2$=0.9987.

### *39.3. Trolox equivalent antioxidant capacity*

The ABTS radical scavenging activity was measured according to the method described by Re et al., 1999. The ABTS stok solution (7mM) and 2.45 mM potassium persulphate were mixtured. The reaction mixture for to obtain the ABTS radical solution was left to stand at room temperature (16 h) in the dark before use. ABTS radical solution was diluted with 80 % ethanol, to give an absorbance value of ~0.70 at 734 nm.

For measuring ABTS radical scavenging activity 20 µl of the sample was mixed with 200 µl of the ABTS radical solution. Absorbance was monitored at 734 nm for 6 min. The decrease in absorption at 734 nm 6 min after addition of ABTS radical solution was used for calculating the TEAC (trolox equivalent antioxidant capacity). The total antioxidant activities were expressed as mM trolox equivalent antioxidant capacity (TEAC). All measurements were performed at least in triplicate. Trolox standards prepared in ethanol (80%) ranging from 100–500 µM. 80 % ethanol was used as blank in measurement.

### *39.4. DPPH free radical scavenging activity*

The DPPH radical scavenging activity was measured according to the method described by Brand-Williams [10] with slight modifications. DPPH (2,2'-diphenyl-1-picrylhydrazyl) stock solution was prepared by dissolving 12 mg in 50 ml 100% methanol and then stored at -20 $^{o}$C until needed. The working solution was obtained by mixing the stock solution (10 ml) with methanol (20 ml) to obtain an absorbance of 1.0 ± 0.02 units at 517 nm using the Multiscan Go Microplate reader (Thermo, USA). The methanolic extract of *Paronchia argyroloba* (15 µl) and 200 µl DPPH were mixed and then shaked and followed by incubation at room temperature in the dark for 10 minutes. The decrease in absorbance in presence of DPPH was measured at 517 nm. Trolox was used as a standard compound. A standard calibration curve is constructed for Trolox at 50-750 µM concentrations. TEAC (trolox equivalent antioxidant capacity) values were calculated by using the standard regression curve.

## 40. RESULTS AND DISCUSSION

The improved $ABTS^{+\cdot}$ method, described by Re et al. [11] was used to determine the antioxidant capacity for the plant species examined in this study. The concentration response curves for $ABTS^{+\cdot}$, as a function of five separetely prepared stock solutions of trolox standards (100, 150, 200, 250 and 500 µM) in terms of trolox equivalent antioxidant capacity (TEAC, mM trolox equivalent per g dry weight of plant). Similarly, concentration response curves for DPPH and TOC five and seven separetely prepared stock solutions of standards (Figure 1).

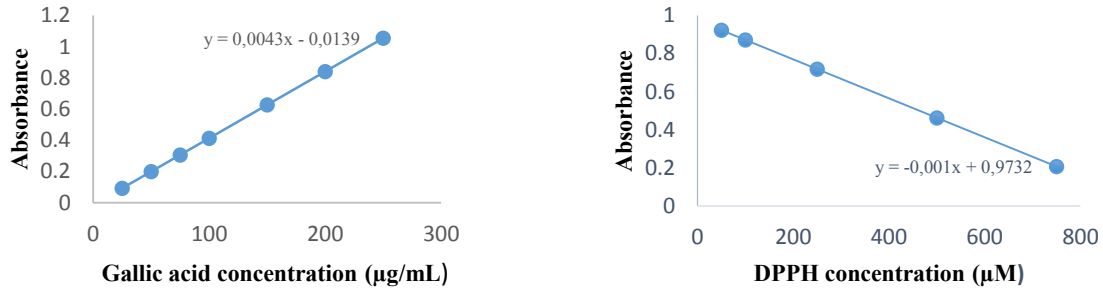


*Figure 1. Concentration-calibration curve for absorbance at 517 nm for DPPH as a function of standard trolox solution at 765 nm for gallic acid standard.*

There was a large variation in the antioxidant and free radical scavenging capacities of the aqueous and methanolic extracts of the plant material tested, as shown in Table 1. We found at 16.23, 23.80 for ABTS and 4.

The results obtained from ABTS and DPPH assays were determined as 16.23, 4.84 for aqueous extracts and 23.80, 22.76 mM TE/g dry weight for methanolic extracts, respectively. Total phenolic content of methanolic extracts were found as 29.12 mg GAE per g weight.

Total phenolic content (TOC) was estimated by Folin-Ciocalteu colorimetric method, based on the procedure of [9], using gallic acid as a standard phenolic compound. A linear calibration curve of gallic acid, in the range 25-250 µg/mL with $r^2$ value of 0.9998, was constructed Figure 1. For methanolic extracts showed the total pheolic content of 29.12 mg gallic acid equivalent per g dry weight of test material.

*Table 6. Antioxidant capacity of P.argyroloba extracts*

| Antioxidant capacity (mM TE/g dry weight)[a] | | | | Total phenolic content (mg GAE/g)[b] |
|---|---|---|---|---|
| ABTS | | DPPH | | |
| Aq.E | Met.E | Aq.E | Met.E | Met.E |
| **16.23** | **23.80±0.72** | **4.84±0.26** | **22.76±1.41** | **29.12±0.57** |

All data are shown as means ± SD from two extraction replicates, each run in dublicate.

Aq.E : Aqueous extracts

Met.E: Methanolic extracts

[a] Data are expressed as mM of trolox equivalents per g dry weight.

[b] Data are expressed as mg of gallic acid equivalents (GAE) per g dry weight.

These results suggested that the phenolic compounds contributed significantly to the antioxidant capacity of the investigated plant species. In many paper, a positive linear correlation between antioxidant capacity and total phenolic content [12] The Folin-Ciocalteu assay gives a crude estimate of the total phenolic compounds present in an extract. It is not specify to polyphenols, but many interfering compounds may react with the reagent, giving elevated apperent phenolic concentrations [13].

As stressed by Frenkel and Meyer, no single method is adequate for evaluating the antioxidant capacity of foods, since different methods can yield widely diverging results. Several methods based on different mechanisms must be used [14]. Therefore, we investigated the antioxidant capacity both ABTS radical cation assay and DPPH free radical scavenging activity.

## ACKNOWLEDGMENT

The authors would like to thank our valuable B.Sc students Ms. Tuğba Tuhan, Merve Alparslan, Esma Özçeliker.

## REFERENCES

[97]. Güner A, Özhatay N, Ekim T & Bafler KHC (2000). Flora of Turkey and the East Aegean Islands, Second Supplement Vol. 11. p. 656.Edinburgh: University Press.
[98]. Davis PH (ed.) (1965-1985). Flora of Turkey and the East Aegean Islands Vol. 1-9. Edinburgh: University Press.
[99]. Ekim T (2000). Herniaria L., In: Güner A, Ekim T, Özhatay N, Baser KHC, editors. Flora of Turkey and the East Aegean Islands (Suppl. 2), Vol. 11. Edinburgh, UK: Edinburgh University Press, pp. 5.

[100]. Afifi, F.U., Al-Khalidi, B., Khalil, E., (2005), Studies on the in vivo hypoglycemic activities of two medicinal plants used in the treatment of diabetes in Jordanian traditional medicine following intranasal administration, Journal of Ethnopharmacology, 100:314–318.
[101]. Al-Bakri, A.G., Affifi, F.U., (2007), Evaluation of antimicrobial activity of selected plant extracts by rapid XTT colorimetry and bacterial enumeration, *Journal of Microbiological Methods*, 68: 19–25.
[102]. Ferreira, A., Proença, C., Serralheiro, M.L.M., Araújo, M.E.M., (2006), The in vitro screening for acetylcholinesterase inhibition and antioxidant activity of medicinal plants from Portugal, *Journal of Ethnopharmacology*, 108: 31–37..
[103]. Avunduk, S., Lacaille-Dubois, M.A., Miyamoto, T., Bedir, E., Senol, S.G., Calişkan, O.A., (2007), Chionaeosides A-D, triterpene saponins from *Paronychia* chionaea, J Nat Prod., 70(11):1830-3.
[104]. Gülcemal, D., Masullo, M., Alankuş-Çalışkan, Ö., Piacente, S., (2014), Oleanane type glycosides from *Paronychia anatolica* subsp.*balansae, Fitoterapia, 92: 274–279.*
[105]. Slinkard K., Singleton V.L. Total phenol analysis: automation and comparison with manual methods. American Journal of Enology and Viticulture, 28 (1977), pp. 49–55.
[106]. Brand-Williams, W., Cuvelier, M.E. and Berset, C. 1995.Use of a free radical method to evaluate antioxidant activity, Lebensmittel-Wissenschaft und-Technologie/Food Science and Technology, 28:25-30.
[107]. Re, R., Pellegrini, N. , Proteggente, A. , Pannala, A. , Yang, M. , Rice Evans, C. , (1999), Anti-oxidant activity applying an improved ABTS radical cation decolorization assay, Free Radic. Biol.Med., 26: 1231-1237.
[108]. Cai, Y. Luo Q, Sun M, Corke H. 2004. Antioxidant activity and phenolic compounds of 112 traditional Chinese medicinal plants associated with anticancer, Life Sciences, 74, 2157-2184.
[109]. Prior R.L., Wu X, & Schaich K. 2005. Standardized methods for the determination of antioxidant capacity and phenolics in foods and dietary supplements. Journal of Agricultural and Food Chemistry. 53, 4290-1302.
[110]. Frankel EN., Meyer AS. The problems of using one-dimensional methods to evaluate multifunctional food and biological antioxidants. J. Sci. Food Agric 2000;80: 1925-41.

# Trolox Equivalent Antioxidant Capacity, Free Radical Scavenging Activity and Total Phenolic Content of *Astragalus flavescens*

***Idris Arslan*[20], Ali Zeytunluoğlu[21]***

***Abstract***

*The genus Astragalus (Fabaceae) is a large genus of about 3.000 species of herbs and small shrubs. It is a largest genus of plants in terms of described species. Astragalus species are native to temperate regions of the Nothern Hemisphere and their common names "geven" in Turkey. Some pale-flowered vetches are similar in apperance, but vetches are more vine-like. Medicinal plants are very important for therapeutical usage. Astragalus species and their extracts have been used for alternative therapy.*

*The main objective of the present study was to test the antioxidant capacity and phenolic content of extracts of Astragalus flavescens ll w Ö ş/İz . H x h l x w x v tsa and TEAC (trolox equivalent antioxidant capacity), TPC (total phenolic content) and DPPH (free radical scavenging activity) of each extracts were incestigated. As a results, a positive correlation was determined between total phenolic content and antioxidant capacity.*

**Keywords: *Astragalus flavescens*, ABTS$^{+\cdot}$ , DPPH, TOC, Fabaceae**

## 41. INTRODUCTION

The genus *Astragalus* is the largest one in the Fabaceae family and is represented by 380 species in the flora of Turkey [1]. Several *Astragalus* species are used in traditional medicine as an antiperspirant, diuretic, and tonic drug and for the treatment of diabetes mellitus, nephritis, and leukemia. [2]. In China, many pharmaceutical preparations containing *Astragalus* extract or isolated compounds have been used: Water decoctions of the roots of *A. membranaceus* and *A. sinicus* were incorporated into pharmaceutical preparations for treatment of toothache or for oral hygiene [3]. Chemical studies on *Astragalus* saponins have provided oleanane-type and cycloartane-type triterpenoid glycosides that exhibited cytotoxic, immunostimulatory, hepatoprotective, or antiviral activities [3].

*Astragalus flavescens,* a compound prescription of Chinese herbal medicine, contains Radix Astragali, Radix Scutellariae and Flavescent Sophora. *Astragalus flavescens* has been utilized in the treatment of chronic liver disease for >10 years and has shown curative effects. It has been clinically demonstrated that *Astragalus flavescens* is effective in receding jaundice, detumescence, retracting the spleen, reducing ascites, lowering transaminase activity, increasing serum albumin levels and improving the prothrombin time. Clinical studies have indicated that *Astragalus flavescens* is able to regulate the immunity and scavenge oxygen free radicals, as well as exhibiting anti-viral and -tumor effects. In addition, the prescription for *Astragalus flavescens* is low in cost and convenient to use; therefore, it has good developmental value. The present study investigated the preventative effects of *Astragalus flavescens* on liver fibrosis in rats and its mechanism of action. The study aimed to provide

a reliable experimental basis for the further application of *Astragalus flavescens* in the treatment of hepatic fibrosis [4].

[20] *Corresponding author: Pamukkale University, Department of Biomedical Engineering, 20170, Pamukkale/Denizli, Turkey.* iarslan@pau.edu.tr

[21] *Pamukkale University, Biomedical Equipment Technology, 20100, Pamukkale/Denizli, Turkey.* azeytun@pau.edu.tr

*Figure 1. (a) Morphological apperance of* Astragalus flavescens

To the best of our knowledge, there is no report on antioxidant capacity and total phenolic content of *A. flavescens* plant species. The main objective of the present study was to analyze the antioxidant capacity and phenolic content of methonolic extracts of *A. flavescens* naturally grows in Anatolia region.

The main objective of the present study was to test the antioxidant capacity and phenolic content of aqueous and methanolic extracts of *A. flavescens* naturally grows in Ödemiş, İzmir region.

## 42. MATERIAL AND METHODS

### *42.1. Plant materials*

*Astragalus flavescens* samples were collected from Bozdağ, Ödemiş, İzmir, Turkey.

3.0 g of the powder plant material was solved in 500 ml of methanol (90 %) (methanolic extract) and distilled water (aqueous extract). The mixture was stirred on the hot-plate in room temperature for 2.5 hours and then then filtered using Whatman filter paper No. 1. The filtrate was concentrated in a rotary evaporator at 60°C. The resulting extracts were stored at −20°C until the analysis.

### *42.2. Total phenolic content*

Total phenolic content of methanolic extract obtained from *Astragalus flavescens* was determined using modified of microscale Folin-Ciocalteau's method described by Slinkard & Singleton with slight modifications [5]. Briefly, 20 µl of plant extract were mixed with 100 µl of Folin–Ciocalteu reagent and the mixture was incubated for 1 min in room temperature and then added of 80 µl of 7.5% (*w/v*) sodium carbonate. The mixture was allowed to stand for a further 30 min in the dark, and absorbance was measured at 760 nm. All measurements were carried out in triplicate and calculations were based on a calibration curve obtained with gallic acid. Total phenolic content was expressed as mg.g$^{-1}$ gallic acid equivalent using the equation obtained from the calibration curve y=0.00427×-0.0138, $R^2$=0.9987.

### *42.3. Trolox equivalent antioxidant capacity*

The ABTS radical scavenging activity was measured according to the method described by Re et al. [6] The ABTS stok solution (7mM) and 2.45 mM potassium persulphate were mixtured. The reaction mixture for to obtain the ABTS radical solution was left to stand at room temperature (16 h) in the dark before use. ABTS radical solution was diluted with 80 % ethanol, to give an absorbance value of ~0.70 at 734 nm.

For measuring ABTS radical scavenging activity 20 µl of the sample was mixed with 200 µl of the ABTS radical solution. Absorbance was monitored at 734 nm for 6 min. The decrease in absorption at 734 nm 6 min after addition of ABTS radical solution was used for calculating the TEAC (trolox equivalent antioxidant capacity). The total antioxidant activities were expressed as mM trolox equivalent antioxidant capacity (TEAC). All measurements were performed at least in triplicate. Trolox standards prepared in ethanol (80%) ranging from 100–500 µM. 80 % ethanol was used as blank in measurement.

### *42.4. DPPH free radical scavenging activity*

The DPPH radical scavenging activity was measured according to the method described by Brand-Williams [7] with slight modifications. DPPH (2,2'-diphenyl-1-picrylhydrazyl) stock solution was prepared by dissolving 12 mg in 50 ml 100% methanol and then stored at -20 $^{o}$C until needed. The working solution was obtained by mixing the stock solution (10 ml) with methanol (20 ml) to obtain an absorbance of 1.0 ± 0.02 units at 517 nm using the Multiscan Go Microplate reader (Thermo, USA). The methanolic extract of *Astragalus flavescens* (15 µl) and 200 µl DPPH were mixed and then shaked and followed by incubation at room temperature in the dark for 10 minutes. The decrease in absorbance in presence of DPPH was measured

at 517 nm. Trolox was used as a standard compound. A standard calibration curve is constructed for Trolox at 50-750 µM concentrations. TEAC (trolox equivalent antioxidant capacity) values were calculated by using the standard regression curve.

## 43. RESULTS AND DISCUSSION

The improved $ABTS^{+\cdot}$ method, described by Re et al. [6] was used to determine the antioxidant capacity for the plant species examined in this study. The concentration response curves for $ABTS^{+\cdot}$, as a function of five separetely prepared stock solutions of trolox standards (100, 150, 200, 250 and 500 µM) in terms of trolox equivalent antioxidant capacity (TEAC, mM trolox equivalent per g dry weight of plant). Similarly, concentration response curves for DPPH and TOC five and seven separetely prepared stock solutions of standards (Figure 1).

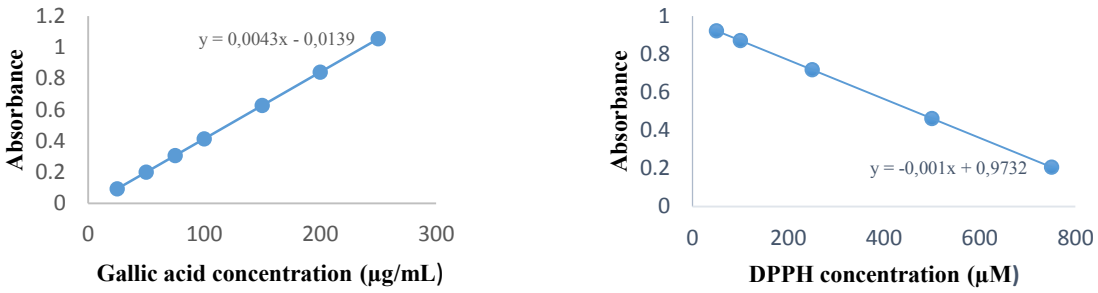


*Figure 1. Concentration-calibration curve for absorbance at 517 nm for DPPH as a function of standard trolox solution at 765 nm for gallic acid standard.*

There was a large variation in the antioxidant and free radical scavenging capacities of the aqueous and methanolic extracts of the plant material tested, as shown in Table 1. The results obtained from ABTS and DPPH assays were determined as 16.04±0.12; 4.85±0.23 for aqueous extracts and 10.10±1.06; 23.75±1.41 mM TE/g dry weight for methanolic extracts, respectively.

Total phenolic content (TOC) was estimated by Folin-Ciocalteu colorimetric method, based on the procedure of [9]. using gallic acid as a standard phenolic compound. A linear calibration curve of gallic acid, in the range 25-250 µg/mL with $r^2$ value of 0.9998, was constructed Figure 1. For methanolic extracts showed the total pheolic content of 29.12 mg gallic acid equivalent per g dry weight of test material.

*Table 7. Antioxidant capacity of A. flavescens extracts*

| Antioxidant capacity (mM TE/g dry weight)[a] | | | | Total phenolic content (mg GAE/g)[b] |
|---|---|---|---|---|
| ABTS | | DPPH | | |
| Aq.E | Met.E | Aq.E | Met.E | Met.E |
| **16.04±0.12** | **10.10±1.06** | **4.85±0.23** | **23.75±1.41** | **29.39±0.97** |

All data are shown as means ± SD from two extraction replicates, each run in dublicate.

Aq.E : Aqueous extracts

Met.E: Methanolic extracts

[a] Data are expressed as mM of trolox equivalents per g dry weight.

[b] Data are expressed as mg of gallic acid equivalents (GAE) per g dry weight.

*Astragalus flavescens* was proposed to be involved in activating blood and dissolving stasis, strengthening body resistance, supplementing qi, heat-clearing and detoxifying, removing dampness and receding jaundice. It may provide multi-channel, -level and -target prevention of and treatment for hepatic fibrosis [4].

These results suggested that the phenolic compounds contributed significantly to the antioxidant capacity of the investigated plant species. In many paper, a positive linear correlation between antioxidant capacity and total phenolic content [12] The Folin-Ciocalteu assay gives a crude estimate of the total phenolic compounds present in an extract. It is not specify to polyphenols, but many interfering compounds may react with the reagent, giving elevated apperent phenolic concentrations [13].

As stressed by Frenkel and Meyer, no single method is adequate for evaluating the antioxidant capacity of foods, since different methods can yield widely diverging results. Several methods based on

different mechanisms must be used [14]. Therefore, we investigated the antioxidant capacity both ABTS radical cation and DPPH free radical scavenging assays.

## ACKNOWLEDGMENT

The authors would like to thank our valuable B.Sc students Ms. Tuğba Tuhan, Merve Alparslan, Esma Özçeliker.

The study was supported by the project TAGEM/13-ARGE/43.

## REFERENCES

[111]. Davis, P. H. Flora of Turkey and East Aegean Islands; Edinburgh University Press: Edinburgh, 1970; *Vol. 4*, pp 49–254.
[112]. Tang, W.; Eisenbrand, G. *Chinese Drugs of Plant Origin*; Springer-Verlag: Berlin, 1992.
[113]. Verrota, L., El-Sebakhy, N. A. In *Studies in Natural ProductsChemistry*; Atta-ur-Rahman, Ed.; Elsevier: Amsterdam, 2001; Vol. 25, pp 179-234.
[114]. Li R, Dai G, Zhao M, Zhang Y, Hui L, Zhang X, Jin B. Preventative effect of *Astragalus flavescens* on hepatic fibrosis in rats and its mechanism of action. Experimental Therapeutical Medicine 2013 Oct; 6(4): 904–908.
[115]. Slinkard K., Singleton V.L. Total phenol analysis: automation and comparison with manual methods. American Journal of Enology and Viticulture, 28 (1977), pp. 49–55.
[116]. Re, R., Pellegrini, N. , Proteggente, A. , Pannala, A. , Yang, M. , Rice Evans, C. , (1999), Anti-oxidant activity applying an improved ABTS radical cation decolorization assay, Free Radic. Biol.Med., 26: 1231-1237.
[117]. Brand-Williams, W., Cuvelier, M.E. and Berset, C. 1995.Use of a free radical method to evaluate antioxidant activity, Lebensmittel-Wissenschaft und-Technologie/Food Science and Technology, 28:25-30.
[118]. Güner A, Özhatay N, Ekim T & Bafler KHC (2000). Flora of Turkey and the East Aegean Islands, Second Supplement Vol. 11. p. 656.Edinburgh: University Press.
[119]. Davis PH (ed.) (1965-1985). Flora of Turkey and the East Aegean Islands Vol. 1-9. Edinburgh: University Press.
[120]. Ekim T (2000). Herniaria L., In: Güner A, Ekim T, Özhatay N, Baser KHC, editors. Flora of Turkey and the East Aegean Islands (Suppl. 2), Vol. 11. Edinburgh, UK: Edinburgh University Press, pp. 5.
[121]. Afifi, F.U., Al-Khalidi, B., Khalil, E., (2005), Studies on the in vivo hypoglycemic activities of two medicinal plants used in the treatment of diabetes in Jordanian traditional medicine following intranasal administration, Journal of Ethnopharmacology, 100:314–318.
[122]. Prior R.L., Wu X, & Schaich K. 2005. Standardized methods for the determination of antioxidant capacity and phenolics in foods and dietary supplements. Journal of Agricultural and Food Chemistry. 53, 4290-1302.
[123]. Cai, Y. Luo Q, Sun M, Corke H. 2004. Antioxidant activity and phenolic compounds of 112 traditional Chinese medicinal plants associated with anticancer, Life Sciences, 74, 2157-2184.
[124]. Frankel EN., Meyer AS. The problems of using one-dimensional methods to evaluate multifunctional food and biological antioxidants. J. Sci. Food Agric 2000;80: 1925-41.

# Electromagnetic Harvesting Based on Pyramid Metamaterial Absorbers

*Mehmet Bağmanci[22], Muharrem Karaaslan[23], Zafer Özer, Emin Ünal*

***Abstract***

*The new metamaterial absorber (MA) based energy harvesting structure composed of pyramid inclusions is numerically presented and investigated in microwave frequency regime. The proposed harvesting mechanism has very simple configuration, scalability and three band responses. The operating frequency values include mobile communication frequencies, WIMAX, WLAN and satellite communications region. The absorption ratios for the proposed structure are higher than %90 for all resonance frequencies. Beside this, polarization (TE/TM) and incident angle independencies of the pyramid model are analysed for the same frequency ranges. The energy harvesting ratios of the system is investigated especially resonance frequencies i.e. maximum absorption frequencies. The energy harvesting potential of the pyramids are as good as the proposed structures in the literature. The proposed structure model can be used to gather widely used microwave signals in environment*

**Keywords: Energy harvesting, Multi-layered SSRs metamaterial absorber.**

## 44. INTRODUCTION

Metamaterials (MTMs) has unnatural properties and draw interest especially in the last decade by electromagnetic (EM) society. Due to their interesting electromagnetic characteristics resultant from the artificially tailored electric [1] and magnetic [2] responses, metamaterials have been used to obtain negative refraction [3], subwavelength image resolution [4, 5], and cloaking effects [6–8]. It is composed of artificial structures of which dimensions are much smaller than the applied signal wavelength. The properties of the metamaterial absorber, especially depends on the bandwidth and the dependency to the polarization of incident wave. Metamaterials can be adjusted to absorb energy for a specific region of the electromagnetic spectrum. The periodic inclusions can also be rearranged to restrain the electromagnetic energy perfectly. Realization of this duty, the imaginary parts of the permittivity and permeability could be manipulated to obtain a perfect absorption [9].

These metamaterial absorbers (MAs) can also provide polarization angle independency at multiple frequency ranges by arranging symmetrical with respect to centre of the structure [10–14]. Both the polarization and the incident angle insensitivity can be realized by these absorber structures [15]. With this adaptability characteristic of MAs, MAs can be useful for some kind of engineering application such as long distance radio communication, sensor, solar cell, medical imaging etc.[10–14]. In this study SSRs (Square Shape Resonator) based absorbers are utilized to provide multi-band absorption response [16]. Although SSRs can provide multiband response, band-width is not wide enough at resonance frequency due to resonance characteristics.

Hence the combination of SSR placed different substrate layers are designed to enhance absorption band and efficiency in this study.

## 45. DESIGN AND NUMERICAL SETUP OF PROPOSED STRUCTURE

In this study, we simulated a structure to get a multi-band layered MA and to investigate the harvesting capability. The proposed structure has three SSRs on three different layers of dielectric substrate which are used to achieve resonance at three different- frequencies. The number of the resonance frequencies provide resonances depending on the number of the different resonators [17]. The resonance number is directly related with number of resonators, gaps, orientation of gaps and dimensions. [18]

MSRR inclusions and unit cell is shown in Fig. 1(a) and Fig. 1(b), respectively. The proposed structure is assigned on FR4 ($\varepsilon$ = 4.3 and tan $\delta$ = 0.025) substrate. The metal film designed as MSSRs is copper with an electric conductivity of $5.8 \times 10^7$ S/m.

[1]*Iskenderun Technical University, Department of Electrical and Electronics Engineering, Iskenderun, Hatay 31200, Turkey, mbagmanci88@gmail.com*

[2]*Iskenderun Technical University, Department of Electrical and Electronics Engineering, Iskenderun, Hatay 31200, Turkey, muharrem.karaaslan@iste.edu.tr*

The size and thickness of each SSR of the proposed structure are presented in Table 1. Each resonator possess two gaps with equal dimensions with a width of 1 mm. the dimensions of each resonator in Table 1 is determined by using parametric sweep to obtain high absorption ratio at a certain frequency.

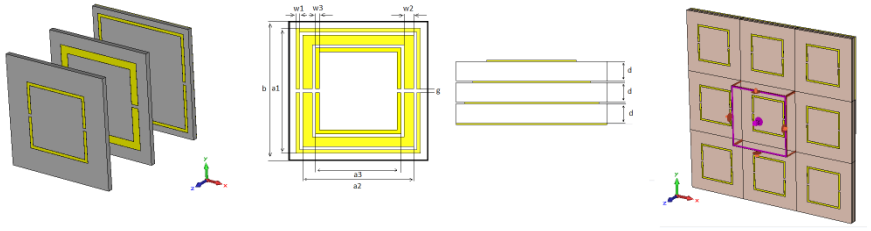

*(a)* *(b)* *(c)*

*F . 1 ( ) F b , (b) l z h SSR l ' h k ( ) l p with unit cell boundary conditions*

*Table 1-Typical size of Structure*

| | | |
|---|---|---|
| Bottom SSR(mm) | a1 =33 | w1=1 |
| Middle SSR(mm) | a2 =29 | W2=2.5 |
| Top SSR(mm) | a3 =22 | w3=1 |
| Others(mm) | b=37 | d=1.6 |
| | g=1 | Copper Thickness=0.035 |

## 46. SIMULATION RESULTS AND DISCUSSION

In this study, the simulations are realized by using Finite Integration Technique (FIT) to obtain the absorption mechanism. The boundary conditions are assigned as unit cell x, y directions and open (add space) z direction. In Fig. 1 (c), the proposed MA structure to achieve energy harvesting is presented. The frequency absorption properties of structure (A (w)) can be evaluated by the equation; A (w) =1-R (w)-T (w). In order to increase the absorption ratio of structure both reflection R (w) =$|S_{11}^2|$ and transmission T (w) =|S212| must be decreased at the resonance frequency band. The transmission ratio is vanish due to the blocking metallic plate located at back side of structure as shown in Fig. 1(a) Hence, evaluation of the absorption is only dependent to the the reflection S11 parameter. Therefore, the optimization and simulation results of the MSSRs structure is realized with the absorption equation A(w)=1-R(w) where |S212|=0 since T(w)→0.

The frequency response of each SSRs on different dielectric layer is investigated to observe their behaviours separately as shown in Fig. 2.

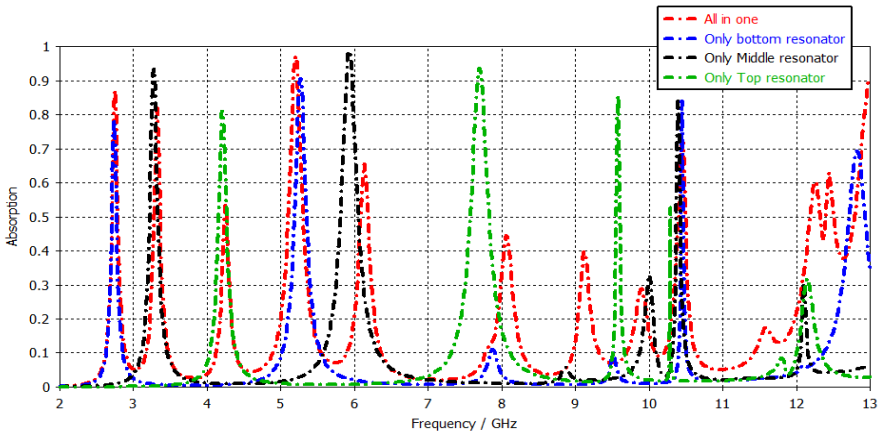


*Fig. 2 The resonance frequency of top, middle, bottom resonator and the actual frequency of all resonators on one dielectric*

The resonance frequencies of the only bottom resonator are 2.8 GHz, 5.4 GHz and 10.5 GHz with absorption coefficients of 0.8, 0.9 and 0.85, respectively. Each resonance frequency of the suggested structure is in conventional range, such as GSM, WIMAX and satellite communications. The resonance frequencies are low due to the higher dimensions of the bottom resonator with respect to the wavelength of incident angle. The resonance frequencies of the middle resonator are 3.4 GHz, 6GHz and 10.5 GHz with absorption coefficients of 0.95, 0.98 and 0.83, respectively. The resonance frequency of the middle

resonator shift to the higher frequency due to wavelength effects. The first resonance frequency of the top resonator is at higher value (4.2 GHz) due to lower dimensions. The two other resonances are 7.7GHz and 9.6 GHz with absorption values of 0.94 and 0.85, respectively. The combination of the overall structure includes three resonators in one layer has resonances in almost all resonance frequencies of individual resonator. Hence combined structure can be used as an absorber for all conventional communication frequencies.

The absorption response of the three resonator structure on three layer and three resonators on the same layer with the same size as presented in Table-1 is demonstrated in Fig. 3. Since we aim to realize a structure with an absorption characteristic for WIMAX, WLAN and satellite communications ranges , we firstly investigated these operating frequencies. The three layered structure has better absorption properties and bandwidth according to three resonator systems on one layer. The resonance frequencies and absorption rates of the suggested structure are 92.36% at 2.62 GHz, 90.90% at 5.03 GHz, 99.41% at 10.54 GHz, 86.14% at 2.14 GHz, 99.45% at 6.19 GHz, 86.13% at 7.98 GHz and 89.22% at 9.05 GHz. The resonance frequencies of the structure can be used to absorb all conventionally used frequencies in environmental. Hence the three layered structure has an impressive potential for harvesting of EM energy for WIMAX range with 92.36% at 2.62 GHz and 86.14% at 2.14 GHz for WIFI range with 90.90% absorption at 5.03 GHz and for direct broadcast satellite services with 99.41% absorption at 10.54 GHz.

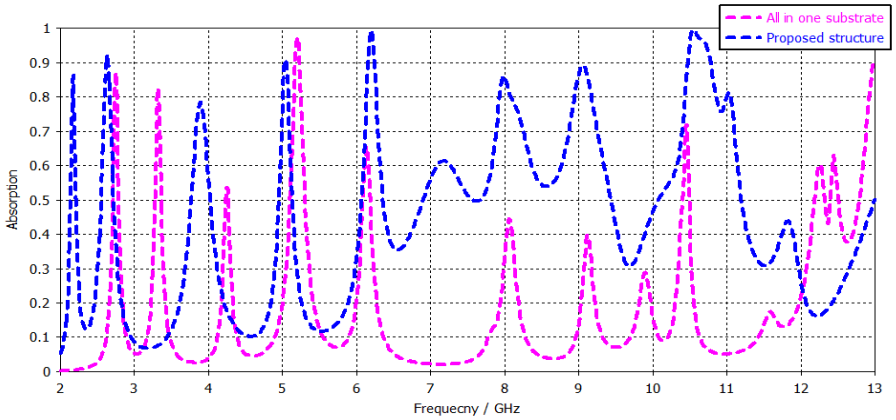


*Fig. 3 All in one substrate and proposed structure comparison.*

The angle dependency of three layer resonator based absorber structure is also investigated by changing phi angle between $0^o$ and $45^o$. the polarization angle response of the suggested structure is revealed in Fig.4. The proposed structure shows almost angle independency with respect to the phi angle. This is due to the centre symmetry of the proposed configuration.

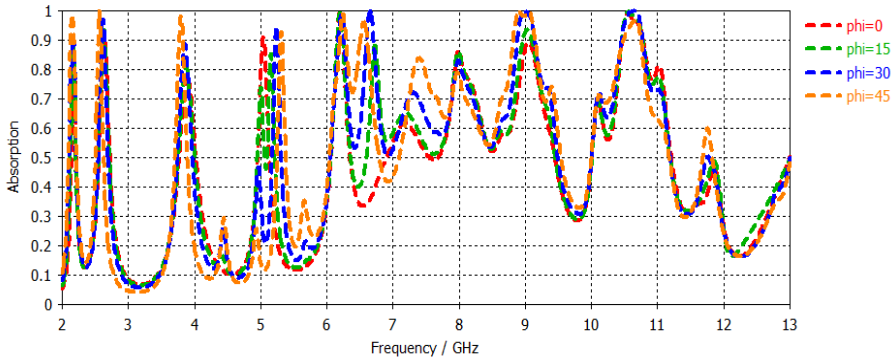


*Fig. 4 Response of polarization angle independency of structure*

## 47. CONCLUSION

The new metamaterial absorber based energy harvesting structure composed of inclusion of pyramid inclusions is numerically presented and investigated in microwave frequency regime. According to the results of numerical simulations, the proposed structure shows and maintains perfect absorption characteristics both two-layered SSRs and three layered SSRs case for WIMAX, WLAN and satellite communications region and it can be used for harvesting in for the same frequency ranges. Proposed structure is also polarization insensitive. After all, proposed structure could be utilized more to be a good candidate for several engineering applications such as spectroscopic imaging, medical imaging, sensor and so on.

## REFERENCES

[125]. J. B. Pendry, A. J. Holden, W. J. Stewart, and I. Youngs, "Extremely low frequency plasmons in metallic mesostructures," Physical Review Letters, Vol. 76, No. 25, 4773–4776, Jun. 1996.
[126]. J. B. Pendry , A. J. Holden, D. J. Robbins, and W. J. Stewart, "Magnetism from conductors and enhanced nonlinear phenomena," IEEE Transactions on Microwave Theory and Techniques, Vol. 47, No. 11, 2075–2084, Nov. 1999. Progress In Electromagnetics Research B, Vol. 14, 2009 427
[127]. R. A. Shelby, D. R. Smith, S. Schultz, "Experimental verification of a negative index of refraction," Science, Vol. 292, No. 5514, 77–79, Apr. 2001.
[128]. J. B. Pendry, "Negative refraction makes a perfect lens," Physical Review Letters, Vol. 85, No. 18, 3966–3969, Oct. 2000.
[129]. A. Grbic and G. V. Eleftheriades, "Overcoming the diffraction limit with a planar left-handed transmission-line lens," Physical Review Letters, Vol. 92, No. 11, Mar. 2004.
[130]. J. B. Pendry, D. Schurig, and D. R. Smith, "Controlling electromagnetic fields," Science, Vol. 312, No. 5781, 1780–1782, Jun. 2006.
[131]. D. Schurig, J. J. Mock, B. J. Justice, S. A. Cummer, J. B. Pendry, A. F. Starr, and D. R. Smith, "Metamaterial electromagnetic cloak at microwave frequencies," Science, Vol. 314, No. 5801, 977– 980, Nov. 2006.
[132]. H. S. Chen, B. I.Wu, B. Zhang, and J. A. Kong, "Electromagnetic wave interactions with a metamaterial cloak," Physical Review Letters, Vol. 99, No. 6, Aug. 2007.
[133]. L. Huang, H. Chen : Multi-band and polarization insensitive metamaterial absorber. Prog. Electromagn. Res. 113, 103–110 (2011)
[134]. C. Sabah, F. Dincer, M. Karaaslan, E. Unal, O. Akgol, E. Demirel : Perfect metamaterial absorber with polarization and incident angle independencies based on ring and cross-wire resonators for shielding and a sensor application Optics Communications 322, 137-142
[135]. F. Dincer, O. Akgol, M. Karaaslan, E. Unal, C. Sabah : Polarization angle independent perfect metamaterial absorbers for solar cell applications in the microwave, infrared, and visible regime. Prog. Electromagn. Res. 144, 93–101 (2014)
[136]. F. Dincer, M. Karaaslan, E. Unal, K. Delihacioglu, C. Sabah: Design of polarization and incident angle insensitive dual-band metamaterial absorber based on isotropic resonator. Prog. Electromagn. Res. 144, 123–132 (2014)
[137]. F. Dincer, M. Karaaslan, E. Unal, O. Akgol, E. Demirel, C. Sabah ; Polarization and angle independent perfect metamaterial absorber based on discontinuous cross-wire-strips Journal of Electromagnetic Waves and Applications 28 (6), 741-751
[138]. F. Dincer, O. Akgol, M. Karaaslan, E. Unal, C. Sabah : Polarization angle independent perfect metamaterial absorbers for solar cell applications in the microwave, infrared, and visible regime Progress In Electromagnetics Research 144, 93-101
[139]. O.M. Ramahi, T.S. Almoneef, M. Alshareef, M.S. Boybay : Metamaterial particles for electromagnetic energy harvesting. Appl. Phys. Lett. 101, 173903-1-5 (2012)
[140]. O. T. Gunduz, C. Sabah : Polarization angle independent perfect multiband metamaterial absorber and energy harvesting application
[141]. C. Sabah : Multiband metamaterials based on multiple concentric open-ring resonators topology. IEEE J. Sel. Top. Quantum 19, 8500808-1-8 (2013)
[142]. C. Sabah : Novel dual-band, single and double negative metamaterials:nonconcentric delta loop resonators. Prog. Electromagn. Res. 25, 225–239 (2010)

# Metamaterial Based Absorber Design

*Muharrem Karaaslan[24], Mehmet Bağmancı[25],Emin Ünal*

***Abstract***

*In this study, a new type of metamaterial absorber composed of gammadion and square inclusions are numerically investigated in microwave range by using finite integration technique based EM solver. This absorber can be easily fabricated and has good absorption characteristic at two different frequency bands. This resonance frequencies are around 3GHz and 6 GHz which are important for telecommunication technologies. The absorption levels at these frequencies are around %90. Incident angle and polarization effects on absorption ratios are also investigated for the same resonance frequencies. The proposed structure performance can be used for stealth technology and new generations of solar cells.*

**Keywords: Energy harvesting, Multi-layered SSRs metamaterial absorber.**

## 48. INTRODUCTION

Metamaterials (MTMs) has important application areas in the last decade by electromagnetic (EM) community. It demonstrate unnatural properties in electric [1] and magnetic [2] responses. Hence it is used to produce negative refraction [3], subwavelength image resolution [4, 5], and cloaking effects [6–8]. The novel properties of MMs stem from the artificial inclusions which can be adopted in the electric and magnetic response. MMs can be defined as effective medium with negative permittivity (ε) and permeability (μ), simultaneously [9]. the researches on MTMs has focused on the real parts of permittivity (ε) and permeability (μ), and characteristically it is desirable to reduce the loss represented by the imaginary parts of ε and μ [10]. But loss in MTMs can be used to create convenient phenomena and devices. Recently, Landy et al. have suggested a thin metamaterial absorber (MA), in which electric and magnetic field sustain resonance and absorber has matched impedance with incident medium to minimize the reflection, so the proposed structure strongly absorbs the incident wave [11].This area is enlarged and , many different types of MAs have been realized from microwave to optical frequencies. But absorption bandwidth of typical structure is around 10% at resonance frequencies. The enlargement of the absorption band is the main task to make the MA units resonate at several neighbour frequencies [12, 15]. Mostly,MAs includes a processed metal film above homogeneous metal film with a dielectriclayer . Although some studies have been made to extend the absorption band of MAs, absorption band is not wide enough or the absorption spectra are composed of discontiguous absorption peaks [16].

## 49. DESIGN AND NUMERICAL SETUP

we investigated a wide band structure in the microwave frequency range. The proposed structure consist of multi-layered metallic-dielectric truncate cones. The proposed structure is shown in Fig. 1(a), which consist of a periodic array of twenty truncate cones with metal film as the ground to block transmission wave. A unit cell of the proposed structure is shown in Fig. 1(b). The cone type inclusions is chosen to realize angular independency. A truncate cone with 20 metal films of which width tapered linearly to obtain wide band

absorption characteristics. All metal film layers are separated by dielectric layer. Copper is choosen as metal in structure with an electrical conductivity of σ=5×107s/m. FR4 is the dielectric layer with relative permittivity of $\epsilon_r$= 4.3 and loss tangent of tan δ = 0.025. The suitable dimensions of the structure are investigated by parametric study.

[1]*Iskenderun Technical University, Department of Electrical and Electronics Engineering, Iskenderun, Hatay 31200, Turkey, muharrem.karaaslan@iste.edu.tr*

[2]*Iskenderun Technical University, Department of Electrical and Electronics Engineering, Iskenderun, Hatay 31200, Turkey, mbagmanci88@gmail.com*

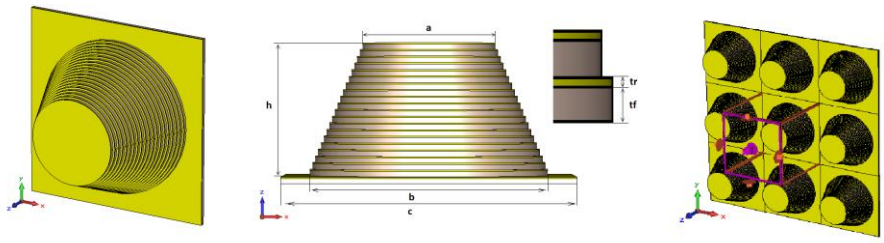


*(a)* *(b)* *(c)*

*Fig. 1 (a) schematic of the proposed structure, (b) typical size of the truncate cone and thickness of layers and (c) simulation setup with unit cell boundary conditions. The optimized dimensions of a unit a=5 mm, b=8.99 mm, c=11mm, h=5mm, tr=0.05mm (copper film thickness) and tf=0.2mm (Fr-4 layer thickness).*

## 50. SIMULATION RESULTS AND ASSESSMENT

In this study, the simulations are achieved by CST Microwave Studio based on Finite Integration Technique. A numerical simulation is used for the structure to investigate reflection and absorption properties as shown in Fig. 1(c). Periodic boundary conditions are assigned along x and y directions and open (add space) boundary condition along z direction along which the plane wave is incident toward on the structure. The electric field polarization is along y-direction (TE) as the incident source component. The absorption value (A (w)) in the frequency band can be evaluated by the equation; A (w) =1-R (w)-T (w). Maximization of the absorption ratio can be realized by minimizing both reflection R (w) $=|S_{11}^2|$ and transmission T (w) $=|S_{21}^2|$ coefficients at the resonance frequency range. The transmission coefficient is nearly zero due to the the metallic plate located at its back side in Fig. 1(a), Therefore the absorption coefficient is only effected by reflection ratio with S11 parameter. So, the absorption is evaluated by simplified equation A (w) =1-R (w) where $|S_{21}^2|=0$ since T (w) $\rightarrow 0$. Absorption and reflection characteristic of the proposed structure is shown in Fig. 2.

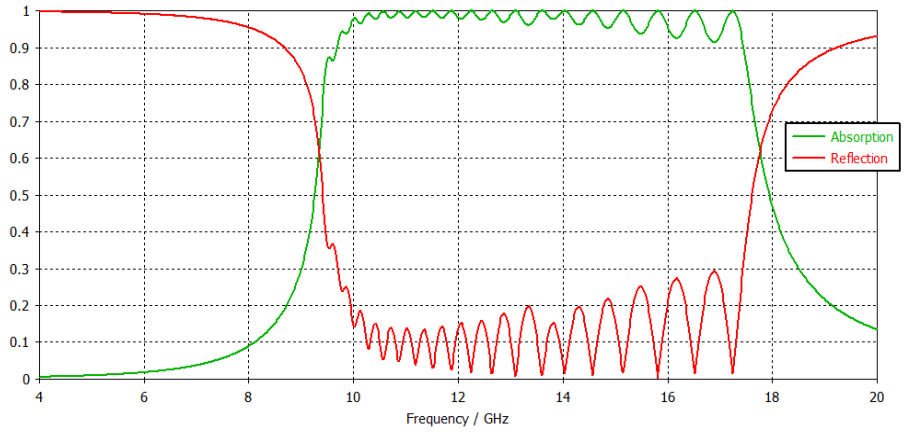


*Fig. 2 Absorption and reflection graph of proposed structure*

## 51. CONCLUSION

In conclusion, a wide band absorber is realized and utilized as an harvesting device of electromagnetic energy in a RF spectrum, it is also researched to obtain for stealth applications of military radars. In respect of the the numerical results, the suggested structure have perfect absorption characteristic with 90% absorptivity in the frequency range of 9.68- 17.45 GHz and 95% in the frequency range of 9.91-14.86 GHz with a good harvesting characteristics. Proposed structure demonstrate polarization and angular independency for all angles of TE and TM incident case . As a result proposed structure exhibits different and specific characteristics with respect to the other broad band structures in literature.

## REFERENCES

[143]. J. B. Pendry, A. J. Holden, W. J. Stewart, and I. Youngs, "Extremely low frequency plasmons in metallic mesostructures," Physical Review Letters, Vol. 76, No. 25, 4773–4776, Jun. 1996.
[144]. J. B. Pendry, A. J. Holden, D. J. Robbins, and W. J. Stewart, "Magnetism from conductors and enhanced nonlinear phenomena," IEEE Transactions on Microwave Theory and Techniques, Vol. 47, No. 11, 2075–2084, Nov. 1999. Progress In Electromagnetics Research B, Vol. 14, 2009 427
[145]. R. A. Shelby, D. R. Smith, and S. Schultz, "Experimental verification of a negative index of refraction," Science, Vol. 292, No. 5514, 77–79, Apr. 2001.
[146]. J. B. Pendry "Negative refraction makes a perfect lens," Physical Review Letters, Vol. 85, No. 18, 3966–3969, Oct. 2000.
[147]. A. Grbic, and G. V. Eleftheriades, "Overcoming the diffraction limit with a planar left-handed transmission-line lens," Physical Review Letters, Vol. 92, No. 11, Mar. 2004.
[148]. J. B. Pendry, D. Schurig, and D. R. Smith, "Controlling electromagnetic fields," Science, Vol. 312, No. 5781, 1780–1782, Jun. 2006.
[149]. D. Schurig, J. J. Mock, B. J. Justice, S. A. Cummer, J. B. Pendry, A. F. Starr, and D. R. Smith, "Metamaterial electromagnetic cloak at microwave frequencies," Science, Vol. 314, No. 5801, 977– 980, Nov. 2006.
[150]. H. S. Chen, B. I. Wu, B. Zhang, and J. A. Kong, "Electromagnetic wave interactions with a metamaterial cloak," Physical Review Letters, Vol. 99, No. 6, Aug. 2007.
[151]. D. R. Smith, J. B. Pendry," Homogenization of metamaterials by field averaging", J. Opt. Soc. Am. B 23, 391 (2006).
[152]. N. I. Zheludev, " The Road Ahead for Metamaterials",Science 328, 582 (2010).
[153]. N. I. Landy, S. Sajuyigbe, J. J. Mock, D. R. Smith and W. J. Padilla, Phys. Rev.Lett. 100, 207402 (2008).
[154]. C. Sabah, F. Dincer, M. Karaaslan, E. Unal, O. Akgol, E. Demirel : Perfect metamaterial absorber with polarization and incident angle independencies based on ring and cross-wire resonators for shielding and a sensor application Optics Communications 322, 137-142
[155]. F. Dincer, O. Akgol, M. Karaaslan, E. Unal, C. Sabah : Polarization angle independent perfect metamaterial absorbers for solar cell applications in the microwave, infrared, and visible regime. Prog. Electromagn. Res. 144, 93–101 (2014)
[156]. F. Dincer, M. Karaaslan, E. Unal, , K. Delihacioglu, C. Sabah : Design of polarization and incident angle insensitive dual-band metamaterial absorber based on isotropic resonator. Prog. Electromagn. Res. 144, 123–132 (2014)
[157]. F. Dincer, M. Karaaslan, E. Unal, O. Akgol, E. Demirel, C. Sabah : Polarization and angle independent perfect metamaterial absorber based on discontinuous cross-wire-strips Journal of Electromagnetic Waves and Applications 28 (6), 741-751
[158]. Y. Q. Ye, Y. Jin, and S. L. He, " "Omnidirectional, polarization-insensitive and broadband thin absorber in the terahertz regime", J. Opt. Soc. Am. B 27, 498 (2010).
[159]. F. Ding, Y. Cui, X. Ge, F. Zhang, Y. Jin, and S. He : Ultra-broadband Microwave Metamaterial Absorber
[160]. O. T. Gunduz, C. Sabah : Polarization angle independent perfect multiband metamaterial absorber and energy harvesting application

# A Comparative Design of the Surface Mounted Permanent Magnet Synchronous Motors

*Mümtaz MUTLUER*[26]

***Abstract***

*Permanent magnet synchronous motors are recently popular in industrial fields. These motors enable different applications with great precision and efficiency through their structural features. It needs to provide a good design approach to provide a high-performance permanent magnet synchronous motor. So in this study, the surface mounted inner and outer rotor permanent magnet synchronous motors were investigated. A number of stator slots per pole and per phase were selected to achieve high efficiency. Analytical designs were made and then to evaluate the optimal geometric parameters genetic algorithm was used. The obtained results were compared with each other and the results were sufficient. This study contains useful comparisons for motor designers and industry eventually.*

**Keywords:** design optimization, genetic algorithm, inner rotor, outer rotor, permanent magnet synchronous motor

## 52. INTRODUCTION

Electric motors are one of the largest energy consumers. Therefore, the energy efficiency of the electric motors is very important. The design studies on electric motors have focused on efficiency [1]. In this case, the design that should be done by selecting the structure of the energy efficient motors is of great importance.

Permanent magnet synchronous motors (PMSMs) have compact structures, high torque/volume ratio and efficiency. One of the most important advantages of the PMSMs is also no need the gearbox [2]. PMSMs have different structures in reviews and in many industrial fields. In low-speed applications, the most popular motor is the surface mounted PMSM with inner rotor, so that the permanent magnets can be protected from centrifugal forces. But for high speed the inner rotor structure are not suitable [3]. The most appropriate ones are the outer rotor PMSM. Moreover power density of them based on the diameter of the air gap is greater. However the stator winding of outer rotor PMSM is a disadvantage because of thermal considerations. Production costs of the surface mounted PMSMs with inner rotor and outer rotor are lower than the other PMSMs because of their simple design features. In the surface mounted motors, inner rotor and outer windings contributes cooling but of weakness of power density, on the other hand outer rotor and inner windings contributes power density but of weakness of cooling.

In order to benefit from the design optimization, sufficient design parameters should be chosen. These variables may be generally geometrical parameters. Another issue with the design parameters is about objective of the design optimization. Surely, the objective function determines the number and the kinds of the parameters.

The stochastic methods have been used for engineering optimization problems in recent years. They search the great solution space very rapidly and they often convergence the global results [1], [4], [5]. One of the optimization methods is genetic algorithm may be the most popular. The most outstanding aspects of these methods are that the initial solution or population do not require. But the objective function of the optimization problem should be established very carefully to be used in the method. The objectives of the design optimization of the PMSMs are especially to minimize the torque harmonics and the weight of the motor or to maximize the efficiency and torque/volume ratio of the motor [4]-[7].

This paper proposes the designs of the surface mounted PMSMs for the certain slot number per pole and per phase. Then to increase the efficiency of the motors the design optimization of them was investigated with the genetic algorithm. Therefore pre-analytical design equations based on the geometrical design parameters were firstly obtained. Then the genetic algorithm was run to provide the optimal efficiency values. Finally, the obtained efficiency results and the analytical results were compared by using tables or graphics. The results are absolutely acceptable and useful.

## 53. DESIGN PARAMETERS OF THE PMSM AND THE OBJECTIVE FUNCTION

The placement of the permanent magnets in the surface mounted PMSMs, the stator slot number per pole per phase and the stator windings schemas are the significant issues for the design. In this study, the investigated PMSMs are the surface mounted, the number of stator slots per pole per phase is 0,4 and 12/10, 24/20, and 36/30 slot/pole numbers, and the winding layout is the double layer concentrated winding. Therefore the geometric, electrical and magnetic properties of the surface mounted PMSMs herein are generally similar. In this case the most important point for different stator slots and pole numbers of the surface mounted PMSMs is to examine the efficiency. Winding layout for 12/10 slot/pole numbers was shown in Figure

[26]*Corresponding author: Necmettin Erbakan University, Department of Electrical and Electronics Engineering, 42090, Meram/Konya, Turkey. mmutluer@konya.edu.tr*

1 and for the other motors it is periodically. The winding factor that is an effective value for the motor performance and it is 0,933 [2], [8].

$$\begin{array}{c|c|c|c|c|c|c|c|c|c|c|c|c} SLOTS & 1 & 2 & 3 & 4 & 5 & 6 & 7 & 8 & 9 & 10 & 11 & 12 \\ \hline COILS & \overbrace{C'A} & \overbrace{A'A'} & \overbrace{AB'} & \overbrace{BB} & \overbrace{B'C} & \overbrace{C'C'} & \overbrace{CA'} & \overbrace{AA} & \overbrace{A'B} & \overbrace{B'B'} & \overbrace{BC'} & \overbrace{CC} \end{array}$$

*Figure 5.Winding layout for 12/10 slot/pole number*

### *53.1. The Geometric Parameters*

An electric motor design is a nonlinear study and there are a lot of geometric parameters. Some of these parameters are the dependent variables while others are the independent variables and constants. Therefore, the selection of the parameters which will affect the obtained efficiency is important in terms of ease and accuracy of the design. These variables for each PMSM were selected as the rotor diameter for the inner rotor or stator diameter for outer rotor $D_{rc}$, magnet thickness $l_m$, air gap length $\delta$, slot wedge height $h_{sw}$, stator tooth width $b_{ts}$, stator slot height $h_{ss}$, ratio of the slot opening over the slot width $k_{open}$ [2], [4]. The two dimensional geometries of the PMSMs were given for the motors have 12/10 slot/pole numbers in Figure 2.

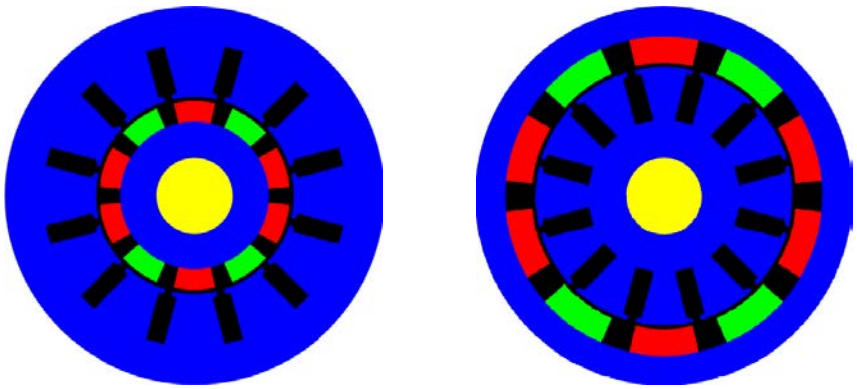

*Figure 2.Two dimensional geometries of the PMSMs*

### *53.2. The Invariable Parameters*

The diameter and the stack length are identical as well as the half pole angle, these quantities are constraints. For each motor the outer diameter is 322mm, the stack length is 120mm, and the pole angle is 126°.

Other quantities for each PMSM such as the supply, power and speed values are 340V, 2400W, and 250rpm. The remanence flux density and the relative permeability of the permanent magnets are 1.2T and 1.03.

### *53.3. The Objective Function*

Permanent magnet synchronous motors have three torque terms in Equation 1. The last term is mutual torque that is desired for PMSMs. The others are parasitic components. On the other hands the current of the motor affects the copper losses namely the efficiency [8].

$$T = \frac{1}{2} i^2 \frac{dL}{d\theta} - \frac{1}{2} \phi^2 \frac{d\mathcal{R}}{d\theta} + Ni \frac{d\phi}{d\theta} \quad (1)$$

where, $i$ is motor current, $L$ is self inductance, $\phi$ is magnet flux, $\mathcal{R}$ is reluctance, and $N$ is coil number.

A primitive performance indicator is described as motor constant which is the ratio of the torque to the copper losses in Equation 2. This ratio in inner rotor PMSM is 1.19 for 12/10 slot/pole number and 1.37 for 24/20 slot/pole number [8].

$$K_m = \frac{T}{\sqrt{3I^2 \times R_{Cu}}} \quad (2)$$

To obtain the objective function namely the efficiency, copper and iron losses of the motor were calculated by using the other design parameters. The efficiency equation was acquired as follows.

$$P_{out} = T \times \omega_{mech} \quad (3)$$

$$P_{Cu} = 3I^2 \times R_{Cu} \quad (4)$$

$$P_{Fe} = P_h + P_e \quad (5)$$

$$\eta = \frac{P_{out}}{P_{out} + P_{Cu} + P_{Fe}} \times 100\% \quad (6)$$

where, $\omega_{mech}$ is mechanical angular velocity, $P_{out}$ is output power, $P_{Cu}$ is copper loss, $P_{Fe}$ is iron loss, and $\eta$ is efficiency of the permanent magnet motor.

## 54. THE GENETIC ALGORITHM

The basic principle of the genetic algorithms is to select the best individuals. Genetic algorithms (GAs) do not produce only one solution to solve the optimization problem. Instead, the endeavor performance is a finding the optimal solution of the optimization problem in the search space. Thanks to these features as soon as genetic algorithms can scan a very large solution space. As a structural in genetic algorithms, populations are composed of individuals are independently of each other, the individuals are composed of genes which includes the solution of the problem. Every individual in the population is a solution of the optimization problem. Population size and the number of genes directly are related to the input parameters [1], [4].

In GAs the moving of genetic characteristics of individuals to the future populations is provided by using the fitness function. The individuals which high fitness values will be effective in the development of the current population and the weak individuals will remain outside. This situation occurred in each iteration will provide to converge to the optimum solution in GAs.

Genetic algorithms do not guarantee to find the optimal solution. However, the GAs may converge to a local solution. But also they do not require the solution of the initial solution. Genetic algorithms have reproduction, crossover and mutation operators. The reproduction chooses the individuals with high fitness values to continue the struggle for life by using roulette wheel, tournament or other selection criteria. Crossover operator exchanges the genes of the selected two individuals at random. Mutation operator changes randomly the string's bit from a "1" to a "0" or vice versa. In this way, the convergence of the algorithm to the local solutions is prevented. The common flowchart of the genetic algorithm is shown in Figure 3.

*Figure 3.Flowchart of the genetic algorithm*

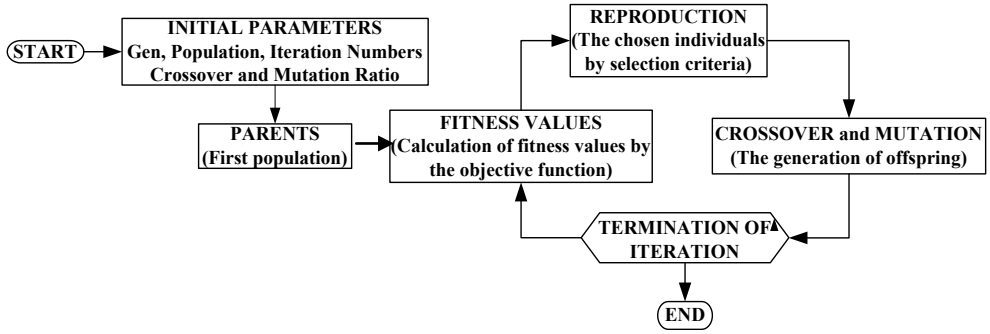


## 55. THE DESIGN

## APPLICATION AND THE EVALUATION OF THE RESULTS

First of all, this study notes to make some assumptions about the design optimization. These are that the mechanical strength, thermal loadability, manufacturability, and the armature reaction have been neglected. At the same time the only constraints are the saturation on the stator teeth and stator and rotor yokes. The constraints are 1.6T for the teeth and 1.2T for the yokes which are small by the normal standards. The design parameters were mentioned as geometric parameters.

Pre-analytical design was firstly made for each motor. The outer diameter of the motor is kept constant and the dimensions of the stator teeth, the stator yoke and the rotor yoke value were adjusted according to saturation. The efficiency, ohmic loss, and iron losses results were given in Table 1. The investigated motors have very high efficiency but the external rotor PMSMs which has 12 slots and 10 poles is generally more efficient. However it is may be said that, for the same stator slot number per phase and per pole, while the slot number and the pole number of the inner or the outer PMSM decreases the efficiency increases. Changes in ohmic loss are not very effective, but the frequency is directly proportional to the number of the motor poles. Therefore, the number of poles increases iron losses vary significantly.

*Table 8.Pre-analytical design results*

| PMSMs | Slot/Pole Numbers | Ohmic Loss (W) | Iron Losses (W) | Efficiency (%) | $K_m$ |
|---|---|---|---|---|---|
| Inner Rotor | 12/10 | 69.3 | 63.7 | 94.75 | 1.32 |
| Inner Rotor | 24/20 | 40.7 | 133.9 | 93.22 | 2.25 |
| Inner Rotor | 36/30 | 33.6 | 210.8 | 90.76 | 2.73 |
| Outer Rotor | 12/10 | 79.4 | 41.7 | 95.20 | 1.15 |
| Outer Rotor | 24/20 | 47.4 | 79.0 | 95.00 | 1.93 |
| Outer Rotor | 36/30 | 37.7 | 123.9 | 93.69 | 2.43 |

Then the genetic algorithm for the design optimization was run five times to obtain the reliable results. For the genetic algorithm, the population number, iteration number, crossover ratio, and mutation ratio was chosen 25, 25, 0.85, and 0.01 respectively. Iteration number was assigned as the termination criterion of each run. The genetic algorithm has binary codes and each gene was composed of ten bits. The design optimization studies were made for only motors which have 12/10 slot/pole numbers and the obtained efficiency, ohmic loss, and iron losses results were compared with the analytical results Table 2.

*Table 2.Design optimization results*

| PMSMs | Slot/Pole Numbers | Ohmic Loss (W) | Iron Losses (W) | Efficiency (%) | $K_m$ |
|---|---|---|---|---|---|
| Inner Rotor | 12/10 | 76.5 | 39.7 | 95.37 | 1.20 |
| Outer Rotor | 12/10 | 82.0 | 36.7 | 95.29 | 1.12 |

Industrial manufacturability of the PMSMs was neglected in the genetic algorithm results. The efficiency of the external rotor PMSMs did not notably improve, but the inner rotor PMSM improved because of the constraints of the design parameters. The analytical and the optimization efficiency results are 94.75% and 95.37% for the inner rotor and 95.20% and 95.29% for the outer rotor. The genetic algorithm may be fallen in a local solution that is absolutely weakness. The graphics of the genetic algorithms were shown in Figure 4.

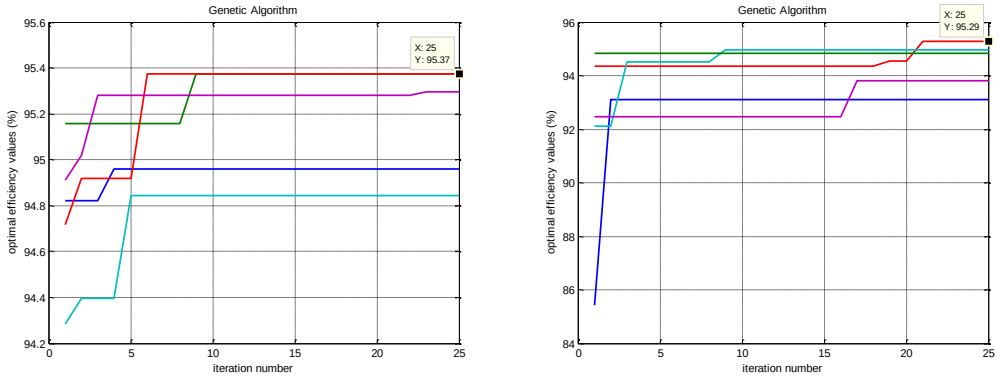


*Figure 4.The graphics of the genetic algorithms*

The motor constant of the inner rotor PMSM has 12/10 slot/pole numbers was mentioned as 1.19. In the analytical design this value was calculated as 1.32 and then in the optimization it is evaluated as 1.2. This value is very close to the reference value. This is the benefit of the optimization and the machine is closer to the ideal design values. The motor constant of the outer rotor PMSM changed from 1.15 to 1.12.

## 56. CONCLUSION

The design optimization of the surface mounted PMSMs with inner rotor and outer rotor were investigated by pre-analytical design and then by using genetic algorithm. The obtained results for the same fractional slot motors, namely for the same stator slot number per pole and per phase, show that if the slot and pole numbers for the constant external PMSM diameter decreases the efficiency of the PMSM increases. The ohmic loss is more important in the low pole numbers and the iron losses are more important in the large pole numbers. Eventually, the design optimization study of the permanent magnet synchronous motor is satisfactory.

## ACKNOWLEDGMENT

This study is supported by The Coordinator of Scientific Research Projects of Necmettin Erbakan University.

## REFERENCES

[161]. B. N. Cassimere, S. D. Sudhoff, “Population-based design of surface-mounted permanent-magnet synchronous machines,” IEEE TRANSACTIONS ON ENERGY CONVERSION, VOL. 24, NO. 2, JUNE 2009.
[162]. F. Libert, J. Soulard, “Design study of a direct-driven surface mounted permanent magnet motor for low speed application,” in Proceedings of Symposium on Advanced Electromechanical Motion Systems (Electromotion), 2003.
[163]. F. Libert, J. Soulard, “Design study of different direct-driven permanent-magnet motors for a low speed application,” in Proceedings of the Nordic Workshop on Power and Industrial Electronics (NORpie), 2004.
[164]. M. Mutluer, O. Bilgin, “Design optimization of PMSM by particle swarm optimization and genetic algorithm,” in International Symposium on Innovations in Intelligent Systems and Applications, Pages 1-4, 2012.
[165]. D. Wu, W. Fei, P. C. K. Luk, B. Xia, “Design considerations of outer-rotor permanent magnet synchronous machines for in-wheel electric drive train using particle swarm optimization,” in 7th IET International Conference on Power Electronics, Machines and Drives (PEMD), p. 1-6, 2014.

[166]. M. Morishita, I. Miki, M. Nakamura, "Efficiency improvement for IPMSM of outer rotor type," in International Symposium on Power Electronics Electrical Drives, Automation and Motion (SPEEDAM), p. 115-118, 2010.
[167]. J. A. Güemes, A. M. Iraolagoitia, M. P. Donsión, J. I. Del Hoyo, "Analysis of torque in permanent magnet synchronous motors with fractional slot windings cogging torque," in Proceedings of The International Conference on Electrical Machines, p. 1-4, 2008.
[168]. D.C.Hanselman, *Brushless permanent magnet motor design*, 2nd ed., Magna Physics Publishing, Lebanon, Ohio, 2006.

# Nutshell as Reinforcing Filler in Thermoplastic Composites

*MürşitTufan*[27], *Nadir Ayrılmış*[28]

***Abstract***

*Mechanical properties of recycled polyethylene composites filled with nutshell flour (NSF) were investigated. Polymer composites were formed by single screw extrusion compounding. All polymer composites formulations were compression molded into a hot press for 3 min at 170 ℃. Compression molded composites were prepared from NSF and recycled high density polyethylene (R-HDPE) with and without maleic anhydride-grafted polyethylene (MAPE) at 30, 40, 50 and 60 wt % contents of the NS flour. The flexural and tensile modulus of the composites significantly increased with increasing the filler content while the flexural and tensile strength significantly decreased. The MAPE improved the interfacial adhesion between nutshell flour and polymer matrix. This study demonstrate that NS has the potential to be effectively recycled as filler in HDPE composites.*

**Keywords:** Nutshell, HDPE, polymer composites, mechanical properties.

## 57. INTRODUCTION

As a result of a growing awareness of the interconnectivity of global environmental factors, principles of sustainability, industrial ecology, eco-efficiency, and green chemistry utilization of renewable resources gained importance. One of the factors affecting the utilization of renewable resources are the environmental pollution caused by fossil fuels and the regulations imposed to control such emissions. Renewable resources like wood is the most abundant and widely utilized renewable material on earth. However rising with population has increased the need for wood materials. On the other hand some countries like Turkey faces the problem of lack of woody raw material by reason of its forested areas (21.6million ha) are unproductive by 46.7% like the most of the countries [1,2]. As a result, many agricultural waste has been used as an alternative to wood material. In addidition to utilization of agricultural waste became more practical in some countries, such as Turkey, which has very limited forest resources.

Numerous experimental studies have focused on the use of agricultural waste as reinforcement in composite with thermoplastics polymer matrices. Wood plastic composites (WPCs) have attracted considerable attention from industry in recent years. WPCs can be made from wood or agriculturel waste fiber or flours mixed with polymers such as high density polyethylene (HDPE), polypropylene (PP) and polyvinylchloride (PVC). The advantage of using agricultural waste in WPC are that the low density, good thermal insulation and mechanical properties, low price, lower density per weight of raw material, non abrasive and recyclable [3,4].

Hazelnut (Corylus avellana) is an important crop that is cultivated which plantations cover 690.000 hectares of land in Turkey and nearly 70% of the world hazelnut production is in Turkey and 660.000 tons of nuts are produced annually. Produced nuts constitute 45-50% of the nutshell. This waste is used for heating purposes in

[27] *Corresponding author:Department of Forest Industrial Engineering, Forestry Faculty, ArtvinÇoruh University, 08000, Artvin, Turkey.* mtufan35@hotmail.com

[28]*Department of Forest Industrial Engineering, Forestry Faculty, Istanbul University, Bahcekoy, Sariyer, 34473, Istanbul, Turkey.* nadiray@istanbul.edu.tr

household, but there is limited information on nutshell utilization [5,6]. This study, investigated the mechanical properties of nutshell polyethylene composites produced with and without maleic anhidrite-grafted polyethylene at 30, 40, 50, 60 wt% contents of the nutshell flour.

## 58. MATERIALS AND METHODS

### *2.1.Materials*

Recycled High density polyethylene (R-HDPE), nutshell flour (NSF), maleic anhydride grafted polyethylene (MAPE) coupling agent were used as thermoplastic matrix, organic filler and coupling agent, respectively. The polymer matrix, R-HDPE, was supplied by Ayan Plastic Co. Ltd.,Turkey, and MAPE (PE MA 4351 GR) was provided by Clariant International Ltd. Nutshell waste was supplied from Espiye, Giresun. The experimental design of the study is presented in Table 1.

***Table 1.****Composition of thepolymercompositesfilledwithdifferentamounts of NSF.*

| Compositegroupcode | NSF (%wt) | R-HDPE (%wt) | MAPE (%wt) |
|---|---|---|---|
| **A** | 30 | 70 | - |
| **B** | 30 | 67 | 3 |
| **C** | 40 | 60 | - |
| **D** | 40 | 57 | 3 |
| **E** | 50 | 50 | - |
| **F** | 50 | 47 | 3 |
| **G** | 60 | 40 | - |
| **H** | 60 | 37 | 3 |

### *2.2.Preparation of polymer composites*

The air dried nutshell waste was milled using a laboratory type Willey mill. The flour screened to 60- and 80-mesh size and this particles were dried for 24 h at 103 ± 2 °C. NSF mixed with R-HDPE and MAPE laboratory mixer (Shini SVM-80U, China). This mixture was compounded in a single-screw laboratory extruder (Rondollinear 30, UK, L/D ratio30:1). The temperature profile was set at the die end for 170-175-180-185 °C. The screw speed was calibrated at 70 rpm. The extrudates samples were cooled and cut into pellets. Finally, the pellets were compressed into 150 (L) mm × 170 (W) mm × 5 (T) mm size composites for 3 min at 170 °C.

### *2.3.Mechanical properties*

The flexural and tensile properties of all samples were determined according to ASTM D790 and ASTM D683 standards, respectively, using a Zwick 10KN universal testing machine. In the three-point flexural test, specimens with dimensions of 150 (L) mm × 12.7 (W) mm × 3.5 (T) mm were used at a crosshead speed of 2 mm/min. For the tensile test (dogbone, type III) the crosshead speed was 5 mm/min. Seven replicate specimens of each polymer composite group were tested for flexural and tensile properties.

### *2.4.Scanning electronmicroscopy*

The fracture surface of the tensile test bars was observed with a scanning electronic microscope (Zeiss scanning electron microscope (SEM) (ZeissEvo/LS10) under an acceleration voltage of 10 kV. The specimen was coated with gold under vacuum prior to scanning. The morphology such as filler dispersion and interfacial adhesion of the components was investigated.

## 59. RESULTS AND DISCUSSION

The tensile properties of the polymer composites produced from different NSF loadings with and without MAPE are presented in Table 2. The tensile strength of the WPC specimens decreased with increasing amount of NSF content, while the tensile modulus increased. Tensile strength values decreased by 45.6% when NFS flour content increased from 30 to 60 wt% without MAPE samples. It is well known that the mechanical properties of composites depend on mainly interaction between lignocellulosic filler and the thermoplastic materials. Because plastics are hydrophobic substances that are not compatible with hydrophilic lignocellulosics, resulting poor adhesion between polymer matrix and NSF in composites. This weak interfacial adhesion between the lignocellulosic material and the polymer matrix resulted in lower tensile strength.

Particularly, the tensile modulus of the WPC significantly increased as the amount of NFS increased from 30 to 60 wt% without MAPE samples. Statistical analysis showed that the filler rate significantly affected the tensile properties ($p < 0.05$).Lignocellulosic material has higher modulus values than HDPE, thus adding NSF reduced the ductility of the composites and increased the modulus [7,8].

One way to improve this to incorporate a coupling agent as an additive. The addition of coupling agent improved the tensile properties of all groups in this study. Similar results reported by the others [9,10].

The flexural strength and modulus values of the composites are presented in Table 2. Flexural modulus of the WPCs were enhanced with the increase in the amount of NSF material. Lignocellulosic fiber have a higher modulus compared with polymer matrix. As a result, flexural modulus increased gradually with increasing NSF content. The same trend has also been reported in other studies [11,12].

***Table 2.*** *Mechanical properties of NSF composites.*

| Composite group code | Tensile Strength (MPa) | Tensile Modulus (GPa) | Flexural Strength (MPa) | Flexural Modulus (GPa) |
|---|---|---|---|---|
| **A** | 21.02 ***e***<br>(0.37) | 1.03 ***a***<br>(0.04) | 27.53 ***d***<br>(2.20) | 1.04 ***a***<br>(0.28) |
| **B** | 26.17 ***g***<br>(0.87) | 1.21 ***b***<br>(0.15) | 30.77 ***e***<br>(0.97) | 1.39 ***bc***<br>(0.16) |
| **C** | 17.78 ***d***<br>(0.62) | 1.10 ***a***<br>(0.07) | 24.70 ***c***<br>(2.56) | 1.24 ***ab***<br>(0.17) |
| **D** | 23.09 ***f***<br>(0.98) | 1.36 ***c***<br>(0.04) | 27.57 ***d***<br>(0.68) | 1.61 ***de***<br>(0.18) |
| **E** | 14.84 ***c***<br>(1.01) | 1.37 ***c***<br>(0.16) | 19.89 ***b***<br>(3.15) | 1.52 ***cd***<br>(0.09) |
| **F** | 17.51***d***<br>(0.75) | 1.62 ***d***<br>(0.06) | 23.46 ***c***<br>(3.36) | 1.83 ***e***<br>(0.14) |
| **G** | 11.42 ***a***<br>(1.22) | 1.70 ***d***<br>(0.04) | 16.01 ***a***<br>(2.27) | 1.71 ***de***<br>(0.23) |
| **H** | 13.44 ***b***<br>(0.94) | 1.93 ***e***<br>(0.03) | 20.34 ***b***<br>(3.27) | 2.11 ***f***<br>(0.19) |

-The value in parenthesis is the standard deviation.

-Each value is the average of seven samples tested.

-Groups with same letters in column indicate that there is no statistical difference ($p < 0.05$).

The result of the flexural strength test are similar to the result of the tensile strength test. The flexural strength values of the WPCs decreased when the NSF addition level increased from 30% to 60%. The decreasing rate was around 42% without MAPE samples. The reduction in the flexural strength of the WPCs as a function of the NSF content was mainly attributed to the poor compatibility between polar NSF and non polar polymer matrix, which forms the weak interfacial regions. The weak interfacial region results lower flexural strength as the amount of filler was increased in the composites. The addition of coupling agent enhanced flexural properties of all groups in this study. Surface adhesion was improved by the addition of 3% MAPE [13]. Figure 1 shows the void areas for the WPC samples in the composite group E. Figure 2 shows a reduction of the voids and better surface adhesion in the composite group F resulting from the addition of 3% MAPE. NSF particles were well dispersed in the polymer matrix (Figures 1 and 2). Indicating, good encapsulation of the lignocellulosic matrix.

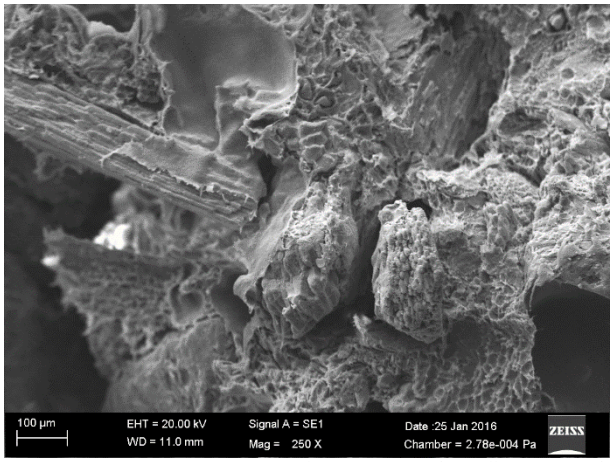


***Figure 1.*** *SEM imagesshowingpoorsurfaceadhesion of thecompositesproducedwithoutMAPE (Group code: E).*

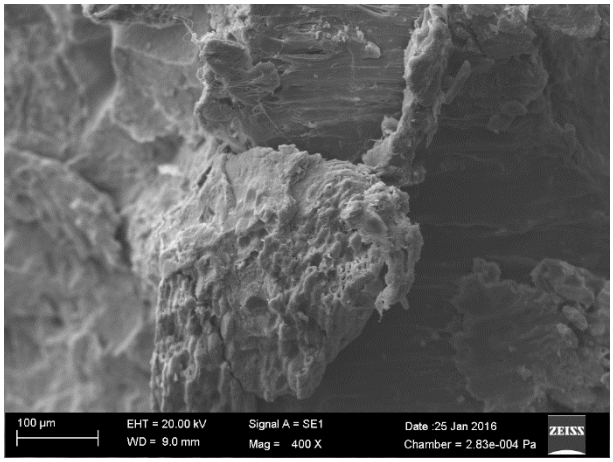


***Figure 2.*** *SEM imagesshowinggoodsurfaceadhesion of thecompositesproducedwith MAPE (Group code: F).*

## 60. CONCLUSIONS

The tensile and flexural modulus values of the composites improved with increasing content of NSF flour, whereas tensile and flexural strength decreased. Tensile and flexural properties were enhanced by the addition of MAPE. The results revealed that the NSF had a potential as filler for WPCs. The results of the present study showed that the 40 wt% nutshell flour as filler could be efficiently used in the production of R-HDPE.

## 61. ACKNOWLEDGEMENTS

This research was supported by The Scientific Technological Research Council of Turkey (Project number: 214O737).

## 62. REFERENCES

[1]. Y. Top, "Waste Generation and Utilization in Micro-Sized Furniture-Manufacturing Enterprises in Turkey,"*Waste Management*., 35:3-11, 2015.

[2]. A.R. Sanadi, D.F. Caulfield, R.M. Rowell, "Reinforcing polypropylene with natural fibers".*PlasticsEngineer.*,(4): 27-30, 1994.

[3]. A. Kaymakci, N.Ayrilmis, F. Ozdemir, and T. Gulec, "Utilization of Sunflower Stalk in Manufacture of Thermoplastic Composite,"*J Polymer Environ*., 21:1135-1142, 2013

[4]. U. Buyuksari, N. Ayrilmis, T. Akbulut, "Compression wood as a source of Reinforcing filler for Thermoplastic Composites" *J Applied Polymer Sci.*, 123: 1740-1745, 2011.

[5]. (2016) Turkish Ministry of Customs and Trade Report [Online]. Available: http://koop.gtb.gov.tr/data/Raporu.pdf.

[6].M. Tufan, S. Akbas, T. Gulec, C. Tascioglu, andM.H. Alma, "Mechanical, Thermal, Morphological Properties and Decay Resistance of Filled Hazelnut Husk Polymer Composites,"*MaderasCiencia y Technol.,* 17(4):865-874, 2015.

[7].C. Taşçıoğlu, M. Tufan, M. Yalcın, S. Şen, "Determination of Biological Performance,Dimensional Stability, Mechanical and Thermal Properties of Wood Plastic Composites Produced From Recycled ChromatedCopper Arsenate Treated Wood". *J Thermoplastic Composite Materials.,*1-19. DOI: 10.1177/0892705714565704, 2014.

[8]. D. Kocaefe, S.Poncsak, Y. Boluk, "Effect of thermal treatment on thechamical composition and mechanical properties of birch and apsen," *BioResources*., 3, 517-537, 2008.

[9].S. He, L. Zhou, H. He, "Preparationandproperties of woodplasticcompositesbased on tearesidue," *PolymerComposites*, 36(12), 2265-2274, 2014.

[10].M. Tufan, T. Gulec, E. Peşman, N. Ayrilmis, "Technological and ThermalProperties of ThermoplasticCompositesFilledwith Heat-Treated Alder Wood", Bioresources.,11(2), 3153-3164, 2016.

[11].A. Ashori, S. Sheshmani, "Hybridcompositesmadefromrecycledmaterials: moistureabsorptionandthicknessswellingbehavior," *BioresourceTechnology*.,101, 4717-4720, 2010.

[12]. N. Ayrilmis, S. Jarusombuti, V. Fueangvivat, P. Bauchongkol, "Effect of thermal-treatment of woodfibers on properties of flat-pressedwoodplasticcomposites," *PolymerDegradationandStability*., 96, 818-822, 2011.

[13].M. Tufan, T. Gulec, U.Cukur, S. Akbas, S.Imamoglu, "Some Properties of WoodPlasticCompositesProducedfromWasteCups", KastamonuUniv Journal of Forestry Faculty., 15(2),176-182, 2015.

# Obtaining the Ground Seismic Vulnerability Indexes Using Microtremor Method

*Aykut Tunçel[29], Mustafa Akgün[1]*

***Abstract***

*It is important to have an idea about the damages of an earthquake at any place. Vulnerability indexes called K values for ground ($K_g$) give a chance to estimate the earthquake damage before the earthquake occurs. K values have been proposed by Nakamura (1996) for estimating earthquake damage of surface ground. Here in this study, $K_g$ will given as an example of application of microtremor method. Main goal of this study is to obtain the $K_g$ values and the distribution of the values at the study area additionally to determine the zones may be damaged after an earthquake. The parameters to calculate $K_g$ values are obtained using microtremor method. Microtremor measurements were collected using Guralp CMG-6TD sensor model seismograph equipped with a three component high sensitive seismometers, which have a flat instrument response between 0.02 and 30 seconds. At each site, microtremor measurements were recorded for 30 minutes within 100 Hz sampling interval at 112 different locations in order to identify predominant frequency of the ground. Microtremor measurements were estimated according to Nakamura HVSR technique. $K_g$ values were calculated using the predominant frequency and amplification values obtained by using HVSR technique. Nakamura proposed the use of a Kg to identify sites where seismic hazards and damage may be expected. The study after the 1989 Loma-Prieta Earthquake offers pretty big ground deformations where Kg values are bigger than 20 and no damages where $K_g$ values are very small. Consequently, southern parts of the study area have $K_g$ values bigger then 20. It is expected less earthquake damage at the northern parts of the study area because this part produces smaller $K_g$ values.*

**Keywords:** Vulnerability index, $K_g$ values, Mikrotremor

## 63. INTRODUCTION

During the past fifty years, many destructive earthquakes in different regions of the world have occurred. These earthquakes have killed many people, caused social and economic detriments. Damaged points due to earthquake motions are weak points revealed by earthquake itself. If weak points are investigated in advance, it is possible to reinforce the weak structures damaged by earthquake. One of the essential factors in urban disaster management is being able to recognize the extent of damage caused during an earthquake. In a vulnerability management study, the value of human life should always be precious than the cost of reinforcing the buildings.

Occurrence of earthquake damage depends on strength, period and duration of seismic motions. These parameters, of course, depend upon earthquake itself but they are also strongly influenced by the seismic response characteristics of ground and structures. Thus, the weak points can be found by investigating seismic characteristics of ground and structures. Significant damage from large earthquakes is related to local ground response and structure status. Therefore, obtaining both ground characteristics and the condition of structures is very considerable in earthquake risk analysis. Ultimately, identifying the vulnerability index that is related to ground parameters and structure status simultaneously is very important in the context of disaster management of an urban region.

Many empirical studies have been carried out to establish the reliability of the horizontal to vertical (H/V) spectral ratio method as a transfer function. The latest method was suggested by Nakamura [8]. This method was used to identify the predominant resonant frequency of a ground layer using the H/V of the Fourier transform from microtremor data. The comparison between the fundamental frequency obtained from microtremor H/V spectral ratios and the receiver functions of earthquake recordings or explosion data have allowed researchers to conclude that microtremor H/V spectral ratios provide reliable estimates of the fundamental frequencies of ground layers. Many researchers have studied to determine the H/V spectral ratio in ground characterization, in addition to microzonation and urban vulnerability studies [6-14-5-2-7].

Microtremor measurements were collected using Guralp CMG-6TD sensor model seismograph equipped with a three component high sensitive seismometers, which have a flat instrument response between 0.02 and 30 seconds. At each point, microtremor measurements were recorded for 30 minutes within 100 Hz sampling interval. Locations of these 112 points are given in Figure 2. With these measurements, characteristics of surface ground are investigated with H/V of microtremor [8]. From the preliminary analysis of the data, fundamental natural frequency F, amplification factor A and vulnerability index for ground Kg values (Kg = A2/F) are estimated.

[29] *Corresponding author: Dokuz Eylul University, Department of Geophysical Engineering, 35160, Buca/Izmir, Turkey.* aykut.tuncel@deu.edu.tr

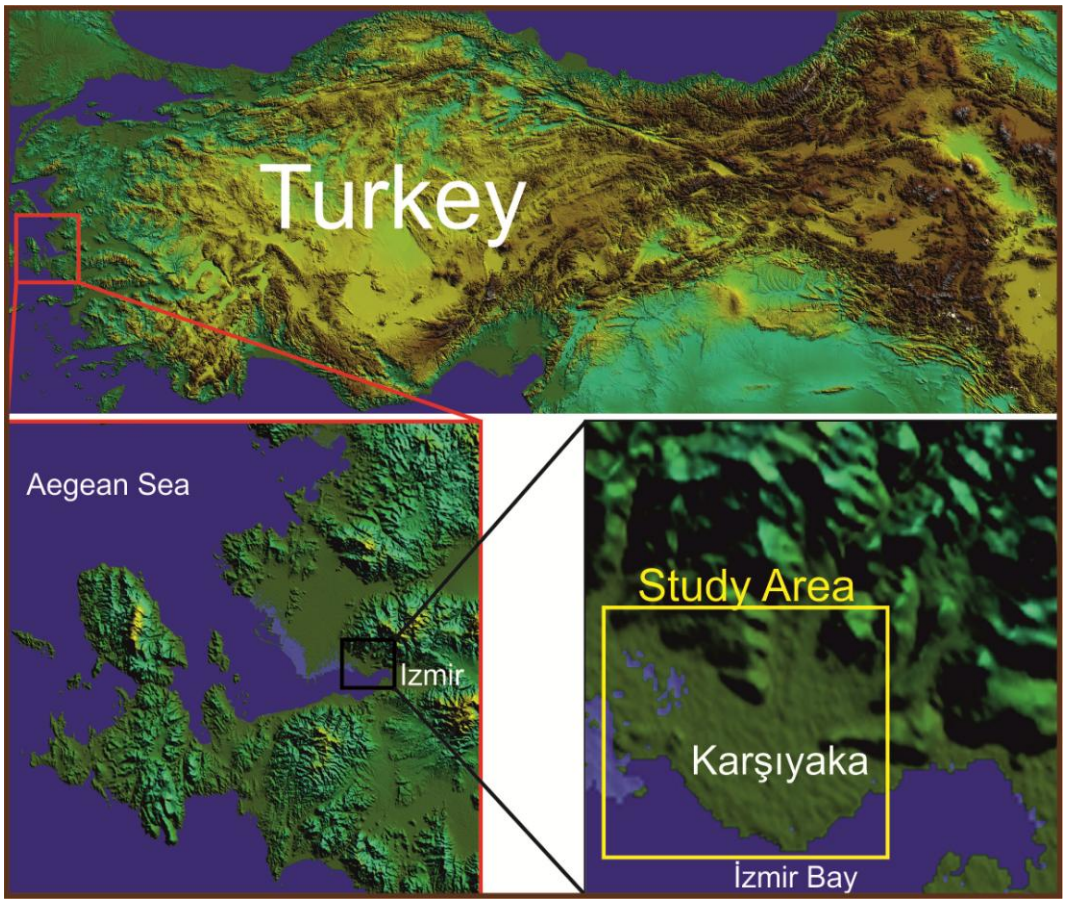


*Figure 6. Location map of the study area with topography.*

## 64. GEOLOGY

Volcanic rocks containing mineralizations in the study area divided into three types as dacites, andesites and andesitic dykes [3]. These volcanics are accepted as "Yamanlar volcanites" by Akdeniz et al. [1], while the ore bearing volcanites named as "Altıntepe volcanites" by Dönmez et al. [4]. Volcanites overlie İzmir flysch [13] in near vicinity of the study area. İzmir flysh is named for the first time as "Crystalline schists" by Dora [3] and mapped as phylitte, clay bearing schists and low grade metamorphosed quartzite, greywacke and very low grade metamorphosed arkose alternating with schists and phyllites. The age of crystalline schists is Paleozoic. Lateron, this unit is described as "flysch association" of Upper Cretaceous age according to regional correlations made by Oğuz [12]. This unit is made up of chlorite schists, phyllite, metasandstone, albitepidote schists, actinolite schists spilite, cherty limestone, meta-conglomerate, bituminous schists and other kind of schists which metamorphosed under greenschist facies. Limestones and serpantinite exotic blocks of Permian, Triassic, Jurassic and Lower Cretaceous age occur in this unit. This unit is called as "Bornova complex" of Maastrichtian Danien age by Dönmez et al. [4].

The northern part of the Izmir bay between Bayraklı and Karşıyaka district is bounded by the Karşıyaka fault zone (KFZ) which is an antithetic fault to the İzmir fault zone (IFZ). It is an approximately N80°W- to E–W trending normal fault zone 0.5–2.5 km wide and 20 km long, characterized by a concave, curvilinear range-front fault trace to the south. The hanging wall of the KFZ contains modern basin fill units, while the footwall includes the Bornova mélange and volcano-sedimentary rocks of the lower sequence. The fault zone displays a well-developed step-like morphology. There is also a series of actively growing lateral alluvial fans aligned parallel to the fault [15].

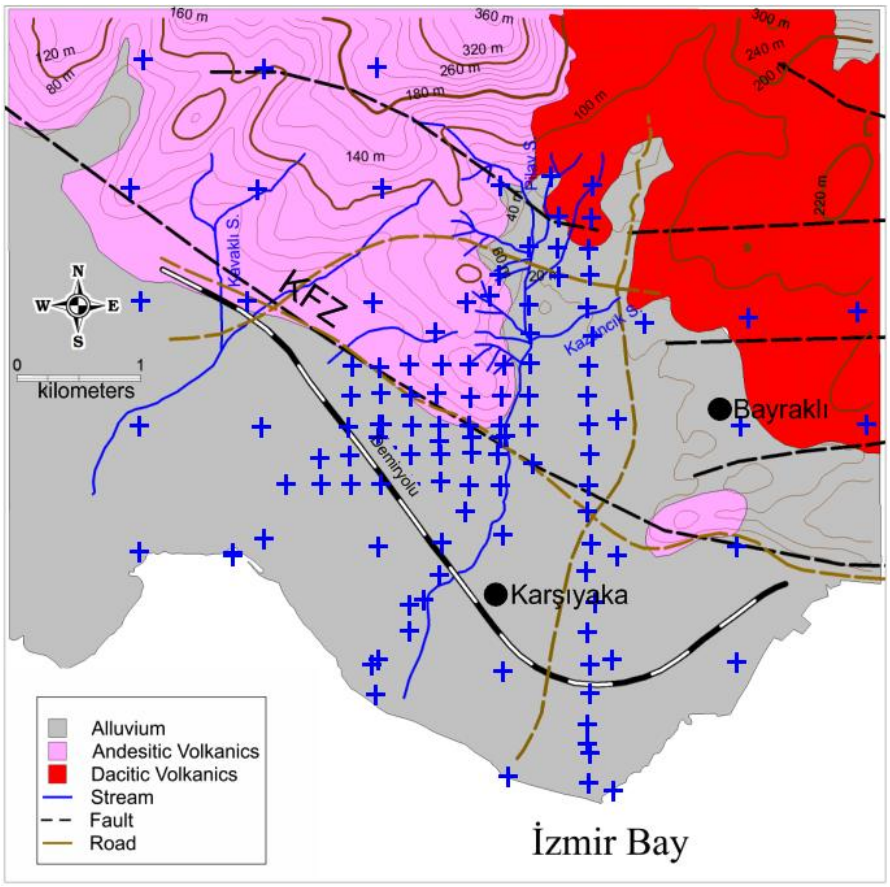


*Figure 2. 1/25000 scale geological map of the study area (modified from MTA 2000), blue pluses show mikrotremor method measuring points.*

## 65. METHOD

In order to evaluate the vulnerability of ground, Nakamura [10] suggested an approach in which he defines the Kg vulnerability index for ground and Kb for various structures based on specifications pertaining to the H/V spectral ratio.

Regarding the formulations described in detail by Nakamura [10-11] a brief description vulnerability index for ground ($K_g$) is introduced in Equation (1)

$$K_g = (A_g)^2/F_g \quad (1)$$

Here, $F_g$ and $A_g$ are the predominant frequency and amplification factor on the ground surface. These parameters were estimated using the H/V spectral ratio. Predominant frequency ($F_g$) and amplification factor ($A_g$) which represents dynamic characteristics of the ground are found from microtremor analysis and Vulnerability index (Kg) are calculated as explained above.

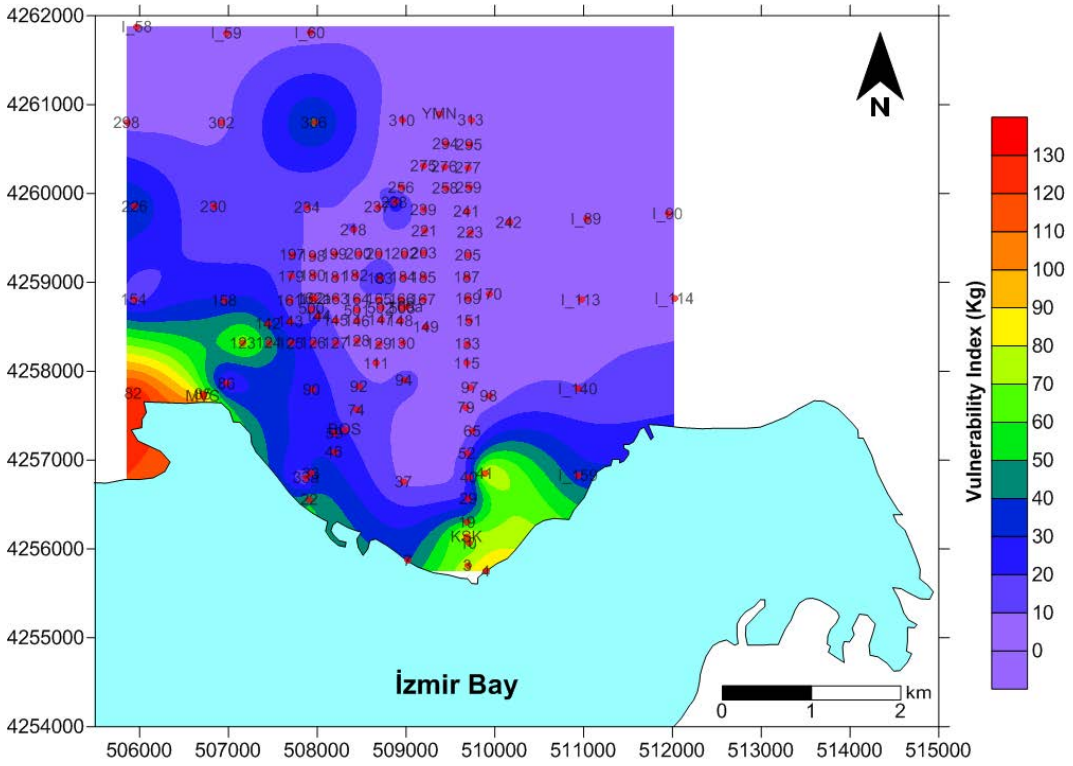


*Figure 3. Calculated vulnerability index distribution map using microtremor method data*

## 66. RESULTS AND COCLUSIONS

It has been proved in many studies [9-10] that K value is high where the damage risk is high. Since this approach is possible to apply before the earthquake, this information can be useful tool for damage estimation. Main target of this approach is using this information for earthquake disaster prevention. Site effect and vulnerability of ground and structures is an important issue for earthquake disaster mitigation, and also detailed microzonation of any city which is waiting for the earthquake is still needed.

After confirming dynamic characteristics of ground, in the present study, the vulnerability index (Kg) of each measurement points which makes possible to estimate the weak points of the ground surface were also calculated. Kg values are directly calculated from the predominant frequency ($F_g$) and amplification factor ($A_g$) parameters.

Consequently, southern parts of the study area that are mostly located on alluvium have $K_g$ values bigger then 20. It is expected less earthquake damage at the northern parts of the study area because this part produces smaller $K_g$ values. Smaller vulnerability values are coincide with the volcanic units likewise alluvium units shows bigger vulnerability. According to these results we can clearly mention that the $K_g$ index values are compatible with the geological units.

## REFERENCES

[169]. Akdeniz, N., Konak, N., Öztürk, Z., and Çakır, M.H., "İzmir-Manisa dolayının jeolojisi", MTA Report. no. 7929, Ankara, 1986.
[170]. Diagourtas, D., Tzanis, A., and Makropoulos, K., "Comparative study of microtremor analysis methods", In Earthquake Microzoning, Birkhäuser Basel, 2463–2479, 2002.
[171]. Dora, Ö., "Geologisch-lagerstâttenkundliche Untersuchungen im Yamanlar-Gebirge nördlich vom Karşıyaka (Westanatolien)", MTA Enst. Publicaiton., Vol. 116, 1964.
[172]. Dönmez, M., Türkecan, A., Akçay, A.E., Hakyemez. Y. and Sevin, D., "İzmir ve kuzeyinin jeolojisi, Tersiyer volkanizmasının petrografik ve kimyasal özlikleri", MTA Report. no. 10181, Ankara, 1998.
[173]. Kobayashi, H., Midorikawa, S., Tanzawa, H., and Matsubara, M., "Development of portable measurement system for ambient vibration test of building", J. Struct. Constr. Eng. 378, 48–56,1987.
[174]. Lachet, C., and Bard, P.Y., "Numerical and theoretical investigations on the possi- bilities and limitations of Nakamura's technique", J. Phys. Earth 42 (5), 377–397, 1994.
[175]. Mokhberi, M., Davoodi, M., Haghshenas, E., and Jafari, M., "Experimental evaluation of the H/V spectral ratio capabilities in estimating the subsurface layer characteristics", Iran. J. Sci. Technol. – Trans. Civil Eng., 37, 457–468, 2013.

[176]. Nakamura, Y., "A Method for Dynamic Characteristics Estimation of Subsurface using Microtremor on the Ground Surface", Quarterly Report of Railway Technical Research Institute (RTRI), Vol. 30, No.1, 1989.
[177]. Nakamura, Y., "Real Time Information Systems for Seismic Hazards Mitigation UrEDAS, HERAS and PIC", Quarterly Report of RTRI, Vol. 37, No. 3, 112-127, 1996.
[178]. Nakamura, Y., "Seismic vulnerability indices for ground and structures using microtremor." World Congress on Railway research, Florence, Italy, 16.-19. November, 1997.
[179]. Nakamura, Y., "Clear identification of fundamental idea of Naka- mura's technique and its applications", Proceedings of the 12th WCEE, New Zealand, paper no. 2656, 2000.
[180]. Oğuz, M., " Manisa dağının kuzey ve kuzeybatısının jeolojisi (Geology of the northern and northwestern part of Manisa Dağ)", Engl. Summary: Fac. Sci., 1966.
[181]. Öngür, T., "İzmir Urla jeotermal araştırma sahasına ilişkin jeolojik rapor", MTA Report no. 4835, Ankara, 1972.
[182]. Scherbaum, F., Hinzen, K.G. and Ohrnberger, M., "Determination of shallow shear wave velocity profiles in the Cologne, Germany area using ambient vibrations", Geophys. J. Int. 152, 597–612, 2003.
[183]. Uzel, B., Sözbilir, H. and Özkaymak, Ç. , " Neotectonic evolution of an actively growing superimposed basin in western Anatolia: the inner bay of İzmir Turkey." Turkish Journal of Earth Sciences, 21, 439-471, 2012.

# A Survey of Web Service Attacks and Countermeasures

*Hatice Çataloluk*[30]

***Abstract***

*Through the arise of web services technology, e-commerce and e-business systems are performing efficiently. Web services simplifies communication with devices and people by standardizing the flow of information and by breaking down the barriers of discrete systems. However, they have some security issues. Due to the nature of web services, they cause the need for bridged firewalls, and go down to application environment of an enterprise, increase vulnerability to malicious attacks and confront companies with security risks. Therefore this paper presents a survey on different specific attacks of web services. For each attack a description of the attack execution, the effect on the target and some simple examples are given. Additionally, some of the important general countermeasures for preventing web service attacks are discussed.*

**Keywords: Web Services, SOA, Security, Attacks, Countermeasures**

## 67. INTRODUCTION

The Internet has begun to make change in the method of businesses perform. The Web is being used for selling products, finding suppliers or trading partners, and for connecting existing applications to other applications by companies. Through the arise of e-commerce and e-business systems, web services are expeditiously becoming the technology in order to provide commerce. Nevertheless, they have some problems. Because of the ability of passing through firewalls and accessing APIs (Application Program Interfaces), security issues are come with web services [11].

It is important that the security of web services be assured for web services technologies in order to keep their promise. They must have confidentiality, integrity, availability, and digital identity management. Thus, people can be assured that interactions with services over the Internet are kept confidential and the privacy of their personal information is protected. They should be sure that the information used for searching and selecting services is true and the integrity is assured. Also people want services to be available when they needed. Providing these requirements is a difficult challenge, especially with open distributed applications [11].

In this paper, we aimed to provide a survey on some of most significant attack types and general countermeasure approaches for these attacks. We have given descriptions on the concepts of attacks and a brief summary on countermeasures.

## 68. BACKGROUND OF SCOPE

### *68.1. Service Oriented Architecture (SOA)*

A Service Oriented Architecture (SOA) can be defined as a collection of services. These services are in communication with each other. SOA specifies an interactivity between software agents as an exchange of

messages between service requesters and service providers. Clients are software agents and they request the execution of a service. Providers are software agents too and they provide the service. The basic SOA is a relationship that consists of three roles: a service provider, a service requester and a service registry. The interactivity contains publish, find and bind operations [12].

[30] *Corresponding author: Yildirim Beyazit University, Department of Computer Engineering, 06050, Al ğ/A k , T k .*
*hcataloluk@ybu.edu.tr*

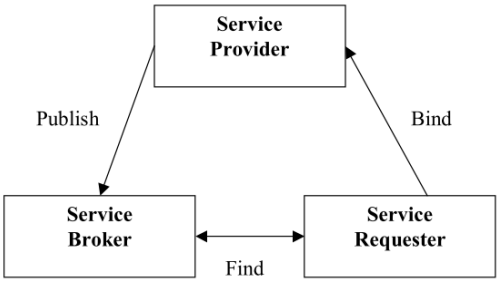


*Figure 7. Web services architecture [7].*

In a SOA, functionality is published on a network where two important capabilities are provided: discovery and binding. Discovery is the ability to find the functionality. Binding is the ability to connect to the functionality. These activities correspond to three roles: Web Service provider, Web Service requester and Web Service broker [7].

### *68.2. Web Services*

A web service is an application which can be described, published, located, and invoked over the Internet. URI identifies web services and its public interfaces, and bindings are defined, and described by using XML in a WSDL (Web Service Description Language) file [14].

Web services are XML (eXtensible Markup Language) based messages delivered by means of Internet standard protocols and deployed in Service-Oriented Architectures (SOAs). Thus web services established upon the XML, the Simple Object Access Protocol (SOAP), and related standards. One of the specific definitions of web services is "A web service is an application that exists in a distributed environment, such as the Internet" [5]. According to another definition; "A web service is an interface that describes a collection of operations that are network accessible through standardized XML messaging." [4].

The main object of web services is to allow applications on dissimilar platforms to interchange business data.

The technologies that make the organization of Web services are SOAP, WSDL, and UDDI.

Simple Object Access Protocol (SOAP) is utilized for communication in between different Web Services. SOAP messages flow from source to a final receiver through a SOAP message path. A SOAP message consists of Soap: Envelope and it contains a Soap: Body element and an optional Soap: Header element. The Soap: Header element can involve a set of child elements that describe message processing that the sender expects a receiver to perform [12].

Web Service Description Language (WSDL) is utilized to describe the functionalities of the services. When the requester receives the WSDL file for the candidate web service, it must be validated [12].

Universal Description Discovery and Integration (UDDI) is utilized as a registry of information for web services. UDDI specifies a group of standard interfaces for accessing a database of web services. The object of UDDI is to allow users to find available web services and interact with them dynamically [12].

## 69. ATTACKS ON WEB SERVICES

In this section, we describe some of the possible important attacks on web services. These are the coercive parsing, WSDL access and scanning, oversize payload, command injections and schema poisoning.

### *69.1. Coercive Parsing*

Parsing the SOAP message and transforming the content of it is one of the first steps in processing a Web service request. XML documents may be more verbose and complicated in parsing, particularly when using namespaces. Then, the XML parsing process allows the coercive parsing attacks [6][10].

The main object of coercive parsing attacks is to exploit XML based portions of web services. Replay attacks, Recursive Payloads attacks, and Oversize Payloads attacks are the subclasses of Coercive Parsing attacks and coercive parsing is the subclass of DoS attacks.

In Replay attacks, attackers send repeated SOAP messages to overwhelm web services. It is really difficult to detect this kind of attacks because of well formed HTTP requests and validity of IP addresses and network packets [15].

The ability of nesting of XML elements in documents causes to Recursive Payloads attacks. In this attack, an attacker may make a document with a large number of nested elements deep to break XML parsing [15].

### *69.2. WSDL Access and Scanning*

WSDL supplies information about methods such as a service's operations including parameters, data types and network bindings etc. that can be exploited by the attackers and lead to potential disaster on web services. WSDL file must be provided with restricted access while WSDL Scanning enables to identify various vulnerabilities in the application [3].

If the generated WSDL file contains all operations (internal and external), in this case, an external client can gain knowledge of the internal operations and can invoke them [6].

In order to avoid WSDL Scanning, a separate access from WSDL to clients that contains just the external operations, can be provided. Thus attackers could try to estimate the excluded operations and call them [2],[3].

### *69.3. Oversize Payload*

Querying a service using a huge request message is another method in order to perform a resource exhaustion attack. This attack is named as Oversize Payload attack [6].

Oversize Payloads attacks happen when an attacker creates a huge SOAP message document and there is not sufficient system buffer for a XML parser to process it [15].

Figure 2 shows an example of Oversized Payload attack [3]:

```
<Envelope>
<Body>
<getLength>
<item> hello </item>
<item> hello </item>
<item> hello </item>
...
</getLength>
</Body>
</Envelope>
```

*Figure 8. Example of Oversized Payload attack [3].*

A straightforward countermeasure approach against this type of attacks is the limitation of the total buffer size in bytes for incoming SOAP messages by controlling the actual message size and rejecting if any message exceeding the predefined limit [6].

### *69.4. Command Injection*

The Web service engine parses SOAP message requests and turns into extracted parameters to native types. Command Injection attacks change parameters within SOAP request messages [16].

SQL Injection attack is a category of Command Injection attacks. In SQL Injection attack, an attacker tries to manage the database by using SQL statements arbitrarily. With SQL injection attacks, attackers aim to access and retrieve private information and data that are not exposed to everyone in applications [3].

If SQL statements are dynamically created while application executes, it means that there is an opportunity for a security violation. In this case, an attacker can break security and pass fixed inputs into the SQL statement. The way of generating SQL injections is inserting spatial values or characters into SOAP requests, Web form submissions, or URL parameters [14].

Through SQL injection attacks, an attacker can gain access to privileged data, log-in to password-protected areas without a proper log-in, remove database tables, add new entries to the database, or even log-in to an application with admin privileges [14].

Another category of Command Injection attacks is XML Injection attack.

> XML injection attacks change SOAP messages by modifying existing XML tags or inserting contents like operation parameters with XML tags using special characters. If the special characters such as "<" and ">" are not escaped appropriately, occurring of this kind of attacks is more possible [6].
>
> Figure 3 presents an example of XML Injection attack against a .NET web service. In this example, the deployed service method has two parameters a and b. Both of these parameters are of type xsd:int. The service has been invoked by using the following message [6]:

```
<Envelope>
 <Body>
  <HelloWorld>
   <a> <b>1</b> </a>
   <b> 2 </b>
  </HelloWorld>
 </Body>
</Envelope>
```

*Figure 9. XML injection example [6].*

In the SOAP message, 1 was inserted as a parameter content and so, the attacker was able to change the value of b by changing the content of a [6]. At the Web Service server side, this content is regarded as part of the SOAP message structure and can lead to undesired effects.

XML injection attacks happen when user input is passed to the XML stream. Because of the capability of parsing the XML documents by the second-tier application or the database, XML code can be injected to database. Then it becomes the part of the stream when it is retrieved from the database [15].

Prevention of xml injection attacks can be provided by rigid validation and check on SOAP messages [3].

### *69.5. Schema Poisoning*

A web service client retrieves all information about a web service such as message format, network location, security requirements, etc. from the metadata documents like schemas provided by the Web Service server. This metadata usually is distributed by using communication protocols like HTTP or mail and these circumstances create new attack possibilities aiming at poisoning these metadata documents [6].

In schema poisoning attack, the attacker can damage the XML Schema document or replace it with a similar but changed one. Then it would allow the parser to process malicious SOAP messages [13].

Figure 4 presents an example of XML schema for an order shipping application [13]:

```
<?xml version="1.0" encoding="ISO-8859-1" ?>
<xs:schema xmlns:xs="http://www.w3.org/2001/XMLSchema">
  <xs:element name="ship_order">
            <xs:complexType>
                      <xs:sequence>
                       <xs:element name="order" type="xs:string"/>
                        <xs:element name="shipping">
                         <xs:complexType>
                          <xs:sequence>
                           <xs:element name="name" type="xs:string"/>
                           <xs:element name="address" type="xs:string"/>
                           <xs:element name="zip" type="xs:string"/>
                           <xs:element name="country" type="xs:string"/>
                          </xs:sequence>
                </xs:complexType>
  </xs:element>
  ...
</xs:schema>
```

*Figure 10. Example of a XML schema [13].*

Figure 5 shows the schema after a simple poisoning attack [13]:

```
<?xml version="1.0" encoding="ISO-8859-1" ?>
<xs:schema xmlns:xs="http://www.w3.org/2001/XMLSchema">
  <xs:element name="ship_order">
              <xs:complexType>
                          <xs:sequence>
                            <xs:element name="order"/>
                            <xs:element name="shipping">
                             <xs:complexType>
                              <xs:sequence>
                               <xs:element name="name"/>
                               <xs:element name="address "/>
                               <xs:element name="zip"/>
                               <xs:element name="country"/>
                              </xs:sequence>
                  </xs:complexType>
  </xs:element>
...
</xs:schema>
```

*Figure 11. The schema file after a simple poisoning [13].*

In this example, by deleting the some schema conditions and limitations, the attacker is free to send a malicious XML message that may include content types [13].

To avoid Schema Poisoning attack, all metadata documents must be controlled carefully for authenticity. Nevertheless, the mechanisms for securing metadata documents are not standardized unlike for securing SOAP request messages [6].

## 70. PREVENTION OF WEB SERVICE ATTACKS

There are various suggested countermeasures for web services attacks in literature. In this section, some of the general methods are presented. These are the schema validation, XML signature, XML encryption and the use of WS-Security.

### *70.1. Schema Validation*

Schema validation is the easiest countermeasure approach. This approach is based on validation of incoming SOAP messages with XML schema. If there are SOAP messages that diverge from web service specification, they are declined.

Because of the validation of every incoming SOAP messages, system performance can be reduced in terms of CPU and memory consumption. And this is the disadvantage of schema validation countermeasure approach [3].

### *70.2. Schema Hardening*

Main object of schema hardening approach is to examine a schema file for constructions which allow unlimited large or complicated XML trees. Then these constructions are altered for restricted boundaries [6].

If there is a definition for an unbounded list of elements in web service description, this list is turned into a list with bounded number of elements. This restriction is used to limit the memory which is necessary for processing the message [3].

For instance, if there is an entry like <element maxOccurs="unbounded"> in the XML schema, this is replaced by <element maxOccurs="n">. Here n is a finite number [6].

### *70.3. XML Signature*

A mechanism for digitally signing XML documents or some parts of XML documents is presented by XML Digital Signature. Signatures do not have to be in the document being signed. By the way XML signature can be used also to sign non-XML documents [14].

XML Digital Signature determines how to digitally sign XML content and how to represent the resulting information in conformity with an XML schema. Information integrity and non-repudiation are given by XML Digital Signature [17].

```
<Signature Id="MyFirstSignature" xmlns="http://www.w3.org/2000/09/xmldsig#">
    <SignedInfo>
        <CanonicalizationMethod
              Algorithm="http://www.w3.org/TR/2001/REC-xml-c14n-20010315"/>
        <SignatureMethod
              Algorithm="http://www.w3.org/2000/09/xmldsig#dsa-sha1"/>
        <Reference URI="http://www.w3.org/TR/2000/REC-xhtml1-20000126/">
            <Transforms>
                <Transform
                    Algorithm="http://www.w3.org/TR/2001/REC-xml-c14n-20010315"/>
                </Transforms>
                <DigestMethod Algorithm="http://www.w3.org/2000/09/xmldsig#sha1"/>
                    <DigestValue>j6lwx3rvEPO0vKtMup4NbeVu8nk=</DigestValue>
                </DigestMethod>
        </Reference>
    </SignedInfo>
    <SignatureValue>MC0CFFrVLtRlk=...</SignatureValue>
    <KeyInfo>
        <KeyValue>
            <DSAKeyValue>
                .....
            </DSAKeyValue>
        </KeyValue>
    </KeyInfo>
</Signature>
```

*Figure 12. XML Signature example [7][8].*

XML Digital signatures are much more complicated to perform than encryption. Because XML signatures depend on the representation of the data being signed. So signature processing is too sensitive to alteration in data representation and processing order. The representation of the signed data and the verified data must be consistent and thus necessary caution must be taken. Although the signature was valid at the moment it was created, it cannot be verifiable because of differences that happened when the SOAP message was routed. [5]

### *70.4. XML Encryption*

A model for encryption, decryption and representation of XML document elements is provided by W3C XML encryption. The problem of confidentiality of SOAP messages exchanged in web services is solved with W3C XML encryption. It describes the structure and syntaxes of the XML elements and it provides rules for encryption or decryption of an XML document [17].

In XML encryption, an entire XML document or only selected parts of an XML document can be encrypted. Also it supports the super encryption of data which means that encrypted data can be encrypted again [5].

Figure presents an example of encrypted data in XML document. This represents a payment information. In this example, while the name on the credit card and the credit limit are being transmitted clearly, the credit card number is encrypted. The encrypted data looks as "CipherValue" [5].

```
<PaymentInfo xmlns='http://example.org/paymentv2'>
  <Name>John Smith</Name>
  <CreditCard Limit='5,000' Currency='USdollars'>
      <EncryptedData xmlns='http://www.w3.org/2001/04/xmlenc#'
           Type='http://www.w3.org/2001/04/xmlenc#Content'>
           <EncryptionMethod
              Algorithm='http://www.w3.org/2001/04/xmlenc#3des-cbc'/>
           <ds:KeyInfo xmlns:ds='http://www.w3.org/2000/09/xmldsig#'>
               <ds:KeyName>MyCompany</ds:KeyName>
           </ds:KeyInfo>
           <CipherData>
                <CipherValue>A23B45C56</CipherValue>
           </CipherData>
       </EncryptedData>
   </CreditCard>
</PaymentInfo>
```

*Figure 13. Example of encrypted data [5].*

### *70.5. WS-security*

WS-security is a family of specification developed by Microsoft and IBM, which are under OASIS standardization process. It is the most significant specification which addresses the security requirements of web services [1].

WS-Security defines mechanisms for the integrity and confidentiality of web service messages. WS-Security also describes security tokens for authentication, which can be used for access control systems [6].

The WS-Security specification describes a group of XML elements and attributes which can include security tokens in the SOAP messages. It also specifies how to use XML Signature and XML Encryption for the confidentiality and integrity of these tokens (username token and binary security token) [7].

A security element in the header of the SOAP message that carries the WS-Security extensions, is defined by WS-security to provide per-message authentication, as well as end-to-end message confidentiality by using XML Encryption and end-to-end message integrity by using XML Digital Signature in a web services environment. WS-Security also describes the use of time stamps to block message replay [9].

WS-Security is one of the important countermeasure approaches for attacks. But it has to be applied carefully. Because the usage of WS-Security itself enables new kinds of DoS attacks. [6]

## CONCLUSIONS

Web services are exposed to many various attacks by attackers. In this paper, the important web service attacks by describing along with possible effects and the general available countermeasures to these attacks of web services have been presented.

By the way, it has been shown that these attacks have a serious effect on web services and can cause to complicated problems for web services. Thus, securing of web services is of great importance.

## REFERENCES

[184]. Nadalin A., Kaler C., Monzillo R., Hallam-Baker P., Web Services Security: SOAP Message Security 1.1, 2006.
[185]. Jensen M, Gruschka N, Luttenberger N, “The Impact of Flooding Attacks on Network-based Services”, Proceedings of the IEEE International Conference on Availability, Reliability and Security, 2008.
[186]. Tiwari S., Singh P., "Survey of potential attacks on web services and web service compositions", 3rd International Conference on Electronics Computer Technology ICECT, Volume: 2, Pages: 47-51, 2011.
[187]. H. Kreger, Web Services Conceptual Architecture (WSCA 1.0), IBM Software Group, 2001.
[188]. Bret Hartman, Donald J. Flinn, Konstantin Beznosov, Shirley Kawamoto, "Mastering Web Services Security", New York, USA, John Wiley Sons, Inc., ISBN 0-471-26716-3, January, 2003.
[189]. Meiko Jensen, Nils Gruschka, Ralph Herkenhöner "A survey of attacks on web services classification and countermeasures countermeasures”, Springer Verlag, CSRD (2009) 24: 185–197
[190]. Yan L., "Web Services Security Using SOAP, WSDL and UDDI", 2006.
[191]. Mark Bartel, John Boyer, Barb Fox, Brian LaMacchia, and Ed Simon.“XML-Signature Syntax and Processing. W3C Recommendation 12 February 2002. http://www.w3.org/TR/xmldsig-core/.
[192]. Martin Naedele, "Standards for XML and WebServices Security", ABB Corporate Research.
[193]. Lindstrom P (2004) Attacking and Defending Web Service. A Spire Research Report.
[194]. Bertino E., Martino L. D., Paci F., Squicciarini A. C., "Security for Web Services and Service-Oriented Architectures", Springer, 2010.
[195]. Sinha S., Sinha S. K., Purkayastha B. S., "Security Issues in Web Services : A Review and Development Approach of Research Agenda", Assam University Journal of Science & Technology : Physical Sciences and Technology, Vol. 5 Number II,134-140, 201
[196]. Orrin S., "The SOA/XML Threat Model and New XML/SOA/WEB 2.0 Attacks &Threats", Dir of Security Solutions, SSG-SPI, Intel Corp.
[197]. Rami Jaamour, "Securing Web Services".
[198]. Artem Vorobiev and Jun Han, "Security Attack Ontology for Web Services"
[199]. Vipul Patel, Radhesh Mohandas and Alwyn R. Pais, "Attacks On Web Services And Mitigation Schemes".
[200]. Carlos Gutiérrez, Eduardo Fernández-Medina and Mario Piattini, "A Survey of Web Services Security".

# Reluctance Network Model Circuit Analysis and Optimization of Permanent Magnet Brushless DC Motor

*İsmail TOPALOĞLU[31], Fatih KORKMAZ[1], Hayati MAMUR[1]*

***Abstract***

*The main idea of this study is to optimize the performance of brushless DC motor (BLDCM). The originality of this work concerns on the use of a Reluctance Network (RN) method, which furnishes the harmonics of output parameters such as torque and back-emf. Then, precise and very fast optimizations are performed by gradient method as Sequential quadratic programming (SQP) which is an iterative method for nonlinear optimization. The results of the study are also compared to Finite Element Analysis (FEA) and several optimizations are presented. Optimization process has been focused on minimizing weight of BLDCM and ohmic loss. That is why; objective functions of BLDCM have been developed and presented in the paper. The optimal BLDC motor design with slot/pole combinations 24/8 has been obtained. The motor with 24 slots and 8 poles yields the highest torque density with the lowest mass of active parts copper, laminations, and magnets respectively. Finally, the proposed method helps engineers to have a better sense of machines behaviour and to quickly optimize the dimensions of their machines during preliminary design process.*

**Keywords:**

## 71. INTRODUCTION

Brushless DC motor is widely used in industry because of having many advantageous from other motors such as high torque in small volume, high efficiency, usable in high-speed applications. Some researcher have been studied to optimizing brushless DC motor using finite element analysis [1-3]. Some of them have been studied using optimization techniques such as genetic algorithm, pattern search and global optimization methods [4-7]. Each optimization process has been focused on minimizing or maximizing a parameter. In this study, optimization process has been focused on minimizing weight of BLDCM and ohmic loss. Electromagnetic equivalent circuit has been used for solution of optimization problem [8-10]. Permanent magnet shape values determined using two dimensional finite element analysis in literature [11-13]. Solving this kind of optimization problem has been taken long time [14-15]. Sequential quadratic programming (SQP) which is an iterative method for nonlinear optimization, is suitable for this kind of optimization problem. It provides wide solution area for using reluctance network model of proposed motor. Besides reluctance network model has been obtained for 24/8 brushless dc motor. Extended and forced optimization solutions can be obtain by using special techniques such as parametric approach, however, this techniques are not allowed to get satisfactory results. In this case, authors preferred reluctance network model of proposed motor with using sequential quadratic programming (SQP) to obtain better results. In addition, results show that used techniques generates better results. Several optimizations, which used reluctance network model, are presented in the study. BLDCM equations for torque, sizing equations, etc. can be found in literature [16-17]. In this study, objective functions of optimization problem have been developed and presented.

## 72. RELUCTANCE NETWORK MODEL

Reluctance network model can be define simply by using non saturated air gap reluctance sign, saturated iron reluctance sign, magnet sign, and MMF sign. Model use flux, which occur in the motor. This method provides to calculating electromagnetic characteristic of machine as a unique model for various positions. Element based structure of machine is obtained and presented.

$$\Re_{PM} = \frac{L}{\mu_0 \mu_r S} \tag{1}$$

[31] *Corresponding author:İ l TOPALOĞLU, C k K k U v , El El E , 18100, Merkez/Cankiri, Turkey. itopaloglu@karatekin.edu.tr*

Where, L is length and S is section of permanent magnet, and $\mu_r$ relative magnetic permeability. Eq. 1 is describe reluctance of permanent magnets in reluctance network model. Eq. 2 describe reluctance of stator core in reluctance network model.

$$\Re_{Stator} = \frac{l}{\mu_0 \mu_r S} \quad (2)$$

Finally, reluctance network of brushless dc motor has been carried out. A unit magnetic circuit as shown in Fig. 2 can express the divided elements.

### *2.1. Characteristics of the BLDCM*

The main characteristics of the BLDCM are given in Table 1:

TABLE 1

MAIN FEATURES OF THE BLDCM

| | |
|---|---|
| **Number of stator slots** | 24 |
| **Number of rotor poles** | 8 |
| **Max. Power** | 3.5 kW |
| **Max. torque @ 1,500 rpm** | 18 N.m. |
| **Max. current (RMS)** | 35 A |
| **Number of turns (coils)** | 48 |
| **Outer diameter** | 124 mm |
| **Depth (Stack length)** | 84 mm |
| **Air-gap** | 0.85 mm |

### *2.2. Machine's geometry*

Optimization process and finite element analysis of machine have been carried out by using electromagnetic design software. So obtained machine scheme is presented in Fig. 1.

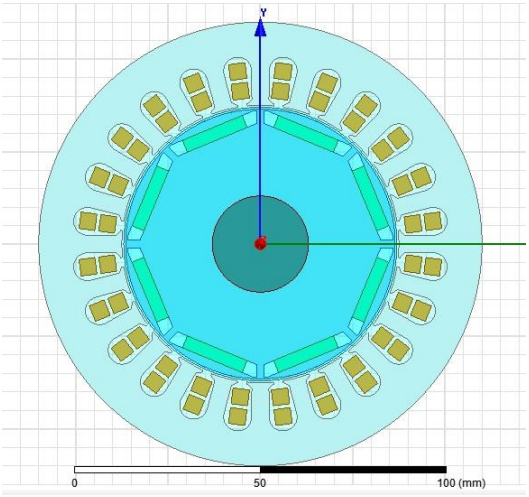


Fig. 1. General view of proposed BLDC motor

### *2.3. Reluctance network of the machine*

For the multistatic model, the RN of the 24/8 machine is modelled and is represented in Fig. 2. This model use as a unique model for various positions in optimization problems. Moreover, analysis results presented in Fig. 3, Fig. 4, Fig. 5, Fig. 6, and Fig. 7, respectively. In addition, transient analysis of machine has been carried out. Results are compared each other.

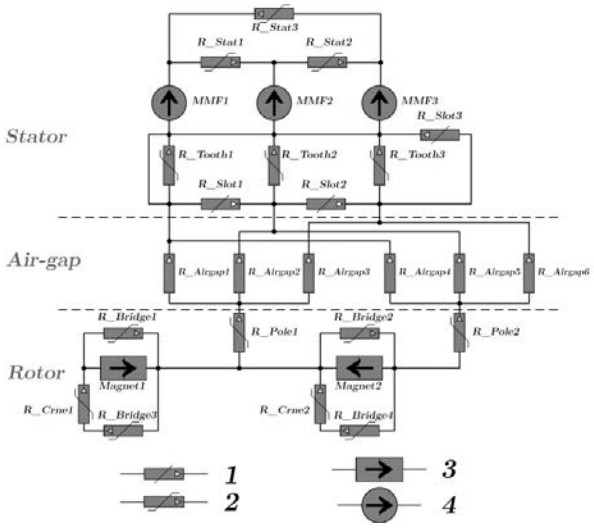


Fig.2. Reluctance network of the 24/8 BLDCM (1- non saturated air gap reluctance sign, 2- saturated iron reluctance sign, 3- magnet sign, 4- MMF sign)

**73. MULTI-OBJECTIVES OPTIMIZATION**

Developed objective functions of BLDCM, which is included cost function for optimization process is represented in Eq.3- Eq.11. Performances of BLDC with optimizations are presented in Table 2.

Stator teeth volume= $$V_t = \left(d_0^2 - d_i^2\right)\left(\left(d_s\left(\pi\left(d_0 + d_i\right)N_h N_m N_{sp} N W_{sb}\right)\right)\right) + \left(\left(\left(W_{sh} d_l\right) + \left(W_{sh} + W_{sb}\right)\frac{d_2}{2}\right)0.001\right)N_h N_m N_{sp} N \quad (3)$$

Stator back iron volume= $V_b = \pi\left(d_0^2 - d_i^2\right)\left(T_s - \left(d_s + \left(d_1 + d_2\right)0.001\right)\right)$ (4)

Stator iron volume= $V_s = V_t + V_b$ (5)

Weight of stator= $W_s = 2V_s\rho_s$ (6)

Magnet weight= $W_{PM} = 2\rho_{PM}\left(d_0^2 - d_i^2\right)\pi T_M$ (7)

Total active material weight of machine can be described as sum of weight of stator, magnet weight, rotor steel weight, and wire weight.

Rotor steel weight= $$W_R = \left[\pi d_s^2 \frac{1}{2}\left(T_m + T_s\right) + L_e + 2\pi\left(d_0 + \frac{\tau_r}{2}\right)\tau_r\left(\left(2T_m + \tau_t\right) + \pi\left(d_0^2 - d_i^2\right)\tau_r\right)\right]\rho_R \quad (8)$$

Wire weight= $$W_W = \frac{2N_h N_p N_w N_c N_{sp} L_m W_l}{48000} \quad (9)$$

Total active material weight= $W_{Total} = W_S + W_{PM} + W_W + W_R$ (10)

Total active material cost= $C_{Total} = W_S C_S + W_{PM} C_{PM} + W_W C_W + W_R C_R$ (11)

TABLE 2
EFFICIENT OF INITIAL & OPTIMAL MACHINES

| | Initial geometry | Optimal geometry |
|---|---|---|

| | | |
|---|---|---|
| **1,500 rpm** | 88.4 % | 92.5 % |
| **3,000 rpm** | 90.9 % | 96 % |

Table 2 shows that efficiency of machine differs under different speed. For instance, efficiency of machine is optimized 4.1 % at 1500 rpm but efficiency is 5.1% changed at 3000 rpm.

## 74. FEA ANALYSIS OF MOTOR

Finite element analysis has been carried out with using Ansfot Maxwell. Simulations realized under different configurations such as transient and magneto static. This is very important to analysis of machines because of machine characteristic is seen under load conditions. Fig. 3 show winding currents under load at transient analysis conditions.

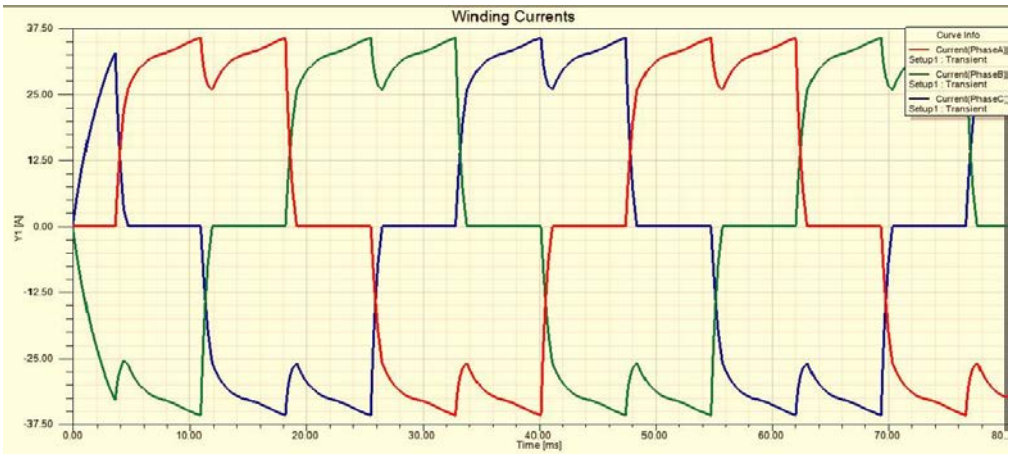


Fig. 3. Winding currents under load at transient conditions

Fig. 4 shows that winding current sunder load at magnet static conditions. Both transient and magneto static analysis results close match. In addition this, just only source current wave shape is different because of transient analysis is not included with this source. Proposed system does not contain any smart control algorithm, in this case speed parameters is not controllable in this stage. Both cost function and material weight is taken in account. Multi-objective optimization process include two limitation points. One of them is cost function and the other is material weight.

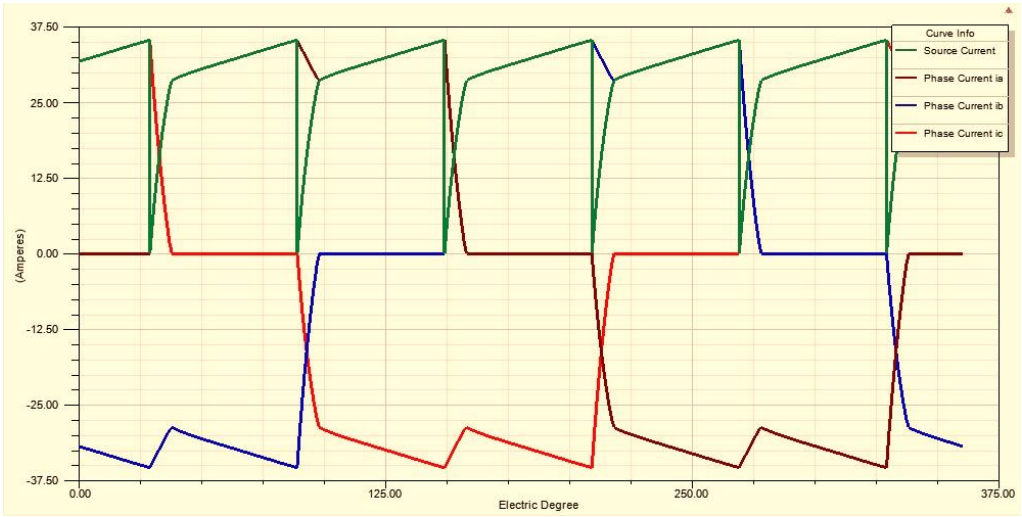


Fig. 4. Winding currents under load

Fig. 5 shows that phase voltages and line voltages under load. Fig. 6 shows that torque variation under load at transient conditions. At transient conditions torque of motor produced has ripples because of system has no vector control or specific control algorithms. Fig. 7 shows that efficiency of motor.

Efficiency is differ under transient conditions because of under this conditions have a lots of undefined variable in the analysis environment. In addition, voltages wave shape is include also some notch. This is occur because of magnet shape will affect directly the voltages wave shape.

$$I = \frac{V - E}{R + sL_s} \tag{12}$$

Eq. 12 is represent stator phase current. Where, $E$ is back emf of motor, $Ls$ is synchronous inductance, and $V$ is terminal phase voltage.

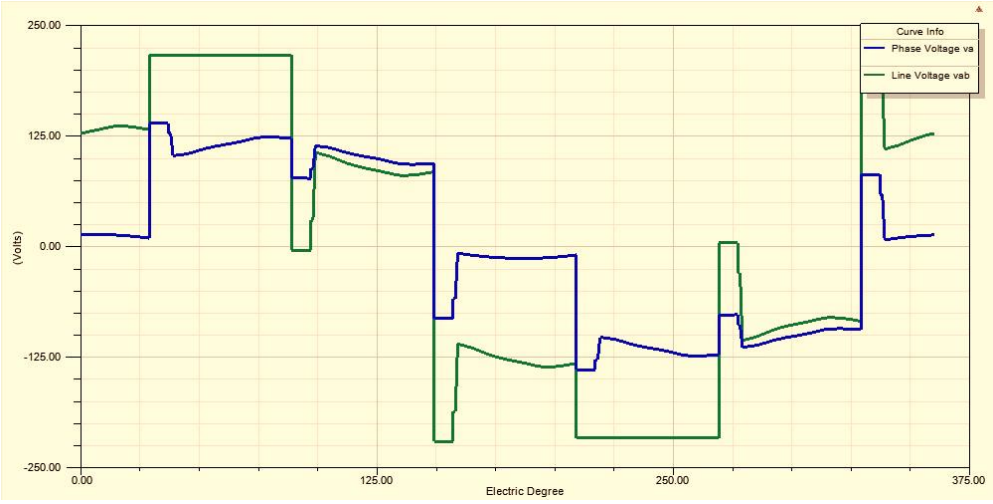


Fig. 5. Voltages under load

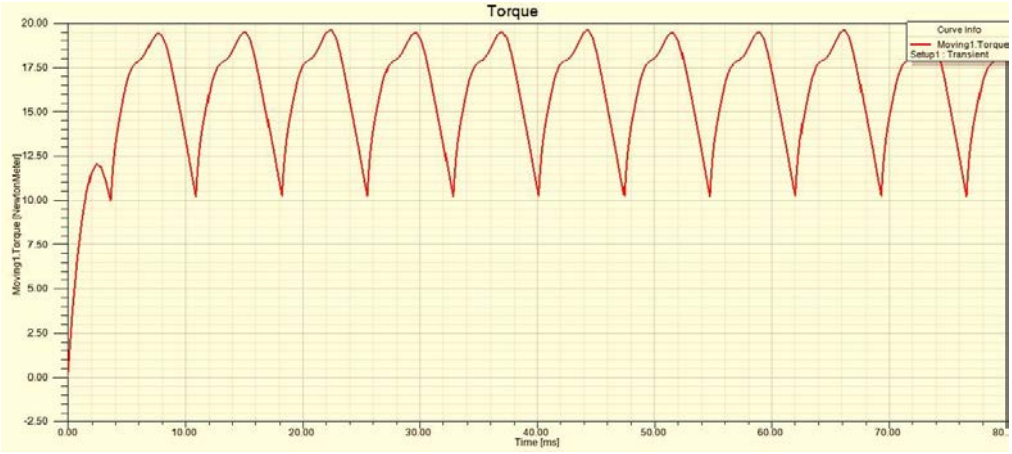


Fig. 6. Torque under load at transient conditions

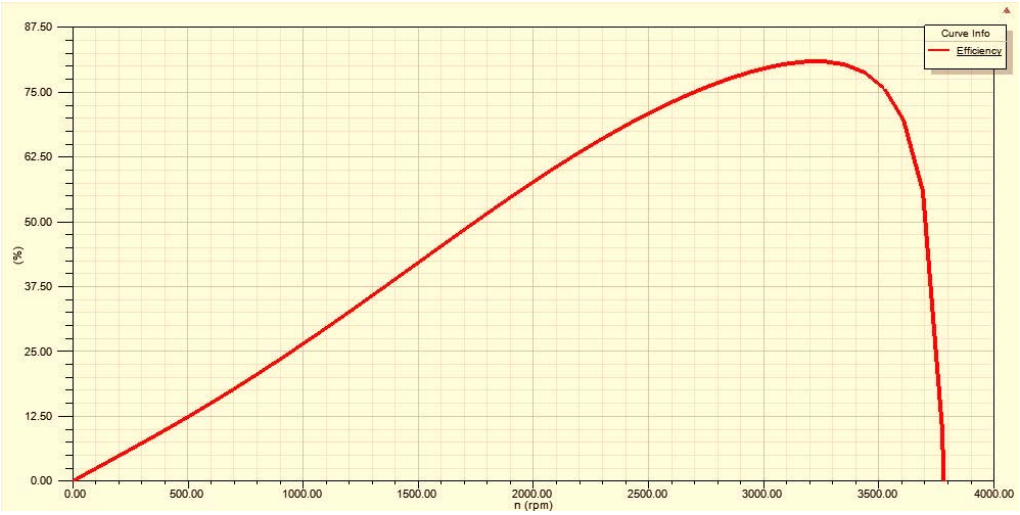


Fig. 7. Efficiency of designed motor at transient conditions

## 75. CONCLUSION

In this study, optimization and analysis of BLDC motor have been carried out by using reluctance network method. In addition, transient analysis has been realized. Developed objective functions of BLDC motor presented in the study. Optimum design for 24/8 BLDC motor configuration is obtained. Results show that very close match between transient simulations and magneto static simulations. Several optimization with multi-objective limiting points have been carried out. Proposed method provides a lot of advantageous for engineers to designing better machine. Finally, smart control algorithm can be added to system, then system will contain less voltages notch and torque ripples.

## ACKNOWLEDGMENT

The scientific research projects unit of Cankiri Karatekin University under grant (MF050315B15) supported this work.

## REFERENCES

1. Olorunfemi, O., 1991. “Multiobjective Optimum Design of Electrical Machines for Variable Speed Motor Drives”, IEEELAS Ann. Meet. Conf. Rec.,vol.1, pp 163-168. [doi: 10.1109/IAS.1991.178149]
2. Boules, N., and Wey, H., 1980. “Machine Constants and Design Consideration of a High Power Synchronous Machine of the Disc Construction Type”, Electric Machine & Electromagnetic, Vol. 5, pp 25-37.
3. Krishan, R., and Baradwaj, A.S., 1991. ‘‘A Comparative Study of Various Motor Drive Systems for Aircraft Applications”, IEEEAAS Ann. Meet. Conf. Rec., pp 252-258. [doi: 10.1109/IAS.1991.178163]
4. Bohon, H. R., Liu Y. D., and Mallinson, M. M., 1986. “Investigation Into a Class of Brushless DC Motor with Quassisquare Wave Voltages and Currents”, IEE Proceedings, Vol. 133, No. 2, pp 103-111.[doi: 10.1049/ip-b:19860015]
5. Chan, C. C., 1987. “Axial Field Electrical Machines Design and Applications”, IEEE Transactions on Energy Conversion, EC. Two, No. 2, pp: 294-300. [doi: 10.1109/TEC.1987.4765844]
6. Slemon, G. R., 1992. “On the Design of High Performance PM Motors”, IEEEiIAS Ann. Meet. Conf. Rec., pp 279-285. [doi: 10.1109/IAS.1992.244283]
7. Boules, N., 1987. “Design Optimization of Permanent Magnet DC Machines”, IEEEiIAS Ann. Meet. Conf. Rec., pp 27-34.
8. Amaratunga, G., Acarnley, P., and McLaren, P., 1985. “Optimum Magnetic Circuit Configuration for Permanent Magnet Aerospace Generators”, IEEE Transactions on Aerospace and Electronics Systems, Vol. AES 121, No. 2, pp 230-254. [doi: 10.1109/TAES.1985.310620]
9. Hippner, M., and Harley, R. G., 1992. “Looking for an Optimal Rotor for High Speed Permanent Magnet Synchronous Machine”. IEEEAAS Ann. Meet. Conf. Rec., pp 265-270. [doi: 10.1109/IAS.1992.244285]
10. Wang R., Gieras J., 1998. “Analysis of characteristics of a permanent magnet hybrid linear stepping motor”. Proceedings of ICEM, Istanbul, Turkey, 2-4, pp. 833-838. [doi: 10.1109/AFRCON.1996.563106]
11. Silvester P., 1967. “Network analog solution of skin and proximity effect problems”. IEEE Transactions on Power Apparatus and Systems, Vol. 86, No. 2, pp. 241- 247. [doi: 10.1109/TPAS.1967.291841]
12. Sewell P., Bradley K., Clare J., Wheeler P., Ferrah A., Magill R., Sunter S., 1998. “Dynamic reluctance mesh modelling of induction motors”. Proceedings of ICEM, Istanbul, Turkey, pp. 1324-1329. [doi: 10.1109/ICELMACH.2008.4799896]

13. Rasmussen C., Ritchie E., 1997. “Improved reluctance-mmf network for calculation of magnetic field distribution in surface-mounted permanent-magnet motors”. Electromotion, No. 4, pp. 55-61.

14. Topaloglu, I., Gürdal, O., 2013. “Design of Linear Electromagnetic Launcher System and Dimension Optimization Using Equivalent Circuit Model of Linear Electromagnetic Launchers to Improve Launching Performance" Journal of the Faculty of Engineering and Architecture of Gazi University, Vol (No); 28(1) pp: 103-113.

15. Topaloglu, I., Gürdal., O. 2010. “A Second Order Sensitivity Analysis Based Numerical Approach Developed for Dimension Optimization, in Electric Machine Design by Electromagnetic Design Programme”, Journal of The Faculty of Engineering and Architecture of Gazi University, Vol (No); 25 (2) pp: 363-369.

16. Topaloglu, I., Korkmaz, F., Mamur, H., Gürbüz, R., 2013. "Closed-Loop Speed Control of PM-BLDC Motor Fed by Six Step Inverter and Effects of Inertia Changes for Desktop CNC Machine", Electronics and Electrical Engineering. – Kaunas: Technologija, vol. 19, no:1, p. 7-10. [doi: 10.5755/j01.eee.19.1.3244]

17. Korkmaz, F, Topaloglu, I., 2013, “Comparative performance evaluation of foc and dtc controlled pmsm drives” IEEE IV. International Conference on Power Engineering, Energy and Electrical Drives,.

# Air Gap Optimization of Iron Core Shunt Reactions with Discretely Distributed Air Gaps for UHV Systems

*İsmail TOPALOĞLU*[32]

***Abstract***

*This paper proposed optimal design of iron core Shunt reactors with discretely distributed air gaps that can suppress over-voltages of high voltage transmission line in various situations, such as, the power frequency over-voltage regulation. It needs very hard optimization process to optimizing discretely distributed air gaps in shunt reactors. Precise and very fast optimizations are performed by gradient method as Sequential quadratic programming (SQP) which is an iterative method for nonlinear optimization. The results of the study are also compared to Finite Element Analysis (FEA) and several optimizations are presented. Optimization process has been focused on minimizing weight of shunt reactor and ohmic loss. The magnetic circuit structure and working principle of shunt reactor are analyzed as well as the technical features in the paper. The proposed method helps engineers to have a better sense of voltage control and reactive power regulation of ultra-high voltage transmission line.*

**Keywords:**

## 76. INTRODUCTION

Shunt reactors to prevent voltage fluctuations that occur from changes in load and capacitive load of high-voltage lines are used to absorb. Shunt reactors at power transmission lines according to the load condition remains active as they can be switched on continuously. Shunt reactors are composed transients entering the circuit and inrush current is the most important of them. In this study, Shunt reactors intended use of the transmission lines to reduce the voltage rise. Shunt reactors suppress excessive capacitive loads which are formed by energy transmission lines, underground cables can be activated partially or altogether. In this way, they can provide extra reactive power into the power transmission line. However, when shunt reactors startup that bring transient events occurring on the power system in the high voltage lines. Many researcher have been investigated transient situations on shunt reactor. [1-5]. Shunt reactor controllability, operating characteristics and effects of different connection types were examined [6-10]. Traditional power compensation equipment, low voltage shunt capacitor banks, static VAR compensator and generator groups; do not provide the required reactive power regulation and voltage spikes [11-13]. Many researchers have studied reactor design since early 1900's. A method of designing air-gap in transformers and chokes to obtain a constant inductance has been introduced in [14] by experimental studies with superimposed dc and ac excitations. Calculation of apparent inductance of a gapped iron-core reactor under superimposed dc and ac excitation has been presented in [15]. An analytical design approach to gapped C-core inductor has been described using flowcharts in [16] for superimposed dc and ac currents. The behavior of the magnetic flux in a shunt reactor with a toroidal core, neglecting leakage flux, has been studied by 3D FEM analysis in [17]. In [18] optimization of smoothing

inductors for electric traction by 6 obtaining the magnetic field distribution using FEA has been introduced for only single air-gap case. A foil winding model for FEA simulations has been developed and introduced in [19]. The reluctances of a gapped core inductor has been calculated in [20] using Schwarz-Christoffel Transformation. Effect of fringing flux has been

[32] *Corresponding author: İ l TOPALOĞLU, C k K k U v , El El E , 18100, Merkez/Cankiri, Turkey. itopaloglu@karatekin.edu.tr*

considered and inductance calculated by FEA, however distribution of air-gap and leakage inductance have not been defined in [20].

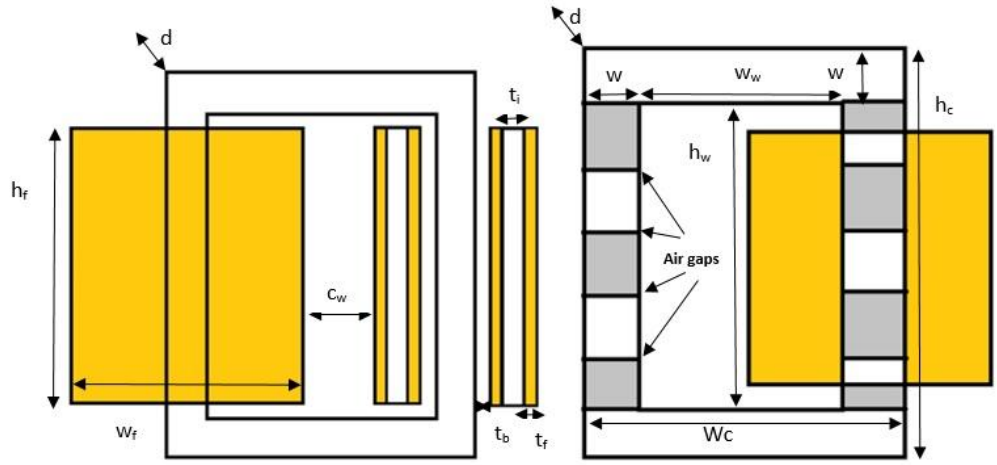


Fig. 1. Illustration of core and winding dimensions

Here, in Fig.1, $c_w$ is clearance between two windings, d is depth of the core, $h_c$ is total height of the core, $h_f$ is height of the coil, $h_w$ is height of the window, $t_b$ is thickness of the tube, $t_f$ is thickness of the copper (each turn), $t_i$ is thickness of the insulation material between each turn, w is width of the limb and the yoke, $w_c$ is total width of the core and $w_w$ is width of the window.

## 77. SEQUENTIAL MIXED INTEGER NONLINEAR PROGRAMMING METHOD

In the design model, this optimization technique permits identification each variable depending each other in continuous space. Linear variables used in this technique definable in Eq. 1.

$$\sum_i \alpha_{ij} x_i < c_j \forall_j \tag{1}$$

Here; $\alpha_{ij}$ represents coefficients, $c_j$ is comparison value for linear variable $J^{th}$ and $x_i$ is design parameter of $i$. The objective function is minimized using the variable to meet the following constraints Eq.2 and Eq. 3.

$Min\, f(y(x_k))$ or $Max\, f(y(x_k))$ for;

$$\begin{aligned} h_i(y(x_k)) &= 0, \quad i = 1,2,3,\ldots\ldots,m \\ g_j(y(x_k)) &= 0, \quad i = 1,2,3,\ldots\ldots,n \end{aligned} \tag{2}$$

$$x_k^u \geq x_k \geq x_k^l \qquad k = 1,2,3,\ldots\ldots,j \tag{3}$$

Here; $f(y(x_k)) = \{f_1(y_1(x_k)), f_2(y_2(x_k)), f_3(y_3(x_k)), \ldots\ldots, f_n(y_n(x_k))\}$ is objective function vector. $g_j$ and $h_i$ are inequality and equality constraint functions respectively. $x_k^u$ and $x_k^l$ are upper and lower limits. $y$ is the second variable depends on the variable $x_k$. Figure 2 shows the solution domain and focus range of the variable.

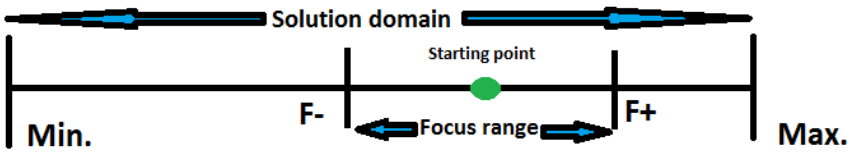


Fig. 2. Solution area of sequential mixed integer nonlinear programming optimization method.

### *77.1. Definition of shunt reactor electrical behavior*

When shunt reactors operating in the energy system, the shunt reactor system behavior demonstrated by the following equations; Eq.4, 5, 6 and 7. In addition, these equations are fundamental equivalent circuit parameters.

$$e = i_L R + u_L \;\Rightarrow i_L = \frac{e - u_L}{R} \tag{4}$$

$$u_L = L\frac{di_L}{dt} \tag{5}$$

$$i_L = \frac{e - L\frac{di_L}{dt}}{R} \Rightarrow i_L^{'} + \frac{R}{L}i_L - \frac{e}{L} = 0 \tag{6}$$

$$e = E_{\max} Sin(\omega t + \alpha) \tag{7}$$

Equation 8 shows that when switches are open or closed for shunt reactor. As seen here, when the switches are open, shun reactor is not running so in this case transient and steady state situations are equal to zero.

$$\begin{aligned} &i_L = i_{Transient} + i_{Steady} \Rightarrow i_{Transient} + i_{Steady}\big|_{t=0} = 0, \\ &i_{Transient} + i_{Steady}\big|_{t=\infty} = i_{Steady} \end{aligned} \tag{8}$$

$$|Z| = \sqrt{R^2 + (\omega L)^2} \tag{9}$$

$$\arctan(\varphi_U - \varphi_Z) \cong \arctan(-\varphi_Z) = -\frac{\omega L}{R} \quad \{\varphi_Z = 0, \varphi_Z = \pi, \varphi_Z = 2\pi, K\} \tag{10}$$

Circuit impedance and phase angle calculations are given in Equation 9 and 10.

$$i_L(t) = i_{Transient} + i_{Steady} = A \cdot e^{-\frac{R}{L}ts} + \frac{e}{\sqrt{R^2 + (2\pi fL)^2}} \sin(2 \cdot \pi \cdot ts + \varphi_U - \varphi_Z) \tag{11}$$

$$A = -\frac{e}{\sqrt{R^2 + (2\pi fL)^2}} \sin(2 \cdot \pi \cdot ts + \varphi_U - \varphi_Z) e^{-\frac{R}{L}ts} \tag{12}$$

The steady state and transient current conditions are given equations 11 and 12. A factor in this equation is given by equation 12. When shunt reactor's switches are closed and opened that occurred voltage and current are given equation 13, 14, 15 and 16 respectively.

When switches are closed;

$$i_L(t) = \left\{ \begin{array}{l} -\dfrac{e}{\sqrt{R^2 + (2\pi fL)^2}} \sin(2 \cdot \pi \cdot ts + \varphi_U - \varphi_Z) e^{-\frac{R}{L}t - ts} \\ +\dfrac{e}{\sqrt{R^2 + (2\pi fL)^2}} \sin(2 \cdot \pi \cdot t + \varphi_U - \varphi_Z) \end{array} \right\} \tag{13}$$

$$u_L = \left\{ \begin{array}{l} -R \cdot \dfrac{e}{\sqrt{R^2 + (2\pi fL)^2}} \sin(2 \cdot \pi \cdot ts + \varphi_U - \varphi_Z) e^{-\frac{R}{L}t - ts} \\ +2\pi fL \dfrac{e}{\sqrt{R^2 + (2\pi fL)^2}} \cos(2 \cdot \pi \cdot t + \varphi_U - \varphi_Z) \end{array} \right\} \tag{14}$$

When switches are open;

$$i_L(t) = \left\{ -\frac{e}{\sqrt{R^2 + (2\pi fL)^2}} \sin(2 \cdot \pi \cdot ts + \varphi_U - \varphi_Z) e^{-\frac{R}{L}t - ts} \right\} \tag{15}$$

$$u_L = L\frac{di_L}{dt} = \left\{ -R \cdot \frac{e}{\sqrt{R^2 + (2\pi fL)^2}} \cdot \sin(2 \cdot \pi \cdot ts + \varphi_U - \varphi_Z) e^{-\frac{R}{L}t - ts} \right\} \quad (16)$$

## 78. OBJECTIVE FUNCTIONS OF IRON CORE SHUNT REACTORS WITH DISCRETELY DISTRIBUTED AIR GAPS

The problem considered in this work is to design a shunt reactor to be used in an ultra-high voltage power system (UHV). The system is composed of iron core, windings and discretely distributed air gaps. Design parameters used are as follows: air gaps of shunt reactor, total air gap ($l_g$) and air gap inductance ($L_g$).

$$L_g = N^2 \frac{\mu_r \mu_0 A}{l_g} \Rightarrow l_g = \frac{\mu N^2 A}{L_g} \quad (17)$$

Here, Eq.17 used in objective function vector, then Eq. 18 optimization function has been obtained for shunt reactor.

$$f\left(l_g\left(\frac{\mu N^2 A}{L_g}\right)\right) = \left\{ f_1\left(l_{g1}\left(\frac{\mu N^2 A}{L_g}\right)_1\right), f_2\left(l_{g2}\left(\frac{\mu N^2 A}{L_g}\right)_2\right), \ldots\ldots f_n\left(l_{gn}\left(\frac{\mu N^2 A}{L_g}\right)_n\right) \right\} \quad (18)$$

Eq. 5 used in the optimization process minimizing the operational cost and production cost. The operational cost and production cost functions are seen in Eq. 19 and Eq. 20.

*Production Cost= ($(N_{core}$*$N_{pr}$)+($C_{copper}$ *$C_{pr}$))*1.65*1.20*1.20*
(19)

*Operational Cost=Total loss*Electrical price (kWh)*24*30*Year*
(20)

## 79. OPTIMIZATION RESULTS

Each optimization work has been performed for four different peak flux density values (0.85 T, 1.05 T, 1.25 T and 1.35 T), therefore several iterations were needed to be performed to obtain the target inductance. If the target inductance has not been satisfied in the first iteration, next iteration has been performed by increasing the number of turns or decreasing the total length of the air-gap sections in the core or vice versa. Inductance parameters and core losses have been calculated by using Maxwell 2D optimization work. Finally, the results of these three different design criteria obtained from FEA have been compared. A further objective of this work is to investigate the effects of number of discretely distributed air-gaps, AG on the OC and PC of the optimum reactors. For this purpose, each design work is carried out for two different number of air-gaps i.e., AG=4 and AG=16.

Table 1. shows that production cost and operation cost of shunt reactor are small under 480kVAR, 2.2 kV and 75 $C^o$ for other compensation equipment. Optimization problem parameters such as *N(turns)*, *A(mm$^2$)*, and $L_g$ (*total air gap length*) that changed under solution process are presented in table 1. These parameters are varied because of shunt parameters operating values changed before the optimization solution process. Flux density of shunt reactor is directly affected the operation and production cost. Figure 3 shows that 2D air gap optimization of shunt reactor model core magnetic flux density and windings magnetic field intensity.

Table 1. Optimization results under different air gaps and flux density

| Name of parameters | Distributed air gaps=4 | Distributed air gaps=16 | Flux density=0.85 T | Flux density=1.05 T | Flux density=1.25 T | Flux density=1.35 T |
|---|---|---|---|---|---|---|
| *Production* | 4225 | 4325 | 3824 | 4207 | 4465 | 4682 |

| | | | | | | |
|---|---|---|---|---|---|---|
| *Cost $* | | | | | | |
| *Operational Cost $* | 1832 | 1245 | 2465 | 2365 | 1978 | 1454 |
| % leakage | 5 | 5 | 14.5 | 15 | 16.5 | 17 |
| $L_g$ (mm) | 12 | 20 | 18.8 | 15.6 | 14.3 | 11,7 |
| N (turns) | 180 | 200 | 184 | 196 | 228 | 264 |
| A ($mm^2$) | 12935,91 | 52597,87 | 13221,23 | 11727,45 | 11527,43 | 11021,03 |

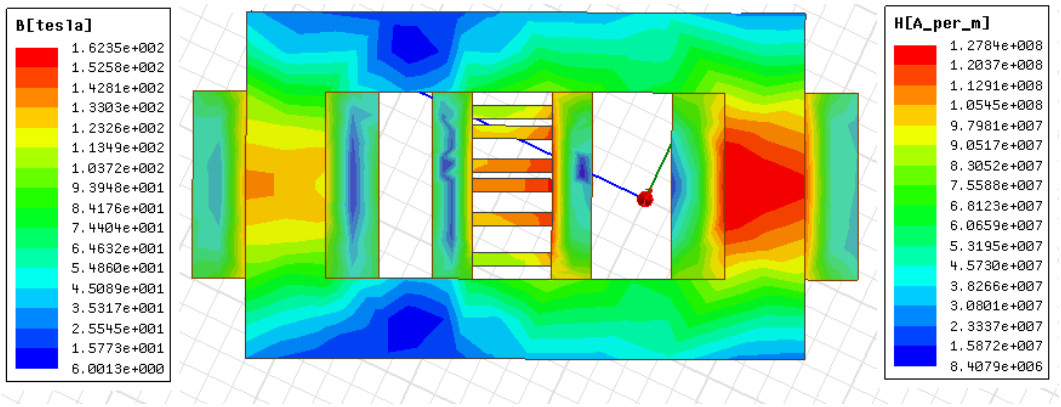


Fig. 3. Air gap optimization of shunt reactor 2D model.

## REFERENCES

[201]. Bossche, V., Cekov, A., Vencislav, V., Inductors and Transformers for Power Electronics. Boca Raton, FL, USA: Taylor & Francis Group
[202]. All circuit models were made in "Tina for Windows – the Complete Electronics Lab" software made by DesignSoft: http:// www.designsoftware.com
[203]. Quad Tech. LCR Primer Measurement Instruction Manual. Massachusetts USA. http:// www.quadtech.com
[204]. Ramli, M.S., 2008, Investigation of Circuit Breaker Switching Transients for Shunt Reactors and Shunt Capacitors, Master thesis, Avustralya.
[205]. Chen Weixian, Chen He, Lu tiecheng, and Zhou Wenjun, 2005, Ultra-high Voltage Controllable Shunt Reactor, High Voltage Eengineering, 31, (11), pp.26-27.
[206]. Hasibar R M, Legate A C,Brunke L, 1981, The application of highspeed grounding switches for single-pole reclosing on 500kV power systems,. IEEE Trans on PAS, 100(4), pp:1512-1515.
[207]. Chen, B., Kokermak, J, M, Torrey, D, A, 1999, Harmonicfree single-phase controlled saturable reactor using active filtering, IEEE international Conference on Power Electronic and Drive System, PEDS'99, pp.1037-1042.
[208]. Zhou, Q, Guo, Q, Guangquan B., Liangeng B., 2007, Application of controllable reactors in China's power grid at extra and ultra voltage level, Proceeding of the CSEE, 27(7), pp.1-6.
[209]. Donuk, A. 2012, Modeling and Design of Iron-Core Shunt Reactors with Discretely Distributed Air-Gaps, Ph.D. Thesis, METU, pp:4-6.
[210]. Xu, W, Chen, S, Jinliang H., 2005, Research on switching over-voltage caused by faults in 1000kV UHV ac transmission line, Power System Technology, 29(21), pp.10-13.
[211]. Chen, H, Chen, W., 2002, Choice of inductance on neutral of shunt reactors,"High Voltage Engineering, 28(8), pp.9-10.
[212]. Zhou, L., Zhu, Y., Zhou, Z, 2006, Regulating range of UHV controlled shunt reactor, Transactions of China Electro technical Society, 21(12) pp.116-120.
[213]. Zhang, L., Xu, Y., 2007, Application and devdlopment of shunt reactors in EHV & UHV transmission lines, Electric Power Automation Equipment, 27(4), pp.75-78.
[214]. F. W. Lanchester, The Air-Gap Transformer and Choke, Proceedings of the Institution of Electrical Engineers - Wireless Section, Vol. 8, Issue 24, pp.195- 200, 1933.
[215]. MIT Members, Magnetic Circuits and Transformers, MIT press, 1943.
[216]. Anil K.Ohri, Thomas G. Wilson, Harry A. Owen, Jr., Design of Air-Gapped Magnetic-Core Inductors for Superimposed Direct and Alternating Currents, IEEE Transactions on Magnetics, Vol. Mag-12, No. 5, pp. 564-574, 1976.
[217]. Y. Ishihara, T. Morino, T. Todaka, Analysis of Magnetic Fields of a Delta Type Shunt Reactor, IEEE Transactions on Magnetics, Vol. 25, No. 4, pp. 2846-2848, 1989.
[218]. C.M. Arturi, M. Ubaldini, Finite Element Analysis and Calculation of the Magnetic Field Distribution in Smoothing Inductors for Electric Traction, IEEE Transactions on Magnetics, Vol. 25, No. 4, pp. 2864-2866, 1989.

[219]. H.D. Gersem, K. Hameyer, A Finite Element Model for Foil Winding Simulation, IEEE Transactions on Magnetics, Vol. 37, No. 5, pp. 3427-3432, 2001.
[220]. A. Balakrishnan, W.T. Joines, T.G. Wilson, Air-Gap Reluctance and Inductance Calculations for Magnetic Circuits Using a Schwarz-Christoffel Transformation, IEEE Transactions on Power Electronics, Vol. 12, No. 4, pp. 654-663, 1997.

# Investigation of Anti-Termite Activity of Wood Treated with Geothermal Fluids from Different Regions of Turkey

*Mesut Yalçın[1*], Çağlar Akçay[1], Teresa de Troya[2], Hüseyin Sivrikaya[3], Hediye Ceylan[1]*

***Abstract***

*The objective of this study was to investigate the anti-termite activity of geothermal fluids supplied from different regions of Turkey. Scotch pine treated with fluids either evaporated or non-evaporated obtained from Ankara, Afyon, Denizli and Eskişehir regions in Turkey. The increasing in the concentration of geothermal fluids significantly decreased the mass loss caused by termite, and increased the termite mortality. Mass losses of all wood samples treated with geothermal fluids were found lower than those treated with pure water. The highest mass losses were found in pure water and non-concentrated fluids provided from Denizli and Afyon (0%) while the lowest mass losses were found in wood treated with thermal fluid from Denizli (75%). The highest and lowest termite mortality was found in the samples treated with evaporated fluid from Denizli (75%) and pure water, respectively. This study indicated that geothermal fluids might be evaluated to protect wood material against termites when it was evaporated.*

**Keywords:** *Geothermal fluid, termite, Scotch pine, wood protection*

## 1. INTRODUCTION

Wood is one of the oldest and most common used materials in various purposes such as building construction. Due to thermal properties of wood, easy workability, absorption of sound, better acceptance of paint and varnish, being more aesthetic than other materials, the need for and usage of wood material is increasing day by day [1]. However, wood has some disadvantages such as combustibility, moisture change, and vulnerability to degradation by termites as well as fungi and insects. In order to protect the wood material against biological organism, it must be impregnated with wood preservatives [2].

Recently, some traditionally wood preservatives such as CCA (copper chrome arsenic) have been banned or restricted due to their harmful effects of on the environment in many European countries, Japan and United States of America. Scientists have tended to develop new environmentally friendly wood preservatives [3].

Few studies have been done on usability of geothermal fluids for wood protection. Var et al. (2012) [4] found that geothermal fluids can be used against wood-degrading fungi. However, yet there is no published study on geothermal fluids that might be effective against termites that degrade the wood.

Turkey has an important position in the world in terms of geothermal resources [5,6]. Geothermal energy is a heat flow that rise to the surface from the depths of the earth's crust by the effecting of high temperature formed from natural degradation of pluton and radioactive elements in magma in the earth's crust. Geothermal resource is dry or wet steam/water extracted from earth's crust [5,6,7]. This water contains some minerals like boron (B), chloride (Cl), potassium (K), sodium (Na), fluoride (F), silicondioksit ( $SiO_2$), ammonia ($NH_3$) and sulfate ($SO_4$), and most of them are found in the wood preservatives in large quantities to protect wood against biological organisms [8].

In the current study, we investigated the anti-termitic properties of geothermal fluids provided from four different regions of Turkey. This study is the first to evaluate the using of geothermal fluids in wood treatment against the termites in the laboratory scale.

## 2. MATERIAL AND METHODS

* [1]*Corresponding Author:* Duzce University, Department of Forest Industry Engineering, 81620, Düzce, Turkey. mesutyal@hotmail.com
[2]*INIA-CIFOR Forest Products Department, wood protection Laboratory, Madrid, Spain*
[3]*Department of Forest Products Engineering, Faculty of Forestry, Bartın University, Bartın, Turkey*

### *2.1. Evaporation of Geothermal Fluids*

The geothermal fluids used in this study were obtained from Ankara, Denizli, Afyon and Eskişehir region in Turkey. To increase the concentration of the active ingredients in geothermal fluids, each natural geothermal fluid was evaporated by 75%. The Scots pine samples either treated with non-concentrated fluids (natural) or evaporated to 75% of geothermal fluids. The distillated (pure) water was used as reference to compare with geothermal fluids in wood treatment

### *2.2. Termite Test*

Wood samples treated with geothermal fluids and pure water that were subjected to *Reticulitermes grassei* (Blattodea, Rhinotermitidae) termites in the forest product department laboratory of INIA- CIFOR according to the EN 117 (2005) [9]. After termite test, termite mortality as well as mass losses occurred in Scots pine samples were determined. A test specimen was placed into a cylindrical test container. Totally 80 workers, 3 nymphs and 3 soldiers were placed into the container. Three replicate were used for each treatment against termites. Termite test environment was set up as 28 °C and 85% for 8 weeks. After the test exposure period, the exposed wood samples were weighed to determine the post exposure weight. Percent mass loss and termite mortality were calculated as follows:

$$\text{Mass loss } (\%) = \left[\frac{M1-M2}{M1}\right] x100 \quad (1)$$

Where, M1: the weight of the test samples before exposure against termites (g), M2: The weight of the test samples after termite test (g), Termite mortality was calculated as follows:

$$\text{Termite mortality } (\%) = \left[\frac{T1-T2}{T1}\right] x100 \quad (2)$$

Where, T1 is the number of termites alive at the beginning of the test and T2 is the number of termites alive after the termite test.

### *2.3. Statistical Analysis*

The SPSS software (SPSS 19, 2010) [10] was used as statistical tool. As a result of multiple analyses of variation (ANOVA) tests, the geothermal sources, concentration levels and their interactions on mass losses and termite mortality were evaluated. In addition, a Duncan test was used to compare values.

## 3. RESULTS AND DISCUSSION

The results obtained from termite resistance test are shown in Table 1. According to the results, 22% mass losses occurred in the samples treated with pure water (control samples). The mean weight losses in the Scotch pine wood impregnated with 4 different geothermal fluids used in the study were lower than the control samples. Table 1 indicates that mass loss due to the termite activity significantly decreased in wood treated with fluids from Denizli and Afyon when evaporated to 75 %. Although low weight losses were detected in the samples treated with Eskisehir geothermal fluids, no significant change was found in the case of concentrated level. The lowest weight loss were occurred in treated with Denizli geothermal fluid evaporated by 75%.

*Table 1. The mass losses caused by R. grassei termite in Scotch pine treated with geothermal fluids*

| Regions | Evaporated ratio | Mass losses (%) | H.G | Min. | Max. |
|---|---|---|---|---|---|
| Pure water | | 22,2 (0,5) | *d* | 21,7 | 22,7 |
| Denizli | 0% (X) | 20,7 (3,1) | *d* | 17,9 | 24,0 |
| | 75% (T) | 10,9 (1,6) | *a* | 9,2 | 12,4 |
| Afyon | 0% (X) | 20,1 (4,4) | *d* | 16,9 | 25,1 |
| | 75% (T) | 12,9 (0,8) | *ab* | 12,0 | 13,5 |
| Ankara | 0% (X) | 16,6 (1,4) | *c* | 15,5 | 18,1 |
| | 75% (T) | 15,4 (1,4) | *bc* | 14,4 | 17,0 |
| Eskişehir | 0% (X) | 13,3 (2,3) | *abc* | 11,9 | 15,9 |
| | 75% (T) | 13,4 (1,6) | *abc* | 11,5 | 14,3 |

H.G: Homogeny groups

Figure 1 shows the percent preventing effect of geothermal fluids against *R grassei* according to control samples (pure water) in terms of mass loss. It can be seen that the best performance was obtained in the samples treated with fluid evaporated to 75% (Denizli) with regard to mass loss as shown in Figure 1. Among the natural fluids, Eskisehir was also found efficient in relation to termite performance, whereas fluid from Denizli showed the lowest effect. It means that evaporating process significantly increases the performance of fluid from Denizli against termite activity.

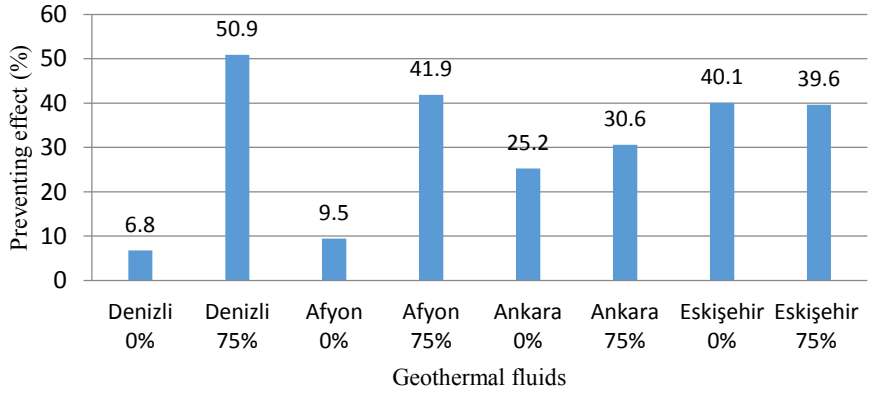


*Figure 1. Preventing effect of geothermal fluids against R grassei compare with control sample (pure water) in terms of mass loss*

The results of termite mortality were shown in Table 2. As it can be seen in the table, the lowest termite mortality occurred in control samples treated with pure water. Additionally, higher ratio were detected in termite mortality when the wood samples treated with fluid from Afyon evaporated to 75 % and geothermal fluids from Ankara. The highest termite mortality (60 %) occurred in the wood treated with evaporated fluid (75 %) from geothermal source in Denizli.

*Table 2. Termite mortality caused by R. grassei termite in Scotch pine treated with geothermal fluids*

| Regions | Evaporated levels | Termite Mortality (%) | H.G | Minimum | Maximum |
|---|---|---|---|---|---|
| Pure water | | 10,7 (11,6) | *a* | 23 | 0 |
| Denizli | 0% (X) | 19,7 (4,0) | *ab* | 15 | 22 |
| | 75% (T) | 60,3 (17,7) | *c* | 40 | 72 |
| Afyon | 0% (X) | 26,0 (8,7) | *ab* | 16 | 32 |
| | 75% (T) | 37,0 (8,5) | *b* | 29 | 46 |
| Ankara | 0% (X) | 29,3 (11,2) | *ab* | 21 | 42 |
| | 75% (T) | 29,3 (4,5) | *ab* | 25 | 34 |
| Eskişehir | 0% (X) | 34,3 (17,8) | *b* | 15 | 50 |
| | 75% (T) | 30,0 (9,5) | *ab* | 24 | 41 |

Figure 2 shows the percent increasing in termite mortality according to the control samples. For instance, 75 % evaporated Afyon geothermal fluid increased the termite mortality (71,08%) while it was increased up to 58,85 % without evaporation.

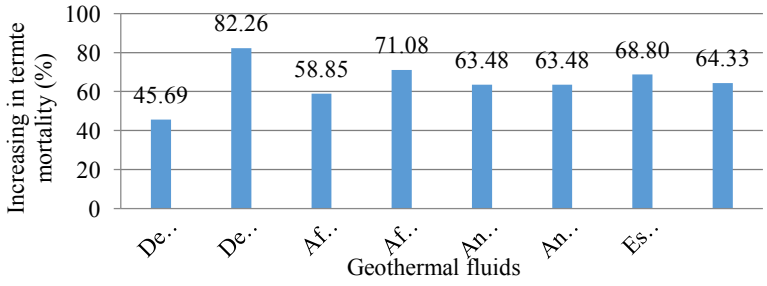


*Figure 2. Increasing in termite mortality (%) in Scots pine treated with different concentration levels of geothermal fluids.*

In literature, it was reported that many compounds that can be effective against biotic factors were identified in the chemical analyzes results of geothermal fluids. A linear relationship between activities of geothermal fluids against biotic factors and the amount of compounds in the contents were found [4].

According to multiple variance analyses test results, the geothermal source (A), the concentration (B) and their mutual interactions (A*B) for mass losses and termite mortality were determined. While B and AxB were found to be significant, A was not significant for the mass losses. Likewise, B was found to be significant, A and AxB were not significant for the termite mortality.

Table 3. Multiple variance analysis for the mass losses and termite mortality

| Experiment | Factor | Sum of squares | Degrees of freedom | Mean square | F-value | P-value |
|---|---|---|---|---|---|---|
| Mass losses | Geothermal source (A) | 24,6 | 3 | 8,2 | 2,2 | 0,114 |
| | Concentration (B) | 488,2 | 2 | 244,1 | 65,6 | 0,000 |
| | Interaction (A*B) | 114,4 | 6 | 19,1 | 5,2 | 0,002 |
| Termite mortality | Geothermal source (A) | 260,6 | 3 | 86,8 | 0,6 | 0,582 |
| | Concentration (B) | 4920,2 | 2 | 2460,1 | 18,8 | 0,000 |
| | Interaction (A*B) | 1980,4 | 6 | 330,1 | 2,5 | 0,149 |

## 4. CONCLUSIONS

This study dealt with the potential effect of geothermal fluids supplied from different regions of Turkey against the wood degrading termites. The highest anti-termite activity (the lowest mass losses and the highest termite mortality) was found in 75% evaporated geothermal fluid supplied from Denizli region. Mass losses of all samples treated with geothermal fluids were found lower than treated with pure water ones. Likewise, termite mortality of the samples treated with geothermal fluids was found higher than control samples.

It has been increased awareness about the environment and human health In today's world, the development of environmentally friendly wood preservative has become is an essential situation. Particularly, in the protection of the interior wood is need for non-biocidal treatments which should be developed in this direction. The fluids used in this study might be evaluated by increasing their concentration levels with evaporation process in wood protection, because the fluids have no adversely effect on human and environment.

## REFERENCES

[1]. O. Perçin, G. Özbay, M. Ordu, “The ınvestıgatıon of the mechanıcal properties of wooden materıals lamınated wıth varıous glues” *Journal of Science of Dumlupınar University*, vol.19, pp. 109-119, 2009.

[2]. T.P. Schultz, D.D. Nicholas, “Development of environmentally-benign wood preservatives based on the combination of organic biocides with antioxidants and metal chelators”, *Phytochemistry*, vol.61, pp. 555-560, 2002

[3]. L. Helsen, E. Van den Bulck, “Review of disposal technologies for chromated copper arsenate (CCA) treated wood waste, with detailed analyses of thermochemical conversion processes” *Environmental Pollution*, vol.134, pp. 301-314, 2005.

[4]. A.A. Var, M. Yalcin, S. Sen, C. Tascioglu, “Antifungal activity of geothermal fluids from different regions of Turkey”, *BioResources*, vol.73, pp. 4226-4236, 2012.

[5]. R. Ilgar, “The View of Dualist Approach on Geothermal Sources” *Elektronik Sosyal Bilimler Dergisi*, www.e-sosder.com, vol.13, pp.88-98, 2005.

[6]. M. Gürü, “Jeotermal enerji kaynaklarının değerlendirilmesi” *Çevreye Genç Bakış*, vol. 7, 2005.

[7]. A.A. Var, D. Göncü, F. Karsantıözü, "Investigation of absorption, retention and swelling in Izmir-Doğanbey geothermal waters-treated pine wood (*Pinus brutia* Ten.)" *Turkish Journal of Forestry*, vol. 14, pp.127-133, 2013.

[8]. A. A. Var, "Quantities potential wood preservatives in Geothermal fluids and their suitableness for wood impregnation treatment." Journal of Faculty of forestry SDU, vol.A, pp. 184-197, 2009.

[9]. European Committee for Standardization. EN 117, "Wood preservatives – Determination of toxic values against Reticulitermes species (European termites)", 2005.

[10]. SPSS 19, Statistical Analysis Programe, 2010.

# Histochemical Evidence for Copper Accumulation in the Kidneys of Loggerhead Sea Turtle Hatchlings from Dalyan Beach, Turkey

*Pinar Ili[1], Fikret Sari[2], Nazan Keskin[3], Yakup Kaska[4]*

***Abstract***

*Heavy metals such as copper (Cu) and zinc (Zn) have toxic effects on marine organisms. In this study, Cu accumulation in h k l h h hl l B h, M ğl , T k w v h h l technique. Cu associated proteins were seen as dark purple deposits mostly in the apical portions of the cells of the lining h l l h b l ' l x l v l b l (PCT) l v l b l ( CT) as extruded structures. Some of the hatchlings from different nests laid by different mothers showed high-density of Cu in PCT and DCT, whereas the others showed low-density. Our histochemical results has shown that Cu is maternally transferred to the hatchlings, the amount of transferred Cu depends on the amount of Cu accumulated by the female sea turtle, and the density of the metals in the tissues can be used to estimate the pollution status of the water.*

**Key words: Cu accumulation, *Caretta caretta*, Dalyan Beach, Heavy metal, Histochemistry**

## 1. INTRODUCTION

Heavy metals such as copper (Cu), zinc (Zn), lead (Pb), nickel (Ni), and cadmium (Cd) [1] accumulate in food chains with the increasing concentrations [2]. Therefore, diet has the greatest influence on the accumulation of metals in animal tissues and generally, metal concentrations are higher in larger animals that are end members of a trophic chain [3].

Most of the marine organisms accumulate heavy metals mainly in their liver, kidneys, muscle and gills [4]-[7]. The level of metals in animal's body usually provides information about the pollution of the water [3]. Besides, heavy metals on fishes and aquatic invertebrates can cause reduction of the developmental growth, increase of developmental anomalies, and DNA damage [8]-[10].

Some elements such as Cu are important constituents of enzymes and other compounds [11]. Although these elements are necessary for metabolism, above a threshold availability they have toxic effects on organisms. One of the detoxification strategies of organisms against toxic heavy metals is to bind them with proteins such as metallothioneins (MT) which plays an important role in metal detoxification and to turn them into insoluble metal-rich granules to be stored or excreted [11], [12]. MT occurs particularly in liver, kidneys, intestine and pancreas in varying amounts [13]. It specifically binds zinc (Zn) and copper (Cu) and controls the concentrations of these toxic elements [14]. It has been reported that the quantification of metals and MT in liver and kidneys may be a valid biomarker of metal exposure in the aquatic environment to assess the health of sea turtles [15].

1 Corresponding author: Pamukkale University, Vocational School of Health Services, Medical Laboratory Techniques, Kinikli/Denizli, Turkey. pili@pau.edu.tr
2 Pamukkale University, Department of Biology, Faculty of Arts & Sciences, Kinikli/Denizli, Turkey. fikretsari1@gmail.com
3 Pamukkale University, Department of Histology and Embryology, Faculty of Medicine, Kinikli/Denizli, Turkey. nkeskin@pau.edu.tr
4 Pamukkale University, Department of Biology, Faculty of Arts & Sciences, Kinikli/Denizli, Turkey. caretta@pau.edu.tr

Sea turtles have long lifespan and can accumulate contaminants from their food, sediment, and water [16]. Some communities consume sea turtle products (e.g., meat, adipose tissue, organs, blood, eggs) as food. Therefore, the consumption of the heavy metals and organochlorine compounds with sea turtle edible tissues could result in toxic effects (neurotoxicity, kidney disease, liver cancer, and developmental effects in fetuses and children) on human [17]. Loggerhead sea turtle (*Caretta caretta*) is one of two sea turtle species nesting in the Mediterranean [18], and the Mediterranean coasts of Turkey are important nesting grounds for them [19].

Cu discharged from navy facilities and ships into the marine environment is one of the most ubiquitous contaminant [20]. The aim of this study is to investigate the Cu accumulation in the kidneys of loggerhead sea turtle hatchlings from Dalyan Beach using histochemical method.

## 2. MATERIALS AND METHODS

### *2.1. Study Site and Sample Collection*

Dalyan Beach (Muğla) has a length of 4.5 km located in the southwest of Turkey. It is one of the most important reproductive sites of the loggerhead turtles in terms of annual nest numbers, nesting density and regular sea turtle surveys not only for Turkey but also for the Mediterranean region [21]. In this study, 25 dead loggerhead hatchlings were collected from 4 nests found during patrolling the beach or checking the nest surfaces for emergence and in nests during their excavation.

### *2.2. Histochemistry*

One kidney from each hatchling was dissected and fixed in Bouin's solution [22]. They were embedded in paraffin after routine tissue processing. 5 µm sections were stained with hematoxylin and eosin (H&E) for general histology, and orcein (http://library.med.utah.edu/WebPath/HISTHTML/MANUALS/ORCEIN.PDF) for Cu associated proteins [23]. Olympus BX53 light microscope and Olympus DP2-BSW microscope digital camera system were used for photography.

## 3. RESULTS

### *3.1. General Histology*

Histological study of the kidney of the hatchlings show normal kidney architecture with normal glomerulus surrounded by the Bowman's capsule, proximal and distal convoluted tubules. Two components of juxtaglomerular apparatus, juxtaglomerular cells and the macula densa, are easily identified. The podocytes overlap the glomerular capillary. Capillary endothelial, mesangial and podocyte cells nuclei are in the glomerulus. Bowman's space is interposed between podocytes and parietal epithelium. The vascular pole and the urinary pole which usually situated opposite the vascular pole, are observed. Proximal convoluted tubules (PCT) have a brush-border eosinophilic epithelium, whereas distal convoluted tubules (DCT) have less acidophilic cytoplasm and smaller cubic cells and diameter (Figure 1).

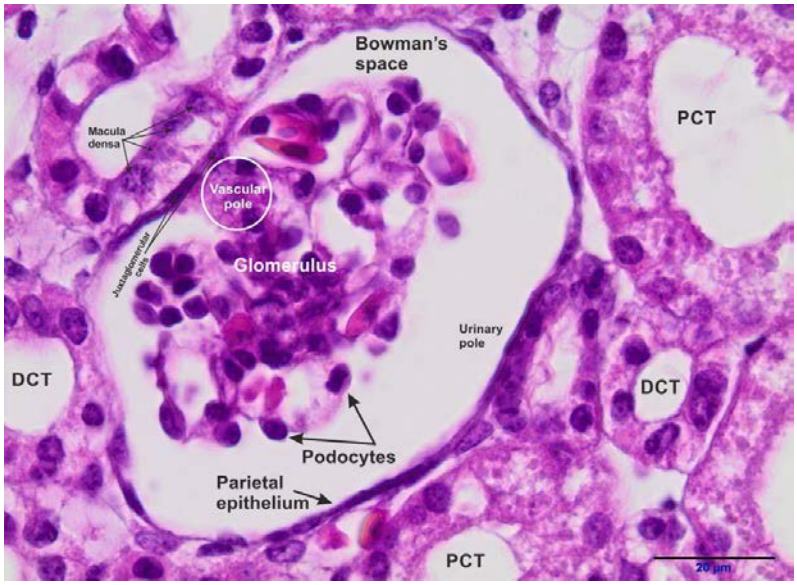


*Figure 1. General histology of the kidney. PCT: Proximal convoluted tubule; DCT: Distal convoluted tubule, H&E, scale bar = 20 µm.*

### *3.2. Histochemical Findings*

Cu associated proteins, possibly MT, are seen as dark purple deposits in globular or granular forms in the cytoplasm of the lining epithelium of some PCT and DCT. They were localised not only in the apical portions of the cells but also in the tubules' lumen as extruded structures (Figures 2 and 3). Kidneys of some of the hatchlings from different nests laid by different mothers show high Cu staining, whereas the others show low Cu staining in PCT and DCT (Figure 4).

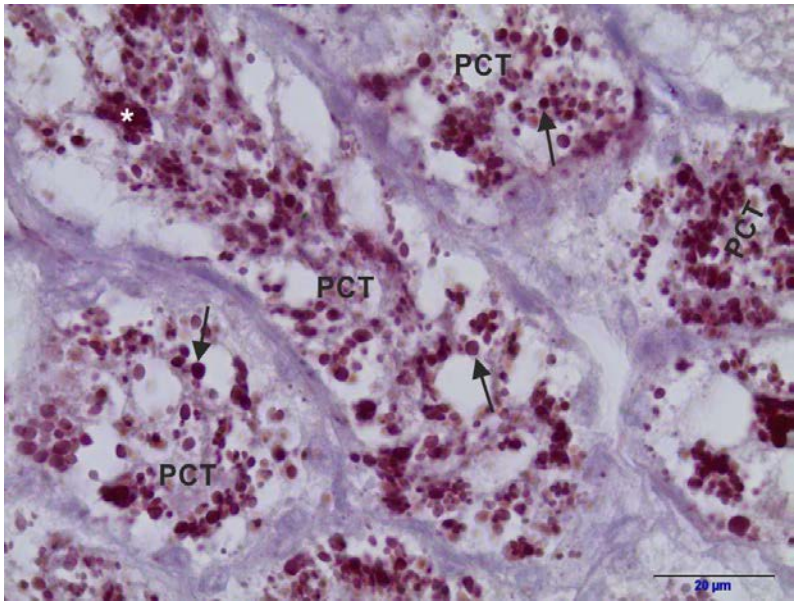


*Figure 2. Particular Cu associated protein deposition within the apical part of the cytoplasm (arrow) and extruded structures (*) in the tubules of the proximal convoluted tubules. PCT: Proximal convoluted tubules, orcein, scale bar = 20 µm.*

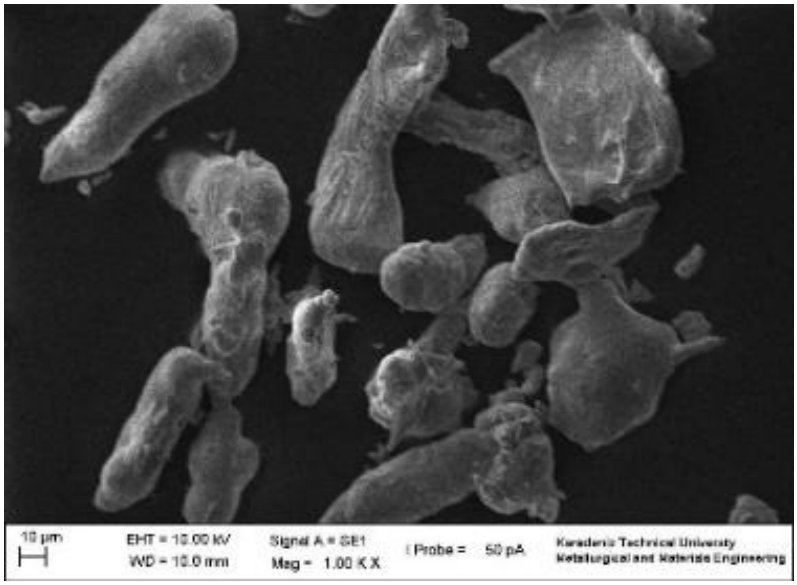


*Figure 3. Extrusion of Cu associated proteins into the lumen (*) of distal convoluted tubules, and Cu associated protein deposition within the apical part of the cytoplasm (arrow) both in the proximal and distal convoluted tubules. DCT: Distal convoluted tubules, PCT: Proximal convoluted tubules, orcein, scale bar = 20 µm.*

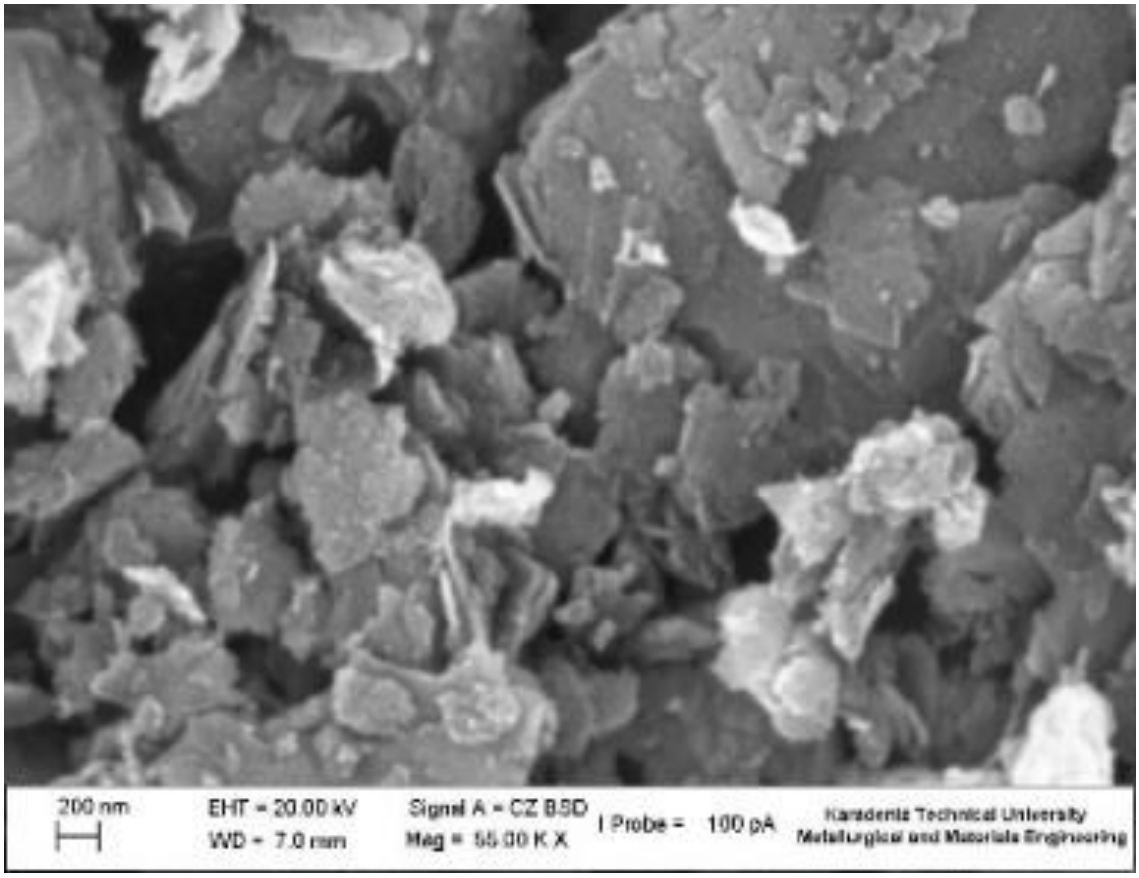


*Figure 4. Low (A) and high (B) densities of the Cu associated proteins in convoluted tubules in hatchlings from two different nests. G: Glomerulus; PCT: Proximal convoluted tubule; DCT: Distal convoluted tubule. Cu associated proteins (arrow), orcein, scale $BAR = 100$ µm (A and B), and 20 µm (insets).*

## 4. DISCUSSION

The presence of the metals in sea turtle eggs has been shown in several studies. It has been reported that the concentration of heavy metals (Mn, Cu, Zn, Cd and Pb) in fresh and un-hatched green turtle (*Chelonia mydas*) eggs are significantly different from each other and that the yolk of rotten eggs can be used as heavy metal indicator for future studies instead of fresh eggs [16]. Metals in the eggs of sea turtles are mainly present in the yolk (significantly higher concentration of mercury (Hg), Cu, Zn and Fe were found in yolk than in albumen) and shell contains highest levels of Mn and Cu [24]. Similarly, in a study in which the concentrations of Cd, Pb, Fe, Cu and Zn in loggerhead hatchling samples (eggshells, remaining yolk and liver) were investigated [25], it was found that Cd, Pb, Fe and Cu concentrations were higher in embryo liver than in yolk, whereas Zn concentration was higher in yolk. In this study, we demonstrated Cu associated proteins in PCT and DCT of the kidneys of loggerhead sea turtle hatchlings from Dalyan Beach, Muğla, Turkey.

Furthermore, the maternal transfer of the heavy metals to the eggs has been also studied by investigators. In a study, the relationships between essential [Cu, Zn, Selenium (Se)] and non-essentials elements [Cd, Pb, Hg] concentrations in blood and in eggs and maternal transfer of these elements to eggs in leatherback (*Dermochelys coriacea*) females were examined [26], and it was observed that significant relationships between blood and egg concentrations of Se and Cd. Trace elements levels in the samples from multiple clutches of each female were also investigated, and it was reported that no change was observed in egg concentrations of Cu levels, while changes were observed in blood concentrations in female turtle [26]. It was also shown that Cu and Zn in the blood are maternally transferred into the eggs and that Cu is found the only element which is positively correlated with breeding age in flatback turtles (*Natator depressus*) [27]. Noteworthy, it was found that Cu concentrations in eggs are positively correlated with female Cu concentrations in the kidneys of turtles [28]. In this study, different densities of the Cu associated proteins in the kidneys of hatchlings from different nests laid by different mothers were observed. Our finding which points out the maternal transfer of Cu to sea turtle hatchlings is consistent with and supports the results of the studies mentioned above. It was also reported that the level of metals in animal's body usually indicates information about the status of heavy metal pollutants in the water [3]. In light of this data, the Cu accumulation results of the current study can be used to estimate the pollution status of the aquatic environment where the mothers of the hatchlings use as foraging area.

The correlation of the standard carapace length and the concentrations of heavy metals were investigated previously. Almost no variation of the major and trace plasma elements in captive hawksbill sea turtles (*Eretmochelys imbricata*) with carapace parameters was reported, and it was suggested that marine pollution could cause the increase in plasma elements seen in wild sea turtles [29]. However, while significant negative correlations were shown between standard carapace length and the concentrations of Cu, Zn, and Se in the kidney in green and hawksbill turtles [30], positive correlations were detected in straight carapace length of loggerhead turtles with the concentrations of Cd, Cu and Ni [5]. When these results mentioned above are taken into account, we can assume that the hatchlings which have heavy Cu staining in their kidneys may belong to older mother, whereas the other hatchlings which have weak Cu staining in their kidneys belong to younger mother.

The heavy metal accumulation into the tissues and the eggs of sea turtles has been extensively studied using spectroscopic methods, such as Atomic Absorption Spectrometer (AAS) [31], [32], Flame Atomic Absorption Spectrophotometry (FAAS) [33] and Coupled Plasma Optical Emission Spectrometer (ICP-OES) [34]. The spectroscopic methods give quantitative results; however, they require expensive and specialised equipment. Some of the investigators use the histochemical techniques to determine the heavy metals in the animal tissues. For instance, accumulations of Hg and Cd salts in liver and kidney of fresh water cat fish (*Clarias batrachus*) [35], localization of the Hg in the ovary of crucian carp (*Carassius auratus gibelio*) [36], and Cu accumulation and excreation in the renal PCT in rats [37] were demonstrated using histochemical techniques. Similarly, we demonstrated the Cu associated protein accumulation in the kidneys of the loggerhead sea turtle hatchlings using histochemical method in this study.

In conclusion, despite our relatively small sample size, our results show that (1) Cu is maternally transferred to the hatchlings, (2) the amount of transferred Cu depends on the amount of Cu accumulated by the female sea turtle, (3) histochemical techniques are useful in demonstrating the density of the metals in the tissues of the marine organisms and in estimating the pollution status of the water. Nevertheless, further analyses are needed to understand the correlation between the copper levels in the water and in the tissues of marine organisms.

## ACKNOWLEDGEMENTS

The study was approved by the Pamukkale University Animal Ethics Committee (No: PAUHDEK-2014/016). We would like to thank Turkish Ministry of Environment and Urbanization General Directorate of the Protection of Natural Assets.

## REFERENCES

[1]. R. Singh, N. Gautam, A. Mishra, and R. Gupta, "Heavy metals and living systems: an overview", *Indian Journal of Pharmacology*, vol. 43(3), pp. 246-253, May-Jun. 2011.
[2]. M. Boran, and I. Altınok, "A review of heavy metals in water, sediment and living organisms in the Black Sea", *Turkish Journal of Fisheries and Aquatic Sciences*, vol. 10(4), pp. 565-572, Dec. 2010.
[3]. A. Jakimska, P. Konieczka, K. Skóra, and J. Namieśnik, "Bioaccumulation of metals in tissues of marine animals, part II: metal concentrations in animal tissues", *Polish Journal of Environmental Studies*, vol. 20(5), pp. 1127-1146, Jun. 2011.
[4]. F. Caurant, P. Bustamante, M. Bordes, and P. Miramand, "Bioaccumulation of cadmium, copper and zinc in some tissues of three species of marine turtles stranded along the French Atlantic Coasts", *Marine Pollution Bulletin*, vol. 38(12), pp. 1085-1091, Dec. 1999.
[5]. S. C. Gardner, S. L. Fitzgerald, B. A. Vargas, and L. M. Rodríguez, "Heavy metal accumulation in four species of sea turtles from the Baja California peninsula, Mexico", *Biometals,* vol. 19(1), pp. 91-99, Feb. 2006.
[6]. B. Jezierska, and M. Witeska, "The metal uptake and accumulation in fish living in polluted waters", In: *Soil and Water Pollution Monitoring, Protection and Remediation*, edited by I. Twardowska and H. E. Allen, Eds. Häggblom, MM & Stefaniak S (Springer, Netherlands), pp. 107, 2006.
[7]. S. S. Waghmode, and D. V. Muley, "Accumulation of heavy metals in fish after chronic exposure to the industrial effluent", *Universal Journal of Environmental Research and Technology*, vol. 3(6), pp. 690-694, 2013.
[8]. S. R. Desai, X. N. Verlecar, and G. U. Nagarajappa, "Genotoxicity of cadmium in marine diatom *Chaetoceros tenuissimus* using the alkaline Comet assay", *Ecotoxicology*, vol. 15(4), pp. 359-363, May. 2006.
[9]. L. Pan, N. Liu, H. Zhang, J. Wang, and J. Miao, "Effects of heavy metal ions ($Cu^{2+}$, $Pb^{2+}$ and $Cd^{2+}$) on DNA damage of the gills, hemocytes and hepatopancreas of marine crab, *Charybdis japonica*", *Journal of Ocean University of China*, vol. 10(2), pp. 177-184, Apr. 2011.
[10]. D. Senthamilselvan, A. Chezhian, E. Suresh, and R. Ezhilmathy, "Toxic effects of heavy metals (cadmium plus mercury) on haematological parameters and DNA damage in *Lates calcarifer*", *Journal of Toxicology and Environmental Health Sciences*, vol. 4(9), pp. 156-161, Oct. 2012.
[11]. A. Jakimska, P. Konieczka, K. Skóra, and J. Namieśnik, "Bioaccumulation of metals in tissues of marine animals, part I: the role and impact of heavy metals on organism", *Polish Journal of Environmental Studies*, vol. 20(5), pp. 1117-1125, Jun. 2011.
[12]. P. S. Rainbow, "The biology of heavy metals in the sea", *International Journal of Environmental Studies*, vol. 25(3), pp. 195-211, 1985.
[13]. I. Bremner, "Interactions between metallothionein and trace elements", *Progress in Food & Nutrition Science*, vol. 11(1), pp. 1-37, 1987.
[14]. N. Sakulsak, "Metallothionein: an overview on its metal homeostatic regulation in mammals", *International Journal of Morphology*, vol. 30(3), pp. 1007-1012, 2012.
[15]. G. Andreani, M. Santoro, S. Cottignoli, M. Fabbri, E. Carpenè, and G. Isani, "Metal distribution and metallothionein in loggerhead (*Caretta caretta*) and green (*Chelonia mydas*) sea turtles", *The Science of the Total Environment*, vol. 390(1), pp. 287-294, Feb. 2008.
[16]. J. Joseph, S. N. Ali, and H. L. Siang, "Heavy metal compositions in green turtle (*Chelonia mydas*) eggs from nesting beaches in Peninsular Malaysia", *Asian Journal of Conservation Biology*, vol. 3(1), pp. 83-87, Jul. 2014.

[17]. A. A. Aguirre, S. C. Gardner, J. C. Marsh, S. G. Delgado, C. J. Limpus, and W. J. Nichols, "Hazards associated with the consumption of sea turtle meat and eggs: a review for health care workers and the general public", *EcoHealth*, vol. 3(3), pp. 141-153, Sep. 2006.
[18]. J. A. Camiñas, "Sea turtles of the Mediterranean Sea: population dynamics, sources of mortality and relative importance of fisheries impacts". In: *Papers presented at the Expert Consultation on Interactions Between Sea Turtles and Fisheries within an Ecosystem Context*. (Food and Agriculture Organization of the United Nations, Rome) 2004 FAO Fisheries Report 738 Supplement 27, 2004.
[19]. B. Groombridge, Marine turtles in the Mediterranean: distribution, population status, conservation. *Nat Environ Ser (Council of Europe),* No. 48, Strasbourg, 1990.
[20]. P. F. Seligman, and A. Zirino, "Chemistry, Toxicity, and Bioavailability of Copper and Its Relationship to Regulation in the Marine Environment" Space and Naval Warfare Systems Center, San Diego, 1998.
[21]. F. Sarı, and Y. Kaska, "Loggerhead sea turtle hatchling sex ratio differences between two nesting beaches in Turkey", *Israel Journal of Ecology & Evolution*, doi: 10.1080/15659801.2015.1047681, 2015.
[22]. B. Guigui, P. Mavier, M. C. Lescs, Y. Pinaudeau, D. Dhumeaux, and E. S. Zafrani, "Copper and copper-binding protein in liver tumors", *Cancer*, vol. 61(6), pp. 1155-1158, Mar. 1988.
[23]. H. Dancygier, and P. Schirmacher, "Cellular adaptation, intracellular inclusion and deposits", In: *Clinical Hepatology: Principles and Practice of Hepatobiliary Diseases*, H. Dancygier Ed. Netherlands: Springer, pp. 219, 2010.
[24]. M. M. Storelli, and G. O. Marcotrigiano, "Heavy metal residues in tissues of marine turtles", *Marine Pollution Bullettin*, vol. 46(4), pp. 397-400, Apr. 2003.
[25]. Y. Kaska, and R. W. Furness, "Heavy metals in marine turtle eggs and hatchlings in the Mediterranean", *Zoology in the Middle East*, vol. 24(1), pp. 127-132, 2001.
[26]. E. Guirlet, K. Das, and M. Girondot, "Maternal transfer of trace elements in leatherback turtles (*Dermochelys coriacea*) of French Guiana", *Aquatic Toxicology*, vol. 88(4), pp. 267-276, Jul. 2008.
[27]. M. P. Ikonomopoulou, H. Olszowy, C. Limpus, R. Francis, and J. Whittier, "Trace element concentrations in nesting flatback turtles (*Natator depressus*) from Curtis Island, Queensland, Australia", *Marine Environmental Research*, vol. 71(1), pp. 10-16, Feb. 2011.
[28]. S. Yu, "Metal Accumulation and Abundance of Turtles on the West Kentucky Wildlife Management Area/DOE Paducah Gaseous Diffusion Plant Complex", Msc thesis, University of Southern Illinois, Carbondale, Dec. 2009.
[29]. K. Suzuki, J. Noda, M. Yanagisawa, I. Kawazu, M. Asakawa, and H. Yokota, "Relationships between carapace sizes and plasma major and trace element status in captive hawksbill sea turtles (*Eretmochelys imbricata*)", *The Journal of Veterinary Medical Science / The Japanese Society of Veterinary Science*, vol. 74(12), pp. 1677-1680, Dec. 2012.
[30]. Y. Anan, T. Kunito, I. Watanabe, H. Sakai, and S. Tanabe, "Trace element accumulation in hawksbill turtles (*Eretmochelys imbricata*) and green turtles (*Chelonia mydas*) from Yaeyama Islands Japan", *Environmental Toxicology and Chemistry / SETAC*, vol. 20(12), pp. 2802-2814, Dec. 2001.
[31]. Z. K. Antoniou, D. Dassenakis, D. Panagopoulos, and E. Sofouli E, "Copper and manganese in loggerhead turtles (*Caretta caretta*) tissues in the Mediterranean", *Mediterranean Marine Science*, vol. 5, pp. 109-115, 2004.
[32]. R. C. Bicho, V. M. Mendonca, A. A. Al Kiyumi, A. Al Habsi, and A. Al Kindi, "Accumulation in livers and excretion through eggs of heavy metals in a nesting population of green turtles, *Chelonia mydas*, in the NW Indian Ocean", In: *Proceedings of the 25th Annual Symposium on Sea Turtle Biology and Conservation*, H. Kalb, A. S. Rohde, K. Gayheart, K. Shanker Eds. USA: NOAA Tech Memo NMFS-SEFSC, pp. 59, 2008.
[33]. E. Barbieri, "Concentration of heavy metals in tissues of green turtles (C*helonia mydas*) sampled in the Cananéia Estuary, Brazil", *Brazilian Journal of Oceanography*, vol. 57(3), pp. 243-248, 2009.
[34]. S. H. Al-Rawahy, A. Y. AlKindi, A. Elshafie, M. Ibrahim, S. N. Al Bahry, S. S. Al Siyabi, M. H. Mansour, and A. A. Al Kiyumi, "Accumulation of metals in the egg yolk and liver of hatchling of green turtles *Chelonia mydas* at Ras Al Hadd, Sultanate of Oman", *Journal of Biological Sciences*, vol. 7, pp. 925-930, 2007.
[35]. A. Arya, "Evaluation of biochemical and histochemical changes following the combined treatment of mercury and cadmium in a fresh water cat fish, *Clarias batrachus* (Linn)", *International Journal of Pharmacy and Pharmaceutical Sciences*, vol. 6(10), pp. 356-358, Sep. 2014.
[36]. R. Meşter, and O. Zarnescu, "Histochemical localization of mercury in the ovary of crucian carp, *Carrassius auratus gibello*, after exposure to mercuric chloride", *Review Roumain de Biologie Animals*, vol. 41(1), pp. 25-34, 1996.
[37]. S. Haywood, J., Trafford, and M. Loughran, "Copper toxicosis and tolerance in the rat: IV. Renal tubular excretion of copper", *British Journal of Experimental Pathology*, vol. 66(6), pp. 699-707, Dec. 1985.

# Experimental Assessment of Heat Flux throughout Cylinder Wall in a Compression Ignition Engine

*Mehmet Cakir*[33]

***Abstract***

*Internal combustion engines are a part of our daily lives as indispensable. The large of energy is consumed for engine operations. So the engine loss power and fuel economy is one of the conditions that need to be analysed. In internal combustion engines, the combustion chamber and the cylinder walls keep in touch with hot exhaust gases. This should be examined in terms of thermal stresses for both consistently engine operations and long-lived engine life.*

*This paper aimed to analyse the combustion chamber wall heat flux by the change of engine speed and loads. The experimental study was carried out on a single-cylinder diesel engine. The experimental measurements involved to 1200 and 2000 rpm engine speeds, and 25% (10 Nm) and 50% (20 Nm) engine loads. The Engine block temperatures were measured using the K-type thermocouples for all parameters. Experimental data were computed using Woschni heat transfer model. The variations of in-cylinder pressure and gas temperature, heat transfer coefficient and heat flux with the crank angle is illustrated graphically. The results demonstrate that the engine running conditions have considerable effects to the combustion chamber wall heat transfer.*

**Keywords: Engine Heat Transfer, Diesel Engine, Heat Loss, In-Cylinder Temperature**

## 80. INTRODUCTION

Internal combustion engines are a part of our daily lives as indispensable. Many scientists have researched enhancement of energy efficiency in internal combustion engines [1-6]. A quantity increase in brake power output can be gained by decreasing the heat losses from an engine cylinder [7]. So, cylinder block or liner materials, its design and thermal loads are important for the wall heat flux distribution.

Alkidas and Myers investigated heat-flux measurements at several locations on the cylinder head and liner of a four-stroke, single-cylinder, spark-ignition engine. Eventually, they determined an increase in peak heat flux of about 30 percent, due to an increase in volumetric efficiency from 40 to 60 percent [8]. Chen et al. [9] examined the power output and thermal efficiency relations for an air standard reversible Otto Cycle taking into consideration the heat transfer loss from the cylinder wall. Demuynck et al. [10], measured the instantaneous heat loss inside a spark-ignition engine at three points for methane, gasoline, methanol and hydrogen fuels. Their conclusions showed that the influence of the engine factors is parallel for all the fuels. But, the heat loss to the cylinder walls of hydrogen is only at the same level of that of the other fuels for very lean mixtures.

This paper examines the combustion chamber wall heat flux by the change of engine speed. The variations of in-cylinder pressure and gas temperature, heat transfer coefficient and heat flux with respect to the crank angle are illustrated graphically.

## 81. METHODS

### *81.1. Research Engine*

The experiments were conducted in a single-cylinder, air-cooled, and four-stroke diesel engine. The engine specifications are given in Table 1. K-type thermocouples were used for measuring temperature of the engine block. In-cylinder pressure was measured using a piezoelectric-type transducer and the crank shaft encoder was used to provide crank positional information. All of the data were recorded to a computer through data collection card.

*Table 1. Engine specifications*

| | |
|---|---|
| **Type** | Diesel, air cooled, four stroke |
| **Cylinder number** | 1 |
| **Bore × Stroke** | 102, 5mm×100mm |
| **Compression ratio** | 17:1 |
| **Engine power max.** | 17 hp |

[33] Y l z T h l U v , M E O ,İstanbul, mecakir@yildiz.edu.tr

### *81.2. Governing Equations*

Heat flux in an internal combustion engine is transferred between the combustion chamber gases and the cylinder wall. Fig. 1 illustrates the steady one-dimensional heat transfer for critical points which are in-cylinder gas temperature, wall surfaces temperature and block external side temperature. It is formulated the heat transfer from in-cylinder gas to wall and heat conduction through the engine block wall (7 mm). Newton's law of cooling for convection heat flux, which is between cylinder wall surfaces and in-cylinder gas, is given by [11];

$$\dot{q}_{conv} = h_c(T_g - T_w) \quad (W/m^2) \tag{1}$$

where $\dot{q}_{conv}, h_c, T_g$ and $T_w$ are heat flux in convection, heat convection coefficient, in-cylinder gas temperature and cylinder wall, respectively. Fourier's law of heat conduction for the wall can be expressed as [12];

$$\dot{q}_{cond} = k\frac{\partial T}{\partial x} \quad (W/m^2) \tag{2}$$

where $\dot{q}_{cond}$ and k are heat flux in conduction, heat conduction coefficient.

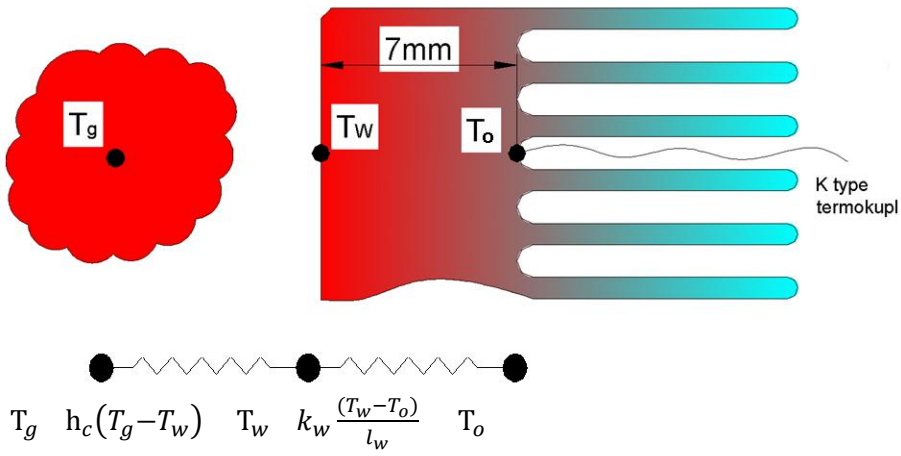


*Figure 1. Heat flow across the combustion chamber wall*

From thermodynamics 1. Law, It can be called that the rate of heat convection into the wall is equal rate of heat conduction through the wall [12]. It can be written as;

$$\dot{q}_{conv} = \dot{q}_{cond} \tag{3}$$

$$\dot{q} = h_c(T_g - T_w) = k_w\frac{(T_w - T_o)}{l_w} \tag{4}$$

where $l_w$ is cylinder liner thickness.

$$\dot{q} = \frac{(T_g - T_w)}{1/h_c} = \frac{(T_w - T_o)}{l_w/k_w} \tag{5}$$

$$\dot{q} = \frac{(T_g - T_o)}{\frac{1}{h_c} + \frac{l_w}{k_w}} \tag{6}$$

The heat flux through the wall can be determined from Equation 6. In-cylinder gas properties are evaluated at the cylinder-average charge temperature $T_g$ is given as [13];

$$T_g(\theta) = \frac{P_g(\theta)V_g(\theta)}{mR} \quad (7)$$

where $\theta, P_g, V_g, m$ and $R$ are crank angle, cylinder gas pressure, cylinder volume, air mass and gas constant, respectively. According to Woschni, with the exponent equal to 0.8, with the cylinder bore B taken as the characteristic length and W as a local average gas velocity in $h_c$ can be written [13];

$$h_c(\theta) = 3{,}26B^{-0,2}P(\theta)^{0,8}T_g(\theta)^{-0,55}W(\theta)^{0,8} \quad (8)$$

The Woschni formula also includes radiation effect in a lumped form [6]. The average cylinder gas velocity was expressed as follows[13];

$$W(\theta) = 2.28\,\bar{S}_p + \left[0{,}00324\frac{V_d T_r}{P_r V_r}\left(P(\theta) - P_{mc}(\theta)\right)\right] \quad (9)$$

where $\bar{S}_p$ is the piston mean velocity and it is expressed as [14]

$$\bar{S}_p = \frac{\text{Stroke x RPM}}{30} \quad (10)$$

## 82. RESULTS AND DISCUSSIONS

The heat transfer across the combustion chamber wall is important in terms of engine performance. In this study, it was investigated heat loss than the combustion chamber wall of working engine at low and high engine speeds and loads. Fig. 2-5 illustrate in-cylinder pressures, heat transfer coefficients and heat flux across cylinder wall depending on the crank angle at 1200 rpm and 2000 rpm under 10 and 20 Nm loads, respectively.

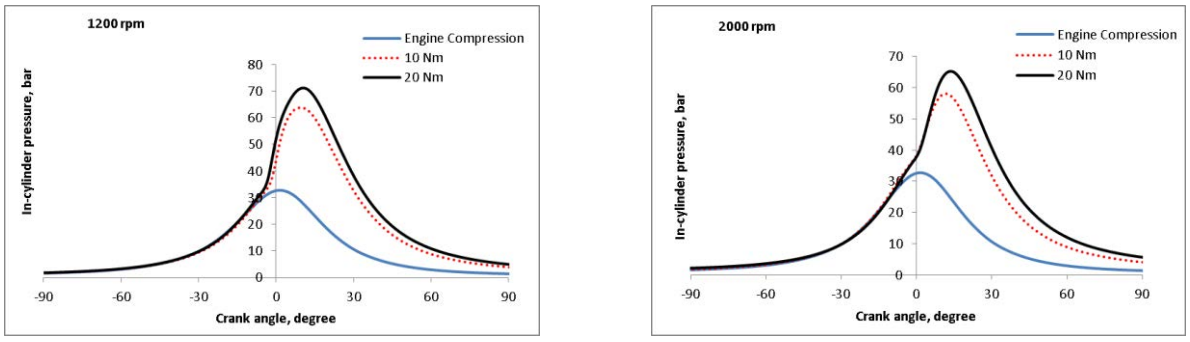


1200 rpm 2000 rpm

*Figure 2. Variation of in-cylinder pressure with respect to crank angle*

Fig. 2 demonstrates the variation of in-cylinder pressure with respect to crank angle and engine speeds for different engine loads. Blue line is engine compressor pressure that approximately is 32 bars. While red dotted lines illustrate to 10 Nm, black lines demonstrate to 20 Nm. It is see that cylinder pressure is increasing with raising engine loads at the same speeds.

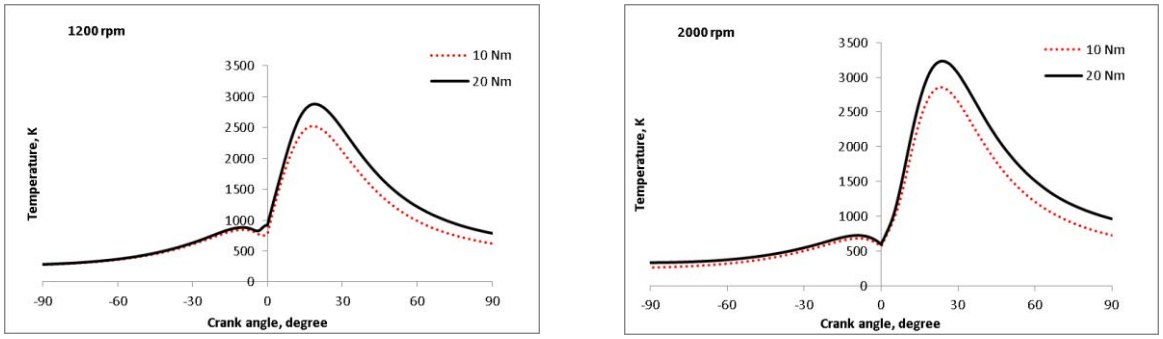


1200 rpm 2000 rpm

*Figure 3. Variation of in-cylinder temperature with respect to crank angle*

Fig. 3 illustrates the variation of in-cylinder temperature with respect to crank angle for different speeds. It is see that in-cylinder temperatures are more increasing at 2000 rpm than values at1200 rpm. Furthermore, the variation of in-cylinder temperature at 20 Nm and 1200 rpm is nearly similar with the variation at 10 Nm and 2000 rpm. But, Fig. 4 and Fig. 5 indicate to not be equal of heat transfer coefficients and heat flux at the same conditions.

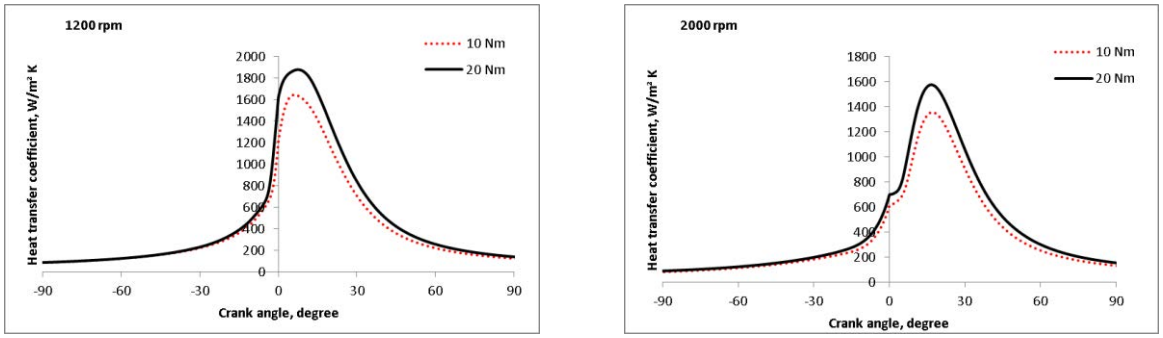


1200 rpm 2000 rpm

*Figure 4. Variation of heat transfer coefficient with respect to crank angle*

Fig. 4 demonstrates the variation of heat transfer coefficient with respect to crank angle. It is seen that the heat transfer coefficient rise with increasing crank angle during the compression process. While the mean peak values are 1600-1800 at low speed conditions, they occur mean 1300-1600 at high speed conditions. So, the variation of heat transfer coefficients increases with decreasing engine speed on the contrary engine load.

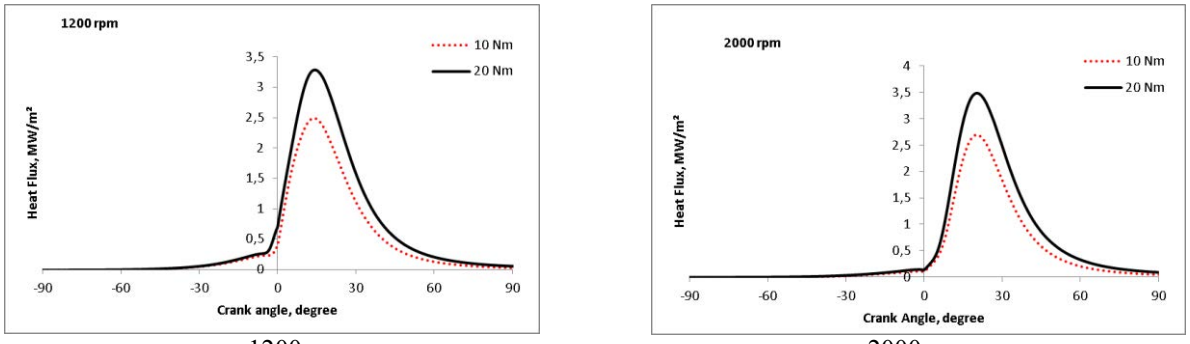


1200 rpm 2000 rpm

*Figure 5. Variation of heat flux with respect to crank angle*

Fig. 5 indicates the variation of heat flux with respect to crank angle for low and high engine speeds. The heat flux at the start of combustion rises with increasing of crank angle. The mean peak values of heat flux under 10 and 20 Nm loads at 1200 rpm condition are 2.5 and 3.3 MW/m2, respectively. In case the 2000 rpm, the mean peak values of heat flux under the 10 and 20 Nm loads are 2.7 and 3.5 MW/m2, respectively. While it is seen that the difference between mean peak values at the both speeds is nearly 0.8 MW/m2, the variation of heat flux at the 2000 rpm is higher than the variation at the 1200 rpm.

## 83. CONCLUSIONS

In this work, the effects of engine speed and load on the heat transfer through combustion chamber wall have been obtained. The experimental measurements involved to 1200 and 2000 rpm engine speeds, and 25% (10 Nm) and 50% (20 Nm) engine loads. The variations of in-cylinder pressure and gas temperature, heat transfer coefficient and heat flux with respect to the crank angle are illustrated graphically and the following points have been reached:

While in-cylinder pressure mean peak value is nearly 65 bars at 10 Nm-1200 rpm and 20 Nm-2000 rpm, the heat flux on cylinder wall are 2.5 and 3.5 MW/m2, respectively. As can be seen from this result in-cylinder pressure is not directly related to cylinder wall heat flux.

Although the variations of in-cylinder pressure at 1200 rpm are higher than the variations of in-cylinder pressure at 2000 rpm, the variations of heat flux at 1200 rpm are lower than variations of heat flux at 2000 rpm. As a result, even if the in-cylinder pressure is higher, the cylinder wall heat transfer can be lower.

## 84. REFERENCES

1. Trujillo E. C., Espadafor F. J. J., Villanueva J. A. B., García M. T., 2011. Methodology for the estimation of cylinder inner surface temperature in an air-cooled engine, Applied Thermal Engineering, 31, 1474-1481.

2. Yamadaa Y., Emia M., Ishiia H., Suzukia Y., Kimurab S., Enomotoa Y., 2002. Heat loss to the combustion chamber wall with deposit in D.I. diesel engine: variation of instantaneous heat flux on piston surface with deposit, JSAE Review, Vol. 23, Issue 4, 415–421.

3. Colaço M. J., Teixeira C. V., Dutra L. M., 2010. Thermal analysis of a diesel engine operating with diesel–biodiesel blends, Fuel, 89, 3742–3752.

4. Barjaneh A., Sayyaadi H., 2015. A new closed-form thermodynamic model for thermal simulation of spark ignition internal combustion engines, Energy Conversion and Management, 105, 607–616.

5. Mohammadi A., Yaghoubi M., 2010. Estimation of instantaneous local heat transfer coefficient in spark-ignition engines, International Journal of Thermal Sciences, 49, 1309-1317.

6. Sanli A., Sayin C., Gumus M, Kilicaslan I., Canakci M., 2009. Numerical Evaluation by Models of Load and Spark Timing Effects on The In-Cylinder Heat Transfer of a SI Engine, Numerical Heat Transfer, Part A, 56, 444–458.

7. Pulkrabek W.W., 2004. Engineering Fundamentals of the Internal Combustion Engine, p.395, New Jersey.

8. Alkidas A. C., Myers J. P., 1982. Transient Heat-Flux Measurements in the Combustion Chamber of a Spark-Ignition Engine, Transactions of the ASME, Vol. 104, p. 62-67.

9. Chen, L., Wu, C., Sun, F., Wu, C., Heat-Transfer Effects on the Net Work-Output and Efficiency Characteristics for an Air Standard Otto Cycle, Energy Convers Mgmt, 39 (1998), 7, pp. 643–648.

10. Demuynck J., Paepe M. D., Verhaert I., Verhelst S., 2012. Heat loss comparison between hydrogen, methane, gasoline and methanol in a spark-ignition internal combustion engine, Energy Procedia, 29, 138 – 146.

11. Incropera F. P., DeWitt D. P., Fundamentals of Heat and Mass Transfer, (4th ed.), New York, 1996.

12. Cengel Y. A., Heat and Mass Transfer, (3th ed.), Mc Graw Hill Book Company, New York 2006.

13. Heywood J.B., Internal Combustion Engine Fundamentals, McGraw Hill Book Company, New York, 1988.

14. Wikipedia: The Free Encyclopaedia, 18 February 2016., 18:20 UTC, <https://en.wikipedia.org/wiki/Mean_piston_speed>

***Biography***: Mehmet CAKIR graduated from Department of Mechanical Engineering at Suleyman Demirel University with PhD degree in 2013. His PhD research project was about investigation of single cylinder internal combustion engine performance by using boronized cylinder liner. Mehmet CAKIR is still working as the Assistant Professor in the Naval Architecture and Maritime Faculty, Yildiz Technical University, Istanbul.

# Moving Object Detection Using an Adaptive Background Modeling in Dynamic Scene

*M.Fatih Savaş[34],Hüseyin Demirel[2],Bilgehan Erkal[3]*

***Abstract***

*Determination of moving foreground objects in dynamic scenes for video surveillance systems is still a problem can not be resolved exactly. In the literature; pixel-based, block-based and texture-based methods have been proposed to solve this problem. The method we propose will be block-based method which can be applied to real time in dynamic scenes. We have created non-overlapped blocks with the averages the pixels in the gray level. We used this average value to generate the background model based on a modified original KDE (Kernel Density Estimation) method. To determine the moving foreground objects and to update background model, we use an adaptive parameter which is determined according to the number of changes in the state of this pixel during the last N frames. Performance evaluation of the proposed method is tested by background methods in literature without applying post-processing techniques. Experimental results demonstrate the effectiveness and robustness of our method.*

**Keywords:** *Background modeling, Moving object, Background update, Adaptive threshold.*

## 85. INTRODUCTION

Background modeling, which aims to classify each pixel as foreground and background, is one of the important processes of video surveillance system. It is a difficult process to determine moving objects in outdoor scenes such as waving trees, rippling water, moving shadow, illumination changes, camera jitters. Most of the studies conducted in recent years aim to minimize the effect of these changes which make difficult to detect efficient moving foreground. Wren et al [1]. have updated the parameters of the function regularly by creating a background model with single gaussian structure. However, this method is inadequate for dynamic background conditions. Gaussian mixture model (GMM) was proposed by Friedman and Russell [2]. and they updated the estimates by using incremental EM. In order to deal with complex scene changes, Stauffer and Grimson [3].expressed GMM with online k average approach. KaewTraKulPong and Bowden's [4]. approach based on Mixture of Gaussians (MOG) improves adaptive background mixture model. To cope with background noise and illumination changes problems, Yan et al [5]. proposed a dynamic learning object determination which synthesizes the methods of background subtraction and adjacent frame difference.

Kim et al [6]. offered a structure called the codebook for real-time applications in one of the studies aimed at coping with the multimodal backgrounds. In this structure, by quantizing sample background

[1]*Corresponding author: Karabuk University, Faculty of Engineering, Electric-Electronic Engineering Department, 78050, Karabük, Turkey, muratfatihsavas@gmail.com*

[2]*Karabuk University, Faculty of Engineering, Electric-Electronic Engineering Department, 78050, Karabük, Turkey hdemirel@karabuk.edu.tr*

[3]*Karabuk University, Faculty of Engineering, Electric-Electronic Engineering Department, 78050, Karabük, Turkey berkal@karabuk.edu.tr*

values of each pixel into the codebook, he updated these codes in certain periods. In this structure, the codes which couldn't be reached for a long time are removed from the code table. To reduce the number of process, by using the color difference, Tu et al [7]. modelled the background with boxed based codebook method. Although codebook structure offers an effective solution for dynamic background modeling, it is not fast while modelling. Maddalena et al [8]. proposed an adaptive learning rate in a neural network background modeling, a self-organizing method that does not contain a prior knowledge and model automatically background.

Elgammal et al [9]. proposed a non-parametric structure by the certain number of framers he accumulated for background modeling that expresses the color distribution of pixels with gaussian function . To eliminate the disadvantages of this structure, adaptive and less computational burden of parzen window structure is used. Ianasi, et al [10]. proposed recursive density estimation with mean shift based mode to reduce the complexity of nonparametric kernel density estimation method. Tanaka et al [11]. proposed a fast PDF calculation function of structure by updating the PDF which partially estimated from the previous frame. By using HSV color values and gradient information, Park et al [12]. created the classification of background or foreground with Bayesian decision rule. Cuevas et al [16]. proposed a real-time spatial-temporal non-parametric method. To create background modeling in this method, by using both spatial and temporal data of pixels, they increased system's immunity to noise. Hoffman et al [13]. proposed the Pixel-Based Adaptive Segment (PBAS) structure by updating the background model which was created as non-parametric, with learning parameters.

Recently, Heikkila et al [10]. have proposed the texture-based background model by using local binary pattern. Although this method is effective against illumination changes, it is not strong in the uniform region. To eliminate the disadvantages of LBP method, which is inadequate in uniform regions. Yao and Odobez [14]. created background modeling by RGB color feature.

## 86. PROPOSED METHOD

Memory burden and process time are the problems that must be solved in Real-time applications. Lee and Park [15]. modified the KDE model to solve this problem. In our study, we based on the modified KDE model for background model.

Moving objects such as sudden illumination change, waving trees, rippling water in the dynamic scenes create too much noise for the background model. To reduce the amount of noise and the computational burden, we connected the pixels by averaging pixels as nxn blocks. These pixel blocks are used for the background model and adaptive parameters. To build an adaptive parameter, we used the counter structure which adaptive Casares et al [16]. used in their studies. By this parameter, the foreground determination and the background update was made. While updating the model, each block is continually involved in background model. Then, normalization process was performed to equal the area to 1, which is under the model's probability function.

### *86.1. Background Subtraction Method*

In background determination algorithms, authors mostly focused on the models such as efficient usage of storage space, reducing process time. Two problems must be solved to use the background model in real-time applications. These problems are; storage space and processing time. In real-time applications, to reduce the processing burden and to use the storage space efficiently, pixels are used as gray level and background model is updated as adaptive. But one of the disadvantages of processing at gray level is that it is open to the noise came up on stage.

A picture frame with the resolution of 160x120 size is made up of 19200 pixel. If these pixels are composed of RGB value, more time and more storage space is required. Processing on these pixels bring a lot of load on the system both in terms of time and the requirements for storage space. Therefore, to create a minimum level for processing time and storage space, the background model we propose was in gray level. However, in literature, to minimize the disadvantage of grayscale structure, kernel density estimation based model which offers an effective solution to background modeling was used.

Lee and Park [15] created the background model as pixel based. In our study, we put the average values created as 2x2 blocks in bins in background model. Instead of evaluating pixels' membership value for bins as 1 or 0, probability values are calculated according to the distance of bins from the center.

| | |
|---|---|
| *I(x, y)* | *I(x,y+1)* |
| *I(x+1,y)* | *I(x+1,y+1)* |

*Figure 1. 2x2 block*

$I(x, y)$ represents the gray level value of each pixel in the image frame. Pixels in the image frame were joined by averaging as 2x2 non-overlap blocks. As computational, mean filter structure which requires less burden is used equation 1.

$$\mu(x, y) = \frac{1}{nxn}\sum_{x=1}^{n}\sum_{y=1}^{n} I(x, y) \quad (1)$$

where μ (x, y), is the average value of the pixels in nxn block.

The following figure shows the change of the pixel at location (39,80) in the time interval 0-30 seconds and shows the gray level changes of the pixels averaged at location (39 + x,80 + y) in the time interval 0-30 seconds from the Wallflower dataset's WavingTrees test sequences. Here x,y={0,1}

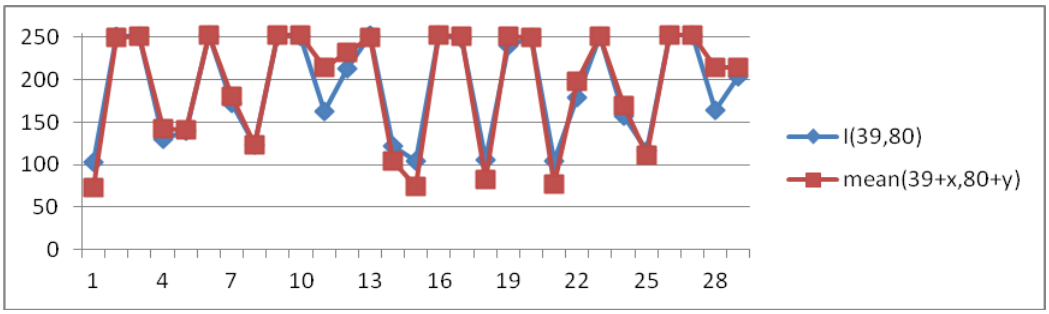


*Figure 2. I(39,80) pixels and 39 + x ,80+ y block of pixels in the range of 0-50 times the change in gray level chart*

The following equation 2. shows the function we used for the background model.

$$p_t(C_k) = \frac{1}{\sqrt{2\pi\left(B_d/_2\right)^2}} exp\left(-\frac{1}{2}\left(\frac{C_k-\mu_t(x,y)}{B_d/_2}\right)^2\right) \quad (2)$$

In equation 2, for each block, the histograms are formed in the width of $B_d$ by bins.$C_k$ is the central point of kth bin which belongs to nxn block pixel, $p_t(C_k)$ is the probability value of block pixel at time index t.

### *86.2. Adaptive Threshold Parameter*

Determining the fixed threshold used for the determination of moving objects in dynamic scenes is difficult. If less values are selected as the parameter, the image may contain a lot of noise, if a large value is selected as the parameter, some values from the image may be lost. To overcome this problem, we created threshold as adaptive in our study. Adaptive threshold is created by counter structure counting the change in each pixel. This counter structure was used to reduce the computational burden.

In this structure, the parameter of $\beta_x, x \in \{1,2,3\}$ is the maximum value of a counter can count that determined by the user. $CC_n, n \in \{1,2,3\}$ shows the number of counter belonging to a pixel. The value of a counter is incremented by 1 at change of each pixel's state. After counting the frame number to be counted, counter values are sequentially reset [16].The value of counters increase or decrease according to the rate of pixels' state changing. $\tau(x,y) = CC_1(x,y) + CC_2(x,y) + CC_3(x,y)$ ) is formed by the total value of counter of pixels. The parameter values of the pixels in moving regions take large $\tau$ value, $\tau$ values of the pixels in quasi-static area take small values. By this approach, at any time index t, we can determine the change number of pixels in past N frame.

### *86.3. Background Update*

The following formulate is used for updating the background model. α is the fixed updating parameter. While updating , all $C_k$ values aren't calculated, only bins interval $p_t(C_{(k-2)})$ and $p_t(C_{(k+2)})$ are updated by considering bins interval $p_t(C_{(k\pm2)})$ [15].The following equation 4.

$$p_t(C_k) = \hat{p}_{t-1}(C_k) + \left(\frac{1}{\alpha+100.\tau}\right)\frac{1}{\sqrt{2\pi\left(B_d/2\right)^2}} exp\left(-\frac{1}{2}\left(\frac{C_k-\mu_t(x,y)}{B_d/2}\right)^2\right) \quad (4)$$

### *86.4. Foreground Detection*

Determination of moving objects in dynamic scenes depends on a robust background modelling structure and the value of parameter to be determined. While determining the foreground, the distance between the bin center which has the largest possibility value at histogram and $\mu_t(x,y)$ is taken into consideration. Equation 5.

$$Distance|C_k - \mu_t(x,y)| \leq threshold + \tau \quad (5)$$

If the absolute value difference between $C_k$, which has the largest possibility value at histogarm and the average value calculated at t time of $\mu_t(x,y)$ is bigger than threshold, foreground is determined. Equation 6.

$$I(x,y)\begin{cases} Foreground & Distance|C_k - \mu_t(x,y)| \leq threshold + \tau \\ Background & otherwise \end{cases} \quad (6)$$

## 87. RESULTS AND DISCUSSION

We tested the performance of our method by wallflower [17]. and Li [18]. datasets. We compared our proposed method with Mixture Of Gaussian V1BGS [4], Pixel Based Adaptive Segmenter [13]. and T2FGMM_UM [22].methods from BGSLibrary which was created by Andrews Sobral [19]. Three different binary classification measurement methods were used while comparing methods. These methods are precision, recall and F-measure. When the recall and precision values are high, it shows that the performance is high. F-measure is the weighed harmonic average of recall and precision [20]-[21].Equation 7.

$$reacll = \frac{TP}{TP+FN} \qquad precision = \frac{TP}{TP+FP} \qquad F = \frac{2.recall.precision}{recall+precision} \quad (7)$$

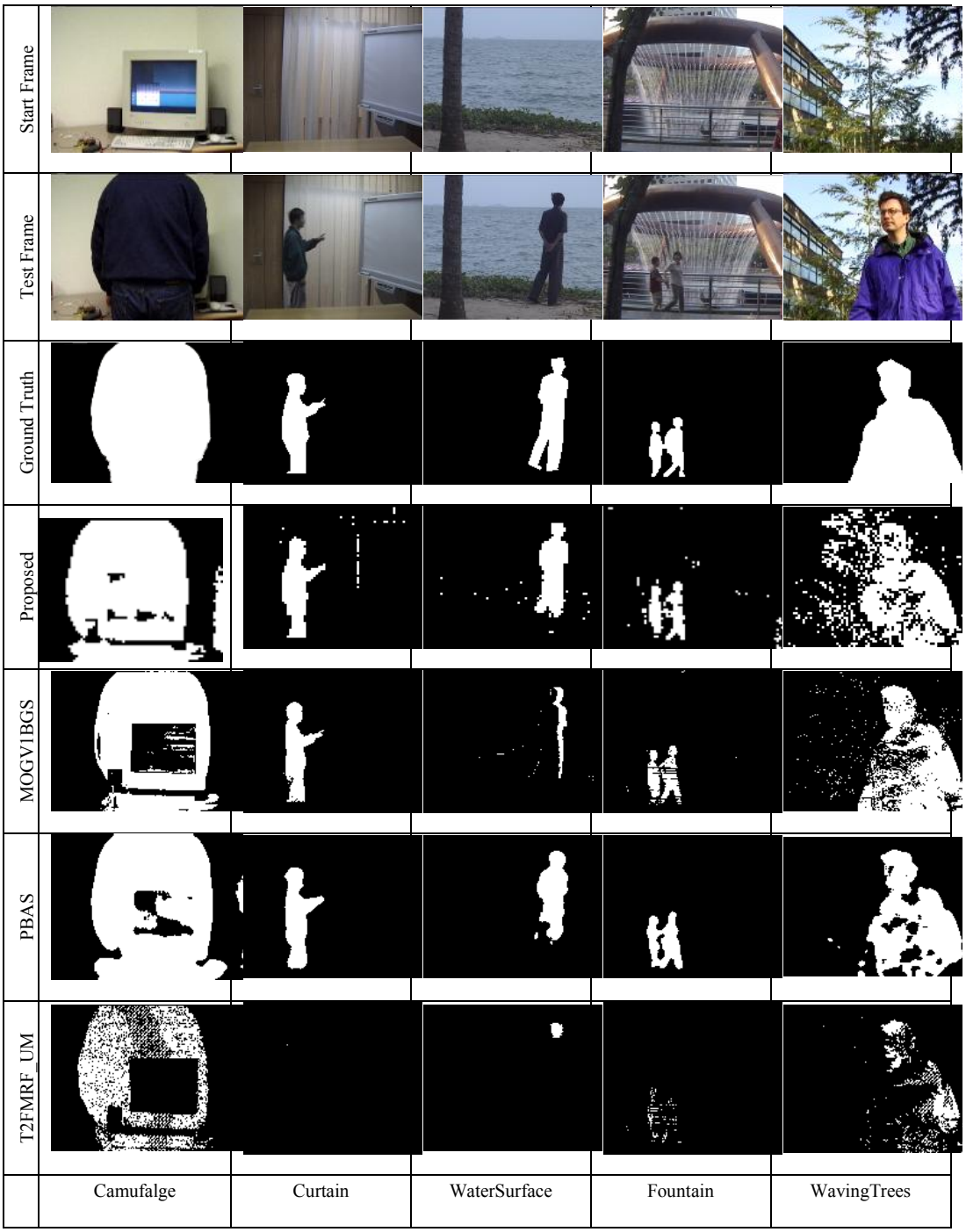


*Figure 3.Experimental Results*

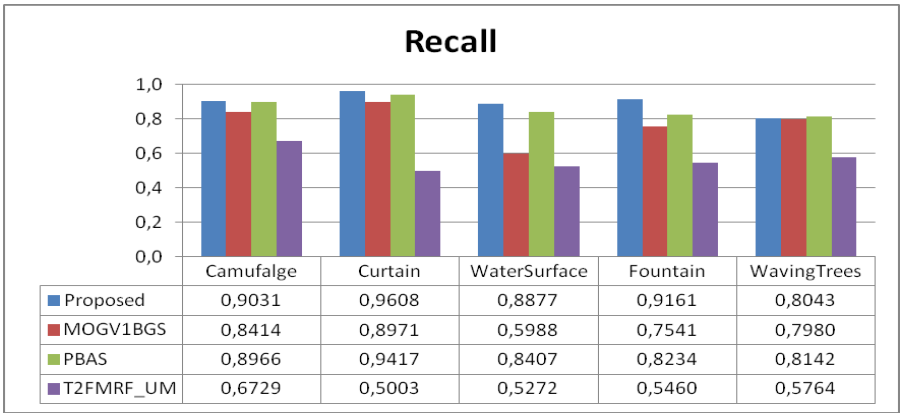


| | Camufalge | Curtain | WaterSurface | Fountain | WavingTrees |
|---|---|---|---|---|---|
| Proposed | 0,9031 | 0,9608 | 0,8877 | 0,9161 | 0,8043 |
| MOGV1BGS | 0,8414 | 0,8971 | 0,5988 | 0,7541 | 0,7980 |
| PBAS | 0,8966 | 0,9417 | 0,8407 | 0,8234 | 0,8142 |
| T2FMRF_UM | 0,6729 | 0,5003 | 0,5272 | 0,5460 | 0,5764 |

*Figure 4.The recall results obtained with the proposed scheme and other methods for the Li and wallflower dataset.*

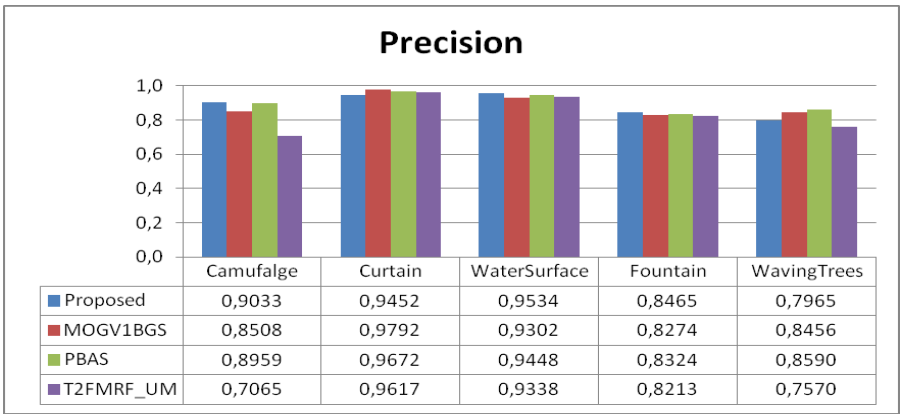


| | Camufalge | Curtain | WaterSurface | Fountain | WavingTrees |
|---|---|---|---|---|---|
| Proposed | 0,9033 | 0,9452 | 0,9534 | 0,8465 | 0,7965 |
| MOGV1BGS | 0,8508 | 0,9792 | 0,9302 | 0,8274 | 0,8456 |
| PBAS | 0,8959 | 0,9672 | 0,9448 | 0,8324 | 0,8590 |
| T2FMRF_UM | 0,7065 | 0,9617 | 0,9338 | 0,8213 | 0,7570 |

*Figure 5.The precision results obtained with the proposed scheme and other methods for the Li and wallflower dataset.*

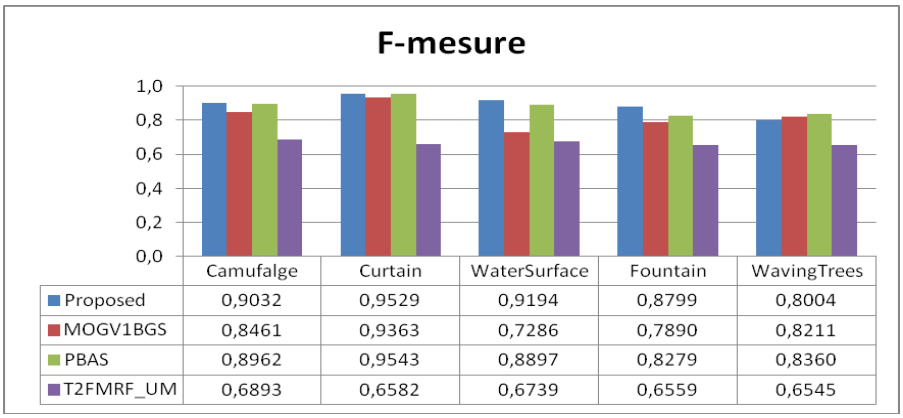


| | Camufalge | Curtain | WaterSurface | Fountain | WavingTrees |
|---|---|---|---|---|---|
| Proposed | 0,9032 | 0,9529 | 0,9194 | 0,8799 | 0,8004 |
| MOGV1BGS | 0,8461 | 0,9363 | 0,7286 | 0,7890 | 0,8211 |
| PBAS | 0,8962 | 0,9543 | 0,8897 | 0,8279 | 0,8360 |
| T2FMRF_UM | 0,6893 | 0,6582 | 0,6739 | 0,6559 | 0,6545 |

*Figure 6.The f-measurement results obtained with the proposed scheme and other methods for the Li and wallflower dataset.*

Recall, also known as detection rate, gives the percentage of detected true positives as compared to the total number of true positives in the ground truth, where TP is the total number of true positives, and FN is the total number of false negatives, which accounts for the number of foreground pixels incorrectly classified as background. Precision, also known as positive prediction, that gives the percentage of detected true positives as compared to the total number of pixels detected by the method, is generally used in conjunction with the recall. Where FP is the total number of false positives.

For five test videos, an evaluation was carried out between the models by calculating Recall, Precision and F measurement values. In test images, no post-processing technic application is performed. Test sequences are Camufalge, Curtain, WaterSurface, Fountain and WavingTrees. Some of these test sequences include continuously changing dynamic background, some of them include changing dynamic background at certain times. These test sequences have the frames with a size of 160 x 120 and 160x128.

The method we proposed in the measurements carried out with these test sequences, obtained robust results in most test data. When the WavingTrees scene was compared with other methods, the amount of noise was seen much more. These noises can be reduced according to the threshold parameter chosen in the process of determining foreground. On the contrary, reducing the noise can cause incorrectly classifying of some pixels belonging to foreground object. In T2FGMM_UM method, the amount of noise was reduced, but pixels belonging to foreground object were evaluated as background. In WaterSurface test sequence, as it is seen in the test data obtained via MOGV1BGS method, if the background model adapts to the scene very fast, the continuance of stopped objects moving at the scene on the screen will be less. The disadvantage of Pixel Based Adaptive Segmenter method which gets similar performance values as our proposed method, it contains too many parameters.

## 88. CONCLUSIONS

In our study, we created an effective model for real time applications by modifying KDE structure of Lee and Park [15]. By dealing with background model as gray level blocks nonoverlap, we reduced both the memory area requirement for model and the time needed for processing pixels. We determined the adaptive parameter by using counter structure of Casares et al. [16], and by determining the condition changing number of pixels in N frame that past at any t time. Thus we created an effective background modeling at grey level in dynamic scenes. The weak point of this method is, as a single band was used for background modeling it can't exactly discriminate the foreground and the background. As background model was created block-based, image belongs to foreground object is coarser than the pixel based methods. In future work, we are going to use this method for RGB band. Test data shows that, our study carried out for single color band is valid.

## REFERENCES

[221]. C. Wren, A. Azarbayejani, T. Darrell, and A. Pentland, " Pfinder: Real-time tracking of the human body," IEEE Trans. Pattern Anal. 1997, 19, 780–785.
[222]. N. Friedman and S. Russell, "Image segmentation in video sequences: a probabilistic approach," In Proceedings of the 13th Conference on Uncertainty in Artificial Intelligence, Morgan Kaufmann Publishers Inc., 1997, pp. 175–181.
[223]. C.Stauffer and W.E.L, Grimson, "Adaptive background mixture models for real-time tracking," In Proceedings of IEEE Conference on Computer Vision and Pattern Recognition, Santa Barbara, CA, USA, June 1998, pp. 246–252.
[224]. P,KaewTraKulPong and R,Bowden, " An improved adaptive background mixture model for real-time tracking with shadow detection," In Proceedings of 2nd European Workshop on Advanced Video-Based Surveillance Systems(AVBS01), September 2001.

[225]. R.Yan, X.Song and S.Yan, "Moving Object Detection Based on an Improved Gaussian Mixture Background Model", Computing, Communication, Control, and Management, 2009. CCCM 2009. ISECS International Colloquium on, Pages: 12 – 15, Year: 2009
[226]. K.Kim, T.H,Chalidabhongse, D.Harwood and L.Davis, "Real-time foreground-background segmentation using codebook model," Real-Time Imaging 2005, 11, 172–185.
[227]. Q.Tu, Y. Xu and M.Zhou, "Box-based Codebook Model for Real-time Objects Detection," Intelligent Control and Automation, 2008. WCICA 2008. 7th World Congress on,2008,Pages: 7621 - 7625
[228]. L.Maddalena and A.Petrosino,"A self-organizing approach to background subtraction for visual surveillance applications," IEEE Trans. Image Process 2008, pages: 1168–1177.
[229]. A.Elgammal, R.Duraiswami, D. Harwood and L.S.Davis, "Background and foreground modeling using nonparametric kernel density estimation for visual surveillance," Proc. IEEE 2002, 90, 1151–1163.
[230]. C.Ianasi, V. Gui, C. Toma and D.Pescaru, " A fast algorithm for background tracking in video surveillance, using nonparametric kernel density estimation," Facta Universitatis (NIS) Ser.: Elec. Energ. 2005, 18, 127–144.
[231]. T.Tanaka, A.Shimada, D. Arita and R.I Taniguchi, "A Fast Algorithm for Adaptive Background Model Construction Using Parzen Density Estimation", Advanced Video and Signal Based Surveillance, 2007. AVSS 2007. IEEE Conference on London. 2007, 528 – 533
[232]. J.G.Park and C.Lee, "Bayesian rule-based complex background modeling and foreground detection, " Opt. Eng. 2010, doi:10.1117/1.3319820.
[233]. M. Hofmann, P. Tiefenbacher, G. Rigoll, "Background segmentation with feedback: The pixel-based adaptive segmenter," IEEE Computer Society Conference on Computer Vision and Pattern Recognition Workshops (CVPRW),2012, pp. 38–43.
[234]. J.Yao and J.M.Odobez, "Multi-Layer Background Subtraction Based on Color and Texture", Computer Vision and Pattern Recognition, 2007. CVPR '07. IEEE Conference on,2007,pp 1 – 8.
[235]. J.Lee and M.Park, "An Adaptive Background Subtraction Method Based on Kernel Density Estimation," Sensors 2012, 12, 12279-12300.
[236]. M.Casares, S.Velipasalar and A.Pinto, "Light-weight salient foreground detection for embedded smart cameras," Computer Vision and Image Understanding,2010, Pages 1223–1237
[237]. Wallflower dataset web site.[Online].Available: http://research.microsoft.com/en-us/um/people/jckrumm/WallFlower/ TestImages.htm
[238]. Li dataset web site.[Online]. Available: http://perception.i2r.a-star.edu.sg/bk_model/bk_index.html

[239]. Andrews Sobral web site.[Online]. Available: https://github.com/andrewssobral/bgslibrary

[240]. S.Brutzer, B.Hoferlin and G.Heidemann, "Evaluation of background subtraction techniques for video surveillance," in: Proceedings of the CVPR, IEEE, 2011, pp. 1937–1944
[241]. EC Funded CAVIAR project/IST 2001 37540, web site.[Online]. Available: http://homepages.inf.ed.ac.uk/rbf/ CAVIAR/
[242]. Fida El Baf, T.Bouwmans, B.Vachon, "Type-2 Fuzzy Mixture of Gaussians Model: Application to Background Modeling," Advances in Visual Computing, Volume 5358, pp 772-78

***Biography***:

**Murat Fatih SAVAŞ**, graduated from Sakarya University Electronic and Computer Education Department in 2002, received master degree from Sakarya University in 2005 and continues his education as a PhD student in Karabuk University. Now, he is a teacher in Kastamonu Vocational High School and is engaged in Background subtraction methods.

**Hüseyin DEMİREL,** graduated from Gazi University Electronic and Computer Education Department in 1997. After that he received MS and PhD from Gazi University in 1999 & 2010 respectively. As an assistant professor in Karabuk University Electrical and Electronic Engineering Department, he is working in digital electronics and thermoelectric modules.

**Bilgehan ERKAL**, graduated from Gazi University Electronic and Computer Education Department in 1997. After that he received M.S. in degree ODTU 2001 and PhD from Karabük University in 2013. He is working as assistant professor in Karabük University Electrical and Electronic Engineering Department, he is working in control systems, satellite Orientation Control, fuzzy Variable Structure Controllers.

ICENS
INTERNATIONAL CONFERENCE ON ENGINEERING AND NATURAL SCIENCES
24-28 May 2016 /Sarajevo

# Effect of Washing with Acidified Sodium Chlorite (ASC) on Quality of Whole Mushroom (*Agaricus bisporus*)

***Fatih Tarlak[1*], Murat Ozdemir[1], Mehmet Melikoglu[1]***

***Abstract***

*Button mushrooms (Agaricus bisporus) are widely consumed all over the world owing to their characteristic taste, aroma and nutritional value. Unfortunately, the shelf life of mushroom is very limited as compared to most vegetables especially at room temperature. In addition, mushrooms can easily be contaminated with microorganisms during their growth and processing. Pseudomonas spp. is the most common spoilage organisms in mushrooms, and the initial count of Pseudomonas spp. on cultivated mushrooms is quite high, ranging from 6.9 to 7.8 log CFU/g. Pseudomonas spp. can be reduced, and shelf life can be prolonged by washing the mushroom with acidified sodium chlorite (ASC) solution. The concentration of washing solution and the treatment time are important factors which can adversely affect the colour and texture of mushroom. Therefore, there exists an optimum washing concentration and washing time in which maximum microbial inactivation occurs, but the colour and texture are not adversely affected. The main objective of this work was to determine the optimum ASC concentration and washing time on the quality parameters (microbial load, colour and texture) of fresh whole mushroom. For this purpose, the whole mushrooms were washed with 0.2-1.2 g/L of ASC solution for 2-10 minutes. Pseudomonas spp. inactivation was the highest when the mushrooms were washed with 1 g/L of ASC solution for 2 minutes in which colour and textural properties were very close to the fresh form. Results show that optimum washing conditions could be used in the mushroom industry to extend the shelf life of mushrooms.*

**Keywords***:* Acidified sodium chlorite (ASC), optimization, washing, whole mushroom

[1]*Department of Chemical Engineering, Gebze Technical University, 41400, Gebze, Kocaeli, Turkey*
*Corresponding author. *E-mail address*: ftarlak@gtu.edu.tr

## 1. INTRODUCTION

The cultivated button mushroom (*Agaricus bisporus*) is the most common edible mushroom in the world. *Agaricus bisporus* has a very short shelf life because it has no cuticle to protect it from physical or microbial attack [1]. After being harvested, mushrooms can be stored only for 1-3 days in the fresh form and lose their commercial value within a few days, because of their high moisture (almost 90%) and enzyme content [2], [3]. This is the biggest limitation of their industrial development since the short shelf life restricts export potential. One or two extra days of shelf life would compensate for time in transit; subsequent extra days of shelf life would give more flexibility to processors, retailers and consumers [1].

Mushrooms can be easily contaminated with microorganisms during growing and processing. The initial count of microorganism on cultivated button mushroom is quite high, ranging from 6.9 to 7.8 log CFU/g [4], [5]. In order to extend shelf life of mushroom and to reduce high initial microbial count of mushroom, they need to be washed with anti-microbial agents that do not adversely affect their sensorial and organoleptic quality [6]. In the last decade washing mushrooms has gained commercial popularity as a means of improving appearance by removing casing soil particles and increasing shelf life. Significant research has been conducted to develop washing processes with many anti-microbial and anti-browning compounds such as, hydrogen peroxide [1], sodium hypochlorite [4], citric acid [6], malic acid [7], acetic acid and ascorbic acid [8].

The effect of washing treatment is basically based on washing concentration and time. Normally, as washing concentration and time are increased, anti-microbial effect increases to certain extend. After a point, anti-microbial effect maintains the same although washing concentration and time are increased. Furthermore, this adversely affects sensorial and organoleptic properties of mushrooms. Therefore, the optimum washing process conditions can be determined. If effective washing processes with anti-microbial and anti-browning agents could be found, combining with proper packaging techniques, could further increase the market value of mushroom [9]. Although significant amount of studies related to extending shelf life of mushrooms were performed, the shelf life of mushrooms is still limited. Therefore, it is necessary to investigate the alternative antimicrobial solution to reduce high initial microbial count of mushrooms and to prolong their shelf life.

The main objective of this work was to determine the optimum ASC concentration and washing time for the quality parameters (colour, microbial load and texture) of fresh whole mushroom. For this purpose, the whole mushrooms were washed with 0.2-1.2 g/L of ASC solution for 2-10 minutes and the effect of washing processes on microbial load, colour and texture of mushrooms were assessed.

## 2. MATERIALS and METHODS

### *2.1. Preparation of food and antimicrobial solution*

The cultivated button mushrooms (*Agaricus bisporus*) were obtained from MUPA Agriculture and Industry Incorporated Company (Izmit, Kocaeli, Turkey). The mushrooms were harvested at the closed cap stage with the cap diameter of 3.5-4.5 cm. After harvesting, mushrooms were immediately transported to the laboratory. Then, mushrooms cleaned with distillate water, stapeses were trimmed at 1 cm.

Acidified sodium chlorite (ASC) was prepared by mixing sodium chlorite (SC) with citric acid immediately before application and used within 30 minutes. Different amount of citric acid was used to obtain ASC solutions with different concentration ranging from 0.2-1.2 g/L. Obtained ASC solutions with central composite experimental design, which was performed using statistical software (Minitab, v.16) and their pH values are shown Table 1.

*Table 1. Prepared acidified sodium chlorite solutions*

| Run Order | Time (minute) | Sodium Chlorite (g/L) | Citric Acid (g/L) | pH |
|---|---|---|---|---|
| 1 | 6.00 | 0.70 | 3.00 | 2.71 |
| 2 | 6.00 | 0.70 | 3.00 | 2.71 |
| 3 | 10.00 | 0.70 | 3.00 | 2.71 |
| 4 | 2.00 | 1.20 | 0.00 | 10.12 |
| 5 | 6.00 | 0.70 | 3.00 | 2.71 |
| 6 | 6.00 | 0.70 | 0.00 | 9.88 |
| 7 | 2.00 | 0.20 | 6.00 | 2.50 |
| 8 | 2.00 | 0.20 | 0.00 | 9.30 |
| 9 | 6.00 | 0.70 | 3.00 | 2.71 |
| 10 | 10.00 | 1.20 | 0.00 | 10.12 |
| 11 | 2.00 | 0.70 | 3.00 | 2.71 |
| 12 | 10.00 | 0.20 | 0.00 | 9.30 |
| 13 | 6.00 | 0.20 | 3.00 | 2.66 |
| 14 | 6.00 | 0.70 | 6.00 | 2.52 |
| 15 | 2.00 | 1.20 | 6.00 | 2.57 |
| 16 | 6.00 | 1.20 | 3.00 | 2.78 |
| 17 | 6.00 | 0.70 | 3.00 | 2.71 |
| 18 | 10.00 | 0.20 | 6.00 | 2.50 |
| 19 | 10.00 | 1.20 | 6.00 | 2.57 |
| 20 | 6.00 | 0.70 | 3.00 | 2.71 |

As can be seen from Table 1, twenty different washing treatments were performed and it was investigated to the effect of these treatments on colour value, texture value and the load of *Pseudomonas* spp. of whole mushrooms.

### *2.2. Colour measurement*

The colour of whole mushrooms was determined using a Chroma Meter (CR-400, Konica Minolta Inc., Tokyo, Japan) equipped with $D_{65}$ illuminant. Prior to colour measurements, the chroma meter was calibrated with its white calibration tile (Y=86.6 x=0.3188 y=0.3364). The $L^*a^*b^*$ colour analysis was performed randomly via twenty different measurements from the external surfaces of whole mushrooms. Colour assessment was performed using $L^*$ values of mushroom surface. The results were given as the average of twenty measurements.

### *2.3. Microbiological analyses*

Twenty-five grams of mushrooms were aseptically weighed and homogenized using Stomacher (Interscience, Bag Mixer 400VW, USA) at high speed for 2 min by adding 0.1% 225 ml of sterile peptone water. Serial dilutions ($10^{-1}$-$10^{-6}$) were made in serial tubes by taking 1 ml sample with 9 ml 0.1% of sterile peptone water. *Pseudomonas* spp. which already exists on natural microflora of mushrooms was determined in King's B medium [10], with an incubation temperature of 25°C for 48 hours. Each experiment was repeated three times and the average of three measurements was expressed as the colony forming units per gram whole mushroom ($\log_{10}$ CFU/g).

### *2.4. Texture measurement*

The firmness of whole mushrooms was measured using TAPlus texture analyser (TA1, Lloyd, USA) equipped with a load cell of 250N. Cylindrical probe with a 12.5 mm diameter was used with the constant speed of 2 mm/s and the contact force of 0.5

N. Samples were penetrated to a depth of 5 mm. The maximum force (Newton, N) was expressed as the firmness of mushroom. Due to the hardness of stipe, this was removed each piece, measuring only the firmness of the cap. Seven samples were analysed for one experiment and the results were given as the average of seven measurements.

## 3. RESULT and DISCUSSION

Whole mushrooms were separated into twenty groups with respect to their washing treatments and following quality parameters of mushrooms were analysed; i) colour, ii) microbial quality and iii) texture. Details of the results were explained in the following subsections.

### *3.1. Colour measurement*

Normally, visual colour assessment of mushrooms is expressed with respect to their colour values ($L^*$) individually, [11]. If $L^*$ value of mushrooms is less than 80, wholesalers cannot accept them [11]. In this regards, to determine the effects of washing treatments on colour quality of mushroom ($L^*$) were assessed after washing application. Figures 1-2 show the change of $L^*$ values on whole mushrooms at different washing treatments.

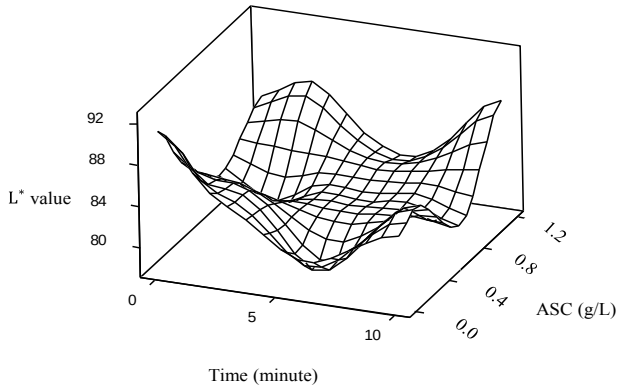


*Figure 1. The effect of time and concentration of washing treatments on $L^*$ values of whole mushrooms*

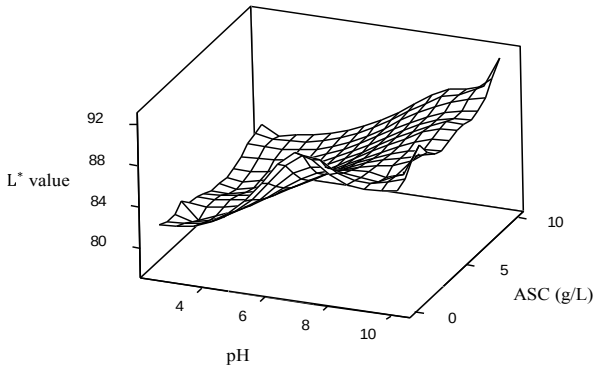


*Figure 2. The effect of pH and concentration of washing treatments on $L^*$ values of whole mushrooms*

As can be seen from Figures 1-2, $L^*$ value of mushrooms decreased with increasing washing time and decreasing pH value. These colour results simply mean that the washing time could be decreased as much as possible and could be avoided from acidity, in order to increase $L^*$ value of mushrooms.

Table 2 show that linear, quadratic and cross product terms affect significantly ($p < 0.01$) the $L^*$ value of mushrooms. The value of lack-of-fit is higher than 0.05 and determination of coefficient value is higher than 0.99. These mean that the prediction performance of response surface model has high reliability for $L^*$ value of mushrooms.

*Table 2. Analysis of variance for Colour value ($L^*$)*

| Analysis of Variance | | Colour value ($L^*$) | | | |
|---|---|---|---|---|---|
| Source | DF | Adj SS | Adj MS | F-Value | P-Value |
| Model | 9 | 395.5 | 43.9 | 596.6 | 0.000** |
| Linear | 3 | 136.4 | 4.5 | 617.1 | 0.000** |
| Quadratic | 3 | 255.7 | 85.2 | 1157.3 | 0.000** |
| Cross product | 3 | 3.4 | 1.1 | 15.4 | 0.000** |
| Lack-of-Fit | 5 | 0.6 | 0.1 | 4.7 | 0.058 |
| Pure Error | 5 | 0.1 | 0.0 | | |
| Determination of Coefficient | $R^2$ =0.9981 | | | | |

** Significant at $p < 0.01$.
*Significant at $p < 0.05$.

### *3.2. Microbiological analyses*

The microbial load on mushrooms is one of the most important parameters affecting their shelf life. According to [12], the microorganism usually responsible for spoilage of mushrooms are gram-negative bacteria, belonging particularly to the *Pseudomonas* spp. Therefore, it was determined that the effects of washing treatments on the load of *Pseudomonas* spp. on whole mushroom. Figures 3-4 show the change of load of *Pseudomonas* spp. on whole mushrooms at different washing treatments.

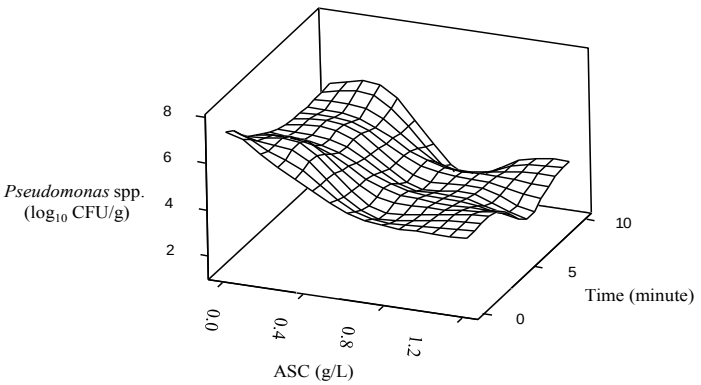


*Figure 3. The effect of concentration and time of washing treatments on the load of Pseudomonas spp. on whole mushrooms*

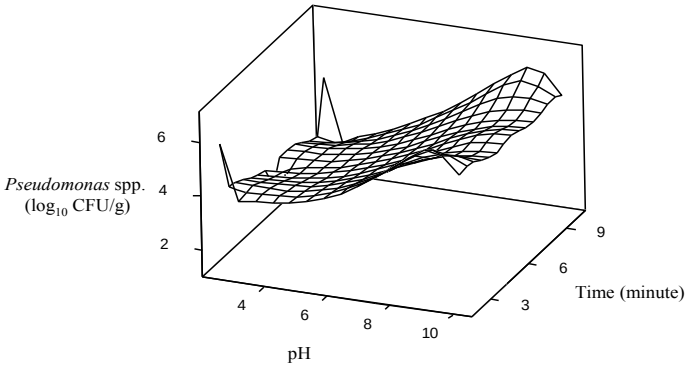


*Figure 4. The effect of pH and time of washing treatments on the load of Pseudomonas spp. on whole mushrooms*

As can be seen from Figure 3-4, the load of *Pseudomonas* spp. on whole mushroom generally decreased with increasing washing time and pH value. These results simply mean that the washing time and acidity of sodium chlorite could be increased as much as possible, in order to decrease the count of *Pseudomonas* spp. on whole mushrooms.

*Table 3. Analysis of variance for the load of Pseudomonas spp. $log_{10}$ (CFU/g)*

| Analysis of Variance | | *Pseudomonas* spp. $log_{10}$ (CFU/g) | | | |
|---|---|---|---|---|---|
| Source | DF | Adj SS | Adj MS | F-Value | P-Value |
| Model | 9 | 52.8 | 5.9 | 65.9 | 0.000** |
| Linear | 3 | 34.3 | 11.4 | 128.3 | 0.000** |
| Quadratic | 3 | 15.3 | 5.1 | 57.1 | 0.000** |
| Cross product | 3 | 3.3 | 1.1 | 12.4 | 0.001** |
| Lack-of-Fit | 5 | 0.7 | 0.1 | 3.1 | 0.117 |
| Pure Error | 5 | 0.2 | 0.0 | | |
| Determination of Coefficient | $R^2$ =0.9834 | | | | |

** Significant at $p < 0.01$.
*Significant at $p < 0.05$.

Table 3 show that linear, quadratic and cross product terms affect significantly ($p < 0.01$) the load of *Pseudomonas* spp. on mushrooms. The value of lack-of-fit is higher than 0.05 and determination of coefficient value is higher than 0.98. These mean that the prediction performance of response surface model has high reliability for the load of *Pseudomonas* spp. on mushrooms.

### *3.3. Texture measurement*

Texture analysis is a testing of physical characteristics of food products, and it gives valuable information about their tactile properties such as firmness. Because tactile properties of mushroom affect consumers' sensory perception and their acceptance, texture analysis was performed to evaluate freshness of mushroom. Figures 5-6 show the change of texture value of whole mushrooms at different washing treatments.

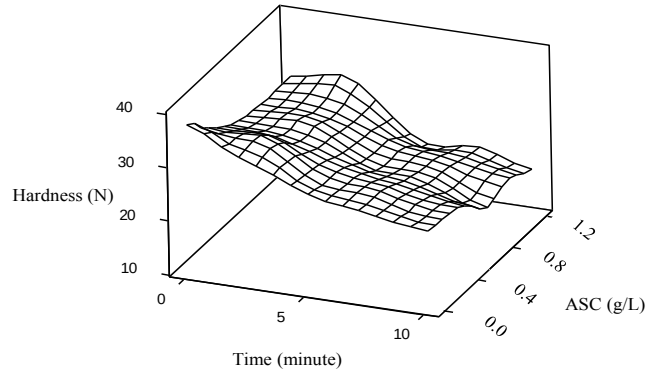


*Figure 5. The effect of time and concentration of washing treatments on the hardness value of on whole mushrooms*

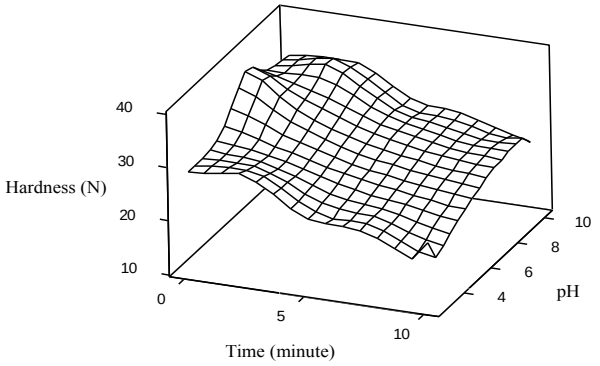


*Figure 6. The effect of time and pH of washing treatments on the hardness value of whole mushrooms*

As can be seen from Figure 5-6, the harness value of whole mushroom generally decreased with increasing washing time and decreasing pH value. These results simply mean that the washing time could be decreased as much as possible and could be avoided from acidity of acidified sodium chlorite, in order to increase the hardness of whole mushrooms.

Table 4 show that linear and quadratic terms ($p < 0.01$), and cross product terms affect significantly ($p < 0.05$) on hardness value of mushrooms. The value of lack-of-fit is higher than 0.05 and determination of coefficient value is higher than 0.98. These mean that the prediction performance of response surface model has high reliability for the hardness value of mushrooms.

*Table 4. Analysis of variance for the hardness value (N)*

| Analysis of Variance | | Hardness (N) | | | |
|---|---|---|---|---|---|
| Source | DF | Adj SS | Adj MS | F-Value | P-Value |
| Model | 9 | 505.6 | 56.2 | 52.7 | 0.000** |
| Linear | 3 | 442.2 | 147.4 | 138.1 | 0.000** |
| Quadratic | 3 | 49.9 | 16.6 | 15.6 | 0.000** |
| Cross product | 3 | 13.6 | 4.5 | 4.2 | 0.036* |
| Lack-of-Fit | 5 | 5.4 | 1.1 | 1.0 | 0.496 |
| Pure Error | 5 | 5.3 | 1.1 | | |
| Determination of Coefficient | $R^2$ =0.9793 | | | | |

** Significant at $p < 0.01$.
*Significant at $p < 0.05$.

The main objective of this study were to found the optimum washing treatment to extend the shelf life of mushrooms. For this purpose, the maximization of $L^*$ and hardness value of mushroom and minimization of the load of *Pseudomonas* spp. on mushroom were simultaneously selected as objective function. Figure 7 shows that the effects of washing conditions on quality parameters of mushrooms (colour value, the load of *Pseudomonas* spp. and hardness).

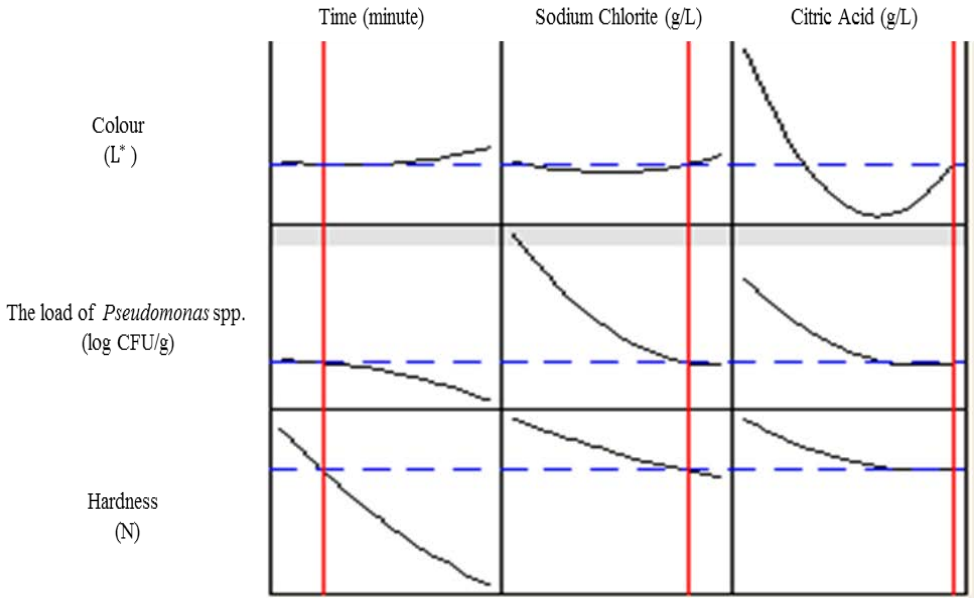


*Figure 7. The effect of significant washing conditions on three quality responses*

Each response was plotted against each significant factor using the predicted models to better understand the relationship between factors and responses (Figure 7). As shown, when the treatment time increased, the hardness of mushrooms decreased fairly linearly from 35.31 to 13.02 N. When sodium chlorite concertation increased to 1 g/L, the load of *Pseudomonas* spp. decreased and then levelled off. When citric acid concentration increased, initially colour value of mushroom decreased then it starts to increase and the maximum $L^*$ value of mushroom was obtained at the concertation of 6 g/L citric acid. When all results are taken in to consideration, sodium chlorite 1 g/L and citric acid 6 g/L for 2 minutes of processing time were determined as the optimum washing process conditions.

## 4. CONCLUSIONS

In this work, the main objective of this work was to determine the optimum ASC concentration and washing time for the quality parameters (microbial load, colour and texture) of fresh whole mushroom. When compared to different washing treatment conditions, *Pseudomonas* spp. inactivation was the highest when the mushrooms were washed with 1 g/L of ASC solution for 2 minutes in which colour and textural properties were very close to the fresh form. Results show that optimum washing conditions could be used in the mushroom industry to extend the shelf life of mushrooms.

## ACKNOWLEDGEMENT

This work was financially supported by Gebze Technical University through Scientific Research Projects (BAP) 2014 A-25 and 2015 A-40. Fatih Tarlak would like to thank The Scientific and Technology Research Council of Turkey (TUBITAK) for granting PhD scholarship (2211-C).

## REFERENCES

[1]. M. Brennan, G.L. Port, and R. Gormley, “Post-harvest with citric acid or hydrogen peroxide to extend the shelf life of fresh sliced mushrooms”, Food Sci. Technol.-LEB., vol. 33, pp. 285-289, 2000.

[2]. T. Jiang, “Effect of Natamycin in Combination with Pure Oxygen Treatment on Postharvest Quality and Selected Enzyme Activities of Button Mushroom (Agaricus bisporus)”, J. Agric. Food Chem., vol. 60, pp. 2562-2568, 2012.

[3]. O. Nerya, R. Ben-Arie, T. Luzzatto, R. Musa, S. Khativ, and J. Vaya, "Prevention of Agaricus bisporus postharvest browning with tyrosinase inhibitors", Postharvest Biol. Tec., vol. 39, pp. 272-277, 2006.

[4]. E. Gonzalez-Fandos, A. Simon, and V. Pardo, "Quality and shelf life of packaged fresh sliced mushrooms stored at two different temperatures", Agri. Food Sci., vol. 15, pp. 414-422, 2006.

[5]. A. Simon, E. Gonzalez-Fandos, and V. Pardo, "The sensory and microbiological quality of fresh sliced mushroom (Agaricus bisporus L.) packaged in modified atmospheres", Int. J. Food Sci. Tech., vol. 40, pp. 943-952, 2005.

[6]. A. Simon, E., Gonzalez-Fandos, M., and Vazquez, "Effect of washing with citric acid and packaging in modified atmosphere on the sensory and microbiological quality of sliced mushrooms (Agaricus bisporus L.)", Food Control., vol. 21, pp. 851-856, 2010.

[7]. R. Singia, A. Ganguli, and M. Ghosh, "Physicochemical and Nutritional Characteristics of OrganicAcid-Treated Button Mushrooms (Agaricus bisporous)", Food Bioprocess Tech., vol. 5, pp. 808-815, 2012.

[8]. N. Sedaghat, and Y. Zahedi, "Application of edible coating and acidic washing for extending the storage life of mushrooms (Agaricus bisporus)", Food Sci. Technol. Int., vol. 18, pp. 523-530, 2012.

[9]. V. Cliffe-Byrnes, and D. O'Beirne, "Process-modified atmosphere and humidity parameters for high-quality sliced mushrooms (Agarıcus bısporus L.)", J. Food Quality., vol. 33, pp. 286-302, 2008.

[10]. E.O. King, M.K. Ward, and R. Ranzy, "Two simple media for the demonstration of pyocyanin and fluorescein", J. Lab. Clin. Med., vol. 44, pp. 301-307, 1954.

[11]. T.R. Gormley, "Chill storage of mushrooms", J. Sci. Food Agr., vol. 26, pp. 401-411, 1975.

[12]. D. Eastwood, and K. Burton, "Mushrooms – a matter of choice and spoiling oneself", Microbiology Today., vol. 29, pp. 18-19, 2002.

## BIOGRAPHY

Fatih Tarlak received his B.Sc. in 2009 from Department of Chemical Engineering, Gazi University, and he received his M.Sc. from Department of Chemical Engineering, Gebze Technical University three years later. He is a Ph.D. student and research assistant in Department of Chemical Engineering, Gebze Technical University at present. His main research areas are optimization and modelling of food microbiology and shelf life.

ICENS
INTERNATIONAL CONFERENCE ON ENGINEERING AND NATURAL SCIENCES
24-28 May 2016 /Sarajevo

# Evaluation of Consulting Firms Selection in Construction Projects by Using Fuzzy Logic

*Aynur Kazaz[35], M. Talat Birgönül[36], Hakan Kaplan[3], Turgut Acıkara[4], Bayram Er[5]*

***Abstract***

*Construction industry brings different specialization-required disciplines together in a common project. This circumstance complicates finishing a project within a desired time, cost and quality. In recent years, especially non-sector investors have started to employ consulting firms for the design and management of the projects to overcome this problem. Unlike contractor selection process, consulting firm selection process is too complicated for a cost-oriented evaluation. In this sense, different organizations such as International Federation of Consulting Engineers (FIDIC) developed new bidding l . "Q l C B S l " (QCBS), wh h ll w v l q l the bids concomitantly, is one of the widely used system in construction industry. In this study, it was aimed to determine which criterions are prioritized in QCBS system by using fuzzy logic. In this context, data of 65 bids belonging to 13 different tenders were investigated and a fuzzy model consisting of 3 input and 1 output variable was developed. The results revealed that, in general consulting firms, which are invited to the tenders, ensures the quality criterions and cost criterion determines the selection.*

**Keywords:** Consulting firm selection, fuzzy logic, fuzzy set theory, construction management

## 89. INTRODUCTION

The construction industry consists of different project types such as building, highway, dam etc. which are constructed for different purposes and requires different expertise. In addition, numerous activities in each project type and different resources with different characteristics used in these activities, forces the project participants to specialize in a specific area. In this sense, the construction industry can be defined as an interdisciplinary sector with a wide range. Nowadays, due to this structure of the sector many project owners prefer to employ consulting firms for the design and management of the projects. Especially for the non-sector investors an effective consulting service is crucial to finish a project within its scope. In this context, "consulting firm selection" concept came to the fore in the sector and many institutions like International Federation of Consulting Engineers (FIDIC) made efforts to standardize the selection process.

Unlike contractor selection, consulting firm selection is too complicated for a cost-oriented selection process. Although the price of consulting service is very low compared to the project cost, the success of design and inspection activities of the consulting firms will prevent time and cost overruns. This circumstance, forced the institutions to develop new methods which enables to evaluate concurrently the quality and cost of the services.

Quality and Cost Based Selection (QCBS), which was introduced by FIDIC is one of the widely used method. In this study, the data of 65 bids belonging to 13 different tenders, at which QCBS was used, were analyzed to determine the prioritized criterions in the selection process.

## 2. QUALITY AND COST BASED SELECTION BID SYSTEM

[35] *Corresponding author: Ak z U v , C v l E , 07058, K l /A l , T k .* akazaz@akdeniz.edu.tr
[36] *M l E T h l U v , C v l E ,06531, İ ö ü B l v /A k , T k ,* birgonul@metu.edu.tr
[3] *Akdeniz University, Department of Civil Engineering, 07058, K l /A l , T k ,* hkaplan79@yahoo.com
[4] *Ak z U v , C v l E , 07058, K l /A l , T k ,* tacikara@akdeniz.edu.tr
[5] *Ak z U v , C v l E , 07058, K l /A l , T k ,* bayramer@akdeniz.edu.tr

QCBS is a competitive method that enables to evaluate the quality of consulting services together with their costs. Besides inducing fewer errors, this method also reduces the contract cost by fewer claims and tender process cycles [1]. The evaluation of the proposals in this method is conducted in 3 steps. In the first step the quality of the proposals are determined after technical evaluations. In context of technical evaluation; consultant firm's project specific experience, methodology proposed for the project, key personnel who will be employed in the project, transfer of knowledge and participation by nationals are considered as criterions. Depending on the scope and features of the project for each criterion a score is determined where the sum of these scores must be 100 (Table 1). As seen from the table, QCBS mainly focuses on methodology and key personnel. Actually, in most of the tenders transfer of knowledge is not evaluated.

*Table 1. Sample scores of criterions in QCBS*

| | |
|---|---|
| Consultant's specific experience | 0-10 |
| Methodology | 20-50 |
| Key personnal | 30-60 |
| Transfer of knowledge | 0-10 |
| Participation by nationals | 0-10 |
| **Sum** | **100** |

In the second step the costs of the proposals which satisfy the quality requirements are evaluated. In general an inverse proportion approach is used for calculating the cost score of each proposal. In this context, the lowest proposal is scored as 100 and the below shown formula is used for determining the cost scores of other participants.

$$Financial\ Score = \frac{lowest\ proposal\ cost}{proposal\ cost}\ x\ 100 \quad (1)$$

Finally, both scores obtained in the first 2 steps are combined and proposal scores of each participant are calculated. For this purpose different weight for both quality and financial scores are determined. Since quality is prioritized in QCBS the weight of financial score must be lower than weight of quality score. In common practice weight of cost is mainly taken as 20%.

## 3. MODEL DEVELOPMENT

After Zadeh [2] introduced fuzzy sets, fuzzy techniques become popular among many research areas in the past decades. In brief, fuzzy logic tries to imitate the human way of thinking [3]. In this context, humans are connected with computers by assessing linguistic statements with numerical values [4]. In classical set theory, each set has sharp boundaries [5]. Therefore, a variable whether belongs to a specific set or not. On the other side, in fuzzy set theory a variable can be a member of more than one set with different membership degrees at the same time [6]. This feature eases modelling complex problems encountered in real world. Fuzzy models are mainly developed based on the developer's experience. Therefore real data is only needed for gaining experience and testing the validity of the model. In this study, 65 proposals belonging to 13 different

tenders in Turkey in which FIDIC documents were taken as a basis were investigated for the model development.

Fuzzy rules are the conditional statements of the model which shows the correlation between input and output variables. In this context, numerous input variables will increase the number of fuzzy rules and hence, extracting an answer for each rule becomes complicated. Therefore, in this study two assumptions were made to decrease the number of input variables;

1. Methodology refers to the method that is proposed by consulting firms based on their previous experiences. In other words, methodology is an outcome of experience. In this context, it was assumed that there is a high correlation between methodology and experience of consulting firms and hence, these criterions were combined as a single variable in the model.
2. Key personnel and participation by nationals are people-oriented criterions. In this sense, it was assumed that employing key personnel from nationals will provide an advantage for consulting firms. Therefore, these two criterions were also combined as a single variable in the model.

Under these assumptions, a fuzzy model consisting of 3 inputs and one output named as "experience-methodology", "key personnel-participation of nationals", "cost" and "outcome", respectively was developed (Figure 1). Since, the purpose was classification, Mean of Maximum (MOM) defuzzification method was used which extracts the output with the highest probability. Maximum scores of "experience-methodology" and key personnel-participation of nationals" in these 13 proposals were 40 and 60, respectively. Similarly, the weight of financial score was taken as 20%

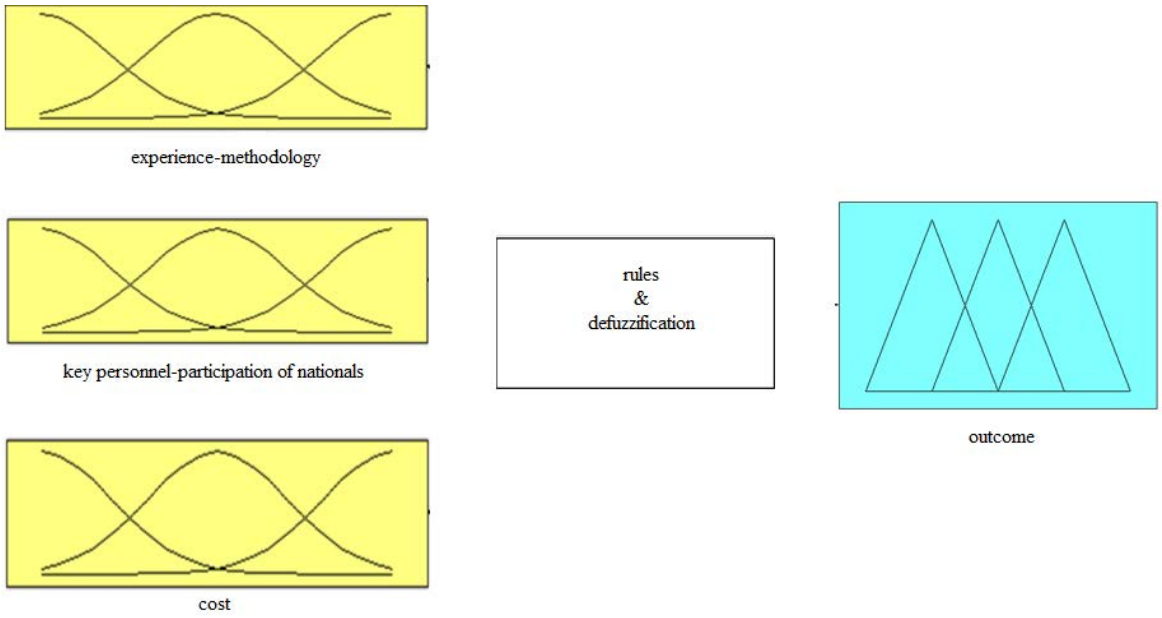


*Figure1. Model structure*

In each input set 3 membership functions (unsuccessful, medium and successful) were used. The intervals of these functions were determined after examining the real data. Membership functions of each set and their intervals are shown in Figure 2, 3, 4 and Table 2, respectively. Similarly, the outcome set included 2 membership functions named as "successful" and "unsuccessful" (Figure 5). Since the model was consisted of 3 input sets and each set had 3 membership functions; 27 fuzzy rules were established which 6 of them extracted "successful" as the outcome.

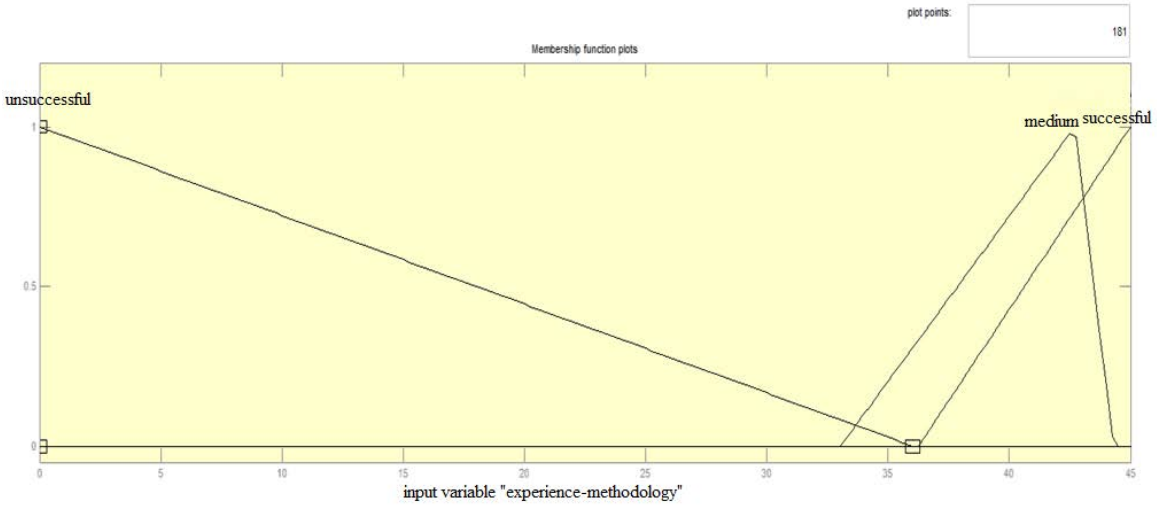


*F 2. M b h "x - h l "*

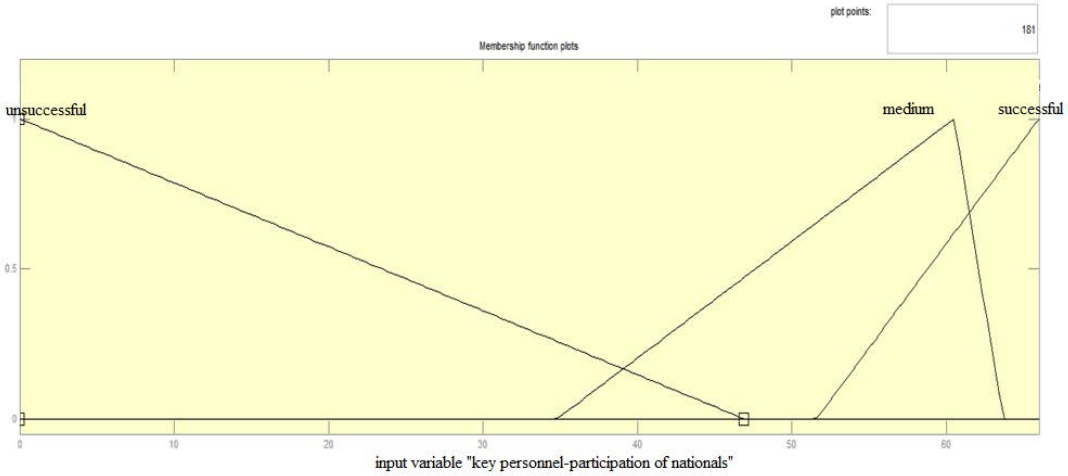


*F 3. M b h "k l- l"*

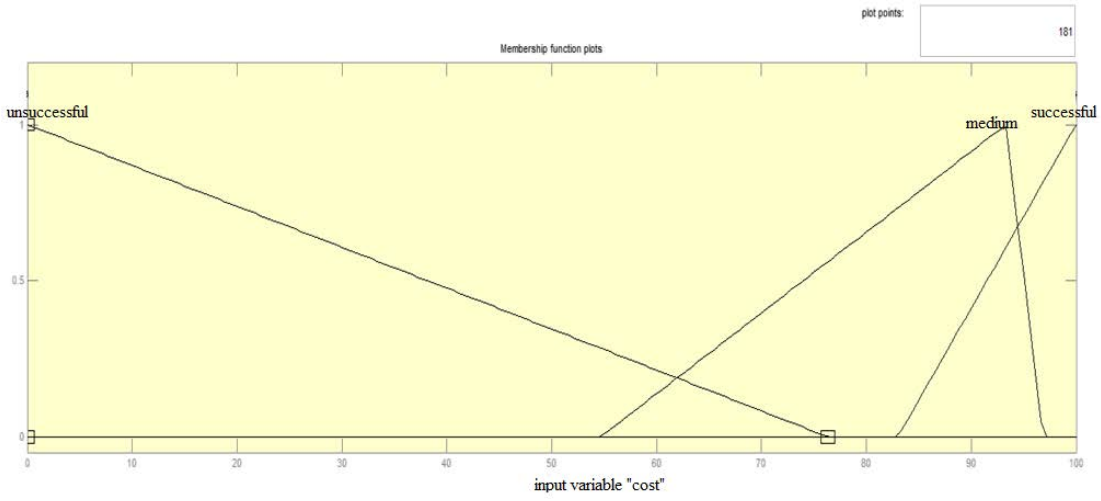


*F 4. M b h " "*

*Table 2. Intervals of membership functions*

| Sets | Unsuccessful | Medium | Successful |
|---|---|---|---|
| Experience-methodology | 0-0-36,1 | 33,04-42,7-44,3 | 36,25-45-45 |
| Key personnel-participation of nationals | 0-0-46,9 | 34,8-60,5-63,7 | 51,6-66-66 |
| Cost | 0-0-76,3 | 54,7-93,3-96,84 | 83-100-100 |

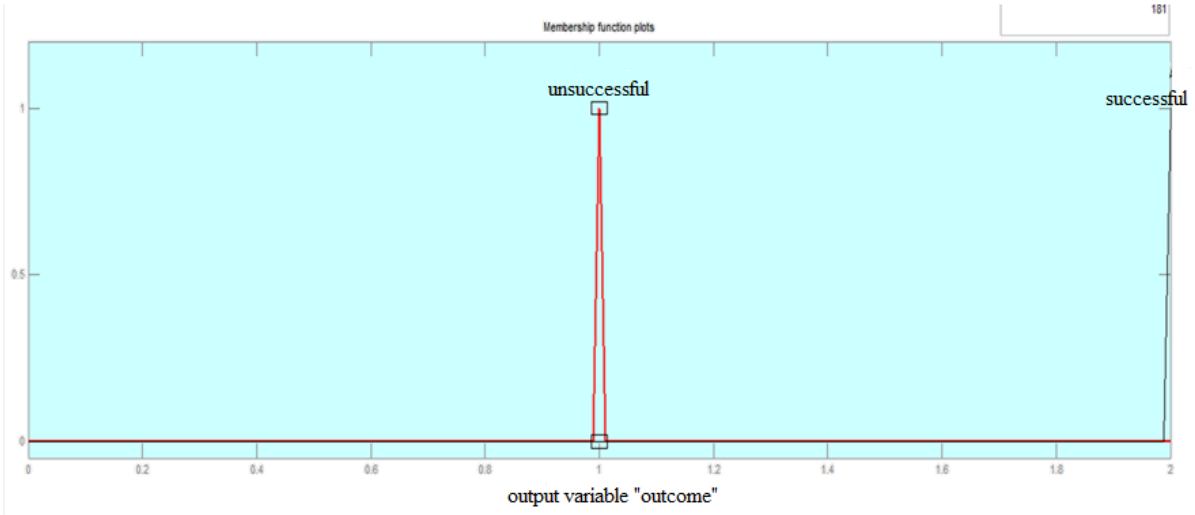


*Figure 5. M b h " "*

## 4. DISCUSSION OF RESULTS

The aim of developing the model was to determine the prioritized criterions in the selection process. To validate the model, data of each proposal were tested and the model results were compared with the actual ones. All of the results extracted by the model overlapped with the actual ones and hence, the validity of the model was confirmed.

In the model it was observed that in 3 successful rules "experience-methodology" was considered as "medium" where in 3 as "successful". As can be seen from Figure 2, medium and successful membership functions were intensified between 36 and 45. The "experience-methodology" scores of 9 winners were placed in this intense area where the other 4 in 33-36 interval. The average "experience-methodology" scores and their standard deviation of all proposals were calculated as 34,95 and 3,60, respectively.

Similarly, "key personnel-participation of nationals" was considered as medium and successful in 4 and 2 successful fuzzy rules, respectively. These two membership functions were intensified in 51-66 interval (Figure 3). In addition, all of the winners were placed in these intervals. The average score of this criterion was 58,25 with a standard deviation of 4,43.

Finally, in 2 successful rules "cost" was considered as medium where in 4 as successful. The intense area of these two membership functions was in 83-100 intervals (Figure 4). All of the winners were placed in this area and 7 of them also proposed the lowest cost in the tenders. The average score and its standard deviation of this criterion were calculated as 78,01 and 18,23, respectively.

To summarize; among the criterions cost had the highest standard deviation. Similarly, experience-methodology and key personnel-participation of nationals scores of the winners were close to the average values of these criterions. Therefore, it can be deduced that the invited firms satisfied the quality requirements in general. In this context, although QCBS focuses mainly on the quality, the success of the bids depended on the proposed cost of the firms. In other words, cost is the prioritized criterion in consulting selection processes.

## 5. CONCLUSION

The interdisciplinary nature of construction industry results in delays, cost overruns and quality losses in construction projects. To overcome these problems, especially non-sector investors have started to employ consulting firms for project design and management. In this context, many institutions such as FIDIC have developed new methods for standardizing the selection process. QCBS is a widely used method which enables to evaluate the quality of consulting services together with their costs.

In this study, it was aimed to determine the prioritized criterion in QCBS. For this purpose, 65 proposals belonging to 13 tenders were investigated and a fuzzy model consisting of 3 input and 1 output was developed. Real data of these 65 proposals were tested in the model and 100% success was achieved. The results of the study revealed that most of the participants satisfied the quality requirements and cost is the main criterion that determines the winner.

## REFERENCES

[1]D.C. Ingram, and B. Peltier, "MTO adopts performance-based consultant selection system", *Engineering Dimensions,* 11-15, March/April 2011.

[2] L.A. Zadeh, "Fuzzy sets." *Information and Control*, Vol. 8(3), pp. 338-353, 1965.

[3] E.E. Elbeltagi, A.A. Hosny, A. Elhakeem, M.E. Abdelrezak, and M.S. El-Abbasy, "Fuzzy Logic Model for Selection of Vertical Formwork Systems." *Journal of Construction Engineering and Management*, Vol. 138(7), pp. 832-840, 2012.

[4] A.P.C Chan, D.W.M. Chan, and J.F.Y. Yeung, "Overview of the application of "Fuzzy Techniques" in construction management research." *Journal of Construction Engineering and Management*, Vol. 135 (11) pp. 1241-1252, 2009.

[5] V. Nguyen, "Tender evaluation by fuzzy sets." *Journal of Construction Engineering and Management*, Vol. 111 (3), pp. 231-243, 1985.

[6] D. Singh, and R. Tiong, "A fuzzy decision framework for contractor selection." *Journal of Construction Engineering and Management*, Vol. 131(1), pp. 62-70, 2005.

# Motivation as a Tool for Ensuring Productivity Improvement in Turkish Construction Industry

*Aynur Kazaz[37], M. Talat Birgönül[38], Turgut Acıkara[3], Bayram Er[4]*

***Abstract***

*Recently, human resource, which is crucial to ensure productivity improvement, became one of the most important competition tools. Employing the labor force in an effective way will provide to benefit from the advantages of productivity improvement. In this aspect, determination and evaluation of the factors affecting labor productivity will ease the right employment of labor force. In the literature, there are numerous researches related with the factors affecting labor productivity. However, in most of these studies motivation theories were neglected and critical factors were not correlated with motivation schemes. The aim of this study is to correlate the factors affecting labor productivity in Turkey with motivation schemes. For this purpose a two-step study was conducted. In the first step, factors affecting labor productivity were categorized under 4 different factors groups named as organizational, economical, socio-physiological and physical, respectively and a questionnaire was administered to craft workers. The results of the questionnaires were evaluated by using Relative Importance Index (RII). In the second step, productivity improvement based on motivation theories was investigated by reviewing the literature. The results revealed that, the most important schemes for craft workers and managers were economical and organizational schemes, respectively*

**Keywords:** Construction Labor Productivity, Productivity Factors, Motivation Theories, Relative Importance Index

## 90. INTRODUCTION

Motivation can be simply defined as a driving force which directs human behavior for realizing a specific goal. Indeed, motivation is a psychological process which appears when a task is planned to execute for a given purpose or a specific wish is fulfilled [1]. In addition, for some researchers motivation is accepted as a human engineering approach which is stimulated by personnel requirements [2]. Depending on the factors motivation can be indigenous or exogenous. Intrinsic motivators create an internal desire in persons to perform a specific task while extrinsic motivators are awards that increases personal satisfactions. For example, self-fulfillment which arises due to high performance is an intrinsic motivator while incentive awards given to the craft worker for his high performance is an extrinsic one.

The researches in the literature have proven the direct relation between motivation and productivity of craft workers [3]. High motivation is one of the most important factors that provide high productivity. Besides

personal productivity, motivation also affects the productivity of team work [4-5]. Therefore, to increase job satisfaction and performance of craft workers, motivation concept must be extensively clarified and investigated [6]. Motivation methods for productivity increasing were structured by different authorities through considering applications of different human relations theories of motivation [7].width and other features. Please make sure that the use of other languages in figures and tables is avoided. Papers should be checked by a native English speaker with expertise in the field prior to submission.

In today's competitive environment, increasing labor productivity became an important goal for the construction industry. Therefore, determining the factors affecting craft workers' motivation is crucial. In this sense many researches were conducted to determine the factors affecting labor productivity. However, in most of these studies motivation theories were neglected. In this study, it was aimed to evaluate the factors affecting labor productivity in Turkey within the context of motivation theories. For this purpose, first motivation theories in the literature were addressed and then factors affecting labor productivity were determined. Since craft workers can better evaluate their own performances [8], their perspectives were used for determining these factors. Finally, these factors were evaluated by using Maslow's hierarchy of needs theory. A better understanding of these factors by using motivation theories will ease to take precautions and hence, a more productive working environment will be created for the Turkish construction industry. .

[37] *Corresponding author: Ak z U v , C v l E , 07058, K l /A l , T k .* akazaz@akdeniz.edu.tr
[38] *M l E T h l U v , C v l E ,06531, İ ö ü B l v /A k , T key,* birgonul@metu.edu.tr
[3] *Ak z U v , C v l E , 07058, K l /A l , T k ,* tacikara@akdeniz.edu.tr
[4] *Akdeniz University, Department of Civil Engineering, 07058, K l /A l , T k ,* bayramer@akdeniz.edu.tr

## 91. OVERVIEW OF MOTIVATION THEORIES

Since 1950s many motivation theories were developed for utilizing in the organizational behavior and management areas [9]. The most known and widely used motivation theories are Maslow's Hierarchy of Needs Theory, Herzbergs' Motivation-Hygiene Theory, McGregor's Theory X and Theory Y, Expectancy Theories of Vroom and Lawler and Ouchi's Theory Z [10-15]. Motivation theories are categorized under 2 groups named as content theories and process theories [16]. Content theories mainly focus on personal needs and determining the factors which are effective on acting or stopping some desired behaviors in persons. On the other side, process theories deal with how and why personal factors are affected from each other during creating a specific behavior pattern. In other words content theories seek an answer for "what" while process theories for "how" and "why".

Maslow's Need Theory is one of the widely used content theories in the literature. This theory became an ideal typology for many sectors to understand motivation types because of its widely understood concept [17]. Indeed, many other content theories in the literature originate from Maslow's Hierarchy of Needs Theory [17]. Maslow assumed that there are 5 basic needs which provide a basis for personal behaviors. In his theory he categorized desires and needs of human beings in an ascending order of importance as physiological, safety, affiliation and social needs, esteem needs and self-actualization needs, respectively. Needs groups and associated samples according to Maslow's Hierarchy of Needs Theory are shown in Table 1 [3, 17, 18, 19].

*Table 1. Examples of classified needs*

| **Physological Needs** | **Safety-Security Needs** | **Social- Affiliation Needs** | **Esteem-Needs** | **Self-actualization Needs** |
|---|---|---|---|---|
| Salary | Safe working conditions/environment | Friendship | Status | The ability to reach one's potential |
| Housing | Freedom from pain and threat | İnteraction | Prestige | İndividual's personal sense of achievement |
| Food | Job security | Affection from friends and family | Respect | Feeling of self-fulfillment |
| Clothing | Absence of illness | Sense of belonging to a group | Recognition | Need for personal growth |
| Water | Shelter | Relationship with others | Positive feedback | Creating challenging tasks that are stimulating |
| Air | Warmth | Team work | Opportunity for advancement | |
| Wage | Stability | Activities to develop relationship between co-workers | | |
| Working conditions | Sick pay | | | |

In general, Maslow's hierarchy of needs is likened to a pyramid where self-actualization and physiological needs are placed on the top and bottom, respectively (Figure 1). Needs in lower level are mainly affected by external factors while needs in higher level from internal ones. According to Maslow's Hierarchy of Needs Theory people seek to be satisfied from the next level only after lower level needs are satisfied. Except esteem and self-actualization needs and as long as a sudden environmental change does not exist, the motivators will lose their effectiveness after the needs are satisfied in a certain level [20].

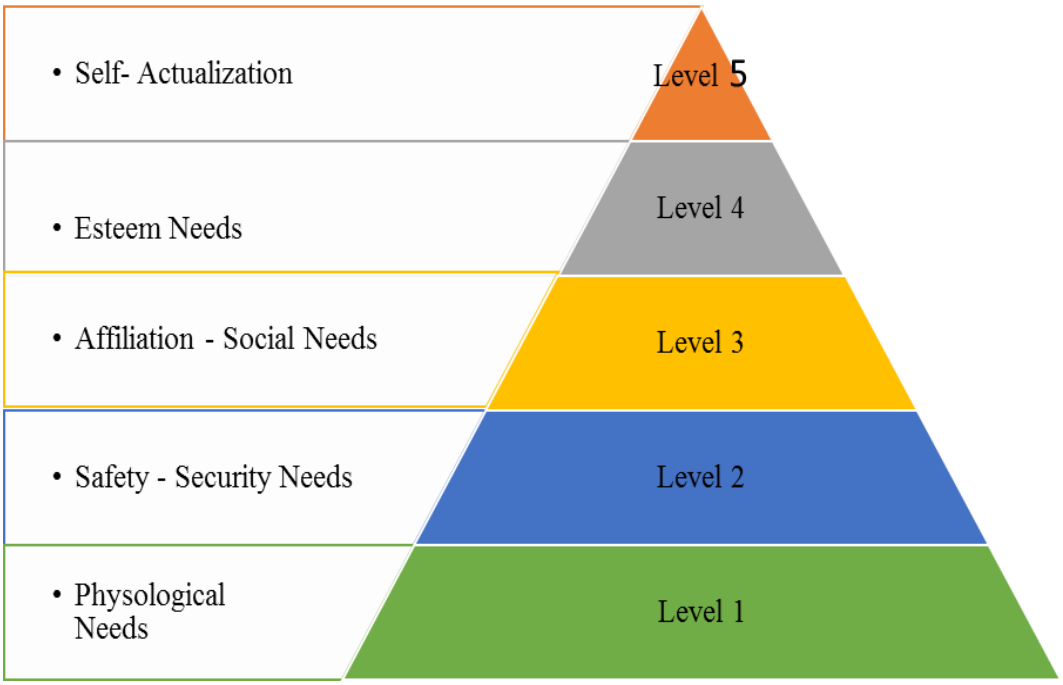


*F l. M l w'*

Maslow's Hierarchy of Needs Theory was a basis for many motivation practice and empirical researches in the literature [21-27]. Schrader's study was one of the preliminary studies related to this topic in which Maslow's theory was applied to construction workers [21]. This study revealed that physiological and safety needs were not motivating factors for the workers [21]. Similarly, Hazeltine and Wilson stated that higher level needs were important for motivating construction workers [22-23]. Olomaiye and Ogunlana, and Zakeri et.al. found out that factors related with financial income are the predominant factors for motivating the workers in both Nigerian and Iranian construction industries, respectively [24-26]. According to Kaming et.al. the higher levels in Maslow's pyramid came forefront among construction workers in Indonesia [27]. In addition, it is also believed that the economic development level of a country affects the needs of the workers [24]. Accordingly, in developed countries the workers require the higher level needs of the pyramid for motivation where in developing countries lower level ones [25, 27].

## 92. METHODOLOGY

Researches related with labor productivity have proven that factors affecting labor productivity vary from region to region. Therefore, region specific researches must be conducted for identifying and evaluating these factors. Kazaz et.al. identified 37 different factors affecting labor productivity in the Turkish construction industry [28]. 18 of these factors were compatible to Maslow's Hierarchy of Needs Theory. In this study it was assumed that considering workers' opinions would provide a more proper evaluation of the factors within the context of Maslow's Hierarchy of Needs Theory. In this sense, a questionnaire involving the 18 compatible factors was prepared and administered to 126 workers face-to-face. Each factor was organized on a 5-point Likert-scale where 1 and 5 represents "not significant" and "extremely significant", respectively. During the interviews necessary interventions were made and thus, all questionnaire results were used in the statistical analysis. The factors were ranked by using the Relative Importance Index (RII) method which represents the relative importance of a variable among other ones. The numeral interval of RII method used for 5-point Likert scale is shown in Table 2.

*Table 2. Numeral Intervals of RII Methods*

| Min RII Points | Definition | Max RII Points |
|---|---|---|
| 1,00 | not significant (NS) | 1,80 |
| 1,80 | somewhat significant (SS) | 2,60 |
| 2,60 | Significant (S) | 3,40 |
| 3,40 | very significant (VS) | 4,20 |
| 4,20 | extremely significant (ES) | 5,00 |

The Test of Internal Consistency was used to determine the reliability of the questionnaire. The Cronbach's Alpha Reliability Test Method is the most widely used method to test the internal consistency. The Cronbach's alpha value varies between 0 and 1 and a questionnaire with a value between 0,600 and 0,900 is accepted as reliable [29].

## 93. DISCUSSION OF RESULTS

The Cronbach's Alpha Reliability Test Method was applied to the factors of each level in Maslow's pyramid separately. The Cronbach's alpha values of physiological, safety, affiliation and social needs, esteem needs and self-actualization were calculated as 0,724, 0,702, 0,604, 0,642 ve 1, respectively. These results confirmed that the questionnaire was reliable.

In Table 3 ranking and RII score of each factor are represented. As seen from the table "Working in social insurance" factor which is categorized under safety needs was the most effective motivator among the craft workers with a RII score of 4,68. This factor satisfies the safety needs by securing the future of workers and their family. The second and third most effective motivators were financial related factors named as "On-time payment" and "Amount of pay" with RII scores of 4,60 and 4,52 respectively. The interesting fact in this result is that craft workers evaluated on-time payment more important compared to their wages. These two factors were categorized under physiological needs in Maslow's pyramid. The least effective motivator according to craft workers was "Sharing problems and their results" factor which was categorized under affiliation-social needs with a RII score of 3,03. Although this factor has the lowest RII score it was evaluated as significant by the workers. According to Maslow's pyramid the most effective motivators of Affiliation-Social Needs and Esteem Needs were "Quality of site management" and "Incentive payments and financial rewards" factors with RII scores of 4,39 and 3,98, respectively. The interviews conducted with the craft workers revealed that the quality of site management affects both their communications between the people and sense of belonging. On the other side, incentive payments and financial rewards are perceived as a positive feedback and accepted as a prestige indicator among the workers. "Work satisfaction" as the only factor investigated under self-actualization turned out to be very significant among workers with a RII score of 3,44.

*Table 3. RII scores of productivity factors*

| Maslow's Need Category | Rank | Productivity Factor | RII Score | RII Effect Level | Factor Group |
|---|---|---|---|---|---|
| Physiological Needs | 1 | On-time payment | 4,60 | ES | Economical |
| | 2 | Amount of pay | 4,52 | ES | Economical |
| | 3 | Camping Conditions | 4,51 | ES | Organizational |
| | 4 | Relaxation allowances | 4,31 | ES | Organizational |
| Safety-Security Needs | 1 | Working in social insurance | 4,68 | ES | Economical |
| | 2 | Health and safety conditions | 4,49 | ES | Socio-Physiological |
| | 3 | Discontinuity of work | 4,18 | VS | Economical |
| Affiliation-Social Needs | 1 | Quality of site management | 4,39 | ES | Organizational |
| | 2 | Social activity opportunities | 4,17 | VS | Socio-Physiological |
| | 3 | Relations with workmates | 3,55 | VS | Socio-Physiological |
| | 4 | Crew size and efficiency | 3,45 | VS | Organizational |
| | 5 | Cultural differences | 3,20 | S | Socio-Physiological |
| | 6 | Sharing problems and their results | 3,03 | S | Socio-Physiological |
| Esteem Needs | 1 | Incentive payments and financial rewards | 3,98 | VS | Economical |
| | 2 | Giving responsibility | 3,53 | VS | Socio-Physiological |
| | 3 | Firm reputation | 3,21 | S | Organizational |
| | 4 | Worker participation in decision making | 3,04 | S | Socio-Physiological |
| Self-actualization | 1 | Work satisfaction | 3,44 | VS | Socio-Physiological |

In context of the study, all of the factors belonging to physiological needs had the impact degree of extremely significant. Indeed, the results revealed that the impact degrees of the factors change from extremely significant to significant as the need levels climbs from bottom to top. In Table 4 the mean RII scores of the

factors investigated in the same need levels and their impact degrees are shown. As seen from the table, physiological and safety-security needs were perceived as extremely significant by the workers with RII scores of 4,49 and 4,45, respectively. This result proves that workers in developed and developing countries give importance to different needs in Maslow's pyramid [25, 27]. Therefore, perceiving the factors in the lower levels as extremely significant in Turkey was an expected result of this study.

*Table 4. Ranking of Maslow pyramid levels*

| Maslow pyramid level | Maslow' needs | Number of investigated factors | Rank | Median RII score | Effect level |
|---|---|---|---|---|---|
| Level 1 | Physiological | 4 | 1 | 4,49 | ES |
| Level 2 | Safety-Security | 3 | 2 | 4,45 | ES |
| Level 3 | Affiliation-Social | 6 | 3 | 3,63 | VS |

| | | | | | |
|---|---|---|---|---|---|
| Level 4 | Esteem | 4 | 4 | 3,44 | VS |
| Level 5 | Self-actualization | 1 | 5 | 3,44 | VS |

## 94. CONCLUSION

Since motivation has a big impact on workers' performance, many researchers give importance on investigating this topic [28]. In this aspect, many theories were developed about motivation. Maslow's Hierarchy of Needs Theory formed a basis for many theories in the literature. This theory, allows understanding human behavior and identifying proper motivational strategies for motivating people. Therefore, evaluating the factors affecting labor productivity within the context of Maslow's Hierarchy of Needs Theory will ease improving labor productivity in the Turkish construction industry.

In this study, factors affecting labor productivity in Turkey were evaluated within the context of Maslow's Hierarchy of Needs Theory. For this purpose 18 factors were categorized by considering Maslow's pyramid and a questionnaire involving these factors were administered to 126 workers. RII method was used for ranking the factors associated with the questionnaire results.

The results of the study revealed that in the Turkish construction industry workers perceive physiological and safety-security needs which are located at the bottom of Maslow's pyramid as extremely significant. Therefore, to improve labor productivity management has to consider the factors belonging to these needs. Evaluating the lowest levels in Maslow's pyramid as extremely significant, which supports the results of the other studies in the literature, was an expected result for Turkey as a developing country.

## REFERENCES

[243]. E. B. Flippo *Personnel Management*, 5th Edition, McGraw hill Inc. London, 1982.
[244]. M. Mee-Edoiye and M.M. Andawei Motivation, "An Alternative to improve workers performance in Today Construction Industry". *The Quantity Surveyor*. vol. 40(3), pp. 2-6, 2002.
[245]. S.Y.W. Lam and C.H.W. Tang "Motivation of Survey Employees in Construction Projects" *Journal of Geospatial Engineering*, vol. 5, No.1, pp. 61-66, 2003.
[246]. R. Butler, *The Economics of Social Insurance and Employee Benefits*, Kluwer Academic, 1999.
[247]. E.M. Rojas and P. Aramvareekul, "Labour Productivity Drivers and Opportunities in the Construction Industry," *Journal of Management in Engineering*, vol. 19:2, pp. 78-82, 2003.
[248]. Y. Zhou, G. Jergeas, and J. Ruwanpura, "Motivation, Performance and Job Satisfaction of Construction Management Professionals – an Expectancy Theory Research Approach", *Proceedings of the IRNOP VII Project Research Conference,* Xi'an, Chian, 2006, pp. 239-249.
[249]. M. S. Khan, "Methods of motivating for increased productivity", *Journal of Management in Engineering* vol. 9(2) pp. 148–156, 1993.
[250]. P.M. Goodrum, J. Dai, and W.F. Maloney "Construction craft workers' perceptions of the factors affecting their productivity." *Journal of Construction Engineering and Management*, Vol.135, 2009.
[251]. R. Ruthankoon and S.O. Ogunlana, "Testing Herzberg's two-factor theory in the Thai construction industry", *Engineering, Construction and Architectural Management*, Vol. 10 Iss 5 pp. 333 – 341, 2003.
[252]. A. Maslow, *"M v l "*, Harper & Row, New York. 1954.
[253]. F. Herzberg, B. Mausner and B. Snyderman, *"Th v w k"*, Wiley, New York. 1959.
[254]. D. McGregor, *"Th h "*, McGraw-Hill, New York., 1960.
[255]. V. Vroom, *"W k v "*, Wiley, New York., 1964.
[256]. E. Lawler, *"M v w k z "*, Books Cole, Monterey, CA., 1973.
[257]. W. Ouchi, *"Th Z: H w A b J h ll "*, Addison-Wesley, Reading, M.A., 1981.
[258]. S, Hollyforde and S. Whiddett, *"Th M v H b k"*. Chartered Institute of Personnel and Development, London, 2002.
[259]. A. Salman and A.R.J. Dainty "Job Motivational Factors for Disparate Occupational Groups Within the UK Construction Sector: A Comparative Analysis" *Journal of Construction Research*, Vol. 6, No. 2 pp. 223–236, 2005.
[260]. A.O. Aiyetan, and A.O. Olotuah, Impact of motivation on workers' productivity in the Nigerian construction industry. *In: Boyd, D (Ed) Procs 22nd Annual ARCOM Conference*, Birmingham, UK, Association of Researchers in Construction Management, pp. 239-248, 2006.
[261]. H.A. Halepota "Motivational theories and their application in construction" *Journal of Cost Engineering*, Vol. 47, pp. 14-18, 2005.
[262]. A.L. Burwash, "Discussion of Motivating Civil Engineers", *Journal of Management in Engineering*, ASCE, pp.173-175, 1988.
[263]. C.R. Schrader, "Motivation of construction craftsmen", *Journal of Construction Engineering Division*, Vol.98(2), pp. 257–273, 1972.
[264]. C.S Hazeltine, "Motivation of construction workers". *Journal of Construction Division*, Vol.102(3), pp. 497–509, 1976.
[265]. A.J Wilson, "Need — Important and Need — Satisfaction for Construction Operatives". M. Eng thesis. Project Report, Loughborough University, Loughborough, UK. 1976.
[266]. P.O. Olomolaiye, and S.O. Ogunlana, "A survey of construction operative motivation on selected sites in Nigeria". *Building and Environment*, vol. 23(3), pp. 179–185, 1988.
[267]. S.O. Ogunlana, and W.P. Chang,"Worker motivation on selected construction sites in Bangkok", *Thailand. Engineering Construction and Architectural Management,* vol.5(1), pp. 68–81, 1998.
[268]. M. Zakeri, P. Olomolaiye, G.D. Holt, and F.C. Harris, "Factors affecting the motivation of Iranian construction operatives", *Building and Environment* vol. 32(2), pp.161–166, 1997.
[269]. P.F. Kaming, P.O. Olomolaiye, G.D. Holt, F.C. Harris, "What motivates construction craftsmen in developing countries? A case study of Indonesia", *Building and Environment* vol. 33(2–3), pp. 131–141, 1998.
[270]. A. Kazaz, E. Manisali and S. Ulubeyli "Effect of basic motivational factors on construction workforce productivity in Turkey", *Journal of Civil Engineering and Management*, vol.14:2, pp. 95-106, Oct. 2010.
[271]. H.F. Kaiser, J. Rice "Little Jiffy, Mark IV" *Journal of Educational and Psychological Measurement* , 1974.

# Some Mechanical and Physical Properties of Plum Fruit

*Selen Alnıak Sezer[39], Mustafa Çetin[40], Hülya Doğan[3]*

***Abstract***

*Exploration in the determination of physical and mechanical properties of plum fruit; a total of 18 Da, built in an area and l (P Eh h.) h h w A U l h harvest period (April 15th - May 1st, May 15th) was carried out. This study aimed to determining the physical and mechanical properties of plums, during different harvest period moisture content, fruit length, width, thickness, geometric mean values of diameter, sphericity, shape index, bulk density, true density, mass, porosity, projection area, and some physical features detachment force compression behavior under load and damage in different situations, such as falls from heights on different surfaces were some of the mechanical properties. The first harvest from the last harvest until the fruit weight and size were generally tends to increase. Plum of fruit mass of 5.491 g with 20.028 g for (throughout) the harvest period, fruit length of 22.92 - 30.01 mm, fruit width 20.84 - 28.88 mm, thickness 20.28 - 27.54 mm, shape index were found between 1.11 - 1.09. Moisture range is 15.22% with 20.86% of the range, bulk density during the harvest period 359.30 $mm^3$ with 278.88 $mm^3$ decreases from and true density increased during the harvest period. Plum of fruit in different harvest periods 0.5 m -1.5 m - 2.5 m in height when he was thrown from injury volume was measured respectively, 0186 $mm^3$, 0.452 $mm^3$, 0.836 $mm^3$. With the increasing height of fall generally have increased sensitivity to shock damage. According to this study the deformation of the second harvest period (May 1st); the other two harvest period (April 15th - May 15th) was determined to be less than.*

**Keywords: Harvest Period, Physical Properties, Plum, Mechanical Properties**

## 95. INTRODUCTION

Plum fruit is a drupe fruit (with a smooth stone/pit) which is from the Prunophore sub-genus of Prunus genus, from Prunoideae sub-family of Rosaceae family, which is from the order of Rosales. It is known that there are nearly 2000 types of fruits which belong to Prunus genus distributed all around the world and the majority of these fruits are located in the northern hemisphere. Plum fruits can be divided into three main groups according to their gene centers, which include European-Asian, Far East and American. The European-Asian species which also include the breeds in our country are also sub-divided into three groups which are Green Plums (Prunus cerasifera Ehrh.) (Papaz, Bekiroğlu, Aynalı), European plums (P. domestica L.) (Karagöynük, Köstendil, Üryani, A'Agen, Giant, Stanley, R.C. Violet, R.C. Verte, Sugar, President), and Japanese Plums (P. salicina Lindel) (Formosa, Santa Rosa, Climax, Red Kinenbol, Red Heart, Burbank, Duarte, Reubennel, Burmosa, Laroda, Nubiana, Wickson) [1].

Despite being a mild climate fruit, plum has spread all around the world with its persistent nature which allow it to grow in either sub-temperate climates or in warm climates easily [2].

Plum ranks as the third most produced drupe fruit in the world. In Turkey however, plum production ranks behind apricot, peach and cherry, however that doesn't stop Turkey to be one of the most important plum producers in the world [3].

Plum fruit can be divided into three types according to the time it takes for it to get ripe which are early bloomers, mid-season and late bloomers, and according to the type of consumption, they can be divided as edible, dryable and for kitchen use (canned, marmalade, jam). Most plums are consumed as green plums. Plums which are going to be green plums are harvested 60 to 70 days before they are in full bloom and this harvest continues till they are fully grown [4].

It is necessary and important to be aware of the biological properties of agricultural products for machinery design, manufacturing, operating and control, determination and analysis of yield, for the release of new animal or plant based products and to evaluate the quality of such products. Being aware of such properties do not just help the engineers, but also food scientists and processers, plant cultivators and other manufacturers and experts who make animal based production [5].

[39] *Corresponding author: Department of Agricultural Machine, Vocational School, Bozok University Yozgat, Turkey.* selenalniak@gmail.com

[40] *Agricultural Faculty Department of Agricultural Machine, Adnan Mende U v A , T k ,*

[3] *Department of Agricultural Machine, Vocational School, Bozok University Yozgat, Turkey.* hulya.dogan@bozok.edu.tr

One of the main tasks of agricultural engineering is to present and apply the most advanced techniques which will be used for the qualitative and quantitative development of agricultural products and to make economical analysis and evaluate their results. One of the main factors to consider while presenting such techniques is the agricultural product itself. Therefore, it is important to wholly know the agricultural products, in other words, the technical properties of the biological material. It is possible to classify the properties of a biological material as physical properties (dimensions, mechanical properties, thermic properties, optical properties, electrical properties etc.), chemical properties and biological properties [6].

In this study; we aimed at presenting some of the physical properties of the plum fruit like their moisture content, length and width, thickness, arithmetic and geometric diameter mean value, sphericity, mass, shape index, bulk density, true density, porosity, projected area and color and also some mechanical properties like picking force, behavior under stress and ratio of damage on impact from various heights to various surfaces.

## 96. MATERIALS AND METHODS

The study took place in Umurlu district of Aydın province, on an 18 decares of production garden which also include "papaz plums". In this garden, the distance between the rows of trees has been established as 5 meters, and the distance between the trees have been established as 4 meters. Attention was paid to not to include any physically deformed or rotten plums to the sample pool of the study, and by using 100 plums from each of the three harvesting periods, the length, width and thickness of the plums have been recorded using digital calipers capable of measuring between 0 to 150 mm, with 0.01 mm precision. The determination of the initial moisture content right after the harvest have been made by drying them in the drying oven for 24 hours in 105±10°C [[7],[8]]. The plums which lost all their moisture were weighed once again and their moisture content was calculated with the following formula [9].

$$M_c(\%) = \frac{w_o - w}{w_0} .100$$

$M_c$: moisture content (%)

$w_0$ : Weight before the drying oven treatment (g)

w : Weight after the drying oven treatment (g)

For presenting the common definitions that could be made according to the shape of a fruit (sphericity, flat, uneven, blunt-end, long, tapered, curved, wavy, ovoid etc.), shape index value is calculated using the following formula [10].

$$\text{Shape index} = \frac{L}{\frac{(W+T)}{2}}$$

T: Thickness (mm),

W: Width (mm),

L: Length (mm)'

The value presented in the dynamometer at the moment of snapping of from the branch was recored. This test was made in 4 different directions, depending on the harvest time. For each direction 100 plums were picked from their branches. The picked fruits have been numbered and tagged depending on their directions. The mass (m) of each plum picked from its branch has been compared to its fruit picking resistance value (R) and m/R ratios have been calculated.

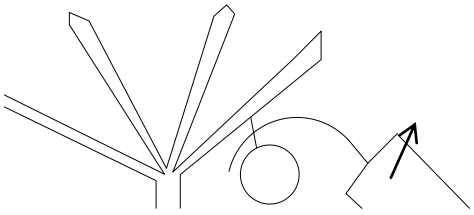

*Image 1. Fruit picking force of plum fruit*

The porosity has been determined using standard weighing methods. This method was carried out by weighing the fruits which are 1000 mm in fixed height in a 2000 ml container [[7],[8]]. For the determination of true density, the plums are dropped 100 mm, to the measuring cylinder which contains pure water and the changing water height in the measuring cylinder gives us the true density of the plums. The density of plums has been calculated as $mm^3$ by using the following formula [8].

$$V = \frac{m}{p_t} .10^6$$

m : mass (g)

$\rho_t$ : True density ($kgm^{-3}$)

In determining the mass; 400 plums from each three harvesting periods have been used. This is defined as the ratio of the volume with porosity compared to the total volume. The following formula has been used to determine in percentage the porosity ($P_f$) values of plum fruits [[5], [8]];

$$\rho_f = \left(1 - \frac{\rho_b}{\rho_t}\right) 100$$

where;

$\rho_b$ : Bulk density ($kgm^{-3}$)

$\rho_t$ : True density ($kgm^{-3}$)

The determination of the projection areas of plum fruits ($A_p$) ($mm^2$), the area that the plum fruit covers on 100 $cm^2$ have been made by using a special set up that includes a scanner connected to a computer and a special software [8]. For the purpose of presenting the damage ratios of plums which fall from various heights (0.5 m- 1,5m -2.5m) to various surfaces (rubber, wood and galvanized steel), a drop stand was established and fruits were dropped as in free fall to these different surfaces with static speeds. The plums were kept in room temperature for 24 hours before the test, in order to spot the color change in the area of impact in order to distinguish the damage marks on the fruits [11]. For the determination of damage volume, definitions and formulas given below were used, which are shown on the idealized damage type image [11].

$$V_z = V_1 + V_2$$

where;

$V_z$ : Damage volume ($mm^3$),

$V_1$ : Damage volume under the contact plane ($mm^3$),

$V_2$ : Damage volume over the contact plane ($mm^3$)'

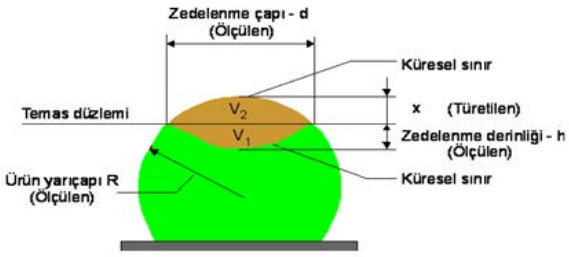


*Image 2. Definitions shown on the idealized damage types which are used for the determination of the damage volume*

For the determination of puncturing, cutting and compression forces, the dynamometer was given a vertical motion and puncturing, cutting or compression forces were measured depending on the attached tip. The dynamometer was connected to the computer with a connection cable and with the help of Data Acquisition Software Multi Channels Model no: SW-U801-WIN, it was possible to process the data and observe the forces graph. The force data transferred from the dynamometer can be stored in the computer and can be seen using MS Excel software. Data logging is done in 2 second intervals.

## 97. RESULTS AND DISCUSSION

Some physico-mechanical properties of plum fruit (Prunus cerasifera Ehrh.) and the mean and standard error values of these properties are given in Table 1. Trials have been made in different harvest periods of the plum fruit (April 15$^{th}$ - May 1$^{st}$, May 15$^{th}$).

The differences of these properties of the plum fruit have been found statistically significant in $p<0,001$ and letter groupings were made in the order of severity. The moisture content of the plum fruit (Prunus cerasifera Ehrh.) have been determined for the three harvesting periods as 20,8%, 18,2% and 15,2% respectively. The fruit length mean values of the plum fruit (Prunus cerasifera Ehrh.) have been determined for the three harvesting periods as 22,920, 28,086 and 30,915 mm respectively. The length values have been found to be higher in the latest harvesting period. The fruit width mean values of the plum fruit (Prunus cerasifera Ehrh.) have been determined for the three harvesting periods as 20,845, 26,624 and 28,886 mm respectively. As the harvesting period progressed the fruit width also increased. The fruit thickness mean values of the plum fruit (Prunus cerasifera Ehrh.) have been determined for the three harvesting periods as 20,283, 25,681, and 27,547 mm respectively.

The geometric mean diameter values of the plum fruit (Prunus cerasifera Ehrh.) have been determined for the three harvesting periods in the 15th of April, 1st of May and 15th of May as 21,306, 26,769 and 30,185 mm respectively. The geometric mean

diameter value has been found higher in the latest harvesting period. The shape index mean values for the plum fruit (Prunus cerasifera Ehrh.) have been determined for the three harvesting periods as 1,11, 1,07 and 1,09 respectively. The ones with a greater shape index than 1,25 have been evaluated as oval in shape and the ones smaller than 1,25 have been identified as round [11]. The mean weight values for the plum fruit (Prunus cerasifera Ehrh.) have been determined for the three harvesting periods as 5,491, 11,123 and 20,028 g respectively.

The weight values increased as the moisture content increased and the harvesting period progressed. The bulk density mean values for the plum fruit (Prunus cerasifera Ehrh.) have been determined for the three harvesting periods as 359,30, 325,68 and 278,88 kg/m$^3$ respectively and the true density have been determined for the same periods as 5,369, 7,966 and 8,367 kg/m$^3$ respectively. The porosity mean value for the plum fruit (Prunus cerasifera Ehrh.) have been determined for the three harvesting periods as 6592,2, 3792,4 and 3400,8% respectively. The projected area of the plum fruit (Prunus cerasifera Ehrh.) have been determined for the three harvesting periods in the 15th of April, 1st of May and 15th of May as 2,350, 2,333 and 2,55 mm$^2$ respectively. It's been determined that as the harvesting periods progressed, the picking force value for the plum fruit (Prunus cerasifera Ehrh.) have been decreased. The picking force values for the plum fruit (Prunus cerasifera Ehrh.) have been determined for the three harvesting periods as 74,408, 50,385 and 34,170 N respectively. The impact force values for the plum fruit (Prunus cerasifera Ehrh.) have been determined for the three harvesting periods as 0,346, 0,648 and 0,446 N respectively. The mean deformation values regarding the puncturing forces for the plum fruit (Prunus cerasifera Ehrh.) have been determined for the three harvesting periods as 1,888, 1,452 and 1,782 mm respectively.

*Table 1. Physico-mechanical properties and the mean and standard error values for these properties*

| **Harvest Period (%)** | **15 April** | **1 May** | **15 May** |
|---|---|---|---|
| | **Mean and Standard Error (X ± SE )** | | |
| **Moisture Content (d.b%)** | 20,86 $^a$±0,201 | 18,22 $^b$± 0,200 | 15,22 $^c$± 0,200 |
| **Length (mm)** | 22,92 $^a$±0,201 | 28,086 $^b$± 0,200 | 30,915$^c$±0,200 |
| **Width (mm)** | 20,845$^a$±0,187 | 26,624 $^b$±0,187 | 28,886 $^c$±0,187 |
| **Thickness (mm)** | 20,283 $^a$±0,179 | 25,681 $^b$±0,179 | 27,547 $^c$± 0,179 |
| **Geometric Diameter (mm)** | 21,306 $^a$±0,644 | 26,769 $^b$±0,642 | 30,185 $^c$± 0,643 |
| **Sphericity (%)** | 0,930 $^a$±0,20 | 0,954 $^a$±0,20 | 0,977 $^a$± 0,20 |
| **Shape İndex** | 1,11 $^a$±0,375 | 1,07 $^b$±0,375 | 1,09 $^c$±0,375 |
| **Mass (g)** | 5,491 $^a$±0,129 | 11,123 $^b$±0,129 | 20,028 $^c$±0,129 |
| **Bulk Density (Kg/m$^3$)** | 359,30 $^a$±10,353 | 325,68 $^b$±10,353 | 278,88 $^c$±10,353 |
| **True Density (Kg/m$^3$)** | 5,369 $^a$±0,306 | 7,966 $^b$±0,291 | 8,367 $^b$±0,283 |
| **Porosity (%)** | 6542,2 $^b$±0,201 | 3792,4 $^a$±0,200 | 3400,8 $^a$±0,200 |
| **Projected Area(mm$^2$)** | 2,350 $^a$±0,066 | 2,333 $^a$±0,067 | 2,55 $^b$±0,066 |
| **Picking Force (N)** | 74,408 $^a$±1,309 | 50,385 $^b$± 1,309 | 34,170 $^c$± 1,309 |
| **İmpact Force (N)** | 0,346 $^a$±0,018 | 0,648 $^b$±0,018 | 0,446 $^c$±0,018 |
| **Puncture forces Deformation(mm)** | 1,188 | 1,452 | 1,782 |
| **Puncture forces Strain Energy(Nmm)** | 21,978 | 26,157 | 27,763 |
| **Puncture Injury forces volume(mm$^3$)** | 3,730 | 4,559 | 5,595 |

| | | | |
|---|---|---|---|
| *P<0,001* **Cutting of forces Deformation(mm)** | 1,617 | 0,726 | 0,957 |
| **Cutting forces Strain Energy(Nmm)** | 33,391 | 12,305 | 18,269 |
| **Cutting forces volume($mm^3$)** | 5,077 | 2,279 | 3,004 |
| **Compression forces Deformation(mm)** | 0,693 | 0,627 | 0,858 |
| **Compression forces Strain Energy(Nmm)** | 6,216 | 11,988 | 16,053 |
| **Compression forces volume($mm^3$)** | 2.176 | 1,968 | 2,694 |

*important*

The mean deformation values regarding the cutting forces for the plum fruit (Prunus cerasifera Ehrh.) have been determined for the three harvesting periods in the 15th of April, 1st of May and 15th of May as 1,617, 0,726 and 0,957 mm respectively. The mean deformation values regarding the compression forces for the plum fruit (Prunus cerasifera Ehrh.) have been determined for the three harvesting periods as 0,693, 0,627 and 0,858 mm respectively.

## 98. *CONCLUSIONS*

In this study of the plum fruit, some physical properties of it like moisture content (Mc), sphericity (k), shape index, bulk density ($\rho_b$), true density ($\rho_t$), mass (m), porosity ($P_f$), projection area ($A_p$), and some mechanical properties like picking force, behavior under compression and ratio of damage have been tried to be identified. The fruit weight and sizes tended to increase starting from the first harvest to the last. Throughout the harvesting periods, the masses of the plums were found to be between 3,95 g and 29,61 g, their length values were found to be between 20,57 mm and 37,55 mm, width values between 17,8 mm and 35,22 mm, thickness between 17,14 mm and 33,89 mm and their shape index values were found to be between 0,90 mm and 1,09 mm. The mean fruit weight was determined as 23,15 g, length as 32,25 mm, width as 34,00 mm, height as 37,20 mm, and shape index as 0,91. [12].

It's been determined that the fruit sizes continued to grow because the cell division within the plum fruits have continued until the last harvest. Also as the mass increased as the harvest progressed, the picking forces decreased. The growth in M/R values is a positive and desired aspect for mechanical harvest. In the trials held by Gezer at al., it's been found out that as the harvest period extended, the mass also increased and picking forces were reduced. [11]. When the moisture content was between 20,86% and 15,22%, bulk density decreased from 359,30 $mm^3$ to 278,88 $mm^3$ as the harvesting period progressed, however, true density increased at the same time. Porosity constantly decreased in the same period.

The damage volume of plum fruit for different harvesting periods has been found to be 0,186 $mm^3$, 0.452 $mm^3$, 0.836 $mm^3$ respectively. It's been seen that as the harvest progressed, the impact damage sensitivity of the fruit has increased. This reduces the fruit quality. Peach is another delicate fruit that is adversely affected from different types of damages during or after the harvest [14]. These kinds of damages lead to loss of quality in peaches. The size properties of fruits like length, width, porosity, bulk density, true density are important for the design of the machinery that will be used for the cultivation, harvest and post-harvest periods. Furthermore, the physical and mechanical properties of agricultural products like density, weight and porosity are also used as design parameters for the storage and drying of the products in which they are in structural stresses. The puncturing and cutting strength of agricultural products are also parameters used to determine the behavior of such products under stress after their harvesting they also are used as parameters for the development of tools and machinery that will be used for storage, transport and packaging. [[15], [16], [17]].

## REFERENCES

[272]. Özvardar. S. and K. Önal., Plum Cultivation, Agricultural Research Support and Development Foundation No:23 Yalova, Turkey 1990.
[273]. Özbek, S., Special Fruit, Cukurova University Faculty of Agriculture Publications. No:128. Adana, Turkey 1978.
[274]. Anonym, 2009a. www.fao.arg.tr, Ankara, Turkey.
[275]. Son, L., Turkey Agricultural Chambers Department of Mersin ISBN: 978-975-8629-62-6. s:12, Mersin, Turkey 2009.
[276]. Mohsenin, N.N. Physical Properties of Plant and Animal Materials. Gordon and Breach Science Publisher, New York, 1970.
[277]. Erdoğan, D. and Yurtlu, B.., Effect of storage time on some mechanical properties and bruise susceptibility of pears and apples. Turkish journal of agriculture and forestry, 2005, 29.6: 469-482.

[278]. Suthar, S. H., and S. K. Das. "Some physical properties of karingda [Citrullus lanatus (Thumb) Mansf] seeds." Journal of Agricultural Engineering Research65.1 (1996): 15-22.
[279]. Özarsalan, C., Physical Properties of Cotton Seed. Bio systems Engineering.(Electronic Journal),vol:83 doi:10.1016/S1537-5110(02)00151-4,[www.idealibrary.com]. 2002.
[280]. Çetin, M. 2006. Physical Properties of Barbunia Bean (Phaseolus vulgaris L. Cv.'Barbunia') seed. Journal of food engineering. (electronic journal), vol:80 [www.elsevier.com/locate/jfoodeng].
[281]. Alayunt, N., Biological Material Information. Ege University Faculty of Agriculture Publications No: 541 İzmir, 2000.
[282]. Yurtlu, Y, Erdoğan D.,. Domates Çeşitlerinde Depolama Süresinin Bazı Mekanik Özelliklere Etkisinin İncelenmesi. Tarım Bilimleri Dergisi 11.2 (2003): 201-206.
[283]. Beyhan; Ö., Darende Standards and Local Plum Varieties Grown In Some of The Pomological, Phonological and a Study on The Determination of Morphological Features 34 (2): 47 – 56, 2005.
[284]. Gezer, İ., Güner, M., Dursun, E., Determination of Physico-Mechanical Properties of Some Vegetables and Fruits Türk-Koop Ekin journal, s. 70-75, Ankara, 2000.
[285]. Vursavuş, K., Özgüven, F., Determining the Strength Properties of the Dixired Peach Variety, Çukurova University, Faculty of Agriculture, Department of Agricultural Machinery, Adana, Turkey, 2003.
[286]. Coskun, M. B., Yalçın, İ., Özarslan, C. Physical Properties of Corn Seed (Zea Mays Saccharata Sturt) Journal of food engineering. (electronic journal), vol:74 [www.elsevier.com/locate/jfoodeng], 2005
[287]. Kabas, O., Yılmaz, E., Ozmerzi, A., Akinci, I. Some Physical and Nutritional Properties of Cowpea Seed (Vigna Sinensis L.) Journal of food engineering. (Electronic Journal), vol:79 [www.elsevier.com/locate/jfoodeng], 2006.
[288]. Isık, E., Ünal, H. Moisture-Dependent Physical Properties of White Speckled Red Kidney Bean Grains. Journal of Food Engineering. (Electronic Journal), vol:82 [www.elsevier.com/ locate/jfoodeng], 2007.

# Prediction of Pull-Out Performance of Chemical Anchors Embedded into Concrete

*Ilker Bekir Topcu[1], Murat Guler[1], Mucteba Uysal[2], Harun Tanyildizi[3]*

[1]Eskisehir Osmangazi University, Department of Civil Engineering, Eskisehir, Turkey

[2]Istanbul University, Department of Civil Engineering, Istanbul, Turkey

[3]Firat University, Department of Civil Engineering, Elazig, Turkey

***Abstract***

This paper summarizes the results of experimental research and prediction model focused on determination of the behavior of pull-out performance limits of what embedded into currently the most widespread concrete type of Turkey as C25/30. Rebars having 14, 16 and 18 mm diameters have been selected as the anchor rod in this study. Epoxy based three component chemical adhesive has been used for the connection between concrete and anchor bar. The depth of holes was in the range of 140 - 220 mm which had been selected various for 14, 16 and 18 mm bar diameters. The effect of the anchor depths, bar diameters and reinforcement diameter on the pull-out capacity of adhesive anchors is product dependent. Moreover, an attempt to predict the pull-out capacity of chemical anchors embedded into concrete using artificial neural networks (ANNs) is presented. The problem is proposed to network models by means of three inputs and one output parameter. A multilayered feed-forward neural network trained with the different algorithm is constructed using 3 design variables as network inputs and the pull-out strength of adhesive anchors as the only output. Experimental results showed that increasing the anchor diameter and the depths of hole have increased pull-out performance of anchors. The best algorithm for collapse load of concrete is the Levenberg-Marquardt backpropagation with $R^2$ of 0.9837. The results indicated that ANNs are useful technique for predicting the pull-out capacity of adhesive anchors.

**Keywords:** Anchor; pull-out performance; rebar diameter; depths of holes; artificial neural networks.

## 1. Introduction

The researches and applications of an anchor embedded in a hardened cementitious material such as concrete have been carried out for many decades. For the convenience of the anchors embedded more efficiently in the concrete, researchers began to adopt post-installation for bonding the reinforcements into the concrete. General operations are drilling a hole in hardened concrete and installing a steel rod into the concrete with adhesive or cement grout.

Chemical anchors are also getting more frequently used to connect structural elements. Anchors that are used to provide the connection between two different elements can be categorized under two categories as cast-in-place and post-installed anchorages. Post-installed anchorages could be manufactured using different methods such as mechanical, grout or chemical. Recently, more researches have focused on adhesive bonded anchors [1-3]. The variables investigated included the condition of the drilled hole, concrete compressive strength, aggregate type, adhesive curing period and loading at elevated temperature. Cook et al. analyzed the behaviors of single adhesive anchors and single headed or unheaded grouted anchors under tensile load in concrete [4-6]. General failure modes of these anchorage systems can be summarized as pullout of a concrete cone, debonding at anchor–adhesive/grout or concrete–adhesive/grout interface, fracture of anchor, and combination of some of these failure modes. Then several design models were recommended taking into account of all the possible failure modes. Moreover, for an adhesive anchor installed into a damp, wet and uncleaned hole, the bond strength between anchor and concrete was generally reduced [7]. An adhesive anchor is installed using a rebar or threaded rod inserted in a drilled hole in

hardened concrete using a polymer-based bonding agent including epoxies, vinylesters and polyesters. Typically, a grouted anchor isa threaded rod, headed bolt or deformed rebar inserted in a drilled hole filled with a cementitious or polymer grout. In this case, the diameter of the predrilled hole is at least 150% larger than that of the fastener [8].

The bond strength of rebars is a function of the geometric and material properties of the concrete member and the rebars. Several factors influence the pull-out performance of anhors. The most important of them are concrete compressive strength, splice length, the relative rib area (the ratio of projected rib area normal to bar axis to the product of the nominal bar perimeter and the center-to-center rib spacing), minimum concrete cover defined as the smallest of clear concrete covers in bottom and/or sides or 12 of the clear spacing between bars, the amount of transverse steel area to spacing ratio and the splice bar size illustrated as ratio of the area of the splice bar to the effective cross section of the beam [9]. Tepfers [10] illustrated that the bond strength increases as cover and bar spacing increase. The mode of failure also depends on cover and bar spacing. For large cover and bar spacing, it is possible to obtain a pull-out failure, but for smaller ones, a splitting tensile failure occurs resulting in lower bond strength.

The approach based on the assumption of separated failure modes generally defines the resistance of an anchor for three load-bearing capacity values. As shown in Fig. 1a, the first failure mode is the tensile failure of the steel anchor element. This failure is clearly defined by the area of the shank of the rebar. The second failure mode is defined as a full concrete failure. This failure typically takes the form of a breakout cone (Fig. 1b). It is usually described as being dependent on concrete strength and the anchorage length. The third failure mode is the extraction of the rebar from the concrete. This can occur via the failure of the concrete–glue interface, the glue–steel interface or via the failure of the glue itself (Fig. 1c). Usually in design methods, the definition of the pull-out resistance for this failure type is related to one of the surfaces of the interface. This is possible because the thickness of the glue layer is small (several millimetres). This failure mode is termed ‘bond failure.

**Fig. 1.** Separated failure modes used in design methods: (a) tensile failure of the steel anchor bolt, (b) full concrete failure, and (c) bond failure: extraction of the steel bolt from the concrete [11].

Their main function is to transfer normal loads (tension and compression) and possible shear loads according to efforts at the base of the structure. The three main anchoring systems are the straight rod, the hooked rod and the headed rod. The tensile load is transferred through a bond between the steel rod and the concrete and/or abutment of the anchor plate or the hook on concrete. Load capacities of the mechanisms depend on the type and dimensions of anchor used. Under tension, the three main failure mechanisms are the breaking of the rod, the sliding of the rod and cone-shaped concrete breakout [12].

The artificial neural networks solve very complex problems with the help of interconnected computing elements. Basically, the processing elements of a neural network are similar to the neurons in the brain, which consist of many simple computational elements arranged in layers. In recent years, the ANNs and other models have been extended extensively and applied to many civil engineering applications such as epoxy-adhesive anchor systems. Similar results were also found in the experimental and numerical simulation studies by Li et al. [13]. James et al. developed an approximate expression to predict the ultimate tensile capacity of the epoxy-adhesive anchors based on the analysis of linear and nonlinear finite element method [14]. Bickel and Shaikh utilized two methods with proper adjustments to predict the shear capacity of single adhesive anchors [15]. Sakla and Ashour introduced artificial neural networks into predicting the tensile capacity of single adhesive anchors and found that the tensile capacity is linearly proportional to the embedment length [8]. Moreover, Beard and Lowe [16] adopted the ultrasonic guided waves to successfully inspect the maximum anchor length for a grouted anchor.

The aim of this study is the investigation of that increasing the anchor diameter and the depths of hole on the performance of pull-out what embedded into currently the most widespread concrete type of Turkey. Furthermore, ANN model is constructed to predict the pull-out performance of chemical anchors embedded into concrete.

## 2. Experimental study

To measure the ultimate load for each anchor, a pullout test was performed to the specimens.

Many strengthening applications are performed on buildings that are made of widespread concrete strength type of a country in order to better represent the practice, the anchors have been embedded in concrete elements. Preliminary data indicated that most concrete existing in Turkey has a compressive strength of 25 MPa for 15x15x15 cm cubic specimens and anchors were embedded in the concrete in scope of the study. Other parameters that have been used in this study are the anchor bar diameter and the anchor depth. In this study, rebars of three different diameters, namely 14, 16 and 18 mm have been embedded in depths that are 140, 150, 160, 170, 180, 190, 200, 210 and 220 mm as can be seen in Table 1. A total of 30 test specimens have been produced. Each data point represents the average of five measurements. The manufactured test specimens have been cured under laboratory conditions. Following this, the holes where the anchor bars will be embedded have been drilled. The holes were cleaned by using pressurized air from an oil-free compressor. The anchor bars have been embedded in the concrete blocks using epoxy resin and necessary precautions have been taken in order to the bars not to move until the epoxy has gained strength. The embedded anchors were covered by a loading block. Testing procedure can be seen in Fig.2a-b-c.

Table 1. Anchor depth, anchor diameter and rebar diameter of the specimens.

**Fig.2.** (a) Drilling, (b) cleaning and (c) embedding of the rebar specimens.

Pattex CF 900 Epoxy was used in this study. Mix proportions and mechanical properties of the epoxy are listed in Table 2.

Table 2. Mechanical properties and mix proportions and of the epoxy.

After emmedding rebar specimens on the curtain wall the bar specimens have been loaded by a hydraulic test apparatus on the curtain wall. Fig.3 shows pull-out of anchor rebar hydraulic test apparatus.

**Fig.3.** Hydraulic test apparatus of anchor rebar.

## 3. Test results

Fig. 4, Fig. 5 and Fig.6 show the results obtained from the anchor pull-out measurements of all the specimens emmebbed into concrete. It is shown in the Fig. 4 that the rebar of 14 mm of diameter has various embedment depths in the range of 140-180 mm. The pull-out strength capacity has been observed to increase with increasing diameters as it was expected. However, with increasing embedment depth, a significant change could be observed in capacity of the specimens. Pull-out strength of the specimens increases with an increasing the depths of hole and there is a notable reduction in pull-out strength of the specimens when embedment diameter decrease from 22 mm to 20 mm. The rebar specimen has 14 mm diameter and 180 mm embedment depth showed pull-out strength performance 18.54 % more than 150 mm embedment depth. Caliskan et al. investigated shear strength of epoxy anchors embedded into low strength concrete and found similar test results [3].

.

**Fig.4.** Test results of pull-out strength of the specimens have 14 mm rebar diameter.

Fig. 5 shows that the rebar of 16 mm of diameter has various embedment depths in the range of 160-200 mm. The pull-out strength capacity has been observed to increase with increasing diameters. However, with increasing embedment depth, a significant change could be observed in capacity of the specimens. Pull-out strength of the specimens increases with an increasing the embedment depth and there is a notable reduction in pull-out strength of the specimens when embedment diameter decrease from 24 mm to 22 mm. The rebar specimen has 16 mm diameter and 200 mm embedment depth showed pull-out strength performance 18.37 % more than 160 mm embedment depth. Xu et al. modelled of anchor bolt pullout in concrete based on a heterogeneous assumption in this context made tests for influence of the embedded depth on the peak pullout load and found similar test results [17]. It can be seen in that research with the increase of the embedded length, the peak pullout load increases.

**Fig.5.** Test results of pull-out strength of the specimens have 16 mm rebar diameter.

**Fig.6.** Test results of pull-out strength of the specimens have 18 mm rebar diameter.

Fig. 6 shows that the rebar of 18 mm of diameter has various embedment depths in the range of 180-220 mm. Pull-out strength of the specimens increases with an increasing the embedment depth and there is a notable reduction in pull-out strength of the specimens when embedment diameter decrease from 26 mm to 24 mm. The rebar specimen has 18 mm diameter and 220 mm embedment depth showed pull-out strength performance 11.69 % more than 180 mm embedment depth.

## 4. Artificial neural network model for prediction of experimental results

ANN can exhibit a surprising number of human brain characteristics [18-26]. The fundamental concept of neural networks is the structure of the information processing system [27, 28]. They are consisting of a large number of simple processing elements called as neurons. A schematic diagram for an artificial neuron model is given in Fig. 7.

**Fig. 7.** Artificial neuron model.

Let $X=(X_1, X_2 \ldots X_n)$ represent the n input applied to the neuron. Where $W_j$ represents the weight for input $X_j$ and b is a bias, then the output of the neuron is given by Eq. 1. These neurons are connected with connection link. Each link has a weight that is multiplied by transmitted signal in network. Each neuron has an activation function to determine the output. There are many kinds of activation functions. Usually nonlinear activation functions such as sigmoid, step are used. ANNs are trained by experience, when an unknown input is applied to the network it can generalize from past experiences and produce a new result [29-32].

$$u = \sum_{j=0}^{m} x_j w_j - b \quad \text{and} \quad V = f(u) \tag{1}$$

Artifical neural networks are systems that are deliberately constructed to make use of some organizational principles resembling those of the human brain [29-32]. They represent the promising new generation of information processing systems.

When designing an ANN model, a number of considerations must be taken into account. At first the suitable structure of the ANN model must be chosen. Then, the activation function need to be determined. The number of layers and the number of units in each layer must be chosen. Generally desired model consists of a number of layers. The most general model assumes complete interconnections between all units. These connections can be bidirectional or unidirectional. ANN can create its own organization or representation of the information it receives during learning time [28-33]. There are many kind of ANN structure. One of these is multilayer feed forward ANN and is shown in Fig. 8.

**Fig. 8.** Multilayer feed forward neural network structure.

In this study, the problem is proposed to network models by means of three inputs and one output parameter. The parameters such as reinforcement diameter, anchor depth, anchor diameter were selected as input variables. The model output variables were the collapse load. A data set including 30 data specimens obtained from experimental studies were used for artificial neural networks. The data were normalized by dividing with max values. ANN architecture used for this study is given in Fig. 9.

**Fig. 9. ANN architecture.**

Some ANN algorithms were used just learning in this study such as the BFGS Quasi-Newton backpropagation, the Powell-Beale Conjugate gradient backpropagation, the Fletcher-Powell conjugate gradient backpropagation, the Levenberg-Marquardt backpropagation, the One Step Secant backpropagation, the Resilient backpropagation, the Scaled conjugate gradient backpropagation. The computer program was performed under MATLAB software using the neural network toolbox. In the training, the number of neuron on the hidden layer changed to find best results. The best result for the BFGS quasi-Newton backpropagation was obtained from the seventeen neurons. The best result for the Powell-Beale conjugate gradient backpropagation algorithm was obtained from the eight neurons. The best result for the Fletcher-Powell conjugate gradient backpropagation was obtained from the eleven neurons. The best result for the Levenberg-Marquardt backpropagation was obtained from the five neurons. The best result for the One step secant backpropagation was obtained from the eighteen neurons. The best result for the Resilient backpropagation was obtained from the twenty-three neurons. The best result for the Scaled conjugate gradient backpropagation was obtained from the fourteen neurons. A data set including 30 data specimens obtained from experimental studies were used for artificial neural networks. From these, 15 data patterns were used for training the network, and the remaining 15 patterns were randomly selected and used as the test data set. Fig. 10-16 present the measured collapse load and the predicted collapse loads by ANN model with $R^2$ coefficients. As it is visible in Figs. 10-23, the values obtained from the ANN models are very close to the experimental results. Furthermore, All of $R^2$ values show that the proposed ANN models are suitable and can predict collapse load of concrete of the experimental values. This can be also observed in the other articles related to predicting concrete properties [26-29]. Fig.12 shows that the best algorithm for collapse load of concrete is the Levenberg-Marquardt backpropagation with $R^2$ of 0.9837. The training performance during the training process is given in Fig. 17-23 where the variation of mean-square error with training epochs is illustrated. Artificial neural networks are capable of learning and modeling using the data obtained from experiments. This makes artificial neural networks a powerful tool for solving some of the complicated civil engineering problems [33].

**Figure 10. Linear relationship between measured and predicted compressive strengths for the BFGS quasi-Newton backpropagation.**

**Figure 11. Linear relationship between measured and predicted splitting tensile strengths for the Powell-Beale conjugate gradient backpropagation.**

**Fig. 12. Linear relationship between measured and predicted compressive strengths for the Levenberg-Marquardt backpropagation.**

**Figure 13. Linear relationship between measured and predicted compressive strengths for the Fletcher-Powell conjugate gradient backpropagation.**

**Fig. 14. Linear relationship between measured and predicted splitting tensile strengths for the One step secant backpropagation.**

**Figure 15.** Linear relationship between measured and predicted splitting tensile strengths for the Resilient backpropagation.

**Figure 16.** Linear relationship between measured and predicted compressive strengths for the Scaled conjugate gradient backpropagation.

**Figure 17.** Training performance for the BFGS quasi-Newton backpropagation.

**Figure 18.**Training performance for the Powell-Beale conjugate gradient backpropagation.

**Figure 19.**Training performance for the Fletcher-Powell conjugate gradient backpropagation.

**Figure 20.** Training performance for the Levenberg-Marquardt backpropagation.

**Figure 21.** Training performance for the One step secant backpropagation.

**Figure 22.**Training performance for the Resilient backpropagation.

**Figure 23.**Training performance for the Scaled conjugate gradient backpropagation.

## 5. Conclusions

In this study, the pull-out strength capacity has been observed to increase with increasing diameters. An ANN prediction model for pull-out capacity of chemical anchors embedded into concrete was devised. From this laboratory and computer work the following conclusions were made:

- A significant change observed in pull-out capacity of the specimens with increasing embedment depth. Pull-out strength of the specimens increases with an increasing the depths of hole and there is a notable reduction in pull-out strength of the specimens when embedment diameter decrease from 26 mm to 20 mm.
- The rebar specimen has 14 mm diameter and 180 mm embedment depth showed pull-out strength performance 18.54 % more than 150 mm embedment depth. Moreover, the specimen has 16 mm rebar diameter and 200 mm embedment depth increased pull-out strength performance 18.37 % more than 160 mm embedment depth. Furthermore, the rebar specimen has 18 mm diameter and 220 mm embedment depth improved pull-out strength performance 11.69 % more than 180 mm embedment depth.
- All of $R^2$ values show that the proposed ANN models are suitable and can predict collapse load of concrete of the experimental values.
- The best algorithm for collapse load of concrete is the Levenberg-Marquardt backpropagation with $R^2$ of 0.9837.

## 6. References

[1] Cook RA, Doerr GT, Klingner RE. Bond stress model for design of adhesive anchors. ACI Struct J 1993;90:514–24.

[2] Eligehausen R, Cook RA, Appl J. Behavior and design adhesive bonded anchors. ACI Struct J 2006;103:822-31.

[3] Çaliskan Ö, Yılmaz S, Kaplan H, Kıraç N. Shear strength of epoxy anchors embedded into low strength concrete. Construction and Building Materials 2013;38:723-730.

[4] Cook RA, Collins DM, Klingner RE, Polyzois D. Load–deflection behavior of castin-place and retrofit concrete anchors. ACI Struct J 1992;89:639–49.

[5] Cook RA, Konz RC. Factors influencing bond strength of adhesive anchors. ACI Struct J 2001;98:76–86.

[6] Eligehausen R, Cook RA, Appl J. Behavior and design adhesive bonded anchors. ACI Struct J 2006;103:822–31.

[7] Wu Z, Yang S, Hu X, Zheng J. Analytical Method for Pull-out of Anchor from Anchor-Mortar-Concrete Anchorage System due to Shear Failure of Mortar. Journal of Engineering Mechanics 2007;133(12):1352-1369.

[8] Sakla S.S. S, Ashour FA. Prediction of tensile capacity of single adhesive anchors using neural networks, Computers & Structures, 2005;(83):1792-1803.

[9] Golafshani EM, Rahai A, Sebt MH, Akbarpour H. Prediction of bond strength of spliced steel bars in concrete using artificial neural network and fuzzy logic. Construction and Building Materials 2012;36:411-418.

[10] Tepfers RA. Theory of bond applied to overlapped tensile reinforcement Splices for deformed bars. Division of concrete structures, vol. 73(2). Goteborg: Chalmers. University of Technology; 1973, p. 328.

[11] Bajer M, Bamat J. The glue-concrete interface of bonded anchors. Construction and Building Materials 2012;34:267-274.

[12] Delhomme F, Debicki G, Chaib Z. Experimental behaviour of anchor bolts under pullout and relaxation tests. Construction and Building Materials 2010;24(3):266-274.

[13] Li YJ, Eligehausen R, Ozbolt J, Lehr B. Numerical analysis of quadruple fastenings with bonded anchors. ACI Struct J 2002;99(2):149-56.

[14] James RW, De la Guardia C, McCreary CRJ. Strength of epoxy-grouted anchor bolts in concrete. J Struct Engng 1987;113(12):2365-81.

[15] Bickel TS, Shaikh AF. Shear strength of adhesive anchors. PCI J 2002;47(5):92-101.

[16] Beard MD, Lowe MJS, Cawley P. Ultrasonic guided waves for inspection of grouted anchors and bolts. J Mater Civil Engng 2003;15(3):212-8.

[17] Xu C, Heping C, Bin L, Fangfang Z. Modeling of anchor bolt pullout in concrete based on a heterogeneous assumption. Nuclear Engineering and Design 2011;(241:5): 1345-1351.

[18] Hanbay D, Turkoglu I, Demir Y. An expert system based on wavelet decomposition and neural network for modeling chua's circuit. Expert Systems with Applications 2008; 34: 2278-83.

[19] Haykin S. Neural networks, a comprehensive foundation, College Publishing Comp. Inc 1994.

[20] Topçu IB, Karakurt C, Saridemir M. Predicting the strength development of cements produced with different pozzolans by neural network and fuzzy logic. Materials and Design 2008;29:1986-1991.

[21] Topçu IB, Saridemir M. Prediction of rubberized concrete properties using artificial neural networks and fuzzy logic. Construction & Building Materials 2008;22:532-540.

[22] Topçu IB, Saridemir M. Prediction of compressive strength of concrete containing fly ash using artificial neural networks and fuzzy logic. Computational Materials and Science 2008;41:305-311.

[23] Topçu IB, Saridemir M. Prediction of mechanical properties of recycled aggregate concretes containing silica fume using artificial neural networks and fuzzy logic. Computational Materials and Science 2008;42:74-82.

[24] Topçu IB, Saridemir M. Prediction of rubberized mortar properties using artificial neural network and fuzzy logic. Journal of Materials Processing Technology 2008;199(1-3):108-118.

[25] Topçu IB, Saridemir M. Prediction of properties of waste AAC aggregate concrete using artificial neural networks. Computational Materials and Science 2007;41(1):117-125.

[26] Saridemir M, Topçu IB, Özcan F, Severcan MH. Prediction of long-term effects of GGBFS on compressive strength of concrete by artificial neural networks and fuzzy logic. Construction and Building Materials 2009;23(3):1279-1286.

[27] Hanbay D, Turkoglu I, Demir Y. Prediction of wastewater treatment plant performance based on wavelet packet decomposition and neural networks. Expert Systems with Applications 2008; 34: 1038-1043.

[28] Bilim C, Atiş CD, Tanyildizi H, Karahan O. Predicting the compressive strength of ground granulated blast furnace slag concrete using artificial neural network. Advances in Engineering Software 2009; 40: 334-340.

[29] Nazari A, Riahi S. Computer-aided design of the effects of $Fe_2O_3$ nanoparticles on split tensile strength and water permeability of high strength concrete. Materials and Design 2011: 32: 3966–3979.

[30] Özcan F. Gene expression programming based formulations for splitting tensile strength of concrete. Construction and Building Materials 2012; 26: 404-410.

[31] Sobhani J, Najimi M, Pourkhorshidi AR, Parhizkar T. Prediction of the compressive strength of no-slump concrete: A comparative study of regression, neural network and ANFIS models. Construction and Building Materials 2010; 24: 709-718.

[32] Erdem H. Prediction of the moment capacity of reinforced concrete slabs in fire using artificial neural networks. Advances in Engineering Software 2010; 41: 270-276.

[33] Uysal M, Tanyildizi H. Predicting the core compressive strength of self-compacting concrete (SCC) mixtures with mineral additives using artificial neural network. Construction and Building Materials 2011;25:4105-4111.

Table 1. Anchor depth, anchor diameter and rebar diameter of the specimens.

| Group Number | Rebar Diameter (mm) | Anchor Diameter (mm) | Anchor Depth (mm) |
|---|---|---|---|
| M1 | 14 | 20 | 140 |
| M2 | 14 | 20 | 150 |
| M3 | 14 | 20 | 160 |
| M4 | 14 | 20 | 170 |
| M5 | 14 | 20 | 180 |
| M6 | 14 | 22 | 140 |
| M7 | 14 | 22 | 150 |
| M8 | 14 | 22 | 160 |
| M9 | 14 | 22 | 170 |
| M10 | 14 | 22 | 180 |
| M11 | 16 | 22 | 160 |
| M12 | 16 | 22 | 170 |
| M13 | 16 | 22 | 180 |
| M14 | 16 | 22 | 190 |
| M15 | 16 | 22 | 200 |
| M16 | 16 | 24 | 160 |
| M17 | 16 | 24 | 170 |
| M18 | 16 | 24 | 180 |
| M19 | 16 | 24 | 190 |
| M20 | 16 | 24 | 200 |
| M21 | 18 | 24 | 180 |
| M22 | 18 | 24 | 190 |
| M23 | 18 | 24 | 200 |
| M24 | 18 | 24 | 210 |
| M25 | 18 | 24 | 220 |
| M26 | 18 | 26 | 180 |
| M27 | 18 | 26 | 190 |
| M28 | 18 | 26 | 200 |
| M29 | 18 | 26 | 210 |
| M30 | 18 | 26 | 220 |

Table 2. Mechanical properties and mix proportions and of the epoxy.

| | |
|---|---|
| Compressive strength (MPa) | 56 |
| Flexural strength (MPa) | 16 |
| Modulus of elasticity | 3034 |
| Number of component | 2 |
| Mixture density ($g/cm^3$, 20 $^oC$) | 1.65 |

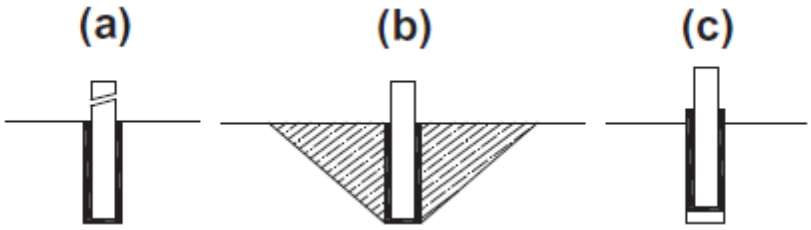


**Fig. 1.** Separated failure modes used in design methods: (a) tensile failure of the steel anchor bolt, (b) full concrete failure, and (c) bond failure: extraction of the steel bolt from the concrete [11].

(a) (b)

(c)

**Fig.2.** (a) Drilling, (b) cleaning and (c) embedding of the rebar specimens.

**Fig.3.** Hydraulic test apparatus of anchor rebar.

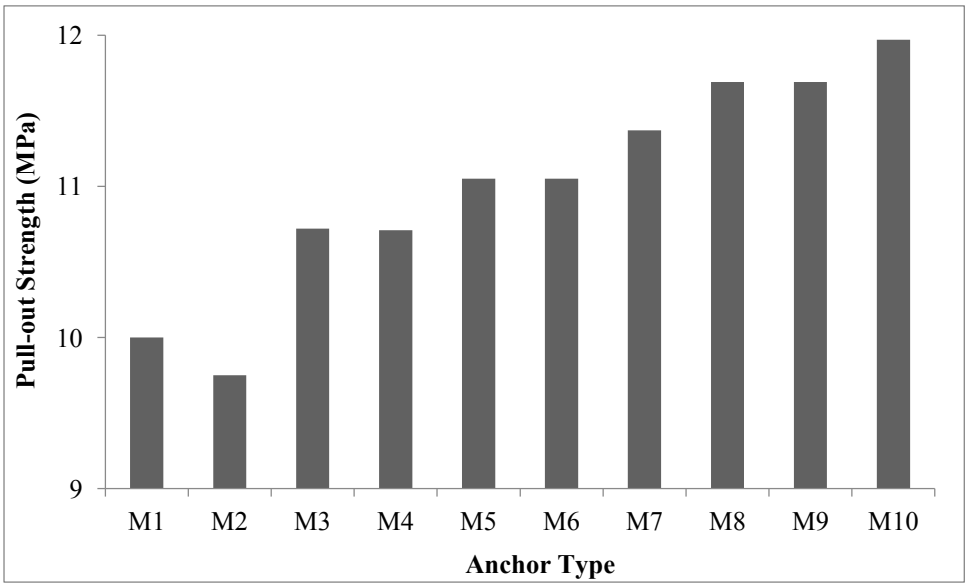


**Fig.4.** Test results of pull-out strength of the specimens have 14 mm rebar diameter.

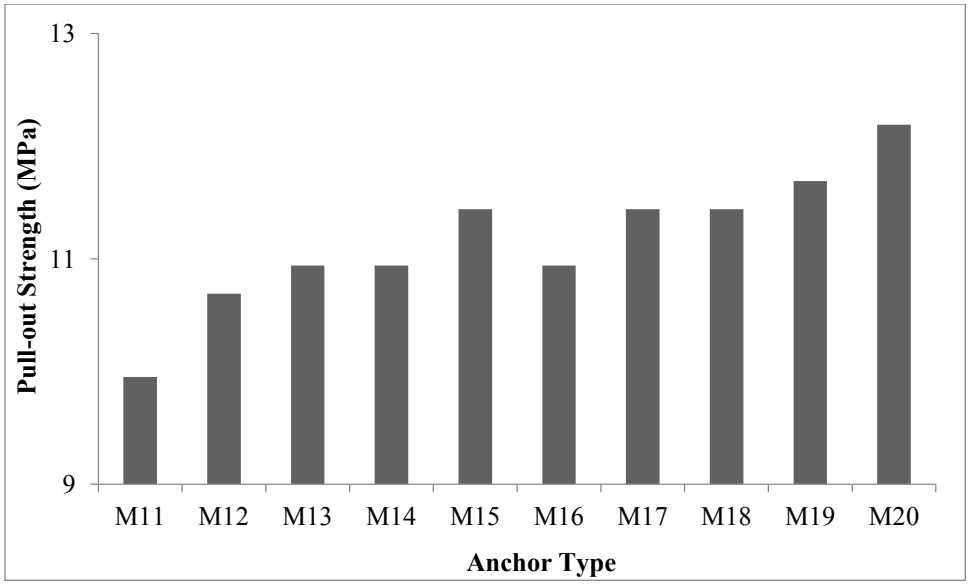


**Fig.5.** Test results of pull-out strength of the specimens have 16 mm rebar diameter.

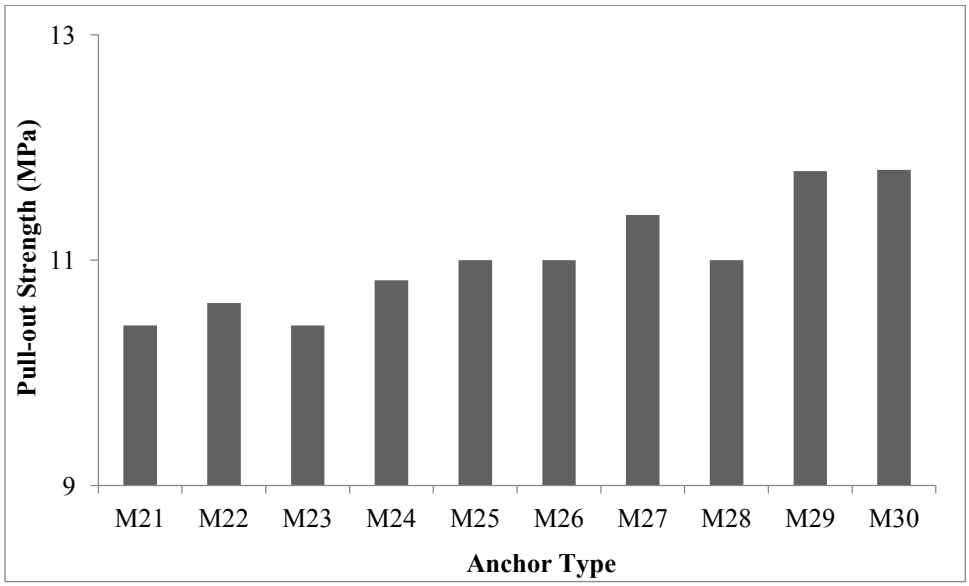


**Fig.6.** Test results of pull-out strength of the specimens have 18 mm rebar diameter.

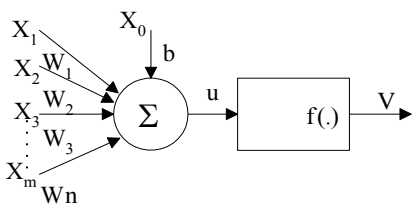


**Fig. 7.** Artificial neuron model

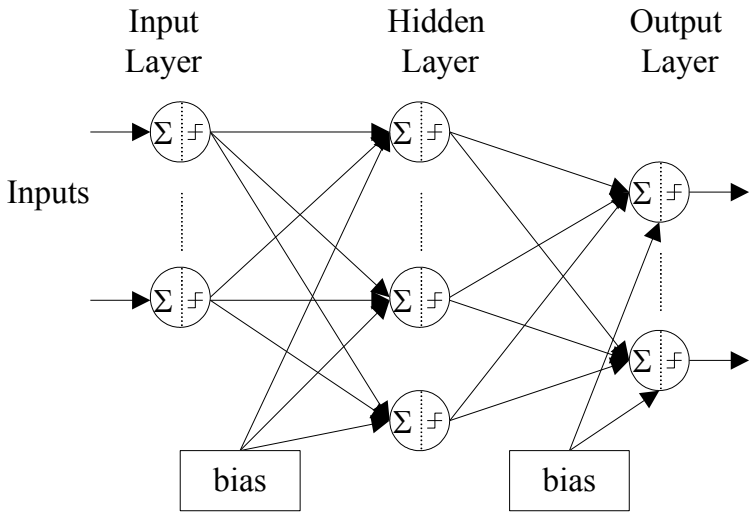


**Fig. 8.** Multilayer feed forward neural network structure.

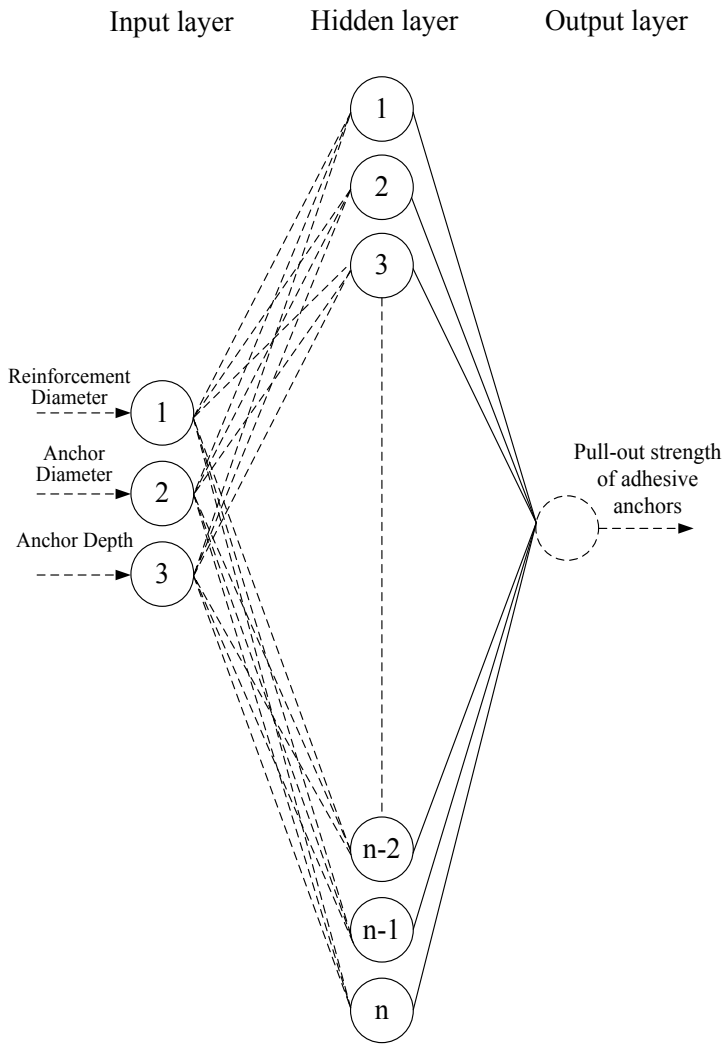


**Fig. 9. ANN architecture.**

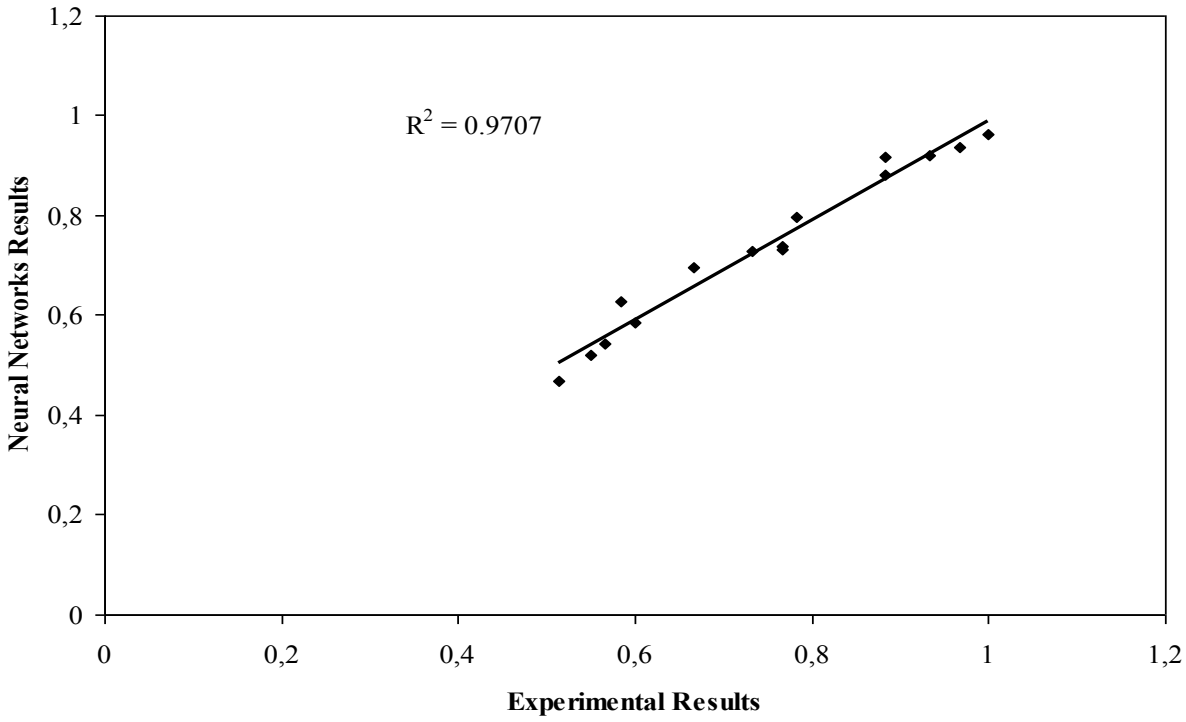


**Fig. 10. Linear relationship between measured and predicted compressive strengths for the BFGS quasi-Newton backpropagation.**

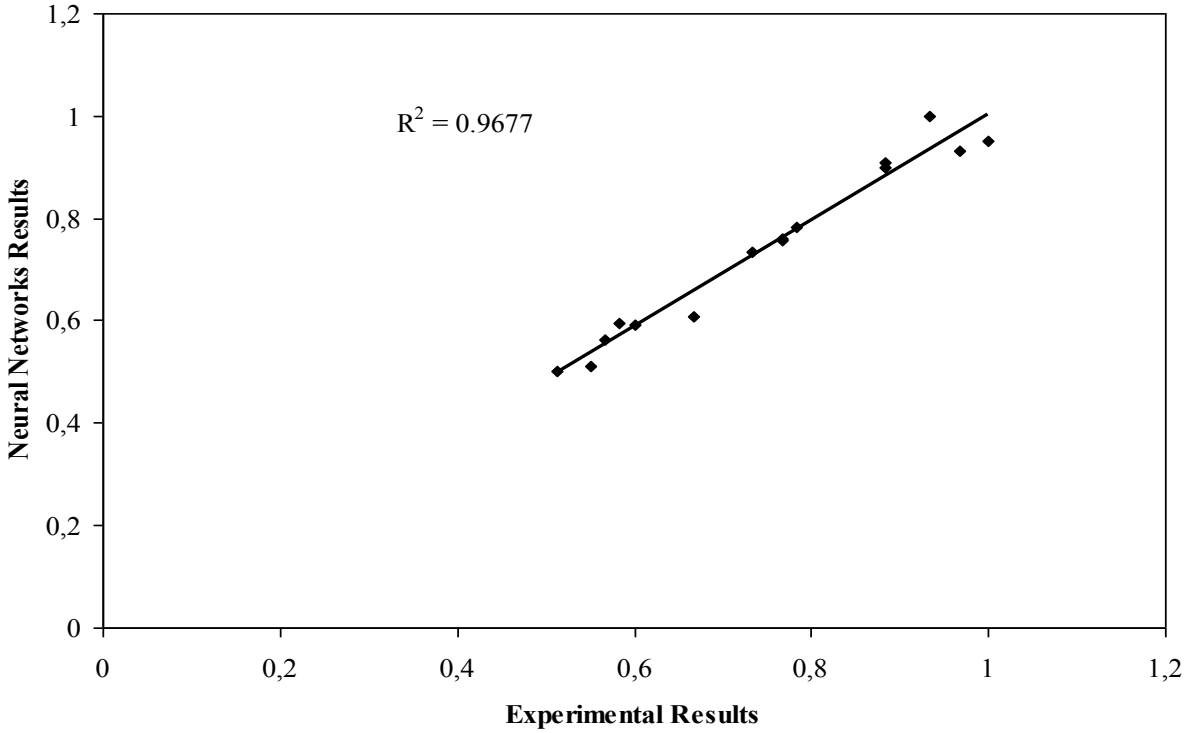


**Fig. 11. Linear relationship between measured and predicted splitting tensile strengths for the Powell-Beale conjugate gradient backpropagation.**

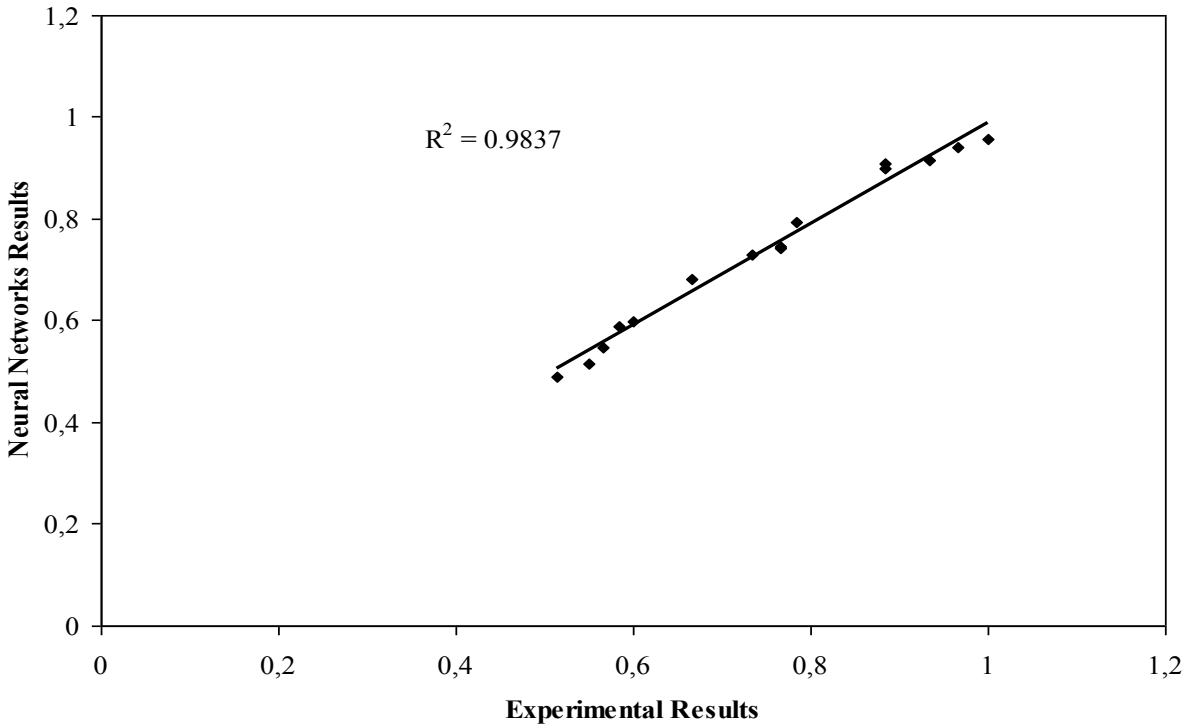


**Fig. 12. Linear relationship between measured and predicted compressive strengths for the Levenberg-Marquardt backpropagation.**

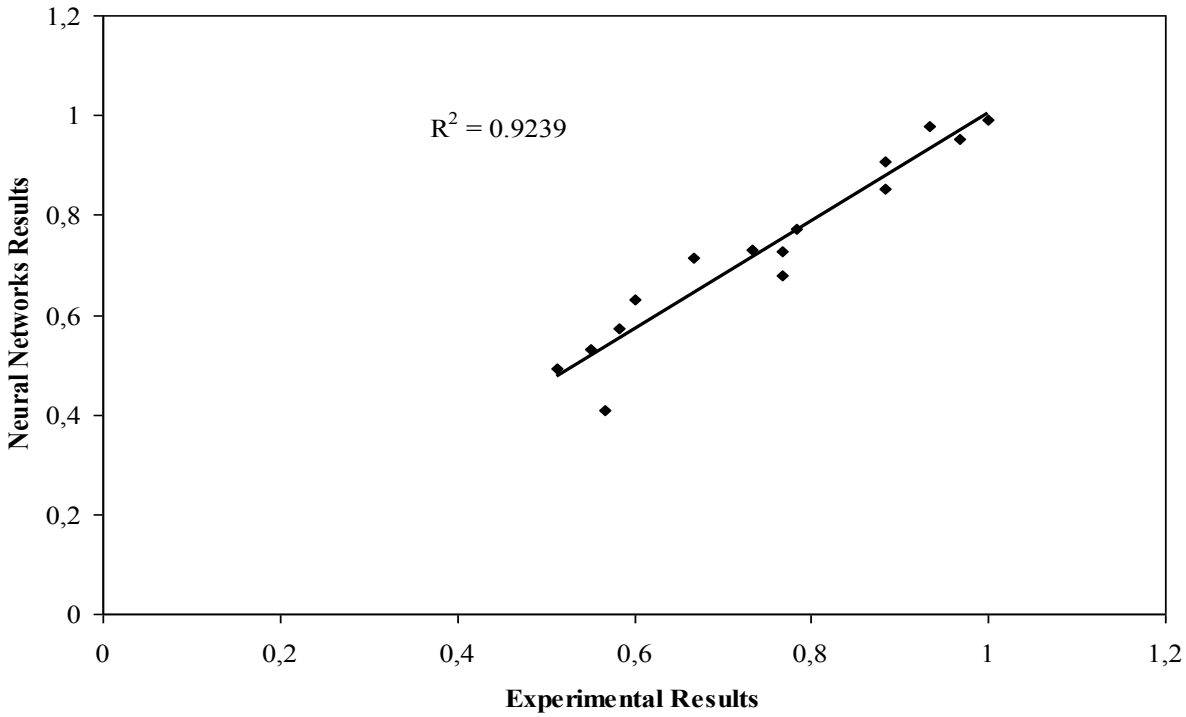


**Figure 13. Linear relationship between measured and predicted compressive strengths for the Fletcher-Powell conjugate gradient backpropagation.**

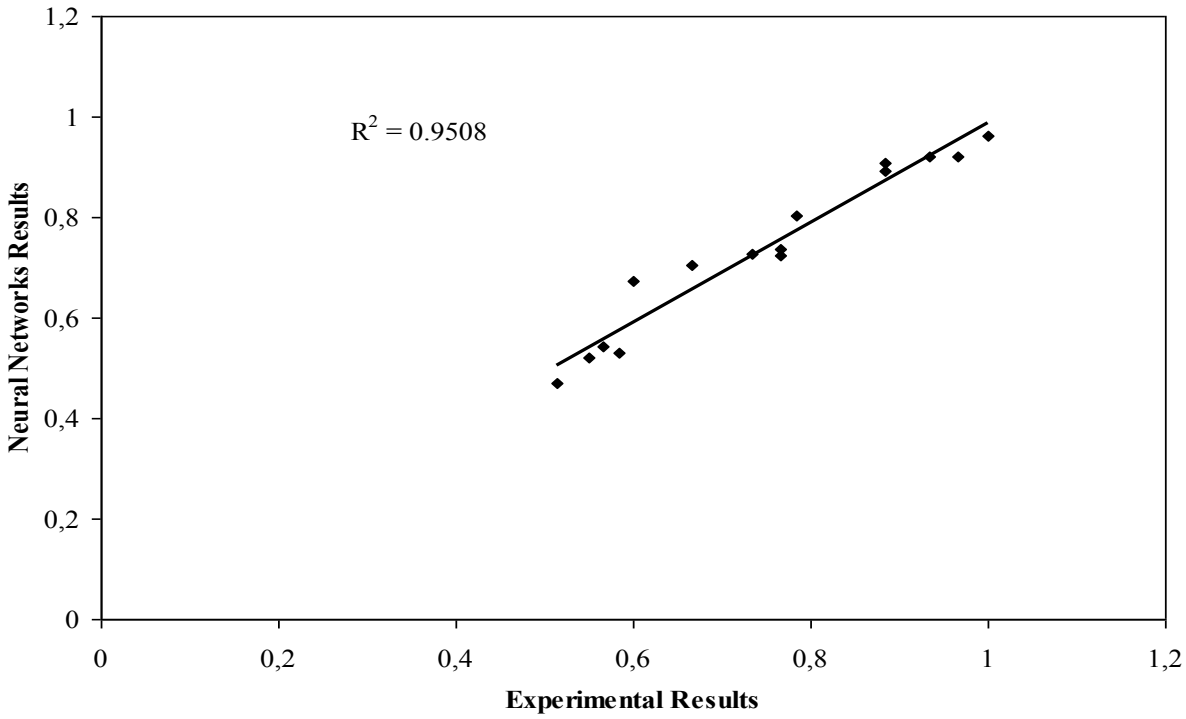


**Fig. 14. Linear relationship between measured and predicted splitting tensile strengths for the One step secant backpropagation.**

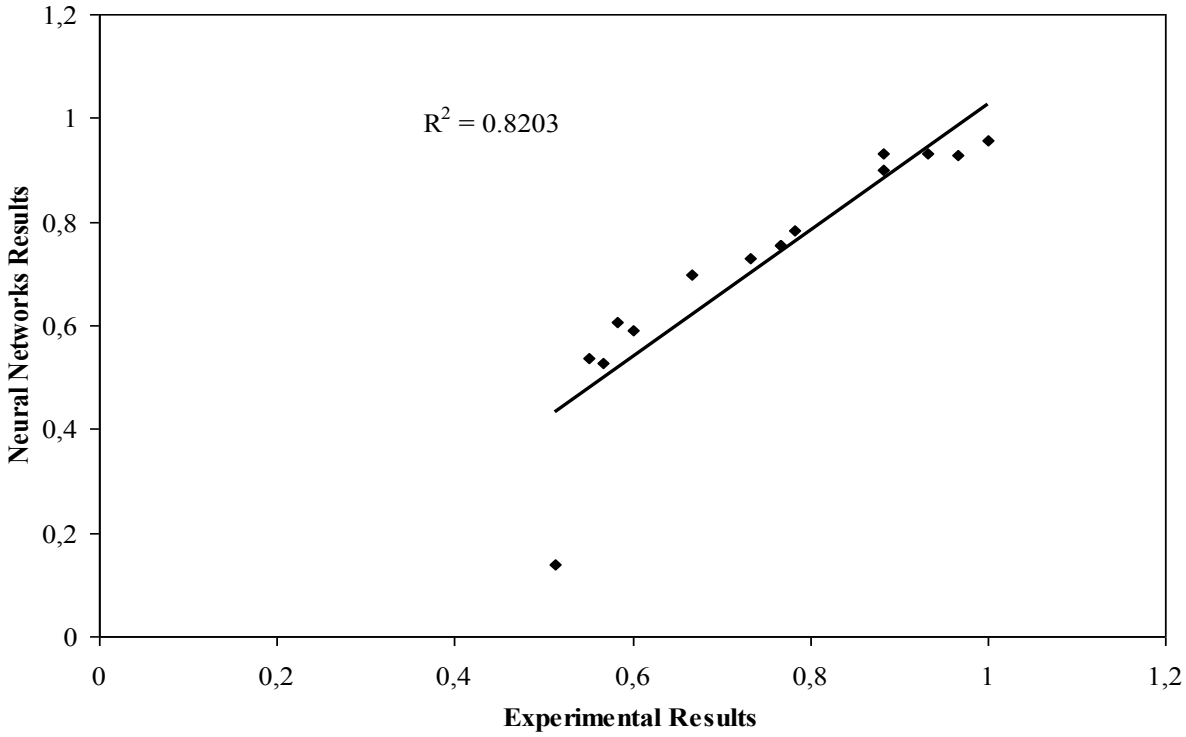


**Fig. 15. Linear relationship between measured and predicted compressive strengths for the Resilient backpropagation.**

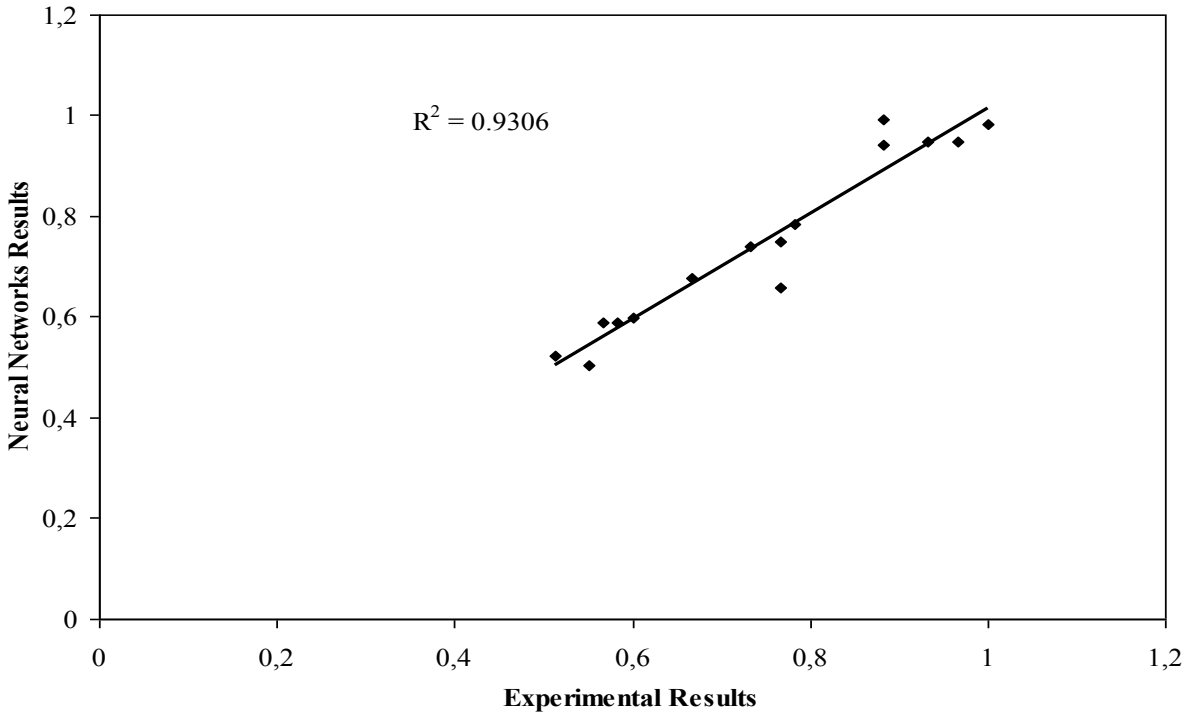


**Fig. 16.** Linear relationship between measured and predicted splitting tensile strengths for the the Scaled conjugate gradient backpropagation.

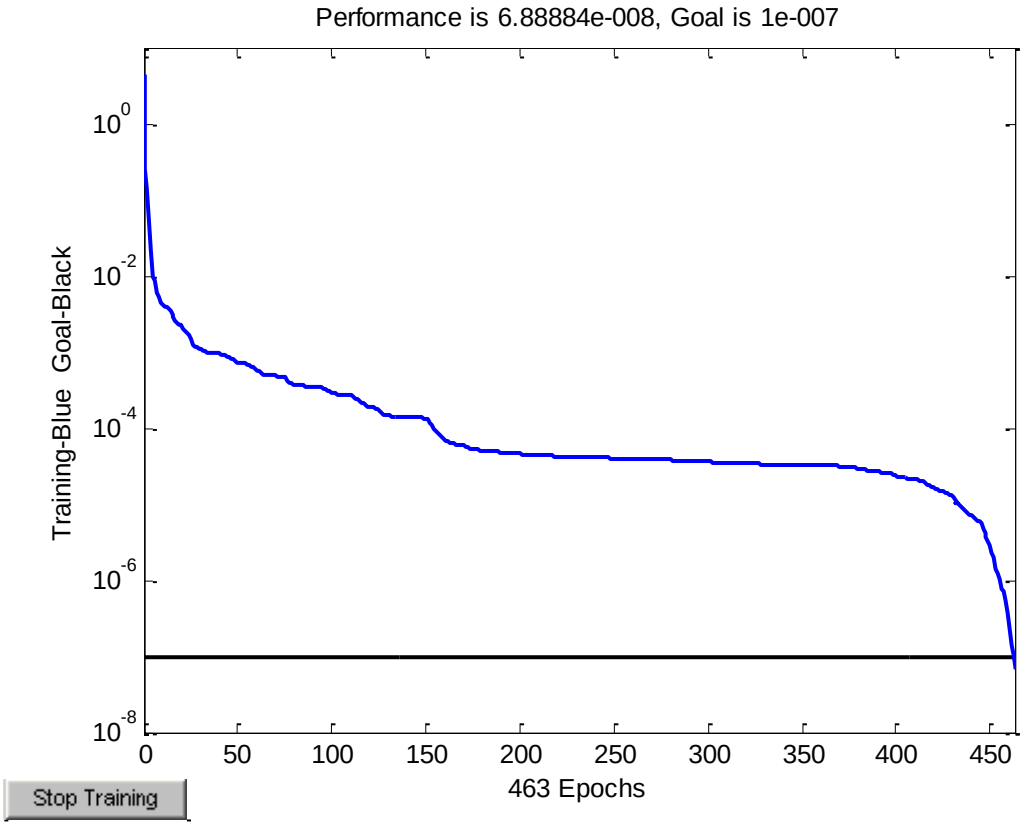


**Figure 17.** Training performance for the BFGS quasi-Newton backpropagation.

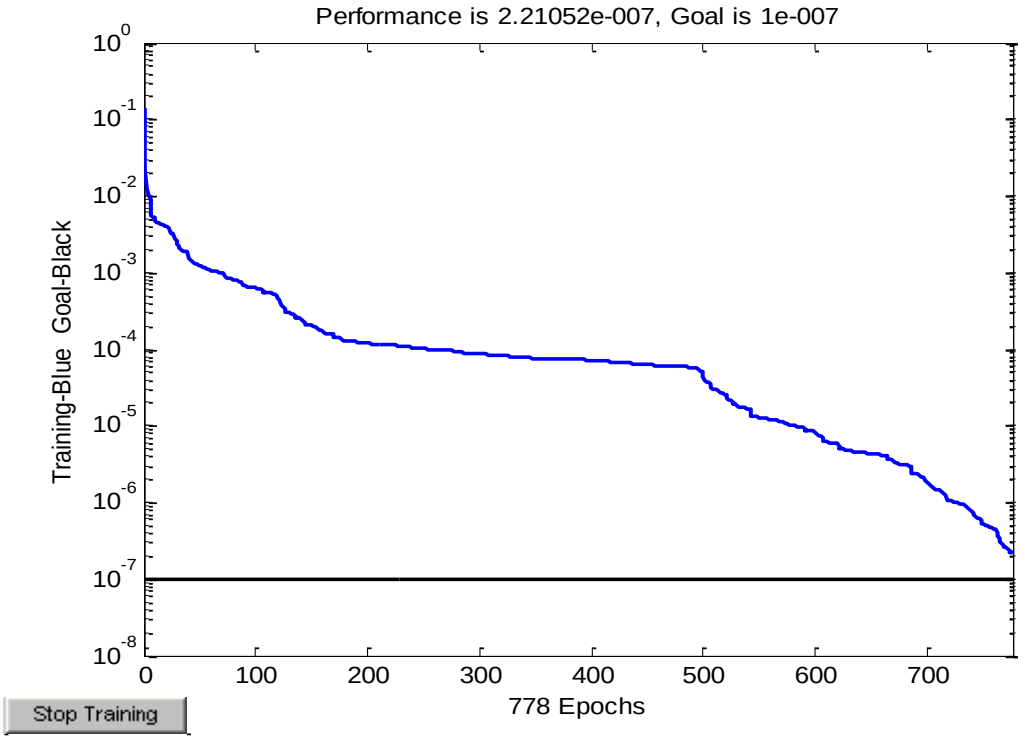


**Figure 18.**Training performance for the Powell-Beale conjugate gradient backpropagation.

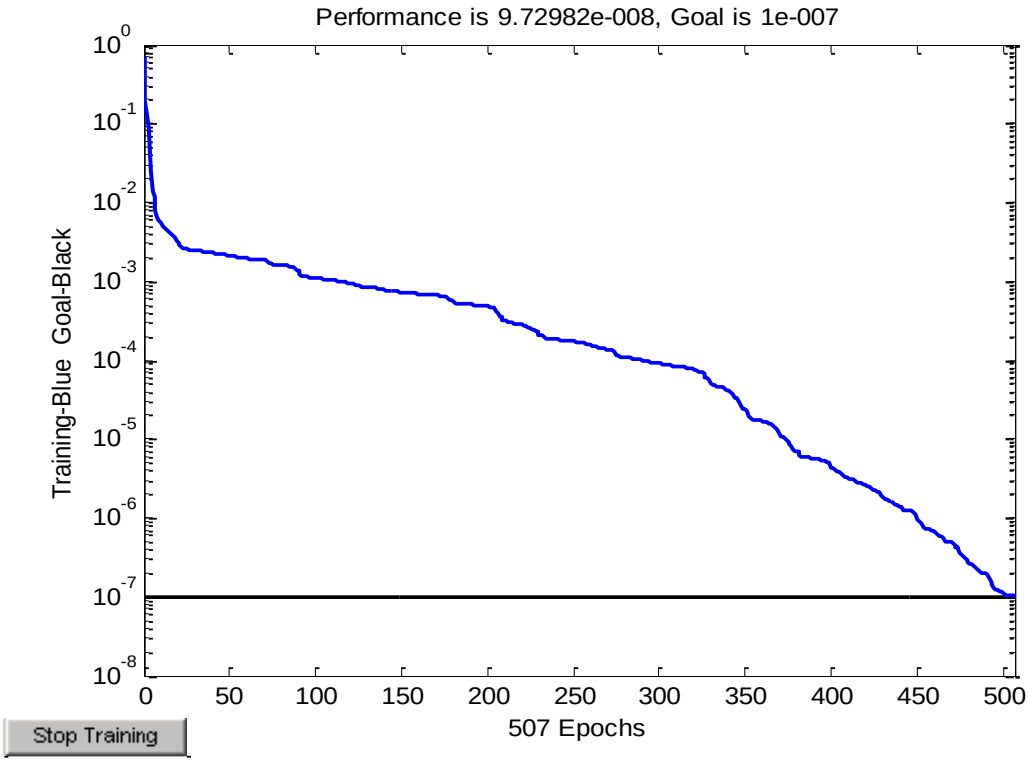


**Figure 19.**Training performance for the Fletcher-Powell conjugate gradient backpropagation.

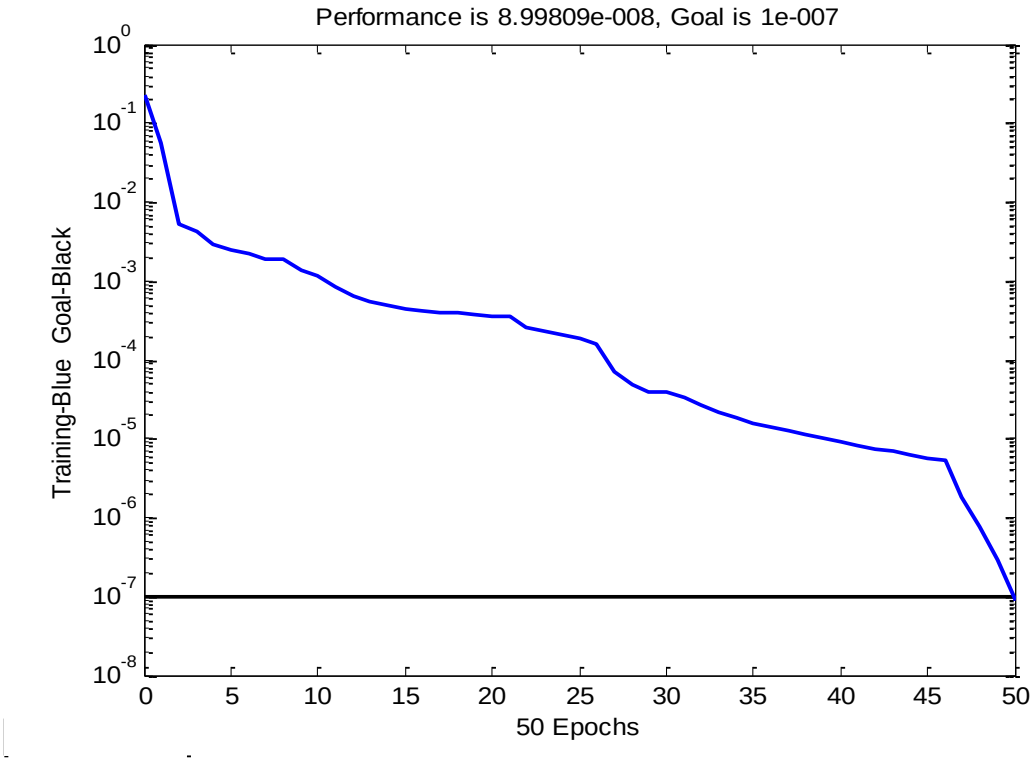


**Figure 20.** Training performance for the Levenberg-Marquardt backpropagation.

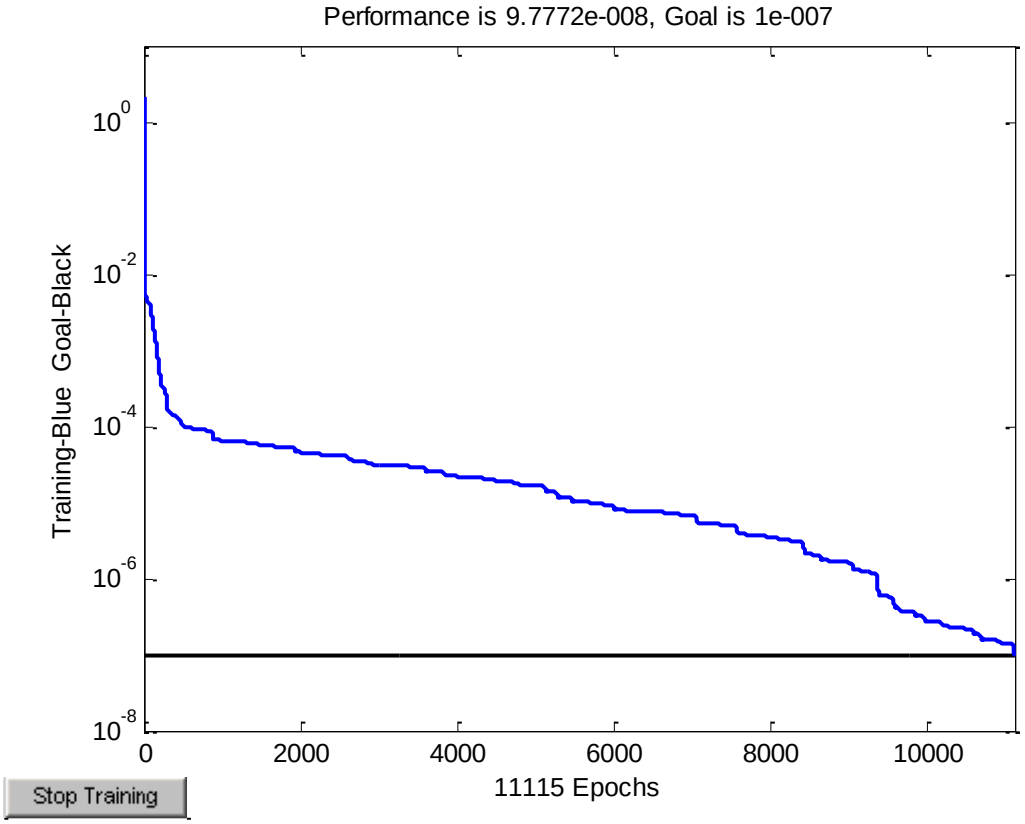


**Figure 21.** Training performance for the One step secant backpropagation.

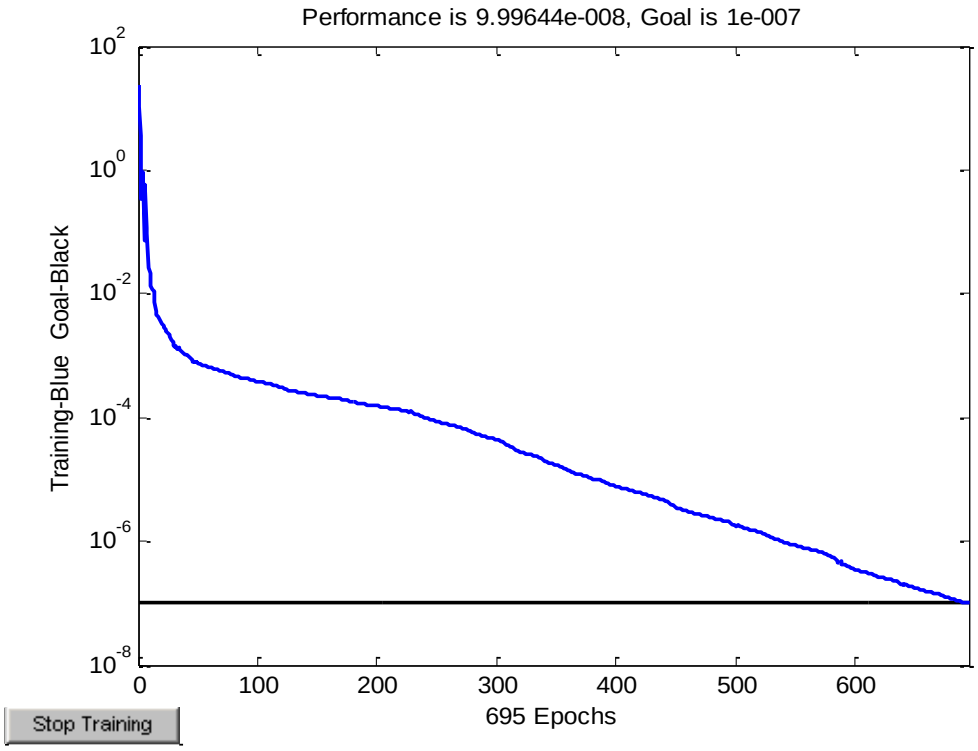


**Figure 22.**Training performance for the Resilient backpropagation.

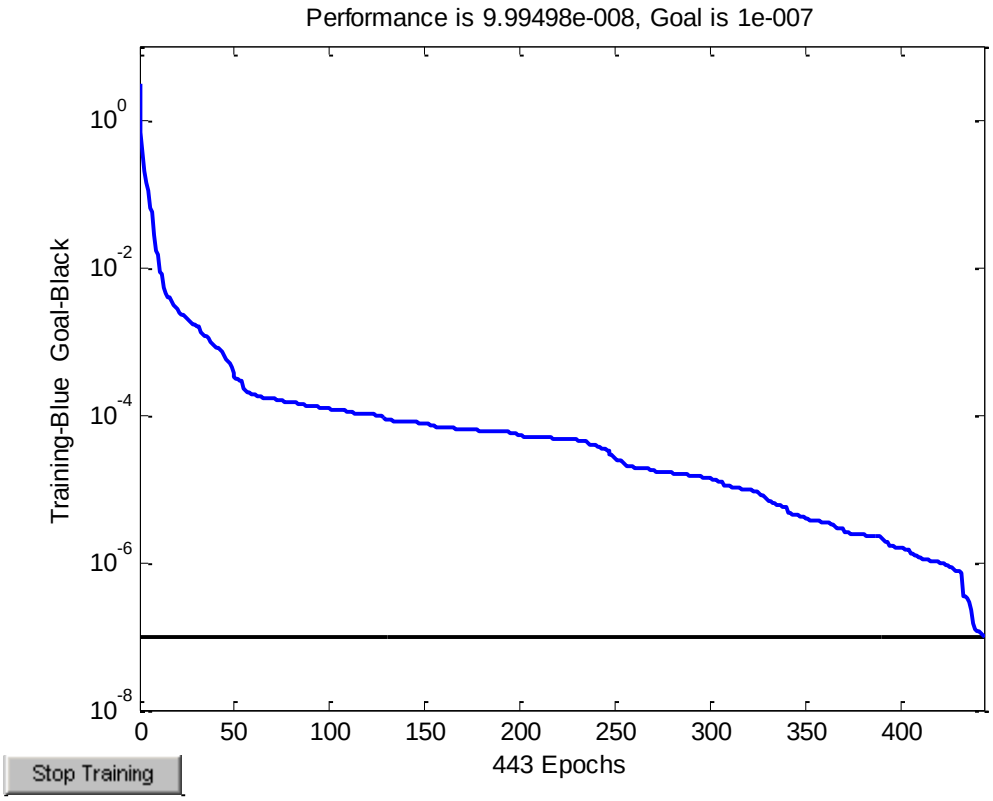


**Figure 23.**Training performance for the Scaled conjugate gradient backpropagation.

# Modeling of a Static VAR Compensator (SVC) as a Voltage Regulator for a Heavy Loaded Transmission Line.

***Bekir Mumyakmaz***[41]

***Abstract***

*In this study, a Static Var Compensator (SVC) is modelled by using Matlab/Simulink in order to regulate the receiving end voltage of a 230 kV transmission line. Only one phase of the transmission system is represented. The SVC consists of one 10 MVAr TCR bank and two 10 MVAr TSC banks connected to each phase of the load bus. The SVC controller monitors the receiving end voltage of the transmission line and successfully sends appropriate pulses to the compensator thyristors to obtain the susceptance required to keep the voltage level of the line end within ± % 5 tolerance limits. The desired voltage regulation at the transmission line end can be achieved in less than a half seconds using the modelled system under changing heavy and light loading conditions.*

**Keywords:** FACTS, SVC, Voltage Regulation, Simulation

## 99. INTRODUCTION

It is known that the shunt reactive compensation can increase the steady-state transmittable power and control the voltage profile along the transmission line, if it is applied appropriately. Reactive compensation changes electrical characteristics of a line to provide compatibility with the load demand. The reactors are used to minimize line overvoltage under light load conditions, and the capacitors are used to maintain voltage levels under heavy load conditions. In practical applications, reactive shunt compensation is often used to provide voltage support for the load or to regulate the voltage at a given bus against load variations. It can also significantly increase the maximum transmittable power. Thus, shunt compensation is able to change the power flow in the system with suitable and fast controls to increase the transient stability limit and provide power oscillation damping [1].

In this study, a Static Var Compensator (SVC) is modelled in order to regulate the receiving end voltage of a 230 kV transmission line. A system consisted of two thyristor switched capacitors (TSC) and one thyristor controlled reactor (TCR) has been used. The line end load has been represented by step by step varying lagging power factor load. One phase equivalent of the system was simulated by Matlab Simulink [2] program.

## 100. VOLTAGE REGULATION USING SVC

The voltage regulation system model is shown in Fig. 1. The circuit in Fig. 1 is a simplified one phase model of a 230 kV power system. The equivalent source is modeled by a voltage source (132.8 kV rms, 60 Hz.) in series with its internal impedance corresponding 2000 MVA short circuit level and X/R=10. Thus, the source inductance is Ls=70.2 mH and source resistance is Rs=2.645 ohms. The transmission line one phase equivalent

model is one single pi section with a branch impedance of R=5.2 ohms and L=138 mH and two shunt capacitances of C=0.967 µF.

[41] *Corresponding author: l U v , El l El E , 43100, Kü h , T k .*
*bekir.mumyakmaz@dpu.edu.tr*

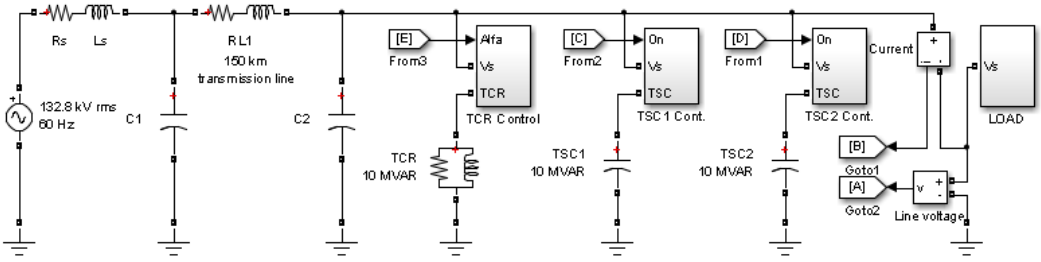


*Fig. 1- The modelled voltage regulation system circuit layout.*

The load at the line end has a total demand of 75 MW and 20 MVAr for each phase as seen in Fig 2. The load in the bottom of Fig. 2 is connected to the line at the beginning of the simulation and disconnected at 4$^{th}$ second. The other two loads in the figure are not connected to the line at the beginning. The load in the middle is connected to the line at 1$^{st}$ second while the other is at 2$^{nd}$. These two loads remain until the end of the simulation.

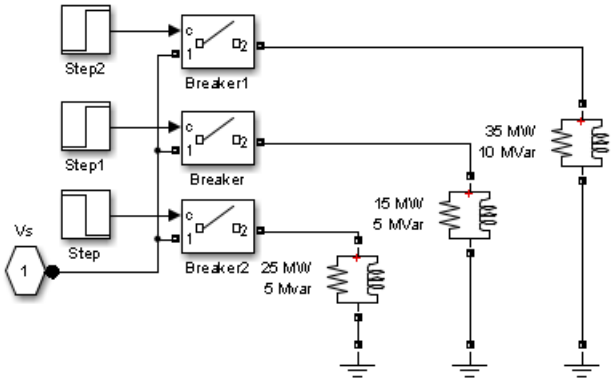


*Fig. 2- The changing load model with a total demand of 75 MW and 20 MVAr.*

The Static VAr Compensator (SVC) consists of two 10 MVAr tyristor switched capacitor (TSC) banks and one 10 MVAr thyristor controlled inductor (TCR) as seen in Fig. 1. The TCR capacity has been chosen to bring line voltage level to the specified limits under light loading conditions. The total TSC capacity is determined according to the full loading condition. The controllers of the TCR and TSC banks are explained in detail in the previous studies of [3 - 5].

The measurement and control block (not shown in Fig. 1.) measures the line voltage and the load current in order to calculate active and reactive power of the load and to decide the necessary number of the TSC units. The open-loop controller has been used to activate TSC banks. The TCR bank is used to regulate line voltage. The controller for the TCR is a "PI" type of controller that compensates the error between the reference line voltage and actual line voltage.

## 101. RESULTS AND DISCUSSION

At the beginning of the study, only source and the line were included in the simulation in order to see the line voltage at no load condition. The voltage of the ideal AC voltage source in Fig. 1 has been chosen as 1.075 per unit (p.u). At no load, the receiving end voltage was 1.117 p.u (257 kV Line to Line) while the sending end voltage was 1.096 p.u (253 kV Line to Line). Then, full load has been added to the simulation to see the voltage profile of the system. The voltage of the ideal AC voltage source in Fig. 1 has kept constant at 1.075 p.u. This time, the voltage at the receiving end of the line is 0.95 p.u. (219 kV Line to Line) and the voltage at the sending end of the line is 1.03 p.u. The voltage level of the load is in the lower limit. Either at no load or at full load the receiving end voltage needs reactive compensation in order to remain inside the allowed limits.

When the 10 MVAr of TCR has been added to the circuit at no load, the receiving end voltage of the line is at upper allowable limit of 1.05 p.u. However, the receiving end voltage of the line is 1.024 p.u. and slightly bigger than rated value of 230 kV at full load when both 10 MVAr of TSC banks are included to the system. The TCR and TSC combination with the appropriate control can provide necessary voltage regulation on the receiving end of the line.

The proposed system in Fig. 1 has been tested in changing load conditions. The total simulation time is 5 seconds. The active and reactive powers of the load and the source are seen in Fig.3 and Fig. 4 respectively. Only 25 MW and 5 MVAr of load has been added in the simulation during the first second. Thus, there is light loading condition on the line and the receiving end voltage of the line is above the rated value (1.03 p.u.) because of the line capacitance as seen on Fig. 5. The only action option for the voltage regulator is using full capacity of the 10 MVAr of TCR. But, this is not enough to bring receiving end voltage to 1.0 p.u. value.

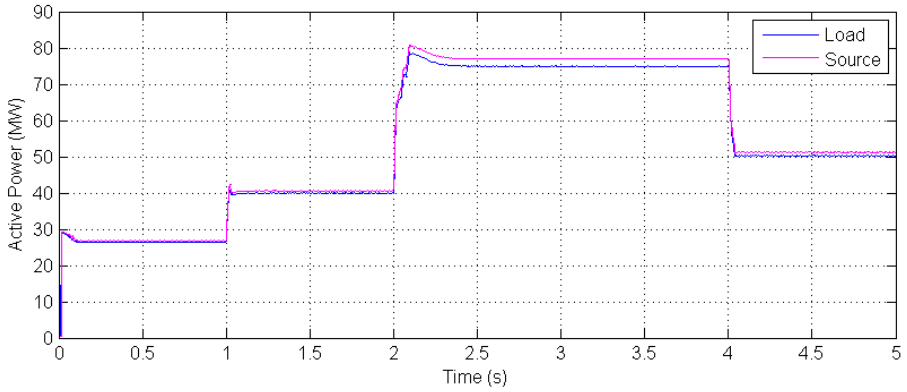


*Fig. 3- The changing active powers of the load and the source during the simulation.*

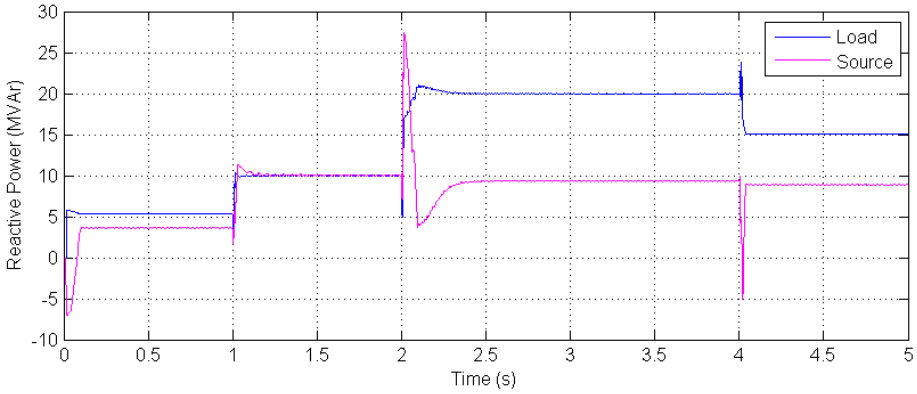


*Fig. 4- The changing reactive powers of the load and the source during the simulation.*

At the 1st. second, additional 15 MW and 5 MVAr of load comes in the simulation. This change causes the voltage to be below the rated value, so the voltage regulator lowers the current in the TCR by changing the ignition angle of the thyristors. Thus, the desired voltage (1.0 p.u) at the receiving end of the line can be achieved in a couple of periods of line frequency as shown in Fig. 5. Another load change occurs in 2nd. second and the demand of the load is now 75 MW and 20 MVAr. In order to bring the voltage within the tolerance limits, the voltage regulator takes both TCS units on then adjusts the ignition angle of the TCR thyristors. The rated voltage on the line-end is achieved in 0.35 seconds.

On the last part of the simulation, the load at the line-end is 50 MW and 15 MVAr. Only one TSC is enough to achieve the desired value on the line with the additional adjustment of TCR current. The current on the TCR is continuously controlled by changing ignition angle of the thyristors during the simulation and the resulting current of the TCR is shown in Fig. 6. The voltage regulation system in this study can affectively keep the voltage level at the receiving end of the transmission line within the specified tolerance limits of ± 5 %.

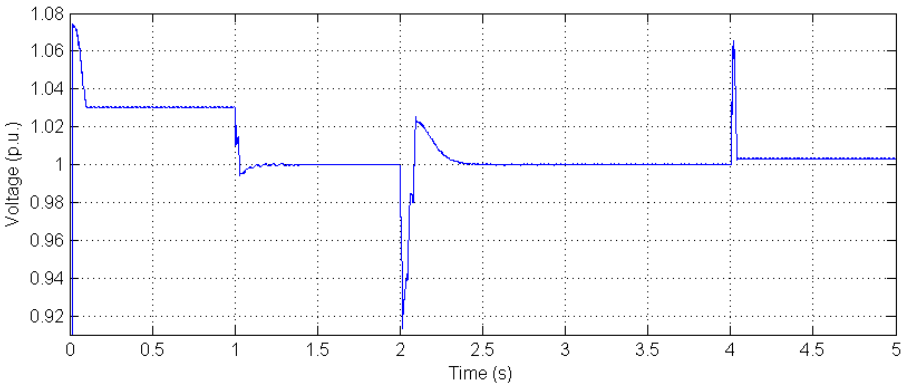


*Fig. 5- The voltage of the receiving end of the line in p.u. during the simulation.*

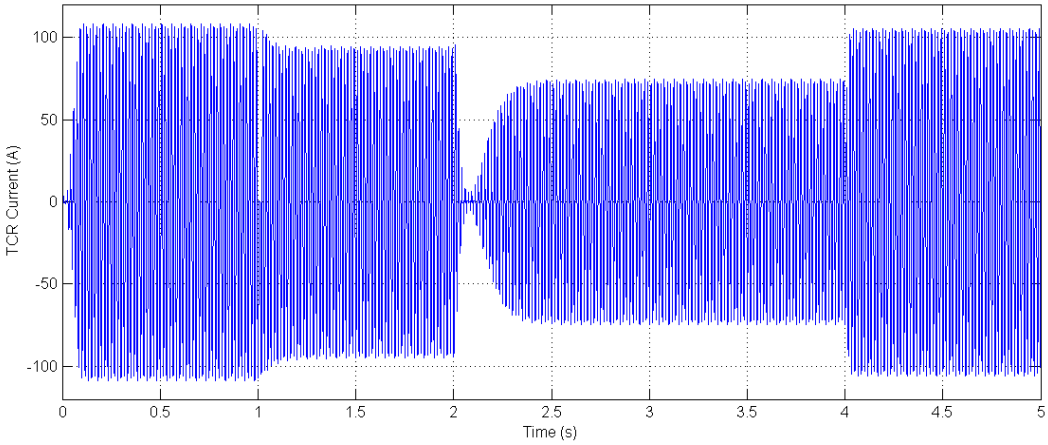


*Fig. 6- The current of the Thyristor Controlled Reactor during the simulation.*

## 102. CONCLUSION

In this study, the voltage regulation of the receiving end of a 230 kV transmission has been made using a Static Var Compensator (SVC). The system that consisted of two thyristor switched capacitors (TSC) and one thyristor controlled reactor (TCR) has been modelled in Matlab Simulink environment. The controller of the static compensator successfully kept the voltage of the receiving end of the line at the specified tolerance limits of ± 5 % by adjusting susceptance of the SVC while the load of the line has changed fast.

## REFERENCES

[289]. Narain G. Hingorani and Laszlo Gyugyi, *Understanding FACTS: Concepts and Technology of Flexible AC Transmission Systems,* December 1999, Wiley-IEEE Press

[290]. Mathworks - MATLAB and Simulink [Online], URL:http://www.mathworks.com, Access date: 15 April 2016.

[291]. Mumyakmaz, B., Vardar, K., "*A k l ç zz k l l k üç k z ö ü* ." ELECO2002 Conference, 2002, Bursa, Turkey.

[292]. Mumyakmaz, B., "*T ö h l l k ö l l k üç k z M l b S l k k ll l k ll* " ELECO2000 Conference, October 2000, Bursa, Turkey.

[293]. Mumyakmaz, B., Jin, X., Wang, C., Cheng, T.C., "*Static Var Compensator with Neural Network Control*" IEEE / PES Transmission and Distribution Conference, April 1999.

# Diagnosis of Power Transformer Incipient Faults Using Electronic Nose

*Bekir Mumyakmaz*[42], *Kerim Karabacak*[43]

***Abstract***

Power transformers are very expensive entities of electrical power systems. Since repairing and maintaining health of a transformer is very difficult and time consuming, their failure will have big negative impact on the system. Thus, any information regarding incipient faults in the transformer is very important. In this study, an electronic nose that is implemented to detect incipient faults of power transformers is presented. The electronic nose has four gas sensors namely hydrogen, carbon monoxide, carbon dioxide and methane with an addition of humidity and temperature sensor. The results of the study show that the proposed detection method can effectively diagnose partial discharge and overheated cellulose type of incipient faults of power transformers.

**Keywords:** Electronic Nose, Power transformer, Incipient fault diagnosis

## 103. INTRODUCTION

Power transformers are very expensive components of electrical power systems. Proper operation of them is crucial to maintain continuity of supply. Therefore, some mechanisms should be developed to predict transformer failures before they may occur.

Certain gases are released in transformer insulating oil due to changing working conditions over time such as overloading, overheating, partial discharge, low energy sparking and arching in the insulation system. The type and amount of the gases generated in the transformer oil provide information about the status of the transformer. Dissolved gas analysis (DGA) is a reliable method to determine incipient faults in a transformer. IEC 60599 [1] and IEEE C57.104 [2] are the standard guidelines for DGA diagnosis.

Classical method for DGA is to take some oil sample from the transformer, take it to the laboratory and put it in the gas chromatography equipment. A modern power transformer may have an online DGA and monitoring system which is very expensive. Some of them may be capable of extracting full DGA gases namely hydrogen ($H_2$), methane ($CH_4$), ethane ($C_2H_6$), ethylene ($C_2H_4$), acetylene ($C_2H_2$), carbon monoxide (CO), carbon dioxide ($CO_2$), nitrogen ($N_2$), and oxygen ($O_2$) [3]. The some others may have only hydrogen and carbon monoxide monitoring [4].

In this study, an electronic nose has been implemented to determine the gases that are released from transformer oil. Various catalytic chemical gas sensors are used in the electronic nose system. The gas samples, that simulate the gas mixtures that of malfunctioned transformers, have been applied to the implemented system and the type of fault has been determined by the sensor responses via information extraction. The chemical sensors that are used in the electronic nose can detect only gases that release in the case of transformer insulating paper deformations and partial discharge events.

## 104. E-NOSE AND DIAGNOSIS OF INCIPIENT FAULTS

Basically, an electronic nose (E-Nose) is a device intended to detect odors and it comprises of gas sensor arrays and pattern recognition systems. The sensors that are commonly used for electronic noses include metal–oxide–semiconductor, conducting polymer, quartz crystal microbalance (QCM), and surface acoustic wave (SAW) type of sensors. The data

[42] *Corresponding author: l U v , El l El tronics Engineering, 43100, Kütahya, Turkey.* bekir.mumyakmaz@dpu.edu.tr

[43] l U v , Kutahya Technical Sciences Vocational School, 43100, Kütahya, Turkey. kerim.karabacak@dpu.edu.tr

interpretation systems that are used for the analysis of results include artificial neural network (ANN), fuzzy logic, and other pattern recognition methods.

The metal-oxide type of gas sensors are used in this study due to suitability of their measurement ranges for incipient faults in transformers. Table 1 lists the sensors that are used in the study. The sensors listed in Table 1 can only be used for transformer insulating paper deformations and partial discharge events. The determination of other type of incipient faults such as arcing is not possible since the sensors for the other three gases mentioned above is not available.

Table 1. The sensors that are used in the E-Nose for diagnosis of incipient faults of transformers.

| Sensor | Gas | Measurement Range |
|---|---|---|
| TGS2442 | CO | 30-1000 ppm |
| TGS3870 | $CH_4$+CO | 500-12500 ($CH_4$);50-1000 (CO) ppm |
| FCM6812 | $H_2$ | 0-14000 ppm |
| TGS821 | $H_2$ | 0- 5000 ppm |
| TGS2611-E00 | $CH_4$ | 500-10000 ppm |
| CDM4160-H00 | $CO_2$ | 400-45000 ppm |
| SHT75 | Humidity and Temperature | RH %20-80 |
| KE-50 | $O_2$ | 0 - %100 |

An E-Nose has been designed and implemented using the sensors above to diagnose transformer incipient faults. The E-Nose is shown in Fig. 1. The sensors are in an aluminum chamber in order to dissipate the heat from the sensors. The purging gas (dry air) and sample gas representing the fault in the transformer are taken from tedlar bags and passed through the chamber using a small pump inside the box. The sensor responses are collected via serial port of a tablet PC as seen in Fig. 1b.

*a) From the inside of the box* *b) From the outside of the box.*

*Fig. 1- The designed and implemented E-Nose.*

Each sensor must be characterized and calibrated before using them for the interpretations. Firstly, the output voltages of the sensors are maximized in the sensing ranges by using adjustable resistances. Secondly, the sensor responses are checked in terms of repeatability. Then, the sensor responses for changing concentrations of the sample gases are recorded in order to calibrate the sensors. One sample of calibration process is shown in Fig. 2.

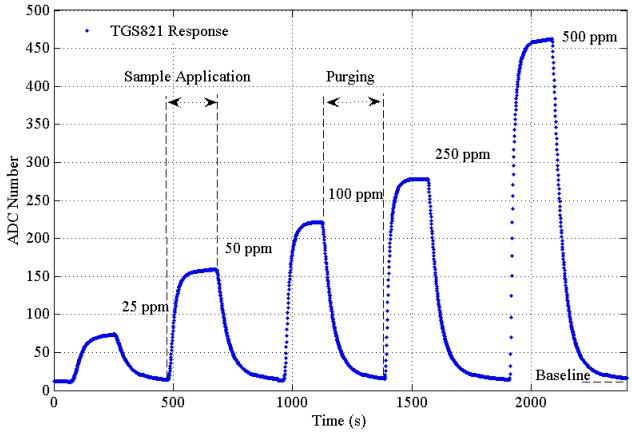


*Fig. 2- The TGS821 response to hydrogen samples in the calibration process.*

Only 4 sensors namely TGS821, TGS4160, TGS2442 and TGS2641 are used to determine the fault types since some of the sensors are redundant. After calibration process of the sensors, the sample gas mixtures that represent incipient faults in power transformers are applied to the E-Nose. The gas mixtures are prepared according to the amounts in certain types of faults determined in power transformers mentioned in [5].

## 105. RESULTS AND DISCUSSION

Figure 3 shows sensor responses for a sample gas mixture after calibration process. At the beginning of the experiment, dry air is applied to the system in order to purge the sensors of the E-Nose for 10 minutes. The prepared gas mixture has been applied to the E-Nose for 5 minutes and then again there has been a purging time. The mixture consists of mainly hydrogen and methane gases with the addition of some carbon monoxide. These gases are dissolved in the transformer oil when there is a partial discharge or thermal cellulose type of faults in the transformer. The steady-state responses of the sensors are on the right side of the Fig. 3.

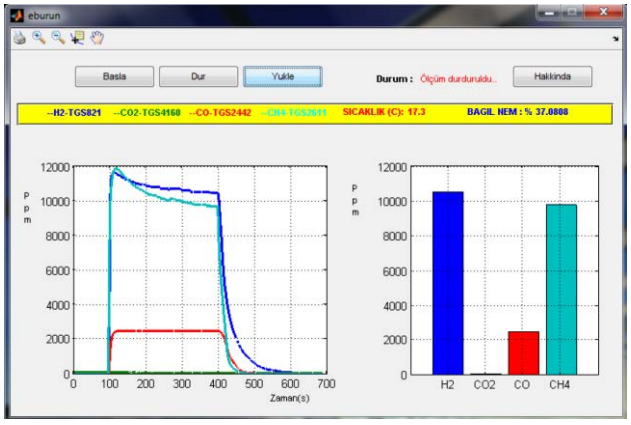


*Fig. 3- Sensor responses for a sample gas mixture after calibration process.*

The sensors clearly show the amounts of the gases in the sample bag in ppm (particles per million). The concentration levels of the gases in the mixture are in the ranges that are seen in partial discharge and overheated cellulose type of incipient faults in a transformer. The E-Nose does not contain ethane, ethylene, and acetylene sensor. Thus, it cannot determine thermal faults in oil or electrical arcing faults.

The pattern recognition part of the E-Nose is explained in detailed in other studies which employ artificial neural networks [6-8].

## 106. CONCLUSION

In this study, an electronic nose that is designed and implemented to detect incipient faults of power transformers is presented. The calibrated electronic nose has four gas sensors namely hydrogen, carbon monoxide, carbon dioxide and methane with an addition of humidity and temperature sensor. The results of the study show that the proposed detection method can effectively diagnose partial discharge and overheated cellulose type of incipient faults of power transformers.

## ACKNOWLEDGMENT

This work was supported by Dumlupınar University (No: 2010-10).

## REFERENCES

[294]. Mineral Oil-Impregnated Electrical Equipment in Service-Guide to the Interpretation of Dissolved and Free Gases Analysis. IEC 60599 - 2007
[295]. IEEE Guide for the Interpretation of Gases Generated in Oil-Immersed Transformers. IEEE Standard C57.104 - 2008
[296]. http://www.energy.siemens.com/us/en/services/power-transmission-distribution/transformer-lifecycle-management/online-dga-monitoring.htm (Accessed April 2016)
[297]. http://www.mte.ch/categorie_26.html (Accessed April 2016)
[298]. Michel Duval, Alfonso de Pablo, (2001) Interpretation of Gas-In-Oil Analysis Using New IEC Publication 60599 and IEC TC 10 Databases
[299]. Mumyakmaz B, Özmen A, Ebeoğlu MA, Taşaltın C. "Predicting gas concentrations of ternary gas mixtures for a predefined 3D sample space." Sensor Actuat B-Chem 2008; 128: 594-602.
[300]. Mumyakmaz B, Karabacak K, "An E-Nose based indoor air quality monitoring system: Prediction of combustible and toxic gas concentrations." Turk J Elec Eng & Comp Sci, 2015, 23(3), 729-740.
[301]. Özmen A, Mumyakmaz B, Ebeoglu M A, Tasaltın C, Gürol I, Öztürk Z Z, Dural D "Quantitative information extraction from gas sensor data using principal component regression (PCR)." Turk J Elec Eng & Comp Sci, 2016, 24: 946-960.

# The Importance and Traditional Uses of *Sideritis* Taxa in Turkey Flora

***Belgin Coşge Şenkal[44], Cüneyt Cesur[1], Cennet Yaman[1], Tansu Uskutoğlu[1]***

***Abstract***

*The genus Sideritis L. (Lamiaceae) is comprised by more than 150 species which are distributed in temperate and tropical regions of the world. For all that, most species are mainly found in the Mediterranean area. Turkey is Turkey is one of the countries having the highest number of Sideritis species. The genus Sideritis is represented in the Flora of Turkey by 45 species and 55 taxa, of which 37 taxa are endemic to Turkey. The rate of endemism is 82%. Sideritis species are known as " , l ", h l h h l h b l and teas. The tea is widespread for stomach ache, indigestion, and common colds such as fever, flu, sore throat and bronchitis. According to some recent researches, extracts and essential oils obtained from some Sideritis species were shown to have antifeedant, antimicrobial, antioxidant, anti-inflammatory, and analgesic. In recent years, the interest in and the demand for these species have increased particularly due to their high antioxidant effect.*

**Keywords: *Sideritis* L., herbal tea, antioxidant capacity**

## 107. INTRODUCTION

The genus *Sideritis* L. belonging to the Labiateae or Lamiaceae family comprises more than 150 species ([1], [2]). These are distributed in temperate and tropical regions of the world. For all that, most species are mainly found in the Mediterranean area. Turkey is one of the countries having the highest number of *Sideritis* species ([2], [3]).

These species are annuals, perennials, and evergreen subshrubs and shrubs. Leaves are often narrow (Figure 1-4). The corolla is mostly yellow, rarely white or red. *Sideritis* species grow optimally in full sun and are adapted to arid conditions. They are found on rocky slopes and pastures, from a few meters above the sea level to more than 3000 m, and require moderately nutrient-rich soils and slightly alkaline ([4], [5]).

*Figure 1. Sideritis germanicopolitana* BORNM. *(Kastamonu/TURKEY-18.07.2009)*

*Figure 2.(a)Sideritis hispida* P. H. DAVIS *(Konya/TURKEY 16.07.2009) (b)Sideritis galatica* BORNM. *(Ankara/TURKEY 17.08.2009)*

[44] *Corresponding author: Bozok University, Agricultural Faculty, Field Crops Department, 66100, Merkez/Yozgat, Turkey. bcosgesenkal@gmail.com*

*Figure 4. Sideritis dichotoma* HUTER (*Karabük/TURKEY- 23.07.2009*)

Many chemical components such as terpenes, flavonoids, essential oil, iridoids, coumarins, lignanes, and sterols have been identified in the aerial parts of *Sideritis* species. Diterpenes, flavonoids and essential oils are the main responsible for the pharmacological activity ([6]).

Leaves are collected in spring, flowering tops as the first open, and dried for infusions. In fact, *Sideritis* species are not rich in essential oil, but their smell and aroma are pleasant. Dried inflorescences of *Sideritis* species are used as a popular herbal tea in Turkey ([4], [7], [8]). Some *Sideritis* species are used widely in the treatment of some diseases in folk medicine ([6]).

## 108. SİDERİTİS TAXA IN THE FLORA OF TURKEY

Turkey has different geographical and climatic features, and is at the intersection of three gene center (the Mediterranean-Europe and Iran-Turan plant geographical regions). Therefore, Turkey is a country rich in plant diversity. On the other hand, a rate of endemic species in Turkey Flora is very high. According to the latest data, 9753 species and 11707 taxa, of which 3649 is endemic (31.82% the rate of endemism) are in the natural flora of our country ([9]).

The genus *Sideritis* is represented in the Flora of Turkey by 45 species and 55 taxa, of which 37 taxa are endemic to Turkey. The rate of endemism is 82% ([9]). The genus *Sideritis* has an important place among the other Lamiaceae genera because of the high percentage of endemism. Also, the Flora of Turkey has very important position in terms of the richness of *Sideritis* species. *Sideritis* taxa in the Flora of Turkey are given in Table 1.

*Table 1. Sideritis taxa in the Flora of Turkey*

| Number | ***Sideritis* Taxa** | **Turkish Name** | **Endemic** |
|---|---|---|---|
| 1 | *S. akmanii* Aytaç, Ekici & Dönmez | Kuyrukçayı | + |
| 2 | *S. albiflora* Hub.-Mor. | Akçiçekçayı | + |
| 3 | *S. amasiaca* Bornm. | Bodurçay | + |
| 4 | *S. arguta* Boiss. & Heldr. | Köyçayı | + |
| 5 | *S. argyrea* P. H. Davis | Boz eşekçayı | + |
| 6 | *S. armeniaca* Bornm. | Yüzükçayı | + |
| 7 | *S. athoa* Papan.& Kokkini | Kedikuyruğu çayı | - |
| 8 | *S. brevibracteata* P. H. Davis | Hacımemetli çayı | + |
| 9 | *S. brevidens* P. H. Davis | Gülnar çayı | + |

| | | | |
|---|---|---|---|
| 10 | *S. bilgerana* P. H. Davis | Altınbaş çayı | + |
| 11 | *S. caesarea* H. Duman, Aytaç & Başer | Topalçay | + |
| 12 | *S. condensate* Boiss. & Heldr. | Kozalıkekik | + |
| 13 | *S. congesta* P. H. Davis & Hub.-Mor. | Başakçayı | + |
| 14 | *S. cilicica* Boiss.&Balansa | Kandilçayı | + |
| 15 | *S. dichotoma* Huter | Çatalçay | + |
| 16 | *S. erythrantha* Boiss. & Heldr. | Morçay | |
| | subsp. *cedretorum* (P. H. Davis) H. Duman | Karlıkçayı | + |
| | subsp. *erythrantha* | Morçay | + |
| 17 | *S. galatica* Bornm. | Kırçayı | + |
| 18 | *S. germanicopolitana* Bornm. | Karakurbağa çayı | + |
| | subsp. *germanicopolitana* | Karakurbağa çayı | + |
| | subsp. *viridis* | Köseçay | + |
| 19 | *S. gulendamii* H. Duman & Karavel. | Hanımçayı | + |
| 20 | *S. hispida* P. H. Davis | Sertçay | + |
| 21 | *S. hololeuca* Boiss. & Heldr. | Çalıçayı | + |
| 22 | *S. huber-morathii* Greuter & Burdet | Şenköy çayı | + |
| 23 | *S. lanata* L. | İpekçayı | - |
| 24 | *S. leptoclada* O. Schwarz & P. H. Davis | Kızlançayı | + |
| 25 | *S. libanotica* Labill. | Gevreğen | - |
| | subsp. *kurdica* (Bornm.) Hub.-Mor. | İnceçay | - |
| | subsp. *libanotica* | Gevreğen | - |
| | subsp. *linearis* (Benth.) Bornm. | Torosçayı | - |
| | subsp. *microchlamys* (Hand.-Mazz) Hub.-Mor. | Zühreçayı | - |
| | subsp. *violascens* (P. H. Davis) P. H. Davis | Topuklu çay | + |
| 26 | *S. lycia* Boiss. & Heldr. | Kemer çayı | + |
| 27 | *S. montana* L. | Karaçay | - |
| | subsp. *montana* | Karaçay | - |
| | subsp. *remota* P. W. Ball | Mor karaçay | - |
| 28 | *S. niveotomentosa* Hub.-Mor. | Duvaklı çay | + |
| 29 | *S. ozaturkii* Aytaç & Aksoy | Paşaçayı | + |
| 30 | *S. perfoliata* L. | Fincançayı | - |
| 31 | *S. phlomoides* Boiss. & Balansa | Tilkiçayı | + |
| 32 | *S. phrygia* Bornm. | Taşlıkçayı | + |
| 33 | *S. pisidica* Boiss. & Heldr. | Eldiven çayı | + |
| 34 | *S. romana* L. | Zarifçay | - |

| | | | |
|---|---|---|---|
| | subsp. *curvidens* (Stapf) Holmboe | Eğriçay | - |
| | subsp. *romana* | Zarifçay | - |
| 35 | *S. rubriflora* Hub.-Mor. | Gülçayı | + |
| 36 | *S. scardica* Griseb. | Pazlak çayı | - |
| | subsp. *scardica* | Pazlak çayı | - |
| 37 | *S. serratifolia* Hub.-Mor. | Fenerli çayı | + |
| 38 | *S. sipylea* Boiss. | Sipil çayı | + |
| 39 | *S. stricta* Boiss. & Heldr. | Tilkikuyruğu çayı | + |
| 40 | *S. syriaca* L. | Amanos çayı | - |
| | subsp. *nusairiensis* (Post) Hub.-Mor. | Amanos çayı | + |
| 41 | *S. taurica* Stephan ex Willd. | Kırımçayı | - |
| 42 | *S. tmolea* P. H. Davis | Sivriçay | + |
| 43 | *S. trojana* Bornm. | Sarıkız çayı | + |
| 44 | *S. vulcanica* Hub.-Mor. | Madençayı | + |
| 45 | *S. vuralii* H. Duman & Başer | Babaçayı | + |

## 2. TRADITIONAL USES

The consumption of herbal tea made from different medicinal and aromatic plants is quite common in Turkey (Figure 5). One of the most commonly used plants for herbal tea is *Sideritis* species ([7]). *Sideritis* species are known as “dag cayi, yayla cayi or adacayi”, and the aerial parts of them are used in the preparation of traditional herbal medicines and teas ([1], [2], [5]-[7], [10]) (Table 2 and Table 3).

*Figure 5. The several Sideritis species collected from natural area are sold by local people in Turkey.*

*Table 2. Some Sideritis taxa as herbal tea in Turkey*

| ***Sideritis* taxa** |
|---|
| *S. amasiaca* |
| *S. brevidens* |

*S. caesarea*

*S. cilicica*

*S. erythrantha* subsp. *erythrantha*

*S. libanotica* subsp. *libanotica*

*S. libanotica* subsp. *linearis*

*S. ozaturkii*

*S. rubriflora*

*S. serratifolia*

*S. stricta*

*S. trojana*

The tea is widespread for stomach ache, indigestion, and common colds such as fever, flu, sore throat and bronchitis. Except herbal tea prepared with infusion and decoction methods using the aerial parts of these plants, there are also different methods of use. For example, the leaves of *S. pisidica* are boiled with barley flour, grated onions and pine tar, and the poultice prepared is useful in treating abdominal pain in our country [11]. Table 3 is given traditional use of some *Sideritis* species in Turkey ([2], [3], [12-19]).

*Table 3. Traditional use of some Sideritis species in Turkey*

| **Sideritis species** | **Traditional Use** |
|---|---|
| *S. arguta* | Diuretic, common cold |
| *S. caesarea* | Gastroptotective |
| *S. condensate* | Flu, sore throat |
| *S. galatica* | Aperitif, carminative |
| *S. leptoclada* | Expectorant |
| *S. lycia* | Common cold |
| *S. pisidica* | Abdominal pain |
| *S. scardica* | Flu, cold, cough, bronchitis |
| *S. stricta* | Common cold, respiratory system, carminative |
| *S. trojana* | Chest and throat illness |

According to some recent researches, extracts and essential oils obtained from some *Sideritis* species were shown to have antifeedant, antimicrobial, antioxidant, anti-inflammatory, anti-ulcerogenic, antispasmodic, digestive, diuretic, and analgesic ([2], [5], [6], [10]).

## 3. CONCLUSIONS

Herbal tea (infusion or decoction) made from leaves, flowers and stem of *Sideritis* species have been also used as folk remedies to treat various ailments. On the other hand, many studies based on their biological, phytochemical and pharmacological properties are conducted on these plants. In recent years, the interest in and the demand for these species have increased particularly due to their high antioxidant effect.

The products derived from plants have very few side effects unlike synthetic drugs, and the plant products are more reliable than synthetic ones. Therefore, their consumption and the market volume are increasing parallel to the developments in the use of medicinal and aromatic plants worldwide. On the other hand, the healthier and living longer wishes of people has been increased significantly the consumption of herbal tea. From this perspective, *Sideritis* species is significant potential plants, and they are economically promising.

## BIOGRAPHY

**Belgin Coşge Şenkal** was born in Turkey in 1972. She received the B.E., M.E., and Ph. D. Degrees from Faculty of Agriculture, Ankara University, Ankara, Turkey, in 1994, 1996, and 2001, respectively. She worked in Abant İzzet Baysal University, Bolu, Turkey from 2008 to 2013. Since 2013, she has been with Faculty of Agriculture, Bozok University, Yozgat, Turkey, where she is currently a Professor. Her main areas of research interest are cultivation and breeding of medicinal and aromatic plants and oil crops.

## REFERENCES

[302]. Y. Tekeli, "Antioxidant activities and phenolic compounds of two endemic taxa of Labiatae *Sideritis*," *REV.CHIM*. (*Bucharest*), vol. 63, pp. 465-469, 2012.
[303]. E. González-Burgos, M.E. Carretero, and M. P. Gómez-Serranillos, "*Sideritis* spp.: Uses, chemical composition and pharmacological activities-A," *Journal of Ethnopharmacology*, vol. 135, pp. 209-225, 2011.
[304]. A. Güvenç, P. J. Houghton, H. Duman, M. Coşkun, and P. Şahin, "Antioxidant activity studies on selected *Sideritis* species native to Turkey," *Pharmaceutical Biology*, vol.43, pp. 173-177, 2005.
[305]. D. Bown, *The Royal Horticultural Society New Encyclopedia of Herbs & Their Uses*, Great Britain: A Penguin Company, 2002.
[306]. Ö. Kılıç, "Essential oil composition of two *Sideritis* L. taxa from Turkey: A Chemotaxonomic approach," *Asian Journal of Chemistry*, vol. 26, pp. 2466-2470, 2014.
[307]. G. Özkan, "Comparison of antioxidant phenolics of ethanolic extracts and aqueous infusions from *Sideritis* species," *Asian Journal of Chemistry*, vol. 21, pp. 1024-1028, 2009.
[308]. G. Topçu, A. Barla, A.C. Gören, G. Bilsel, M. Bilsel, and G. Tümen, "Analysis of essential oil composition of Sideritis albiflora using direct thermal desorption and headspace GC-MS techniques," *Turk. J. Chem*., vol. 29, pp. 525-529, 2005.
[309]. T. Askun, G. Tümen, F. Satıl, and M. Ateş, "Characterization of the phenolic composition and antimicrobial activities of Turkish medicinal plants," *Pharmaceutical Biology*, vol. 47, pp. 563-571, 2009.
[310]. A. Güner, S. Aslan, T. Ekim, M. Vural, and T.M. Babaç, *Türkiye Bitkileri Listesi* ( *l B k l* ), İstanbul: Nezahat Gökyiğit Botanik Bahçesi ve Flora Araştırmaları Derneği Yayını, 2012.
[311]. Ö. Kılıç, E. Bağcı, G. Doğan, E. Yüce, Ş. Hayta, A. Demirpolat, and S. Eser, "Essential oil composition of endemic Sideritis dichotoma Huter (Lamiaceae) from Turkey," *B l k Ş hE b l Ü v F B l l* , vol. 1, pp. 55-58, 2014.
[312]. E. Yeşilada, G. Honda, E. Sezik, M. Tabata, T. Fujita, T. Tanaka, Y. Takeda, and Y. Takaishi, "Traditional medicine in Turkey V. Folk medicine in the inner Taurus Mountains," *Journal of Ethnopharmacology*, vol. 46, pp. 133-152, 1995.
[313]. I. Gürbüz, A. M. Özkan, E. Yeşilada, and O. Kutsal, "Anti-ulcerogenic activity of some plants used in folk medicine of Pinarbasi (Kayseri, Turkey)," *Journal of Ethnopharmacology*, vol. 101, pp. 313-318, 2005.
[314]. B. Dulger, A. Gonuz, and V. Aysel, "Inhibition of clotrimazole-resistant *Candida albicans* by some endemic *Sideritis* species from Turkey," *Fitoterapia*, vol. 77, pp. 404-405, 2006.
[315]. N. Sarac and A. Ugur, "Antimicrobial activities and usage in folkloric medicine of some Lamiaceae species growing in Mugla, Turkey," *EurAsian Journal of Bio-Sciences*, vol. 4, pp. 28-37, 2007.
[316]. Y. Akços, N. Ezer, I. Çalis, R. Demirdamar, and B.C. Tel, "Polyphenolic compounds of *Sideritis lycia* and their anti-inflammatory activity,"*Pharmaceutical Biology*, vol. 37, pp. 118-122, 1999.
[317]. Z. Tunalier, M. Kosar, N. Ozturk, K. H. C. Baser, H. Duman, and N. Kirimer, " Antioxidant properties and phenolic composition of *Sideritis* species," *Chemistry of Natural Compounds*, vol. 40, pp. 206-210, 2004.
[318]. E. Küpeli, P. Şahin, I. Çaliş, E. Yeşilada, and N. Ezer, "Phenolic compounds of *Sideritis ozturkii* and their in vivo ant-inflammatory and antinocicptive activities," *Journal of Ethnopharmacology*, vol. 112, pp. 356-360, 2007.
[319]. E. Küpeli, P. Şahin, E. Yeşilada, I. Çaliş, and N. Ezer, "In vivo anti-inflammatory and antinocciceptive activity evaluation of phenolic compounds from *Sideritis stricta*," *Zeitschrift für Naturforschung*, vol. 62c, pp. 519-525, 2007.
I. Arslan, T. Kiliç, A. Gören, and G. Topçu, "Toxicity of acetone extract of *Sideritis trojana* and 7-epicandicandiol diacetate and 18-acetylsideroxol against stored pests *Acanthoscelides obtectus* (Say), *Sitophilus granaries* (L.) and *Ephestia kuehniella* (Zell)," *Industrial Crops and Products*, vol. 23, pp. 171-176, 2006.

# Tribological Properties of Boron Carbide Reinforced Copper Based Composites

*Hüseyin İpek[45], Hamdullah Çuvalcı,[46] Cemal Çelebi[3]*

***Abstract***

*In this study, a boron carbide ($B_4C$) reinforced copper based Metal Matrix Composites (MMCs) manufactured by powder metallurgy method and tribological behavior of compacted composites were investigated. $B_4C$ reinforcement was selected at different ratio from 2%wt to 10%wt. Powders was compacted under 735±1 MPa pressure in a die with cold pressing method. Sintering of the samples was performed at two different sintering time as 1 hour and 3 hours under Ar gas atmosphere at 900 °C. Tribological tests were performed by using a computer aided pin-on-disc experimental setup under dry sliding conditions. Tribological tests were performed from 1 hour to 5 hours. And wearing surfaces were investigated in a Scanning Electron Microscope SEM) and mechanisms of the wear were detected. In addition to that tribological behavior and porosity properties of the manufactured samples were investigated. It was found that the porosity of the samples was increased with increasing $B_4C$ content. Nevertheless, wear resistivity increased with increasing reinforcement content.*

**Keywords:** Metal Matrix Composites (MMC's), $B_4C$, Tribology, Copper Based Composites

## 109. INTRODUCTION

Because of the unique properties of the Metal Matrix Composites (MMCs) have many application in industry [1, 2]. Most of the studies in industrial components should have good mechanical properties with better tribological properties [3]. The need for a recent wear resistant material for high performance tribological applications has been one of the major propellant power for the tribological development of ceramic particulate reinforced materials [4]. The introduction of hard, non-deformable ceramic particles into matrix alloy causes a loss in ductility and toughness of MMCs [5]. But the optimum ratio usage of the reinforcement particles could assist wear performance with a toughness. Matrix materials of the MMCs generally selected for their high thermal conductivity and ductility properties as copper, nickel and aluminum [6]. And reinforcement materials should be harder than matrix for the supporting the structure of composite as SiC, $B_4C$ $Si_3N_4$, $Al_2O_3$ and TiC [7].

In this study, copper and $B_4C$ was selected as a matrix and reinforcement materials, respectively. Copper-based materials are widely used in many industrial applications because of their good wear resistance and friction ductility, remarkable corrosion resistance, as well as self-lubrication properties, such as sliding bearings, sleeves, brushes and other components [8-10]. $B_4C$ reinforcement material was selected for its tribological and mechanical properties [4, 11]. Moreover, $B_4C$ particles have high impact and wear, low density, high melting

point, and excellent resistance to chemical agents as well as high capability for neutron absorption make boron carbide attracting much attention as an acceptable reinforcement [12].

Wear and friction are the common problem in industry [13, 14]. And wear shows itself in two different way, abrasive and adhesive. [15, 16]. Adhesive wear cause surface deformation with separation of the surface by layers but the abrasive wear cause separation of the particles from surface by scratching [17]. Main motivation and the novelty of the study was determine of the wearing performance of the Cu-$B_4C$ MMCs with a pin-on-disc wearing test machine.

[45] *Corresponding author: Karadeniz Technical University, Department of Metallurgical and Materials Engineering, 61100, Ortahisar, Trabzon, Turkey.hipek@ktu.edu.tr*

[46] *Ortahisar, Trabzon, Turkey. hcuvalci@ktu.edu.tr*

[3] *Cemal Çelebi, Gaziantep, Turkey*

## 110. EXPERIMENTAL DETAILS

In this study, MMCs was manufactured. Copper as matrix and boron carbide ($B_4C$) as reinforcement were selected at different ration (2%, 4%, 6%, 8% and 10%). 0,1mg precisions balance was used for weighting operations. Composites were mixed about 8-10 min. with mechanically. Mold was lubricated with a solid lubricant before molding. Manufacturing parameters and wearing parameter was given Table 1.

*Table 1. Manufacturing and wearing parameters.*

| | Sintering Time (h) | Molding Pressure (MPa) | Sintering Temperature (ºC) | Wearing Time (h) | Wearing Load (N) |
|---|---|---|---|---|---|
| Cupper (pure) | 1 | 735 | 900 | - | - |
| | 3 | | | | |
| Composites (2%, 4%, 6%, 8% and 10%) | 1 | | | 1-5 | 50 ±5 |
| | 3 | | | | |

Samples were sintered at 900 ºC. Argon atmosphere were selected for preventing the dirtiness during sintering process. Different sintering time and molding pressure were applied. Hardness of the samples was measured with Brinell Hardness method. Porosity of the samples was calculated with experimentally.

Samples experimental density was measured with formula 1.

$$\rho=m/V \quad (1)$$

Where, ρ (g/cm3) density, m (g) mass and V (cm3) volume. Composites theoretical density was calculated with formula 2.

$$\rho T= [(\%\ wt\ Cu\ .\ \rho\ 1\ )+ (\%\ wt\ B_4C.\ \rho\ 2)] \quad (2)$$

Where, ρT theoretical density, wt (g) mass, ρ1 and ρ2 ($g/cm^3$) copper and $B_4C$ densities. Then formula 3 can be used for calculate the porosity of the samples.

$$\%\ porozite = (\Delta\rho/\rho_0)x100 \quad (3)$$

Where, Δρ difference between theoretical density and experimental density, $\rho_0$ theoretical density.

Pin-on-disc wear method was run for wearing process. Samples were cut suitable for sample (pin) holder about 10mm x 10mm x40mm. Pin track diameter was selected as 100 mm. with 100 rpm working speed (≈0,5m/s). Cold work tool steel disc was used for wearing. Running in process was applied before wearing. Running in and experiments were carried out 50±5 N load

## 111. RESULT and DISCUSSIONS

### *111.1. Structural Investigation*

Structural investigations of the composites were performed with a Leica named optical system and the images of the structures were given in Figure 1. Figures show the different reinforcement ratio of the $B_4C$.

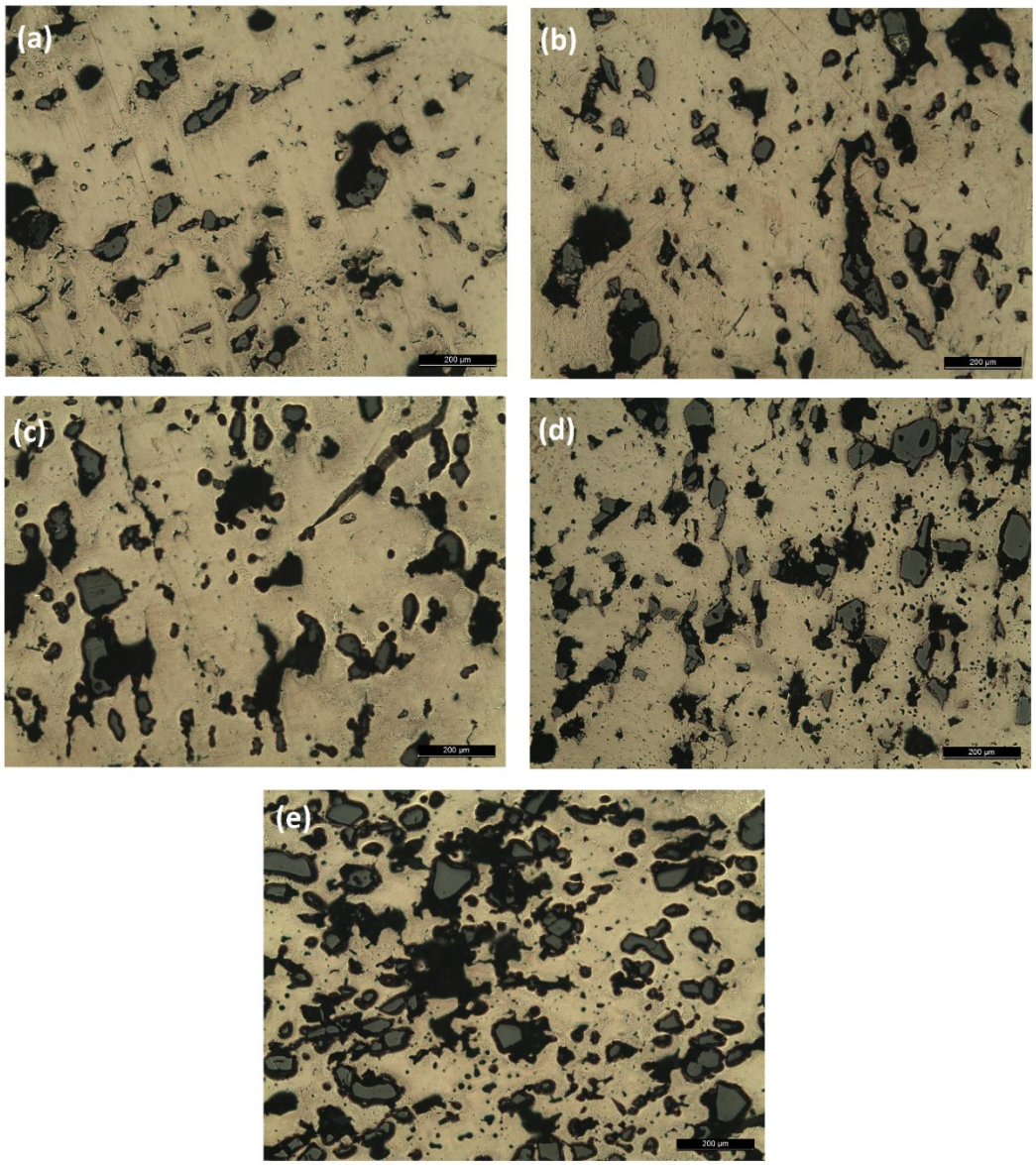


*Figure 1. Optical microscope images of the composites (1 hour sintering time)*

*(a-2%, b-4%, c-6%, d-8%, e-10%) (10x)*

Investigated macrostructure images show that the effect of reinforcement. Images show that porosity (dark areas) was increased with increasing reinforcement $B_4C$ particles (grey areas).

### *111.2. SEM Investigation*

Scanning Electron Microscope (SEM) investigations was imaged after wear tests. And Figure 2 shows the worn surface of the composites under dry sliding conditions.

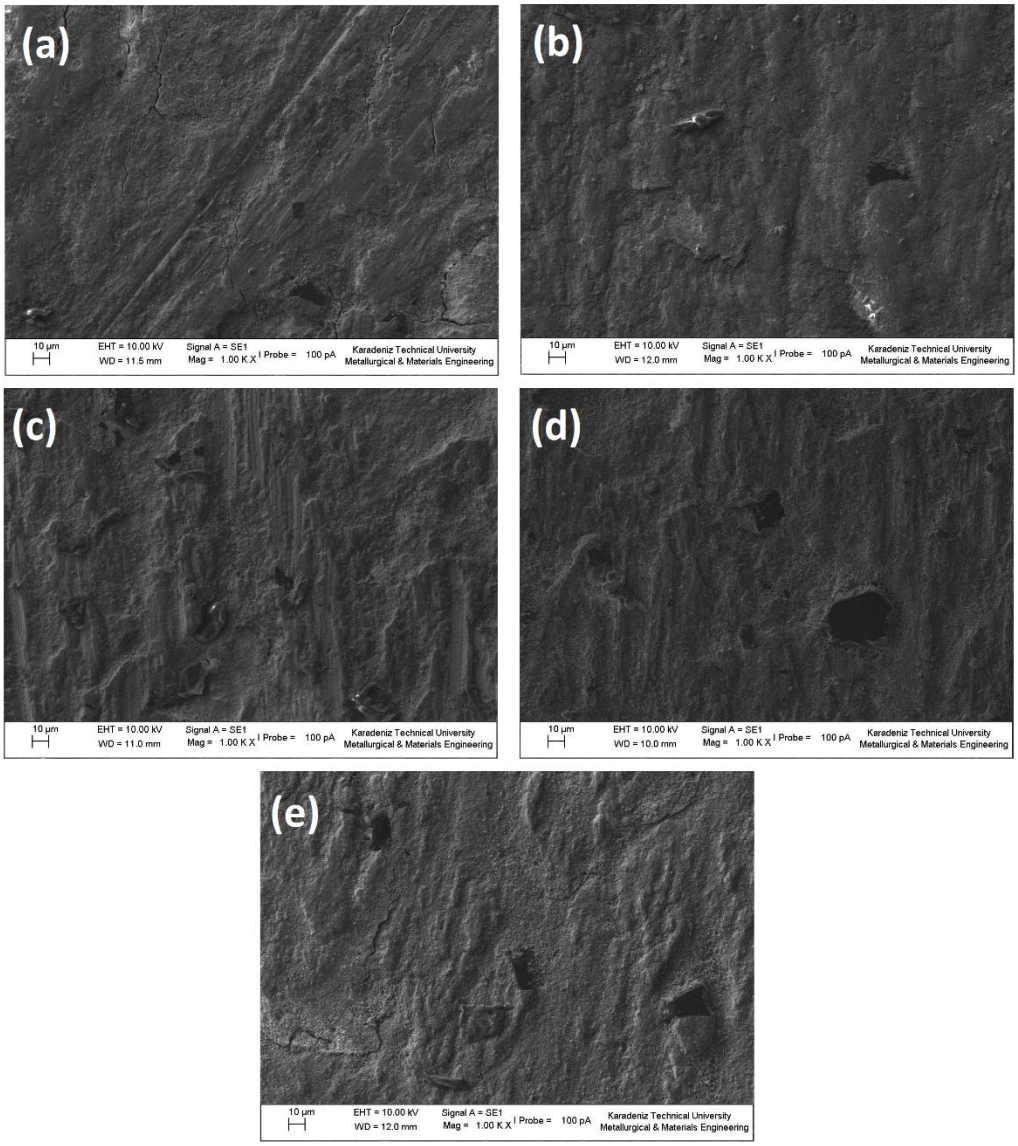


*Figure 2. Worn surface of the composites which was manufactured with 1 hour sintering time (*a-2%, b-4%, c-6%, d-8%, e-10%) (1000x)

### *111.3. Porosity*

Porosity of the samples was calculated with formulas 1, 2 and 3. The graphical explanation was given in Figure 3.

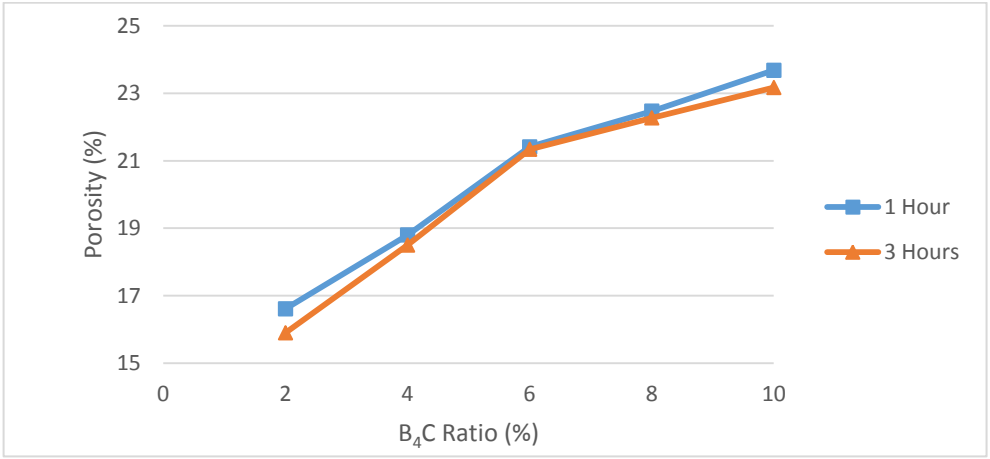

*Figure 3. Porosity ratio of the samples*

Porosity of the samples was increased with the increasing reinforcement ratio. And pure compacted copper porosity was calculated as 10.05%

### *111.4. Hardness*

Hardness of the samples was measured with Brinell Hardness test method. And the hardness of the samples was given in Table 4.

*Table 2. Hardness value of the samples*

| Sample | HB | |
|---|---|---|
| | 1 hour sintering time | 3 hour sintering time |
| Pure compacted copper | 32 | 24 |
| 2 % | 42 | 33 |
| 4 % | 51 | 53 |
| 6 % | 53 | 55 |
| 8 % | 56 | 84 |
| 10 % | 57 | 86 |

### *111.5. Wear loss*

The wear investigation of the samples was performed under dry sliding conditions. Wear loss was measured hour by hour and mass loss was found. Finding of the mass loss was converted to the wear rate. Wear rate formula was given in Formula 4.

$$\text{Wear Rate } (mm^3\ m^{-1}) = \text{mass loss } (g) / [\text{density } (g/mm^3) \text{ x sliding distance } (m)] \quad (4)$$

With the conversion of mass loss to the wear rate Figure 4 and 5 was obtained.

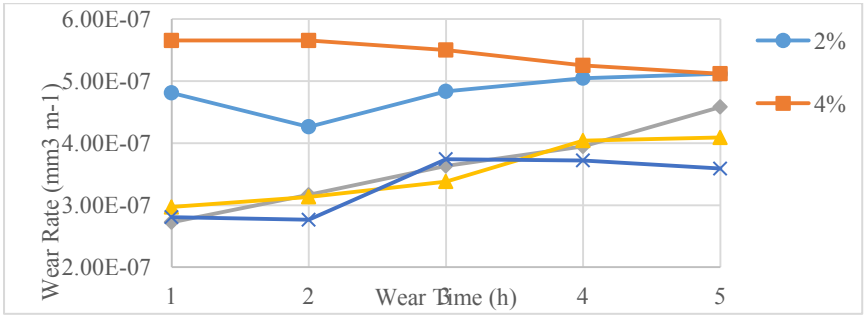


*Figure 4.Effect of the sintering time to the wear rate (1 h sintering time)*

Average wear rate of the samples was showed that minimum wear rate for 10% reinforced sample. 2% and 4% samples was showed higher wear rate and the ratio of the wear was decreased with increasing wear time. By the contrast with, samples which was reinforced in proportion as 6%, 8%, 10% showed that increasing wear rate with the increasing wear time. It means, $B_4C$ particles was removed from surface with the vibration and cause some deep scratching and erosion.

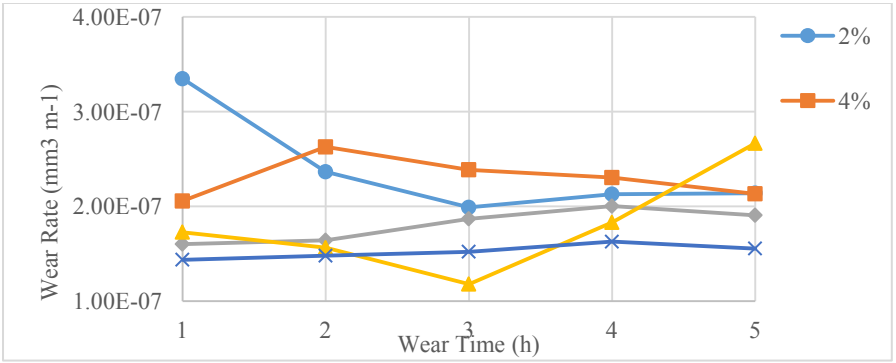


*Figure 5. Effect of the sintering time to the wear rate (3 h sintering time)*

Figure 5 shows that the sintering effect on the samples and it was detected decreasing wear rate with increasing sintering time. Average wear rate was showed minimum wear rate for 10% reinforced sample as Figure 4. But the average wear rate was less than Figure 4 about almost 46%. And all samples difference was less according the 1 hour sintered. Also Figure 3 showed that sintering effect on porosity. So increasing sintering time cause less pore, high hardness and high wear resistivity.

## 112. CONCLUSIONS

Copper and $B_4C$ reinforced copper based metal matrix composites was manufactured with different sintering time. Hardness and porosity measurement was performed for all samples. But tribological tests was applied for the composites and the conclusion was found:

1.) Porosity of the composites were increased with increasing reinforcement ratio.

2.) Hardness of the composites were increased with increasing sintering time.

3.) Wear loss was decreased with increasing sintering time.

## REFERENCES

1. A. Baradeswaran, A.E.P., *Influence of B4C on the tribological and mechanical properties of Al 7075–$B_4C$ composites.* 2013.
2. Varol, T. and A. Canakci, *Effect of particle size and ratio of $B_4C$ reinforcement on properties and morphology of nanocrystalline Al2024-B4C composite powders.* Powder Technology, 2013. **246**: p. 462-472.
3. A. Baradeswaran, S.C.V.b., A. Elaya Perumal, N. Selvakumar, R. Franklin Issac, *Experimental investigation on mechanical behaviour, modelling and optimization of wear parameters of $B_4C$ and graphite reinforced aluminium hybrid composites.* 2014.
4. M. Uthayakumara, S. Aravindan b, K. Rajkumarb, *Wear performance of Al–SiC–$B_4C$ hybrid composites under dry sliding conditions.* 2013.
5. R. Sathıskumar, N.M., I.Dınaharan, S.J. Vıjay, *F b A Ch z O C /$B_4C$ S S h C U F S P* . 2014.
6. Huiying Zhu, Y.N., Chucheng Lin, Liping Huang, Heng Ji, Xuebin Zhengn, *Microstructures and tribological properties of vacuum plasma sprayed $B_4C$–Ni composite coatings.* 2013.
7. Gode, C., *Mechanical properties of hot pressed SiCp and $B_4C$p/Alumix 123 composites alloyed with minor Zr.* Composites Part B-Engineering, 2013. **54**: p. 34-40.
8. Canakci, A., et al., *Synthesis of novel CuSn10-graphite nanocomposite powders by mechanical alloying.* Micro & Nano Letters, 2014. **9**(2): p. 109-112.
9. Sathiskumar, R., et al., *Characterization of boron carbide particulate reinforced in situ copper surface composites synthesized using friction stir processing.* Materials Characterization, 2013. **84**: p. 16-27.
10. H.R. Akramifard, M.S., ⇑, M. Sabbaghian a,b, M. Esmailzadeh b,c, *Microstructure and mechanical properties of Cu/SiC metal matrix composite fabricated via friction stir processing.* 2014.
11. L. M. Manocha, G.P., and S. Manocha, *Carbon-Ceramic Composites for Friction Applications.* 2014.
12. Ali Mazahery, M.O.S., *Influence of the hard coated $B_4C$ particulates on wear resistance of Al–Cu alloys.* 2012.
13. Canakci, A., et al., *Microstructure and Abrasive Wear Behavior of CuSn10-Graphite Composites Produced by Powder Metallurgy.* Powder Metallurgy and Metal Ceramics, 2014. **53**(5-6): p. 275-287.
14. Unal, H. and A. Mimaroglu, *Friction and wear performance of polyamide 6 and graphite and wax polyamide 6 composites under dry sliding conditions.* Wear, 2012. **289**: p. 132-137.
15. Cuvalci, H. and H.S. Celik, *Investigation of the abrasive wear behaviour of ZA-27 alloy and CuSn10 bronze.* Journal of Materials Science, 2011. **46**(14): p. 4850-4857.
16. Cuvalci, H. and H. Bas, *Investigation of the tribological properties of silicon containing zinc-aluminum based journal bearings.* Tribology International, 2004. **37**(6): p. 433-440.
17. Patnaik, A., et al., *Tribo-performance of polyester hybrid composites: Damage assessment and parameter optimization using Taguchi design.* Materials & Design, 2009. **30**(1): p. 57-67.

# Evaluation of a Potential Wildlife Crossing in the City of Burdur

*Latif Gürkan Kaya*[47], *Cengiz Yücedağ*[48]

***Abstract***

*Especially highways and expressways affect populations in numerous ways, from habitat loss and fragmentation, to barriers to animal movement, and wildlife mortality. For this reason, wildlife crossing has been established on the roads to protect the wild animals and them to breed, feed and to meet water needs in recent years. In this study, a wildlife crossing is designed for two fragmented areas (Mehmet Akif Ersoy Urban Forest and 607th Burdur Forest Compartment) located in the City of Burdur. For this purpose, computer software has been used to maintain a map that has been supported with photographs. This wildlife crossing is supported by samples established in the developed countries. The research team also reviewed studies that assess the efficiency of crossings and in doing so, learned what was working well. It has been thought that such a crossing is essential for the living in these areas. Moreover, this kind of crossing should be established in the whole fragmented areas in Turkey.*

**Keywords: Fragmentation; Protection; Roads; Wildlife crossing; Burdur; Turkey**

## 113. INTRODUCTION

Development pressures of countries including rapid population and unplanned growth necessitate the expansion of transportation infrastructure to prevent negative effects of roads on wildlife. The effects of roads on wildlife populations are habitat loss, reduced habitat quality and landscape connectivity and road-related mortality. They also have both immediate and cumulative deleterious effects. These include the degradation of remaining habitat, the disruption of ecological processes including animal migration and breeding, and the reduction or local extinction of wide-ranging species [1]. A research conducted in Hungary has showed that current expressways or an expressway under construction not only changes the frequency of deer crossings, but affects their distribution as well [2]. In reality, wildlife needs to move across the landscape to meet their basic survival needs (Figure 1). Therefore, ecosystems and landscapes must be connected and permeable to support sustainable wildlife population [3]. For these reasons, wildlife crossing has been set up on the roads to protect the wild animals and them to breed, feed and to meet water needs nowadays.

Wildlife crossings have evolved since the first crossings were established in Florida, almost 70 years ago. Wildlife crossing is a patch of wildlife habitat, generally vegetated, which joins two or more larger areas of wildlife habitat [3]. Namely, it has facilitated the living of wild animals by providing a connection between two fragmented areas. Vegetation helps animals get used to it and increase the chances of it being used. Vegetation is especially important for an overpass because it makes the overpass more natural, and it will decrease the noise and light of the traffic as well, eliminating most of the disturbances [2]. Studies have shown that crossing structures can mitigate habitat fragmentation, facilitate wildlife passage, reduce wildlife mortality from vehicle collisions, improve highway safety, and improve habitat connectivity [4, 5].

*Figure 1.* Wildlife needs to move across the landscape [6]

The general categories of wildlife crossings include underpasses (e.g. culverts and tunnels) and overpasses (i.e. bridges). Crossings have also been segmented by their height. Small and large underpasses are differentiated by a height or diameters of

[47] *Mehmet Akif Ersoy University, Department of Landscape Architecture, 15030, Burdur, Turkey. lgkaya@gmail.com*

[48] *Corresponding author: Mehmet Akif Ersoy University, Department of Landscape Architecture, 15030, Burdur, Turkey. yucedagc@gmail.com*

1.5 m. Other characteristics that can also be used to differentiate wildlife crossings include structure materials (e.g. concrete or metal) and shape (e.g. box, circular, elliptical, or open-span underpasses; and hourglass or box overpasses). Overpasses are usually designed for large vertebrates such as carnivores and hoofed animals. Their length is about 200 m and width range 0.3 to 0.5 m [7-9].

The design choices for a particular wildlife crossing are often unique from location to location [8]. Proper placement of wildlife crossing structures is one of the most important considerations for successful mitigation. Most studies indicate that placing the crossing structure near traditional movement routes will increase effectiveness. Studies conducted in Florida determined that structures placed without regard to traditional movement paths failed [10]. Sometimes a few years are necessary for wildlife to get used to the crossing structures, and a few years with low use can be followed by sudden and significant increase [11]. Downs et al. [5] have indicated that using the maximal covering location problem (MCLP) allows planners to objectively choose the best locations for new crossing structures as well as to quantify the benefits of building each successive facility. Considered the information mentioned-above, in this study a wildlife crossing is designed for two fragmented areas (Mehmet Akif Ersoy Urban Forest and 607$^{th}$ Burdur Forest Compartment) located in the City of Burdur.

## 114. MATERIAL AND METHOD

The study is conducted on the Turkish D350 and D650 expressways, in Burdur (Southern West of Lake Burdur) between the kilometric posts 2.75 and 74.25. The highway runs across SW Turkey (Antalya), and it is built in 1993-2000. Climate has a transition between the Mediterranean climate and terrestrial climate with an average temperature of 13ºC and approximately 405 mm precipitations [12]. There are forest lands on both side of the expressways, consisted of mostly Brutian pine (*Pinus brutia* Ten.).

In this study, a wildlife crossing is designed for two fragmented areas (Mehmet Akif Ersoy Urban Forest and 607$^{th}$ Burdur Forest Compartment) located in the city of Burdur (Figure 2). For this purpose, computer software has been used to maintain a map that has been supported with photographs.


*Figure 2. Location of the case area*

## 115. RESULTS AND DISCUSSION

In the study, a wildlife crossing has been designed for two fragmented areas in the city of Burdur. Figure 3 has illustrated the previous and future form of the landscape. Width and length of wildlife crossing designed as overpass are 30 m and 50 m, respectively. Vegetation of wildlife crossing is natural. Namely, it consists of Brutian pine and maquis plants (e.g. *Phillyrea latifolia, Spartium junceum, Erica manipuliflora, E. arborea, Paliurus spina-christi, Styrax officinalis*) growing naturally in the province. As a matter of fact, Özçelik et al. [13] have reported that the main vegetation formation of province is maquis forming under the influence of the general climate type. As many smaller forest-dwelling species appear to be reluctant to

cross roads, the construction of this vegetated wildlife overpass appears to have facilitated opportunities for movement that has been exploited by local species [14].

The choice of location for wildlife crossing has been noted to be the narrowest part of the expressway for more comfortable passage of animals. For example, crossing structures, built with the shortest dimensions possible, have been suggested for the most effective passage of mule deer under Utah highways [15]. The other aim of location selected for wildlife crossing is to provide the best connection between two fragmented forest areas. On the other hand, wildlife funneling, typically using fences, can be beneficial for effective use of wildlife crossing. Wildlife crossing signs encouraging drivers to slow down and be more observant of the expressway should be used.

Wildlife overpasses appear to accommodate more species of wildlife that do underpasses. Primary advantages relative to underpasses are that they are less confining, quieter, and can maintain ambient conditions of rainfall, temperature and light. Furthermore, overpasses can serve both as passageways for wildlife and intermediate habitat for small animals such as reptiles, amphibians and small mammals. By providing intermediate habitat, overpasses may provide a feasible alternative for various species to cross highways, especially small animals [4]. On the other hand, the most important drawback is that they are expensive. The availability of adequate funding is one of the primary limiting factors to establish a wildlife crossing structure.

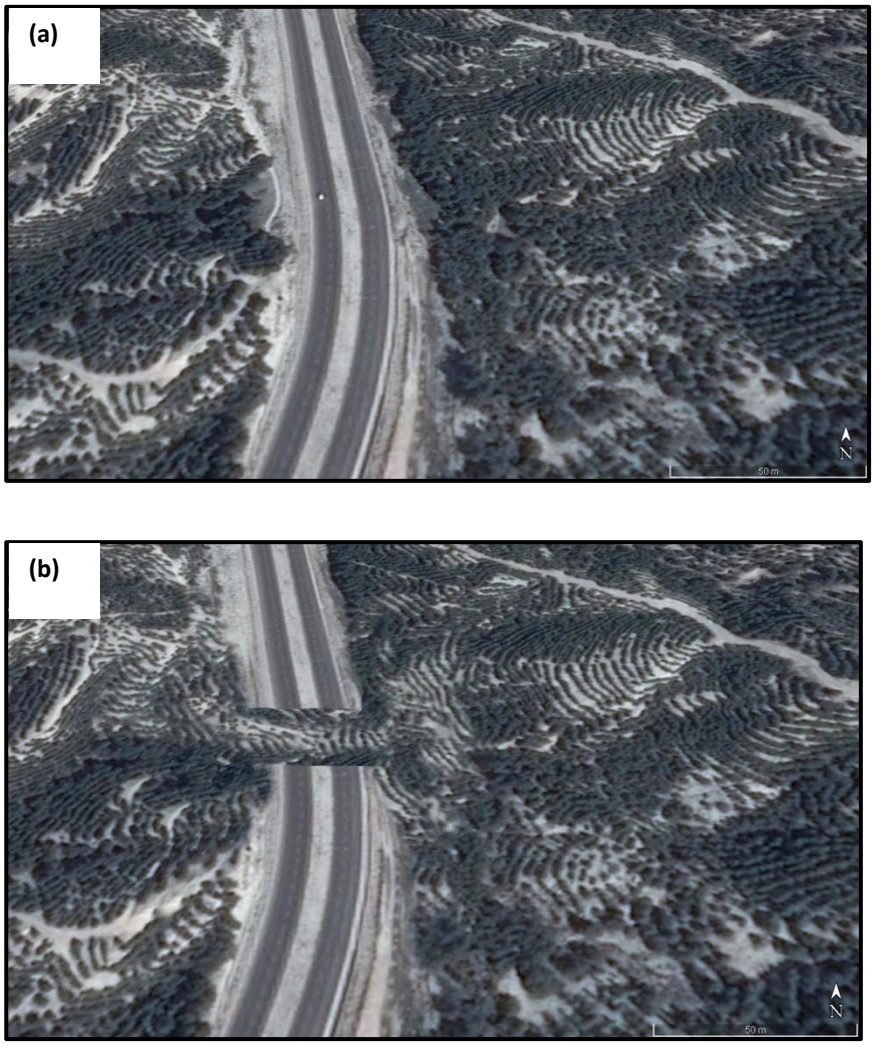


*Figure 3. (a) Expressway before wildlife crossing; (b) Expressway after the suggested wildlife crossing*

In conclusion, this is a preliminary study for the region. The different initiatives, environmental regulations, magnitude of the installation, target species, maintenance issues, budgets, and stakeholder attitudes toward such a project have influenced the decision to establish a wildlife crossing. Building wildlife crossings requires a considerable amount of funds, so it is essential to know their effectiveness and to monitor how often they are used by different species. In the further studies, a detailed study on the flora and fauna of the forest on both sides of the wildlife crossing needs to be conducted. Monitoring and maintenance plans should be prepared to ensure that mitigation systems continue to function over time.

## REFERENCES

[320]. A. Sott, *The Efficacy of Wildlife Crossings as Constructed Corridors: Lessons for Planning Natural Heritage Systems in Ontario*, Queen's University Kingston, Ontario, Canada, 2012.

[321]. Z. Ballok, A. Nahlık, and T. Tarı, Effects of Building a Highway and Wildlife Crossings in a Red Deer (*Cervus elaphus*) Habitat in Hungary, *Acta Silv. Lign. Hung*., Vol. 6, pp. 67-74, 2010.

[322]. P.C. Cramer, and J.A. Bissonette, *Wildlife crossings in North America: the state of the science and practice*. IN: Proceedings of the 2005 International Conference on Ecology and Transportation, Eds. Irwin CL, Garrett P, McDermott KP. Center for Transportation and the Environment, North Carolina State University, Raleigh, NC: pp. 442-447, 2006.

[323]. L. Cavallaro, K. Sanden, J. Schellhase, M. Tanaka, Designing Road Crossings for Safe Wildlife Passage: Ventura County Guidelines, A Group Project submitted in partial satisfaction of the requirements for the degree of Masters of Environmental Science and Management for the Donald Bren School of Environmental Science and Management, University of California, 2005.

[324]. J. Downs, M. Horner, R. Loraamm, J. Anderson, H. Kim, and D. Onorato, Strategically Locating Wildlife Crossing Structures for Florida Panthers Using Maximal Covering Approaches, Transactions in GIS, Vol. 18, pp. 46-65, 2014.

[325]. E. Chan, Wait – Don't Swerve! How to Safely Share the Road with Wildlife. CTVNews.ca, 2014. (access date: 22.04.2016).

[326]. S.D. Jackson, and C.R. Griffin, A strategy for mitigating highway impacts on wildlife. In: Messmer, T.A., West, B. (Eds.), Wildlife and Highways: Seeking Solutions to an Ecological and Socio-economic Dilemma. The Wildlife Society, Bethesda, MD, pp. 143–159, 2000.

[327]. R.T.T. Forman, D. Sperling, J.A. Bissonette, A.P. Clevenger, C.D. Cutshall, V.H. Dale, L. Fahrig, R. France, C.R. Goldman, K. Heanue, J.A. Jones, F.J. Swanson, T. Turrentine, and T.C. Winter, *Road Ecology; Science and Solutions*. Island Press, Washington DC, 2003.

[328]. D.J. Glista, T.L. DeVault, and J.A. DeWoody, *A review of mitigation measures for reducing wildlife mortality on roadways*, USDA National Wildlife Research Center - Staff Publications. Paper 846, 2009.

[329]. M. Hartmann. (2005) Evaluation of Wildlife Crossing Structures: Their Use and Effectiveness [Online]. Available: Wildlands CPR website.

[330]. A.P. Clevenger, and N. Waltho, *Long-term, year-round monitoring of wildlife crossing structures and the importance of temporal and spatial variability in performance studies*, Proceedings of the International Conference on Ecology and Transportation 2003, pp. 293–302, 2003.

[331]. H. Yiğitbaşıoğlu, and A. Uğur, Burdur Gölü Havzasında Arazi Kullanım Özelliklerinden Kaynaklanan Çevre Sorunları. *Ankara Üniversitesi Çevrebilimleri Dergisi*, Vol. 2, pp. 129-143, 2010. (in Turkish)

[332]. H. Özçelik, İ. Çinbilgel, A. Koca, and B. Muca, B. Mermer Ocaklarının Burdur Florası Üzerine Etkileri. Ulusal Mermer ve Taş Ocakları Onarım Teknikleri Sempozyumu, 18-20 Eylül 2014, Isparta, 2014. (in Turkish)

[333]. D.N. Jones, and J. Pickvance, Forest Birds Use Vegetated Fauna Overpass to Cross Multi-Lane Road, *Oecologia Australis*, Vol. 17, pp. 147-156, 2013.

[334]. M. Schwender, Mule Deer and Wildlife Crossings in Utah, USA. All Graduate Theses and Dissertations. 2013, Paper 1465.

***Assoc. Prof. Dr. Cengiz Yücedağ***

*Presenting Author*

I have been working at Department of Landscape Architecture, University of Mehmet Akif Ersoy, Burdur-Turkey. My research interests are urban forestry, protected areas and population genetic.

# The Use of Conditional Probability and Expected Value Functions to Maximize Earnings on Betting Games

*Nurhayat Varol*[49], *Serkan Varol*[50]

***Abstract***

Betting on sport games has become a rife habit since the invention of gambling software that allows online monetary transactions. Despite its glamour and intense imaginative power of being wealthy, people lose billions of dollars in total. The purpose of this research is to promote a new approach that people can utilize to maximize their earnings based on the use of conditional probability and expected value theorem on a bet. The proposed approach measures how often the individuals' predictions are accurate versus the actual results on betting games which finds the intersection of probability of the initial prediction and the final score of a game. The validity of the model is proven with a practical example. The results of the study are presented, and recommendations are made to help individuals to achieve the best practice in terms of maximizing their earnings on a bet.

**Keywords: Conditional Probability, Expected Value, Maximize Earnings, Betting, Gamble**

## 116. INTRODUCTION

Winning at sports betting is a desired outcome that most people would be motivated to success. It is usually performed through internet outlets and bookmakers. There are many domestic and international organizations that run betting activities on sport games, but as far as the history, Software System LTD is known as the first company to create a gambling software in 1994 while the CyptoLogic is recognized as the first company who allowed online monetary transactions in 1995 [1].

According to Hing et al. [2] commercial arrangements between gambling operators and sport organizations yield extensive promotion of gambling during televised sports. They applied a survey on 544 Australian sports bettors with varying degrees of problem gambling severity indicate that problem gamblers have highest approval of these promotions. They concluded that frequent exposure of sports bettors to the proliferation of gambling and sports betting promotions that are now firmly integrated into televised sports broadcast may supply marketing cues that steer additional consumption, especially amongst problem gamblers. They claimed that problem gamblers report viewing these gambling promotions more favorable compared to non-problem and at-risk gamblers and to feel more encouraged and effected to bet by this type of marketing [2].

Canale et al. [3] have investigated the impact of online gambling on gambling problems in a large-scale nationality representative sample of Italian youth, and to determine and examine a subgroup of online gamblers that reported higher rates of gambling problems. They used data from ESPAD®Italia2013 (European School Survey Project on Alcohol and others), a national school survey applied every year to observe risk-attitudes among Italian young population. Participation in eight various gambling activities was assessed, including football pools, sport betting. The result shows that adolescent participation in online gambling is significantly relevant to greater problem severity. Rates of adolescent problem gambling were five times higher among online gamblers than non-online gamblers [3].

Lorentziadis [4] has investigated the game theoretic perspective in auction bidding. He claims that the predictive power of auction theory remains in many cases limited. So, he concentrated to improve the applicability of auction theory yielding to

[49] *Corresponding author: Firat University, Vocational School of Technical Sciences, 23119, Elazig, Turkey, nurhayat_varol@yahoo.com*

[50] *Lamar University, Texas, US, serkanvarol23@gmail.com*

more realistic descriptions of bidding attitudes. He concluded that the growing application of auctions as a means of economic trading will certainly give rise to new unanticipated problems yielding to unchartered research ways [4].

Gainsbury et al. have studied [5] on consumer attitudes towards Internet gambling that contributes to difficulties in developing regulations to encourage the use of regulated online gambling sites. They have concerned the issues of player protection, policies and responsible gambling. They summarized that policy makers should take continues actions to ensure that consumer protection measures are sufficiently rigorous and appropriate [5].

Thanks to the rapid development in internet era, the number of betting sites have increased dramatically and as a result, people bet more than ever despite the prolonged economic downturn. According to survey performed by ESPN, there are about 180 million American gambled on sports as of 2008. Also, a recent survey has stated that 44% of 12$^{th}$ grade males had bet on sport gambling at least once, also 42% of Americans are ready to vote for legal sports betting in all states, if legalized sports betting is expected to generate more than $10 billion per year, also $100 million taxes per state. Surprisingly, gambling produce more revenue than movies, theme parks etc. In the down side, American has lost $119 billion gambling in 2013, followed by China for $76 billion [6].

Since betting has been a lifestyle of many people in the world, people are seeking for useful methods to maximize their earnings. In this research, the study of conditional probability (CP) and expected value (EV) are combined to evaluate sport betting, thus bring a new approach in terms of maximizing earnings.

## 2. THE PROPOSED MODEL WITH AN EXAMPLE

Let's assume a gambler who wants to bet on soccer games at Liga BBVA (Spain) and Serie A (Italy) is accessing betting odds as given below (Table 1 and Table 2).

Table 1. Soccer games at Liga BBVA, Spain

| **GC** | *Liga BBVA(L)* | | | *ODDS* | | |
|---|---|---|---|---|---|---|
| | **Home** | | **Away** | **1** | **0** | **2** |
| **L1** | Gatefe | **vs** | Malaga | 2.20 | 2.90 | 2.50 |
| **L2** | Real Madrid | **vs** | Granada | 1.35 | 4.75 | 4.00 |
| **L3** | Valencia | **vs** | R.Betis | 1.35 | 3.60 | 5.50 |
| **L4** | Eibar | **vs** | At.Madrid | 5.00 | 3.50 | 1.40 |
| **L5** | R.Sociedad | **vs** | Espanyol | 1.80 | 3.10 | 3.10 |
| **L6** | Sevilla | **vs** | Celta Vigo | 1.65 | 3.30 | 3.40 |
| **L7** | D.La.Coruna | **vs** | Sporting Gijon | 1.85 | 3.00 | 3.10 |
| **L8** | Villarreal | **vs** | Bilbao | 1.80 | 3.20 | 3.00 |
| **L9** | Barcelona | **vs** | Levante | 1.35 | 4.75 | 4.00 |
| **L10** | Las Palmas | **vs** | Vallecano | 1.80 | 3.10 | 3.10 |

The given odds ($GC_R$) are the conversion of implied probabilities where $R$ is the probability of each event in a game as home-win (1), draw (0) and away-win (2). Implied probabilities are calculated as $IP_{GC_R} = 1/GC_R$. Hence, when $GC_R = L1_1$, $IP_{GC_R} = \frac{1}{2.20} = 0.45\%$. It basically implies that the betting company assumes that Getafe has a 46% of probability of winning game L1 against Malaga whereas $L1_0 = 34\%$ and $L1_2 = 40\%$. When $IP_{L1_1} + IP_{L1_0} + IP_{L1_2} = 110\%$ which proves that the betting

company makes a certain profit out of any given bet, therefore $GC_R$ is reduced by the amount of profit percentage.

Table 2. Soccer games at Serie, Italy

| GC | *Seria A(S)* | | | *ODDS* | | |
|---|---|---|---|---|---|---|
| | **Home** | | **Away** | **1** | **0** | **2** |
| **S1** | Udinese | **vs** | Empoli | 1.85 | 3.00 | 3.10 |
| **S2** | AC Milan | **vs** | Palermo | 1.50 | 3.30 | 4.30 |
| **S3** | Chievo | **vs** | Inter | 3.20 | 3.00 | 1.80 |
| **S4** | Atalanta | **vs** | Verona | 1.80 | 3.00 | 3.20 |
| **S5** | Bologna | **vs** | Frosinone | 1.80 | 3.10 | 3.10 |
| **S6** | Genoa | **vs** | Juventus | 3.75 | 3.20 | 1.60 |
| **S7** | Roma | **vs** | Sassuolo | 1.30 | 3.75 | 6.25 |
| **S8** | Torino | **vs** | Sampdoria | 1.70 | 3.20 | 3.30 |
| **S9** | Capri | **vs** | Fiorentina | 3.50 | 3.10 | 1.70 |
| **S10** | Napoli | **vs** | Lazio | 1.70 | 3.20 | 3.30 |

In this research, it is assumed that the betting company decides not to make any profit from games, thus offer original odds. Therefore, in order to access initial implied probabilities ($OIP_{GC_R}$), the first step is to find the profit rate, also named as bet profit (BP*) that the company implied on bets.

$BP_{L1_1}$=$L1_1/\sum(GC_R */ GC_R)$ where R=1,0,2 and $BP *_{L1_1} = 1 - BP_{L1_1}$

Then, original given odds ($OGC_R$) are calculated as follows

$OGC_R$=$L1_1/ BP_{L1_1}$

After all, original implied probabilities can be found:

$OIP_{GC_R}$=$1/OGC_R$

Assume that $L1_1$ is taken as a sample unit, then $BP *_{L1_1} = 16.4\%$, $OGC_R$=2.64 and $OIP_{GC_R}$ is measured to be 37.8%. In theoretical explanation, the original calculated odds are 37.8% (Getafe wins). However, the betting company adds 16.4% profit on every bet that they offer, thus the implied probabilities are artificially increased and set to be 45%. Original implied probabilities equal to 1. ($OIP_{L1_1} + OIP_{L1_0} + 0IP_{L1_2} = 100\%$).

In order to consolidate the problem and make it more understandable, conditional probabilities which is an important concept on probability theory that measures the probability of an event by assuming that another event has already occurred of predicting games scores and results are given as illustrated on Table 3 below. It is based on research predictions that reflect the relationship between predicting and final scores, represented as $CP_{xy}$ where x is initial predict and y is final score of the selected game. For example: $CP_{11}$ gives the interaction between the initial predict of home win and the actual result of home win. It is often illustrated on a tree diagram to ease understanding of problems.

Table 3: Conditional Probability that measures the probability of an event

| Conditional Probability | | Initial Predict | | |
|---|---|---|---|---|
| | | **1** | **0** | **2** |
| $CP_{xy}$ FINAL SCORE | **1** | $CP_{11}$ | $CP_{01}$ | $CP_{21}$ |
| | **0** | $CP_{10}$ | $CP_{00}$ | $CP_{20}$ |
| | **2** | $CP_{12}$ | $CP_{02}$ | $CP_{22}$ |

| Conditional Probability | | Initial Predict | | |
|---|---|---|---|---|
| | | **1** | **0** | **2** |
| $L1$ FINAL SCORE | **1** | 46% | 28% | 26% |
| | **0** | 32% | 20% | 48% |
| | **2** | 7% | 40% | 53% |

## 3. FINDING INTERSECTION OF BOTH PREDICTIONS AND IMPLIED PROBABILITIES OF A BET

This part of research aims to find the intersection of probability of the initial prediction and the final score of a game. This gives vital information to users to find how often individuals' predictions are $R$ using the Table 4 below and it ties in predictions of game scores to return which the odds of winning money from a game (It basically measures how often is individuals predictions are accurate versus the actual results).

Table 4. Intersection of probability of initial prediction

| $F_{xy}$ | **1** | **0** | **2** |
|---|---|---|---|
| **1** | $F_{11} = CP_{11}\ x\ OIP_{L1_1}$ | $F_{01} = CP_{01}\ x\ OIP_{L1_1}$ | $F_{21} = CP_{21}\ x\ OIP_{L1_1}$ |
| **0** | $F_{10} = CP_{10}\ x\ OIP_{L1_0}$ | $F_{00} = CP_{00}\ x\ OIP_{L1_0}$ | $F_{20} = CP_{20}\ x\ OIP_{L1_0}$ |
| **2** | $F_{12} = CP_{12}\ x\ OIP_{L1_2}$ | $F_{02} = CP_{02}\ x\ OIP_{L1_2}$ | $F_{22} = CP_{22}\ x\ OIP_{L1_2}$ |

The following table explains when predictions are made to score $R$, how often the final score turns out be $R$ (Table 5 and Table 6).

Table 5. Actual probabilities of winning game

| 1=Home Win<br>0=Draw<br>2=Away Win | | **Actual Probabilities of Winning Game** | | |
|---|---|---|---|---|
| | | **1** | **0** | **2** |
| **Predictions** | **1** | $F_{11}/(F_{11}+F_{10}+F_{12})$ | $F_{10}/(F_{11}+F_{10}+F_{12})$ | $F_{12}/(F_{11}+F_{10}+F_{12})$ |
| | **0** | $F_{01}/(F_{01}+F_{00}+F_{02})$ | $F_{00}/(F_{01}+F_{00}+F_{02})$ | $F_{02}/(F_{01}+F_{00}+F_{02})$ |
| | **2** | $F_{21}/(F_{21}+F_{20}+F_{22})$ | $F_{20}/(F_{21}+F_{20}+F_{22})$ | $F_{22}/(F_{21}+F_{20}+F_{22})$ |

Table 6. Results of actual probabilities of winning game and expected value

| Game:L1 | | Actual Probabilities of Winning Game | | | Expected Value |
|---|---|---|---|---|---|
| | | **1** | **0** | **2** | |
| **Predictions** | **1** | 60% | 32% | 8% | 1.20 |
| | **0** | 36% | 19% | 45% | 1.19 |
| | **2** | 24% | 33% | 43% | 1.14 |

An assumption has been made that Min ($OIP_{L1_R}$) = 1 where R is 0, then $OIP_{L1_1}$/ $OIP_{L1_0}$ and $OIP_{L1_2}$/ $OIP_{L1_0}$ give the corresponding factors of each $OIP_{L1_R}$. Therefore, when $OIP_{L1_0}$ is equal to 1 unit, $OIP_{L1_1}$ can bring 1.32 unit and $OIP_{L1_2}$ can bring 1.16 unit. ($L1_1 = 1.32$ nd $L1_{0=}1$ and $L1_2$=1.16)

## 5. RESULTS AND CONCLUSION

The proposed model help subjects to choose from complicated bets based on their own observation with given odds. The result of the sample indicates that the person should select draw over away win in such given case despite initial odds suggested that away win must be chosen by margin.

Combining conditional probabilities with expected value enhance the chance of getting more accurate results in betting games. The model can be expanded to where an actual survey is made and predictions are obtained from subjects and initiated with odds, which even give more accurate results to users.

## REFERENCES

[335]. Banks, James (2012). Online gambling and crime: a sure bet? The ETHICOMP Journal
[336]. Hing, N., Lamot, M., Vitartas, P., Fink, E., (2015), Sports bettors' responses to sports-embedded gambling implications for compulsive consumption, Journal of Business Research 68 (2015) 2057-2066.
[337]. Canale, N., Griffiths, M. D., Vieno, A., Siciliano, V., (2016), Impact of internet gambling on problem gambling among adolescents in Italy: Findings from a large-scale nationally representative survey, Computers in Human Behavior 57 (2016) 99-106.
[338]. Lorentziadis, P. L., (2016), Optimal bidding in auctions from a game theory perspective, European Journal of Operational Research 248 (2016) 347-371.
[339]. Gainsbury, S., Parke, J., Suhonen, N., (2013), Consumer attitudes towards internet gambling: Perceptions of responsible gambling policies, consumer protection, and regulation of online gambling sites, Computers in Human Behavior 29 (2013) 235-245.
[340]. REAP, (2016), Sport Gambling Facts and Statistics, http://www.ncpgambling.org/wp-content/uploads/2015/01/Sports-Gambling-Facts-and-Statistics.pdf, last accessed date: March 16, 2016.

# Research on Retinal and Iris Identification Systems

***Yeşim Ülgen Sönmez[51], Asaf Varol[52]***

***Abstract***

*Biometrics is the science that analyzes biological data and also the technology that measures biological data. Biometric systems make identification or identity verification by using measurable, distinctive physical and behavioral properties of humans. The most widely used biometrics techniques rely on finger prints, palm, hand geometry, iris, retina, face, ear shape, vein, signature, hand writing and voice identification of an individual. Iris identification systems and retina identification systems are the most accurate and reliable identifying techniques. Iris is a circular structure surrounding the pupil, which determines eye color. The iris is a very rich tissue and it has a unique texture. This texture is different for each individual and it will stay same throughout their lives. Iris identification systems use the mathematical pattern-identification algorithms and statistical methods on v l ' . R , l , q h h an unchanging texture throughout the life, except for some side effects of diseases. Retina that is located in the back side of the eye is responsible for vision. The mesh of blood vessels in retina is very complicated and distinctive. In retina identification systems, firstly, infrared light is radiated into the eye and blood vessels create unique reflections of this light. Retina identification is used in many areas from security systems to medical applications. This study examines and presents similarities and differences between two ocular biometric systems which are iris identification systems and retina identification systems. Analysis has also been carried out suing the findings of this study.*

**Keywords: Biometrics, Iris identification System, Retina identification System.**

## 1. INTRODUCTION

Biometric systems work with the principle of examining and identifying some unique physiological and behavioral characteristics of each person. The way the human brain works is taken as the basis of biometric systems. In such systems, there are two phases called identification and verification. In identification phase, data is collected and saved in the database as computer codes (which are digital codes). In the verification phase, the data collected is compared with the data of the person who requests access and a conclusion is reached by the system.

Iris and retina identification systems are among ocular identification systems. However, they do have different structures and they are different biometric systems. Iris and retina tissues are unique and distinctive for each and every human being. The structure of iris does not change from birth to death. Retina tissue also does not change, however it is affected by some diseases like diabetes, high blood pressure, MS and leukemia. Thus, iris and retina identification systems are the highest grade biometric systems in their field with the properties of uniqueness, accuracy, universality and permanence. The rich texture of iris is essential for the iris identification systems. The shape of capillaries is taken into account for retina identification systems.

[51] S w E , T h l F l , F U v , El z ğ, T k , yesimulgen123@gmail.com
[52] C h : S w E , T h l F l , F U v , El z ğ, T k , v l. @ il.com

This study examines and presents similarities and differences between two ocular biometric systems which are iris identification systems and retina identification systems. Analysis has also been carried out suing the findings of this study.

### *1.1. Biometric System Characteristics and Criteria*

There are unique characteristics used in biometric systems which are unique for each and every human being. These can be finger prints, palm structure, hand shape, vein patterns, finger joint prints in hands, ear shape, teeth, tongue print in face area, retina, iris and sclera in the eyes, and as with biological properties go, DNA, bodily scent, heart sound, or behavioral features such as voice, signature, keystroke patters and style of walking. [1].

Biometric traits must have some criteria. These criteria can be listed as follows [1, 2].

- Universality: Every person should have that particular trait [1-5]. It should exist in every individual.
- Distinctiveness/Uniqueness: The trait should be effectively different for each person [1-5].
- Permanence: The characteristic should not change as time goes by, it should permanently stay the way it is [1-5].
- Collectability: The trait which will be measured should be easily acquired by suitable devices. [1-5].
- Measurability: The quantitative measurability of the trait.
- Performance: Performance is accuracy and speed, and also robustness of the technology used [1-4]. It is the relative success of defining the biometric trait [1].
- Acceptability: The approval rating of the technology used [1-5]. This can be defined as agreeable of acquisition and assessment of the biometric characteristic [1-5].
- Circumvention: The ease of using a substitute [1-4]. The biometric system can be fooled easily by unauthorized persons.
- If the human trait carries the permanence, universality, uniqueness, collectability criteria, it can be used for querying within a biometric system. If a system uses such a biometric trait and appropriate and robust technological equipment, it can be accepted as a reliable and powerful biometric system.

Table 1 shows the comparison of iris and retinal biometrics, according to biometric trait criteria, under suitable conditions [1, 2]. In the table, H means "high", L means "low" and M means mediocre.

Table 1. Comparison of iris and retina characteristics [1, 2, 6].

| | Uniqueness | Universality | Permanence | Measurability | Performance | Acceptability | Circumvention |
|---|---|---|---|---|---|---|---|
| Iris | H | H | H | M | H | L | L |

| | | | | | | | |
|---|---|---|---|---|---|---|---|
| Retina | H | H | M | L | H | L | L |

The measurements used in biometric systems are called biometric measurements. There are international standards for the use of these systems in passwords. These standards are set by INCITS, International Committee for Information Technology Standards [2, 7]. Thanks to these standards, any person with a bank account who can reach his account with iris or palm identification systems, can reach his bank account in his home country from anywhere around the world and make a transaction [2].

### *1.2. Comparison of Iris and Retinal Biometrics*

In table 2, ease of use, possible problems, performance and security requirements of iris and retinal biometric systems under appropriate conditions have been compared.

Retina identification systems are systems with high accuracy and speed; however, because they need focus of the camera, they are not widely used biometrics [1, 4, 8].

Table 2. Comparison of iris and retina biometric systems [1, 8].

| Biometric Trait | Ease of Use | Problems | Accuracy | Security Requirements |
|---|---|---|---|---|
| Retina | Low | Glasses | Very high | High |
| Iris | Medium | Light | Very high | Very high |

### *1.3. Areas in Which Retina and Iris Biometrics are used*

In table 3, the most common usage areas for iris and retinal biometrics have been listed. The most widely used biometric traits that are used for border security application are iris and retina. In ID cards and passports however, iris is used more in comparison to retina.

Table 3. Fields of application for iris and retinal biometrics [1, 9].

| | Iris | Retina | Sclera |
|---|---|---|---|
| Border Security | x | x | |

| | | | |
|---|---|---|---|
| Forensics | | | |
| Identification of Criminals | x | x | |
| ID Cards | x | | |
| Passports | x | | |
| Computer Logon Processes | x | | x |
| Access Control | x | x | x |
| Electronic Trade | x | | x |
| Smart Phones | | | |
| Imaging Systems | x | | |
| Watching Videos | | | |
| Missing Child Identification | x | | |
| Crowd Tracking | | | |
| Electronic Banking | | | |

## 2. OCULAR BIOMETRICS

Because of relatively more accurate and permanent characteristics of ocular biometric traits, many different approaches have been developed regarding ocular identification [1, 9]. The most important biometric traits in the ocular area are iris, sclera and retina. In iris based biometric systems, identification is done by benefiting from color, shape and the properties of iris tissue. Besides the distinctive property of iris, as these character based systems are relatively expensive and prone to attacks, they are not very widely used [1, 10].

In retina based biometric systems, the attributes of blood vessels which filter the light and optical field in retina are used as the distinctive traits [1, 9]. As the retina identification systems are expensive and it is rather difficult to obtain the data, they are not also widely used.

The sclera of the eye consists of blood vessels. The particular patterns of these blood vessels are used in sclera based biometric systems. [1, 9].

### *2.1. The Structure of the Eye and Eyesight*

Eyes are very special and important organs which take in the light that is originated from the sun, and reflected from objects. The light that is visible to human eye is called visible light. It is the light in between wavelengths of 400 and 700 nanometers. Human eyes cannot perceive X rays, ultraviolet rays and infrared rays [11, 12]. Eye consists of two types of structures, one for sight, and others for the protection of these structures. The protective structures are the eyelids, eyebrows, eyelashes, lacrimal glands, and the muscles that connect the eyes to their circular orbits and provide movement [11]. The structure of a human eye is made up of three layers. These layers are the sclera on the outer layer, choroid in the middle and retina in the inner layer [11].

Sclera is the white part of the eyeball. Sclera is a structure that surrounds and protects the eye. It becomes the transparent cornea on the front side of the eye and lets the light enter.

Choroid is beneath the sclera. Its exact place in the eye is shown in figure 1. It consists of blood vessels that feed the eye. It also absorbs excess light and prevents damage to the eye. Choroid gets thicker in the front side of the eye and becomes the round and colorful structure called iris [11].

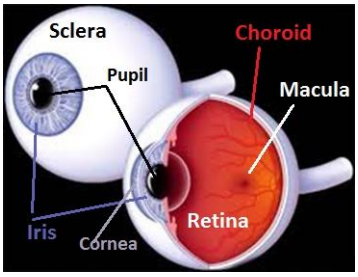


*Figure 1. Anatomy of the eye [39]*

Iris can be in different colors according to the color material that it possesses. Iris color can be black, brown, blue, green or hazel.

In the middle of iris is the pupil, which is a gap. The light enters the eye through this gap and goes to the back of the eye, to retina. As shown in figure 2, iris either enlarges or shrinks the pupil, according to the amount of light entering the eye. Thus, pupils constrict in bright light and they dilate in darkness.

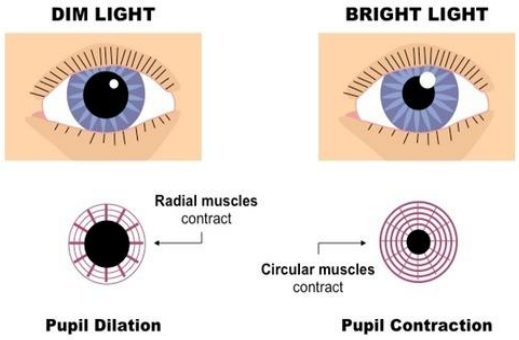


*Figure 2. Constriction and dilation of the pupils [40].*

Retina is the inner layer of the eye. It receives colors and impulses and provides vision. As there are networks of nerve endings in this layer, it is called the retina [11].

### *2.2. The phases in which the vision is realized*

Vision starts with the rays of light coming from the sun which are reflected from the objects to come to our eyes. Any ray of light reflected from an object, gets refracted by the cornea and passes through the pupils and reaches to the lens [11].

The light that reached to the lens is refracted once again and passes on to vitreous body and reaches to the retina. The rays of light that reached the retina create electrical pulses on optic nerves. These electrical impulses allow the formation of a reverse image in the macula [11]. Optic nerve transmits this reverse image to the brain. The part of the brain which manages sight rotates the image and, thus seeing occurs.

Figure 3 shows how seeing works, how the light is refracted, where the vision is created, and how it is transmitted to the brain. The role of iris in seeing is to control the size of pupils and adjust the amount of light entering into the eye [13].

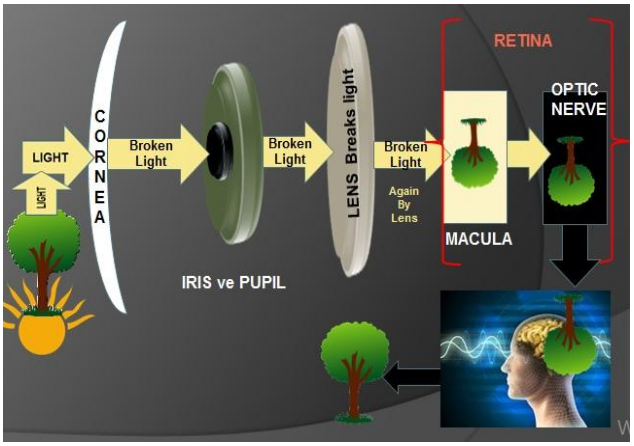


Figure 3. The phases of seeing

## 3. IRIS IDENTIFICATION SYSTEMS

Iris identification system is one of the most accurate and reliable biometric systems because it uses the unique and unchanging structure of iris. It was first introduced by John Daugman in 1993. J. Daugman, in 1994, introduced a prototype that delivers excellent results over databases with many different images and developed a human identification system based on iris analysis [13].

Iris identification is a highly reliable biometric method used for identification. The iris pattern of the person whose iris is scanned is mapped and converted into a digital code in various ways. This digital iris code is matched with the other ones in the database in order to make identification [14].

### *3.1. The Unique Structure of Iris*

In 1985, Leonard Flom and Aran Safir have proven that iris pattern of each and every human being is different [14]. This part is also the part which gives the eye its color. The color of iris depends on cell density and pigment concentration. For example, brown eyes have more cell density and pigment count compared to blue eyes. The structure of iris is not hereditary, however its color is.

*Figure 4. Different iris structures*

The features related to the unique structure of iris which enables it to be a biometric trait are as follows;

- The structure of each person's irises is unique. Even though DNA structures in twins are the same, their irises are still different.
- There are even differences between the right and left irises.

- Iris is much less affected by genetic factors.
- Iris structure does not change with genetic diseases.
- Race, gender or skin color does not affect the characteristics of the iris.
- It is an internal organ which can be seen and measures externally.
- The structure of iris does not change. Due to its permanence, it is a secure biometric trait.
- Eye is the organ which loses its viability the quickest after death.

Figure 4 illustrates different iris tissues. Iris possesses the tissue properties of sclera and retina [13]. In biometric systems, this rich tissue's structure is converted into digital codes using various methods [14].

For a clear visibility of the iris tissue, the eye should be photographed using 750 nm infrared light. Because with visible daylight (400-700 nm), these tissues can't be seen clearly [14].

### *3.2. The Way the Iris Identification Systems Work*

#### *3.2.1. Photographing the Iris*

There are stages of iris identification systems. In the first stage, digital photographs of the person who requests access to the system are taken using video cameras. This stage requires the person to willingly look at the camera. This biometric system is not intrusive as there is no contact with the eye by the camera, thus it is healthy. This way of it increases its adoption level by the people.

#### *3.2.2. Localization – Locating the Iris and the Pupil*

The captured image is processed using visual processing methods. Meanwhile, iris and pupil is distinguished in the image taken and the remaining parts are removed from the image. The purpose for doing that is to separate eyebrows, eyelashes etc. from the iris in order to create a code and make a healthy analysis. At this stage, the center of the pupil is also determined [13]. Various edge detection methods are applied in this stage.

#### *3.2.3. Segmentation*

At this stage, as shown in Figure 5, the circular edge between the iris and the pupil, and the circular edge between the iris and the sclera is determined.

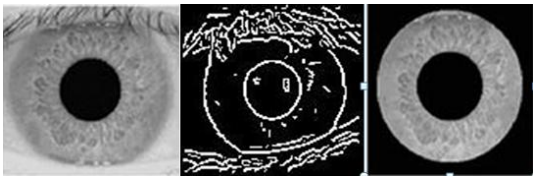

Figure 5. Determining circular borders and noise [13, 41]

The noise on the iris image is removed using a variety of image processing techniques. The noises over the iris image are factors like eyebrows, eyelashes, eyelids and light reflections etc. The removal of

such factors from the image is called noise detection [13, 45, 46]. In figure 5, the pupil, iris and sclera is separated from each other using circular edge detection methods.

#### *3.2.3.1. John Daugman Segmentation Method*

Daugman used circular edge detection methods to determine the borders of iris, pupil and sclera. Especially to separate sclera from the iris, he used maximum gradient integrodifferential equation in iris images [13].

$$max_{r,x_0,y_0}\left|\frac{\partial}{\partial r}\, G(r) * \oint_{r,\ x_0,y_0} \frac{I(x,y)}{2\pi r}\ ds\right| \quad (1)$$

$$G(r) = \left(\frac{1}{\sqrt{2\pi}\,\sigma}\right) e^{-\left(\frac{(r-r_0)^2}{2\sigma^2}\right)} \quad (2)$$

*G(r)*, is the radial Gaussian function. *I(x, y)* is the input iris image. The firs equation looks for the maximum value with fuzzy partial derivative for increasing radius and (0, 0) $x_0$ , $y_0$ central coordinate. This method is also called active contour fitting [13, 15].

#### *3.2.3.2. John Daugman Polar Conversion Method*

The system generates a coordinate system on the localized iris image. The center of the coordinate system is the center of the circular pupillary boundary. Figure 6 shows the cartesian form of the iris image [13, 41].

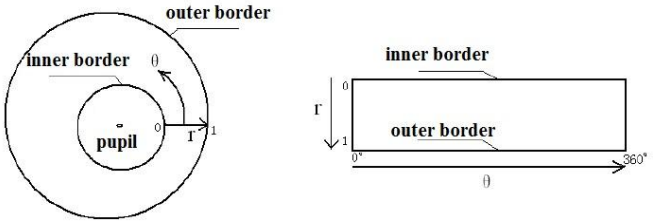


**Figure 6.** Cartesian form of the iris image, normalization and polar form [41, 42, 46].

#### *3.2.4. Normalization - Polar Transformation*

At this stage polar transformation is applied to the image and it is converted into dimensionless form polar from cartesian form. Daugman used radial scaling method for polar conversion [13, 46].

$$x(r,\theta) = (1-r)x_p(\theta) + rx_1(\theta) \quad (3)$$

$$y(r,\theta) = (1-r)y_p(\theta) + ry_1(\theta) \quad (4)$$

As shown in figure 6, the image is converted from (x, y) form into polar (r, θ) form, using image radial scaling and polar transformation [13]. Figure 7 shows (a) the image of iris area, (b) the iris image after the application of polar transformation and normalization. Daugman's polar transformation method is called Rubber Sheet model [42].

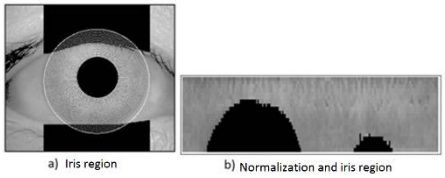


Figure 7. Normalized iris image [46].

In this stage, in order to compose a clearer iris code, histogram equalization and noise reduction methods are applied once again on the polar image.

### *3.2.5. Demodulation - Formation of Iris Code*

After the normalization, feature vector (digital code) of the polar iris image is created during the demodulation stage. Pattern identification methods are used for image identification. In the first iris identification system, the digital code of the image is reduced to a size between 256 and 512 bytes, using a function called "2D Gabor wavelet transform" [13,16]. The created iris template in other words iris feature vector is matched with other iris templates in a huge database, for the identification and verification. During all these processes, the iris code is password protected and it is impossible to use them in any other way [16].

At this stage, feature extraction is performed using Gabor wavelet filter. Gabor wavelet filter is applied on the normalized image and a binary iris code like the one seen in figure 8 is created, which is in a fixed size and universal format.

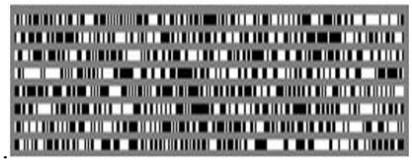

Figure 8. Binary iris code [13, 44, 45].

In the field of iris identification, there are many different feature extraction methods in literature, for converting iris images into digital codes. Some of these methods are as follows [13];

- 1-D Gabor Wavelet Transform
- 2-D Gabor Wavelet Transform
- Correlation Filter
- Haar wavelet transform
- Dydatic wavelet transform
- Discrete Cosine transform
- Log Gabor wavelet transform
- Zero-Crossing wavelet transform

### *3.2.6. Iris Identification Methods According to Iris Encoding*

Iris identification Methods according to Iris Encoding are separated into 4 different classes [13]. These classes are as follows;

- Phase based methods [17]
- Zero pass method [18, 19]
- Tissue analysis method [ 19, 20, 21,22]
- Density gradient analysis [23]

### *3.2.7. Comparison of Iris Codes*

After the iris image of the person who demands access to the system passes the segmentation, normalization and demodulation processes, it is matched with the iris templates in the database and then identification is done. For this comparison, different methods and classifiers are used.

The comparison method of Daugman was Hamming Distance [13]. Hamming distance is the comparison of two binary codes XOR and AND. It calculates the difference between the bits of two iris codes [13, 43, 45].

$$HD = \frac{(IrisCodeA \oplus IrisCodeB) \cap MaskA \cap MaskB}{MaskA \cap MaskB} \quad (5)$$

Normalized Hamming distance

$$HD = \frac{1}{2048} \sum_{j=1}^{2,048} A_j \oplus B_j \quad (6)$$

System makes matching according to the results of the Hamming distance results. It reaches to yes or no decisions. Figure 9 shows the matching in between three iris samples. Hamming distances have been calculated. The iris with the smallest value of distance matches with the code [24]. It produces a "yes" result. Without any match, a "no" answer is produced.

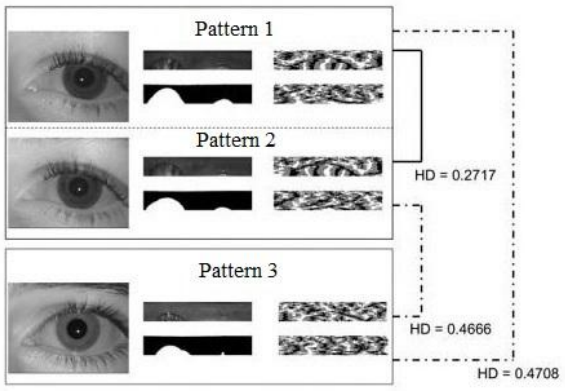


*Figure 9. Hamming distance [24].*

When the studies in the literature are examined, the classifiers used for the comparison of iris codes are as follows [13];

- Hamming Distance
- Euclid Distance
- Support Vector Machine (SVM)
- Artificial Neural Networks (NN)
- Nearest Neighbor Clustering (kNN)
- Self-Organized Feature Maps (SOM)
- Vector Quantization Learning (LVQ)
- Bayes Classifier

The iris codes derived from the iris images of a living eye are matched with another iris code which was previously saved in the database, within a few seconds. If there is any damaged bit on the iris code, the system detects it and only matches the valid ones [16].

**4. IRIS IDENTIFICATION STUDIES IN LITERATURE**

Wildes [21, 25, 26] used different methods from what John Daugman used for iris identification. Wildes first used a histogram based approach for the detection of circular edges of the iris and pupil, then, he used Hough transform [26]. Eyelids were identified as parabolic arcs.

$$H\,(x_0\,,y_0\,,r) = \sum_{j=1}^{n} h\,(x_j\,,y_j,x_c,y_c\,,r\,) \tag{7}$$

$$h\,(x_jy_jx_0y_0\,,r) = \begin{cases} 1, & if\ \ g(x_jy_jx_0y_0,r\,) \\ 0, & otherwise \end{cases} \tag{8}$$

$$g\,(x_j\,,y_j,x_0\,,y_0,r) = \\ = (x_j - x_0)^2 + (y_j - y_0)^2 - r^2 \tag{9}$$

Wildes uses image saving technique for the scaling and rotation.

$$\int_x \int_y (I_d\ (x,y) - I_a\ (x-u\,,y-v\,))^2\ \mathrm{dxdy} \tag{10}$$

$$\begin{pmatrix} x' \\ y' \end{pmatrix} = \begin{pmatrix} x \\ y \end{pmatrix} - sR(\emptyset)\begin{pmatrix} x \\ y \end{pmatrix} \tag{11}$$

Matching function that minimizes the similarity transformation which transforms (x, y) coordinates into (x', y') is used [21, 25]. Instead of capturing the spatial details of the iris, isotropic band-pass derived with Laplacian of Gaussian is made. For the matching in between the obtained pattern and the patterns in the database, normalized correlation is used.

In the literature, in different stages of iris identification, there are studies carried out for the systems to perform better [13]. These are as follows;

- Systems have been developed which use iris code as biometric secret key. These keys were more secure than crypto-graph based keys [27].

- In order to improve real time localization (iris and pupil separation), methods which are based on particle swarm optimization have been developed [28].

- 2D Haar wavelet transform was used, which separates iris images into 4 different phases and this 4 phases of high frequency information was quantized in 87 bits code form. For classification, vector quantized learning (LVQ) has been applied [29]. In another study, iris identification systems have been produced which are based on the zero pass of wavelet transform [30].

- Iris identification systems combining wavelet transform and support vector machines have been developed. Support vector machine wavelet transform method reduced the error rates.

Methods using support vector machines have given much better results compared to methods using feed-forward artificial neural networks, nearest neighbor clustering, Hamming and Mahalanobis distance classifiers [13].

As a result of the research, it's been determined that Haar wavelet transform does better feature extraction compared to Gabor filter [20]. Image 10 shows the iris code with applied 5-D Haar wavelet transform. Haar WT is used in visible light photos.

*Figure 10. Iris code with Haar wavelet transform applied [31].*

## 5. RETINAL IDENTIFICATION SYSTEMS

Retinal identification systems are biometric systems which convert the retinal pattern which consists of capillaries, into a digital code.

### *5.1. The Unique Structure of the Retina*

Retina is located behind the eyeball and is the most inner layer of the layers of the eye. It is rich in capillaries. These blood vessels absorb the excess light and protect the eye from damages. While working on ocular diseases in 1935, Dr. Carleton Simon and Dr. Isodure Goldstein found that each eye has a unique blood vessel structure [33]. Later on, it's also seen that although twins have the same genetic code, have different retinal patterns [34].

After the discovery that the retinal structure is unique and different for each and every human being, and is also universal, it's been understood that it could be used for identification and studies for a retinal identification system has been started. Retina can be affected by diseases like diabetes, high blood pressure, blood and cardio vascular diseases. This diminishes its reliability as a biometric system a little bit. In figure 11, (a) original photo of the retina, (b) blood vessel network of retina.

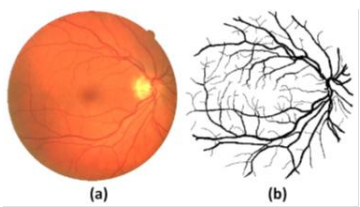

*Figure 11. (a) Original retinal image (b) Blood vessels [34, 35].*

### *5.2. Working Methods of Iris Identification Systems*

Retinal identification system consists of the following stages: obtaining retinal image, segmentation, blood vascular pattern extraction, feature extraction and filtering, finally biometric pattern matching. The flowchart of retinal identification is given in figure 12.

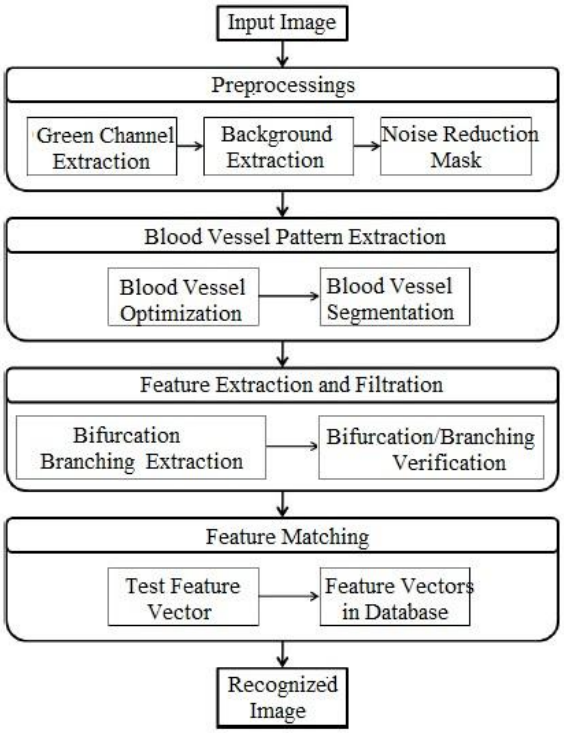


*Figure 12. Flowchart of retinal identification system [32].*

#### *5.2.1. Obtaining the Retinal Image - Acquisition*

The eye of the person who wants access to the system is photographed from close proximity. As the retina is behind the eye, the person has to stay close to the camera. The infrared ray of light is shone to the eye. This light passes the lens and follows the retinal path and reaches the capillaries in the retina. Meanwhile, the capillaries undergo changes as the light reaches them. They take different shapes and forms. These characteristic shapes are reflected to a video camera. System obtains the image from this reflection.

#### *5.2.2. Preprocessing, Segmentation and Optimization*

There are green, red and blue levels in digital photos. A photo can be viewed in different levels. Green channel has a higher density compared to red and blue channels. Thus green channel is extracted from the photo. The green channel is located with the following mathematical formula.

$$G = \frac{G}{R+G+B} \tag{12}$$

R means the red channel, G means the green channel and B means the blue channel [38]. In figure 13, retinal images have been given according to the techniques applied in the preprocessing stage.

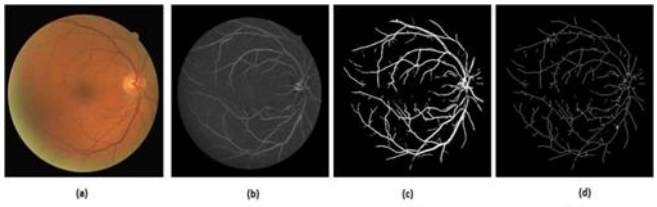


*Figure 13. (a) green channel image (b) optimized capillaries (c) Segmented image (d) Refined capillaries [34, 35].*

Preprocessing stage includes the detection of noise and separation of background from the retinal image and to highlight the blood vessel pattern. The correction of retinal identification depends on the extraction of the features of capillaries. The preprocessing includes the following actions;

- First, optimization of the image is done using wavelet transform in order to extract capillary pattern.
- A multi layered thresholding is applied on the optimized retinal image.
- Wavelet transform method is used for feature extraction. The used transform methods are as follows [34].
- Constant wavelet transform (CWT) $T\psi\ (\ b, \theta, a)$
- Fourier wavelet transform (FWT)
- 2-D Gabor wavelet transform

With Gabor wavelet transform, optimized vascular pattern can be obtained [34].

### *5.2.3. Feature Extraction and Bifurcation*

Bifurcation means branching. The main features of vascular patterns are vascular endings and branching points [35]. The system uses the crossing number method which is shown in figure 14, for the extraction of the vascular endings and branching [35]. Figure 15 shows the vascular features and branching which are obtained using this method.

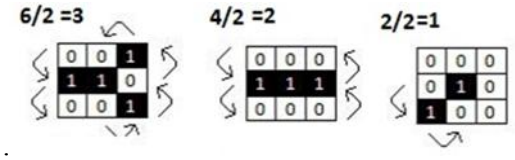


Figure 14. Crossing number method [36].

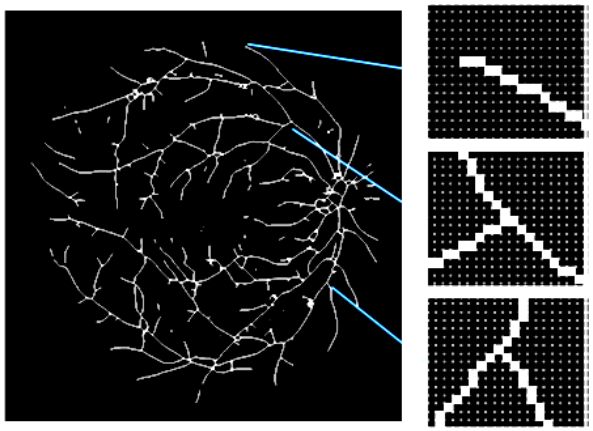

*Figure 15. Vascular features, endings and bifurcation [34].*

The mathematical expression of this method:

$$C(p) = \frac{1}{2}\sum_{i=1}^{8}|g(p_{imod8}) - g(p_{i-1})| \quad (13)$$

$g$ is the refined retinal image and $p$ represents each vascular pixel. Pixels between $p_0$ and $p_7$ are the pixels in clock wise which define the 8 neighboring of $p$ and $g(p)$ is the pixel value [34]. For vascular pixels $g(p) = 1$, for others $g(p) = 0$. $C(p) = 3$ $and$ $C(p) = 1$ are branching and vascular endings. Feature spots obtained with this algorithm are the correct ones. In order to determine the wrong spots, 9x9 windowing method is used. Figure 16 shows the wrong spots like bling spots, breaks and short blood vessels.

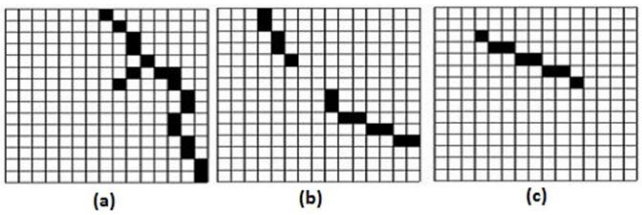


Figure 16. Wrong spots, (a) blind spots, (b) breaks, (c) short Blood vessels [36].

While obtaining the retinal vascular patterns, the purpose is to find the correct branching. After the blind spots, breaks and short blood vessels are found using windowing technique, these are eliminated [36]. Thus, correct endings and branching feature spots can be determined.

### *5.2.4. Comparison of Vascular Patterns*

This is the identification phase. The retinal image taken from the person who wants access is processed using various processing, recognition etc. methods and feature vector (digital code) is generated for the retina. This digital template is matched with other retinal templates in the big database. This comparison can be made using various methods. These methods are as follows;

- Mahalanobis distance

- Vascular pattern correlation
- Matching which use branching spots.

## 6. PERFORMANCE CRITERIA OF BIOMETRIC SYSTEMS

Performance is an important concept for computerized systems. Any computerized system should operate fast and accurate. The most important performance criteria in biometric systems are total processing time, false acceptance rate (FAR) and false rejection rate (FRR) [2, 37, 45].

The total processing time is the time elapsed between the person's request to access, and the time the access is given. This should take 1-2 seconds in a good system [2, 37]. False acceptance rate is the possibility of access being granted for an unauthorized person, with a faulty decision. False rejection rate is the possibility of access not being granted for an authorized person. The aim for all biometric systems is to reduce both FARs and FRRs below 1%. [2, 37, 45].

## 7. RESULTS

In this study, different iris and retinal identification methods have been examined, and the similarities and differences of these systems have been identified. It's been seen that these systems are much more reliable, accurate and fast, compared to other biometric systems available. However, their high cost prevents them to be widely adopted.

The similarities between iris and retinal identification can be listed as follows;

- False acceptance rate is low in both.
- False rejection rate is very low, almost 0.
- Highly reliable, because the iris or retinal patterns are unique for everybody.
- Identification is very fast in both.

The differences between iris and retinal identification can be listed as follows;

- The accuracy of retinal scanning can be affected by various diseases, however, the rich texture of the iris is fixed for life and immutable.
- Iris scanning is not different from a normal photo shoot, shots are taken from a short distance. Retinal scanning requires the person to be much more close to the camera.
- Iris is an internal organ which can be seen externally, but retina is on the back of the eye. Therefore, photographs are taken from different distances.
- Iris scanning is more commercially accepted than retinal scans. Retinal scanning is considered to be harmful.

Retina and iris can be used in cryptography with their unique structures. With smart cards that carry both iris and retinal codes, both users and the system owners or institutions can have a more security.

When the properties of retinal and iris identification are analyzed, it is expected that these two systems can perform better compared to other biometric based systems like finger print, face or vascular identification systems. Apart from that, it's also been understood that with a combination of iris and retinal pattern prototype can be one of the most secure identification systems available.

## REFERENCES

[1]. Turhan C., Ceyhan, E., Sağıroğlu Ş., Biyometrik Sistemlerde Güvenlik Üzerine Bir İnceleme, www.iscturkey.org, access: 03.03.2016.

[2]. Yalçın, N., Gürbüz, F., 2015. Biyometrik Güvenlik Sistemlerinin İncelenmesi, Düzce Üniversitesi Bilim ve Teknoloji Dergisi, cilt

3, no. 2, pp.

[3]. Elumalai, K., Kannan, M., 2011. Multimodal Authentication For High End Security, International Journal on Computer Science and Engineering (IJCSE), 3(2), 687-692.

[4]. Jain, K., Bolle, R., Pankanti, S., 1999. Biometrics: Personal identification in Networked Society, Springer Science and Business Media.

[5]. Ergen, B., Çalışkan, A., 2011. Biyometrik Sistemler ve El Tabanlı Biyometrik Tanıma Karakteristikleri, 6th International Advanced Technologies Symposium, Elazığ-Türkiye.

[6]. Jain, A.K., Ross, A., Prabhakar, S., 2004. An Introduction to Biometric identification, IEEE Transaction on Circuits and Systems for Video Technology, vol.14, no.1, pp.4-20.

[7]. Şamlı, R., Yüksel, M. E., 2009. Biyometrik Güvenlik Sistemleri, Akademik Bilişim, Şanlıurfa-Türkiye.

[8]. Liu, S., Silverman, M., 2001. A Practical Guide to Biometric Security Technology, IT Professional, vol. 3, no. 1, pp. 27-32.

[9]. Unar, J., Senga, W., Abbasia, A., 2014. A Review of Biometric Technology Along with Trends and Prospects, Pattern identification, vol. 47, pp.2673-2688.

[10]. Monrose, F., Rubin, A., 1997. Authentication via Keystroke Dynamics, 4th ACM Conference on Computer and Communications Security, Switzerland, pp. 48-56.

[11]. http://www.biyolojisitesi.net/tum%20uniteler/denetleme_ve_duzenleme/gorme_nasil_gerceklesir.html, access: 6.1.2016.

[12]. Yücel, E. Işık, Renk ve Elektromanyetk Spektrum,http://www.akat.org/sizin_icin/elektromagnetik_tayf.pdf, access: 6.1.2016.

[13]. Alkoot, Fuad M., 2012. A Review On Advances In Iris identification Methods, International Journal of Computer Engineering Research, vol. 3(1), pp. 1-9, Kuwait.

[14]. http://www.biltek.tubitak.gov.tr/haberler/tip/s528_5.pdf, access: 6.1.2016.

[15]. Tasyapi Celebi A., Güllü, Kemal M., Ertürk, S., 2009. Low-complexity Iris identification Using One-bit Transform and Angular Radial Partitioning, 2009 IEEE 17th Signal Processing and Communications Applications Conference.

[16]. http://www.ergosis.com.tr/iris-tanima-teknolojisi.html, access: 6.1.2016.

[17]. Daugman, J., 2003. Demodulation by Comlex-Valued Wavelets for Stochastic Pattern identification, Int. J. Wavelets, Multi-Res. and ınfo. Processing. 1(1): 1-17.

[18]. Daugman, J., Downing, C., 1995. Demodulation, Predictive Coding and Spatial Vision, J. Opt. Soc. Am. A 12: 641-660.

[19]. Sanchez-Avila, C., Sanchez-Reillo, R., 2002. Iris-Based Biometric identification Using Dyadic Wavelet Transform, IEEE Aerosp. Electron. Sys. Mag., 17:3-6.

[20]. Lim, S., Lee, K., Byeon, O., Kim, T., 2001.Efficient İris identification Through İmprovement of Feature Vector and Classifier, ETRI J. 23(2): 1-70

[21]. Wildes, R., Asmuth, J., Green, G., Hsu, S., Kolczynski, R., Matey, J., McBride, S., 1996. A Machine-Vision System for Irıs identification, Mach. Vis. Applic., 9: 1-8.

[22]. Zhu, Y., Tan, T., Wang, Y., 2000. Biometric Personal identification Based On Iris Patterns, Int. Conf. Pattern identification, II:805-808.

[23]. Ma, L., 2003. Personal identification Based On Iris identification, Ph.D dissertation, China.

[24]. Jain, A., Ross, A., Nandakumar, K., İntroduction to Biometrics, https://books.google.com.tr/, access: 6.1.2016.

[25]. Wildes, R., 1994. A System for Automated Iris identification, 2nd IEEE Workshop Applicat. Comput. Vision, pp.121-128.

[26]. Jones, M. J., Guo, G., 2008. Iris Extraction Based on Intensity Gradient and Texture Difference, IEEE Workshop on Applications of Computer Vision Conference.

[27]. Ziauddin, S., Dailey M., 2010. Robust Iris Verification for Key Management, Pattern identification Letters, 31(9).

[28]. Perez, C. A., Aravena, C. M., Vallejos, J. I., Estevez, P. A., Held, C. M. 2010.Face and Iris Localization Using Templates Designed by Particle Swarm Optimization, Pattern identification Letters, 31(9): 857-868.

[29]. Lim, S., Lee, K., Byeon, O., Kim, T., 2001. Efficient Iris identification Through Improvement of Feature Vector and Classifier. ETRI J. 23(2): 1-70.

[30]. Boles, W., Boashash, B., 1998. A Human identification Technique Using Images of Iris and Wavelet Transform, IEEE Transaction on Signal Processing, 46(4).

[31]. Murty, P. C., Reddy, E. S., Babu, I. R., 2009, Iris identification System Using Fractal Dimensions of Haar Patterns International, Journal of Signal Processing, Image Processing and Pattern identification, vol. 2, No.3.

[32]. Akram, U. M., Tariqy, A., Khan, S. A., 2011. Retinal identification: Personal identification using Blood Vessel, 6th International Conference on İnternet Technology and Secured Transactions, United Arab Emirates.

[33]. Simon, C., Goldstein, I., 1935. A New Scientific Method of identification, New York State Journal of Medicine, vol. 35, No. 18, pp. 901-906.

[34]. Qamber, S., Waheed, Z., Akram, U., 2012. Personal identification System Based on Vascular Pattern of Human Retina, Cairo International Biomedical Engineering Conference (CIBEC), Egypt.

[35]. Fatima, J., Syed, M., Akram, U., 2013. A Secure Personal identification System Based on Human Retina, 2013 IEEE Symposium on Industrial Electronics and Applications, Malaysia.

[36]. Fatima, J., Syed, M., Akram, U., 2013. Feature Point Validation for Improved Retina identification, IEEE Workshop on Biometrics Measurements and Systems for Security and Medical Applications, Italy.

[37]. http://elektroteknoloji.com/Elektrik_Elektronik/Teknik_Yazilar/Biyometrik_Sistemler_Fiziksel_Ozelliklerden_Yararlanarak_Kimlik_Tespit_Etme_bilgisayar_destekli.html, access::6.1.2016.

[38]. Patwari, Manjiri B., Manza, Ramesh R., Rajput, Yogesh M., Saswade, M., Deshpande, M.,2014. Personal Identification Algorithm Based on Retinal Blood Vessels Bifurcation, 2014 International Conference on Intelligent Computing Applications, India.

[39]. http://www.evrenvebilim.com/kotu_tasarim_yanilgisi.html,

access: 11.3.2016.

[40]. http://pmgbiology.com/2014/05/31/understanding-the-functioning-of-the-eye-to-a-biology-gcse-part-1/

access: 11.3.2016.

[41]. Rashad, M. Z. Shams ,M. Y., Nomir, O., El-Awady, R. M., 2011. Iris Recognition Based on LBP and Combıned LVQ Classıfıer, International Journal of Computer Science & Information Technology (IJCSIT), vol 3, No 5, DOI : 10.5121/ijcsit.2011.

[42]. Bendre, Sandip M., Shivarkar, Raosahe A., An Improved Approach for Iris Authentication System by Using Daugman's Rubber Sheet Model, Segmentation, Normalization and RSA Security Algorithm, International Journal of Computer Technology and Electronics Engineering (IJCTEE) vol. 1, Issue 3 102.

[43]. Latha, L., Thangasamy, S., 2010. A Robust Person Authentication System based on Score Level Fusion of Left and Right Irises and Retinal Features, Procedia Computer Science 2 (2010) 111–120.

[44]. Daugman, J., 2007. New Methods in Iris Recognition, IEEE Transactıons on Systems, Man, and Cybernetıcs—part b: Cybernetıcs, vol. 37, no. 5.

[45]. Abhyankar, A., Hornak, L. and Schuckersa, S.,2005. Biorthogonal-Wavelets-Based Iris Recognition, Proc. SPIE 5779, Biometric Technology for Human Identification II,59; doi:10.1117/12.604212.

[46]. Tian, Q., Qu, H., Zhang, L. and Zong, R., Personal Identity Recognition Approach Based on Iris Pattern,2011. http://cdn.intechweb.org/pdfs/16589.pdf, access: 11.3.2006.

# What Sustainability and Sustainable Development Mean for Mining

*Necmettin Çetin*[53]

***Abstract***

Mineral productions and processing are important economic activities in many parts of the world. Growth in world population, together with improvements in standards of living in many countries and development of new uses for minerals has fueled the pace of exploitations. This has been facilitated by advances in technology that allows lower-cost and more-efficient extraction along with increased recycling. Improved mining equipment, methods and technology have placed an important role in reducing the risk faced by mine workers, partly through reducing the risk of human error**.** Sustainability requires collaboration and communication with the local and the wider community. Strategic partnerships with communities should be fostered to optimize social and economical benefits from its activities. The wisdom of sustainable development requires optimal outcomes for the industry, economy, society and the environment. Sustainable development for the mineral sector is broad and it encompasses for both public and private property, the sustaining of natural resources, ecosystem, communities and economies as they relate to the processes and products of the sector. For mineral sector, it involves minimizing rather than optimizing the negative effects of production and maximizing the potential benefits of the sector's current capacity.

**Keywords:** Sustainability**,** Sustainable Development, Mining, Mineral Industry

## 117. INTRODUCTION

Mining and mineral resources have the potential to be important sources of income and driving forces behind boarder economic development. A mining project can be more successful when guided by targeting the highest possible standards in technical, safety, and environmental issues. Sustainability is really a simple concept. It requires only that something be maintained at its current level, for example, environmental quality or economic well being. This term originally referred to the management of renewable resources such as a fishery or a forest; a resource was being managed in a sustainable manner if the harvest rate was greater than the natural or biological rate of regeneration. Sustainable development is more recent, and more complicated. It requires that development be sustained. But what is development? It is first and foremost a multidimensional concept. One dimension is economic, reflecting the desire to improve economic well being, which may estimated by as per capita income of a nation. A second dimension is environmental and reflect the desire that improvements in economic well being not come at the cost of diminished environmental quality. A third dimension is socio-cultural and reflects the desire that improvements in economic well being occur in manner that is socially just. Social justice relates primarily to fairness in the distribution of the benefits and burdens (i.e. economic, environmental and social) that result from economic growth. Sustainable development requires that human beings act in ways that simultaneously sustain or enhance economic well being, the quality of environment and

[53] *Corresponding author: l U v , M E , 43200, Evl Ç l b Y l şk T vş l Y l 10 km/Kütahya, Turkey. necmettin.cetin@dpu..edu.tr*

social justice. It is well accepted that the environmental and socio-cultural aspects must be an integral part of the way the minerals industry operates. Sustainability requires economic growth, environmental protection of our ecosystem, and social responsibility. The dynamic interplay of these three components is a prerequisite for achieving the goals of sustainability [1], [2], [3].

How do mining and mineral resources fit into this picture of sustainability and sustainable development? At first glance, mining and mineral resources seem to be quintessential unsustainable activities. Individual mines have finite reserves that once mined are gone. The earth crusts contain a limited supply of any mineral resources. Since through mineral exploration and development, mining companies replace reserves that mining depletes, mining is more sustainable than it appears. Also, through technological innovation, mining companies are able to discover or mine mineral resources that otherwise would be technically and commercially unfeasible to mine. Second, recycling sustains the benefits of materials made possible by mining, even if a mine itself is not sustainable. Third and most importantly, even if a mine is unsustainable, in principle the economic benefits created by mining can be sustained indefinitely through appropriate investment in education, health care, infrastructure, and other activities that create well being long after mining ceases. In other words, a depleting mineral resource can, in effect, be converted into a sustainable, renewable source of human well being through appropriate investment [4], [5], [6].

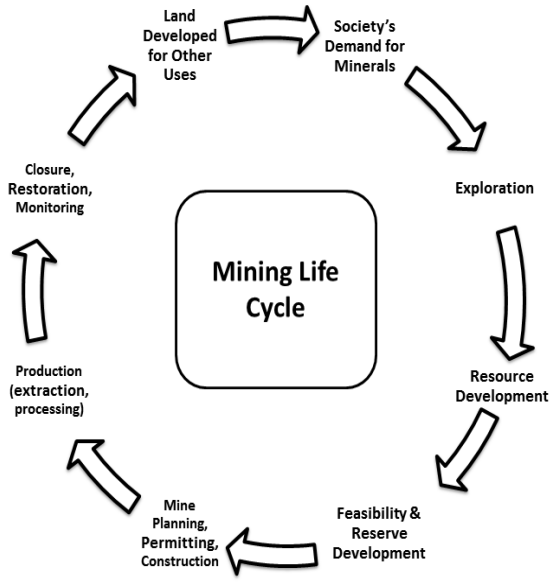


Figure1. The Mining Lifecycle after Kogel [1]

## 118. METHODOLOGY

The life of a mine consists of discrete phases or activities that together comprise the mining lifecycle (Figure 1). Exploration focuses on the discovery of new mineral deposits. The next step is towards bringing a deposit into production. Feasibility studies are detailed engineering and economic analyses that include mine design, cash-flow analysis (capital cost, operational cost, and revenue), mineral processing flow-sheets, closure plans, reclamation plans and plant design. Mine design and planning encompasses a broad range of activities that are mainly concerned with determining the size of the mine, mine

layout, mining method, production requirements, and equipment needs. After the ore has been removed, the mine is closed and the land is graded, re-vegetated and developed for a variety of post mining uses that, if managed appropriately, will bring long term value to the local community.

### *118.1. Four Principles for Mining*

What do these broad concepts of sustainability and sustainable development mean for mining sector? What they certainly do not mean is that a mine should not be sustained forever, which of course is impossible. Also, these concepts do not mean that a mine should be sustained forever and at all costs the life an individual community. The concept of sustainability and sustainable development suggest the following principles or social goals associated with mining:

- Facilitate the creation of mineral wealth
- Ensure that mineral development occurs in an economically (socially) efficient manner
- Distribute the surpluses from mining fairly; and
- Sustain the benefits of mining even after a mine closes.

### *118.2. Sustainable Mining Practices*

Mineral development can be viewed as supporting the concept of sustainable development if the extraction of minerals takes place in a manner that minimizes the environmental impacts; equitably shares the benefits from the new wealth created; utilizes the capital obtained to provide adequate healthcare, education, and other social services; and reduces the level of waste through recycling and improved technologies to optimize recoveries. Sustainable mining practices are a concept that embeds the principles of sustainable development into a mining and minerals context. At its core is the belief that through the responsible development of the world's mineral resources, the global population will be able to access the mineral resources they demand for both a higher standard of living and better access to energy. It is an important tool in alleviating poverty. Companies that exhibit sustainable mining practices demonstrate:

- Environmental leading practices
- Community engagement and support
- Economic development
- Safety excellence
- Optimum resource utilization

As a result of embedding these practices into the way of work, the operation will be sustained (premature mine closure avoided) and enduring benefits will flow to the community (Figure 2). An emerging standard of best practices in mining industry aims at resulting in net positive benefits across social, economic, and environmental areas that are sustainable after closure.


Figure2. Five Pillars of Sustainability of Mining after Laurence, [2]

## 119. RESULTS AND DISCUSSIONS

Since mining is necessary to sustain economic prosperity and quality of life, a continued exploration for new mineral deposits is required. Before minerals can contribute to sustainability or sustainable development, mineral wealth needs to be created. The creation mineral wealth requires human activities to acquire sufficient knowledge of a mineral occurrence (or the chance of occurrence) that someone is willing to purchase explorations, development, or mining rights. Exploration is the most strategic activity of any mining company and efficient management of exploration portfolio is essential to sustainability. The success of a mining company is determined by its capacity to transform today's exploration targets into tomorrow' cash flows. Sustainable exploration strategies should be focused on controlling risks considering risk as chance of failure or loss (Figure 3).

The key idea or goal of economic efficiency is to maximize net benefits, in this case from mining. The definitions of benefits and costs need to be broad enough to include full social benefits and costs. Starting points estimating benefits and costs are the revenues received and costs incurred by profit-seeking mining companies. In addition when evaluating sustainability and sustainable development, one needs to consider the possible spillover benefits and costs associated with mining. Spillover benefits may include local purchases of inputs by a mining company, local spending of mine workers salaries, health improvements experienced by local communities from clinics, roads or other infrastructures. Spillover costs may include environmental damage, cultural impacts associated by mining development. Economic efficiency requires that decision-makers acknowledge and recognize the unpaid nature of spillover costs and overall incorporates at least conceptually the environmental and social problems that lead to the concern that these activities are unsustainable.

Mining often generates surpluses or economic profits even after mining companies pay the spillover costs either by compensating local communities or others by bearing these costs or through activities such as expenditure on environmental protection that reduce or eliminate the creation of these costs. How these surpluses are distributed among the owners and worker of private mining companies, government and communities is a key issue in social and cultural sustainability and sustainable development. This issue is a critical aspect of the social justice.

Investing appropriate portion of the revenues from mining in sustainable assets can in effect make the benefits from mining permanent. This principle is perhaps the key lesson from the concept of economic sustainability. The idea is simple: save and invest a portion of current income each period, spend at most the investment's income each period and in doing so sustain the fund spending indefinitely into the future.

In an ideal world, governments acting on behalf of society at large should establish appropriate legal and regulatory frameworks that facilitate achievement of the four principles of sustainable mineral development identified previously. In particular, most economists argue that government intervention in specific markets, including mining, be limited to activities that facilitate market activity, promote fairness in the distribution of burdens and benefits, and promote economic efficiency by correcting imperfections in actual markets that would prevent them from being well-functioning or economic efficiency. In mining, governments should facilitate mineral exploration, mine development, and mining through policies that define property rights, create processes for private companies to obtain approvals for exploration and development, and outline and describe the rights and responsibilities of private companies during extraction activities and after mining ceases (Figure 4).

**120. CONCLUSIONS**

Sustainability and sustainable development mean that mining companies and mine managers should continue to work with local communities and governments to integrate environmental and social issues into technical and commercial decisions about mining. They mean that processes though which companies and all other interested parties to mine development identify, discuss, and resolve issues that require integrating the technical, commercial, environmental, and social aspects of mining should continue to be important issues. More broadly, it is hoped that the growing experience of mining companies and communities interacting with one another should lead to broader agreement about what is to be sustained, for whom, and through what process. To date, there has been little consensus on how to put the broad concepts of sustainability and sustainable development into practice. There are limits to what extend that one can expect worldwide agreement to emerge since what is sustainable to a community in one part of the world may not be sustainable in any other community in any other part of the world. Sustainability and sustainable development are all about social preferences for the appropriate balance among the economic, environmental, and socio-cultural dimensions of human activities. In the foreseeable future, there will be growing pressure to ensure that mining projects and operations are managed for sustainability and sustainable development.

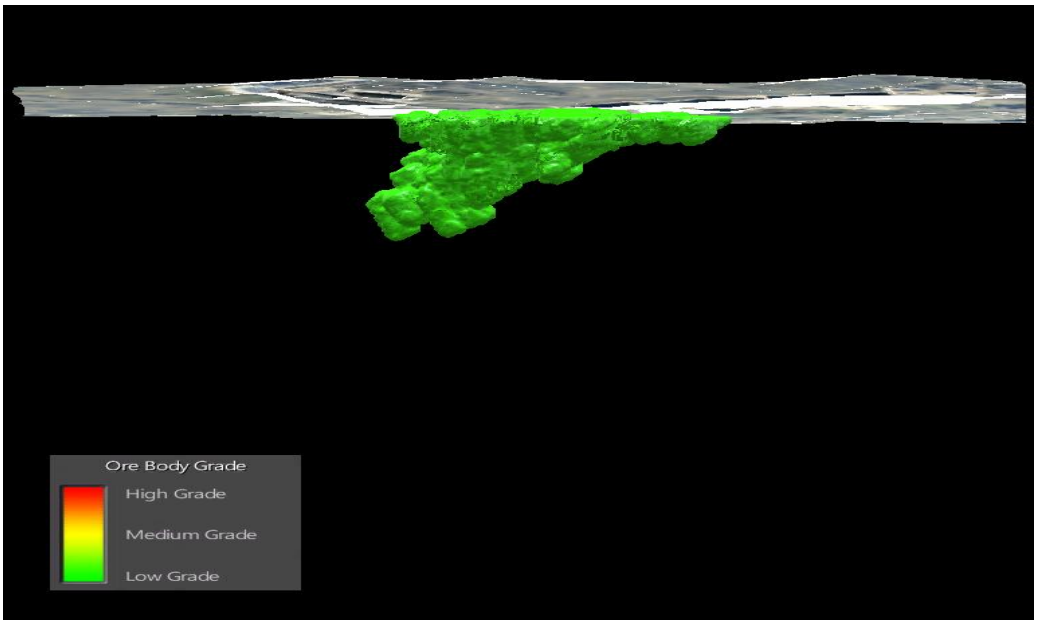


Figure3. A View of an Ore Deposit in Australia [7]

Figure4. A View of an Operating Open Pit Mine in Australia. [8]

## REFERENCES

[341]. J. E., Kogel. (2003) EPD Congress webpage on WFEO. [Online]. Available: http://www.wfeo.org/wp-content/uploads/stc-environment/Sustainable_Development_Practices_and_the_Minerals_Industry.pdf
[342]. D. C., Laurence, "Establishing a Sustainable Mining Operation—an Overview"," Journal of Cleaner Production, Elsevier Science Ltd.vol. 19 Issue 2-3, Jan/Feb 2011.
[343]. V.Rajaram, S. Dutta, K. Parameswaran, Sustainable Mining Practices: A Global Perspective, 1st ed., Taylor and Francis Group, London, UK, 2005.
[344]. R. G., Eggert, "Mining, Sustainability and Sustainable Development", Australian mineral Economics, monograph 24, ed. Philips Maxwell (Carlton, Victoria: Australian Institute of Mining and Metallurgy), pp. 187-194, 2006.
[345]. R. G., Eggert, "Sustainable Development and Mineral Industry", Sustainable Development and the Future of Mineral Investment, eds. J.M. Otto and J. Cordes (Paris: United Nations Environment Programme and Metal Mining Agency of Japan), 2000.
[346]. J. A., Botin, Sustainable Management of Mining Operations, 1st ed., SME, Englewood, Colorado, USA, 2009.
[347]. http://www.engineering.unsw.edu.au/mining-engineering/files/vm1b/VimineThirdYear.html
[348]. https://www.austrade.gov.au/ArticleDocuments/1358/Sustainable-Mining-ICR.pdf

## BIOGRAPHY

Dr. Necmettin Çetin got his PhD from Middle East Technical University, METU, Ankara in 2004. His areas of specialization include Open Pit Mining, Simulation and Optimization.

# Wave Hindcasting for Wave Energy Assessments in the Black Sea

*Adem Akpinar[54], Bilal Bingölbali[55], Halid Jafali[56]*

***Abstract***

*Assessment of wave energy potential in sea areas is considered to be of great importance all over the world and the number of studies in this way has increased rapidly. For the Black Sea, however, only a limited amount of studies has been carried out so far, providing only a crude estimate of its wave energy potential. This paper summarises performance of the developed nested models to investigate spatial and temporal variability of wave energy potential in the Black Sea within the TUBITAK research project [1]. For this purpose, the third-generation numerical wave hindcast model SWAN results forcing with CFSR wind data were compared with the buoy measurements at six buoy locations (Hopa, Gelendzhik, Gloria, Sinop, Filyos, and Karaburun). Focusing on the south-western coast of the Black Sea, a set of nested SWAN model with increasing spatial resolutions (a coarse grid, then a fine grid, and then three sub-grids) was established. SWAN model with a coarse grid was calibrated and validated with the measurements at Gelendzhik, Sinop, and Hopa. Then, SWAN model with a fine grid was calibrated and validated at Gloria. And finally, each of SWAN model with three sub-grids was calibrated and validated at Karaburun, Filyos, and Sinop, independently. Thus, the numerical and physical settings of the SWAN model for the Black Sea by calibrating source term settings for deep and shallow water was optimised. The results show that SWAN model hindcasts match well with the measurements. Therefore, the setting of the nested SWAN models will be applied to the Black Sea during 31 years to obtain a data base including some wind and wave parameters and to correctly assess the wave energy potential of the south western part of the Black Sea.*

**Keywords: SWAN, Wind-wave modelling, Wave Energy Potential, Black Sea**

## 121. INTRODUCTION

SWAN wave model, which stands for Simulating Waves Nearshore, is a 3rd-generation numerical model. It can compute wind-generated waves both in coastal areas and inland waters such as lakes and it is the most used model globally at the moment. As a system, it has different formulations of source terms that help to drive it, some of which are optional. For wind input, Komen et al. [2], which is the default in the SWAN, Janssen [3, 4], and Yan [5] are the used formulations. For bottom friction, JONSWAP (Hasselmann et al. [6]), which is the default in the SWAN, Madsen et al. [7] and Collins [8] options are available. Therefore it is important to conduct a test on how different options affect the performance of the SWAN model, thus, ending up with the most suitable model for a given area. In this study, depth-induced wave breaking effect, triad and quadruplet wave-wave interactions, different bottom friction, wind input, and whitecapping options are examined with measured data at several stations over the Black sea. Besides, effects of some tunable parameters in the physical processes along with effects of some parameters for numerical setting to the SWAN model performance were also investigated for each nested SWAN model.

## 122. DATA COLLECTION AND PRE-PROCESSING

Two main inputs needed for wave model simulations were firstly obtained and processed. Globally preferred bathymetry data, the General Bathymetric Charts of the Ocean (GEBCO) data produced by the British Oceanographic Data Centre (BODC) is used. The data has the same resolution (30 seconds) in both latitude and longitude and was requested from BODC via their website. A few processes were performed on the data to make it detectable by the numerical model. The other main input is wind field. For this data, CFSR winds produced by NOAA were used based on a study carried out by Van Vledder and Akpinar [9] using the SWAN model for the Black Sea. They examined the effects of 6 different atmospheric models on wave hindcast and concluded that CFSR wind were most appropriate for the Black sea since they showed more accurate results.

Since a long-term (31 years) analysis was carried out in our study, 31-year (1979-2009) data was obtained from the NOAA website in GRIB format. The data has u and v wind components of spatial resolution of 0.3125 °, 1 hour temporal resolution and at a height of 10 m. As in bathymetry data, a few processes were also performed on all 31-year wind data set in order to get it in a format detectable by the SWAN model.

[54] Ul ğ U v , C v l E , 16059, N lü /B , T k . ademakpinar@uludag.edu.tr
[55] Ul ğ U v , C v l E , 16059, N lü /B , T k . arda_bilal_49@hotmail.com
[56] Ul ğ U v , C v l E , 16059, N lü /B , T k . halidjfone@gmail.com

**123. DEVELOPMENT OF NUMERICAL MODEL**

After acquiring and processing these two main input files, a numerical wave prediction model code was prepared. Considering that our model consists of nested grids (coarse, fine and 3 sub-grids) (see Figure 1), each grid was calibrated separately.

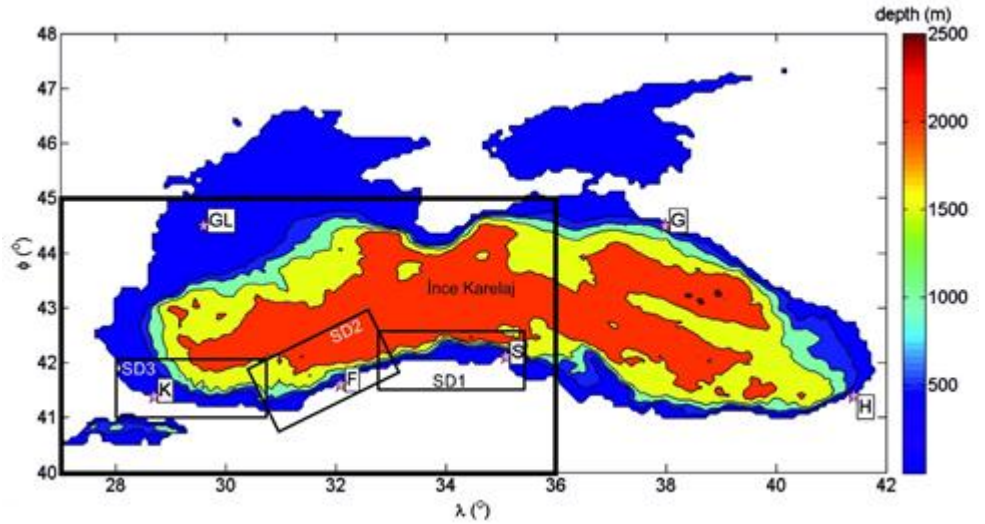


*Figure 1. Bathymetry for coarse, fine and finer sub-grids used in the SWAN model and stations (K: Karaburun, F: Filyos, S: Sinop, H: Hopa, GL: Gloria, G: Gelendzhik) used for model calibration and verification of hindcasted data.*

In the calibration, we focused on the least known event in numerical wave modeling called whitecapping. Since SWAN model contains different formulations for wind input and whitecapping, five different combinations defining the two physical processes were formed. The performance of these combinations and the effect of tunable whitecapping coefficient in each combination were examined. Combinations created for calibration are as follows in the form of wind input formulation & whitecapping formulation:

- Komen et al [2] & Komen et al [2]
- Komen et al [2] & Janssen [3, 4]
- Janssen [3, 4] & Janssen [3, 4]
- Janssen [3, 4] & Komen et al [2]
- Yan [5] & Westhuysen et al [10].

During the calibration process, we first started off with the main/coarse grid covering the entire Black sea as a whole using measurements from Hopa, Sinop and Gelendzhik stations collected in 1996. The performance of SWAN models developed for the above listed combinations were determined using statistical error parameters, after which whitecapping parameters were set using try and error method by increasing and decreasing their value in each combination. Thus, the model showing the highest correlation, lowest bias, rmse and mae errors and lowest scattering index (si) was determined as the best model. Comparisons of developed SWAN models' scatter index values at all three stations are presented in Figure 2.


*F 2. C v l SWAN l' x v l ll h*

*(0 index represents default set-up scenario for each combination)*

After benchmarking the results, the best SWAN model setup was determined as C3.2 numbered SWAN model with the formulations of Komen for wind input and Janssen for whitecapping where the whitecapping dissipation parameter value ($C_{ds}$) is setup to 1.5. Apart from the calibration process, sensitivity analysis was conducted for some parameters and physical processes. The cases performed for sensitivity analysis of physical and numerical parameters are as follows:

- Depth-induced wave breaking ( active and non-active cases)
- triad wave - wave interactions ( active and non-active cases)
- Quadruplet wave - wave interactions ( active and non-active cases)
- Bottom friction ( active, non-active cases and different formulations)
- Delta parameter which determines the dependence of the whitecapping on wave number
- Coefficient of the wave steepness for a Pierson - Moskowitz spectrum (stpm)
- Coefficient of Jonswap formulation (cfjon)
- Proportionality coefficient of the rate of dissipation (alpha)
- The ratio of the maximum individual wave height over depth (gamma)
- Collins bottom friction coefficient (cfw)
- Equivalent roughness length scale of the bottom (kn)

- Density of water (rho)
- Computational grid's spatial resolution
- Computational grid 's frequency range
- Computational grid's frequency resolution
- Computational grid's directional resolution
- Correction of wind speeds using a coefficient (increased winds)
- The time step of the non-stationary computation

In the previous study [11], sensitivity of calculation of non-stationary time interval (time step) were examined for 6 hours, 3 hours, 1 hour, 30 minutes and 15 minutes in the simulations, and 30 minutes setting was determined to be the most suitable. Therefore, 30 minutes time interval is considered for coarse grid computation in this study. The effect of the delta coefficient that represents dependence of whitecapping on the wave number was examined and based on the error statistics in three buoy stations, it is effective and therefore delta equaling to 1.0 was chosen as the suitable (Figure 3). SWAN model simulations for the above mentioned conditions and other parameters in sensitivity analysis were conducted. Different stpm coefficient values which are Pierson - Moskowitz spectrum's values of wave steepness, were used to run the SWAN model but no any improvement in model performance was obtained. In addition, different values of cfjon, cfw and kn parameters and alpha and gamma were also used in SWAN model with no improvement in model performance. Furthermore, different values of computational grid spatial resolution, frequency range, frequency resolution and directional resolution were also used to run SWAN model but still no improvement was made in the model at the three stations. In addition, CFSR winds used as an input in the model were increased by 5% and 10% to examine their impact on the performance of the model. From the model results, by increasing the wind, there is an improvement in estimating both wave parameters at Gelendzhik station and an improvement in wave period estimation at Hopa while at Sinop both parameters, and wave height estimation at Hopa worsen. Therefore, it has been decided not to increase winds on the coarse grid. The effects of depth-induced wave breaking, triad and quadruplet wave-wave interactions and bottom friction processes on SWAN model was also investigated by taking into consideration active or inactive cases for each processes. The results show that the model worsens when these processes are closed so they were left active. SWAN model performances developed for the parameters and cases examined in the sensitivity analysis are not presented here because they do not cause any change in comparison with the default model performance. Ultimately, after all the SWAN test analyses were carried out, the best model for the coarse grid was set.

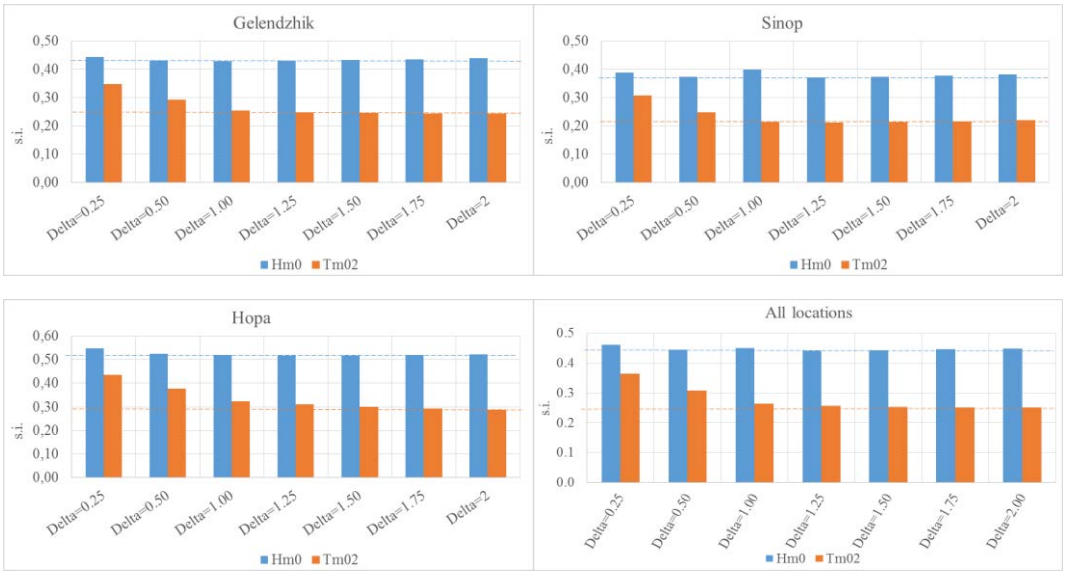


*Figure 3. Comparison of results for SWAN models using different delta values in three buoy stations*

All test simulations, including calibration and sensitivity analysis carried out with the coarse grid were also performed separately for both fine and innermost 3 sub- grids. SWAN model setting using the combinations mentioned above used in the calibration process of the fine grid, was run using boundary conditions from the best model setting of the coarse grid, after which its results were tested for accuracy using measurements from Gloria station. Statistical error indicators in all the developed SWAN model estimates of both wave parameters for each combination of fine grid calibration process were computed for Gloria station. Comparisons of scatter index values at Gloria station for all developed SWAN models for the fine grid are presented in Figure 4. Based on the results presented here, the best SWAN model setting for the fine grid is determined as Janssen formulation for wind input and Janssen formulation for whitecapping where $C_{ds}$ equals to 3.0.

Analyzing sensitivity testing for fine grid, no change occurred in the performance of models developed to examine all parameters.

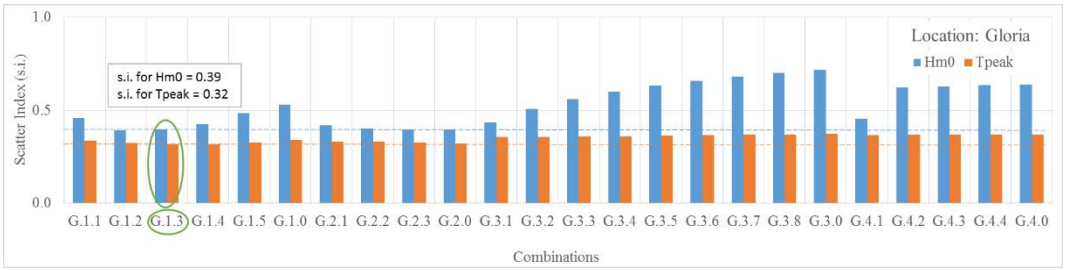


*F 4. C v l SWAN l' x v l Gl*

*(0 index represents default set-up scenario for each combination)*

The performance of the five individual calibration combinations mentioned above in each sub- grid namely SD1, SD2 and SD3 has been examined and tested using try and error method and effect of the whitecapping dissipation parameter on the model has been investigated for each combination in each sub-grid. Scatter index comparisons of both wave parameters hindcasted for all developed SWAN models for three sub-grids are given in Figure 5. According to calibration process' results, the SWAN model settings with the best performance are as follows: Komen for wind input and Janssen formulation for whitecapping where $C_{ds}$ equals to 3.0 for SD1 sub-grid, Komen for wind input and Janssen for whitecapping where $C_{ds}$ equals to 9.0 for SD2 sub-grid and Komen for wind input and Janssen for whitecapping where $C_{ds}$ equals to 2.0 for SD3 sub-grid.


*Figure 5. C h v l SWAN l' x v l h h b-grids*

The effect of some parameters and cases on the model results are discussed separately for each sub- grid with sensitivity analysis. SWAN models set according to the follows combinations were run; alpha coefficient values of 0.8, 0.9, 1.0, 1.1 and 1.2 in the physical process of depth-induced wave breaking and gamma parameters of 0.53 , 0.63 , 0.73 , 0.83 and 0.93 but no change was seen in the results. Again no change was detected in model set-up results with cfjon parameter values of 0.02, 0.03, 0.038 and 0.05 for the bottom friction formula, cfw values of 0,005, 0,015, 0.01 and 0.02, and kn values of 0.02, 0.03, 0.04 and 0.05 combinations. Furthermore, no change was observed in computational grid for the frequency range 0.03 - 1, 0.04 – 0.625, 0.04 - 1, 0.01 – 1.2 and 0.04 – 1.2 values, computational grid for the spatial resolution of 750 x 300, 500 x 200 and 934 x 444, computational frequency resolution grid of values 18, 24, 30 and 35, and computational grid for directional resolution of values 10, 20, 30 and 36 combinations. Wind in each of the three sub-grids was increased by 5% and 10 %, but the results did not show any significant improvement. A small but important worsening change (increase in error value) was detected after triad and quadruplet wave-wave interactions were inactivated. Lastly, calculation of non-stationary time interval (time step of computation) impact on the model results are discussed for each of the three sub- grids. Models for each of the three grids were run for 30 min, 20 min, 15 min 10 min and 5 min intervals. Wave parameter statistical errors of model results at Sinop station for SD1 sub-grid, at Filyos station for SD2 sub-grid and at Karaburun station for SD3 sub-grid are given in Tables 1 and 2. Based on these results; SWAN models with 10 min computational time step for SD1 sub-grid, with 30 min computational time step for SD2 sub-grid and 20 min computational time step for SD3 sub-grid are determined to achieve the most accurate results.

*Table 1. $H_{m0}$ error statistics for different computational time steps in 3 sub-grids*

| | | **$H_{m0}$ error statistics at Sinop** | | | | | | | |
|---|---|---|---|---|---|---|---|---|---|
| | **Time step (min)** | **n** | **r** | **Bias** | **rmse** | **mae** | **$X_{mean}$** | **$Y_{mean}$** | **si** |
| **Wind input: Komen Whitecapping: Janssen $C_{ds}$=3** | 5 | 2164 | 0.84 | 0.01 | 0.27 | 0.20 | 0.80 | 0.79 | 0.33 |
| | 10 | 2164 | 0.84 | 0.01 | 0.27 | 0.20 | 0.80 | 0.79 | 0.34 |
| | 15 | 2413 | 0.83 | 0.01 | 0.28 | 0.21 | 0.80 | 0.79 | 0.34 |
| | 20 | 1828 | 0.83 | 0.01 | 0.28 | 0.21 | 0.81 | 0.79 | 0.35 |
| | 30 | 1249 | 0.82 | 0.02 | 0.28 | 0.21 | 0.81 | 0.79 | 0.35 |
| | | **$H_{m0}$ error statistics at Filyos** | | | | | | | |
| | **Time step (min)** | **n** | **r** | **bias** | **rmse** | **mae** | **$X_{mean}$** | **$Y_{mean}$** | **si** |
| **Wind input: Komen Whitecapping: Janssen $C_{ds}$=9** | 5 | 1335 | 0.56 | 0.00 | 0.44 | 0.30 | 0.59 | 0.59 | 0.75 |
| | 10 | 1335 | 0.56 | 0.00 | 0.44 | 0.30 | 0.59 | 0.59 | 0.75 |
| | 15 | 1335 | 0.56 | 0.00 | 0.44 | 0.30 | 0.59 | 0.59 | 0.75 |
| | 20 | 4003 | 0.55 | 0.00 | 0.45 | 0.30 | 0.59 | 0.59 | 0.76 |
| | 30 | 1335 | 0.56 | 0.00 | 0.44 | 0.30 | 0.59 | 0.59 | 0.75 |
| | | **$H_{m0}$ error statistics at Karaburun** | | | | | | | |
| | **Time step (min)** | **n** | **r** | **bias** | **rmse** | **mae** | **$X_{mean}$** | **$Y_{mean}$** | **si** |
| **Wind input: Komen Whitecapping: Janssen $C_{ds}$=2** | 5 | 771 | 0.87 | -0.02 | 0.23 | 0.16 | 0.63 | 0.65 | 0.37 |
| | 10 | 771 | 0.87 | -0.02 | 0.23 | 0.16 | 0.63 | 0.65 | 0.37 |
| | 15 | 1019 | 0.88 | -0.01 | 0.22 | 0.15 | 0.64 | 0.66 | 0.35 |
| | 20 | 734 | 0.88 | -0.01 | 0.22 | 0.15 | 0.65 | 0.66 | 0.34 |
| | 30 | 531 | 0.87 | -0.02 | 0.23 | 0.16 | 0.66 | 0.68 | 0.36 |

*Table 2. $T_{m02}$ and $T_{peak}$ error statistics for different computational time steps in 3 sub-grids*

| | | **$T_{m0s}$ error statistics at Sinop** | | | | | | | |
|---|---|---|---|---|---|---|---|---|---|
| | **Time step (min)** | **n** | **R** | **bias** | **rmse** | **mae** | **$X_{mean}$** | **$Y_{mean}$** | **si** |
| **Wind input: Komen** **Whitecapping: Janssen** **$C_{ds}$=3** | 5 | 2164 | 0.73 | 0.08 | 0.73 | 0.59 | 3.79 | 3.71 | 0.19 |
| | 10 | 2164 | 0.73 | 0.08 | 0.73 | 0.59 | 3.79 | 3.71 | 0.19 |
| | 15 | 2413 | 0.72 | 0.09 | 0.74 | 0.59 | 3.79 | 3.70 | 0.20 |
| | 20 | 1828 | 0.72 | 0.10 | 0.74 | 0.59 | 3.80 | 3.70 | 0.19 |
| | 30 | 1249 | 0.71 | 0.12 | 0.74 | 0.59 | 3.80 | 3.68 | 0.19 |
| | | **$T_{peak}$ error statistics at Filyos** | | | | | | | |
| | **Time step (min)** | **n** | **R** | **bias** | **rmse** | **mae** | **$X_{mean}$** | **$Y_{mean}$** | **si** |
| **Wind input: Komen** **Whitecapping: Janssen** **$C_{ds}$=9** | 5 | 1335 | 0.52 | 0.11 | 1.24 | 0.95 | 5.46 | 5.35 | 0.23 |
| | 10 | 1335 | 0.51 | 0.11 | 1.23 | 0.95 | 5.46 | 5.35 | 0.23 |
| | 15 | 1335 | 0.52 | 0.10 | 1.23 | 0.95 | 5.46 | 5.36 | 0.23 |
| | 20 | 4003 | 0.50 | 0.09 | 1.27 | 0.96 | 5.46 | 5.37 | 0.23 |
| | 30 | 1335 | 0.52 | 0.08 | 1.22 | 0.94 | 5.46 | 5.38 | 0.22 |

## 124. CONCLUSION

In this study, SWAN model calibration and sensitivity analysis process for coarse, fine and 3 sub-grids of the nested grid system has been performed. The physical and numerical settings for each grid have been carried out by using the measured buoy data at six locations along the Black sea coasts were investigated. Based on the derived results, it was determined that the whitecapping process has the most effect on the SWAN model performance while the other processes and tunable parameters had less impact on the model results. The SWAN model setups for each grid are as below.

For coarse grid:

- Komen et al [2] & Janssen [3, 4]

  Delta = 1.0

  $C_{ds}$ = 1.5

  The time step of the non-stationary computation: 30 min
  Other physical processes are active in default mode

For fine grid:

- Janssen [3, 4] & Janssen [3, 4]

  Delta = 1.0

  $C_{ds}$ = 3.0

  The time step of the non-stationary computation: 30 min

Other physical processes are active in default mode
Boundary conditions are from SWAN model with the coarse grid

For SD1 sub-grid:

- Komen et al. [2] & Janssen [3, 4]

  Delta = 1.0

  $C_{ds}$ = 3.0

  The time step of the non-stationary computation: 10 min
  Other physical processes are active in default mode
  Boundary conditions are from SWAN model with the fine grid

For SD2 sub-grid:

- Komen et al. [2] & Janssen [3, 4]

  Delta = 1.0

  $C_{ds}$ = 9.0

  The time step of the non-stationary computation: 30 min
  Other physical processes are active in default mode
  Boundary conditions are from SWAN model with the fine grid

For SD3 sub-grid:

- Komen et al. [2] & Janssen [3, 4]

  Delta = 1.0

  $C_{ds}$ = 2.0

  The time step of the non-stationary computation: 20 min
  Other physical processes are active in default mode
  Boundary conditions are from SWAN model with the fine grid.

Validation of the SWAN model results, which will be performed using data not used in the calibration, is still ongoing. After validation, 31-year long term simulations for three sub-grids will be carried out to correctly assess wave energy potential along the south western coasts of the Black Sea.

**ACKNOWLEDGEMENT**

We would like to thank the NCEP CFS team for providing the CFSR winds, the NOAA (General Bathymetric Chart of the Oceans, GEBCO) for the providing the bathymetry data, the Turkish Ministry of Transport (General Directorate of Railways, Ports and Airports Construction) for the providing the wave measurements at Filyos and Karaburun, and the NIMRD (Oceanography Department) for the providing the wind and wave measurements at Gloria.

The authors would like to acknowledge Prof. Dr. Erdal Özhan of the Middle East Technical University, Ankara, Turkey, who was the Director of the NATO TU-WAVES, for providing the buoy data at Gelendzhik, Hopa, and Sinop, and the NATO Science for Stability Program for supporting the NATO TU-WAVES project.

Special thanks from the author go to TUBITAK (The Scientific and Technological Research Council of Turkey) for its supporting our Project under the grant number 214M436.

## REFERENCES

[349]. A. Akpınar, S. Bekiroglu, G.Ph. Van Vledder, B. Bingölbali, H. Jafali, *Temporal and Spatial Analysis of Wave Energy Potential Along the Southern west Coasts of the Black Sea*, Project Number: 214M436, TUBITAK Project, 2015 (In Progress).

[350]. G.J. Komen, L. Cavaleri, M. Donelan, K. Hasselmann, S. Hasselmann, P.A.E.M. Janssen, *Dynamics and Modelling of Ocean Waves*. Cambridge University Press, 1994.

[351]. P.A.E.M. Janssen, *Quasi-linear theory of wind-wave generation applied to wave forecasting*, Journal of Physical Oceanography, 21, 1631-1642, 1991a.

[352]. P.A.E.M. Janssen, *Consequences of the effect of surface gravity waves on the mean air flow*, Int. Union of Theor. and Appl. Mech. (IUTAM), Sydney, Australia, 193-198, 1991b.

[353]. L. Yan, *An improved wind input source term for third generation ocean wave modelling*, Scientific report WR-No 87-8, De Bilt, The Netherlands. 1987.

[354]. K. Hasselmann, T.P. Barnett, E. Bouws, H. Carlson, D.E. Cartwright, K. Enke, J.A. Ewing, H. Gienapp, D.E. Hasselmann, P. Kruseman, A. Meerburg, P. Müller, D.J. Olbers, K. Richter, W. Sell, H. Walden, *Measurements of wind-wave growth and swell decay during the Joint North Sea Wave Project (JONSWAP)*, Dtsch. Hydrogr. Z. Suppl., 12, A8, 1973.

[355]. O.S Madsen, Y.-K Poon, H.C. Graber, *Spectral wave attenuation by bottom friction*: Theory, Proc. 21 th Int. Conf. Coastal Engineering, ASCE, 492-504, 1988.

[356]. J.I. Collins, *Prediction of shallow water spectra*, Journal of Geophysical Research, 77 (15), 2693-2707, 1972.

[357]. G.Ph. Van Vledder, A. Akpınar, *Wave model predictions in the Black Sea: Sensitivity to wind fields*. Applied Ocean Research, 53, 161-178, 2015.

[358]. A.J Westhuysen, M. Zijlema, J.A. Battjes, *Nonlinear saturation based whitecapping dissipation in SWAN for deep and shallow wate*r, Coastal Engineering, 54, 151-170, 2007.

[359]. A. Akpınar, G.Ph. van Vledder, M.İ. Kömürcü, M. Özger, *Evaluation of the numerical wave model (SWAN) for wave simulation in the Black Sea*, Continental Shelf Research, 50-51, 80-99, 2012.

ICENS
INTERNATIONAL CONFERENCE ON ENGINEERING AND NATURAL SCIENCES
24-28 May 2016 /Sarajevo

# Modeling of Pyrolysis Products by Multiple-Linear Regression Model

***Hasan Merdun***

*Akdeniz University, Faculty of Engineering, Environmental Engineering Department, 07058 Antalya – TURKEY.*
***E-mail:*** *merdun@alumni.clemson.edu*

***Abstract***

*Pyrolysis is probably the most commonly applied conversion process in which biomass is heated to moderate temperatures in an oxygen free atmosphere to yield solid (biochar), liquid (bio-oil) and gaseous (gas mixtures) products. The yield and quality of pyrolysis products depend on several parameters such as feedstock properties and pyrolysis process parameters. The particle size, porosity, humidity, ash and mineral content are typical feedstock properties while pyrolysis temperature, heating rate, residence time, sweeping gas flow rate, and catalyst type are process parameters. Modeling pyrolysis products by using the feedstock and pyrolysis process parameters as input through multiple-linear regression technique is relatively easy, produces acceptable results, and offers trying several scenarios at short time. In this study, after collecting pyrolysis data from the literature, pyrolysis products (bio-oil, biochar or gas mixture) were modeled by multiple-linear regression using pyrolysis process parameters (temperature, nitrogen gas flow, and biomass particle size) as input. The 75% of the data were used for the model derivation and the remaining 25% were used for the model validation. The performances of the derivation and validation models were evaluated by using coefficient of determination ($R^2$) and root mean square error (RMSE). Some of the models had higher performances compared to the others and some of the independent model parameters were significant, whereas the others were not in the modeling processes. It can be said that multiple-linear regression technique is promising in modeling pyrolysis products by using pyrolysis process parameters as input variables.*

**Keywords:** pyrolysis, bio-oil, biochar, gas, modeling, multiple-linear regression

## 125. INTRODUCTION

The importance of energy in our daily life is increasing because it is the basic element or driving force of social and economical development. Renewable energy sources and technologies in Turkey should be improved because fossil fuel resources (coal, oil, and natural gas) are limited and they cause environmental problems such as climate changes, acid rains, and natural resources pollution. Solar, wind, hydraulic, and biomass are main renewable energy sources [1]. Since biomass is available in all over the world, it is produced automatically, therefore, it is cheap, and its conversion technologies into biofuels are well-developed, biomass energy or bioenergy is getting more interest in all over the world.

Biomass is all organic materials that store the solar energy in their chemical bonds [2]. Biomass is defined as all materials which includes terrestrial and aquatic plants, animal wastes, food and forest wastes, and urban wastes. Energy in biomass as in conventional fuels is a chemical energy formed by bonding of carbon and hydrogen atoms [3]. Biomass energy resources can be classified into three main groups: agricultural resources (animal, plant, and aquatic), forest resources (woody resources), urban (municipal solid wastes, sewage sludge), and industrial resources [4].

Biomass can be converted to useful energy forms by using different processes or technologies. Biomass can be converted to three main products: power/heat production, fuel, and useful chemicals. Generally, biomass is directly converted to heat energy through combustion. However, nowadays, the developed countries prefer

biomass not only for converting into heat energy, but also for producing biofuel and useful chemicals through modern technologies Two main processes are available in order to produce energy from biomass: thermochemical and biochemical. Biomass biochemical conversion technologies include two main processes; anaerobic digestion and fermentation, whereas biomass thermochemical conversion technologies include combustion, pyrolysis, gasification, and liquefaction ([3], [5]).

Pyrolysis is a process to obtain organic volatiles from biomass by decomposition of organic molecules under oxygen-free environment. Pyrolysis products are solid (char/biochar), liquid (bio-oil), and gas

(mixture of several gases). The yields of these products depend on biomass type, process parameters, and reactor type [6]. Pyrolysis is an easily applied thermochemical method to produce solid, liquid and geseous fuel from biomass. Liquid product produced by pyrolysis contains quite complex organic compounds and some water. Besides, this liquid is extremely viscous, corosive, and unstable and it has low heating value. Therefore, this pyrolytic liquid should be upgraded to be able to use in vehicles as fuel [7]. Pyrolysis methods are slow pyrolysis, intermediate pyrolysis, and fast pyrolysis [8]. Pyrolysis process parameters that affect the distribution of pyrolysis products are pyrolysis temperature, heating rate, residence time, pyrolysis time, carrier gas flow rate, pressure, biomass particle size, pyrolysis environment, catalyst, and reactor geometry ([9], [3]).

Intensive experimental studies related to biomass pyrolysis are conducted in all over the world, but the modeling studies on pyrolysis are very limited in the literature. Modeling offers chance to investigate the relationships between the pyrolysis parameters and try many scenarios in a short time with limited effort and expense. Therefore, the objectives of this study are to: i) determine the parameters that affect pyrolysis product yield and obtain these parameter values, ii) modeling the pyrolysis product yields through multiple-linear regression, iii) interpreting the modeling results in terms of the parameters affecting the pyrolysis product yields, and iv) assessing the performence of multiple-linear regression model in modeling the pyrolysis product yields by using some statistical parameters.

## 126. MATERIALS AND METHODS

The data used in this study were collected from the thesis and articles produced from pyrolysis studies conducted in Turkey. The data set with the pyrolysis input parameters and products such as temperature, bio-oil, biochar, and gas mixture was composed of 506 samples. The data set with the pyrolysis input parameters and products such as temperature, nitrogen gas flow, biomass particle size, bio-oil, biochar, and gas mixture was composed of 302 samples. Pyrolysis products such as bio-oil, biochar, and gas mixture was modeled by multiple-linear regression by using pyrolysis process parameters like temperature, nitrogen gas flow, and biomass particle size in addition to gas mixture as input data.

Multiple-linear regression model is a mathematical model determined through statistical analysis which investigate the cause and effect relationships between three or more parameters or variables in order to make estimation or prediction of a dependent variable from various number of independent variables. Multiple linear-regression is a method of estimation or prediction of dependent variable from certain values of independent variables. General form of multiple-linear regression models can be expressed as follows:

$$y_i = \beta_0 + \beta_1 x_{i1} + \beta_2 x_{i2} + \beta_3 x_{i3} + \ldots\ldots + \beta_n x_{in} + \varepsilon_i \quad (1)$$

where, $y_i$ is dependent variable, $\beta_0$ is intercept, $\beta_1$, $\beta_2$, $\beta_3$, ..... , $\beta_n$ are regression coefficients, $x_{i1}$, $x_{i2}$, $x_{i3}$, ....., $x_{in}$ are independent variables, and $\varepsilon_i$ is error term. Only main effects, main effects and interactions, and quadratic terms were used in multiple-linear regression models in order to get complete modeling or the best results. The 75% of all data were used for the derivation of multiple-linear regression models, whereas the remaining 25% were used for the validation of the models. All multiple-linear regression analyses were performed by using Statistical Analysis System (SAS) package program. The performences of the multiple-linear regression models were evaluated by two statistical evaluation parameters: coefficient of determination ($R^2$) and root mean square error (RMSE).

## 127. RESULTS AND DISCUSSION

Descriptive statistics of the input and output parameters of derivation and validation of multiple-linear regression models are given in Table 1. The ranges of input parameters such as temperature (T), nitrogen gas flow (N), and biomass particle size (PS) for derivation of models were 400-700$^o$C, 100-800 mL/min, and 0.2-1.5 mm, respectively. The ranges of output parameters such as bio-oil (OIL), biochar (CHAR), and gas mixture (GAS) for derivation of models were 26.8-57.6%, 17.7-51.5%, and 14.1-82%, respectively. The ranges of input and output parameters of validation of models had a similar trends.

*Table 1. Descriptive statistics of input and output parameters of derivation and validation of multiple-linear regression models*

| Parameter | Derivation | | | | Validation | | | |
|---|---|---|---|---|---|---|---|---|
| | Min | Ort | Max | SD | Min | Ort | Max | SD |

| | | | | | | | | |
|---|---|---|---|---|---|---|---|---|
| T* | 400 | 550 | 700 | 110 | 400 | 564 | 700 | 105 |
| N | 100 | 243 | 800 | 115 | 50 | 249 | 400 | 114 |
| PS | 0.2 | 0.62 | 1.5 | 0.4 | 0.2 | 0.68 | 1.5 | 0.5 |
| OIL | 26.8 | 10.6 | 57.6 | 7 | 23 | 40.8 | 52.5 | 5.9 |
| CHAR | 17.7 | 27.4 | 51.5 | 6.9 | 10.3 | 27.1 | 44 | 7 |
| GAS | 14.1 | 30.5 | 82 | 9.4 | 23 | 40.8 | 52.5 | 5.9 |

*T: Temperature ($^oC$), N: Nitrogen gas flow (mL/min), PS: Biomass particle size (mm), OIL: Bio-oil yield (%), CHAR: Biochar yield (%), GAS: Gas yield (%).

Models for bio-oil and their performances for derivation and validation are shown in Table 2. Bio-oil (O) was modeled by using temperature (T), biochar (C), and gas mixture (G) as input parameters. The differences among the models ($O_1$, $O_2$, $O_3$) were the number of samples used in the modeling, where the number of samples were 506, 302, and 172, respectively. Only main affects were used in the models because when main effects and interactions and quadratic terms were included into the models, the models had very bad performances. The models had much better performences in the derivation than in the validation, where $R^2$ values were much higher and RMSE values were lower in the derivation compared to the validation.

*Table 2. Models for bio-oil and their performences for derivation and validation*

| Model | Derivation | | Validation | |
|---|---|---|---|---|
| | $R^2$ | RMSE | $R^2$ | RMSE |
| $O_1$=57.07+0.0260 T-0.341 C-0.693 G | 0.52 | 4.63 | 0.05 | 11.2 |
| $O_2$=52.01+0.0179 T-0.509 C-0.181 G | 0.99 | 4.65 | 0.86 | 13 |
| $O_3$=-159.6+0.537 T +5.656 C-0.573 G | 0.71 | 7.04 | 0.02 | 14.6 |

O: Bio-oil yield (%), T: Temperature ($^oC$), C: Biochar yield (%), GAS: Gas yield (%), $R^2$: Coefficient of determination, RMSE: Roort Mean Square Error.

Models for bio-oil and their performances for derivation and validation are shown in Table 3. Bio-oil (O) was modeled by using temperature (T), nitrogen gas flow (N), and biomass particle size (PS) as input parameters. The first model ($O_1$) had only main effects, the second model ($O_2$) had main effects and interactions, and the third model ($O_3$) had main effects, interactions, and quadratic terms. The second model had the best and similar performances in both derivation and validation based on $R^2$ and RMSE values. However, even though the first model had much better performance in the derivation than in the validation, both derivation and validation had low performances. These results showed that only main effects were not good enough to model bio-oil, but including much terms (quadratic terms) were also not a good idea as shown in the third model to improve the performance of the model.

*Table 3. Models for bio-oil and their performences for derivation and validation*

| Model | Derivation | | Validation | |
|---|---|---|---|---|
| | $R^2$ | RMSE | $R^2$ | RMSE |
| $O_1$=46.21+0.0023 T-0.014 N-5.799 PS | 0.22 | 6.20 | 3.35E-06 | 5.60 |
| $O_2$=40.63+0.0189 T -0.013 N-2.026 PS-3E-5 T N-0.016 T PS+0.0206 N PS | 0.86 | 6.10 | 0.84 | 5.70 |
| $O_3$=-55.63+0.385 T+0.0141 N-12.74 PS-33E-5 $T^2$-21E-6 $N^2$ +9.083 $PS^2$-51E-6 T N-0.018 T PS +0.0127 N PS | 0.50 | 5.10 | 0.37 | 5.20 |

O: Bio-oil yield (%), T: Temperature ($^oC$), N: Nitrogen gas flow (mL/min), PS: Biomass particle size (mm), $R^2$: Coefficient of determination, RMSE: Roort Mean Square Error.

Models for gas mixture and their performances for derivation and validation are presented in Table 4. Gas mixture (G) was modeled by using temperature (T), nitrogen gas flow (N), and biomass particle size (PS) as input parameters. The first model ($G_1$) had only main effects, the second model ($G_2$) had main effects and interactions, and the third model ($G_3$) had main effects, interactions, and quadratic terms. The second and third models had very good performances for both derivation and validation, where $R^2$ values were very high and RMSE values were relatively low. However, the first model had low performances in the derivation and validation. These results showed that only main effects were not good enough to model gas mixture as seen in Table 4.

*Table 4. Models for gas mixture and their performences for derivation and validation*

| Model | Derivation | Validation |
|---|---|---|

| | $R^2$ | RMSE | $R^2$ | RMSE |
|---|---|---|---|---|
| $G_1$=-3.099+0.052 T +0.0111 N+5.401 PS | 0.38 | 7.40 | 0.21 | 6.40 |
| $G_2$=6.650+0.0303 T+0.0024 N-4.117 PS + 328E-7 T N+0.0232 T PS-0.011 N PS | 0.95 | 7.30 | 0.95 | 6.90 |
| $G_3$=68.06-0.200 T-0,011 N-1.572 PS+ 0.0002 $T^2$+144E-7 $N^2$-3.324 $PS^2$+425E-7 T N+0.0259 T PS-0.009 N PS | 0.88 | 7.30 | 0.90 | 6.40 |

GAS: Gas yield (%), T: Temperature ($^o$C), N: Nitrogen gas flow (mL/min), PS: Biomass particle size (mm), $R^2$: Coefficient of determination, RMSE: Roort Mean Square Error.

Models for biochar and their performances for derivation and validation are tabulated in Table 5. Biochar (C) was modeled by using temperature (T), nitrogen gas flow (N), and biomass particle size (PS) as input parameters. The first model ($C_1$) had only main effects, the second model ($C_2$) had main effects and interactions, and the third model ($C_3$) had main effects, interactions, and quadratic terms. The second and third models had very good performances for both derivation and validation, where $R^2$ values were very high and RMSE values were relatively low. And also the first model had good enough performances in the derivation and validation. These results showed that the second and third models should be preferred to the first model in which only main effects were not good enough to model biochar as seen in Table 5.

*Table 5. Models for biochar and their performences for derivation and validation*

| Model | Derivation | | Validation | |
|---|---|---|---|---|
| | $R^2$ | RMSE | $R^2$ | RMSE |
| $C_1$=57.08-0.047 T-0.021 N+0.295 PS | 0.61 | 4.30 | 0.52 | 4.20 |
| $C_2$=55.72-0.043 T-0.037 N+6.620 PS + 232E-7 T N-0.014 T PS+0.0049 N PS | 0.98 | 4.20 | 0.97 | 4.30 |
| $C_3$=124.7-0.302 T-0.038 N+3.939 PS+ 0.0002 $T^2$+481E-8 $N^2$-0.648 $PS^2$+ 269E-7 T N-0.009 T PS+0.0055 N PS | 0.91 | 11.00 | 0.88 | 11.10 |

C: Biochar yield (%), T: Temperature ($^o$C), N: Nitrogen gas flow (mL/min), PS: Biomass particle size (mm), $R^2$: Coefficient of determination, RMSE: Roort Mean Square Error.

## 128. CONCLUSIONS

The relationships between pyrolysis process parameters and pyrolysis products were studied or pyrolysis products were modeled through multiple-linear regression method by using pyrolysis process parameters as input parameters. In general, multiple-linear regression technique was good enough to model pyrolysis products such as bio-oil, biochar, and gas mixture by using pyrolysis process parameters as input. Parameters such as pyrolysis temperature, nitrogen gas flow, and biomass particle size were significant input parameters in all models. The models with the main effects and interactions of input parameter produced the best results, whereas the models with only main effects of input parameters resulted in the worst results. As a conclusion, the application of multiple-linear regression technique is promising in modeling pyrolysis products by using pyrolysis process parameters as input variables.

***Biography***: Dr. Hasan Merdun is currently serving as a faculty member at the Department of Environmental Engineering, Akdeniz University in Turkey. He got his undergraduate degree on Agricultural Engineering in Turkey. He got his MSc degree at Agricultural Engineering Department and PhD degree at Crop and Soil Environmental Sciences in Clemson University, USA, on the subjects of soil and water resources. After getting his PhD degree, he started working at the university as an academician. Around six years ago, he shifted his research interests from soil and water resources to bioenergy production through thermochemical processes / technologies, specifically fast pyrolysis and gasification. He has a specially designed drop-tube reactor for fast pyrolysis and is currently working on several projects. His research mission is to add value to the national and global bioenergy sector by applying an integrated biorefinery approach for the development of renewable energy technologies.

## ACKNOWLEDGMENT

The author expresses his gratitude to undergraduate students (Şevket KILIÇ, Barış KISA, and İsmail DUMAN) for their helps in collecting the data.

## REFERENCES

[360]. K. Kaygusuz K., "Hydropower and the World's Energy Future", *Energy Sources*, 26, 215-224, 2004.
[361]. R. C. Saxena, D. K. Adhikari, H.B. Goyal, H.B., "Biomass-based energy fuel through biochemical routes: A review", *Renewable and Sustainable Energy Reviews*, 13, 167-178, 2009.
[362]. P. Mckendry, "Energy Production from Biomass (Part 2): Conversion Technologies", *Bioresource Technology*, 83, 47-54, 2002.
[363]. S. Demirtaş S., "Avrupa Birliği ve Türkiye'de yenilenebilir enerji kaynakları ve bunlarda biyokütlenin önemi", 46. Dönem AB Temel Eğitim Kursu, Orman Genel Müdürlüğü, Ankara, 2010.
[364]. M. Parikka, "Global Biomass Fuel Resources", *Biomass and Bioenergy*, 27, 613-620, 2004.
[365]. İ. Üçgül, G. Akgül, "Biyokütle Teknolojisi", *Yekarum Dergi*, 1, 3-11, 2010.
[366]. M. Acaroğlu, A. S. Aksoy, H. Öğüt, "The potential of biomass and animal waste of Turkey the possibilities of these as fuel in thermal generating stations", *Energy Sources*, 21, 339-345, 1999.
[367]. D. Mohan, J. Pittman, U. Charles, P. H. Steele, "Pyrolysis of Wood/Biomass for Bio-Oil: A Critical Review", *Energy & Fuels*, 20, 848-889, 2006.
[368]. D. L. Klass, "Biomass for Renewable Energy, Fuels and Chemicals", *Academic Press*, London, 1998.

# Biofuel Production from Municipal Solid Wastes by Fast Pyrolysis

***Hasan Merdun[1], İsmail Veli Sezgin[2]***

*[1,2]Akdeniz University, Faculty of Engineering, Environmental Engineering Department, 07058 Antalya – TURKEY.*
***E-mail:** merdun@alumni.clemson.edu*

***Abstract***

*Municipal solid wastes (MSW) are problematic directly for surface and subsurface waters and indirectly for climate change because of the decomposition of biodegradable part of them, leading to the emission of greenhouse gasses. Nowadays, avoiding negative environmental impacts of biodegradable wastes and evaluate them as an energy source either for the protection of the environment and producing fuel / biofuel are widely discussed in the scientific researches. For this purpose, in this study, yard wastes and food wastes were used as the biodegradable waste material in the fast pyrolysis experimental system in order to investigate the effect of different parameters (catalyst type, biomass particle size, temperature) on bio-oil and biochar yields and bio-oil quality. GC-MS analyses were made to determine the compounds of the obtained bio-oil samples. Based on the study results, different experiments produced different amounts of bio-oil and biochar. The highest bio-oil yield was obtained as 42.73% in the experiment in which the biomass particle size was 1.0-1.5 mm, the temperature was 500°C, and catalyst type of dolomite. Besides, it was observed that bio-oil yield was the highest in case of zeolite usage as a catalyst. GC-MS analysis results showed that bio-oil contained levoglucosan compound in the highest amount. Allose, which is a kind of sugar, was in the second highest amount in bio-oil. Heptanoic acid, butiric acid, and the other acids were also observed in bio-oil.*

**Keywords:** energy, renewable energy, fast pyrolysis, biomass, bio-oil, bioenergy

## 129. INTRODUCTION

Main domestic energy resources of Turkey are coal, hydraulic, and biomass (as traditional fuel) and there are no great oil and natural gas reserves in Turkey. Turkey imports around 75% of its energy demand as fossil fuels such as petroleum and natural gas [1]. Especially after 1973 energy crisis, intensive national and international researches began on renewable (alternative) energy resources. The main parts of these researches were related to biomass energy [2]. Currently, 14% of the world energy consumption is from renewable energy resources and biomass is one of the important parts (around 10%) of these sources [3].

Biomass, known as biorenewable resources, is defined as all materials from biological origins. Biomass energy or bioenergy is conversion of biomass into useful energy forms such as heat, electric, and liquid and gas fuels [4]. Biomass typically contains cellulose, hemicellulose, lignin, extractives, lipids, proteins, simple sugars, starches, water, inorganics (ash), and other compounds [5]. Eelementel composition of biomass (as dry weight %) is 51% carbon (C), 42% oxygen (O), 5% hydrogen (H), 0.9% nitrogen (N), and 0.01-2% chloride (Cl) [6]. Municipal solid wastes (MSW) contains up to 70-75% organic materials such as paper, cardboard, yard wastes, food wastes, plant and forest residues, plastics, etc.

Recently, MSW management is one of the great problems of the world because of the increase in urbans populations, as a result, the production of MSW. The storage of MSW is the most general method of their destroy. However, it confirmed by researchers that this method causes the pollution of the environment and surface and/or subsurface water resources, emission of methane ($CH_4$) gas due to the decomposition of biomass,

bad smelling, emission of harmful gases due to the artificial and natural combustion of biomass, as a result, air pollution and climate change. Therefore, the conversion of MSW into energy attracts an important interest globally. Evaluation of MSW as biomass resources is an important issue of Turkey in general but Antalya Province in special. Since the conversion of MSW into biofuels through biochemical conversion technologies (anaerobic digestion and fermentation) is inefficient due to high lignin content of MSW, thermochemical conversion technologies (combustion, pyrolysis, gasification, liquefaction) are used in quite effective conversion of MSW into biofuels. MSW pyrolysis and gasification technologies compared to the other technologies draw more attention in volarization of MSW by researchers due to the less pollution emission to the environment [7]. In Turkey a number of studies related to the conversion of biomass into biofuels (mostly biogas) through biochemical conversion technologies is available, studies on thermochemical conversion of biomass into biofuels through pyrolysis or gasification are very limited. It is obvious that biomass resources in Turkey should be evaluated by modern and effective technologies in order to prevent the formation of harmful wastes from biomass for the environment and also to get rid of extreme energy deficit by producing biofuels out of biomass.

Therefore, the general objective of this study is to convert organic parts of MSW into biofuel (bio-oil) by fast pyrolysis. The specific objective of the study is to investigate the effects of catalyst type, biomass particle size, and pyrolysis temperature on the yield and quality of bio-oil by using a laboratory scale drop-tube reactor fast pyrolysis experimental system. The yield of bio-oil is determined by mass balance calculations and the quality of bio-oil is determined by GC-MS analysis of bio-oil samples. Optimum fast pyrolysis process parameter values have been determined at the end of such study.

## 130. MATERIALS AND METHODS

### *2.1. Materials*

Since the most common organic matials found in MSW in Antalya Province were paper-cardboard, yard wastes, and food wastes based on the MSW characterization made by Municipality of Antalya Province; yard wastes and food wastes were used as biomass material in this study. After biomass materials were air-dried for one week, they were milled and sieved to get the desired biomass particle size. Biomass sample used in all experiments was 15 g (7.5 g mixture of yard wastes and food wastes)

Catalyst is used to improve improper bio-oil properties such as high oxygen content, low calorific value, high viscosity, and instability. Tar production during pyrolysis process decreases if an inorganic material is mixed with an organik material [8]. Natural catalysts such as dolomite, calcite, and zeolite were used in this study to improve bio-oil quality. Catalyst amount used in all experiments was 7.5 g (1:2 catalyst:biomass).

### *2.2. Methods*

#### *2.2.1. Pyrolysis*

Pyrolysis is conversion of biomass into liquid (bio-oil, tar, organic compounds, water), solid (char or biochar), and gas (CO, $H_2$, $CO_2$, $CH_4$) products under no oxygen and atmospheric pressure around 400-600$^oC$ temperature ([9]-[10]). Even though pyrolysis has different types such as slow, intermediate, and fast pyrolysis; nowadays fast pyrolysis is commonly used because mainly bio-oil can be produced up to 75% in this process. In fast pyrolysis process, biomass is decomposed to mainly produce bio-oil under no oxygen and atmospheric pressure with around constant temperature of 500$^oC$ but very high heating rate (300 $^oC$/s). Main characteristics of fast pyrolysis are: i) small biomass particle size and very high heating and heat transfer rates, ii) good controlled reaction temperature of around 500$^oC$ in vapor phase, iii) keeping pyrolysis vapor in reactor less than a second, and iv) quenching or cooling pyrolysis vapor very fast to obtain bio-oil ([11-[13]).

#### *2.2.2 Experiments*

Fast pyrolysis experiments were conducted in a specially designed laboratory scale drop-tube reactor experimental system (Figure 1). After placing biomass sample (15 g) into biomass bed and reactor temperature reached the desired level, biomass

was dropped into the reactor. Then, pyrolysis vapor passing through the catalyst bed was condensed in condenser as bio-oil, but non-condensable gases were collected in gas bag.

In fast pyrolysis experiments, the effects of catalyst type (dolomite, calcite, zeolite), biomass particle size (0.3-0.5, 0.5-1.0, 1.0-1.5 mm), and pyrolysis temperature (450, 500, 550$^{o}$C) on the yield and quality of bio-oil were investigated. Fast pyrolysis process parameters or experimental plan of this study is shown in Table 1. In all fast pyrolysis experiments, carrier gas (nitrogen) flow rate was 300 mL/min and pyrolysis (reaction) time was 5 min. Bio-oil yield was determined by mass balance of bio-oil collected in condenser. Similarly, biochar yield was determined by mass balance of biochar collected in the reactor after the experiment. Quality of bio-oil was determined through GC-MS by defining the names and amounts (peak areas) of chemical compounds in bio-oil.

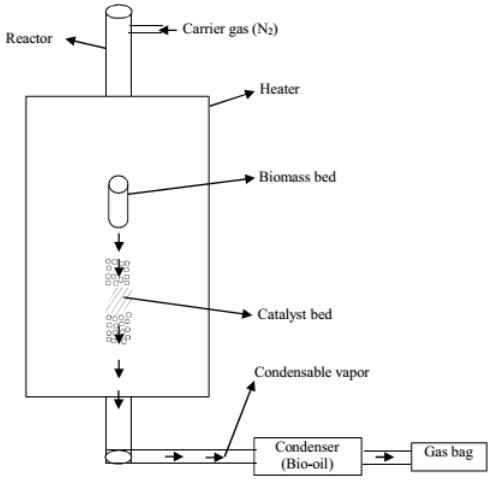


*Figure 1. Fast pyrolysis experimental system*

## 131. RESULTS AND DISCUSSION

In this study, the effects of catalyst type, biomass particle size, and pyrolysis temperature on the yield and quality of bio-oil were investigated by using yard wastes and food wastes as biomass wastes. The results about the effects of fast pyrolysis process parameters on pyrolysis product yields are presented in Table 1.

The highest bio-oil yield was observed as 42.73% in the experiment with the biomass particle size of 1.0-1.5 mm, pyrolysis temperature of 500$^{o}$C, and catalyst type of dolomite. The lowest bio-oil yield was observed as 26.53 in the experiment with the biomass particle size of 0.3-0.5 mm, pyrolysis temperature of 500$^{o}$C, and catalyst type of calcite. The highest biochar yield was observed as 43.40 in the experiment with the biomass particle size of 0.3-0.5 mm, pyrolysis temperature of 450$^{o}$C, and catalyst type of dolomite. The lowest biochar yield was observed as 27.27 in the experiment with the biomass particle size of 0.5-1.0 mm, pyrolysis temperature of 550$^{o}$C, and catalyst types of calcite and zeolite. When considering the overall effect of catalyst type on bio-oil yield it was observed that the order of the mean bio-oil yield from the highest to the lowest was as zeolite > dolomite > calcite with 36.61%, 36.49%, and 35.71%, respectively. It was observed that the overall effect of catalyst type on biochar yield with the mean biochar yield from the highest to the lowest was as dolomite > calcite > zeolite with 33.63%, 33.45%, and 32.17%, respectively. These results were similar to the results in the literature [13]. Biomass to bio-oil conversion got better with the biomass particle size of 1.0-1.5 > 0.5-1.0 > 0.3-0.5 mm in experiments conducted by using dolomite catalyst. Besides, biomass conversion to bio-oil decreased over 500$^{o}$C pyrolysis temperature under the dolomite catalyst. The highest bio-oil yield under calcite catalyst was observed as 40.67% with the biomass particle size of 0.5-1.0 mm, pyrolysis temperature of 450$^{o}$C. Biomass to bio-oil conversion got better with the biomass particle size of 0.5-1.0 > 1.0-1.5 > 0.3-0.5 mm in calcite use as catalyst. The highest bio-oil yield under zeolite catalyst was observed as 38.27% with the biomass particle size of 0.5-1.0 mm, pyrolysis temperature of 500$^{o}$C. Biomass to bio-oil conversion got better with the biomass particle size of 0.5-1.0 > 0.3-0.5 > 1.0-1.5 mm in zeolite use. In general, the yield ranges for bio-oil and biochar are 26-43% and 27-44. The reason of lower biochar yields in temperatures of 500 and 550$^{o}$C than in temperatures of 450 can be explained as that pyrolysis gas yield increases.

Properties of pyrolysis liquid depend on parameters such as biomass type, reactor type, and process conditions [14]. When GC-MS analysis results were examined (not shown here), it was observed that bio-oil contained over 70 chemical compounds. The number of chemical compounds in bio-oil samples determined based on GC-MS peak areas over 2.00 is tabulated in Table 2. A sample GC-MS analysis spectrum is shown in Figure 2. In general, in all fast pyrolysis experiments, most of chemical compounds in bio-oil had the peak area between 2.00 and 5.00, some between 5.00 and 10.00, few between 10.00 and 15.00, and almost no compounds over 15.00 (Table 2). Levoglucosan was the main chemical compound in bio-oil samples in terms of abundance. Levoglucosan is one of six-carbone organic products emerged out of pyrolysis of carbohydrates such as cellulose and starch. The other high amount compound after levoglucosan was allose which is monosaccharid sugar type. The reason of high amount of levoglucosan in bio-oil samples may be explained that half of the

biomass sample was the yard wastes (grass and plant residues), where they have high lignin contents. Besides, bio-oil sample contained high amount of organic structures such as butanoic acid, pentanoic acid, asetik acid, furfural, and 1,2-benzenediol.

*Table 1. Fast pyrolysis process parameters and pyrolysis product yields*

| | Fast Pyrolysis Process Parameters | | | Fast Pyrolysis Product Yields | | | |
|---|---|---|---|---|---|---|---|
| Experiment No | Catalyst | Particle Size (mm) | Temperature ($^{o}$C) | Biyoyağ (g) | Biochar (g) | Biyoyağ (%) | Biochar (%) |
| 1 | | 1-1.5 | 450 | 5.65 | 4.44 | 37.67 | 29.60 |
| 2 | | 1-1.5 | 500 | 6.41 | 5.01 | 42.73 | 33.40 |
| 3 | | 1-1.5 | 550 | 5.47 | 4.46 | 36.47 | 29.73 |
| 4 | Dolomite | 0.5-1 | 450 | 5.7 | 5.79 | 38.00 | 38.60 |
| 5 | | 0.5-1 | 500 | 6.3 | 4.65 | 42.00 | 31.00 |
| 6 | | 0.5-1 | 550 | 5.77 | 4.72 | 38.47 | 31.47 |
| 7 | | 0.3-0.5 | 450 | 4.26 | 6.51 | 28.40 | 43.40 |
| 8 | | 0.3-0.5 | 500 | 5.36 | 5.43 | 35.73 | 36.20 |
| 9 | | 0.3-0.5 | 550 | 4.34 | 4.39 | 28.93 | 29.27 |
| 10 | | 1-1.5 | 450 | 5.39 | 5.97 | 35.93 | 39.80 |
| 11 | | 1-1.5 | 500 | 5.65 | 4.58 | 37.67 | 30.53 |
| 12 | | 1-1.5 | 550 | 5.8 | 4.54 | 38.67 | 30.27 |
| 13 | | 0.5-1 | 450 | 5.66 | 6.10 | 37.73 | 40.67 |
| 14 | Calcite | 0.5-1 | 500 | 5.95 | 5.43 | 39.67 | 36.20 |
| 15 | | 0.5-1 | 550 | 5.9 | 4.09 | 39.33 | 27.27 |
| 16 | | 0.3-0.5 | 450 | 5.28 | 4.65 | 35.20 | 31.00 |
| 17 | | 0.3-0.5 | 500 | 3.98 | 5.07 | 26.53 | 33.80 |
| 18 | | 0.3-0.5 | 550 | 4.60 | 4.73 | 30.67 | 31.53 |
| 19 | Zeolite | 1-1.5 | 450 | 5.31 | 5.22 | 35.40 | 34.80 |
| 20 | | 1-1.5 | 500 | 5.43 | 4.84 | 36.20 | 32.27 |
| 21 | | 1-1.5 | 550 | 5.54 | 4.24 | 36.93 | 28.27 |
| 22 | | 0.5-1 | 450 | 5.58 | 5.25 | 37.20 | 35.00 |
| 23 | | 0.5-1 | 500 | 5.74 | 4.87 | 38.27 | 32.47 |
| 24 | | 0.5-1 | 550 | 5.73 | 4.09 | 38.20 | 27.27 |

| | | | | | | |
|---|---|---|---|---|---|---|
| 25 | 0.3-0.5 | 450 | 5.34 | 5.32 | 35.60 | 35.47 |
| 26 | 0.3-0.5 | 500 | 5.70 | 4.81 | 38.00 | 32.07 |
| 27 | 0.3-0.5 | 550 | 5.05 | 4.78 | 33.67 | 31.87 |

*Table 2. The number of chemical compounds in bio-oil samples based on GC-MS peak area*

| **Experiment No** | **GC-MS Peak Area** | | | |
|---|---|---|---|---|
| | 2-5 | 5-10 | 10-15 | > 15 |
| **1** | 8 | 7 | 1 | - |
| **2** | 11 | 3 | 1 | - |
| **3** | 8 | 1 | 1 | 1 |
| **4** | 6 | 5 | 1 | - |
| **5** | 9 | 1 | 1 | - |
| **6** | 12 | 2 | - | - |
| **7** | 11 | 5 | - | - |
| **8** | 11 | 4 | - | - |
| **9** | 12 | 2 | 1 | - |
| **10** | 14 | 1 | 1 | - |
| **11** | 12 | 2 | - | - |
| **13** | 15 | 3 | - | - |
| **14** | 16 | 2 | - | - |
| **15** | 12 | 5 | - | - |
| **16** | 14 | 3 | 1 | - |
| **17** | 9 | 5 | 1 | - |
| **18** | 11 | 4 | - | - |
| **19** | 10 | 4 | 2 | - |
| **20** | 8 | 3 | - | - |
| **21** | 10 | 2 | 1 | - |
| **22** | 10 | 2 | - | - |
| **23** | 12 | 3 | - | - |
| **24** | 10 | 4 | - | - |
| **25** | 6 | 5 | 1 | - |

| | | | | |
|---|---|---|---|---|
| **26** | 9 | 3 | - | - |
| **27** | 9 | 3 | 1 | - |

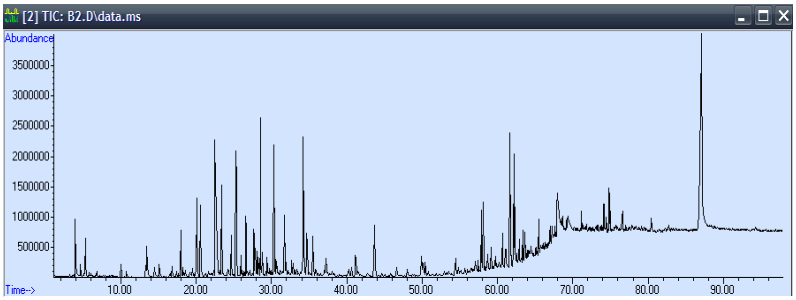


*Figure 2. GC-MS analysis spectrum*

## 132. CONCLUSIONS

In this study, biofuel (bio-oil) was produced from biomass wastes such as yard wastes and food wastes by using laboratory scale fast pyrolysis system. In experiments, the effects of catalyst type, biomass particle size, and pyrolysis temperature on pyrolysis products (bio-oil and biochar) yields and bio-oil quality were studied. The study results showed that pyrolysis temperature was a significant parameter that affects yield and quality. Overall the mean bio-oil yield was the highest with zeolite, but the mean biochar yield was the highest with dolomite. GC-MS analysis results showed that bio-oil contained levoglucosan compound with highest amount. Even though bio-oil yield may reach up to 70-75% of dry biomass weight in literature, in bio-oil yield was relatively low, may be because of low lignin content of biomass used in this study. Besides, fast pyrolysis process parameters should be experimented with smaller changes so that the effects of these parameters on the yield and quality of the products (bio-oil and biochar) may be captured better. And also configuration and control (automation) of fast pyrolysis experimental system may be improved.

***Biography***: Dr. Hasan Merdun is currently serving as a faculty member at the Department of Environmental Engineering, Akdeniz University in Turkey. He got his undergraduate degree on Agricultural Engineering in Turkey. He got his MSc degree at Agricultural Engineering Department and PhD degree at Crop and Soil Environmental Sciences in Clemson University, USA, on the subjects of soil and water resources. After getting his PhD degree, he started working at the university as an academician. Around six years ago, he shifted his research interests from soil and water resources to bioenergy production through thermochemical processes / technologies, specifically fast pyrolysis and gasification. He has a specially designed drop-tube reactor for fast pyrolysis and is currently working on several projects. His research mission is to add value to the national and global bioenergy sector by applying an integrated biorefinery approach for the development of renewable energy technologies.

## ACKNOWLEDGMENT

The authors would like to express their thanks to Scientific Research Projects Coordination Unit of Akdeniz University for the financial support that made this project (No: 2014.01.0102.004) possible.

## REFERENCES

[369]. Z. B. Erdem, “The contribution of renewable resources in meeting Turkey’s energy-related challenges”, *Renewable and Sustainable Energy Reviews*, 14, 2710-2722, 2010.
[370]. M. Acaroğlu, H. Aydoğan, “Biofuels energy sources and future of biofuels energy in Turkey”, *Biomass and Bioenergy*, 36, 69-76, 2012.
[371]. B. A. Ladislao, J. L. T. Gomez, “Second-generation biofuels and local bioenergy systems”, “Biofuels, Bioproducts & Biorefining”, 2, 455-469, 2008.
[372]. R. C. Brown, “Biorenewable Resources: Engineering New Products from Agriculture”, Iowa State Press, Ames, Iowa, 2003.
[373]. M. Siedlecki, W. de Jong, A. H. M. Verkooijen, “Fluidized bed gasification as a mature and reliable technology for the production of bio-syngas and applied in the production of liquid transportation fuels - A review”, *Energies*, 4, 389-434, 2011.
[374]. S. H. Schneider, A. Rosencranz, J. O. Niles, “Climate change policy”, Island Press, 2002.
[375]. M. Juraik, A. Sues, K. J. Ptasinski, “Exergetic evaluation and improvement of biomass-to-synthetic natural gas conversion”, *Energy and Environmental Sciences*, 2(7), 791-801, 2009.
[376]. S. C. N. Tripathi, “Effect of process parameters on production of biochar from biomass waste through pyrolysis”, *Renewable and Sustainable Energy Reviews*, 55, 467-481, 2015.
[377]. P. McKendry, “Energy production from biomass (part 2): conversion technologies”, *Bioresource Technology*, 83, 47-54, 2002.
[378]. M. K. Bahng, C. Mukarakate, D. J. Robichaud, M. R. Nimlos, “Current technologies for analysis of biomass thermochemical processing: A review”, *Analytica Chimica Acta*, 651, 117-138, 2009.

[379]. R. P. Overend, "Thermochemical conversion of biomass, in Renewable Energy Sources Charged with Energy from the Sun and Originated from Earth-Moon Interaction, [Ed. Evald E. Shpilrain], in Encyclopedia of Life Support Systems (EOLSS), Developed under the Auspices of the UNESCO, Eolss Publishers, Oxford ,UK, [http://www.eolss.net], 2004.
[380]. L. Qiang, L. Wen-Zhi, Z. Xi-Feng, "Overview of fuel properties of biomass fast pyrolysis oils", *Energy Conversion and Management*, 50, 1376-1383, 2009.
[381]. A. V. Bridgwater, "Review of fast pyrolysis of biomass and product upgrading", *Biomass and Bioenergy*, 38, 68-94, 2012.
[382]. S. Czernick, A. V. Bridgwater, "Overview of applications of biomass fast pyrolyisis oils", *Energ and Fuels*, 18, 590-598, 2004.

ISBN: 978-605-83575-0-1

# 2016 BOOK OF PROCEEDINGS

**ICENS**
International Conference on Engineering and Natural Sciences
www.icens.eu

**ICOEST**
International Conference on Environmental Science and Technology
www.icoest.eu

**ICSD**
International Conference on Sustainable Development
www.icsd.eu